

ELECTRO-OPTICAL EQUIPMENT FOR SPACECRAFT

A. N. Iznar, A. V. Pavlov, and B. F. Fedorov

- Translation of "Optiko-elektronnyye Pribory Kosmicheskikh
Apparátov," Moscow, "Mashinostroyeniye" Press, 1972, pp. 1-368
(NASA-TT-F-15368) ELECTRO-OPTICAL
EQUIPMENT FOR SPACECRAFT (Kanner (Leo)
Associates)

N74-72985

00/99 Unclass
27525

NATIONAL AERONAUTICS AND SPACE ADMINISTRATION
WASHINGTON, D. C. 20546 January 1974.

REPRODUCED BY
NATIONAL TECHNICAL
INFORMATION SERVICE
U.S. DEPARTMENT OF COMMERCE
SPRINGFIELD, VA. 22161

NOTICE

THIS DOCUMENT HAS BEEN REPRODUCED FROM THE BEST COPY FURNISHED US BY THE SPONSORING AGENCY. ALTHOUGH IT IS RECOGNIZED THAT CERTAIN PORTIONS ARE ILLEGIBLE, IT IS BEING RELEASED IN THE INTEREST OF MAKING AVAILABLE AS MUCH INFORMATION AS POSSIBLE.

ANNOTATION

UDC 629.78.054.001.24

Electro-Optical Devices for Spacecraft. A. N. Iznar, A. V. Pavlov, and B. F. Fedorov, Moscow, "Mashinostroyeniye," 1972, 368 pages.

The book presents the theoretical fundamentals for designing electro-optical instruments for orientation and navigation.

It examines the principles of construction and standard circuitry for electro-optical instruments for various purposes. Methods are presented for calculating parameters with consideration of attenuation of radiation in the atmosphere and the effect of backgrounds, and the special features of calculating the basic parameters of equipment with lasers are also presented.

Methods for calculating the characteristics of radiation sources are given.

The book is intended for specialists engaged in the development and planning of electro-optical instruments and may be useful for students of the higher education institutions.

174 illustrations, 32 tables, bibliography -- 70 titles.

Foreword

To control the movement of a spacecraft (SC) and accomplish various tasks in investigating outer space, information is required on the parameters of movement of the spacecraft itself as well as on phenomena in its surrounding environment. This information can be obtained with the use of measurements based on the use of various physical principles. Along with radio engineering systems, wider and wider application is being found by instruments based on the use of radiations of the optical band of the electromagnetic spectrum.

All instruments of electro-optical automatic equipment, homing systems, electro-optical measurement instruments, and others belong in this category.

These instruments are used for trajectory and orbital measurements, the precise guidance of the carrier rockets of spacecraft during launchings, for the automatic tracking of satellites, for the guidance and homing of SC during approach and docking and orientation of the SC relative to the earth, planets, and other heavenly bodies, and for the correction of orbits or the execution of a landing of the SC, meteorological observations, and weather forecasting.

Present-day Soviet electro-optical instrument making is based on the works of famous scientists N. D. Smirnov, V. V. Meshkov, S. V. Yeliseyev, V. G. Vafiad', L. P. Lazarev, N. G. Basov, A. M. Prokhorov, M. M. Miroshnikov, V. A. Khrustalev, D. M. Khorol, and many others.

In this book, basic attention is devoted to the physical principles of the construction of automatic electro-optical instruments which are employed in space technology, the special features in the construction of schematic diagrams, and to the calculation of the basic parameters which determine their functional properties.

Considering the ever wider use of lasers, the authors presented material in the book which throws light on the principles for the construction of electro-optical instruments with lasers and methods for their design.

The first part of the book outlines fundamentals of the theory of electro-optical instruments and the principles for the construction of instruments for various purposes.

The material of the second part of the book will give the reader the opportunity to calculate the parameters of the electro-optical equipment of a SC in the preliminary design stage.

Chapters 1, 2, 4-6, 9-13, sections 7.4 of Chapter 7, 8.5 of Chapter 8, and the appendix were written by A. V. Pavlov, Chapter 3 and sections 7.1 and 7.2 of Chapter 7¹ by A. N. Iznar, and Chapter 8 except for section 8.5 by B. F. Fedorov.

The authors express their profound gratitude to the Honored Scientist and Technician of the RSFSR [Russian Soviet Federative Socialist Republic], Professor and Doctor of Technical Sciences S. V. Yelisseyev and Doctor of Technical Sciences L. P. Lazarev for the advice which they gave in reviewing the rough draft for the book.

The authors thank the reviewer, Professor and Doctor of Technical Sciences L. A. Novitskiy, for the remarks and recommendations he made on the manuscript.

The authors also thank R. N. Denisov, Yu. F. Sitnikov, and Ye. D. Timoshenko for the assistance which they rendered in preparing the book for publication.

All comments on the book should be sent to the address: Moscow, B-78, 1st Basmanny Alley, 3, "Mashinostroyeniye" [Machine building] Publishing House.

¹ Section 7.3 of Chapter 7 was written by V. D. Permyakov

TABLE OF CONTENTS

	<u>Page</u>
Foreword	111
PART I	
PRINCIPLES OF THE DESIGN OF ELECTRO-OPTICAL INSTRUMENTS OF SPACECRAFT	
Chapter 1. Sources of Radiation and Their Characteristics	1
1.1. Standard Emitters and Their Characteristics	1
1.2. Radiation of Heavenly Bodies	11
1.3. Radiation of Auroras	18
1.4. Characteristics of the Radiation of Lasers	20
Chapter 2. The Propagation of Radiation in the Atmosphere and Space	25
2.1. Radiation Attenuation in a Uniform Medium	25
2.2. Brief Information About the Atmosphere	28
2.3. Characteristics of Outer Space	30
2.4. The Propagation of Radiation in the Atmosphere and Space	33
Chapter 3. Optical System of Electro-Optical Instruments of Space Vehicles	36
3.1. The Purpose and Characteristics of Optical Systems	36
3.2. Scheme of an Optical System and Its Elements	37
3.3. Dimensional Characteristics	40
3.4. Energy Characteristics of an Optical System	44
3.5. Aberration Characteristics	50
3.6. Transmission Characteristics of an Optical System	59
3.7. Classification of Optical Systems	64
3.8. Lens Systems	65
3.9. Mirror and Mirror-Lens Systems	69
3.10. Systems with Fiber Optics	74
3.11. Optical Systems of Equipment with a Laser	78
3.12. Optical Filters	80
Chapter 4. Radiation Receivers	83
4.1. Purpose and Classification	83
4.2. Basic Characteristics of Receivers	85
4.3. Photocells and Photomultipliers	100
4.4. Photoresistors	117
4.5. Photodiodes and Phototriodes	125
4.6. Photocells with a Longitudinal Photoelectric Effect (Inversion Photodiodes)	131
4.7. Thermal Radiation Receivers	136

	<u>Page</u>
Chapter 5. Analyzers and Scanners of Electro-Optical Instruments	145
5.1. Purpose and Classification of Analyzers	145
5.2. Phase Analyzers	147
5.3. Polar Analyzers	156
5.4. Scanning and Search Systems in Optoelectronic Equipment	160
5.5. Scanning and Search Systems Based on the Use of Fiber Optics	176
Chapter 6. Electro-optical Instruments for the Orientation of Spacecraft	181
6.1. The Purpose and Classification of Orientation Instruments	181
6.2. Pulse Sensors of the Horizon	183
6.3. Principles and Equipment for Determining the Local Vertical by the Method of Secants	186
6.4. Principles and Equipment for Determining the Local Vertical by the Method of Tracking the Horizon Line	198
6.5. Electro-optical instruments for Course Orientation of the SC	209
6.6. Orientation Instruments Which Use the Sun as a Reference Point	218
6.7. Electro-Optical Instruments for Orienting Spacecraft by the Stars	233
Chapter 7. Special Electro-Optical Instruments of Space	245
7.1. Types and Purpose of Special Electro-optical Instruments	245
7.2. Principles of Construction of On-Board Radiometric Equipment	246
7.3. Instruments for the Measurement of Thermal Characteristics of the Earth's Surface and the Atmosphere	252
7.4. Instruments for Controlling the Approach of Space Ships	256
Chapter 8. Electro-Optical Locators with Lasers	260
8.1. Block Diagram of an Electro-Optical Locator with a Laser	260
8.2. Electro-optical Locators which Measure Range by the Pulsed Method	265
8.3. Electro-Optical Locators Which Measure Range by the Phase Method	269

	<u>Page</u>
8.4. Electro -Optical Locators with the Use of the Doppler Effect	273
8.5. Electro-Optical Equipment for Docking with a Laser	275

PART 2
PRINCIPLES FOR THE DESIGN OF ELECTRO-OPTICAL INSTRUMENTS
OF SPACECRAFT

Chapter 9. A Method for Calculating the Radiation Characteristics	285
9.1. A Method For Calculating the Amount of Solar Radiation Perceived by the Instruments After Reflection from the Earth's Surface and Clouds	285
9.2. Calculation of the Amount of Solar Radiation Reflected by Artificial Objects and Perceived by the Instrument	290
9.3. A Method for Calculating the Amount of Radiation Intensity with Reflection from Objects of Spherical Form	294
9.4. Calculation of Radiation Intensity with Reflection from Corner Reflectors	
9.5. A Method for Calculating the Functions of the Spectral Density of Selective and Gray Emitters	305
9.6. Determination of the Characteristics of the Radiation of a Source from the Known Value of the Functions of Spectral Density	309
9.7. A Method for Determining the Radiation Characteristics of Emitters Which Are Nonuniformly Heated	312
Chapter 10. Energy Calculations for Electro-Optical Instruments	319
10.1. The Problems of Energy Calculation	319
10.2. Calculations of the Range of Action and Threshold Sensitivity of Instruments in the Absence of a Background	320
10.3. Calculation of the Range of Action and Threshold Sensitivity with the Influence of a Uniform Background	326
10.4. Calculation of the Range of Action and Threshold Sensitivity with the Observation of an Object on a Nonuniformly Radiating Background	342
10.5. Calculation of the Threshold Sensitivity of Instruments Which Operate with Areal Emitters	349

	<u>Page</u>
Chapter 11. Calculation of the Characteristics of Transparency of the Atmosphere	354
11.1. A Method for Determining the Coefficients of Transparency of the Atmosphere for Monochromatic and Complex Radiations	354
11.2. Calculation of the Quantity of Water Vapor on Horizontal, Sloping, and Vertical Paths	358
11.3. A Method for Calculating the Mass of Air and Carbon Dioxide on Horizontal, Sloping and Vertical Paths	361
Chapter 12. Selection of Radiation Receivers and Calculation of their Characteristics	364
12.1. A Method for Calculating Spectral Sensitivity and Monochromatic Threshold Flux of Photocells and Photomultipliers	364
12.2. Calculation of the Characteristics of Radiation Receivers	366
12.3. Quantum Effectiveness and Quantum Threshold Sensitivity and a Method for their Calculation	371
12.4. A Method for Calculating Quantum Effectiveness from the Integral Radiation of a Source	374
12.5. Selection of the Optimum Radiation Receiver	379
Chapter 13. Special Features of Calculating Electro-Optical Instruments with Lasers	388
13.1. Special Features in Calculating Operating Range in the Absence of Background Radiation	388
13.2. Calculation of the Range of Action with the Presence of a Radiating Background	395
Appendix	400
References	409

ABBREVIATIONS

SC	Spacecraft
IBB	Ideal black body
AES	Artificial earth satellite
SFC	Space-frequency characteristic
ASFC	Amplitude-space-frequency characteristic
PM	Photomultiplier
PR	Photoresistor
AGC	Automatic gain control
RVG	Reference-voltage generator
UIP	Unmanned interplanetary probe
FSD	Frequency-sensitive detector
SUE	Sun-spacecraft-earth
CTU	Common time unit
S	Storage
SCR	Silicon-controlled rectifier
PFM	Pulse-frequency modulator

ELECTRO-OPTICAL DEVICES OF SPACECRAFT

A. N. Iznar, A. V. Pavlov, and B. F. Fedorov

PART I PRINCIPLES OF THE DESIGN OF ELECTRO-OPTICAL INSTRUMENTS OF SPACECRAFT

/5*

CHAPTER 1. SOURCES OF RADIATION AND THEIR CHARACTERISTICS

1.1. Standard Emitters and Their Characteristics

The basic energy characteristics are used for the calculation of the parameters of any radiation source: the radiation energy, radiation flux, energy brightness, energy luminosity, energy irradiance, and also the spectral composition and three-dimensional radiation pattern.

The formulas which describe the basic energy characteristics and the tie between them are presented in Table 1.

For a complete description of the radiation source, it is necessary to know not only the integral values of the characteristics, for example, of the radiation flux, but also the spectral composition of the radiation.

For this purpose, use is made of the concept of spectral density of radiation flux $\Delta\Phi_\lambda/\Delta\lambda$.

For an infinitely small interval $\Delta\lambda$, the relationship $\Delta\Phi_\lambda/\Delta\lambda$ (Fig. 1.1) is called the function of the spectral density of radiation flux, i.e.

$$\lim_{\Delta\lambda \rightarrow 0} \frac{\Delta\Phi_\lambda}{\Delta\lambda} = \frac{d\Phi_\lambda}{d\lambda} = \phi(\lambda). \quad (1.1)$$

Integrating it for the entire spectrum, we can find the value of the total radiation flux

$$\Phi = \int_0^\infty \phi(\lambda) d\lambda. \quad (1.11)$$

* Numbers in the margin indicate pagination in the foreign text.

Table 1.1

/6

Basic characteristics		Connections between characteristics	Remarks
Radiation flux	$\Phi = \frac{dW}{dt}$ or $\Phi = \frac{W}{t}$ (1.2)	$\Phi = \pi B A$ (1.3)	W - energy
Energy luminous intensity	$I = \frac{d\Phi}{d\omega}$ or $I = \frac{\Phi}{\omega}$ (1.4)	$dI_{\beta} = B dA \cos \beta$ or $I_{\beta} = B A \cos \beta$ (1.5)	ω - solid angle
Energy brightness	$B_{\beta} = \frac{dI_{\beta}}{dA \cos \beta}$ or $B_{\beta} = \frac{I_{\beta}}{A \cos \beta}$ (1.6)	$B = \frac{R}{\pi}$ (1.7)	A - area of radiative surface
Energy luminosity (radiation density)	$R = \frac{d\Phi}{dA}$ or $R = \frac{\Phi}{A}$ (1.8)	$R = \pi B$ (1.9)	β - the angle between the normal to the radiative surface and the direction under construction
Energy irradiance	$E = \frac{d\Phi}{dA}$ or $E = \frac{\Phi}{A}$ (1.10)	$E = \frac{I}{L^2} \cos \beta$ (1.10a)	A - area of illuminated surface L - distance from source to irradiated source

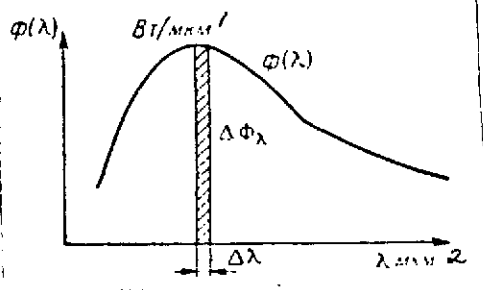


Fig. 1.1. Function of spectral density of radiation flux.

Key: 1. W/μm; 2. μm

By analogy with the function of 7 the spectral density of radiation flux $\Phi(\lambda)$, we write the expressions for the functions of spectral density of the other characteristics:

Energy brightness

$$\lim_{\Delta\lambda \rightarrow 0} \frac{\Delta B_\lambda}{\Delta\lambda} = \frac{dB_\lambda}{d\lambda} = b(\lambda); \quad (1.12)$$

Energy luminous intensity

$$\lim_{\Delta\lambda \rightarrow 0} \frac{\Delta I_\lambda}{\Delta\lambda} = \frac{dI_\lambda}{d\lambda} = I(\lambda); \quad (1.13)$$

Energy irradiance

$$\lim_{\Delta\lambda \rightarrow 0} \frac{\Delta E_\lambda}{\Delta\lambda} = \frac{dE_\lambda}{d\lambda} = e(\lambda); \quad (1.14)$$

Energy luminosity

$$\lim_{\Delta\lambda \rightarrow 0} \frac{\Delta R_\lambda}{\Delta\lambda} = \frac{dR_\lambda}{d\lambda} = r(\lambda). \quad (1.15)$$

The integration of these functions permits obtaining the integral values of the quantities under consideration

$$\int_0^\infty b(\lambda) d\lambda = B; \quad \int_0^\infty I(\lambda) d\lambda = I; \quad \int_0^\infty e(\lambda) d\lambda = E; \quad \int_0^\infty r(\lambda) d\lambda = R. \quad (1.16)$$

The radiation of any object consists of the intrinsic temperature radiation and the radiation of other sources reflected from it.

Intrinsic temperature radiation is determined by the temperature, shape, dimensions, and properties of the radiative surface. The basic characteristics of temperature radiation of ideal black bodies is calculated in accordance with the basic laws of radiation, the analytic expressions for which are given in Table 1.2.

Table 1.2

78

Analytical expression	Remarks
$\frac{R'(T)}{\alpha'(T)} = \frac{R(T)}{\alpha(T)} = \text{const} = R(T) \quad (1.17)$ $\frac{r'(\lambda, T)}{\alpha'(\lambda, T)} = \frac{r''(\lambda, T)}{\alpha''(\lambda, T)} = \dots \text{const} \frac{r(\lambda, T)}{\alpha(\lambda, T)} = r(\lambda, T) \quad (1.18)$ <p>Kirchoff's law</p>	$R'(T) \& R(T)$ - Energy luminosity and IBB (ideal black body at temperature T) $\alpha'(T) \& \alpha(T)$ - Absorptivity of a body and IBB at temperature T
$r(\lambda, T) = C_1 \lambda^{-5} \left(e^{\frac{C_2}{\lambda T}} - 1 \right)^{-1} \quad (1.19)$ <p>Planck's law</p>	$C_1 = 2\pi h c^2, \quad C_2 = \frac{hc}{k} \quad (1.20)$
$R(T) = \sigma T^4 \quad (1.21)$ <p>Stefan-Boltzmann law</p>	$\sigma = 6,455 \frac{C_1}{C_2^4} = 5,67 \cdot 10^{-12}$ <p>Stefan-Boltzmann constant</p>
$\lambda_{\max} T = \text{const} = 2896 \text{ } \mu \cdot \text{deg} \quad (1.22)$ <p>Golitsyn-Wien law</p>	
$r(\lambda_{\max}, T) = 1,315 \left(\frac{T}{1000} \right)^5, \quad \text{W/}(\text{cm}^2 \cdot \mu) \quad (1.23)$	
$y = 142,3 x^{-5} \left(e^{\frac{4,965}{x}} - 1 \right)^{-1} \quad (1.24)$	$x = \frac{\lambda}{\lambda_m}; \quad y = \frac{r(\lambda)}{r(\lambda_{\max})}$ <p>The tables of values of this function by argument are presented in work [20]</p>

Note. The factor ϵ is introduced into the formulas which characterize the emittance of gray bodies.

The share of radiation taken over a comparatively broad interval of the spectrum is calculated by the formula

$$f = Z(x_2) - Z(x_1), \quad (1.25)$$

where $\frac{\int_0^x y(x) dx}{\int_0^\infty y(x) dx} = Z(x)$ is the tabular function. (1.26)

With narrow intervals, considerable errors are possible /9
because of the absence of tables of the function $Z = Z(x)$ with a small step. Therefore, with a narrow spectrum interval, the share of radiation of the IBB can be estimated in the following manner.

If the function of the spectral radiation density $r(\lambda)$ is known, the energy luminosity $R_{\Delta\lambda}$ on the interval $\Delta\lambda$ will be

$$R_{\Delta\lambda} = \int_{\lambda_1}^{\lambda_2} r(\lambda) d\lambda. \quad (1.27)$$

Since it is assumed that the interval $\Delta\lambda$ is extremely small, the function $r(\lambda)$, within its limits for the practical calculations, can be considered constant and equal to the value $r_{\Delta\lambda}(\lambda_{av})$ on the wavelength of the middle of the interval. Then, from (1.27), we have

$$R_{\Delta\lambda} = r_{\Delta\lambda}(\lambda_{av}) \Delta\lambda.$$

Substituting the value $r_{\Delta\lambda}(\lambda_{av})$ from (1.24) in the formula which is obtained, we find

$$R_{\Delta\lambda} = \epsilon r(\lambda_{max}, T) \Delta\lambda.$$

On the other hand, on the basis of (1.21), energy luminosity $R = \sigma T^4$. We designate the relation of $R_{\Delta\lambda}$ to R $f_R = \frac{R_{\Delta\lambda}}{R}$.

Substituting the values R and $R_{\Delta\lambda}$ here and considering (1.23), we find the expression

$$f_R = 0.232 y_{\Delta\lambda} T_{\Delta\lambda} 10^{-3}, \quad (1.28)$$

which permits determining the share of radiation of the AChT taken over an extremely narrow spectrum interval.

For the characteristic of the radiation properties of one or another non-black body, the concept of emittance ε is used:

$$\varepsilon(T) = \frac{R'(T)}{R_{\text{IBB}}(T)} \quad \text{or} \quad \varepsilon_{\lambda}(T) = \frac{r'(\lambda, T)}{r_{\text{IBB}}(\lambda, T)}. \quad (1.29)$$

Hence, it follows:

$$\varepsilon(T) = a(T) \quad \text{or} \quad \varepsilon_{\lambda}(T) = a(\lambda, T). \quad (1.30)$$

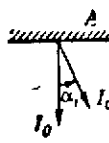
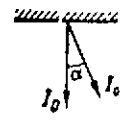
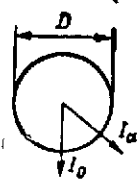
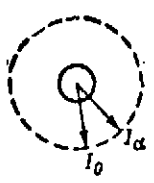
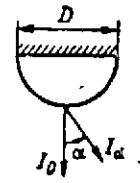
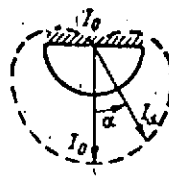
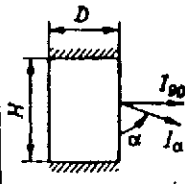

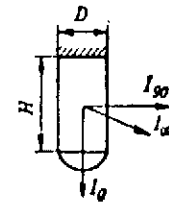
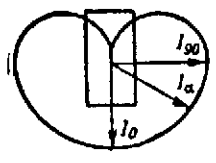
The emittance of all real bodies is always less than 1. If the emittance does not remain constant with a change in wavelength, such bodies possess selective radiation. The degree of selectivity is determined by how much the spectral distribution of the radiation differs from the spectrum of the IBB at the same temperature.

Using the formulas presented in Table 1.1 and 1.2 and, considering the emitters, which follow Lambert's law, we can determine the nature of the distribution of the energy luminous intensity in space and the integral values of the radiation fluxes.

Several characteristics of the radiation of sources of simple form are presented in Table 1.3.

An emitter typical for the electro-optical equipment of space vehicles is the earth with its surrounding atmosphere. In 12 general, its radiation consists of two components: intrinsic temperature radiation of the underlying surface of the earth and the layer of the atmosphere, and also the radiation of heavenly

Table 1.3

Type of emitter		Radiant intensity	Shape of radiation indicatrix	Radiation flux
Disc		$I_\alpha = I_0 \cos \alpha$ $I_0 = BA = \frac{\sigma T^4 \varepsilon A}{\pi} = \frac{\sigma T^4 \varepsilon D^2}{4}$		$\Phi = \pi I_0$ $\Phi = \frac{\varepsilon \sigma T^4 \pi D^2}{4}$
Sphere		$I_\alpha = I_0 = \text{const}$ $I_0 = B \frac{\pi D^2}{4} = \frac{\varepsilon \sigma T^4 D^2}{4}$		$\Phi = 4\pi I_0$ $\Phi = \varepsilon \pi D^2 \sigma T^4$
Hemisphere		$I_\alpha = \frac{I_0}{2} (1 + \cos \alpha)$ $I_0 = B \frac{\pi D^2}{4} = \frac{\varepsilon \sigma T^4 D^2}{4}$		$\Phi = 2\pi I_0$ $\Phi = \frac{1}{2} \varepsilon \pi D^2 \sigma T^4$
Cylinder		$I_\alpha = I_{90} \sin \alpha$ $I_{90} = BHD = \frac{\varepsilon \sigma T^4 HD}{\pi}$		$\Phi = \pi^2 I_{90}$ $\Phi = \varepsilon \pi H D \sigma T^4$
Cylinder with spherical base		$I_\alpha = \frac{I_0}{2} (1 + \cos \alpha) + I_{90} \sin \alpha$ $I_0 = \frac{\varepsilon \sigma T^4 D^2}{4}$ $I_{90} = \frac{\varepsilon \sigma T^4 DH}{\pi}$		$\Phi = 2\pi I_0 + \pi^2 I_{90}$ $\Phi = \varepsilon \pi D \sigma T^4 \left(H + \frac{D}{2} \right)$

bodies (sun, moon, stars) which is reflected from the earth's surface layers and the atmosphere.

The intrinsic radiation of the earth's surface layers and the layer of the atmosphere depends on the temperature and nature of the earth's surface, the composition of the atmosphere and the distribution of the absorbing substances in it, the presence and nature of cloudiness, etc. Besides this, the reflected radiation depends on what source irradiates the earth's cover. The type of function of spectral density of the energy brightness of the side of the earth illuminated by the sun during observation from outer space is shown in Fig. 1.2. From the graph it can be seen that in the windows of transparency of the atmosphere, the energy brightness corresponds to the radiation of an IBB at the temperature of the stratosphere. In the spectral band $\lambda \leq 3 \mu$, the reflected solar radiation is predominant.

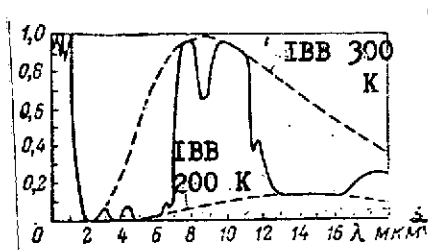


Fig. 1.2. Functions of the spectral density of energetic luminance of the side of the earth illuminated by the sun. Note. The dashed lines show the functions of the spectral density of energy brightness of an IBB at temperatures $T = 300$ and $T = 200$ K.

Key: 1. IBB; 2. μm

The intrinsic radiation of the earth's surface is determined by its temperature and the nature of the underlying surfaces. The temperature of the surface depends on the nature of the earth's cover. In the transition from one cover to another, temperature drops arise (Table 1.4)

The effect of the nature of the surface on the characteristics of radiation is considered by the blackness coefficient (Table 1.5).

In the calculations, the earth's surface covers can be considered as diffuse (equally bright) emitters.

TABLE 1.4

Nature of transition	Field-forest	Plowland-grass	Land-water	City-field
Temperature drop, K	Up to 5.3	Up to 5.0	3-4	1.5-1.0

TABLE 1.5

Type of surface	Soil	Coni- ferous needles	Green Grass	Water Surface	Snow	Sand	Clay
Coefficient	0.95	0.97	0.97	0.96	0.92	0.89	0.85

In the spectral bands of intense absorption, the radiation of the earth's surface is absorbed without emerging beyond the limits of the earth's atmosphere. Energy is radiated into outer space which is emitted by the absorbing molecules of the atmosphere. The larger the absorptance, the higher the layers of the atmosphere radiate into outer space. The spectral composition of such radiation is presented in Fig. 1.3.

Since temperature is reduced with an increase in altitude (up to altitudes of 75-80 km), less is radiated into outer space than is shown in Fig. 1.3. A noticeable reduction is observed in the absorption bands of carbon dioxide and water and ozone vapors. Since the water vapors are concentrated in the surface layer (see Chapter 2) and have a comparatively high temperature, they have a lesser effect on outgoing radiation than carbon dioxide and ozone. Radiation in the absorption bands depends on the temperature of the radiative layers as well as on the change in the distribution of radiating molecules, especially CO_2 and O_3 .

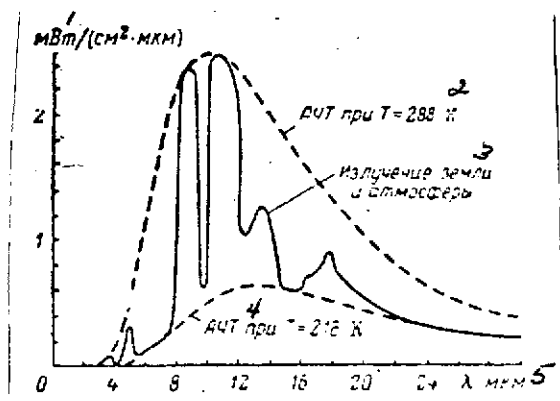


Fig. 1.3. Spectral composition of the earth's radiation into outer space.

Note. The dash lines show the functions of the spectral density of energy brightness of an IBB at temperatures of $T = 288$ and $T = 218$ K.

Key: 1. $\text{mW}/(\text{cm}^2 \cdot \mu)$; 2. IBB with $T = 288$ K; 3. Radiation of the earth and the atmosphere; 4. IBB with $T = 218$ K; 5. micrometers (μm).

The reflected component depends on the nature of the underlying surface as well as on the position of the irradiating source. The reflectances (albedo) of the majority of earth surfaces in the infrared region are

comparatively low. The ground covered with grass reflects approximately 15% of the incident radiation and only in the band of 0.7-1 μ m is the albedo of the grass cover higher than 70-80%. On the average, for the earth's hemisphere the albedo varies from 0.36 to 0.39 in the visible region of the spectrum and comprises approximately 0.3 in the infrared band of the spectrum. If we consider the total radiation, then on wavelengths $\lambda < 3-4 \mu$ m, a large part of the radiation of the earth's surface is caused by a diffusely radiated radiation flux from the sun. On wavelengths $\lambda > 4 \mu$ m, the scattered radiation of the sun becomes negligibly small in comparison with the intrinsic radiation of the atmosphere.

With cloudiness, radiation beyond the limits of the atmosphere goes not from the earth's surface but from the upper boundary of the clouds which radiate as an ideal black body with the temperature of the clouds. This radiation is selectively attenuated by the molecules of the upper layers of the atmosphere. /14

In addition to energy characteristics, illumination characteristics are often employed: luminous flux, luminous intensity, illumination, etc. Their connection with the energy characteristics is established by the formula

$$F = K_{\max}(\lambda) \eta \Phi, \quad (1.31)$$

where

$$\eta = \frac{\int_0^{\infty} \phi(\lambda) V(\lambda) d\lambda}{\int_0^{\infty} \phi(\lambda) d\lambda} \quad (1.32)$$

is the efficiency of the eye or the coefficient of the utilization of the radiation flux of a given source by the eye;

$$V(\lambda) = \frac{K(\lambda)}{K_{\max}(\lambda)} \quad (1.33)$$

is the function of the relative spectral sensitivity of the eye which is known in literature under the name of the function of relative luminous efficiency of the eye;

$$K_{\max}(\lambda) = \frac{F}{\eta_s \Phi_s} = 683 \text{ lm/W.} \quad (1.34)$$

and by the formula

$$E^{cp} = E_{n683} \quad (1.35)$$

(E is expressed in W/m^2).

1.2. Radiation of Heavenly Bodies

The sources of radiation on the celestial sphere are the sun, moon, planets, and stars.

The magnitude of the radiation fluxes of the planets and the moon depends primarily on the absolute temperature of the upper layers of the atmosphere of the planet or its surface. Along with this, they also depend on the nature of the planet's atmosphere. Data on some characteristics of planets connected with their infrared radiation are tabulated in Table 1.6.

TABLE 1.6

Characteristics	Earth		Venus		Moon		Mars	
	Surface	Upper layers of atmosphere	Surface	Upper layers of atmosphere	Illuminated side	Unilluminated side	Equator	Pole
Temperature, K	290	220	430	225	400	120	280	205
Wavelength of maximum radiation λ_{max} , μm	10	13	7	11.5	7.5	24	10	14
Energy brightness $W/(cm^2 \cdot sr)$	0.013	0.004	0.005	0.047	0.0004	0.011	0.011	0.003
Portion of radiation in the spectrum band $\Delta\lambda$ from 1.8 to 18 μm	0.66	0.47	0.85	0.49	0.82	0.09	0.64	0.42
Portion of radiation in the spectrum band $\Delta\lambda$ from 7.5 to 18 μm	0.56	0.45	0.52	0.46	0.54	0.09	0.56	0.41

From the table, it can be seen that the temperature of the radiating surfaces lies within the limits of from 120 to 430 K, as a result of which the main share of the radiation flux emanates in the infrared region of the spectrum on wavelengths of more than 5 μm . Therefore, with the use of the indicated planets as emitters, receivers should be used in electro-optical equipment which possess sensitivity in the band of the spectrum from 5 μ and up to 15-20 μm , and sometimes up to 40 μm . /15

The infrared radiation of the planets is the sum of two components: intrinsic radiation and diffusely reflected solar radiation. The temperature and, consequently, the thermal radiation of the planets which have a comparably dense atmosphere, such as Venus, earth, and Mars are comparatively constant identical over the entire surface of the planet. Characteristic of planets and satellites which have a very rarefied atmosphere or do not have it at all (for example, the moon) are considerable periodic temperature drops, which causes similar drops in radiation fluxes.

The amount of reflected solar radiation varies significantly over the surface of the planet depending on the time. It depends on the position of the terminator and the reflectance (albedo) of the section of the planet. The albedo depends on the character and altitude of cloudiness. The spectral composition of reflected radiation is characterized by a color temperature of $T = 6000 \text{ K}$ (color temperature of the sun). The main portion (95%) of the reflected solar radiation is taken over a band of wavelengths shorter than 2 μm .

In the solution of many practical problems connected with orientation and navigation, stars can be used as astronomic reference points. /16

In selecting a star as an astronomic reference point, it is necessary to consider its position on the celestial sphere and apparent point brilliance.

By the apparent point brilliance of a star (heavenly body) we mean the illumination-engineering value which characterizes the illumination which a given heavenly body creates at the boundary of the earth's atmosphere on a small area perpendicular to the direction of propagation of the rays.

The overall number of stars which comprise our galactic system is approximately 100 billion. However, there are comparatively few stars which possess a sufficiently large visible point brilliance.

The apparent point brilliance of heavenly bodies is evaluated in stellar magnitudes.

The stellar magnitude m which determines the measure of apparent point brilliance of a heavenly body is connected with illumination E , created by the heavenly body, by the relation

$$m = -2.5 \lg E + c, \quad (1.36)$$

where c is a constant value equal to that stellar magnitude m_0 at which the heavenly body creates an illuminance of 1 lx on a small area.

An illuminance of 1 lx at the boundary of the earth's atmosphere can be created by a heavenly body whose apparent point brilliance is characterized by the stellar magnitude $m_0 = -13.89$ and, on the earth's surface, by a heavenly body having a stellar magnitude of $m_0 = -14.2$. Consequently, in working with formula (1.36), it is necessary to take the value of constant c in accordance with the conditions under consideration.

We rewrite expression (1.36) in the form

$$-\frac{m-c}{2.5} = \lg E$$

and solving it for E , we obtain a relationship which enables us to calculate the luminosity from the celestial bodies from their stellar magnitude

$$E = 10^{-\frac{m-c}{2.5}},$$

or, with consideration of the values of coefficient c , we obtain

$$E_s = 10^{-\frac{13.89+m}{2.5}}; \quad (1.37)$$

$$E_e = 10^{-\frac{14.2+m}{2.5}}, \quad (1.38)$$

where E_s and E_e are the illuminances in space and on the earth respectively.

We establish the relation between the illuminations created by heavenly bodies with an apparent point brilliance of different stellar magnitude. If the apparent point brilliance of two heavenly bodies is evaluated by stellar magnitudes m_1 and m_2 and the illuminance which they create is E_1 and E_2 , respectively, then on the basis of (1.36), we write

/17

$$\begin{aligned} m_1 &= -2.5 \lg E_1 + c; \\ m_2 &= -2.5 \lg E_2 + c. \end{aligned}$$

Subtracting one expression from the other, we will have

$$-\frac{m_1 - m_2}{2.5} = \lg E_1 - \lg E_2 \quad \text{or} \quad \lg \frac{E_1}{E_2} = 0.4(m_2 - m_1).$$

Hence, after involution we obtain

$$\frac{E_1}{E_2} = 10^{0.4(m_2 - m_1)} \quad \text{or} \quad \frac{E_1}{E_2} = 2.512^{(m_2 - m_1)}. \quad (1.39)$$

Expression (1.39) shows that with a difference in apparent point brilliance of heavenly bodies by one stellar magnitude the illuminations which they create differ 2.512 times. In this, the greater the stellar magnitude of the heavenly body, the less the illumination which it creates.

We note that prior to the introduction of the principle of the division of stars by magnitude of apparent point brilliance on the basis of equation (1.36), only six groups were distinguished. Stars with the greatest point brilliance pertained to stars of the first magnitude and the weakest but still visible to the eye on a clear moonless night -- to the sixth. After the introduction of the classification, it turned out that there are stars whose apparent point brilliance exceeds the apparent point brilliance of stars of the first magnitude. Therefore, so as not to disturb the classification which had been developed, the scale of stellar magnitudes was extended both to stars weaker than the sixth magnitude and visible only in a telescope and to heavenly bodies having a larger apparent point brilliance than stars of the first magnitude. In this case, the counting is conducted in the direction of negative values. For example, the apparent point brilliance of the star Sirius is evaluated by the stellar magnitude ($-1^m.43$); of Venus with the greatest point brilliance ($-4^m.4$); of the moon at half-moon ($-12^m.6$); and the sun ($-26^m.7$).

Recently, photoelectric photometers have found application and new requirements have arisen for a photometric system in which stellar magnitudes are expressed. Used as the basis in contemporary electrophotometry is the photometric system introduced by Johnson and Morgan and designated by the letters UBV, where U is the ultraviolet rays, B is the dark blue rays, and V is the visual rays. In this system, the stellar magnitudes are measured on wavelengths close to $0.35 \mu\text{m}$, $0.435 \mu\text{m}$, and $0.555 \mu\text{m}$ (Fig. 1.4) with two color indices: U-V and B-V. Taken as zero of the system are several stars of the A0 class, close to the sun, and having color indices equal to zero. The visual stellar magnitudes which are determined in this system differ somewhat in their values from regular visual stellar magnitudes. This can be seen in the example of the brightest stars presented in Table 2 of the Appendix. With the introduction of the new system, the possibility appeared to employ photoelectric photometers which possess high precision in measurement (errors on the order of $\pm 0^m.01$) and objectivity of the results obtained.

/18

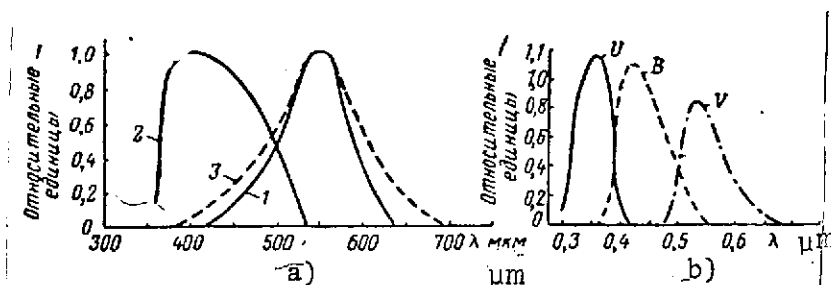


Fig. 1.4. For the determination of luminosity and apparent point brilliance of stars:
1. Eye; 2. Normal photoplate; 3. photo-visual plate.

Key: 1. Relative units

Of the tremendous number of stars presently known, only 4850 are visible to the naked eye. Their number includes all stars with $m < 6$. The number of stars on the celestial sphere increases with an increase in apparent stellar magnitude (Table 7).

The stars are scattered irregularly on the celestial sphere. For convenience in orientation, they are arbitrarily distributed into groups called constellations. Altogether, 88 constellations are presently counted which embrace the entire celestial sphere without overlappings and omissions. Individual stars which are

/19

part of the constellations are designated by Greek letters with the indication of the name of the constellation to which they pertain. The designation of the stars in alphabetic order (α , β , γ , δ , ...), as a rule, corresponds to the decrease in their apparent point brilliance.

TABLE 1.7

m	N _{vis} *	N _{photogr}	m	N _{vis}	N _{photogr}
1.0	13	—	8.0	42000	23000
2.0	40	—	9.0	125000	62000
3.0	100	—	10.0	350000	270000
4.0	500	400	11.0	900000	410000
5.0	1600	1200	12.0	2300000	1100000
6.0	4800	2900	13.0	5700000	2700000
7.0	15000	8300	14.0	14000000	6500000

* Beginning with $m = 6$, the number of stars determined by the photovisual method is presented.

The majority of the bright stars, in particular all stars of magnitudes 1 and 2, also have their own names besides the letter designation (for example, α Orion-Betelgeuse, α Lira-Vega, α Virgo-Spica, and so on).

Star charts, atlases, and catalogs can be used to obtain information on the relative disposition of the stars on the celestial sphere and their basic characteristics.

Besides division into groups according to apparent point brilliance, all stars are subdivided according to spectral composition in accordance with their intrinsic temperature. In accordance with this criterion, the stars pertain to different spectral classes designated in order of temperature decrease by the letters O, B, A, F, G, K, M, R, N, and S. Each class encompasses stars with a specific spectral composition which is characterized by a color temperature of one magnitude or another (Table 1.8).

TABLE 1.8

O	B	A	F	G	K	M
35000—25000	25000—15000	11000	7500	6000	5000	3500—2000

In order to characterize more precisely the spectral composition of radiation, in each class the stars are divided into ten groups from 0 to 9 and have a double designation, for example, O0, B2, A0, A7, G0, F8, and so on. From such designation, one can determine rather precisely the temperature of the radiative surface of a star, and, consequently, characterize the distribution of radiation flux according to the spectrum. Knowing the temperature of the radiative surface and the apparent point brilliance (stellar magnitude) from known relations, we can determine the energy irradiance created by a heavenly body from the formula

$$E = E_{cp} \frac{1}{K_{max}(\lambda) \cdot \eta \cdot 10^4} = \frac{10^{\frac{13.75 - m}{2.5}}}{683 \eta \cdot 10^4}, \quad (1.40)$$

where η is the efficiency of the eye.

Sometimes, to determine the color temperature of a heavenly body use is made of the formula

$$T = \frac{7200}{0.64 + c}, \quad (1.41)$$

where c is the index of the color of the star which is the difference in the photographic and visual stellar magnitudes

/20

$$c = m_{phot} - m_{vis}$$

The distribution of stars by different spectral classes is presented in Table 1.9.

TABLE 1.9

Spectrum of stars	B0-B5	B8-A3	A5-F2	F5-G0	G5-K2	K5-M8	Remainder
Number of star in percent	2	29	9.0	21	33	6	1

The characteristics of some of the brighter heavenly bodies are presented in the Appendix in Table 4.

Of the stars, the closest to the earth is the sun, the average distance to which equals 149,000,000 km. It is a dense nucleus surrounded by an incandescent gaseous shell. The temperature of the upper layers of the sun equals approximately 6000 K. The diameter of the sun is 109 times greater than the diameter of the earth and is 1,391,000 km. The energy irradiance of the sun equals $6.2 \cdot 10^3$ W/cm². Beyond the limits of the earth's atmosphere on a small area perpendicular to the direction of propagation of the radiation, the sun creates energy irradiance $E = 1350$ W/m² or 0.135 W/cm². The latter characteristic is known by the name of solar constant. The overall value of the radiation flux emitted by the sun is $3.8 \cdot 10^{26}$ W. Beyond the limits of the earth's atmosphere, the illumination which it creates is $\sim 135,000$ lx, and on the earth's surface in the middle latitudes $\sim 100,000$ lx. The integral radiation of the sun is extremely constant; however, the intensity of the ultraviolet radiation fluctuates.

In calculations of the characteristics of equipment which operates on solar radiation, the sun as an emitter can be taken as an IBB whose function of spectral density of radiation flux is determined with a temperature of $T \sim 6000$ K. The spectral distribution of the sun's radiation is presented in Fig. 1.5.

1.3. Radiation of Auroras

/21

Auroras arise under the action of powerful corpuscular radiation of the sun at altitudes up to 700-1000 km above the earth's surface. They are observed most often in the polar regions but they sometimes occur in the middle and equatorial latitudes. The maximum number of the auroras observable during a year occurs in the zone of the earth's magnetic pole. The zone of auroras, in which they arise and are observed during darkness almost daily, is at a distance from the world pole of approximately $23.174 \cdot 10^{-2}$ rad (23°). To the south of this zone, the average annual number of auroras is reduced and their intensity weakens.

Translator's Note: The typesetter has obviously made an error since the energy luminosity (энергетическая светимость) is given the symbol "E" and units of W/cm² which could only be energy irradiance

18 (энергетическая освещенность).

Auroras occur most often at altitudes of about 100 km, in which regard the lower boundary of the altitudes depends on their intensity (Table 1.10).

TABLE 1.10

Intensity of aurora	Weak	Average	Strong	Very strong	Arcs with Intensive coloration of lower edge
Average altitude in km	115	108	99	95	65-70

The upper edge of the auroras is less clearly expressed and extends to different altitudes for various forms (Table 1.11).

TABLE 1.11

Form of aurora	Rays	Drapery	Drapery-like	Diffuse arcs
Altitude in km	250	176	174	143
Average vertical extension in km	137	68	68	34

In proportion to the distance from the zone of the auroras toward the southern latitudes, the altitudes of the rayed auroras increases and may reach values of 1000-1100 km.

Bands of radiation of various gases have been discovered in the auroras (oxygen, nitrogen, helium, hydrogen). The range of change of the radiance of the auroras is rather great and in the bands of 0.3914, 0.4278, 0.5577, 0.6300, 0.7200, 0.7900, and 0.8680 μm the radiance changes within limits from $3 \cdot 10^{-7}$ to $1.1 \cdot 10^{-4}$ W/sr m^2 [11]. However, according to data [35], auroras with high luminance are encountered much more rarely than auroras of weak luminance.

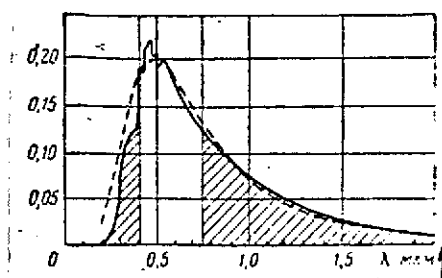


Fig. 1.5. Spectral composition of the sun's radiation beyond the limits of the earth's atmosphere.

Note. The dash line shows the function of the spectral density of an IBB at $T = 6000$ K.

Key: 1. μm

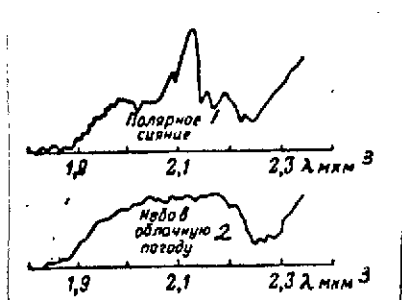


Fig. 1.6. Spectra of radiations of auroras

Key: 1. Aurora; 2. Sky in cloudy weather; 3. μm

The spectra of auroras are a series of lines in the visible region of the spectrum and a small segment of continuous spectrum in the band from $\lambda = 0.65 \mu\text{m}$ to $\lambda = 0.95 \mu\text{m}$ with a clearly separated line on a wavelength of $\lambda = 0.92 \mu\text{m}$, the radiance of which is $(5-6) \cdot 10^{-8} \text{ W}/(\text{sr} \cdot \text{cm}^2)$. In the longer-wave portion of the spectrum, there is also a number of radiation bands. However, in this band of the spectrum, the radiation of the auroras exceeds insignificantly the radiation of the night sky (Fig. 1.6). The values of radiance of the basic bands of auroras in the infrared region of the spectrum are presented in Table 1.12.

Auroras are not distinguished by time or spatial stability. The radiation of the night sky mentioned earlier, as became clear in recent years, is caused to a considerable degree by the radiation of molecules of the OH hydroxyl group. This compound is constantly present in the upper layers of the atmosphere and is a source of extremely strong infrared radiation of the sky [35].

The spectral distribution of the radiation of the upper layers of the atmosphere has the character of bands (Fig. 1.7 a, b). The integral radiance of the upper layers of the atmosphere caused by the radiation of OH molecules is estimated in the spectrum band $\Delta\lambda = 1.2-1.8 \mu\text{m}$ as the value $3 \cdot 10^{-5} \text{ W}/(\text{sr} \cdot \text{cm}^2)$, and in the band $\Delta\lambda = 3.8-4.4 \mu\text{m}$ -- as the value $7 \cdot 10^{-4} \text{ W}/(\text{sr} \cdot \text{cm}^2)$.

1.4. Characteristics of the Radiation of Lasers

In recent years, lasers have been receiving ever wider application in space technology.

Three types of lasers exist: solid state, gas, and semiconductor.

TABLE 1.12

Wavelength in μ	1.45	1.51	1.57	2.13	2.25	2.36
Radiance of bands in $W/(sr \cdot cm^2)$	$1 \cdot 10^{-5}$	$3 \cdot 10^{-5}$	$1 \cdot 10^{-5}$	$1.5 \cdot 10^{-5}$	$1 \cdot 10^{-5}$	$2 \cdot 10^{-5}$

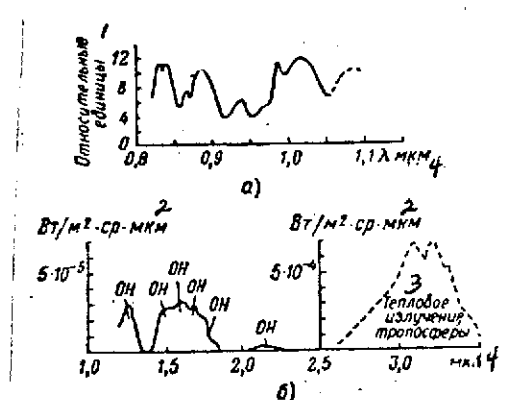


Fig. 1.7. Spectral distribution of radiation of the upper layers of the atmosphere: a - in spectrum band $\lambda = 0.8-1.1 \mu m$; b - in spectrum band from $\lambda = 1 \mu m$ and higher.

Key: 1. Relative units; 2. $W/m^2 \cdot sr \cdot \mu m$ 3. Thermal radiation of the troposphere; 4. μm

Any type of laser has an active material, cavity, source of excitation, and power-supply source (Fig. 1.8). Used as the active substances are:

-- in solid-state lasers: ruby crystals and other crystalline substances (plastics and glass with various admixtures,

-- in semiconductor lasers semiconductor materials (gallium arsenide, arsenic-gallium phosphide, gallium phosphide and indium arsenide).

Data on the materials used in lasers are presented in work [20].

The properties of lasers as emitters are evaluated with the use of their basic characteristics:

-- Radiation flux (equivalent mechanical power) or radiation energy;

-- Direction of radiation, or width of beam;

-- Wavelength λ and band width $\Delta\lambda$ of radiation;

-- Radiation coherence

The radiation power is characterized by the value of the radiation flux emitted by the laser. Lasers which operate in the pulsed mode are characterized most often by the radiation energy which is calculated as the product of the mean value of

the radiation flux in the pulse for the duration of the pulse and is measured in J.

$$W = \Phi \cdot t, J.$$

The power of a continuous-duty laser (gas and semi-conductor) lies within limits from a few mW to a few W, and the power of a solid state laser may reach 10^6 - 10^2 W. Data on the materials and basic characteristics of specific models of lasers of various types are presented in tables (see Appendix).

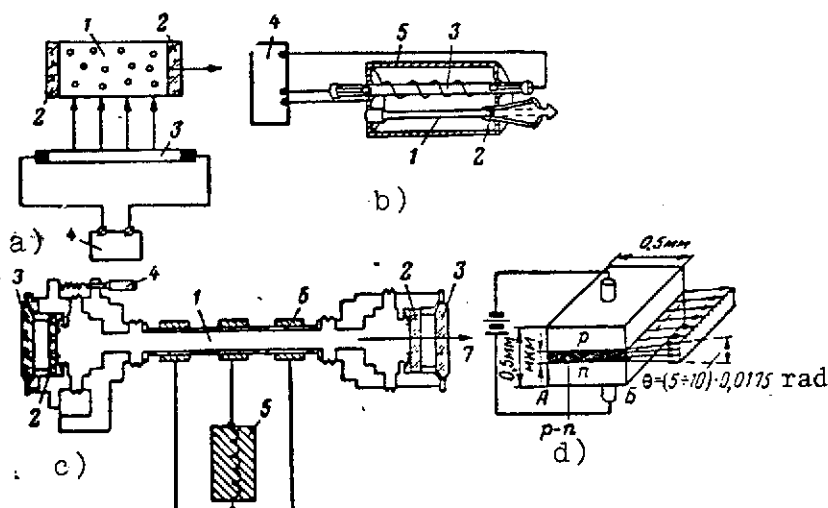


Fig. 1.8. Schematic diagram of lasers: a - Typical schematic diagram of laser: 1 - Active material; 2 - Cavity (mirror); 3 - excitation source (Flash lamp); 4 - power supply source; b - Diagram of ruby laser: 1 - Ruby rod; 2 - Cavity (mirror); 3 - Excitation source (flash lamp); 4 - power supply source; 5 - Reflector; c - Diagram of the construction of a gas laser: 1 - Tube with helium-neon mixture; 2 - cavity (reflecting mirror); 3 - entry windows; 4 - Mechanism for the adjustment of the parallelism of the mirrors; 5 - high-frequency oscillator; 6 - electrodes; 7 - Emergent beam; d - Diagram of semiconductor laser: A and B - Faces with mirror coating (cavity); p-region - Active material.

Direction of radiation is characterized by the value of the angle of divergence of the beam. The least value of this beam, which is limited only by the phenomenon of diffraction, can be the value

$$\theta = 2 \arcsin \frac{\lambda \cdot 0.61}{d}, \quad (1.42)$$

where d is the diameter of the radiation spot.

Since the angle of divergence are small, we can write

$$\theta = \frac{1.22\lambda}{d}, \quad (1.43)$$

from which it follows that very small divergences can be attained. If $\lambda = 0.63 \mu$ ($0.63 \cdot 10^{-4}$ cm) and $d = 2$ mm, then $\theta = 3.8 \cdot 10^{-4}$ rad, which comprises an angle not exceeding $1'15''$.

The divergence of a beam of a gas laser lies within the limits of units of minutes, and of semiconductor and solid lasers, units of degrees.

The width of the line of radiation, measured in λ/c , depends on the radiation flux and the Q of the cavity and can be calculated from the formula

$$\Delta \nu_r = \frac{\tau c}{2\pi l}, \quad (1.44)$$

where τ -- Radiation losses with one-time passage in the active material and reflection from the glass of the cavity; /25
 c -- The speed of light in the active material;
 l -- The distance between the mirrors.

The minimum width of line caused by spontaneous radiation is determined by the expression [16]

$$\Delta \nu_0 = \frac{8\pi h \nu (\Delta \nu_r)^2}{\Phi}, \quad (1.45)$$

where $h = 6.625 \cdot 10^{-34}$ W.s² is Planck's constant.

Thus, if $\Phi = 1$ mW, $l = 100$ cm, $\tau = 0.02$, then with $\lambda = 1.15$ μm , $\Delta\nu_r = 1$ MHz and $\Delta\nu_0 = 10^{-3}$ Hz.

Coherence is the basic property of quantum radiation sources. It is made up of spatial and time components. Time coherence signifies that the maxima of radiation in a wave follow one after the other with period t . With a change in the radiation wavelength (frequency) the intervals between the maxima become irregular and coherence is reduced. With spatial coherence, the waves emitted by the laser form a flat front perpendicular to the axis of the laser. More detailed information on the physical processes which take place in the laser, their construction, and characteristics can be found by the reader in works [6, 10]. The basic characteristics of some models of solid lasers and gas lasers are presented in Tables 3, 4, and 5 of the Appendix.

2.1. Radiation Attenuation in a Uniform Medium

The amount of radiation flux from an object which falls on a radiation receiver depends not only on the power of the emitter but also on the properties of the medium in which this flux is propagated. For approximate calculations, we will consider the optical media in which radiation flux is propagated to be homogeneous. The attenuation of radiation in a medium may be selective as well as non-selective. We will establish the regular laws of attenuation as applicable to a monochromatic radiation flux.

Suppose that a beam of parallel rays of a monochromatic radiation flux $\Phi_\lambda(0)$ enters a homogeneous medium with thicknesses L (Fig. 2.1). Assuming that the particles of the medium attenuate the radiation flux independently, we can present the change in its value with passage through a layer of the medium with thickness dl by the relationship

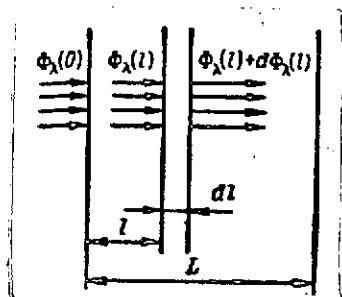
$$d\Phi_\lambda(l) = -\alpha_\lambda \Phi_\lambda(l) dl, \quad (2.1)$$

where α_λ is the attenuation coefficient of a monochromatic radiation flux. Separating the variables in (2.1), we have

$$\frac{d\Phi_\lambda(l)}{\Phi_\lambda(l)} = -\alpha_\lambda dl,$$

whence, after integration, we obtain

$$\ln \Phi_\lambda(l) \Big|_{l=0}^{l=L} = -\alpha_\lambda l \Big|_0^L \quad \text{or} \quad \Phi_\lambda(L) = \Phi_\lambda(0) e^{-\alpha_\lambda L}. \quad (2.2)$$



In this expression, the coefficient α_λ characterizes the total attenuation of the radiation flux by particles of the medium both through scattering as well as through absorption and, therefore, is the sum of the corresponding coefficients

$$\alpha_\lambda = \alpha_{\lambda \text{scat}} + \alpha_{\lambda \text{ab}} \quad (2.3)$$

Fig. 2.1. Derivation of equation for radiation attenuation propagating in a uniform medium.

where $\alpha_{\lambda \text{scat}}$ and $\alpha_{\lambda \text{ab}}$ are the coefficients of attenuation of radiation flux in the medium due to scattering and absorption.

If a complex radiation flux Φ_0 enters a medium whose spectral distribution is characterized by the function $\Phi_0(\lambda)$, then on the basis of (2.2) with consideration of (1.1) we can write

$$\phi_L(\lambda) d\lambda = \phi_0(\lambda) e^{-\alpha_\lambda L} d\lambda. \quad (2.4)$$

Integrating this equality for λ in the entire band of the spectrum, we find the value of a complex radiation flux at the exit from the medium.

$$\Phi = \int_0^\infty \phi_L(\lambda) d\lambda = \int_0^\infty \phi_0(\lambda) e^{-\alpha_\lambda L} d\lambda \quad (2.5)$$

For some narrow intervals of the spectrum, for example for the visible band, the value α_λ can be taken as independent of the wavelength, and then from (2.5) we obtain

$$\Phi' = e^{-\alpha L} \int_{\lambda_1}^{\lambda_2} \phi_0(\lambda) d\lambda = \Phi_0' e^{-\alpha L}, \quad (2.6)$$

where Φ_0 and Φ' are the radiation fluxes at the entry and exit from the medium, respectively.

If we designate $e^{-\alpha_\lambda L} = \tau(\lambda)$; $e^{-\alpha L} = \tau$, then expressions (2.2) and (2.6) will take the form

$$\Phi_\lambda(L) = \Phi_\lambda(0) \tau_0^\lambda(\lambda); \quad (2.7)$$

$$\Phi = \Phi_0 \tau_0^L. \quad (2.8)$$

Coefficients $\tau_0(\lambda)$ and τ_0 are called the coefficients of transmission of radiation flux by a layer of the medium of unit thickness.

In this case, the transparency of the medium is characterized by the function of spectral transmission $\tau(\lambda)$ for a monochromatic radiation flux and the transmission coefficient τ for a complete flux.

The expressions for the determination of $\tau(\lambda)$ and τ can be obtained from formulas (2.7) and (2.8)

$$\frac{(\Phi)_\lambda}{(\Phi)_0} = \frac{(\tau)_\lambda}{(\tau)_0} = (\tau)_\lambda^0 = (\tau)_\lambda \quad (2.9)$$

$$\frac{(0)\Phi}{(7)\Phi} = \frac{0}{7} 1 = 1 \quad (2.10)$$

Since the coefficients α_λ and α and $\tau(\lambda)$ and τ which correspond to them account for attenuation of radiation flux as a consequence of scatter and absorption, the overall transmission of the medium can be presented by the products

$$\tau(\lambda) = \tau_{\text{scat}}(\lambda) \tau_{\text{ab}}(\lambda) \quad (2.11)$$

$$\tau = \tau_{\text{scat}} \tau_{\text{ab}} \quad (2.12)$$

where $\tau_{\text{scat}}(\tau)$ and τ_{scat} are the spectral and integral transmission of the medium with consideration of losses to scattering; $\tau_{\text{ab}}(\lambda)$ and τ_{ab} are the spectral and integral transmission but with consideration of losses only by absorption.

Each of the coefficients in formulas (2.11) and (2.12), in turn, can characterize the transparency of the medium with consideration of losses for scattering or absorption by various components, i.e., each of these components is a product of the type /28

$$\left. \begin{aligned} \tau_p(\lambda) &= \tau_p(\lambda)_1 \tau_p(\lambda)_2 \dots \tau(\lambda)_k = \prod_{j=1}^k \tau_p(\lambda)_j; \\ \tau_n(\lambda) &= \tau_n(\lambda)_1 \tau_n(\lambda)_2 \dots \tau(\lambda)_n = \prod_{j=1}^n \tau_n(\lambda)_j; \\ \tau_p &= \tau_{p1} \tau_{p2} \dots \tau_k = \prod_{j=1}^k \tau_{pj}; \\ \tau_n &= \tau_{n1} \tau_{n2} \dots \tau_n = \prod_{j=1}^n \tau_{nj}. \end{aligned} \right\}$$

With consideration of the latter relations, Eqs. (2.1) and (2.2) will take the form

$$\tau(\lambda) = \prod_{j=1}^k \tau_p(\lambda)_j \prod_{j=1}^n \tau_n(\lambda)_j; \quad (2.13)$$

$$\tau = \prod_{j=1}^k \tau_{pj} \prod_{j=1}^n \tau_{nj}. \quad (2.14)$$

The formulas presented can be employed for calculating the transmission coefficients of various optical media-including the atmosphere and optical materials of parts of electro-optical instruments.

2.2. Brief Information About the Atmosphere

The earth's atmosphere is a medium consisting of a mixture of gases and water vapor with foreign particles suspended in it -- aerosols (droplets of water which appear with the condensation of water vapor, dust particles, smoke particles) whose size fluctuates from $5 \cdot 10^{-6}$ to $5 \cdot 10^{-3}$ cm.

Nitrogen (78%) and oxygen (21%) are the basic permanent components of the ground layer of air. The fraction of the other gases (argon, xenon, hydrogen, carbon dioxide, ozone, and others) is less than one percent of the volume. Of these latter, carbon dioxide and ozone have an influence on the transparency of the atmosphere. The content of carbon dioxide in the ground layer of the atmosphere is irregular and sometimes reaches 0.05%; however, for evaluating transparency, we will consider that carbon dioxide is distributed in the atmosphere approximately uniformly and its concentration by volume is 0.03% at all altitudes. Corresponding to such a concentration is a thickness of CO_2 layer equal to 2.4 meters reduced to normal pressure and temperature. The concentration of ozone O_3 at an altitude of 20-25 km comprises about 10^{-5} - 10^{-6} percent, which corresponds to a reduced thickness of several millimeters. The maximum concentration of ozone is found at an altitude of from 20 to 30 km. In the altitude interval of from 40 to 70 km, ozone is in photochemical equilibrium. At an altitude of 40 km, 1 cm^3 contains $4.6 \cdot 10^{11}$ molecules of ozone, which corresponds to a concentration of $5 \cdot 10^{-6}$, and at an altitude of 70 km, 1 cm^3 contains $6 \cdot 10^8$ molecules (concentration $3.3 \cdot 10^{-7}$), i.e., the concentration of ozone decreases with altitude more rapidly than the overall concentration of air. The content of various components in the atmosphere, expressed in atm-cm, is provided in Table 2.1 [8].

TABLE 2.1.

Component	N_2	O_2	Ar	CO_2	Ne	CH_4	Kr	N_2O	H_2	He	O_3	Xe	CO	H_2O
Content atm-cm	624500	167600	7440	240- 320	14.6	1.2	0.8	0.4	0.4	4.2	0.2- 0.3	0.06	0.0- 0.15	10 ³ - 10 ⁴

The content of water vapor in the atmosphere depends on a number of factors, in particular, on air temperature and pressure and the presence of bodies of water on the given terrain. In this connection, the water vapor content in the atmosphere increases with an increase in temperature. Fluctuations in the mean tension of water vapor in the ground layer of the atmosphere for the middle latitudes occur within limits of from $2 \cdot 10^5$ Pa (2 mm Hg) in January to $10 \cdot 10^5$ Pa (10 mm Hg) in July, which corresponds to an absolute air humidity of 2.3 g/m^3 and 9.9 g/m^3 . The basic quantity of water vapor is concentrated in the lower 5-kilometer layer of the atmosphere and drops sharply with a further increase in altitude.

As shown by data obtained during experimental investigations with the use of AES [artificial earth satellites], meteorological rockets, and other means, up to altitudes on the order of 100 km, the earth's atmosphere remains basically nitrogen-oxygen in its composition. With an increase in altitude, the pressure and density of atmospheric air decrease in accordance with the exponential law. Table 2.2 [3] presents data on a model of the atmosphere which can be used in calculations of attenuation. The table was obtained by the concentration method.

TABLE 2.2. CHANGE IN CHARACTERISTICS OF THE ATMOSPHERE WITH ALTITUDE.

Altitude H (km)	Density $\rho \text{ g-cm}^3$	Pressure p, Pa	No. of Particles in unit of volume, n cm^{-3}	Temper- ature, T, K	Reduced layer atm-cm
0	$1.29 \cdot 10^{-1}$	$133.760 \cdot 10^5$	$2.6 \cdot 10^{19}$	273	$9.1 \cdot 10^5$
60	$3.5 \cdot 10^{-7}$	$2.4 \cdot 10^{-1}$	$7.3 \cdot 10^{15}$	235	$2.63 \cdot 10^2$
70	$8.1 \cdot 10^{-8}$	$4.3 \cdot 10^0$	$1.7 \cdot 10^{15}$	185	$4.6 \cdot 10^1$
80	$1.2 \cdot 10^{-8}$	$6.0 \cdot 10^{-1}$	$2.5 \cdot 10^{14}$	175	$6.6 \cdot 10^0$
90	$1.7 \cdot 10^{-9}$	$9.2 \cdot 10^{-2}$	$3.5 \cdot 10^{13}$	195	$10.3 \cdot 10^{-1}$
100	$2.7 \cdot 10^{-10}$	$1.6 \cdot 10^{-2}$	$5.5 \cdot 10^{12}$	215	$2.08 \cdot 10^{-1}$
110	$5.3 \cdot 10^{-11}$	$4.0 \cdot 10^{-3}$	$1.2 \cdot 10^{12}$	235	$5.4 \cdot 10^{-2}$
120	$1.3 \cdot 10^{-11}$	$1.2 \cdot 10^{-3}$	$3.1 \cdot 10^{11}$	280	$1.75 \cdot 10^{-2}$
130	$3.9 \cdot 10^{-12}$	$4.7 \cdot 10^{-4}$	$9.2 \cdot 10^{10}$	355	$7.10 \cdot 10^{-3}$
140	$1.4 \cdot 10^{-12}$	$2.3 \cdot 10^{-4}$	$3.4 \cdot 10^{10}$	485	$3.7 \cdot 10^{-3}$
150	$6.5 \cdot 10^{-13}$	$1.3 \cdot 10^{-4}$	$1.6 \cdot 10^{10}$	605	$1.20 \cdot 10^{-3}$
160	$3.5 \cdot 10^{-13}$	$8.3 \cdot 10^{-5}$	$8.4 \cdot 10^9$	715	$7.8 \cdot 10^{-4}$
170	$2.1 \cdot 10^{-13}$	$5.6 \cdot 10^{-5}$	$5.1 \cdot 10^9$	800	$5.3 \cdot 10^{-4}$
180	$1.4 \cdot 10^{-13}$	$4.0 \cdot 10^{-5}$	$3.5 \cdot 10^9$	830	$3.8 \cdot 10^{-4}$
200	$6.9 \cdot 10^{-14}$	$2.0 \cdot 10^{-5}$	$1.7 \cdot 10^9$	830	$1.9 \cdot 10^{-4}$

Besides gases and water vapor, the lower layers of the atmosphere constantly have admixtures -- aerosols in the form of dust, smoke, various particles, and droplets of water which make the atmosphere turbid and worsen conditions for the propagation of radiation flux.

2.3. Characteristics of Outer Space

/30

With an increase in altitude above the earth's surface, in its parameters the atmosphere gradually approaches the parameters of an interplanetary gas.¹ Therefore, in the solution of various problems, the influence of the atmosphere is disregarded beginning with the altitude determined for a given case.

As investigations show [26, 27], the parameters of the atmosphere, including its upper layers, being practically circumterrestrial outer space, are unstable. They change with the latitude of the locality, time of year, during a day, and also with a change in solar activity.

At altitudes of more than 100 km, the ratio between nitrogen and oxygen changes. The dissociation of molecules of gases and water vapor occurs, and ions of molecular O₂ and atomic oxygen O, molecular N₂ and atomic nitrogen N, nitric oxide NO, and water H₂O are created.

A notion of the nature of change in the parameters of the upper atmosphere with altitude is given by Table 2.3 compiled on the basis of the processing of experimental data [27].

/31

At the present time, it has been established with sufficient precision [26] that at altitudes of 90-100 km even those small vertical movements of air which could intermix and equalize the gas composition of the atmosphere stop.

However, at altitudes of more than 80-90 km, there are solid particles of cosmic origin (micrometeorites). It is assumed that [28] the drop in the concentration of micrometeorites with altitude conforms to the law $H^{-1.4}$.

In works [27] it is presumed that the upper atmosphere is divided for density of meteoric matter into three zones, for which the distribution of meteoric particles is characterized by the data in Table 2.4.

¹It is assumed that the density of an ionized interplanetary gas expressed by the number of particles in a unit of volume is approximately 10³ particles in 1 cm³.

TABLE 2.3. CHANGE IN PARAMETERS OF THE UPPER ATMOSPHERE WITH ALTITUDE.

Altitude H km	No. of par- ticles in unit of volume, n cm ⁻³	Density ρ g/cm ³	Temperature T K	Pressure p Pa
225	6.01·10 ⁹	2.12·10 ⁻¹³	936	8.3·10 ⁻⁵
230	5.31	1.79	938	7.4·10 ⁻⁵
240	4.17	1.42	946	5.9·10 ⁻⁵
250	3.3	1.10	958	4.7·10 ⁻⁵
260	2.64	8.66·10 ⁻¹⁴	971	3.85·10 ⁻⁵
270	2.12	6.83	987	3.14·10 ⁻⁵
280	1.72	5.44	1005	2.6·10 ⁻⁵
290	1.40	4.36	1026	2.16·10 ⁻⁵
300	1.15	3.53	1048	1.83·10 ⁻⁵
325	7.31·10 ⁸	2.17	1110	1.24·10 ⁻⁵
350	4.82	1.40	1185	1.05·10 ⁻⁵
375	3.31	9.41·10 ⁻¹⁵	1276	4.90·10 ⁻⁶
400	2.36	6.60	1373	5.07·10 ⁻⁶
425	1.73	4.79	1489	4.05·10 ⁻⁶
450	1.32	3.60	1614	3.38·10 ⁻⁶
475	1.03	2.79	1781	2.92·10 ⁻⁶
500	8.24·10 ⁷	2.21	1953	2.60·10 ⁻⁶

TABLE 2.4.

Zone	Frequency of impacts, N ₂ , M ⁻² ·s	Mass of par- ticles per unit area in units of time, 10 ⁻³ g·cm ⁻² ·s	No. of particles in unit volume, n 10 ⁻¹³ ·cm ⁻³	Density ρ 10 ⁻²¹ g·cm ³
100 < h < 400	0.1—1.0	0.1—1.0	4·10 ² —4·10 ³	4·10 ² —4·10 ³
400 < h < 2R ₃	10 ⁻⁴ —10 ⁻²	10 ⁻⁴ —10 ⁻²	0.4—40	0.4—40
h > 2R ₃	5·10 ⁻⁶ —10 ⁻⁴	5·10 ⁻⁶ —10 ⁻⁴	0.02—0.4	0.02—0.4
Zodiacal Cloud	2·10 ⁻⁶ — 12·10 ⁻⁴	10 ⁻⁵ —10 ⁻³	0.01—1.0	0.03—3.0

Cosmic particles enter the earth's atmosphere with tremendous velocities on the order of 11-70 km/s and reach altitudes of 160-140 km experiencing almost no deceleration. Next, they are sharply decelerated and particles with radius $r < 1 \mu\text{m}$ lose their cosmic speed in the altitude interval of 130-95 km. The overwhelming majority of the particles which enter the atmosphere are of small dimensions. Dust particles from 0.30 to $1 \mu\text{m}$ comprise 99% of all arriving particles; among them 60% of the particles have a radius $r \approx 0.3 \mu\text{m}$ and only 1% have a radius of $1 \mu\text{m}$. Particles of rather big dimensions are also encountered. At the high altitudes there are no particles with $r < 0.25 \mu\text{m}$, since they are driven out of the solar system by light pressure. To estimate the density number of particles at various altitudes, we can use the data of B.A. Mirtov [26] presented in Table 2.5. /32

TABLE 2.5.

Altitude H km	Density ρ $\text{g}\cdot\text{cm}^{-3}$	No. of particles in unit vol., n, cm^{-3}	Velocity of flight of particles v, cm/s	nv
80	$2.5 \cdot 10^{-8}$	$5.7 \cdot 10^{14}$	$5.8 \cdot 10^1$	$3.3 \cdot 10^{16}$
90	$4.0 \cdot 10^{-9}$	$8.6 \cdot 10^{13}$	$3.84 \cdot 10^2$	$3.3 \cdot 10^{16}$
95	$1.0 \cdot 10^{-9}$	$2.7 \cdot 10^{13}$	$3.0 \cdot 10^4$	$8.0 \cdot 10^{17}$
100	$5.5 \cdot 10^{-10}$	$1.5 \cdot 10^{13}$	$3.0 \cdot 10^5$	$4.5 \cdot 10^{18}$
110	$1.2 \cdot 10^{-10}$	$3.3 \cdot 10^{12}$	$1.68 \cdot 10^6$	$5.6 \cdot 10^{18}$
120	$3.7 \cdot 10^{-11}$	$1.1 \cdot 10^{12}$	$2.40 \cdot 10^6$	$2.6 \cdot 10^{18}$
130	$1.4 \cdot 10^{-11}$	$4.0 \cdot 10^{11}$	$2.70 \cdot 10^6$	$1.1 \cdot 10^{18}$
140	$7.0 \cdot 10^{-12}$	$2.0 \cdot 10^{11}$	$2.82 \cdot 10^6$	$5.6 \cdot 10^{17}$
150	$4.0 \cdot 10^{-12}$	$1.1 \cdot 10^{11}$	$2.88 \cdot 10^6$	$3.2 \cdot 10^{17}$
200	$6.1 \cdot 10^{-13}$	$1.7 \cdot 10^{10}$	$2.97 \cdot 10^6$	$5.0 \cdot 10^{16}$
225	$3.5 \cdot 10^{-13}$	$1.0 \cdot 10^{10}$	$2.98 \cdot 10^6$	$3.0 \cdot 10^{16}$
275	$7.0 \cdot 10^{-14}$	$2.1 \cdot 10^9$	$3.0 \cdot 10^6$	$6.3 \cdot 10^{15}$
300	$3.4 \cdot 10^{-14}$	$1.1 \cdot 10^9$	$3.0 \cdot 10^6$	$3.3 \cdot 10^{15}$

Micrometeorites influence the operation of electro-optical equipment, attenuating the transient radiation and causing the background component of scattered solar radiation. But because of the comparatively low density, the attenuation of the radiation by micrometeorites can be disregarded in practice. /33

In addition, the prolonged action of meteoric particles can lead to the failure of the optical parts. The nature of the processes which occur on the impact of the micrometeorites with various substances and the degree of change of the surface subjected

to bombardment are considered in work [15]. In it, it is shown that the degree of dulling action which is possessed by the meteoric particles on the optical surfaces of the instruments beyond the atmosphere is not great. A perceptible effect arises during a time on the order of 10 years. The effect is considerably stronger for refractive surfaces than for mirrors.

Data presented in work [15] indicate that the meteoric bombardment of optical surfaces leads to an increase in the scattering component. Calculations which have been conducted show that with an optical instrument which operates in the visible band of the spectrum, the scattered component reaches 50% in 2 hours after the start of bombardment.

For instruments which operate in the long-wave band of the spectrum, the dulling effect is felt less.

Since the basic mass of the atmosphere (99.9%) is concentrated in the layer below 50 km and the concentration of meteoric particles at great altitudes is relatively small, the attenuation of radiation at altitudes of 50 km or higher can be disregarded.

2.4. The Propagation of Radiation in the Atmosphere and Space

During propagation in the atmosphere and space, radiation flux is attenuated due to absorption and scattering by the molecules of various gases, water vapor, and also solid particles and drops of water. The dependence of attenuation due to scattering on the radiation wavelength has a smooth character and the attenuation due to absorption has a selective character.

The radiation flux is absorbed selectively primarily by ozone, carbon dioxide, and water vapor, in which regard the last two are the basic absorbing components (Fig. 2.2).

Ozone absorbs radiation comparatively intensively in zones with centers on wavelengths $\lambda = 4.7$ and $9.6 \mu\text{m}$; carbon dioxide -- in zones characterized by wavelengths $\lambda = 2.05, 2.6, 4.3$ (from 4.0 to 4.7) μm , and especially in the zone of 12.8 – $17.3 \mu\text{m}$.

Water vapor absorbs most strongly in the zones whose centers lie on wavelengths $\lambda = 0.94, 1.13, 1.38$ (1.3 – 1.5), $1.46, 1.87$ (1.7 – 2.0), 2.66 (2.4 – 3.4), $2.15, 6.26$ (4.5 – 8.0), $11.7, 13.5$, and $14.3 \mu\text{m}$.

The zones of absorption of carbon dioxide and water vapor are the reason for the almost complete absorption of infrared radiation in a broad band of the spectrum by the atmosphere, beginning with 14 – $15 \mu\text{m}$.

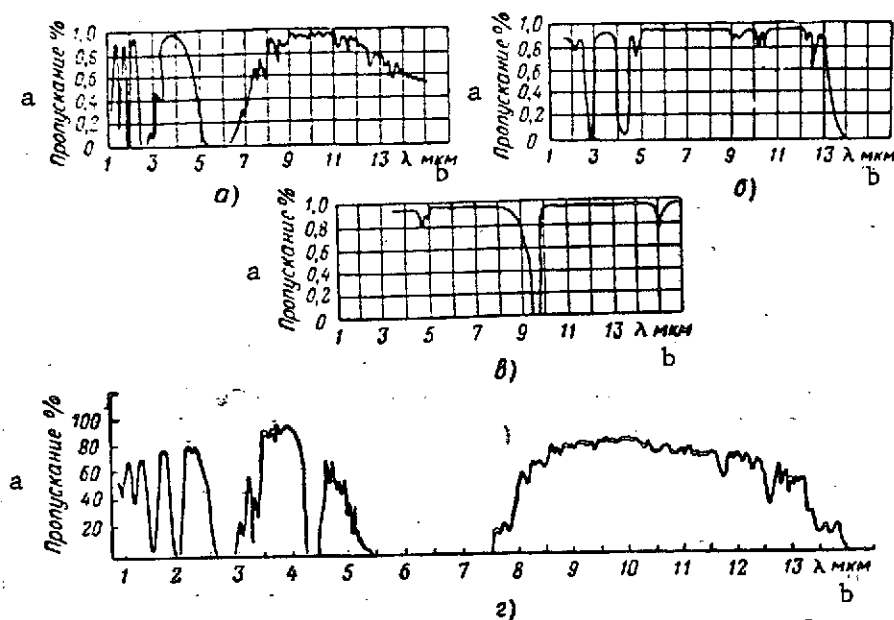


Fig. 2.2. Selective character of attenuation of radiation flux by the atmosphere.

Key: a. Transmission
b. μm

The dependence of the attenuation of radiation flux on the quantity of attenuating matter in the path of propagation of the radiation with normal pressure is illustrated by a table [35] (see Appendix, Table 6.7). With a reduction in pressure, the absorptivity of all components is reduced, i.e., layers of absorbing matter of the same thickness at great altitudes above the earth's surface attenuate radiation less than at low altitudes. This corresponds to a reduction in the effective thickness of the absorbing matter. If we designate by ω_{eff} the effective thickness of an equivalent layer of precipitated water vapor in the path of propagation of radiation flux reduced for absorptivity to the water vapor of the ground layer of the atmosphere, and by ω_n the actual thickness of a layer of precipitated water vapor, the ratio will characterize the reduction in absorptivity of water vapor with altitude. Data on the relative change in the effective thickness of layers of water vapor and carbon dioxide depending on altitude above sea level are presented in Table 2.6.

According to the data in Table 7 (see Appendix), for water vapor the function $f(H)$ is approximated with sufficient precision by the equation

$$\omega_{\text{eff}}/\omega_n = e^{-0.0654 H}, \text{ whence}$$

TABLE 2.6.

Altitude m H	$\omega_{\text{eff}}/\omega_n$		Altitude m H	$\omega_{\text{eff}}/\omega_n$	
	H ₂ O	CO ₂		H ₂ O	CO ₂
0	1.000	1.000	3050	0.819	0.548
305	0.981	0.940	4575	0.739	0.404
610	0.961	0.883	6100	0.670	0.299
915	0.942	0.840	9150	0.552	0.168
1220	0.923	0.774	12200	0.441	0.085
1525	0.904	0.743	15250	0.348	0.042
1830	0.886	0.699	18300	0.272	0.020
2135	0.869	0.660	21350	0.214	0.010
2440	0.852	0.620	24400	0.167	0.005
2745	0.835	0.580	27450	0.134	0.002
			30500	0.105	0.001

$$\omega_{\text{eff}} = \omega_n e^{-0.0654 H} \quad (2.15) \quad /35$$

For carbon dioxide, it is approximated by the equation

$$L_{\text{eff}}/L_H = e^{-0.19 H}$$

then

$$L_{\text{eff}} = L_H e^{-0.19 H} \quad (2.16)$$

where L_H is the distance at which radiation is propagated at altitude H , and L_{eff} the effective distance reduced for absorptivity to the ground layer.

Formulas (2.15) and (2.16) permit calculating, from the known thickness of precipitated water vapors and the distance of propagation of radiation at altitude H , the effective values of the indicated quantities reduced for absorptivity to the ground layer.

CHAPTER 3. OPTICAL SYSTEM OF ELECTRO-OPTICAL INSTRUMENTS OF SPACE VEHICLES

3.1. The Purpose and Characteristics of Optical Systems

Optical systems employed in on-board equipment of artificial earth satellites and space ships are extremely varied in basic circuits and design. They have a common basic purpose -- to collect energy emitted or reflected by the object of observation and, transforming it to an image or specific form of radiation flux, to send it to a radiation receiver. /36

Photoresistors, bolometers, television tubes, photographic materials, and other devices are used as receivers in on-board electro-optical equipment. During recent years, visual optical systems in which the observer's eye is the receiver of the radiations are beginning to find employment on manned artificial earth satellites. The properties and characteristics of the receivers, just as the purpose of a given type of electro-optical equipment, predetermine requirements for the optical system, for example, the nature of conversion of the radiation flux, the necessary transmission in a given region of the spectrum, the form and quality of the image, and so forth. However, in their functional properties and volume of tasks accomplished with their aid, optical systems can be considered as independent devices possessing specific characteristics.

Included among the basic tasks which are accomplished in various types of on-board equipment with the use of optical systems are:

- Survey by means of the discrete or continuous scanning of a specific part of space in which the object of search, reference point, or subject of observation may be located;

- Reproduction of the image of an object of observation in a specific scale with the goal of its subsequent recording with the use of photographic or television devices;

- Provision of the required energy irradiance on the surface of the sensitive element of the receiver;

- Concentration of the radiation flux of artificial emitters, for example, lasers or flash lamps;

- Assuring the determination of angular coordinates and range of the objects of observation.

Moreover, with the use of optical systems, one can accomplish observation with variable magnification and with various fields of view, the transmission of information between space ships and to ground posts, signaling, and a number of other tasks.

An estimate of the properties and qualities of optical systems can be conducted successfully only with the use of a number of special characteristics. The experience of optical instrument manufacturing and the operation of optical and electro-optical equipment provides the grounds for dividing all the characteristics used for this into the following groups: overall size, power, aberrational, and space-frequency or transmission.

Technical-economic and operational characteristics common for instrument manufacture are used for an estimate of the quality, /37 dependability, and economy of the design formulation and the effectiveness of the given equipment in the process of operation.

3.2. Scheme of an Optical System and Its Elements

Common to all optical systems is the fact that the basis of each of them is made up of an aggregate of specific elements (lens, prism, and others), the properties and mutual arrangement of which predetermine the characteristics of a specific system. In designing, when the structural parameters of the parts and units of the optical system are still unknown, its equivalent scheme is constructed. In the theory of optical systems, such a scheme is called ideal because the basic principle of its construction is the condition that it converts the aggregate of points, straight lines, and planes of the space of objects into geometrically similar aggregates of points, straight lines, and planes of the space of images without introducing distortions into the structure of refracted or reflected pencils of rays.

This condition is applicable to real optical systems only for infinitely narrow pencils of rays which pass through the systems at small angles of slope to the optical axis. With the passage of broad pencils of rays, distortions or aberrations arise in the position, geometric form, and coloring of the image in comparison with the object. For an evaluation of the magnitude and character of the aberrations which determine the quality of the image and the degree of perfection of a real optical system, a similar ideal system which possesses the very same parameters and which gives an aberration-free image is used as a standard of comparison. The method of replacing an actual system being designed by its equivalent scheme permits calculating ahead of time the basic optical characteristics of the apparatus being designed.

The equivalent scheme of an optical system also consists of an aggregate of elements; however, they are not optical parts but arbitrary planes and points which possess specific properties.

The basic elements of the scheme are the principal and focal planes.

The principal plane is the geometric locus of the points of intersection of the pencils of rays incident to the system (lens, non-planar mirror) and refracted by it. Thus, in its properties it is seemingly equivalent to the action of a real optical system for the passage of a pencil of rays through it. In the construction of an equivalent system, the optical system is given in the form of two principal planes: front H and back H' (Fig. 3.1) in which regard the principal plane H' determines the influence of the system on the pencils of rays, for example pm , which go from that part of space where the objects being observed or recorded are arranged, and the principal plane H -- the influence on the pencils of rays which go in the reverse direction, from that part of space where the images of these objects are located.

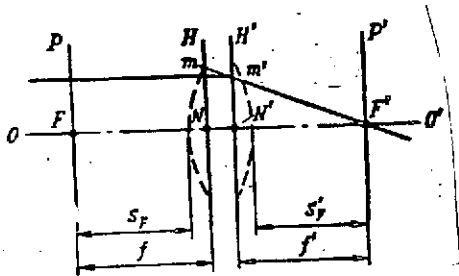


Fig. 3.1. Equivalent scheme of an optical system.

A complex optical system consisting of several simple ones can be presented in the form of a corresponding series of pairs of principal planes of its elements and two principal planes of the entire system which characterize its overall influence on the passing pencils of rays.

The points of intersection of the principal planes with optical axis OO' are called the principal points of the system. The front principal point N corresponds to the front principal plane H , and the back principal point N' to the back principal plane H' .

The principal planes and principal points permit accomplishing the construction of rays which pass through the system without consideration of their actual refraction on the surfaces of the lenses or reflection from the mirror.

The focal plane is the geometric locus of the points of intersection of a pencil of rays from an object refracted or reflected by the system which is located so far away that the rays of the incident pencil can be considered parallel.

The point of intersection of the focal plane with the optical axis OO' is called the principal focus which is the point of intersection of a pencil of rays which have fallen on the system parallel to the optical axis. Depending on the direction of the pencil of rays, just as for the principal planes, the front and back focal planes P and P' are distinguished and, respectively, the front and back principal foci of the system F and F' .

The sections between the principal points and the principal foci are called the focal distances. The section $NF' = f'$ is called the back focal distance and the section $NF = f$ the front focal distance. If the optical system is in a homogeneous environment, i.e., the refractive indices of the medium in front of and following the system are the same, the front and back focal distances are equal.

The principal planes are arranged symmetrically to the real refractive surfaces only with single biconvex or biconcave symmetrical lenses. In real systems, the front and back refractive surfaces are at different distances from the respective front and back principal points. Therefore, besides the focal distances, it is necessary to determine the sections between the principal focus and the corresponding front or back refractive (reflecting) surface of the system. They are called the back foci or, respectively, the front S_F and back S'_F sections. The size of the back section is a design parameter which determines the distance from the back focal length of the plane to the last lens of the system. /39

For an estimate of the transverse dimensions of the system and, in particular, the diameters of the greatest cross sections which transmit the system of pencils of rays, the scheme is supplemented with diaphragms.

With the passage of pencils of rays through the optical system, their solid angles and cross sections are limited by openings in the mountings of the optical parts and special screens installed to cut off the fringe, spurious rays. The mounts of these openings are called diaphragms. The position and size of the diaphragm determine the basic characteristics of the optical system and influence the illumination and sharpness of the image. Three types of diaphragms are distinguished: aperture, field, and auxiliary. The latter is intended to eliminate bright spots and haloes which arise with the incidence of spurious rays in the system.

The operative or aperture diaphragm limits the solid angles or the diameters of the cross sections of the pencils of rays which go from objects located on the optical axis (Fig. 3.2). The area of the operative diaphragm D_a determines the amount of light which passes through the system and is used for the creation of the central portion of the image.

The image of an operative diaphragm in the space of objects is the entrance pupil of the system. In real systems, if there are no additional optical parts in front of the objective lens in the form of mirrors or prisms, usually the operative diaphragm and the entrance pupil coincide with the lens mount. The image of diaphragm D_a following the optical system in the space of the images is the exit pupil.

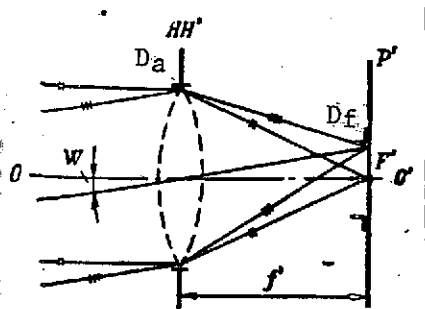


Fig. 3.2. Diaphragms of an optical system.

The diaphragm of the field of view D_f limits the inclined or field pencils of rays which go from the extra-axial objects and which pass into the optical system of the instrument. These pencils of rays create the image of extra-axial sections in the plane of the image; therefore, the position, form, and size of this diaphragm determine the form and size of the field of view of the system.

To obtain sharply defined edges and increase the uniformity of illumination of the image in real optical systems, the field diaphragm is situated in the plane of the image. For example, /40 if a photomultiplier or photoelement is the radiation receiver, the mount of its photocathode is the field diaphragm.

3.3. Dimensional Characteristics

This group of characteristics determines the "optical dimensions," i.e., the length of the system, light diameters of its elements and their mutual disposition, and the degree of influence on the pencils of rays passing through the system.

The basic characteristics of this group are: focal distance, field of view, relative aperture, and resolution.

Moreover, depending on the purpose and basic scheme of the instrument, this group of characteristics is supplemented or some of them are replaced by equivalents. For example, for instruments in which the image of an object observed by the eye or analyzed by other methods is constructed with the use of optical systems, a characteristic such as magnification is used. Instruments with scanning devices which provide a survey of space beyond the limits of the field of view of the basic optical system are characterized by such parameters as viewing angle, instantaneous field-of-vision angle, and so forth. However, all these values are derivatives of the basic dimensional characteristics.

The focal distance f' causes magnification, scale of image, and the optical power of the system.

Magnification determines in linear or angular measure how many times the system reduces or magnifies the image in comparison with the object. Two types of magnification are distinguished: linear and angular.

Linear magnification (β) is the name given to the ratio of the linear dimensions of the image l' to the linear dimensions l of the corresponding part of the object

$$\beta = \frac{l'}{l} = \frac{1}{m}, \quad (3.1)$$

where $1/m$ is the linear scale of the image.

If we designate (Fig. 3.3) the distance from the front principal focus F to the object by x and from the back principal focus F' to the image by x' , then

$$\beta = \frac{f}{x} = \frac{x'}{f'}. \quad (3.2)$$

Angular magnification Γ /41 determines the capability of the optical system to change the direction of the rays passing through it:

$$\Gamma = \frac{\tan u'}{\tan u} \quad (3.3)$$

where u and u' are the angles of slope of the rays to the optical axis before and after the system, respectively.

Fig. 3.3. Diagram of the structure of an image in an equivalent scheme.

The relation between the angular and linear magnification can be found using Fig. 3.3. Since $\tan u' = l'/f'$ and $\tan u = l/f$, and considering that for optical systems in a homogeneous environment $|f| = |f'|$, we obtain $\Gamma = (l/l')(f/f') = 1/\beta$ or

$$\Gamma\beta = 1 \quad (3.4)$$

The optical power of the system ϕ equals:

$$\phi = \frac{1}{F}, \quad (3.5)$$

Note. The sign of optical power, which is determined by the sign of the focal distance, characterizes the capability of the system to collect and scatter refracted (for mirrors, reflected) pencils of rays. Systems with a positive optical power are called collective, and with negative optical power, diffusive.

The sign of the focal distance is taken as positive if it is read off from the principal point along the course of the light rays in the system.

For a compound optical system consisting of two simple ones, the optical power will equal

$$\varphi = \varphi_1 + \varphi_2 - d\varphi_1\varphi_2, \quad (3.6)$$

where ϕ_1, ϕ_2 are the optical power of each of the components, and d is the distance between them.

The field of view determines that part of space which is reproduced by the optical system within limits of the plane of the image limited by the dimensions of the field diaphragm. From Fig. 3.2, it follows that the angle of the field of view $2W$ is /42 determined from the relationship

$$\tan W = \frac{D_f}{2f}, \quad (3.7)$$

where D_f is the diameter of the field diaphragm

If a single photoresistor or bolometer is used as a radiation receiver in an electro-optical system, it is impossible to obtain a large field of view due to the small dimensions of the receiver's sensitive element whose mount is the field diaphragm. In this case, a scanning system is used which deflects the optical axis of the objective lens within the limits of a specific angle (viewing angle). The elementary viewing angle will be the value $2W_0$, called the instantaneous field of vision angle.

The relative aperture (q) is calculated from the formula

$$q = \frac{D_1}{f}, \quad (3.8)$$

accepting approximately that the entrance pupil is combined with the mount of the objective lens. Here D_1 is the light (or operating) diameter of the objective lens.

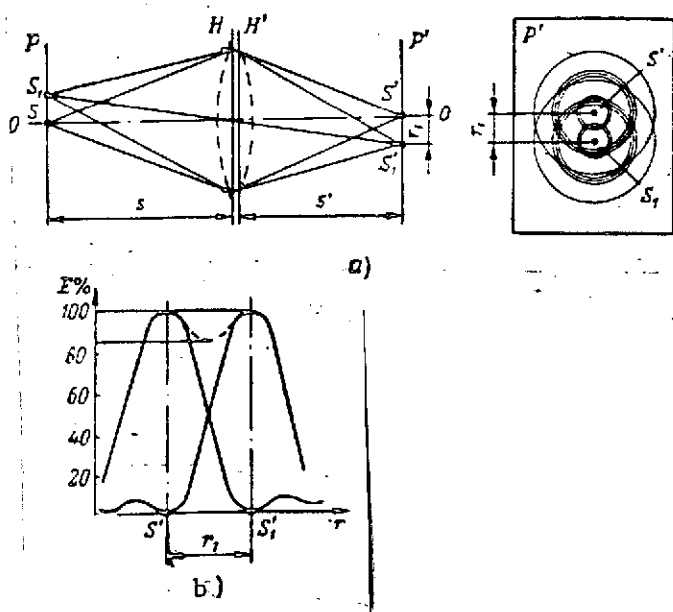
The theoretical limit of the value q is the relation $q \leq 1/0.5$. It can be found by accepting that with small values of the angle u' (Fig. 3.3) $\sin u' \sim D_a/2f'$. Since the maximum value of $\sin u' \leq 1$, consequently $q \leq 1:0.5$. For the fastest objective lenses, the value q lies within limits of 0.5-2.0.

Resolution (V) characterizes the possibilities of the optical system to construct separately (or resolve) the images of individual elements of the surface of an object or point objects which are closely spaced, for example, stars. The higher the resolution, the greater the information capacity and the higher the precision of measurements or the aiming of the electro-optical equipment.

The theoretical resolution of an optical system can be determined using the diffraction theory of the construction of an image. If two luminous points S and S_1 (Fig. 3.4) are located at a specific distance from each other, their image will have the appearance not of points S' and S'_1 but of diffraction circles of confusion, consisting of concentric dark and light rings (see Fig. 3.4a). The distribution of irradiance within the limits of such rings is presented in Fig. 3.4b, in which regard, in the central portion the irradiance will be maximum. These two images S' and S'_1 can be detected separately with the use of /43 any analyzing system only under the condition where the distance between their centers is not less than the radius r_1 of the first dark ring. From the theory of diffraction [44], it is known that this value equals

$$r_1 = \frac{3.83\lambda}{\pi} \frac{1}{q}, \quad (3.9)$$

where λ is the wavelength of the radiation for which the resolution is determined; 3.83 is the coefficient for the first dark ring.



The angular size of the radius of the first dark ring or the minimum angle between the points being resolved at the limit in the plane of the image S' and S'_1 under the condition that $S \rightarrow \infty$ and $s' = f'$ is determined from the expression

$$\sin \varepsilon \cong \varepsilon = \frac{r_1}{f'} = \frac{3.83\lambda}{\pi D_1} = \frac{1.22\lambda}{D_1} \quad (3.10)$$

where angle ε is called the theoretical resolving angle.

For optical systems which operate in the visible region of the spectrum, the mean value of wavelength $\lambda = 0.55 \mu\text{m} = 0.00055 \text{ mm}$. In this regard

$$\varepsilon = \frac{1.22 \cdot 0.00055 \cdot 206000}{D_1} \approx \left[\frac{140}{D_1} \frac{\pi \text{ rad/ang. sec}}{648000} \right]$$

Fig. 3.4. The influence of diffraction on the theoretical resolution of an optical system. a. Course of refracted pencils of rays and the appearance of the image of two points with the presence of diffraction; b. Distribution of irradiance in the image of two points.

If the same optical system is to operate in the near infrared /44 region, with $\lambda = 1 \text{ } \mu\text{m}$, the value of ϵ will be twice as great.

The angle ϵ is connected with resolution V by the relation

$$V = \frac{1}{\epsilon} \frac{\pi}{648000} \text{ rad} \quad (3.11)$$

The resolution of real optical systems is always less than the theoretical, due to the influence of aberrations, defects in the manufacture of the optical parts, and the quality of the assembly and adjustment of the system.

3.4. Energy Characteristics of an Optical System

The energy characteristics determine the properties of an optical system as a converter of radiation flux.

The basic characteristics of this group are: transmission coefficient, aperture ratio, and irradiance in the plane of the image of the optical system.

With the passage of radiation flux through an optical system, losses in radiation energy arise due to reflection on the surfaces of the optical parts and absorption in the metal mirror coatings and in the optical material of the parts.

The transmission coefficient τ characterizes the ratio of radiation flux Φ_τ which has passed through the system to the flux Φ which falls on its entrance

$$\tau = \frac{\Phi_\tau}{\Phi} \quad (3.12)$$

The coefficients of reflection ρ and absorption β will equal, respectively

$$\rho = \frac{\Phi_\rho}{\Phi} \text{ and } \beta = \frac{\Phi_\beta}{\Phi}, \quad (3.13)$$

where Φ_ρ and Φ_β are the values of energy fluxes lost due to reflection and absorption, respectively.

The values of coefficients τ , ρ , and β depend on the spectral composition of the flux, the nature and quality of the surface of the optical part, and the physical properties of its material. Therefore, in a number of cases the spectral values of these coefficients are used. The connection between the general τ and spectral $\tau(\lambda)$ transmission coefficients is expressed by the relation

$$\tau = \int_{\lambda_1}^{\lambda_2} \tau(\lambda) d\lambda. \quad (3.14)$$

In accordance with (2.7), we obtain

45

$$\tau = \frac{\int_{\lambda_1}^{\lambda_2} \Phi_{\tau(\lambda)} d\lambda}{\int_{\lambda_1}^{\lambda_2} \Phi_{\lambda} d\lambda} = \frac{\int_{\lambda_1}^{\lambda_2} \tau(\lambda) \Phi_{\lambda} d\lambda}{\int_{\lambda_1}^{\lambda_2} \Phi_{\lambda} d\lambda}, \quad (3.15)$$

where Φ_{λ} and $\Phi_{\tau(\lambda)}$ are the spectral values for the incident and transmitted fluxes respectively; λ_1, λ_2 are wavelengths which limit the band of the spectrum under consideration.

Similar relations can also be obtained for the coefficients ρ and β .

The connection between coefficients τ, ρ , and β is expressed by the relation

$$\tau = 1 - (\rho + \beta) \quad (3.16)$$

The coefficient of reflection for one surface of an optical part can be determined from the formula

$$\rho = \frac{(n - n_0)^2}{(n + n_0)^2}, \quad (3.17)$$

where n and n_0 are the refraction indices for the optical material of the part and the medium, respectively.

If the optical part is in the air, then $n_0 = 1$ and expression (3.17) takes the form

$$\rho = \frac{(n - 1)^2}{(n + 1)^2}. \quad (3.18)$$

Although the value of ρ depends on the angle of incidence of the rays on the refracting surface, with calculations of regular optical systems, this is often disregarded due to the small angles of slope to the optical axis.

For optical glass and quartz in the visible region of the spectrum $\rho = 0.04-0.06$. For coated optics, the surface of whose parts is coated with special films which reduce losses for reflection, the value of the coefficient ρ does not exceed 0.01-0.005. For special optical materials which are employed in systems which operate in the infrared region of the spectrum, the index of

refraction is usually larger than with optical glass. For example, with TBI crystals $n \approx 2.2-2.46$, with silver chloride, $n = 2.06$, and with germanium crystals, $n \approx 3.56-3.44$. Therefore, in calculations of coefficient ρ (3.18), it is necessary to consider the material of the part and the presence of a transmitting coating.

If there are a number of optical parts in the optical system, with a number of refracting surfaces equal to m , the transmission coefficient τ_p which considers losses for reflection alone will equal /46

$$\tau_p = (1 - \rho)^m \quad (3.19)$$

During reflection from mirrors, losses will arise due to the absorption of radiation energy in the metal coating layer. Table 3.1 presents the reflection coefficients for polished mirror coatings used in electro-optical equipment.

TABLE 3.1.

Mirror Coating	Reflection Coefficient	
	Visible Region	Infrared Region
Gold	0.82-0.89	0.96-0.98
Silver (polished)	0.88-0.96	0.96-0.98
Chromium	0.60-0.70	0.75-0.80
Aluminum	0.65-0.75	0.80-0.85

By analogy with expression (3.19), the transmission coefficient which considers energy losses only on the surface of mirrors will equal

$$\tau_m = \rho_m^{m_m} \quad (3.20)$$

where m_m is the number of mirrors.

The absorption of radiation energy in optical material is determined by the expression

$$\tau_p = e^{-\beta l} = \tau_0^l \quad (3.21)$$

where τ_p is the transmission coefficient which considers only losses by absorption; τ_0 is the specific coefficient of transparency per unit of thickness, and l is the thickness of the optical material.

In calculations, 1 cm is taken as the unit of thickness of a layer of optical material. The value of τ_0 for optical glass is taken as 0.01 per centimeter. For optical materials which are used in the infrared region of the spectrum, the value of τ_0 is taken from reference literature [7].

Thus, the general transmission coefficient of an optical system equals

$$\begin{aligned}\tau &= \tau_p \tau_m \tau_g \text{ or} \\ \tau &= (1-\rho)^m \rho_m^m \tau_0^l\end{aligned}\quad (3.22)$$

For a system with coated parts of optical glass or quartz /47 which operate in the visible region of the spectrum, the formula for the calculation of the transmission coefficient takes the form

$$\tau \approx 0.99^m \cdot 0.99^l \rho_m^m$$

Since the overall quantity of radiation energy which enters the system is determined by the area of the entrance pupil and is inversely proportional to the square of the focal length of the objective lens, for the determination of the relative aperture (H) we use the relation

$$H = \tau \left(\frac{D_{\text{entr. pup.}}}{f} \right) \quad (3.23)$$

In calculations, the diameter of the entrance pupil is often used which is equal to the diameter of the objective lens; then

$$H = \tau q^2 \quad (3.24)$$

Since the value of τ is inversely proportional to the number of lenses and their thickness, in the use of multilens systems with a large relative aperture, the effective relative aperture may be equal to or even less than that of simple systems with a small number of lenses and a smaller relative aperture.

The irradiance of the image (E') depends on the ratio of the radiation flux $d\Phi$ which emerged from an elementary area of the surface of the object and passed through the optical system to the corresponding elementary area $\Delta A'$ of the surface of the image. The magnitude of the irradiance and its distribution over the surface of the image determine the possibility of its recording with the use of photoelectric or other radiation receivers.

For the calculation of the irradiance in the center of image E'_0 we present an optical system (Fig. 3.5) with entrance M and exit M' pupils. Suppose that the plane of object A whose /48 central section is designated ΔA has uniform energy brightness B.

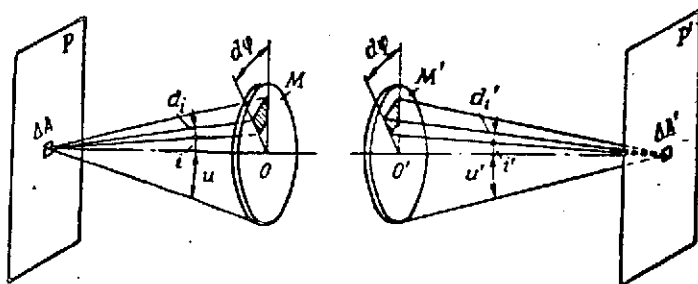


Fig. 3.5. For the derivation of the dependence of irradiance on the dimension characteristics of an optical system.

The elementary flux $d\Phi$ which falls on the entrance pupil within the limits of the solid angle $d\omega$ at angle i to the optical axis equals

$$d\Phi = B \Delta A \cos i d\omega. \quad (3.25)$$

Since $d\omega = \sin i di d\phi$, the total flux will equal

$$\Phi = \int_{i=0}^{i=\tau} \int_{\phi=0}^{\phi=2\pi} B \Delta A \sin i \cos i di d\phi. \quad (3.26)$$

Carrying the constant values B and ΔA outside the integral sign and performing the integration within the indicated limits, we obtain

$$\Phi = \pi B \Delta A \sin^2 u. \quad (3.27)$$

For the transition to the plane of the image we use the known [38] invariant $n l \sin u = n' l' \sin u'$ where l and l' are the linear dimensions of the corresponding elements of the object and its image, and n and n' the refraction indices of the environment before and after the system, respectively. Moreover, from geometric considerations, it is clear that $\Delta A' / \Delta A = l' / l^2$. Then

$$\Delta A \sin^2 u = \frac{n'^2}{n^2} \Delta A' \sin^2 u'.$$

Usually, $n' = n = 1$, therefore expression (3.27) takes the form

$$\Phi = \pi B \Delta A' \sin^2 u'.$$

In accordance with (3.13), flux Φ' which has passed through the optical system equals $\Phi' = \tau \Phi$; consequently

$$\Phi' = \pi B \tau \Delta A' \sin^2 u'. \quad (3.28)$$

The irradiance of the central area of the image will equal

$$E'_0 = \frac{\Phi'}{\Delta A'} = \pi B \tau \sin^2 u'. \quad (3.29)$$

The value $\sin^2 u'$ is called the numerical aperture of the optical system.

If the image is in the focal plane of the objective lens, which corresponds to the removal of the object at a distance equal to or greater than practical infinity, then, taking the condition $\sin u' \sim \tan u'$ for small values of angle u' and considering that ^{/49} for the objective lens its light diameter D_1 equals approximately the diameters of the entrance and exit pupils, we obtain

$$\sin u' \cong \frac{D_1}{2f'}.$$

Thus, the final relation for the calculation of irradiance in the center of the plane of the image takes the form

$$E'_0 = \frac{\pi B}{4} \tau \left(\frac{D_1}{f'} \right)^2 = \frac{\pi B}{4} H. \quad (3.30)$$

The obtained equation establishes the connection between the irradiance in the center of the image and the relative aperture of the system.

The irradiance decreases in proportion to removal toward the edges of the plane of the image. If an elementary radiation flux $d\Phi'$ which falls within the limits of solid angle $d\omega'_0$ on the central element $\Delta S'_0$ of plane P' of the image passes through element dm' of the plane of the exit pupil M' (Fig. 3.6) from (3.25) we have

$$d\Phi'_{\Delta A'_0} = B \Delta A'_0 d\omega'_0. \quad (3.31)$$

A flux which falls on such an area ΔA which is located on the edge of the plane of the image will accordingly equal

$$d\Phi'_{\Delta A'} = B \Delta A' \cos W' d\omega'. \quad (3.32)$$

Considering that $d\omega' = d\omega'_0 \cos^4 W'$ and $E' = \frac{d\Phi'}{\Delta A'}$,

we obtain

$$E'_{AA'} = E'_{AA_0} \cos^4 W. \quad (3.33)$$

(3.33)

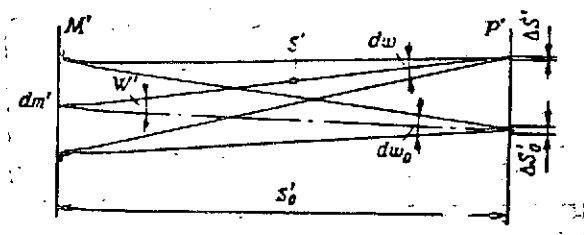


Fig. 3.6. For the derivation of the dependence of irradiance on the angle of slope of the pencil of rays.

This law of the change in irradiance over the plane of the image is valid for systems with small dimensions of the entrance pupil.

but also through all sections of the pupil of the system; therefore, attenuation of irradiance toward the edges of the image will be less intensive.

In regular optical systems /50 with relatively large entrance pupils, the irradiance of each element of the image is caused by radiation fluxes which pass not only through the center

3.5. Aberration Characteristics

In the consideration of dimensional and energy characteristics it was assumed that the optical system is ideal, i.e., in a specific scale it provides an image similar to the object without any distortions introduced by the system itself.

The images obtained with the use of real optical systems differ in geometric form, definition, and spectral composition from the images created by equivalent ideal systems.

These distortions or errors of images are also called aberrations. To estimate the character and magnitudes of aberrations, the corresponding aberration characteristics are used which are a measure of the evaluation of the quality of the optical system.

Aberration characteristics determine the relation between:

- the nature and amount of distortion of the image;
- the conditions for the passage of pencils of rays which create images through the system and the design parameters of the optical parts of the system.

In planning, this permits obtaining the optimum parameters of the optics which satisfy given requirements for image quality.

Depending on the nature of the arising of aberrations, they are divided into monochromatic and chromatic.

Monochromatic aberrations arise as a result of the difference in the conditions of the passage of rays of one wavelength or frequency through an optical system at various heights and at various angles relative to the optical axis. This type of aberrations causes a change in the geometric shape and dimensions of the image of points, lines, and planes.

Chromatic aberrations arise as a consequence of the dispersion of rays of various wavelengths or frequencies in the material of the optical parts. As a result of chromatic aberrations, the coloring of the image arises which leads to a worsening of its definition.

In designing or evaluating the quality of a specific model of electro-optical equipment, in order to consider the aberrations alone which are inherent to a given system, they are divided into axial and field. Axial aberrations arise with the image formation of points in the space of objects, for example stars, which are located 51 on the optical axis and cause the appearance of circles of confusion of a specific diameter instead of point images in the center of the image's plane. Axial aberrations are most dangerous for optical systems with small field-of-vision angles in which the object of analysis or recording is the central portion of the image plane, for example, in star-oriented electro-optical instruments, and so forth.

Field aberrations distort images of extra-axial points of the space of objects embraced by the solid angle of the field of view of the system.

To establish the connection with the parameters of the optical system and its parts, monochromatic aberrations are divided into five types: spherical, coma, astigmatism, curvature of the surface of the image, and distortion.

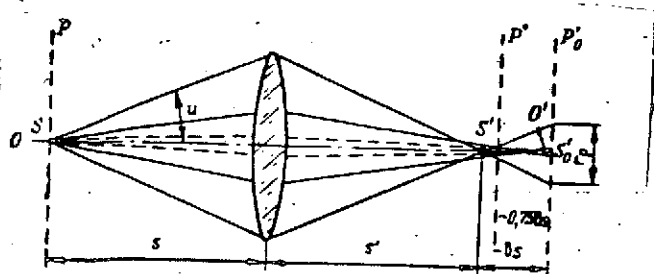


Fig. 3.7. Spherical or aperture aberration.

Spherical aberration (Fig. 3.7) arises with the incidence of a broad pencil on a lens, the rays of which emerge from point S of the object which lies on the $00'$ optical axis. As a result of the difference in the angles of incidence on the surface of the lens and the refraction conditions in it, the rays of the near-axis (shown by the dashed line) and broad pencils (shown by the solid lines) will intersect with the axis at different points S'_0 and S' . As a result

of spherical aberration, the image of point S will have the appearance of a circle of confusion whose diameter changes depending on the locus of the cross section of the pencil within limits of the segment $\delta s' = \overline{S_0' S'}$. The least diameter of $2\rho'$ will be in plane P' removed from plane P'_0 by a distance of approximately $0.75\delta s'$. Plane P' is called the plane of least scatter with which the attempt is made to match the surface of the radiation receiver in adjusting the optical system. The distance $\delta s'$ within the limits of which the points of intersection of the pencil with the axis of refracted rays are disposed is called the longitudinal spherical aberration. It is read from point S_0' ; therefore, for a positive lens (see Fig. 3.7), it has a minus sign. The value r_ρ is called the transverse spherical aberration. It is obvious that $r_\rho = \delta s' \tan u'$. With the removal of point S to distance $s = \infty$, plane P'_0 is matched with the back focal plane of the system and $s' = f'$. Then the value $\delta s' = \delta f'$ will characterize the error in the position of the focus F' and its dispersion depends on the change in angles u or u' . In accordance with the theory of monochromatic aberrations [43, 44], the value of the radius of the circle of confusion of a simple lens can be expressed approximately by the relation

$$r_0 \cong \frac{h^3}{f'^2} S_I, \quad (3.34)$$

where $S_I = \psi(r_i; n_i; d_i; S_i)$ is the coefficient of spherical aberration; $r_i; d_i$ and n_i are the radius of curvature, thickness, and refraction index of the lens material, respectively; s_i are relative spacings of the lens components; h is the height of the outmost ray equal to half the diameter of the entrance pupil.

Equation (3.34) shows that with given dimensional characteristics ($D_{entr.pup.} = \text{diameter of entrance pupil and } f'$) it is necessary to so select the design parameters of the parts of the system that, in reducing coefficient S_I , the required value of the radius of the circle of confusion is attained.

For a negative lens (Fig. 3.8a) and spherical mirror (Fig. 3.8b), the longitudinal spherical aberration has the reverse sign in comparison with the aberration of a positive lens since the focus F'_0 is displaced relative to F' in the direction from which the rays fall.

In calculating aspherical mirrors which have a parabolic or elliptical shape of reflecting surface, it is necessary to include in coefficient S_I (3.34) additional parameters which characterize the deviation of the mirror surface from a sphere. This permits the more successful elimination of spherical aberration in using aspherical mirrors. /53

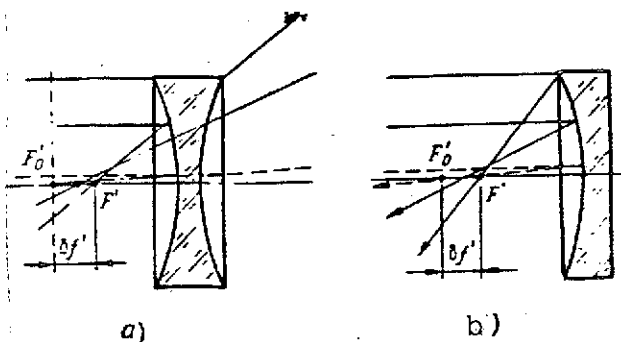


Fig. 3.8. Spherical aberrations. a. Negative lens. b. Spherical mirror.

The different signs of spherical aberration of positive and negative lenses and mirrors permit using the aberration compensation method, i.e., the components of the system are selected so that their aberrations are approximately equal in magnitude but have reverse signs.

Spherical aberration is evaluated by the amount of longitudinal spherical aberration $\delta f'$ or the circle of confusion r_0 and the curve for change in $\delta f'$ as a function of the height of incidence of the ray on the optical system (Fig. 3.9). To illustrate the method of compensation, presented on the chart are curves of aberrations of positive and negative lenses and the resulting curve which characterizes the residual aberration of a two-lens component.

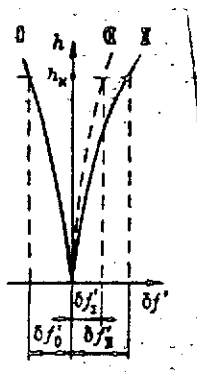


Fig. 3.9. Chart of the dependence of longitudinal spherical aberrations on the height of incidence of rays on the surface of a lens.

Just as in the case of spherical aberration, the reason for the arising of a coma (Fig. 3.10) is the different conditions for the incidence and refraction of the central (dashed line) and outermost (solid line) rays. As a result, the construction of a refracted pencil becomes asymmetrical and in plane P' , instead of the image of a point, a spot of scatter is created (with a shape like a drop) whose pointed end is elongated in a direction toward the edge of the plane of the image. Figure 3.10 shows a view of the plane of the image with the presence of a coma. Shown in the center is a circle of confusion $2\rho'$ caused by

spherical aberration. The coma is evaluated by the greatest longitudinal dimension of the scatter figure ($\delta g_k'$) and the coma chart. /54

The value of $\delta g_k'$ is connected with the dimensional characteristics and the design parameters of the system by the relationship [44]:

$$\delta g_k' = \frac{3h^2}{f'} \tan W_{STT} \quad (3.35)$$

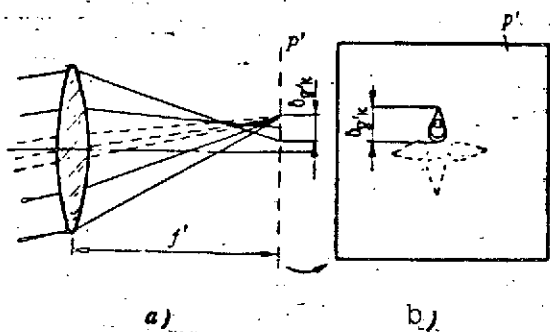


Fig. 3.10. Course of refracted coma worsens the quality along the edges of the image plane, especially in wide-angle systems. The value of a refracted pencil of rays. b. Image of extra-axial points with a coma.

where W is the angle of slope of the pencil to the optical axis of the system; S_{II} is the coefficient of the coma which depends on the design parameters and the mutual position of the optical parts.

This equation shows that the value of k' is equal or close to zero.

$$k' = \frac{h}{\sin u'} - f' \quad (3.36)$$

is called the measure of the coma k' . In the absence of a coma, $k' = 0$. Therefore, in designing optical systems, the parameters of their parts are calculated so that for all rays of inclined pencils, Eq. (3.36) is equal or close to zero. The diagram of the coma is constructed by analogy with the diagram of spherical aberration, but the value k' is laid off along the abscissa and the angle u' along the ordinate.

Astigmatism causes disruption of the symmetry of a pencil refracted by a lens or reflected by a mirror and inclined by the angle W whose rays lie in various planes which intersect along the axis of the pencil $O''O'''$. As a result of the astigmatism, the extra-axial points of the plane of the object (Fig. 3.11) are depicted in the form of two mutually perpendicular lines which lie across the $O''O'''$ axis of the refracted (reflected) pencil at a distance of $\delta s'_A = F'_M F'_S$.

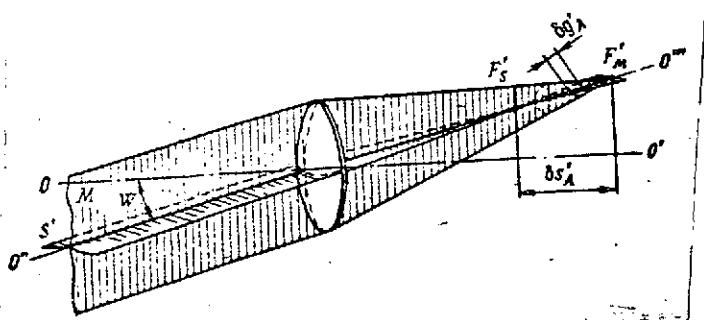


Fig. 3.11. Diagram of a refracted pencil of rays with the astigmatism aberration.

Astigmatism arises from the fact that the rays which lie in one plane, for example S , will be refracted (or reflected) when falling on a spherical surface differently from rays which lie in another plane, for example M , because of the difference in curvature of the cross sections formed where the surface of the sphere is intersected by these planes. Astigmatism is evaluated by the astigmatic difference $\delta s'_A$ and the transverse dimensions of the scatter figure $\delta g'_A$ formed by a point of the

object in the focal plane. For a simple lens, this value equals approximately $\delta g_A \approx \tan^2 W S_{III}$ where S_{III} is the astigmatism coefficient which depends on the design parameters of the system. Since astigmatism is a field aberration, its diagram (Fig. 3.12) is constructed depending on the angle of the field of view W . Curves X_S and X_M are the geometric locus of astigmatic foci F'_S and F'_M , and the distance between them along the horizontal characterizes the value $\delta s'_A = \psi(W)$.

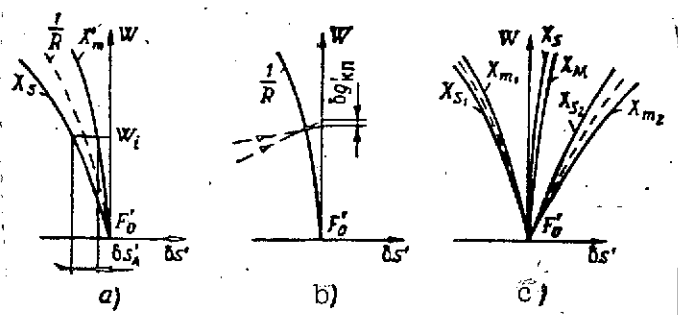


Fig. 3.12. Diagrams of aberrations inclined toward the axis of pencils of rays: a. astigmatism; b. surface curvature of image in elimination of astigmatism; c. diaphragm for a two-component optical system corrected for astigmatism and image surface curvature.

If the design parameters of the system are selected so as to eliminate astigmatism, i.e., $\delta s'_A = 0$, the aberration of the surface curvature arises, as a result of which the geometric locus of point images will be a surface with curvature $1/R$ (see Fig. 3.12b). As a result, instead of point images scatter diagrams $\delta g'_{\text{curv.surf.}}$ will be created on the plane surface of the radiation receiver matched with the focal plane. The value of $1/R$ can be found from the equation

$$\frac{1}{R} \approx \sum_{i=1}^k \frac{\varphi_i}{n_i}, \quad (3.37)$$

where φ_i are the optical powers of the system's components, and k is the number of components.

These two aberrations are eliminated simultaneously by selecting the characteristics of the components so that their astigmatic differences and curvature of the image mutually compensate each other (see Fig. 3.12c).

Dispersion causes distortion of the scale of the image as a result of the disruption of the constancy of the linear magnification over the plane of the image. As a result of the dispersion, the object, for example in the form of a square, is depicted in the form of a barrel-shape or pin-cushion shape. Since the amount of distortion is proportional to $\tan^3 W$, it is most dangerous for wide-angle lenses. The measure of distortion is the value:

$$V = \frac{\gamma_W - \gamma_0}{\gamma_0} = \frac{\Delta \gamma}{\gamma_0}, \quad (3.38)$$

where γ_0 and γ_W are the linear magnifications in the center and on the edge of the plane of the image, respectively.

The distortion diagram is constructed in the form of the relationship $V = \phi(W)$. Distortion is eliminated by methods of selecting parameters and mutual compensation.

Chromatic aberrations are divided into chromatic aberration of position and chromatism of magnification.

Chromatic aberration of position arises as a result of the dispersion of rays in the optical material of the lens. In this, the pencil of rays of complex spectral composition following the lens (Fig. 3.13) is separated into components and instead of one focus F' , a number of foci arise for rays of corresponding wavelengths. Since the refraction index of optical material is inversely proportional to the radiation wavelength, rays with the smallest

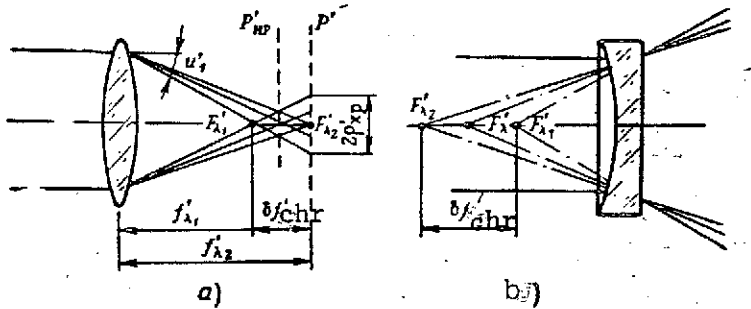


Fig. 3.13. Chromatic aberrations:
a. positive lens; b. negative lens.

wavelength are refracted most intensively and vice versa. If, for example, the spectrum of an incident pencil lies in the visible region, F'_{λ_1} will be the focus for violet rays, and F'_{λ_2} for longer-wave rays, i.e., red. This aberration is axial since it distorts the image in the center of the plane of images. /57

The distance $\delta f'_{chr} = F'_{\lambda_1} - F'_{\lambda_2}$ within the limits of which the foci are located and, consequently, also the corresponding focal planes of a chromatic pencil of rays is called the chromatic aberration of position. From the diagram of the path of the rays (see Fig. 3.13), it can be seen that

$$\delta f'_{chr} = f'_{\lambda_1} - f'_{\lambda_2}, \quad (3.39)$$

i.e., for positive lenses this value has a negative sign, and for negative lenses a positive sign.

The dependence of $\delta f'_{\text{chr}}$ on the dimensional and design parameters of the system is expressed by the equation [38]:

$$\delta f'_{\text{chr}} = -f'^2 \sum_{i=1}^{l-m} \left(\frac{h_i}{h_1} \right)^2 \frac{\varphi_i}{v_i}, \quad (3.40)$$

where h_i is the height of incidence of a ray on a given lens; v_i is the dispersion coefficient of the lens material; m is the number of lenses in the system.

The value of the dispersion coefficient is expressed by the formula

$$v = \frac{n-1}{dn}, \quad (3.41)$$

where $dn = n_{\lambda_1} - n_{\lambda_2}$ is the difference in the refraction indices of the optical material for the extreme wavelengths.

Accepting that $h_1 \approx h_2 = \dots = h_m$, from (3.40) we obtain

$$\delta f'_{\text{chr}} = -f'^2 \sum_{i=1}^m \frac{\varphi_i}{v_i}. \quad (3.42)$$

Thus, for the achromatization of the system, i.e., the elimination of the chromatism of the position of the focus, it is necessary to so select the optical materials and values of φ_i of the components that the sum

$$\sum_{i=1}^m \frac{\varphi_i}{v_i} = 0.$$

For example, the condition of complete achromatization for a two-lens objective consisting of a positive and negative lens will have the appearance

$$\frac{\varphi_1}{v_1} = -\frac{\varphi_2}{v_2}.$$

Chromatic aberration of position is often characterized by a circle of confusion $2\rho'_{\text{chr}}$ (see Fig. 3.13a) which arises in the plane of the image. The value of $2\rho'_{\text{chr}}$ depends on the position of the plane of the image within limits of $\delta f'_{\text{chr}}$ and has a minimum value in the plane P'_0 , called the plane of least scatter, equal to

$$2\rho'_{\text{chr min}} \approx 0.78 \delta f'_{\text{chr}} \log u'$$

In the alignment of the system with this plane, usually the surface of the radiation receiver is matched. With the use of a single photoresistor with a diameter of the operating surface of d_s as a receiver, the initial condition for achromatization will be $2\rho'_{chr} \leq d_s$. Substituting in (3.42) the value f' given by the technical specifications, and considering that $\tan u'$ depends on the relative aperture of the objective lens $\tan u' = D_{ob}/f'$, we obtain the achromatization condition

$$df'_{chr} = \frac{2\rho'_{chr} \min}{0,75 \tan u'} = \frac{2d_s f'}{0,75 D_{ob}} \text{ and } \sum_{i=1}^k \frac{\varphi_i}{v_i} = \frac{2d_s f'}{0,75 D_{ob}}$$

The diagram of chromatic aberration of position is constructed similar to the diagram of spherical aberration, but for values of wavelengths: two extreme λ_1, λ_2 and average λ . The distance along the horizontal between these curves provides the value of df'_{chr} as a function of the height of incidence of a ray on the lens. For objective lenses of photographic systems, the diagrams of chromatic aberration (Fig. 3.14) are constructed as the function $\delta f'_{chr} = \psi(\lambda)$, which provides the most graphic impression for evaluating the degree of achromatization.

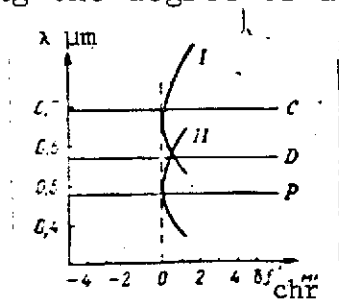


Fig. 3.14. Diagram of chromatic aberration depending on wavelength.

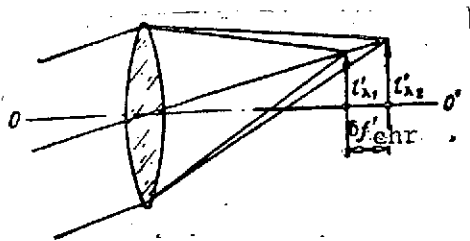


Fig. 3.15. Chromatic aberration of magnification.

With the transmission of the rays which go from extra-axial points (Fig. 3.15), as a result of dispersion, chromatism of magnification arises which consists of the fact that images l'_{λ_1} and l'_{λ_2} of object 1 have different magnification. This field chromatic aberration is also maintained in the case where chromatism of position is eliminated. Chromatism of magnification of an optical system is reduced by the appropriate selection of the types of optical materials and the design parameters of the parts of the system.

Monochromatic and chromatic aberrations also arise with the passage of convergent rays inclined toward the optical axis through prisms and plane-parallel plates. The basic parameter which influences the amount of aberration is the thickness d of the plate or prism. For example, the circle of confusion of a spherical (aperture) aberration equals

$$\delta g'_{\text{sph}} = \frac{d}{2} \left(\frac{n^2 - 1}{n^3} \right) \{g^3 W\},$$

where n' is the index of refraction of the material of the prism; W is the angle of slope to the axis of the pencil of rays.

In this case, the chromatic aberration of position equals

$$\delta f'_{\text{chr}} = d \left(\frac{n - 1}{n^2 v} \right).$$

Therefore, aberrations are considered only for prisms and plates having considerable thickness and standing in sloping, convergent, or divergent pencils of rays.

In addition to aberrations, the quality of image is also influenced by defects in the manufacture of optical parts and the precision of their placement in the design position. The basic criterion for estimating the quality of the image, which determines the requirements for residual aberrations and tolerances for manufacture and assembly, is the linear or angular resolution of the radiation receiver which operates with a given optical system. For example, if a single photoresistor or a mosaic of several with a specific diameter of the sensitive element is used as the receiver, the circle of confusion of allowable total aberration should have a smaller or equal diameter. Similar requirements are also put forth in the use of other receivers, for example photo materials where the limit of the dimensions of the circle of confusion is determined by the grain of the emulsion.

3.6. Transmission Characteristics of an Optical System

For the evaluation of the quality of optical systems of on-board electro-optical equipment, the method of space-frequency transmission functions is widely used. This method permits evaluating the resolution of an optical system depending on the degree and character of change in contrast properties, luminance, and other parameters of the object. /60

The quality of an image created by an optical system is determined in this case with the aid of special functions which

connect the contrast properties of the object and its image depending on the characteristics of the optical system.

Suppose that an object possessing a specific distribution of luminance over its surface is given by the function $B(x,y)$ (Fig. 3.16). The field of luminance of the object can be presented in the form of a set of sine functions, each of which is characterized by amplitude and spatial frequency, i. e., by a value inverse to the period of a given harmonic.

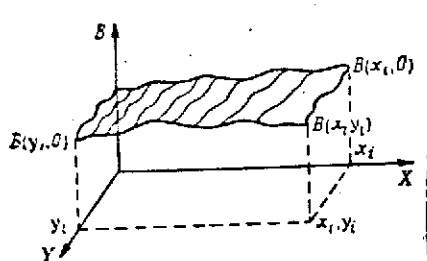


Fig. 3.16. Spatial distribution of luminance over the surface of an object.

In an ideal system, one point in the plane of the image with coordinates x, y will correspond to each point of the object with coordinates x_0, y_0 .

In actual systems, as a result of the influence of dispersion, monochromatic aberrations, and other reasons, the image of a point has the form of a scatter figure with a specific distribution of irradiance over its surface. This distribution is called the scattering function of a point or, after normalization, the function of the weight of the optical system. In this case, normalization consists of the fact that the integral of the scattering function $H(x',y')$ is equated to unity:

$$\iint_{-\infty}^{\infty} H(x', y') dx' dy' = 1. \quad (3.43)$$

If we accept that in the central portion of the plane of the image the scatter figure is determined only by axial aberrations and its form and dimensions change little, the image of any point of the object can be presented by the function $H(x' - \beta x_0, y' - \beta y_0)$ where β is the linear magnification of the system. Substituting $\beta x_0 = x$ and $\beta y_0 = y$, we obtain the expression for the scattering function within the limits of the section of the plane of the image $H(x-x, y'-y)$ considered.

In this, the distribution of irradiance $E(x', y')$ in the plane of the image will be expressed by the relation

$$E(x', y') = \iint_{-\infty}^{\infty} B(x, y) H(x' - x, y' - y) dx dy. \quad (3.44)$$

Thus, the resultant integral of the convolution of these two ^{/61} functions shows that the distribution of irradiance of the image with a given change in brightness of the object $B(x,y)$ is determined by the aggregate of the scattering functions of each point of the image.

Transformation of the Fourier function $E(x',y')$ permits obtaining the frequency spectrum $\varepsilon(v_1, v_2)$ of the distribution of the irradiance of the image:

$$\varepsilon(v_1, v_2) = \iint_{-\infty}^{\infty} E(x', y') e^{-2\pi i(x'v_1 + y'v_2)} dx' dy'. \quad (3.45)$$

In this expression, v_1 and v_2 are spatial frequencies along the X and Y axes, i.e.,

$$v_1 = \frac{1}{\xi} \text{ and } v_2 = \frac{1}{\eta}$$

where ξ and η are the periods of the first harmonics along the corresponding axes.

Substituting variables $X = x' - x$ and $Y = y' - y$ and transforming expression (3.45), we obtain

$$\begin{aligned} \varepsilon(v_1, v_2) = & \iint_{-\infty}^{\infty} B(x, y) e^{-2\pi i(xv_1 + yv_2)} dx dy \times \\ & \times \iint_{-\infty}^{\infty} H(X, Y) e^{-2\pi i(Xv_1 + Yv_2)} dX dY. \end{aligned} \quad (3.46)$$

Expression (3.46) shows that the frequency spectrum of the distribution of irradiance in the plane of the image equals the transformation of the Fourier function of the distribution of luminance of the object and the scattering function (weight function) of the optical system.

Introducing abbreviated designations for two terms of the right side, expression (3.46) can be rewritten in the form

$$\varepsilon(v_1, v_2) = b(v_1, v_2) h(v_1, v_2). \quad (3.47)$$

Function $b(v_1, v_2)$ is called the space-frequency characteristic (SFC) of the distribution of the object's luminance. The function $h(v_1, v_2)$, which determines the influence of the optical system on the change of the space-frequency spectrum of the object in the process of creation of the image, is called the complex space-frequency transmission function of the optical system.

From (3.47), it follows that the transmission function of an optical system can be obtained as the relation of frequency 62 spectra of irradiance of the image and the luminance of the object:

$$h(v_1, v_2) = \frac{\varepsilon(v_1, v_2)}{b(v_1, v_2)} \quad (3.48)$$

The determination of function $b(v_1, v_2)$ for actual objects and its calculation is a difficult task since a spatial spectrum should be selected as the object which would contain a set of all frequencies transmitted by the optical system. Therefore, one of the methods of calculating the transmission function of an optical system is the use of a point emitter which possesses the properties of a delta-function, the space-frequency characteristic of which is constant and equals

$$b(v_1, v_2) = 1$$

This means that the spectrum of such a source contains a set of all frequencies of the same amplitude. In this, the transmission function can be calculated or determined experimentally in the form

$$h(v_1, v_2) = \varepsilon_T(v_1, v_2), \quad (3.49)$$

where $\varepsilon_T(v_1, v_2)$ is the frequency spectrum of the distribution of irradiance in a scatter spot from the point source or a Fourier transform of the weight function.

Function $h(v_1, v_2)$ is complex. Its modulus $|h(v_1, v_2)|$ is called the modulation transmission function of the optical system.¹ The initial value for the determination of the modulation transmission function is the scattering function which characterizes the distribution of irradiance and the geometry of the circle of confusion in the form of which each point of the object is portrayed. This permits the most complete evaluation of the influence of dimensional, energy, and aberration characteristics of a given optical system on the quality of the image which it creates.

Let us present an example which shows the influence of the modulation transmission function on the change in the contrast-frequency spectrum. Suppose that the distribution of luminance over the plane of the object along the X axis has the form of a sine function with a constant component.

¹In the literature, this value is also called the amplitude-space-frequency characteristic (ASFC) or contrast-frequency characteristic.

$$B(x) = B_0 + B_1 \sin 2\pi v_1 x.$$

The modulation transmission function $h(v_1)$ is given by the graph (Fig. 3.17). If this function is normalized, i.e., the transmission factor for a constant component B_0 equals one, the distribution of irradiance in the plane of the image of the optical system will be expressed by the relation 763

$$E(x) = B_0 + h(v_1) B_1 \sin 2\pi v_1 x. \quad (3.50)$$

The contrast in the plane of the object k_0 and in the plane of the image k_1 is expressed by the known relationships

$$\begin{aligned} k_0 &= \frac{B_{\max} - B_{\min}}{B_{\max} + B_{\min}}; \\ k_1 &= \frac{E_{\max} - E_{\min}}{E_{\max} + E_{\min}}. \end{aligned} \quad (3.51)$$

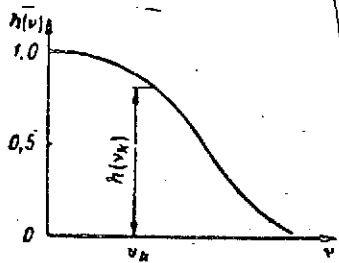


Fig. 3.17. Graph of the relation for the transmission function of an optical system.

Using expressions (3.50) and (3.51) and Fig. 3.18, we obtain

$$\begin{aligned} k_0 &= \frac{B_1}{B_0}; \\ k_1 &= \frac{B_1 h(v_1)}{B_0} \end{aligned}$$

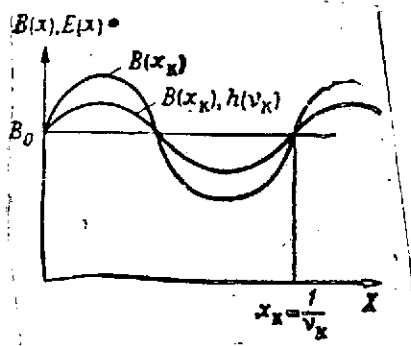


Fig. 3.18. Graph of the change in luminance or irradiance along the axis.

and consequently

$$v_1 = k_0 h(v_1) \quad (3.52)$$

Formula (3.52) was obtained for one spatial frequency. In the general form with consideration of the functional dependence of k_1 and k_0 on v_1 and v_2

$$k_1(v_1, v_2) = k_0(v_1, v_2) h(v_1, v_2). \quad (3.52a)$$

Thus, the image contrast can be determined knowing the contrast in the plane of the object and the value of the modulation transmission function of the optical system.

Optical systems are divided into several groups depending on the purpose, schematic diagram, and special features of the device.

If the change in the convergence of the pencil of rays which passes through the system is accomplished with the use of a lens, the system is called a lens system. A system in which spherical or aspherical mirrors are used for this purpose is called a mirror system. If parts with refracting or reflecting surfaces are used simultaneously in an optical system, i.e., lenses and mirrors, the system is called a mirror-lens system.

Depending on the magnitude and sign of the optical power, three groups of optical systems are distinguished: positive, negative, and afocal.

Positive systems which have an optical power greater than zero press the pencil of rays passing through the system toward the optical axis and create a real image of the object at the exit from the system. Objective lenses are typical examples of such systems. Negative systems which have an optical power less than zero deflect the pencils of rays which pass through them from the optical axis and create virtual images of the objects.

A virtual image can be constructed graphically (or analytically), extending the lines of direction of the rays which diverge after the negative system to their mutual intersection.

Negative systems are used individually only for the solution of particular problems, for example, to expand a cone of rays to fill the entire area of a radiation emitter. Usually, negative systems are connected with positive ones to compensate for aberrations.

Afocal optical systems are systems which have an optical power equal to zero, i.e., with an infinitely large focal length. Afocal systems do not change the form (convergence) of the pencils of rays which pass through them but, depending on the multiplicity factor, they accordingly increase or decrease their diameter and angle of slope to the axis. Typical examples of such systems are telescopic systems.

Depending on the purpose and schematic diagram, optical systems can be projection, telescopic, collimator, and so forth.

Projection optical systems create actual images of observed objects or emitters in the plane of the image with which the surface of the sensitive element of the radiation receiver is usually combined. The basic type of projection systems in on-board equipment of an artificial earth satellite and space ship are lens and mirror objectives.

Telescopic systems form the basis of all types of observation instruments including the sights of manned earth satellites. /65 Recently, telescopic systems have begun to be used to change the transverse cross section of laser rays in on-board optical location equipment.

Collimator systems serve for matching the image of scales, sights, or sighting markers with the field of view of the observation or photographic system. Collimators find wide employment in control-and-adjustment and checking equipment.

Besides the enumerated basic types of optical systems, other types of optical systems are also beginning to find application in the special instrumentation of artificial earth satellites and space ships, for example, of fiber optics, spectral optics, and so forth.

3.8. Lens Systems

Lens systems are divided into simple and compound. A simple system consists of two or three lenses. Compound systems often contain several dozen lenses. Lenses (Fig. 3.19) are usually distinguished by the shape of their refracting surfaces. Spherical, aspherical, and cylindrical lenses are employed most often. Because of the different curvature along the XX and YY axes, a cylindrical lens (Fig. 3.20) creates the image of a point object in the form of a line perpendicular to the plane of the cross section of greatest curvature.

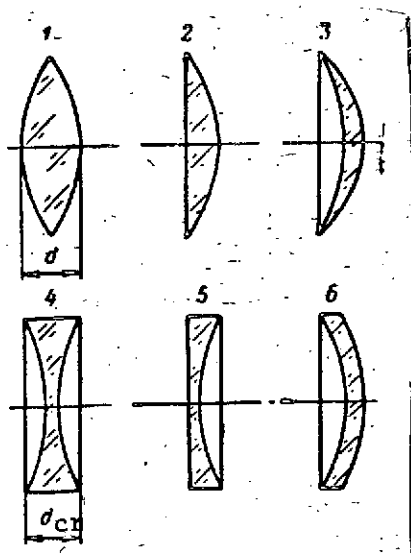


Fig. 3.19. Types of lenses.

In determining the parameters of a lens, at the first stage of the calculation its thickness is usually disregarded and the radii of curvature are calculated for a /66 so-called "thin" lens. After obtaining satisfactory results, the design and aberration characteristics are finally calculated with consideration of the thickness of the cylindrical lens.

A thin lens (Fig. 3.21) is characterized by five basic parameters: focal length, light diameter, two radii of curvature, and the refraction index of the optical material. Taking the thickness of the lens $d \approx 0$, we unambiguously give the position of its principal planes which coincide in this case

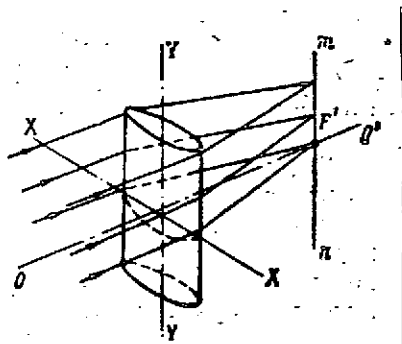


Fig. 3.20. Cylindrical lens.

with the apexes of the refracting surfaces.

From physical optics it is known that if a lens is in a homogeneous medium, for example in air, i.e., $n_1 = n_3 = 1$ and $n_2 = n$, then

$$\frac{1}{s'} - \frac{1}{s} = (n-1) \left(\frac{1}{r_1} - \frac{1}{r_2} \right), \quad (3.53)$$

where s' and s are the distances to the image and the object, respectively.

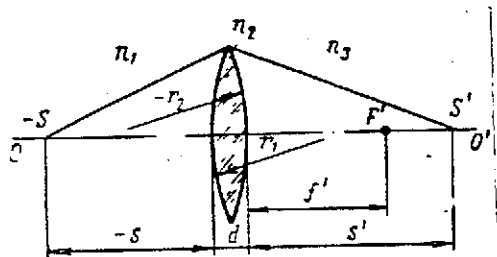


Fig. 3.21. For the derivation of the equation of a thin lens.

Equation (3.53) is called the equation of a thin lens. It permits determining the position of an image with known lens parameters or solving the inverse problem for the determination of the lens parameters depending on the required distance to the image plane. Setting $s = \infty$, Eq. (3.53) permits determining the focal length of the lens

$$\frac{1}{f'} = (n-1) \left(\frac{1}{r_1} - \frac{1}{r_2} \right)$$

or

$$f' = \frac{r_1 r_2}{(n-1)(r_2 - r_1)}.$$

(3.54)

With the equality of the refraction indices before and after the lens, the front and back focal lengths are equal but have different signs.

If we accept that air is in front of and behind the lens and ⁶⁷ the refraction index of the optical material of the lens equals n , then for the back focal length of the first surface f_1' and the front focal length of the second surface f_2 , we will have

$$f_1' = -\frac{nr_1}{n-1} \quad f_2 = \frac{nr_2}{n-1}.$$

Two refracting surfaces which limit the lens are located at distance d (see Fig. 3.21) from each other and comprise a complex system whose optical interval Δ , i.e., the distance between F_1' and F_2 with consideration of signs, will equal $\Delta = d + f_2 - f_1'$.

Substituting the values f_1' and f_2 , we obtain

$$\Delta = \frac{n(r_2 - r_1) + (n-1)d}{n-1}. \quad (3.55)$$

The focal length of a compound system will equal

$$f' = -\frac{f_1' f_2'}{\Delta} = -\frac{n r_1 r_2}{(n-1)[n(r_2 - r_1) + (n-1)d]}. \quad (3.56)$$

Expressing in (3.56) the radii of curvature $\rho_1 = 1/r_1$ and $\rho_2 = 1/r_2$, we find a simple formula for the optical power of a lens of finite thickness

$$\varphi = \frac{1}{f'} = (n-1)(\rho_1 - \rho_2) + \frac{(n-1)^2}{n} d \rho_1 \rho_2. \quad (3.57)$$

Calculation in accordance with the obtained formula provides the value of the optical power in diopters if the radii of curvature are expressed in meters.

Most often, the lens systems in electro-optical on-board ment accomplish the functions of objectives and condensers.

The objective is the lens system which, in the overall scheme of the instrument, is disposed closer to the object than the other lens parts and units. In accordance with the number of lenses, objectives are divided into two-lens (glued and unglued), three-lens, and multilens.

For a wide-angle objective, the main characteristic is the angle of the field of view (in some models, it equals $20.88 \cdot 10^{-2}$ rad or more). Wide-angle objectives are used in photographic and television cameras to obtain images of extended terrain sectors.

Wide-angle objectives have small focal lengths up to 200-300 mm with a relative aperture of no more than $1/3 - 1/4$.

Long-focus objectives possessing a small field-of-vision angle/68 ($8.7 \cdot 10^{-2} - 17.4 \cdot 10^{-2}$ rad) with a relative aperture less than $1/5 - 1/6$ form an image of an object with large linear magnification, which permits obtaining its small-scale image. According to design, long-focus objectives are divided into regular and telephoto. A regular long-focus lens objective has a length of housing which is approximately equal to its back focal length; therefore, with

the use of such an objective, the dimensions of the apparatus increase sharply. A telephoto objective, consisting of two lens components, positive and negative (Fig. 3.22), is distinguished by the fact that its back principal plane is moved forward, into the space of the objects; therefore, the length of its housing is two or three times shorter with the same focal length as with a similar long-focus objective.

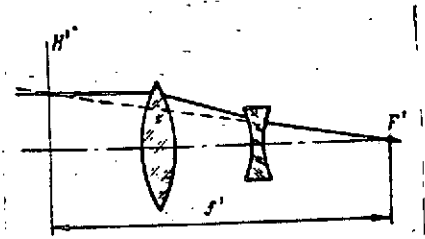


Fig. 3.22. Diagram of a telephoto lens.

The group of fast objectives is made up of compound multilens objectives having a relative aperture of at least $1/2 - 1/2.5$, i.e., possessing a large entrance pupil with comparatively small focal lengths.

In electro-optical equipment, where radiation flux modulators or screens installed in the back focal plane of the objective are employed, a condenser is usually located directly behind the focal plane of the objective in front of the receiver.

If the receiver is disposed at distance s' from the focal plane P' of the objective (Fig. 3.23a), with its transverse dimensions AB , a radiation flux will fall on its surfaces from element $\Delta s'$ of the image within the limits of solid angle $2u_0$. If a condenser with light diameter D_c is placed between the radiation source, in this case element $\Delta A'$, and the receiver, the solid angle of the effectively used radiation flux will be increased to value $2u$. (Fig. 3.22b). As a result, the irradiance of the surface of the receiver will be proportionally greater. Using expression (3.23) without consideration of losses in the condenser, i.e., $\tau \approx 0$, we obtain for the cases being considered the equations

$$F_0 = \pi B \Delta A \sin^2 u_0$$

$$F = \pi B \Delta A \sin^2 u$$

where B is the luminance of the element ΔA .

Since the irradiance is proportional to the relationship F/A_r where A_r is the area of the receiver, the degree of intensification of irradiance with the use of a condenser is determined by the relation

$$\frac{E}{E_0} = \frac{\sin^2 u}{\sin^2 u_0} \quad (3.58)$$

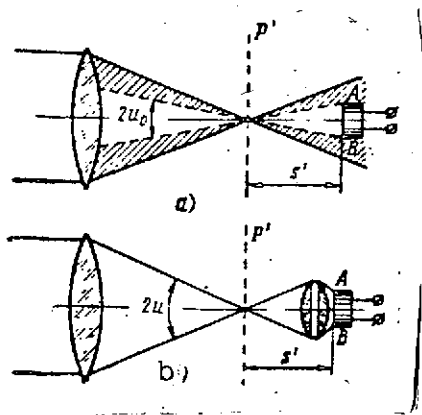


Fig. 3.23. Diagram of the path of rays: a. without condenser; b. with condenser.

A single-lens condenser provides a sufficiently uniform irradiance of small areas of the receiver with a size of aperture angle of $2u$ up to $60.9 \cdot 10^{-3} - 78.3 \cdot 10^{-3}$ rad ($35^\circ - 45^\circ$). A symmetrical two-lens condenser whose lens arrangement is shown in Fig. 3.23b is employed more often. Such a condenser permits obtaining an aperture angle up to $104.40 - 95.70$ rads ($55^\circ - 60^\circ$).

Lens systems are usually used in electro-optical equipment intended for operation in the visible region of the spectrum, since, in this case, optical glass can be used for the lens material.

3.9. Mirror and Mirror-Lens Systems

Mirror and mirror lens systems are usually used in electro-optical equipment as objectives. Their basic advantages over lens objectives with similar parameters are higher lens speed and the absence of chromatic aberrations at the mirrors which are the main optical parts of such systems. In addition, mirror objectives do not contain refracting parts; therefore, they are convenient for use in the infrared or ultraviolet regions of the spectrum. The shortcomings of mirror and mirror-lens systems which limit their employment are difficulty in manufacture, especially aspherical mirrors, increase in the construction dimensions and complication of adjustment in comparison with lens systems, and also the necessity of using protective glass for hermetic sealing in individual 70 cases.

The mirror objective (Fig. 3.24) consists of two mirrors, primary 1 and secondary 2. The light diameter of the primary mirror determines the relative aperture of the objective. The secondary mirror serves to change the convergence of a pencil of rays refracted by the primary mirror. The rear side of the secondary mirror diaphragms the area of the light aperture of the primary mirror; therefore, the area A_1 of the effective aperture of the objective is computed from the formula:

$$A_1 = \frac{\pi}{4} (D_1^2 - D_2^2).$$

where D_2 is the diameter of the secondary mirror.

In this, the speed of the mirror objective will equal

$$H = \tau_m q = \frac{\tau_m^2}{f'^2} (D_1^2 - D_2^2), \quad (3.59)$$

where τ_m is the coefficient which determines the value of the light flux reflected from the surface of the mirror; q is the relative aperture of the objective.

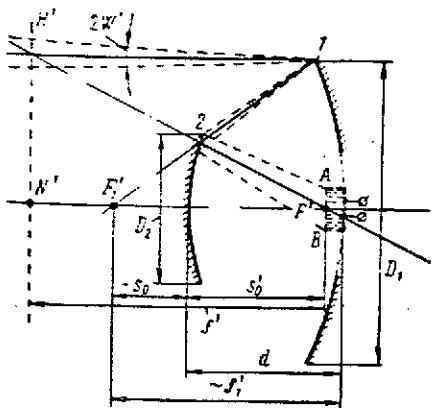


Fig. 3.24. Diagram of a mirror objective.

be found graphically by extending the line of direction of a ray which has passed through the objective to the intersection with the incident ray and constructing the back principal plane H' . Since segment $N'F' = f'$ and $N'K' = D_1/2$, then $f' = D_1/2 \tan u'$ where u' is the angle of the aperture ray with its optical axis after the objective. If the size of the secondary mirror is so selected that it does not cut off the aperture rays which have passed through the primary mirror, then in the absence of additional diaphragms, the plane of the entrance pupil coincides with the edges of the primary mirror, and its diameter $D_{entr.pup.} = D_1$. The angle of the field of view $2W$ depends on the focal length and the transverse cross section l of the field diaphragm. For example, if a photomultiplier, the diameter of whose photocathode is d_{pc} , is placed in the focal plane of the objective, the angle of the field of view of the instrument will equal

$$\tan W = \frac{d_{pc}}{2f'_1} \quad (3.60)$$

Since the primary principal plane of the objective is carried 71 out into the space of objects, the mirror objective is similar to a telephoto lens.

The shape of the surface and the curvature of the mirrors of the objective depend on the requirements for the size of the focal length and the residual aberrations. Since the spherical mirrors provide comparatively large values of residual aberrations, one of the mirrors is often made aspherical, in which regard an attempt is made to so calculate the parameters of the objective that the aberrations of the primary and secondary mirrors compensate each other.

The connection between the main parameters of the mirror objective is established with the use of two coefficients

$$\alpha = \frac{f_1'}{s_0} = \frac{\dot{R}_1}{2s_0} \approx \frac{h_1}{h_2}; \quad \zeta = \frac{s_0}{s_0'} \quad (3.61)$$

where h_1 and h_2 are the height of incidence of the ray on the primary and secondary mirrors respectively; R_1 is the radius of curvature of the mirror surface along the optical axis [22].

Geometrically, coefficient α determines the position of the secondary mirror relative to the primary one, and coefficient ζ the position of the back principal focus of the objective.

With the use of the well-known formula for focal length of a spherical mirror $f_1' = R_1/2$ from (3.61) and the expression for conjugate segments of a spherical mirror

$$s' = \frac{2R}{2s + R} - h^2 \frac{(s + R)^2}{R(2s + R)^2}$$

we find the equation for the determination of the radius of curvature of the secondary mirror

$$\dot{R}_2 = \frac{\dot{R}_1}{\alpha(\zeta - 1)} \quad (3.62)$$

The focal length of the objective will equal

$$f' = -f_1' \frac{s_0'}{s_0} = -\frac{f_1'}{\zeta} = \frac{\dot{R}_1}{2\alpha} \quad (3.63)$$

From geometric considerations, we find the size of the conjugate segments

$$s_0 = \frac{\dot{R}_1}{2\alpha} \quad \text{and} \quad s_0' = \frac{\dot{R}_1}{2\alpha\zeta}$$

The distance between the apexes of the mirrors will equal 72

$$d = \frac{\dot{R}_1}{2} \left(\frac{\alpha - 1}{\alpha} \right) \quad (3.64)$$

Telemagnification of the mirror objective $\gamma_T = f'/d$ is determined from expressions (3.63) and (3.64):

$$\gamma_T = \frac{R_1}{2\zeta} : \frac{R_1}{2} \left(\frac{\alpha-1}{\alpha} \right) = \frac{\alpha}{\zeta(\alpha-1)} \quad (3.65)$$

The value of coefficient α usually lies within limits of 3-4 with consideration of the sign for a given type of mirror objective. With $\alpha < 3$, the quality of the image worsens as a result of the increase in the iris action of the secondary mirror. The increase in α of more than 4 causes an increase in the dimensions of the secondary mirror and its aspherical quality with a given value of ζ . The coefficient ζ is usually within limits of 0.2-0.8. The relations presented above permit calculating all basic dimensional parameters of the objective. However, precise results are obtained only for the paraxial region and they will be approximate for wide pencils. The values of the obtained parameters are refined with consideration of the aspherical quality of the mirrors.

Besides axially symmetric mirror systems having one axis of symmetry which coincides with the optical axis of the system, extra-axial aspherical systems, for example parabolic systems, are beginning to find application in electro-optical equipment. Characteristic of them is the fact that the axis of symmetry, for example of a paraboloid of revolution, is located in space non-parallel with the optical axis of the system. This permits increasing the geometric relative aperture, changing the shape of the field of view giving it, for example, a concentric form, and varying the design outlines of the instrument being planned.

Mirror objectives usually have mirrors with an external reflecting layer applied to glass, metal, or plastic bases of the required form, which reduces losses to reflection and lowers the requirements for the precision of manufacture of the rear side of the base. Thin films of gold, chromium, aluminum, rhodium, and silver are used for the reflecting coatings. The selection of the coating depends on the band of the spectrum in which the objective should operate, on the design of the objective, and on the technology of its manufacture. The greatest reflection coefficient in the visible and near infrared regions of the spectrum is possessed by silver (about 96-98%); however, a polished silver surface darkens quickly. To eliminate the influence of atmospheric moisture, silver coats are protected by a thin layer of transparent protective film. Coatings of gold, aluminum, and chromium are more stable but the reflection coefficients of such layers are usually no more than 78-85% /73

To increase the reflection coefficient of the mirrors in the effective region of the spectrum, the protective films are applied to their surface in the form of two- or three-layer coatings, so

selecting the chemical composition and thickness of the film as to obtain the maximum spectral coefficient of reflection in a given region of the spectrum. This method is especially advantageous in objectives intended for operation in the infrared region of the spectrum in which additional filters are used to cut off visible radiation. Figure 3.25 shows a curve which characterizes the spectral coefficient of reflection of such a mirror covered with a four-layer film.

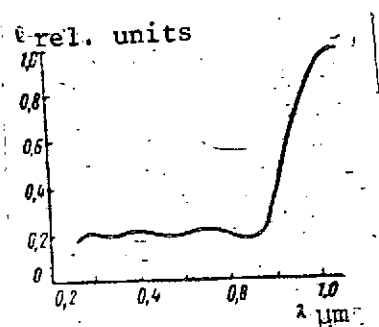


Fig. 3.25. Spectral coefficient of reflection of a mirror coated with a special film which absorbs the visible region of the spectrum.

An objective with such mirrors in the infrared region, beginning with 0.9-1.0 μm, does not require the employment of an additional filter since all radiations of the visible region are absorbed by the interference surface film.

The relative apertures of fast mirror objectives reach 1:1.1 - 1:0.8 with focal lengths of 150-180 mm. With a relative aperture of 1:1.4 and a focal length of about 600 mm, the mirror objective permits obtaining a magnification of 5x - 7x with a field of view of $(5.22-8.7 \cdot 10^{-2})$ rad (3-5°). Wide-angle mirror

objectives with a field of view of $69.6 \cdot 10^{-2}$ rad (40-50°) have focal lengths of about 50 mm, in which regard the diameters of the mirrors are usually: primary -- 200-220 mm and secondary -- 30-35 mm.

To protect the internal cavities and reflecting surfaces from the effect of the external environment, the mirror objectives should have protective glass. If the protective glass is flat, then in designing the objective only the increase in light losses by reflection and absorption in the glass are considered. If the design of the instrument requires the use of spherical or aspherical protective glass rather than flat glass, it is necessary to consider its influence on the dimensional and aberrational characteristics of the objective. In the latter case, the objective ceases to be purely mirror and is now a mirror-lens objective.

Mirror-lens systems are used if it is more advantageous, from the technological and economic points of view, not to use aspherical mirrors for the correction of aberrations of a two-mirror system but to introduce correction lenses in the objective, one of which can simultaneously accomplish the role of a protective glass.

Depending on the position and curvature of the mirrors, the ^{/74} objective may have different focal lengths. Relative apertures of such objectives reach 1:1.2 with an effective geometry aperture ratio up to 1:1.45. The field of view of mirror objectives usually does not exceed $17.4 \cdot 10^{-2} - 20.88 \cdot 10^{-2}$ rad ($10-12^\circ$).

In Maksutov's objectives, an achromatic meniscus having a positive spherical aberration capable of compensating for the negative aberration of two mirrors of the objective is used as the correction lens. In this case, these mirrors can have a spherical form. The secondary mirror can be built up on the central portion of the outermost surface of the meniscus, which provides the required sphericity in the process of preparation.

The basic dimensional parameters are determined with the use of a table [22], assigning the required value q and one of the design parameters, for example D_2 .

3.10. Systems with Fiber Optics

Fiber optics are parts and units of optical systems consisting of a large quantity of fine flexible fibers or threads of glass or another optical material transparent in a given band of the spectrum. Each fiber has a diameter on the order of several micrometers and is a light conductor over which radiation flux can be transmitted from only one element of the plane of the image with which the end of the fiber is matched. To transmit a group of elements or the entire image, the fibers (sometimes numbering up to 200,000-250,000 fibers) are assembled in a flexible bunched conductor, the diameter of whose end determines the size of the image or portion of space of the objective which can be transmitted to the radiation receiver or to any other portion of the optical system. The fibers can have a cylindrical or conical form. In the latter case, with the aid of the bunched conductor one can change the linear dimensions or the scale of the image and also concentrate the radiation flux falling on the end of the bunched conductor on a smaller area, increasing its irradiance. Dividing one of the ends of the bunched conductor, for example the exit end, into several parts, it is possible to include several radiation receivers in the optical system simultaneously or to collect on one receiver the radiation fluxes from various sections of the space of objects. Redistributing the fibers along the bunched conductor or changing the geometric form of its entrance and exit ends, one can change the geometric parameters, improve the quality of the image, and accomplish the coding and decoding of the transmitted information.

The operating principle of fiber optics (Fig. 3.26) is based on the use of the phenomenon of total internal reflection which arises with the passage of a radiation flux from an optically denser ^{/75}

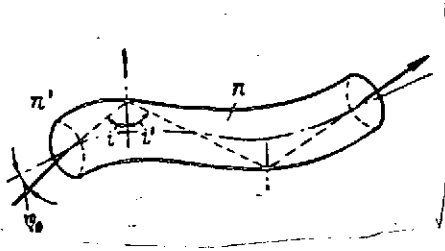


Fig. 3.26. Diagram of the path of a ray in an optical fiber.

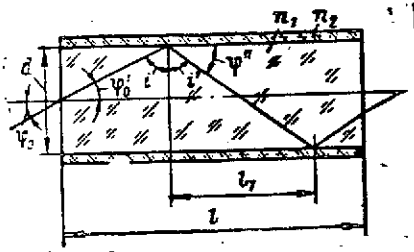


Fig. 3.27. Path of a ray in an optical fiber with a jacket.

medium to a less dense medium. The fiber (Fig. 3.27) is a transparent core with a smooth surface; therefore, the rays which have entered through one of the ends emerge through the opposite end after repeated reflections. In this, it is necessary that the angle of incidence i of each ray on the internal surface of the fiber wall be greater than the angle of total internal reflection i_0 . Using the invariant of refraction $n \sin i = n' \sin i'$ known from physical optics, we assume that the reflected ray can have the maximum angle $i' = 156.6$ rad (90°), i.e., it will go along the fiber wall; therefore, $\sin i = \sin i_0 = n'/n$.

If the material for the fiber is glass with a refraction index $n \sim 1.5$, then accepting $n' = 1$ for air we obtain $i_0 \sim 71.34$ rad ($41^\circ 48'$). The value of the angle of incidence $i \geq i_0$ determines the degree of permissible bending of the fiber in the bunched conductor and the greatest aperture angle ϕ_0 of a pencil of rays which passes through a fiber of the bunched conductor with total internal reflection.

With the close packing of the fibers in the bunched conductor, optical contact arises between their outer surfaces in a number of places, and a portion of the rays of the pencil which is passing through the fiber may land in other fibers and be scattered in the bunched conductor.

Therefore, the surface of each fiber is covered with a jacket of another optical material with a smaller refraction index.

The maximum value of angle ϕ_0 can be found from the following considerations. Since

$$\sin \varphi_0 = \sin \varphi'_0 \frac{n_1}{n_0} = \sin \varphi'_0 n_1,$$

where $n_0=1$ is the refraction index of the air, and considering that $\sin \phi'_0 = \cos i_1$ and $\sin i_1 = n_2 - n_1$, we obtain

$$\cos i_1 = \frac{\sqrt{n_1^2 - n_2^2}}{n_1};$$

/76

$$\sin \varphi_0 = \sqrt{n_1^2 - n_2^2}$$

and finally

$$\varphi_0 = \arcsin \sqrt{n_1^2 - n_2^2}.$$

(3.66)

Using glass of the flint type for the fiber ($n \sim 1.7$) and a jacket of glass ($n \sim 1.5$), we obtain $\phi_0 \sim 92.22 \cdot 10^{-2}$ rad (53°).

As a result of repeated reflections, path L of a ray in a fiber is considerably greater than its length l :

$$L = \frac{l}{\cos \varphi_0} = l \sec \varphi_0.$$

The number m of reflections of the ray from the internal surface of the fiber depending on its length l and the maximum angle of incidence of the rays on the end is determined by the equation

$$m = \frac{l}{l_1} = \frac{l}{d} \operatorname{tg} \varphi_0 = \frac{l}{d} \operatorname{tg} [\arcsin (\sqrt{n_1^2 - n_2^2})].$$

(3.67)

Thus, with $l = 280$ mm, $d = 0.7$, $n_1 = 1.7$ and $n_2 = 1.5$, the value of m is ≈ 2000 . The number of reflections of the rays of the pencil from the internal surface of the fibers, even with a not very long length, may be fairly high. Therefore, very high demands are made on the quality of fiber surface. To increase the resolution, an attempt is made to make the number of fibers in the bunched conductor maximum; however, a reduction in the diameter of fibers less than $2\text{--}5 \mu\text{m}$ leads to the appearance of diffraction which causes the scattering of light energy in the bunched conductor.

The basic parameter which determines the effectiveness of employment of fiber optics is the light transmission coefficient. Its value depends on the degree of absorption of radiation energy during reflection from the fiber walls, absorption and scatter in the fiber material, losses to reflection during refraction on the ends, and on the density of filling of the cross-sectional

area of the bunched conductor with fibers. With consideration of expressions (3.21) and (3.22), the general formula for calculating the transmission coefficient has the form

$$\tau = (1 - \rho)^2 (1 - \rho_\alpha)^m e^{-\alpha L} k_f$$

where ρ is the coefficient of reflection from one surface of the end; ρ_α is the coefficient of losses in reflection from the fiber walls; α , the coefficient of absorption in the fiber per unit of optical length; and k_f is the coefficient of filling, considering the effective cross-sectional area of the bunched conductor.

The values of coefficients α and ρ are determined by the optical material of the fibers. The value ρ_α depends on the refraction index and the quality of manufacture of the fiber and its jacket. The filling coefficient is calculated depending on the shape of the cross section of the bunched conductor and the scheme for packing the fibers. Its approximate value equals $k_f \approx (0.8-0.9)(D_1/D)$, where D_1 is the light diameter of the fiber and D is the diameter of its jacket. In practice, we can consider $k \approx 0.73-0.80$. For a glass fiber bunched conductor 1500 mm long with a cross-sectional diameter of 30 mm, with the number of fibers $1 \cdot 10^7$ with a diameter of 2.5 μm , the specific coefficient of light transmission will equal $\tau = 0.15(1/\text{m})$. In the manufacture of fibers from optically denser materials which are used, for example, for the infrared region of the spectrum, radiation energy losses will be even greater.

For the visible region of the spectrum, fibers are made of optical glass of the crown grade ($n \approx 1.55$) with a jacket of flint ($n \approx 1.7$). For the infrared region of the spectrum, the fibers are made from special grades of glass and also from some artificial crystalline materials and optical plastics.

In electro-optical equipment, fiber optics are used for the accomplishment of the following tasks:

-- For the concentration of the radiation flux from different objects (or different sections of the field of view) on one receiver and, conversely, from one object on a number of receivers;

-- For the transmission of an image or energy of radiation flux between those sections of the optical system of an instrument which cannot be connected with the use of regular optical methods;

-- For the discrete or continuous change of the entrance and exit pupils of an optical system;

-- For the transformation of the geometric form of an image without violating the principle of operation of the system and without lowering its resolution;

-- For the coupling on non-planar, for example, spherical surfaces of photocathodes of photoemission radiation receivers with the image plane of the preceding optical system, and so forth.

3.11. Optical Systems of Equipment with a Laser

One of the new and rapidly developing directions is systems with lasers. They are beginning to find application as optical locators, rangefinders, and other devices which assure the precise determination of relative values of velocity, linear and angular coordinates, rendezvous or docking of space ships, altimeters for determination of the distance to the earth or planets, and in communication and signaling systems. Regardless of the purpose, the basic elements of the block diagram of such systems are the transmitter and receiver. A laser ray of a transmitter, after reflection from an object or directly, should be received by the receiver. To increase the operating range and raise the precision of the measurements, it is necessary that the aperture angle of the laser beam of the transmitter be as small as possible. In receivers, it is necessary to assure the capture of the maximum portion of the incident flux of radiation energy and concentrate it on the surface of the receiver's sensitive element. 778

Special optical systems serve for the solution of tasks on the formation of a laser beam and its reception. They can be divided into two basic groups: systems which serve to reduce the divergence of the beam and systems which increase the surface density.

In the general case, optical system L located at distance l from end AB of the laser emitter (Fig. 3.28) converts the pencil of rays falling on it at an angle of $2u$ into a converging, parallel, or diverging pencil. In the first case, the rays of the pencil are focused in plane P' with which the surface of the irradiated object or radiation receiver is matched. The degree of convergence of the entire pencil is determined by the value of the angle $2W'$, and the irradiance at each point of the plane P' by the angle $2u'$. For optical systems of the first group, the angle $2W'$ should be reduced to the minimum. For systems of the second group, the basic task is increasing angle $2u'$.

The basic relations which show the influence of the parameters of an optical system on the shape of a pencil of rays and the irradiance which it creates are determined on the basis of general dimensional characteristics (see Section 3.2). Accepting that in plane P' image A'B' of emitter end AB is created, with consideration 779

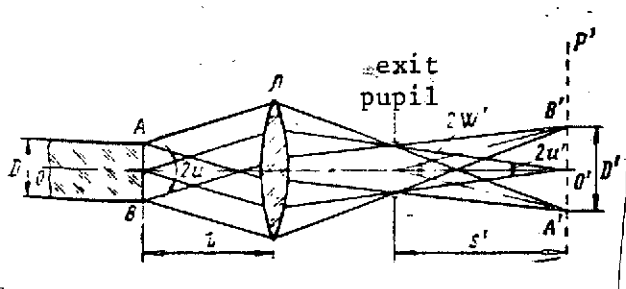


Fig. 3.28. Diagram of the influence of an optical system L on the path of laser rays.

condition $s' \gg d_{\text{exit pup.}}$. In this case,

$$\frac{D'}{2s'} d_{\text{exit pup.}} = D \tan u$$

or

$$d_{\text{exit pup.}} = \frac{2s' D \tan u}{D'} \quad (3.68)$$

Angle W' is determined from the expression

$$\tan W' = \frac{D'}{2s'} = \frac{D}{2s'} \beta.$$

To obtain a diverging pencil $D' > d_{\text{exit pup.}}$, converging pencil $D' < d_{\text{exit pup.}}$, and parallel pencil $D' = d_{\text{exit pup.}}$, we determine the linear or angular magnification, dimensions of the pupils, and other parameters of the system depending on the distance to the object (receiver) and the dimensions of the laser emitter.

Typical examples of systems of the first group are mirror (Fig. 3.29a) and lens (Fig. 3.29b) telescopic systems in which the back focus F'_1 of the first component 1 is matched with the front focus F_2 of the second component 2 and the distance $F'_1 F_2 = \Delta$ (optical interval) equals zero. Therefore, in accordance with (3.4), the focal lengths of the system will equal infinity and the system is afocal. If a pencil whose rays are parallel falls on one of the components of the system, then the beam leaving the system is also of parallel rays with diameter $D_{\text{exit}} = G D_{\text{entr.}}$, where $D_{\text{entr.}}$ is the diameter of the incident pencil. A reduction in the angle of divergence of the laser rays is also determined by an increase in G of the system and is connected

of (3.1) and (3.3), we obtain

$$\beta = \frac{D'}{D} = \frac{\tan u}{\tan u'}.$$

For the central portion of the pencil $\tan u' =$

$$= \frac{d_{\text{exit pup.}}}{2s'}. \quad \text{For the out-}$$

most rays, this is approximately valid under the con-

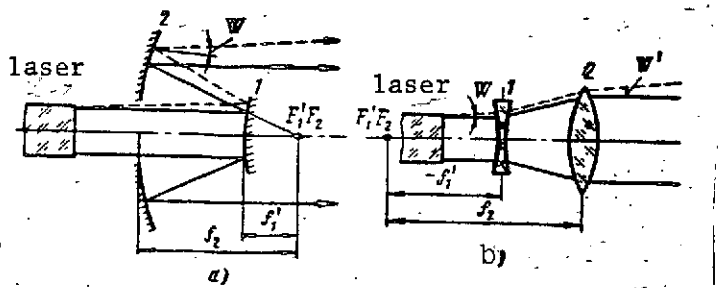


Fig. 3.29. Diagrams of optical systems employed to reduce the divergence of a pencil of laser rays: a. mirror; b. lens.

required parameters of the equipment. Mirror systems are more suitable for the infrared region of the spectrum, but they iris the central portion of the pencil. Lens systems preserve it but increase losses of radiation energy in the glass.

Condensers are used as systems of the second group. Fast mirror or lens objectives are used in receivers.

3.12. Optical Filters

Optical filters in electro-optical equipment serve to attenuate or change the spectral composition of a radiation flux to reduce the hindering influence of backgrounds and provide the best conditions for distinguishing the signal from the object.

In accordance with the nature of influence on the passing radiation flux, filters are divided into neutral and selective. Neutral or gray filters attenuate the intensity of the radiation flux without changing its spectral composition. Selective filters serve to change the spectral distribution of energy of the radiation flux, segregating a specific band of its spectrum by the absorption, reflection, or the scattering of the energy of the remaining sections (bands) of the spectrum.

Depending on the width of the transmission band, selective filters are divided into broad-band, narrow-band and monochromatic (interference) types. The latter group of filters is typical of an extremely narrow transmission band, on the order of tens of angstroms, which is attained by the use of the phenomenon of the interference of monochromatic rays on the interface of the filter layers.

with the focal length of its components by the relation

$$\tan W' = \frac{\tan W}{\Gamma} = \frac{\tan W f_1}{f_2}$$

Usually, in telescopic systems of this type magnification $G = 3x - 4x$, which permits reducing accordingly the angle of divergence of the laser beam.

The selection of one system or another is determined depending on the

According to design, optical filters can be solid, powder, liquid, and gaseous. Solid filters are made of colored glass, optical crystals, or films. The material of the filter and its thickness determine the optical properties of the filter. Powder filters are made by the deposition of thin layers of metals, for example germanium, selenium, and others, or metal oxides on bases which are transparent in a given band of the spectrum. In a number of cases, such filters are applied directly to the surface of the optical parts of the equipment. /81

Liquid and gaseous filters in the form of a vessel with an absorbing substance are usually used in laboratory practice.

The basic characteristics of a filter are the general or integral transmission coefficient, its spectral distribution, i.e., the spectral or spectrophotometric characteristic of the filter, and also its geometric and design parameters. For a more detailed evaluation of the quality of a filter, in some cases such values as optical density, effective transmission coefficients, effective width of transmission band, gradient of spectral characteristic, and so forth are also used.

A general or integral transmission characteristic equals

$$\tau = \frac{\Phi_e}{\Phi_0} = e^{-\alpha l}.$$

The value of the coefficient α for neutral filters depends on the physical properties of the filter material, for example the concentration of dye, heat losses, and scatter of radiation energy in the filter but it remains constant for a given filter in the effective band of wavelengths. For selective filters, this value is a function of the wavelength.

The spectral transmission coefficients τ_λ are the ratio of the monochromatic fluxes $d\Phi_{\tau_\lambda}$ and $d\Phi_{0_\lambda}$ in the spectral section $\Delta\lambda$:

$$\tau_\lambda = \frac{d\Phi_{\tau_\lambda}}{d\Phi_{0_\lambda}}.$$

The connection between the general and spectral transmission coefficients with consideration of the spectral distribution of the flux Φ_λ is expressed by relation (3.15). In calculations of electro-optical systems, to consider the degree of use, by the receiver, of the radiation flux transmitted by the filter, instead of the general transmission coefficient its effective value is used:

$$\tau_{\text{eff}} = \frac{\int_0^{\infty} \Phi_{\lambda} S_{\lambda} \tau_{\lambda} d\lambda}{\int_0^{\infty} \Phi_{\lambda} S_{\lambda} d\lambda}, \quad (3.69)$$

where S_{λ} is the spectral sensitivity of the receiver.

For instruments in which the eye is the radiation receiver, ^{/82} the values of spectral sensitivity of the eye V_{λ} are substituted in place of the value S_{λ} in formula (3.69).

Filters which are used in photographic equipment are usually evaluated from the value of the optical density d which is expressed by the relation

$$D = \log \frac{1}{\tau} = \log \tau \quad (3.70)$$

In this, the spectral optical density will equal accordingly

$$D_{\lambda} = \log \frac{1}{\tau_{\lambda}}$$

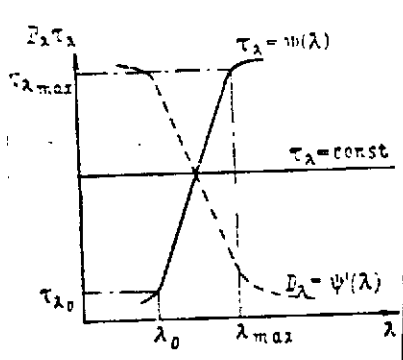


Fig. 3.30. Spectral or spectrophotometric characteristics of an optical filter.

A more detailed analysis of the properties of a filter can be conducted from its spectral characteristic by the determination of such of its parameters as gradient, and width of transmission band and boundary and maximum values of the spectral transmission coefficient. The gradient of spectral characteristic (Fig. 3.30) is determined by the tangent of

the angle of slope of the initial (final) section of the curve within limits from λ_0 to λ_{\max} which corresponds to the largest value of transmission coefficient $\tau_{\lambda \max}$ or by the ratio $\Delta\lambda/\lambda_0$ where $\Delta\lambda = \lambda_{\max} - \lambda_0$ is the width of the transmission band. The maximum wavelength λ_0 is considered to be that at which the transmission coefficient $\tau_{\lambda 0} = a\tau_{\lambda \max}$. The value of coefficient a is given depending on the purpose of the filter, for example, 0.4-0.5 for photographic systems, 0.1-0.05 for electro-optical equipment, and so on.

4.1. Purpose and Classification

Elements and devices which react to the influence of a radiation flux are called radiation flux receivers or indicators.

The radiation energy which falls on a receiver is converted to some other type of energy: electrical, thermal, energy of chemical processes, and so forth. Depending on the character of the physical processes which occur in the receivers during the conversion of the energy, they are divided into the following basic groups: photoelectric, thermal, optical-acoustical, photochemical, luminescent, and others.

Photoelectrical and thermal radiation flux receivers find widest employment in electro-optical equipment.

Photoelectric receivers possess selective radiation absorption and, consequently, selective sensitivity to radiation with different wavelengths. With receivers of this group, the magnitude of the absorbed radiation flux can be estimated either from the change in electrical conductivity of the material of the sensitive layer or from the value of the photocurrent or photoemf.

The photoelectric action of radiation can be manifested in various ways.

If electrons are emitted into a vacuum from a substance under the influence of an absorbed radiation flux, a photoemissive effect occurs. With a photoemissive effect, the radiation energy absorbed by the sensitive layer is imparted to the electrons of the substance. A portion of them overcome the forces within the substance which are restraining them and, leaving the substance, they form a flux of free charges in the vacuum.

The internal excitation of the crystal lattice of the semiconductor material under the action of the absorbed radiation flux which causes the conversion of the electrons from bound states to free states without escaping to the outside is called the photoconductive effect.

The appearance of free charges capable of moving within a solid leads to a change in the electrical conductivity of the material of the sensitive layer. The photocells which are based on photoconductivity, i. e., on a change in electrical conductivity under the influence of an incident radiation flux, are called photoresistors.

The phenomenon of photoconduction arises in systems consisting of two different contacting substances (metal-semiconductor, two semiconductors) and causes the initiation of a photo-emf on the boundaries of the system with the irradiation of the contact region. This phenomenon of photoconduction is known as the barrier-layer photoeffect. The photocells which are based on the phenomenon of the formation of a photo-emf on the boundary of two substances are called barrier-layer cells or photocells with a barrier layer. The photocurrent in the circuit of the barrier-layer cells arises in the absence of an external supply voltage.

If semiconductors with different types of conductivity are used as the contacting substances in the barrier-layer cell, then along with the arising of the difference in potentials between the layers with p and n conductivity, a difference in potentials is formed along the p-n junction. This photo-emf is called longitudinal or lateral. Photocells based on the use of a longitudinal photo-emf are called photocells with a longitudinal or lateral photoelectric effect. A longitudinal photoelectric effect is manifested only with the uneven illumination of the sensitive layer. In this regard, the phenomenon of a regular transverse photoelectric effect is also observed in photocells with a longitudinal photoelectric effect. /84

Barrier-layer cells on the base of electron-hole junctions which operate with the application of an external voltage are called photodiodes.

Moreover, devices similar to photodiodes but possessing the property of internal amplification of photocurrent can be receivers of radiation flux. They are called phototriodes or phototransistors.

Thermal receivers of radiation flux react to an increase in the temperature of the sensitive layer and require thermal equilibrium with each measurement. In this group of receivers, the energy of the quanta of incident radiation is distributed between all particles of the substance of the sensitive layer uniformly.

Therefore, as a rule, they possess nonselective sensitivity, i.e., they react equally to the radiation of all wavelengths. The heating of a sensitive layer is detected from generation of a thermoelectromotive force in the thermoelements and from the change in resistance in the bolometers and thermistors which are part of the group of thermal receivers.

4.2 Basic Characteristics of Receivers

The following characteristics are used to evaluate the technical properties and effectiveness of radiation flux receivers:

- Spectral sensitivity;
- Integral sensitivity;
- Sensitivity to current and voltage (spectral and integral);
- Utilization factor;
- Threshold flux or detecting capability;
- Quantum effectiveness;
- Quantum threshold sensitivity;
- Time constant;
- Frequency-response curve;
- Energy (light) characteristic;
- Voltage or current-voltage characteristics;
- Temperature characteristics.

Any characteristic of sensitivity is estimated from the value of the receiver's reaction to a monochromatic or complex radiation flux.

If a reaction is evaluated from the change in some parameter ^{/85} of the receiver with a change in the value of the incident flux, integral or spectral sensitivity of the receiver is obtained. For example, one can use the change in relative resistance caused by a change in the value of the incident radiation flux as such a parameter. However, integral and spectral sensitivity in such a treatment for a practical evaluation of radiation flux receivers has not yet received wide dissemination.

In the majority of cases, integral or spectral sensitivity is used (sensitivity to current or voltage). In accordance with these characteristics, the reaction of the receivers is evaluated as applicable to an actual connection scheme from the magnitude of the electrical signal (voltage or current) on the output of the receiver which is caused by the radiation flux which has fallen on it.

The spectral sensitivity equals

$$S_{\lambda} = \frac{dU_{\lambda}}{d\Phi_{\lambda}} \quad (4.1)$$

where dU_{λ} is the reaction of the receiver caused by the monochromatic radiation flux $d\Phi_{\lambda}$ falling on it.

With many radiation flux receivers, the value of S_{λ} changes depending on the wavelength λ and attains its greatest value at

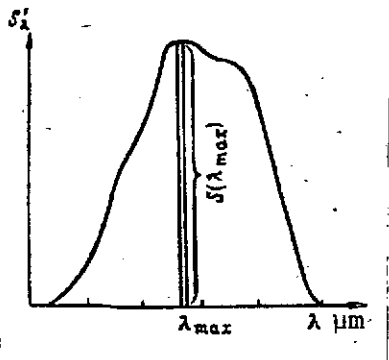


Fig. 4.1. For the determination of spectral sensitivity of radiation receivers.

some specific wavelength λ_{\max} , called the wavelength of maximum sensitivity (Fig. 4.1).

The concept of spectral sensitivity is completely clear and simple, but its measurement presents certain difficulties. Therefore, instead of spectral sensitivity use is made of relative spectral sensitivity $s(\lambda)$, which is the ratio of the function S_λ to its maximum value $S_{\lambda\max}$:

$$s(\lambda) = \frac{S_\lambda}{S_{\lambda\max}}. \quad (4.2)$$

With the presence of several maximums with the function S_λ , the ordinate of the largest of them is arbitrarily taken as unity.

The relative spectral sensitivity $s(\lambda)$ is the spectral characteristic of the receivers and is usually presented in the form of graphs from which one can judge the applicability of a given receiver for operation with one or another radiation source. However, the graphs permit evaluation only of the spectrum in which the receiver under consideration may be used.

/86

The integral sensitivity of the receiver S is the measure of its reaction to a complex radiation flux and is determined as the relation

$$S = \frac{U}{\Phi}, \quad (4.3)$$

where U is the reaction of the receiver to the complex radiation flux Φ . A fully specific connection exists between spectral and integral sensitivities. From formula (4.1), we have

$$dU_\lambda = S_\lambda d\Phi_\lambda,$$

whence, with consideration of the equality $d\Phi_\lambda = \Phi(\lambda)d\lambda$, we obtain

$$dU_{\lambda} = S_{\lambda} \phi(\lambda) d\lambda \quad (4.4)$$

This relation permits calculating the value of the reaction of the receiver to a monochromatic radiation flux. For a complex radiation flux, the value of the reaction is determined by integration of expression (4.4) for the entire spectrum

$$U = \int_{\lambda} dU_{\lambda} = \int_0^{\infty} \phi(\lambda) S_{\lambda} d\lambda \quad (4.5)$$

Since on the basis of (4.2) $S_{\lambda} = s(\lambda) S_{\lambda \max}$, from (4.5), we have

$$U = S_{\lambda \max} \int_0^{\infty} \phi(\lambda) s(\lambda) d\lambda \quad (4.6)$$

On the other hand, since $d\Phi_{\lambda} = \phi(\lambda) d\lambda$, then $\Phi = \int_0^{\infty} \phi(\lambda) d\lambda$.

Substituting the found values for U and Φ in formula (4.3), we obtain

$$S = \frac{\int_0^{\infty} \phi(\lambda) S_{\lambda} d\lambda}{\int_0^{\infty} \phi(\lambda) d\lambda} = S_{\lambda \max} \frac{\int_0^{\infty} \phi(\lambda) s(\lambda) d\lambda}{\int_0^{\infty} \phi(\lambda) d\lambda} \quad (4.7)$$

The integral of the numerator of expression (4.7) is that value of a complex flux which falls on the receiver which, with the sensitivity of the receiver constant for the entire spectrum and equal to its maximum value, would cause on its output such a signal as the entire complex radiation flux which falls on it causes with real spectral sensitivity. This value has received the name of effective (for a given receiver) radiation flux and is designated Φ_{eff} (Fig. 4.2):

$$\Phi_{\text{eff}} = \int_0^{\infty} \phi(\lambda) s(\lambda) d\lambda \quad (4.8)$$

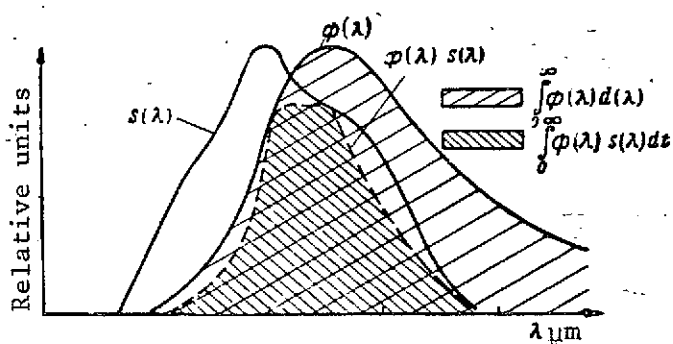


Fig. 4.2. For the concept of the effective radiation flux for a given receiver.

The integral of the denominator is the entire complex flux which falls on the radiation receiver.

From formula (4.7), it can be seen that the integral sensitivity of a receiver depends on the character of the function of the spectral density of the flux $\phi(\lambda)$ of the emitter. Consequently, the integral sensitivity depends not only on the

properties of the receiver but also on the radiation characteristics of the object. Therefore, along with the value of integral sensitivity, the parameters of the emitter from which the sensitivity was determined are indicated.

In this case, the characteristics of the receivers which are sensitive in the visible band of the spectrum are evaluated from the influence of the luminous flux F and with receivers which possess sensitivity in the infrared and ultraviolet regions of the spectrum -- from the influence of the radiation flux Φ . Evaluation from the influence of the radiation flux is more universal.

The values of integral sensitivity presented in the receiver certificates are usually measured from the radiation of standard sources:

- Source A ($T = 2848K$) -- for photoemissive cells and other receivers sensitive in the visible region of the spectrum:

- Source B ($T = 2500K$) and C ($T = 2360K$) -- for types of 88 receivers indicated above.

An ideally black body (IBB) with a temperature of 373K or 573K is for radiation flux receivers which are sensitive in the long-wave region of the spectrum.

In the United States, the parameters of photoresistors are measured most often from the radiation of an IBB with a temperature of $T = 500K$.

The utilization factor K is the relation of the integrals in formula (4.7), i.e.,

$$K = \frac{\int_0^{\infty} \phi(\lambda) s(\lambda) d\lambda}{\int_0^{\infty} \phi(\lambda) d\lambda} \quad (4.9)$$

This factor shows the fraction of the complex radiation flux which falls on a receiver which is comprised by the effective flux for this receiver.

Inasmuch as the function $s(\lambda)$ has no analytical expression but is given graphically, the utilization factor is computed by numerical (graphic) integration. For this, it is necessary to plot the functions $\phi(\lambda)$ and $s(\lambda)$ on a graph in relative units and the same scale, find the product $\phi(\lambda)s(\lambda)$, calculate the corresponding areas (see Fig. 4.2), and take their ratio.

For calculations of utilization factors by receivers of radiation of an IBB, formula (4.9) can be simplified considerably.

Since $\phi(\lambda) = r(\lambda)A = y(\lambda)r_{\max}(\lambda)A$, the following equality is valid

$$K = \frac{\int_0^{\infty} \phi(\lambda) s(\lambda) d\lambda}{\int_0^{\infty} \phi(\lambda) d\lambda} = \frac{\int_0^{\infty} r(\lambda) s(\lambda) d\lambda}{\int_0^{\infty} r(\lambda) d\lambda} = \frac{\int_0^{\infty} y(\lambda) s(\lambda) d\lambda}{\int_0^{\infty} y(\lambda) d\lambda} \quad (4.10)$$

Using the relation

$$K = \frac{\int_0^{\infty} r(\lambda) s(\lambda) d\lambda}{\int_0^{\infty} r(\lambda) d\lambda}$$

and considering that $\int_0^{\infty} r(\lambda) d\lambda = \sigma T^4$, a $r(\lambda) = y(\lambda)r_{\max}(\lambda)$, we obtain

$$K = \frac{r_{\max}(\lambda) \int_0^{\infty} y(\lambda) s(\lambda) d\lambda}{\sigma T^4} \quad (4.11) \quad /89$$

$$r_{\max}(\lambda) = 1.315 \left(\frac{T}{1000} \right)^5$$

where

Substituting numerical values here, we will have

$$K = \frac{1.315 \cdot 10^{-15} T^5}{5.7 \cdot 10^{-12} T^4} \int_0^{\infty} y(\lambda) s(\lambda) d\lambda = 0.232 \frac{T}{1000} \int_0^{\infty} y(\lambda) s(\lambda) d\lambda \quad (4.12)$$

Replacing the integral by the summation symbol and assigning the integration step $\Delta\lambda$, we obtain the final formula for the calculation of the utilization factors of the receivers from the radiation of an IBB

$$K = 0.232 \cdot 10^{-3} T \Delta\lambda \sum_{i=1}^n y(\lambda_i) s(\lambda_i) \quad (4.13)$$

The calculation in accordance with formula (4.13) is reduced to the determination of the sum of the products of two functions with given values of λ on the section of the spectrum where both functions differ from zero and to the multiplication of the found sum by a constant previously computed value which stands in front of the summation symbol.

If the integral sensitivity and utilization factor for some emitter are known for a given receiver, the spectral sensitivity can also be determined in absolute units. Actually, considering (4.9) and (4.7), we have

$$S = S_{\lambda_{\max}} K \quad \text{or} \quad S_{\lambda_{\max}} = \frac{S}{K} \quad (4.14)$$

i.e., the relation of the integral sensitivity of the receiver for a given emitter to the utilization factor of the radiation of the same emitter is a constant value and equals the maximum spectral sensitivity of the receiver.

Replacing $S_{\lambda_{\max}}$ in (4.14) with its value from (4.2), we obtain the desired relation

$$S_{\lambda} = \frac{S}{K} s(\lambda) \quad (4.15)$$

In some cases, instead of the utilization factor, we use the derivative characteristic from it -- the effective width of the sensitivity zone -- for the calculations.

The effective width of the receiver sensitivity zone is the width of the spectrum band where the entire effective radiation flux which falls on it would be concentrated for a given receiver under the condition that in this interval of the spectrum the function of spectral density is constant and equal to its maximum value, i.e.

$$\Delta\lambda_{\text{eff}} = \frac{\int_0^{\infty} \phi(\lambda) s(\lambda) d\lambda}{\phi(\lambda_{\text{max}})}$$

or, changing to relative units by division of the numerator and denominator by $\phi(\lambda_{\text{max}})$,

$$\Delta\lambda_{\text{eff}} = \frac{\int_0^{\infty} y(\lambda) s(\lambda) d\lambda}{1} \quad (4.16)$$

The necessary graphical constructions are shown on Fig. 4.3; in this regard, the shaded areas A_1 and A_2 are equal.

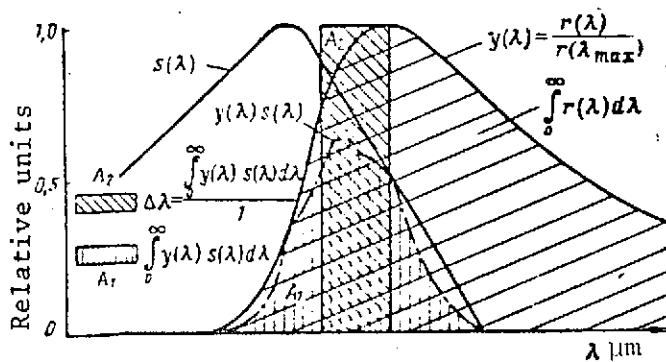


Fig. 4.3. For the determination of the effective width of a receiver's zone of sensitivity.

$$\Delta\lambda_{\text{eff}} = K \frac{\int_0^{\infty} \phi(\lambda) d\lambda}{\phi(\lambda_{\text{max}})} = K \frac{\phi}{\phi(\lambda_{\text{max}})} \quad (4.17)$$

Comparing the expressions with each other for $\Delta\lambda_{\text{eff}}$ and K , where

$$\Delta\lambda_{\text{eff}} = \frac{\int_0^{\infty} \phi(\lambda) s(\lambda) d\lambda}{\phi(\lambda_{\text{max}})}$$

$$\text{and} \quad K = \frac{\int_0^{\infty} \phi(\lambda) s(\lambda) d\lambda}{\int_0^{\infty} \phi(\lambda) d\lambda},$$

it is not difficult to establish the connection between these characteristics in the form

If an IBB is the emitter, then formula (4.17) is transformed on the basis of (4.10) to the type /91

$$\Delta\lambda_{\text{eff}} = K \frac{R}{r(\lambda_{\text{max}})} = \frac{\sigma T^4}{1,315 \left(\frac{T}{1000}\right)^5},$$

whence we finally have

$$\Delta\lambda_{\text{eff}} = 4310 \frac{K}{T}. \quad (4.18)$$

Formulas (4.17) and (4.18) establish the rather simple connection between the utilization factor and the effective width of the sensitivity zone.

The threshold flux Φ_t is the minimum radiation flux which causes a signal on the receiver output equivalent to the level of intrinsic noises.

Replacing in (4.3) the reaction of the receiver through the mean square value of the noise as applicable to Φ_t , we obtain

$$S = \frac{\sqrt{U_n^2}}{\Phi_t}, \quad \text{whence } \Phi_t = \frac{\sqrt{U_n^2}}{S}. \quad (4.19)$$

The threshold flux of the receiver is measured from the radiation of a fully specific source and, just as the integral sensitivity, depends on the characteristics of its radiation. Therefore, indicated in technical documents along with the value Φ_t is the type of source according to whose radiation it was measured.

In contrast to the threshold flux, which depends not only on the properties of the receiver, but also on the parameters of the emitter, a characteristic of the threshold sensitivity of the receiver itself is the monochromatic threshold flux $\Phi_{\lambda t}$ or the spectral distribution of threshold sensitivity. Let us establish the connection between Φ_t and $\Phi_{\lambda t}$. For this, we substitute in formula (4.19) the value S from (4.15) and obtain

$$\Phi_t = \frac{\sqrt{U_n^2}}{KS_\lambda} s(\lambda) \quad (4.20)$$

On the other hand, by analogy with (4.19) for a monochromatic threshold flux we can write

$$\Phi_{\lambda t} = \frac{\sqrt{U_n^2}}{S_\lambda} \quad (4.21)$$

Expressing $\sqrt{U_n^2}$ from (4.20) and substituting its value in (4.21), we obtain

$$\Phi_{\lambda t} = \Phi_t \frac{K}{s(\lambda)} \quad (4.22)$$

From this formula, it can be seen that the monochromatic threshold flux will be minimum with $s(\lambda) = 1$, i.e., in maximum spectral sensitivity

/92

$$\Phi_{\lambda t \min} = \Phi_t K, \quad (4.23)$$

and the current value of the monochromatic threshold flux will be

$$\Phi_{\lambda t} = \Phi_{\lambda t \min} \frac{1}{s(\lambda)} \quad (4.24)$$

The threshold sensitivity of radiation receivers of the same type depends on the dimensions of the area of the sensitive layer A. Therefore, for a more objective comparison of various receivers of radiation flux, it is necessary to reduce their threshold fluxes to a unit area through the formulas

$$\Phi'_t = \Phi_t \frac{1}{\sqrt{A}} \quad \text{and} \quad \Phi'_{\lambda t} = \Phi_{\lambda t} \frac{1}{\sqrt{A}}, \quad (4.25)$$

where Φ'_t and $\Phi'_{\lambda t}$ are the threshold fluxes of the receivers reduced to a unit area of the sensitive layer.

Besides this, as follows from (4.19) and (4.21), the threshold fluxes of the receivers depend on the level of noise signals at the output of the receivers whose value, in turn, depends on the transmission band of the amplifier channels.

The threshold fluxes of receivers, with a narrow transmission band for the circuit, depend on the width of the transmission band Δf . Therefore, for a comparison of the threshold fluxes of the receivers, they are reduced to a unit transmission band. With consideration of this, the sensitivity threshold of the receiver reduced to a unit area and unit transmission is expressed in the form

$$\Phi_t^t = \Phi_t \frac{1}{\sqrt{A \Delta f}}; \quad (4.26)$$

$$\Phi_{\lambda t}^t = \Phi_{\lambda t} \frac{1}{\sqrt{A \Delta f}}. \quad (4.27)$$

These values have dimensionality ($\text{W} \cdot \text{cm}^{-1} \cdot \text{Hz}^{-1/2}$) or ($\text{lm} \cdot \text{cm}^{-1} \cdot \text{Hz}^{-1/2}$). Sometimes, in a comparison of radiation flux receivers, it is more convenient to use the reciprocal of Φ_t^t

This characteristic was first introduced in the United States and is called detectivity.

On the basis of (4.26) and (4.27), we obtain the expressions for detectivity D^* :

$$D^* = \frac{1}{\Phi_t^t} = \frac{\sqrt{A \Delta f}}{\Phi_t} \quad \text{or} \quad D^* = \frac{S \sqrt{A \Delta f}}{\sqrt{U_n^2}} \quad (4.28)$$

and for spectral detectivity D^*_λ :

$$D^*_\lambda = \frac{1}{\Phi_{\lambda t}^t} = \frac{\sqrt{A \Delta f}}{\Phi_{\lambda t}} \quad \text{or} \quad D^*_\lambda = \frac{S_\lambda \sqrt{A \Delta f}}{\sqrt{U_n^2}}. \quad (4.29) \quad \underline{93}$$

From the obtained expressions, it follows that with given dimensions of the sensitive layer and width of transmission band the threshold sensitivity of the radiation flux receivers depends

on the noise level. The noise of the receivers is evaluated from their mean square value. The arising of noise is explained by many reasons, in which regard some of them are still insufficiently investigated. Common to all receivers are thermal noises, radiation noises, and noises caused by current fluctuations.

The finite time for the course of the processes for the transformation of radiation current by the receivers causes the necessity to consider their inertial properties. Considering the receiver as a linear system (this is valid with small values of incident radiation flux), its inertial properties can be characterized by the pulse sensitivity, frequency response, and time constant.

By pulse sensitivity $S_p(t)$, we mean the ratio of the pulse reaction of the receiver $U(t)$ to the value of radiation energy W of the input pulse

$$S_p(t) = \frac{U(t)}{W}. \quad (4.30)$$

With the influence of a pulse with a power of $\Phi(t)$ on a receiver, the value of the energy in it is determined as

$$W = \int_{-\infty}^{\infty} \Phi(t) dt, \quad (4.31)$$

in which regard, the Fourier transform for the power of flux $\Phi(t)$ has the form

$$E(f) = \int_{-\infty}^{\infty} \Phi(t) e^{-2\pi i f t} dt. \quad (4.32)$$

If all the energy reaches the receiver instantaneously, then $\delta(t)$ can be introduced -- a function which connects the power with the energy: $\Phi(t) = W\delta(t)$.

With the noninstantaneous arrival of a radiation flux at the receiver, we find its reaction with the use of the integral of convolution

$$U(t) = \int_{-\infty}^{\infty} S_p(\tau) \Phi(t-\tau) d\tau, \quad (4.33)$$

In this case, we will have in mind that $S_p(\tau) \equiv 0$, when $t \leq 0$.

If a radiation flux which falls on a receiver changes in accordance with a sine law, it can be presented in the form of a complex function $\Phi(t) = \Phi_0 e^{2\pi j f_1 t}$ where f_1 is the modulation frequency of the radiation flux. Substituting this value in the expression for $U(t)$, we obtain /94

$$U(t) = \int_{-\infty}^{\infty} S_p(\tau) \Phi_0 e^{2\pi j f_1 (t-\tau)} d\tau = \Phi_0 e^{2\pi j f_1 t} \int_{-\infty}^{\infty} S_p(\tau) e^{-2\pi j f_1 \tau} d\tau. \quad (4.34)$$

Designating the integral $\int_{-\infty}^{\infty} S_p(\tau) e^{-2\pi j f_1 \tau} d\tau = S(jf_1)$, we rewrite expression (4.34) in the form

$$U(t) = \Phi_0 e^{2\pi j f_1 t} \cdot S(jf_1). \quad (4.35)$$

Thus, with a sinusoidal change in the radiation flux, the signal at the output of the receiver also changes in accordance with a sine law, but thanks to the multiplier $S(jf_1)$, this change for a given frequency will have the corresponding amplitude and another phase. Since the integral sensitivity of the receiver is determined as the ratio of the reaction to the value of the incident radiation flux, with a sinusoidal change in the flux and the transition to absolute values, from expression (4.35) it follows that $S(jf_1)$ is the integral sensitivity of the receiver at a given frequency f_1 for the modulation of the radiation flux. The dependence of the integral sensitivity on frequency is the frequency response of the receiver (Fig. 4.4).

On the basis of the frequency response, with the use of the Fourier transform, we can obtain the relation of the pulse sensitivity

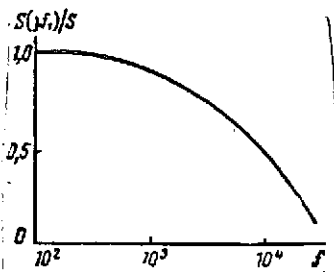
$$S_p(t) = \int_{-\infty}^{\infty} S(jf_1) e^{2\pi j f_1 t} df_1. \quad (4.36)$$

Using the Fourier transform, we present the value of the pulse of radiation flux in the form

$$\Phi(t) = \int_{-\infty}^{\infty} \Phi(jf) e^{2\pi jft} df \quad (4.37)$$

and, substituting the obtained expression in (4.33), we find

$$\begin{aligned} U(t) &= \int_{-\infty}^{\infty} S_p(\tau) d\tau \int_{-\infty}^{\infty} \Phi(jf) e^{2\pi jf(t-\tau)} df = \\ &= \int_{-\infty}^{\infty} \Phi(jf) e^{2\pi jft} df \int_{-\infty}^{\infty} S_p(\tau) e^{-2\pi jf\tau} d\tau = \int_{-\infty}^{\infty} \Phi(jf) S(jf) e^{-2\pi jf\tau} d\tau. \end{aligned} \quad (4.38) \quad /95$$



Inasmuch as the reaction of the receiver as a function of time $U(t)$ is connected with the reaction of the receiver as a function of frequency $U(jf)$ by the Fourier transform

$$U(t) = \int_{-\infty}^{\infty} U(jf) e^{2\pi jft} df, \text{ on the basis of (4.38)}$$

we can write that

$$U(jf) = \Phi(jf) S(jf). \quad (4.39)$$

Fig. 4.4. Frequency response of a receiver

Thus, on the basis of (4.39), the spectrum of the reaction on the output of the receiver is determined by the frequency spectrum of the signal on the input and the frequency response of the radiation flux receiver.

The time constant τ of the receiver is determined by the time interval during which the signal at the output of the receiver reaches a specific amount of the established value with constancy of the amount of incident radiation flux. The time constant can be calculated from the transient function of the receiver which is the relation of the reaction to the unit flux

Φ_1 . We find the reaction of the receiver to the influence of the unit flux Φ_1 with the use of the integral of convolution

$$U(t) = \int_{-\infty}^t S_p(\tau) \Phi_1 d\tau = \Phi_1 \int_{-\infty}^t S_p(\tau) d\tau. \quad (4.40)$$

Then, the transient function of the receiver will be

$$S_p(t) = \frac{U(t)}{\Phi_1} = \int_{-\infty}^t S_p(\tau) d\tau,$$

whence

$$S_p(t) = \frac{dS_p(t)}{dt}. \quad (4.41)$$

With the irradiation of the photoresistors by square pulses of radiation flux, in many cases their reaction changes according to the law

$$U = U_0(1 - e^{-kt}), \quad (4.42)$$

where U_0 is the established value of the reaction (signal at the output).

The energy (light) characteristic $S = f(\Phi)$ expresses the dependence of integral or spectral sensitivity of the receiver on the magnitude of the radiation flux which falls on it.

/96

Sometimes, the energy characteristic is the dependence of the voltage or current at the receiver output on the magnitude of the incident radiation flux.

The energy characteristics are linear with small values of incident flux. With an increase in incident flux, the linearity is destroyed. With an increase in the flux which falls on the sensitive layer, the sensitivity of the receiver is reduced.

Therefore, with sufficiently large values of radiation flux directed at the receiver, changes in its sensitivity should be considered utilizing the energy characteristic.

The current-voltage characteristics -- $I = f(U)$ and $I_T = \phi(U)$ -- determine the electrical properties of the radiation flux receivers. The linearity of the current-voltage characteristics can be destroyed in the region of voltages which are high for a given receiver. This is manifested especially clearly with gas-filled photocells. In addition, extremely important dependences are the voltage characteristics. They reflect the connection between the sensitivity of the receiver and the magnitude of the supply voltage.

$$S = f(U); U_n = \varphi(U) \text{ and } \Phi_p = \psi(U).$$

Inasmuch as both the integral sensitivity and the noise increase with an increase in supply voltage, to assume optimum conditions for the operation of the receiver, the value of the supply voltage should be specially selected in the circuit.

In order to exclude the dependence of sensitivity on the value of the supply voltage in calculations, use is made of the concept of specific sensitivity, relating it to a voltage equal to 1 V:

$$S_{sp} = \frac{U}{\Phi} \frac{1}{U_{sup}} \quad (4.43)$$

Then the sensitivity with an operating supply voltage U_0 will be

$$S = S_{sp} U_0 \quad (4.44)$$

Besides the designated characteristics, in the selection of a radiation flux receiver it is necessary to consider the dependence of its parameters on temperature for use in the circuit of a specific instrument. These dependences are presented in the form of temperature characteristics which indicate how the parameters of the receiver change (sensitivity, threshold flux, noise, resistance) with a change in the temperature of the sensitive layer.

4.3. Photocells and Photomultipliers

In this group of photocells, photoemissivity is used in which the radiation flux which falls on the surface of the material causes the emission of electrons which have received the name of photoelectrons. They are absorbed by the external electrical field created by the applied voltage. The role of the cathode is played by the photosensitive layer, called the photocathode. The second electrode is the anode. A least radiation frequency exists for each material

/97

$$\nu_0 = \frac{\varphi_0}{h}, \quad (4.45)$$

at which emission of photoelectrons still arises. This frequency or the wavelength corresponding to it

$$\lambda = \frac{c}{\nu_0} = \frac{1.242}{\varphi_0} \mu\text{m} \quad (4.46)$$

is called the "threshold," which characterizes the long-wave limit of the sensitivity of the material.

Photocathodes of contemporary photocells have a composite structure. A monomolecular layer of atoms of electropositive metal, which reduces the operation of the output, is applied to the surface of the basic metal. In this, an intermediate semiconductor layer is usually created between the basic metal (backing) and the surface layer of adsorbed atoms.

Composite photocathodes [36, 48, 51], in contrast to pure metal ones, possess high sensitivity in the visible and ultraviolet and infrared regions of the spectrum close to it (Table 4).

Such photocathodes have a film of several hundreds or even thousands of atomic layers applied to a metal or insulating base. Antimony-cesium and silver-oxygen-cesium photocathodes have received wide popularity in practice. The atoms of the alkaline metal (cesium) which are part of the composition of the photocathode are contained both inside the semiconductor layer in chemically bound and adsorbed states and on its outer surface. The basic photoelectric properties of the cathode are determined by the structure of the intermediate layer.

/98

TABLE 4.1

Substance	ϕ_0 , J	λ_0 , μm
Nickel	$5.01 \cdot 1,6 \cdot 10^{-19}$	0.246
Silver	$4.54 \cdot 1,6 \cdot 10^{-19}$	0.270
Potassium	$2.25 \cdot 1,6 \cdot 10^{-19}$	0.550
Cesium	$1.46 \cdot 1,6 \cdot 10^{-19}$ $1.37 \cdot 1,6 \cdot 10^{-19}$	0.660
Oxidized silver with an admixture of cesium	$0.9 \cdot 1,6 \cdot 10^{-19}$ $0.7 \cdot 1,6 \cdot 10^{-19}$	1.50—1.35
Oxidized antimony with an admixture of cesium	$1.27 \cdot 1,6 \cdot 10^{-19}$ $1.22 \cdot 1,6 \cdot 10^{-19}$	0.75—0.70

Fig. 4.5 shows a diagram of the structure of a silver-oxygen-cesium photocathode. Applied to the silver backing is an intermediate layer consisting of cesium oxide, reducing finely dispersed particles of silver, and internal adsorbed cesium atoms. The structure of this photocathode can be expressed symbolically by the formula

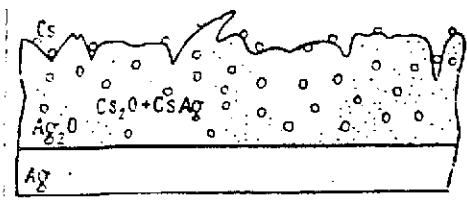


Fig. 4.5. Structure of a silver-oxygen-cesium photocathode.

Silver-oxygen-cesium photocathodes are most often used in work in the near infrared and visible regions of the spectrum. Antimony-cesium photocathodes are used in instruments which operate in the visible region of the spectrum [38].

In addition, the following types of photocathodes find employment in various types of photocells: antimony-sodium, antimony-potassium, antimony-lithium, bismuth-cesium, antimony-potassium-sodium (multi-alkaline), antimony-potassium-cesium (multialkaline), copper-sulfur-cesium, and others. Depending on the thickness of the layer, the backings of the photocathodes are divided into solid and semitransparent. With the latter, the thickness of the backing layer is reduced practically to zero and the photocathode operates on transillumination.

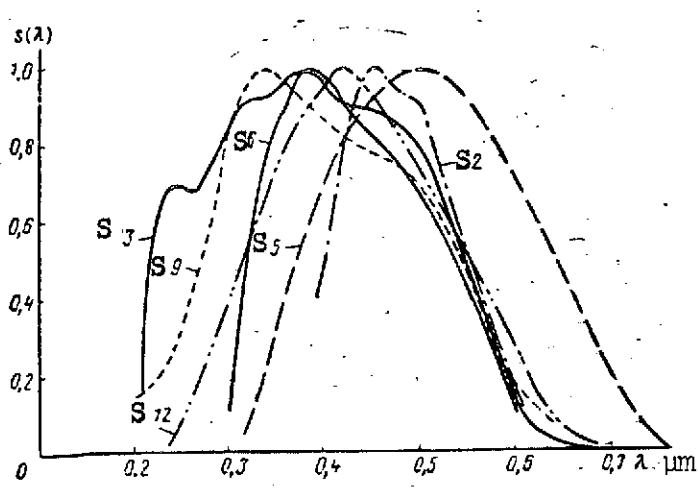
We note that the increase in the sensitivity of the photocathodes by means of a reduction in the operation of the output causes a sudden increase in the thermionic and cold (autoelectronic) emissions when, under the influence of the ambient temperature and the intensity of the field, an electron current arises at the surface of the photocathode in the absence of an incident flux..

A modern photoemissive cell is a glass envelope out of which the air has been pumped. The photocathode is deposited on one of the walls of the envelope. The role of the anode is accomplished by a metal plate or ring located in the center of the envelope.

A supply voltage is applied between the photocathode and the anode. With the incidence of radiation flux on the photocathode, photoelectrons are knocked out of it. Under the influence of the applied voltage, they flow to the anode and cause the appearance of a signal across the load resistance. The amount of supply voltage depends on the design of the photocell, and can reach 300-400 V.

Depending on their purpose, photocathodes are made from various materials which also determine the region of spectral sensitivity of the photocells. In this regard, the short-wave limit of sensitivity is determined by the transparency of the envelope material and the long-wave limit by the work function of the photocathode. The characteristics of the relative spectral sensitivity of various photocathodes are presented on Figs. 4.6-4.8 [20].

/99



Even in the absence of the irradiation of the sensitive layer, a dark current made up of the current of thermoemission of the cathode and the leakage current between the electrodes flows in the circuit of the photocell. The values of the densities of the thermocurrents for various types of photocathodes are presented in Table 4.2 [49].

Fig. 4.6. Graph of the relative spectral sensitivity of photocells with photocathodes: S2 S3
S5 S6
S9 S12

TABLE 4.2

Photo-cathode	Silver-oxygen-cesium	Antimony-cesium	Multi-alkaline	Sb-Na, K and Sb-Na, Cs
Density of thermocurrent in A/cm ²	10 ⁻¹¹ —10 ⁻¹³	10 ⁻¹⁴ —10 ⁻¹⁵	10 ⁻¹⁵ —10 ⁻¹⁶	10 ⁻¹⁶

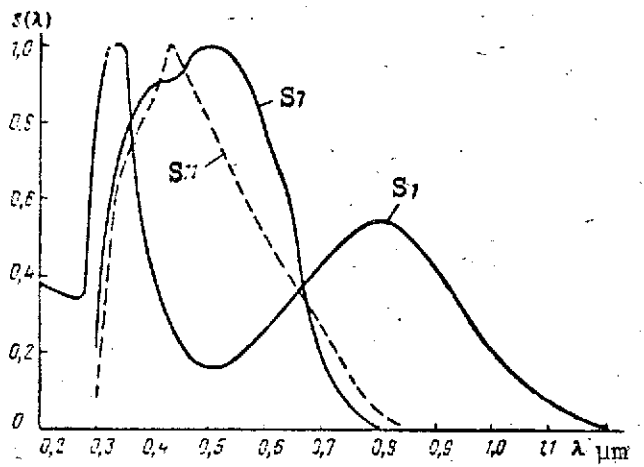


Fig. 4.7. Graph of the relative spectral sensitivity of photocells with photocathodes:

S1 S7
S11

The total leakage current depends on the amount of area of the photocathode. It can be reduced by a reduction in the area and the cooling of the photocathode.

The value of the second, more significant component of the dark current (leakage current) between the electrodes depends on the resistance of the insulation of the material of the envelope and base. With the presence of a base, the total leakage current for the base and glass of the envelope is 10⁻⁸–10⁻⁷ A. This component can be reduced either by increasing the

distance between the cathode and the anode or by introducing a protective ring [38].

Usually, a reduction in the influence of dark current is also attained by the modulation of the radiation flux and the use of alternating current amplifiers. However, its influence cannot be completely excluded since, in working with small currents, it determines several types of noise and, consequently, the threshold sensitivity of the photocells. /101

External and internal noises are distinguished. The reasons for external noises may be inductions from extraneous fields, vibrational noises, and so forth. They can be reduced to the minimum. External noises which cannot be eliminated include radiation noise which arises due to fluctuations in the radiation which falls on the receiver. For a radiating body with area A

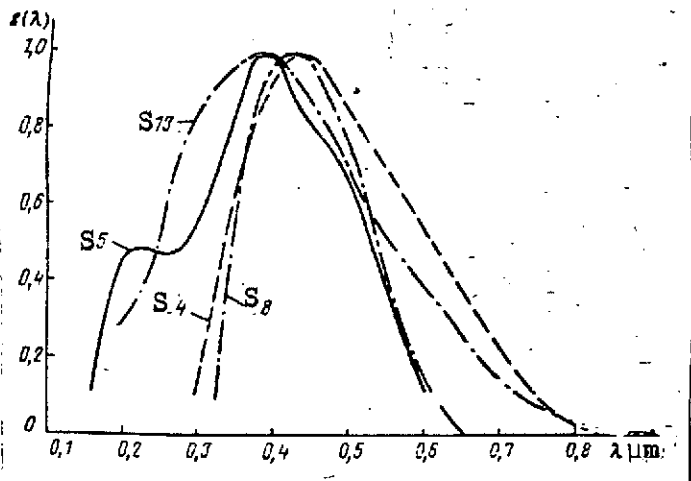


Fig. 4.8. Graph of relative spectral sensitivity of photocells with photocathodes:

S4	S8
S13	S15

having a blackness coefficient ϵ , fluctuations in the power of radiation are determined from the formula

$$\overline{\Delta\Phi_o^2} = 8kT^{\epsilon_s} A \Delta f = 8kT\Phi\Delta f, \quad (4.47)$$

where K is the Boltzmann constant; Δf is the width of the frequency band.

We find the noises at the output of the receiver caused by the radiation noises of the emitter from the expression

$$\sqrt{\overline{i_n^2}} = S \sqrt{\overline{\Phi_o^2}} = S \sqrt{8kT\Phi\Delta f}. \quad (4.48)$$

The internal noises of the photocells are basically non-removable. Their origin is explained by the corpuscular nature of light and electricity. The internal noises of the photocell itself are the noises of the shot effect and the scintillation noise.

Inasmuch as an electric current is an electron flux, i.e., a flow of discrete particles, and the value of the current is determined by the number of these particles, by virtue of the fluctuations in the number of particles with time the noise of the shot effect arises. The mean square value of the current of the shot effect is found from statistical considerations and is calculated from the Schottky formula

$$\sqrt{\overline{i_s^2}} = \sqrt{2ei_0\Delta f}, \quad (4.49)$$

where e is the electron charge; $i_0 = i_t + i_{fc}$ is the total current of the photocathode; i_{fc} is the constant component of the photocurrent; i_d is the dark current.

The scintillation noise (flicker effect) is caused by the fluctuations in photocurrent due to the inconstancy of sensitivity with time. This inconstancy of sensitivity is called the random

changes in the emission of the photocathode. The processes which cause a change in emission proceed slowly. Therefore, the scintillation noise is manifested only in the region of low frequency where it can exceed the level of the shot noise by approximately an order of magnitude. This noise drops with an increase in frequency. The equation for the scintillation noises has the form /102

$$\overline{\Delta i_{sc}^2} = 2ei \left(1 + \frac{Bi}{A_{pc} f_{sc}} \right), \quad (4.50)$$

where B is a constant which characterizes the nature of the photocathode; A_{pc} is the area of the photocathode; f_{sc} is the frequency.

Along with the intrinsic noises of the receiver, noises arrive at the input of the amplifier which are caused by fluctuations in the volume density of the current carrier in the material of the load (input) impedance and the shot effect of the anode current.

The noise of the input impedance of the amplifier is the thermal noise connected with the thermal motion of the current carrier in the material of the substance. The mean square value of the thermal noise caused by the chaotic motion of the electrons in the conductor can be calculated from Nyquist's well-known formula:

$$\overline{U_i^2} = \sqrt{4kT \int_0^{f_2} R(f) df}, \quad (4.51)$$

where $R(f)$ is the function which describes the dependence of the conductor's resistance on the frequency.

With R not dependent on frequency

$$\overline{U_i^2} = \sqrt{4kTR\Delta f} \quad \text{or} \quad \overline{i_d^2} = \sqrt{\frac{4kT\Delta f}{R}} \quad (4.52)$$

The noises of the shot effect of the anode current of an electron tube (primarily tubes of the first stage of an amplifier)

are similar to the noise of the shot effect of the photocathode. In practice, this noise component is not great and is considered by the introduction into the calculation of an equivalent resistance R_{eq} in the grid circuit of the tube which creates a noise equal to the shot noise of the tube. Then the total noise introduced by the amplifier will be

$$\overline{U_{\text{ampl}}^2} = 4kT(R_{\text{load}} + R_{eq})\Delta f \text{ or } \overline{i^2} = \frac{4kT\Delta f}{R_{\text{load}} + R_{eq}}. \quad (4.53)$$

The total mean square value of the noise acting on the output of the amplifier is expressed through components independent of each other by the formula

$$\sqrt{\overline{i^2}} = \sqrt{\overline{i_o^2} + \overline{i_s^2} + \overline{\Delta i_{sc}^2} + \overline{i_{\text{ampl}}^2}} \quad (4.54)$$

With the detection of small radiation fluxes modulated at a comparatively high frequency, components $\overline{i_o^2}$ and $\overline{\Delta i_{sc}^2}$ can be disregarded. Then

$$\sqrt{\overline{i_n^2}} = \sqrt{\overline{i_s^2} + \overline{i_{\text{ampl}}^2}} \sqrt{\left(2ei_0 + 4kT \frac{1}{R_{\text{load}} + R_{eq}}\right) \Delta f}$$

or, approximately considering that $R_{eq} \ll R_{\text{load}}$

$$\sqrt{\overline{i_n^2}} = \sqrt{\left(2ei_0 + \frac{4kT}{R_{\text{load}}}\right) \Delta f} \quad (4.55)$$

In this formula, the first term of the sum under the radical characterizes the intrinsic noise of the photocell, and the second characterizes the noise introduced by the amplifier.

In accordance with the definition, the luminous threshold flux of the photoelement can be calculated by the formula

$$F_t = \frac{\sqrt{i_n^2}}{S^l} \quad (4.56)$$

where S^l is the luminous integral sensitivity of the photocell measured in A/lm.

Here substituting the value $\sqrt{i_n^2}$, from (4.55), we find

$$F_t = \frac{\sqrt{\left(2ei_0 + \frac{4kT}{R_{load}}\right) \Delta f}}{S^l} \quad (4.57)$$

If the constant component of the photocurrent is small in comparison with the dark current, which is valid with the operation of the photocell with luminous fluxes close to the threshold flux, then

$$F_t = \frac{\sqrt{\left(2ei_T + \frac{4kT}{R_{load}}\right) \Delta f}}{S^l} \quad (4.58)$$

With the use of a sufficiently large value of load resistance R_{load} , the second term of the radicand becomes small in comparison with the first:

$$\frac{2kT}{R_{load}} \ll ei_T \quad \text{or} \quad \frac{2kT}{e} \ll R_{load} i_T. \quad (4.59)$$

At room temperature $\frac{2kT}{e} \approx 0.05$ V. Thus, if the measured photocurrent creates a voltage drop which considerably exceeds 0.05 V across load resistance R_{load} , the noise of the amplifier in comparison with the shot noise of the photocell can be disregarded.

Then, the threshold flux of the photocell will be /105

$$F_t = \frac{\sqrt{2ei_T \Delta f}}{S^l} \quad (4.60)$$

Condition (4.60) is satisfied if $i_d = 10^{-8}$ A and $R_{load} = 10^8$ ohms.

Selecting load resistance R_{load} , one should consider the limitations imposed on the upper frequency limit of the input capacitance C_{in} of the amplifier. This frequency depends on the value of the product $R_{load}C_{in}$ and is determined from the expression

$$f_u = \frac{1}{R_{load}C_{in}2\pi} \quad (4.61)$$

with $R_{load} = 10^8$ ohms and $C_{in} = 30$ pf $f_u = 50$ Hz. Such frequency modulation of a radiation flux may prove to be insufficient. Then, depending on the value of R_{load} , the threshold flux is calculated either from formula (4.58), where both noise components are comparable with each other, or from the formula

$$F_t = \frac{2\sqrt{kT/R_{load}\Delta f}}{S\lambda} \quad (4.62)$$

for the case of $i_d R_{load} \ll \frac{2kT}{e}$

The basic characteristics of the photocells are measured from their response to a luminous flux of a standard source A_{lm} with $T = 2848K$. Therefore, in reference books, their integral sensitivity is given in A/lm, and threshold flux in lm. The characteristics of several standard vacuum photocells are presented in Table 4.3.

From the table, it can be seen that the greatest integral sensitivity is possessed by antimony-cesium photocathodes; however, they operate in a comparatively narrow band of the spectrum [38]. With the expansion of this band, as occurs with composite photocathodes, their integral sensitivity decreases.

Sometimes, to raise the integral sensitivity of the photocells, recourse is had to the amplification of the primary photocurrent. At present, two general methods exist for increasing the sensitivity of the photocell within the instrument. In the first of them, this is attained with the aid of the ionization of an inert gas with which the envelope of the photocell is filled (gas-filled photocells), and in the second, through the use of the phenomenon of secondary electron emission (photomultipliers).

In gas-filled photocells, the photoelectrons which have been knocked out of the photocathode, on collision with neutral gas particles, cause their ionization. As a result, an increasing

TABLE 4.3

Photo-cell	Photo-cathode	Region of spectral sensitivity	Band of possible positions of maximum spectral sensitivity, μm	Operating voltage, V	Integral sensitivity $\mu\text{A}/\text{lm}$			Dark current	Number of spectral characteristic
					Minimum	Nominal	Maximum		
STsV-4	Sb-Cs	0.40—0.60	0.45±0.05	300	80	with $U=240\text{B}$ 100	170	$1 \cdot 10^{-7}$	S2
STsV-51	Sb-Cs	0.40—0.60	0.45±0.05	300	80	with $U=240\text{B}$ 100	140	$1 \cdot 10^{-8}$	S2
F-1	Sb-Cs	0.215—0.60	0.38±0.05	100—300	70	with $U=100\text{B}$ 100	130	With $U=80\text{B}$ $1 \cdot 10^{-14}$	S3
F-2	Sb-Cs	0.30—0.60	0.39±0.05	100—300	15	with $U=100\text{B}$ 30	70	$1 \cdot 10^{-8}$	S6
F-3	Bi-Ag-Cs	0.32—0.75	0.50±0.05	50—100	40	with $U=100\text{B}$ 70	115	with $U=50\text{B}$ $1 \cdot 10^{-9}$	S7
F-5	Ag-O-Cs	0.60—1.10	0.80±0.10	100—300	0.82 (0.0124)	with $U=100\text{B}$ 0.77 (0.05)	14 (0.4)	with $U=30\text{B}$ $7.5 \cdot 10^{-11}$	S1
F-6	Bi-Ag-Cs	0.32—0.75	0.50±0.10	100—300	40	with $U=100\text{B}$ 50	80	with $U=30\text{B}$ $1 \cdot 10^{-11}$	S7
F-8	Sb-Cs	0.40—0.60	0.45±0.05	300	—	with $U=150\text{B}$ 80	—	$1 \cdot 10^{-8}$	S2
F-9	Sb-K-Na-Cs	0.30—0.85	0.43±0.05	100	—	80	—	with $U=60\text{B}$ $1 \cdot 10^{-12}$	S11
TsG-4	Ag-O-Cs	0.60—1.10	0.80±0.10	240	100	200	400	$1 \cdot 10^{-7}$	S1

cascade of electrons will move from the cathode to the anode and, /106 in the reverse direction, a flux of positive ions. This causes an increase in the current in the circuit of the photocell and a raising of its integral sensitivity.

A natural advantage of gas-filled photocells in comparison with vacuum photocells is their large integral sensitivity.

The shortcomings of these photocells include their greater inertness, the absence of a saturation current [38], and the dependence of their parameters on the fluctuations of the applied voltage caused by this, and also the possibility of the appearance of nonlinear distortions with the modulation of the incident radiation flux. The characteristics of one of the models of gas-filled photocells are presented in Table 4.3.

The other method of increasing sensitivity -- the use of secondary electron emission -- moreover permits reducing the effect of thermal noises in the load resistors. This method is realized in the photomultipliers.

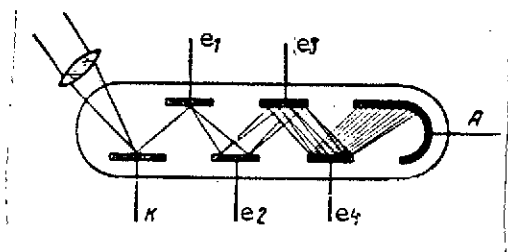


Fig. 4.9. Operating principle of a photomultiplier.

In a photomultiplier, the electrons emitted by a photocathode go under the influence of an electrical field not to the main but to intermediate anodes (emitters) between which an accelerating field is created (Fig. 4.9). The ratio of the number of electrons emitted by the emitter n_2 to the number of electrons which fall on it n_1 is called the coefficient of secondary emission

$$m_e = \frac{n_2}{n_1} .$$

The values of the coefficient m_e for several materials are given in Table 4.4.

In accordance with the number of amplification stages, which correspond to the number of emitters, single-stage and multi-stage (photomultipliers) (PM) are distinguished.

Emitters with 10-14 stages which are employed in contemporary photomultipliers assure a current amplification which reaches

10^6 – 10^8 . In the first approximation, the amplification coefficient of a PM is determined as $M = m_e^n$, where n is the number of stages.

TABLE 4.4

Material	Ni	Cu ₂ O	Cu–Be	Ag–Be	Cu–Al	Sb–Cs	MgO	BeO
m_e Electron energy, J	1.27 $500 \cdot 10^{-7}$	1.19–1.25 $500 \cdot 10^{-7}$	2.6 $200 \cdot 1.6 \cdot 10^{-19}$	2.6 $200 \cdot 1.6 \cdot 10^{-19}$	6.8 $200 \cdot 1.6 \cdot 10^{-19}$	5.9 $200 \cdot 1.6 \cdot 10^{-19}$	3.8–3.9 $100 \cdot 1.6 \cdot 10^{-19}$	3.9–4.3 $100 \cdot 1.6 \cdot 10^{-19}$

The threshold sensitivity of a photomultiplier is higher than that of photocells and is limited by dark currents and noises.

In photomultipliers, just as in a photocell, with the supply of the power supply voltage and the absence of illumination, a dark current flows in the anode circuit. It is the sum of the following components:

- The current of thermo-ionic emission of the photocathode /107 and the first emitter amplified by the multiplier system;
- Autoelectronic emission of the electrodes;
- Feedback currents (optical and ionic).

The values of the thermocurrents of photocathodes are presented in Table 4.2.

If we consider that the amplification coefficient of a PM equals 10^6 – 10^8 , the dark current in the anode circuit of a PM with different photocathodes can reach rather large values (up to 1 μ A).

Leakage currents in PM are caused by the conductivity of films of excess metal which condense on the glass of the envelope and the interelectrode insulators and also by films of contamination and moisture on the external surface of the envelope. Reductions in leakage currents are achieved by fastening the anode on special glass insulators separately from the emitters.

The raising of the stage voltages causes an autoelectronic emission at points of the closest approach of electrodes. This emission is often accompanied by the ionization of cesium vapors (discharge) and the appearance of scintillations. With large power supply voltages, such discharge scintillations cause sudden surges of anode current and the unstable operation of the photomultiplier. Autoelectronic emission can be avoided by the selection of the power supply voltage.

Photons appear with the discharges and luminescence within the PM. If they fall on the photocathode, optical feedback arises. Simultaneously with the luminescence, positive ions appear which fall on the photocathode. They cause ionic feedback. Both feedbacks lead to a sharp increase in the anode current.

The exclusion of the last component can be attained; however, the first two remain. The dark current which they cause and its fluctuations are one of the factors which determine the threshold sensitivity of the PM. As other factors, we can point to external and internal noises, similar to the noises of the photocells. As applicable to the PM, the basic types of noise are shot current and thermal noises of the load resistors. The remaining components can be disregarded under actual conditions. /108

Since in photomultipliers the current of the shot effect of the photocathode is amplified in each stage on a level with useful signals, with consideration of the shot current of the first emitter at the output of the first stage, we will have

$$\overline{i_{s1}^2} = (\overline{i_s \cdot m_{1e}})^2 + 2e i_{11} \Delta f, \quad (4.63a)$$

where $i_s = 2ei\Delta f$ is the current of the shot effect of the photocathode; m_{1e} is the amplification current of the first stage of the PM; $2ei_{11}\Delta f$ is the current of the shot effect of the first emitter; $i_{11} = im_{1e}$ is the current of the first emitter; i is the current of the photocathode.

Expanding the first component in (4.63a), we find the current of the shot effect at the output of the first stage

$$\overline{i_{e1}^2} = 2ei\Delta f m_{1e}^2 + 2eim_{1e}\Delta f = \overline{i_s^2} \cdot m_{1e}(1 + m_{1e}). \quad (4.63b)$$

It can be shown that the shot current at the output of the second stage will be

$$\overline{i_{s2}^2} = \overline{i_s^2} m_{1e} m_{2e} (1 + m_{2e} + m_{1e} m_{2e}),$$

and at the output of the n-th stage

$$\overline{i_{s_n}^2} = \overline{i_s^2} m_{1e} m_{2e} \dots m_{ne} (1 + m_{ne} + \dots + 1 + m_{ne} m_{(n-1)e} \dots m_{2e} m_{1e}).$$

If we consider that $m_{1e} = m_{2e} = \dots = m_{ne} = m_e$ and $m_e^n = M$, then for the calculation of the mean square shot current at the output of the n-th stage, we obtain the expression

$$\overline{I_s^2} = 2ei\Delta f M \frac{m_e^{n+1} - 1}{m_e - 1}. \quad (4.64)$$

Inasmuch as $m_e^n + 1 \gg 1$, expression (4.64) is transformed to the type

$$\overline{I_s^2} = 2ei\Delta f M^2 \frac{m_e}{m_e - 1}. \quad (4.65)$$

In the ideal case, where the shot effect on the emitters is absent, there is no multiplier $m_e/m_e - 1$ in (4.65). Under actual conditions, the shot effect of the emitters has an influence on the value of the shot current of the multiplier and is considered /109 by the factor $(1 + B) = m_e/(m_e - 1)$, and then

$$\overline{I_s^2} = 2ei\Delta f M^2 (1 + B). \quad (4.66)$$

In photomultipliers with electrostatic focusing, the value of the factor $(1 + B)$ fluctuates within limits of 1.5-3 and is taken as equal to 2.5.

The thermal noise on the load resistance of the PM is calculated from formula (4.52).

Then the mean square value of the total current on the amplifier input will be

$$\overline{I_n^2} = \overline{I_s^2} + \overline{I_t^2} = 2ei\Delta f M^2 (1 + B) + 4kT\Delta f R_{load}^{-1} \quad (4.67)$$

In this formula, just as in (4.55), the first component characterizes the intrinsic noises of the photomultiplier and the second, the noise introduced by the amplifier.

By analogy with (4.65), the luminous threshold flux of the PM is determined by the expression

$$F_t = \frac{\sqrt{I_n^2}}{S_{PM}^1}, \quad (4.68)$$

where S_{PM}^1 is the integral sensitivity of the photomultiplier measured in A/lm.

Substituting in this formula the value $\overline{I_n^2}$ from (4.67), we obtain

$$F_t = \frac{\sqrt{2 [ei\Delta f M^2 (1+B) + 2kT\Delta f R_{load}^{-1}]}}{S_{PM}^1} \quad (4.69)$$

It can be shown that in actual circuits, for the majority of the photomultipliers, the second component of the radicand is sufficiently small in comparison with the first, i.e., the condition is satisfied

$$2 \frac{kT}{R_{load}} \gg eiM^2(1+B) \quad (4.70)$$

or

$$2 \frac{kT}{e} \ll R_{load} i M^2 (1+B).$$

Actually, if $i = 10^{-10}$ A and $M = 10^5-10^6$, the indicated condition is satisfied with $R_{load} > 10^4-10^5$ ohms.

Disregarding the second component (thermal noises) from (4.69), we have the expression for the threshold flux of the PM

$$F_t = \frac{\sqrt{2ei\Delta f M^2 (1+B)}}{S_{PM}^1} \quad (4.71)$$

It is completely obvious that the detection and measurement of small fluxes commensurate with the threshold values is limited by the dark current in comparison with which the constant component of the photocurrent can be disregarded, then

$$F_t = \frac{\sqrt{2e i_d M^2 (1+B) \Delta f}}{S_{PM}^{\ell}} \quad (4.72)$$

The obtained formula is basic for the calculation of threshold sensitivity (threshold flux) of the photomultipliers.

The values of the anode dark current are presented in reference books and certificates for photomultipliers, and formula (4.72) includes the dark current of a photocathode, which are interconnected by the relations

$$I_d = i_d M \text{ or } i_d = \frac{I_d}{M} \quad (4.73)$$

Similarly connected are the integral sensitivities of the photocathode and the entire PM

$$S_{PM}^{\ell} = S_{PC}^{\ell} M. \quad (4.74)$$

With consideration of (4.73) and (4.74), from (4.72) for the calculation of the value of the threshold flux, of a photomultiplier, we obtain the relations with transmission band Δf :

$$F_t = \sqrt{\frac{2I_d e (1+B) \Delta f}{S_{PM}^{\ell} S_{PC}^{\ell}}} = \sqrt{\frac{5I_d e \Delta f}{S_{PM}^{\ell} S_{PC}^{\ell}}} \quad (4.75)$$

and with a unit transmission band ($\Delta f = 1 \text{ Hz}$)

$$F_t^{(1)} = \sqrt{\frac{2I_d e (1+B)}{S_{PM}^{\ell} S_{PC}^{\ell}}} = \sqrt{\frac{5I_d e}{S_{PM}^{\ell} S_{PC}^{\ell}}} \quad (4.76)$$

For example, for the FEU-31 photomultiplier for which $S_{PC}^l = 20 \text{ } \mu\text{A/lm}$,

$$S_{PM}^l = 10 \text{ A/lm}, I_d = 5 \cdot 10^{-7} \text{ A},$$

we obtain,

$$F_t^{(1)} = \sqrt{\frac{5 \cdot 5 \cdot 10^{-7} \cdot 1,6 \cdot 10^{-19}}{10 \cdot 20 \cdot 10^{-6}}} \simeq 4,5 \cdot 10^{-11} \text{ lm} \cdot \text{Hz}^{-1/2}$$

When the modulated luminous flux is discovered against the background of a constant flux F_{const} (illumination of the photomultiplier) which creates a noticeable constant component of the photocurrent I_{fc} , the threshold value of the modulated luminous flux can be calculated from the formula

$$F_t = \sqrt{\frac{2(I_d + I_{fc})e(1+B)\Delta f}{S_{PM}^l S_{pc}^l}} = \sqrt{\frac{5(I_d + S_{PM}^l F_{\text{const}})e\Delta f}{S_{PM}^l S_{pc}^l}} \quad (4.77)$$

If we express the luminous flux of the constant illumination F_{const} by the value of the threshold flux of the PM in accordance with the standard emitter $F_{s,t}$:

$$F_{\text{const}} = bF_{s,t},$$

where b is the coefficient for the reduction of the luminous flux to the flux of a standard source, then after several transformations from (4.77), we obtain the expression

$$\begin{aligned} F_t &= \sqrt{\frac{5I_d e \Delta f}{S_{PM}^l S_{pc}^l} + \frac{5b F_{s,t} S_{PM}^l e \Delta f}{S_{PM}^l S_{pc}^l}} = \\ &= F_{s,t} \sqrt{1 + \frac{b F_{s,t} S_{PM}^l}{I_d}} \end{aligned} \quad (4.78)$$

which permits calculating the threshold flux of the photomultiplier on the detection of a modulated or pulsed signal against the background of permanent illuminations.

The characteristics of several models of standard photomultipliers produced by Soviet industry are presented in Table 8 of the appendix.

4.4. Photoresistors

Semiconductor instruments whose action is based on the phenomenon of photoconductivity (change in electrical conductivity with their excitation by a radiation flux) are called photoresistors.

The electrical conductivity of semiconductors depends on the number of free electrons and holes formed in the basic zone as a result of the passage of electrons into the zone of conductivity. Such passages are caused both by the absorption of quanta of radiation energy which is accompanied by the appearance of photoconductivity and due to the chaotic thermal motion of the electrons which causes dark conductivity.

Photoconductivity may arise only under the condition where the energy of the radiation quantum $h\nu$ is sufficient for an electron to overcome the forbidden band

$$h\nu \geq \Delta W, \quad (4.79)$$

where ΔW is the width of the forbidden band in J.

From this relation, it follows that the long-wave limit of sensitivity which corresponds to the least frequency $\nu_0 = \Delta W/h$ for photoconduction lies in the longer-wave portion of the spectrum than for photoemission since, for the accomplishment of the latter, it is necessary for the electron to impart additional energy to overcome the potential barrier. Among the semiconductors, there are materials whose photoconductivity begins with extremely small quantum energies (radiation with wavelengths of a few dozen μm).

Data on the width of the forbidden band and the long-wave limit of sensitivity of several semiconductors are presented in Table 4.5.

Semiconductor materials are used for the making of sensitive layers of photoresistors in the form of polycrystals, pure single crystals, or single crystals with additions of alloying admixtures.

/112

TABLE 4.5

Semiconductor material	Se	PbS	PbSe	PbTe
Width of forbidden band $\Delta W, \text{J}$	$1.55 \times 1.6 \cdot 10^{-19}$	$0.4 \cdot 1.6 \cdot 10^{-19}$	$0.25 \times 1.6 \cdot 10^{-19}$	$0.34 \times 1.6 \cdot 10^{-19}$
Long-wave limit of sensitivity $\lambda_0, \mu\text{m}$	0.8	3.1	5.0	3.65

Continuation

Semiconductor material	InAs	InSb	Ge	Ge-Au
Width of forbidden band, $\Delta W, \text{J}$	$0.3 \cdot 1.6 \cdot 10^{-19}$	$0.26 \times 1.6 \cdot 10^{-19}$	$0.7 \times 1.6 \cdot 10^{-19}$	$0.15 \times 1.6 \cdot 10^{-19}$
Long-wave limit of sensitivity $\lambda_0, \mu\text{m}$	4.1	7.8	1.8	8.2

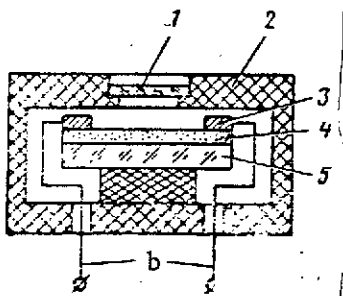


Fig. 4.10. Diagram of the design of a photoresistor: 1. protective window; 2. housing; 3. contacts; 4. sensitive layer; 5. backing; 6. leads.

The design of a photoresistor is presented in Fig. 4.10. To protect the photoresistor from the external influences, the inlet to the housing is covered by a protective window of a material which is transparent in the required band of the spectrum. Sometimes, the role of the protective plates is fulfilled by special filters. The diagram of the photoresistor presented on Fig. 4.10 reflects only the principle of its design; the constructional formulation of real models of photoresistors is extremely varied.

The spectral sensitivity of photoresistors, depending on the material used for the sensitive layer, lies within very broad limits from the visible to the far infrared region of the spectrum. /113

The threshold sensitivity of the photoresistors is limited by the noises inherent to them, to which thermal, generation-recombination, current ($1/f$ - noise), and radiation (photon) noises pertain.

Thermal noise is caused by thermal fluctuations in the concentration of the current carriers and is manifested in the form of random fluctuations in the voltage across the leads of the photoresistor. The mean square value of the thermal noise is calculated from formula (4.52).

Generation-recombination noise arises as a consequence of fluctuations in the number and lifetime of the current carriers which appear in the sensitive layer of the photoresistor with its excitation by an incident radiation flux. The nature of this noise is similar to the shot effect of electron emission. At frequencies comparable with the value $1/2\pi\tau_c$, the dispersion of the noise current is described by the formula

$$\overline{I_{gr}^2} = 4eI_0 \frac{\tau_c}{T_s} \Delta f \frac{1}{1 + (2\pi f\tau_c)^2},$$

where e is the electron charge; I_0 is the mean value of the current which flows in the circuit of the photoresistor; τ_c is the lifetime of the carrier; T_s is the time of drift of the carrier from one electrode to another.

In the frequency interval where $f \ll 1/2\pi\tau_c$, the generation-recombination noise is white

$$\overline{I_{gr}^2} = 4eI_0 \frac{\tau_c}{T_s} \Delta f.$$

Sometimes [51], this type of noise is considered one of the components of current noise. In practice, neither the magnitude nor the frequency spectrum of the noise agrees exactly with the conclusions of the theory.

The true value of the noise considerably exceeds (sometimes by 2-3 orders of magnitude) the calculated values of the thermal and generation-recombination noise. This excess noise is called the current or $1/f$ -noise.

It is assumed that its composition includes modulation noise and contact noise, and sometimes generation noise pertains here (with frequencies comparable with the value $1/2\pi\tau_c$).

The modulation noise is described by the relation

$$\overline{U_m^2} = A_m \frac{I^2 R^2}{f^i} \Delta f,$$

and the contact noise depends on the quality of the contacts and /114 is expressed in the form

$$\overline{U}_c^2 = A_c \frac{I^2 R^2}{f^\xi} \Delta f,$$

where A_M and A_K are constants; R is the resistance of the sensitive layer of the receiver.

Inasmuch as $\zeta \rightarrow 2$ and $\xi \rightarrow 1$, we take as the expression of the current noise

$$\overline{U}_i^2 = A_T I^2 R^2 \frac{\Delta f}{f}, \quad (4.80)$$

where $A_T = 10^{-11} - 10^{-13}$ is a constant whose value is determined for each type of receiver.

In the calculations, a number of additional relations are used which can be obtained if, on the basis of the presented information about the current noise, we consider that the function of spectral density for it is described by the expression

$$G(f) = \frac{c}{f}, \quad (4.81)$$

where

$$c = A_T I^2 R^2.$$

The mean square value of the current noise is found from the equation

$$\sqrt{\overline{U}_i^2} = \sqrt{\int_{f_1}^{f_2} G(f) df} = \sqrt{c \ln \frac{f_2}{f_1}}. \quad (4.82)$$

Inasmuch as in the measurements of the characteristics of photoresistors the radiation flux is modulated with frequency f_0 , from (4.82), we obtain

$$\overline{U_i^2} = \frac{c}{f_0} f_0 \ln \frac{f_2}{f_1}. \quad (4.83)$$

If the receiver is connected to the input of a circuit with a narrow-band filter, i.e., Δf is small, then within the limits of this frequency band the function of spectral density of the current noise can be taken as constant and equal to $G(f_0) = c/f_0$; then, from (4.82) we have

$$\overline{U_i^2} = \frac{c}{f_0} \Delta f. \quad (4.84)$$

Thus, the expression presented earlier for current noise is valid as applicable to a narrow frequency interval, and with a wide frequency band, it is necessary to use relation (4.83).

The mean square value of current noise in the band $\Delta f = 1 \text{ MHz}$, /115 on the basis of (4.84), will be

$$\sqrt{\overline{U_{\Delta f}^2}} = \sqrt{\frac{\overline{U_i^2}}{\Delta f}} = \sqrt{\frac{c}{f_0}}. \quad (4.85)$$

Thus, the mean square value of the current noise in a narrow band must be calculated by the formula

$$\sqrt{\overline{U_i^2}} = \sqrt{\overline{U_{\Delta f}^2}} \sqrt{\Delta f}, \quad (4.86)$$

and in a wide frequency band, the relation

$$\sqrt{\overline{U_i^2}} = \sqrt{\overline{U_{\Delta f}^2}} \sqrt{f_0 \ln \frac{f_2}{f_1}}. \quad (4.87)$$

must be used.

If the frequency of modulation of radiation flux f_M in an actual apparatus differs from the frequency of modulation f_0 on which the measurement of the characteristics were conducted, then on the basis of (4.84), we can write

$$\overline{U_i^2}(f_M) = \frac{c}{f_M} = \frac{c}{f_0} \frac{f_0}{f_M} = \overline{U_i^2}(f_0) \frac{f_0}{f_M}. \quad (4.88)$$

The obtained formula permits calculating the current noise with a new modulation frequency from the value of the noises at a given modulation frequency.

The value c is often determined experimentally, using formula (4.84), from which

$$c = \frac{\overline{U_i^2} f_0}{\Delta f} \quad (4.89)$$

With the given measurement conditions (values Δf and f_0 are known), we experimentally determine the mean square value of noise $\overline{U_i^2}$ and from formula (4.89) we calculate the constant c .

Besides the noises examined, the threshold sensitivity of the photoresistors will be influenced by radiation noise caused by random fluctuations in radiation flux and causing fluctuations in current or voltage in the receiver circuit. If the temperature of the emitter on which the receiver operates is T kelvins, the mean square value of fluctuation of radiation flux Φ falling on the receiver, on the basis of (4.47), equals

$$\overline{\Delta \Phi^2} = 8kT\Delta f\Phi \quad (4.90)$$

Inasmuch as the temperature of the sensitive layer of the photoresistor $T_{pr} > 0$, and it itself is the emitter, the total value of the fluctuation of radiation flux will be

$$\overline{\Delta \Phi_F^2} = 8k(T\Phi + T_{pr}\Phi_{pr})\Delta f \quad (4.91)$$

The mean square value of the voltage due to radiation noise /116 can be calculated from the formula

$$\sqrt{\overline{U_F^2}} = S\sqrt{\overline{\Delta \Phi_F^2}} = S\sqrt{8k(T\Phi + T_{pr}\Phi_{pr})\Delta f} \quad (4.92)$$

In general, all indicated noises cause voltage fluctuations at the input of the amplifier, the mean square value of which is determined as

$$\sqrt{\overline{U_n^2}} = \sqrt{S^2\overline{\Delta \Phi_F^2} + \overline{U_i^2} + \overline{U_r^2}} \quad (4.93)$$

It has been established that at low frequencies (up to tens of kHz), in the majority of cases, thermal noise is small in comparison with current noise and need not be considered in calculations. Then

$$\sqrt{U_n^2} = \sqrt{S^2 \Delta \Phi_f^2 + U_i^2} \quad (4.94)$$

With frequencies in tens of kHz and higher, the main noises will be thermal and radiation noises. In many cases, with low modulation frequencies we can disregard the component caused by radiation noise. Therefore, in practice, current noises are often considered the basic noises of the photoresistors. In this case, for the solution of the problem of which noises can be disregarded and which should be considered in the calculation of threshold sensitivity, it is necessary to know their spectral distribution. A typical dependence of the mean square noise on the frequency of modulation of radiation flux is presented Fig. 4.11.

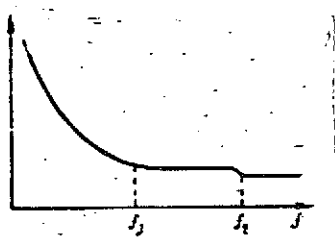


Fig. 4.11. Dependence of mean square noise of a receiver on frequency.

Current noise predominates in the region of low frequencies. The limit of this region f_1 lies within limits up to 1000 Hz. In the frequency band up to tens of kHz, generation-recombination noise is predominant, and with frequencies of tens of kHz and higher, the basic noises will be thermal and radiation.

The characteristics of several types of general-purpose photoresistors produced by industry are presented in table [20].

The frequency responses for a number of models of photoresistors which are presented in the tables in work [20] are shown in Fig. 4.12, and the character-

istics of relative spectral sensitivity of these receivers are given in Fig. 4.13.

To raise the sensitivity of the photoresistors, recourse is had to a reduction in the equilibrium concentration of the current carrier by means of the deep-freezing of the photosensitive layer. The parameters of photoresistance during cooling change rather significantly. Thus, with lead sulfide photoresistors, depending on the degree of cooling of the photolayer, the long-wave limit of sensitivity is shifted to the right up to 4-5 μm (Fig. 4.14), the dark resistance increases considerably, and the time constant increases.

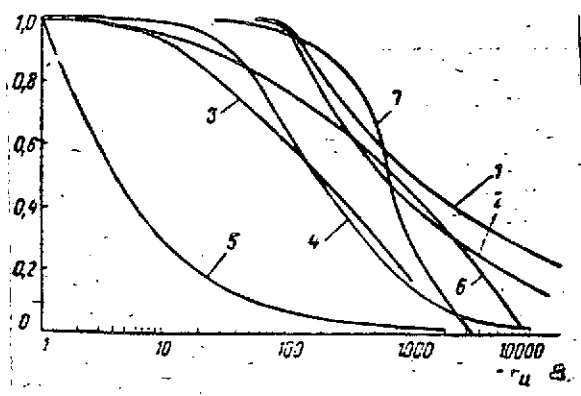


Fig. 4.12. Frequency characteristics of photoresistors: 1. FS (photoresistor; PK) K-1; 2. PRK-2; 3. PRA; 4,5. PRK-M1; 6. PbSe; 7. CdSe; 8. kHz.

The cooling of the sensitive layers of the photoresistors can be accomplished ^{/117} by special coolants having a sufficiently low temperature of melting or evaporation. Various substances are used as coolants which are in a liquid or solid state; dry ice, liquid nitrogen, liquid air, and liquid helium, whose temperatures of evaporation are respectively 195, 90, and 77K.

In cooling the sensitive layers the photoresistors are fastened in the inner cavity of a Dewar vessel (Fig. 4.15) in which a specific quantity of cooling substance

is placed during operation. Heat removal from the receiver is accomplished with the use of a metal screen.

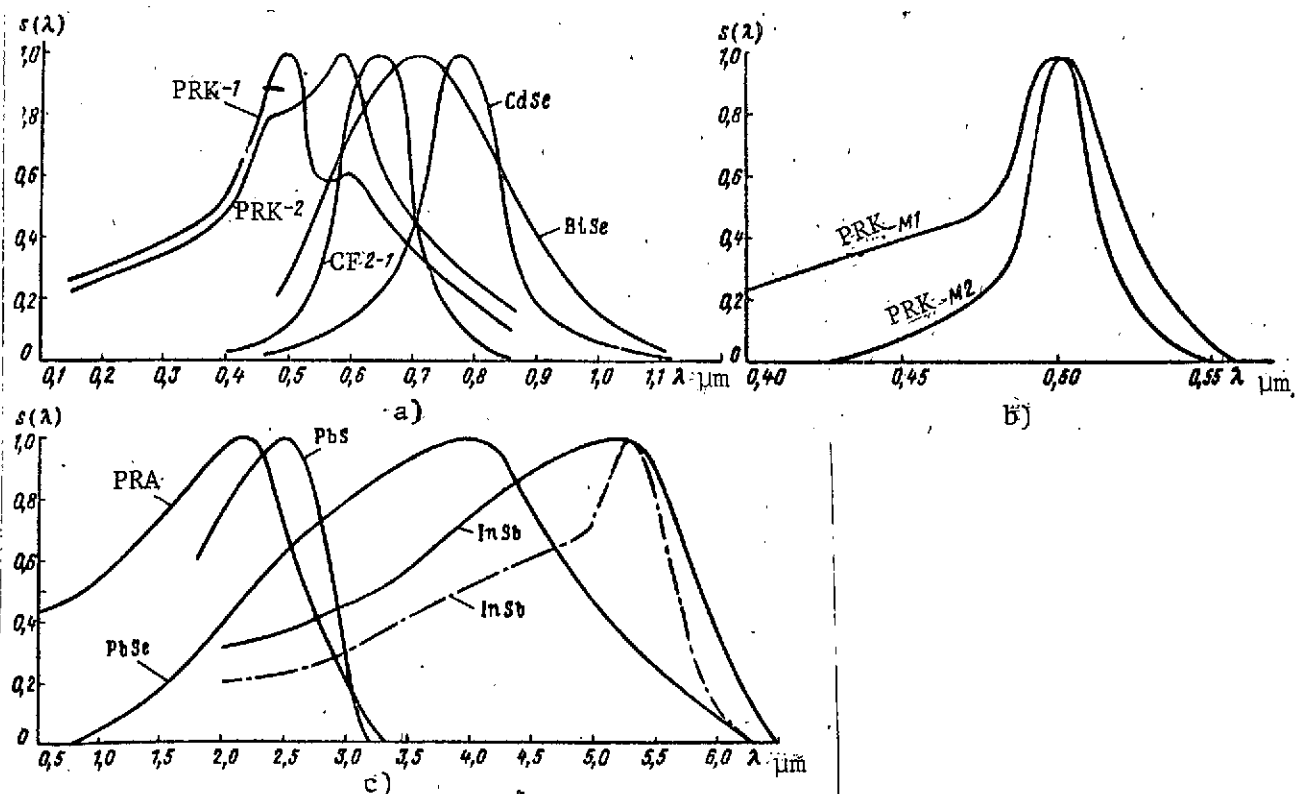


Fig. 4.13. Relative spectral sensitivity of photoresistors: a and b - for the short-wave region of the spectrum; c - for the long-wave region of the spectrum

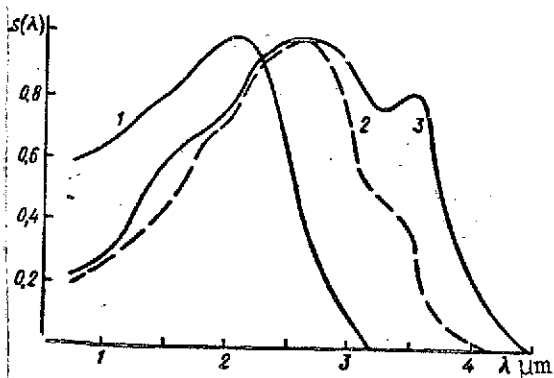


Fig. 4.14. Change in spectral sensitivity in the cooling of a sensitive layer: 1. PbS (293K); 2. PbS (195K); 3. PbS (90K).

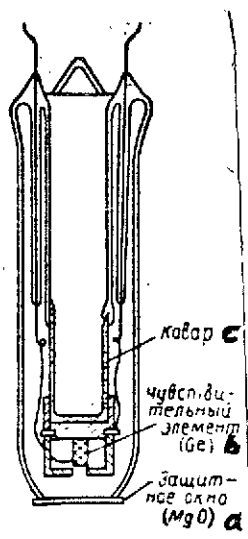


Fig. 4.15. Diagram of the design of a cooled photoresistor.

Key: a. Protective window (MgO); b. sensitive element, (Ge); c. Kovar

Besides the indicated method, the sensitive layers are cooled by means of the expansion of gas under high pressure. The cooling of the photoresistor to the required temperature will occur under the condition where the temperature of the expanding gas is lower than the temperature of inversion. In this case, the gas expanding in the cavity will be cooled itself and will cool the sensitive layer of the receiver and the gas brought up to the cavity. The in-

indicated process will continue until the establishment of a state of equilibrium in which some quantity of liquified gas will always be located on the sensitive layer and the temperature of the layer will equal the evaporation temperature of this gas.

The thermoelectric method based on the Peltier effect may also find application for cooling the sensitive layers. Especially intensive cooling occurs at soldered joints which consist of electronic and p-type semiconductors. One stage of such a cooling device provides a temperature drop of up to 50K. With the use of several stages, a temperature drop of up to 150K can be achieved.

/119

4.5. Photodiodes and Phototriodes

Photodiodes are based on the use of one-way conductivity of a p-n junction. They can operate both in a valve mode (without an external power-supply source) and in a photodiode mode where a considerable power supply voltage is applied in the opposite direction.

The operating principle of a photodiode consists of the following. When the photodiode is not illuminated and a reverse voltage is

fed to the p-n junction, a small current will flow through it which is caused by the minority carrier-electrons in the p region and the holes in the n region of the semiconductor.

With the illumination of the photodiode (Fig. 4.16) electron-hole pairs arise on the boundary of the n region. The holes,

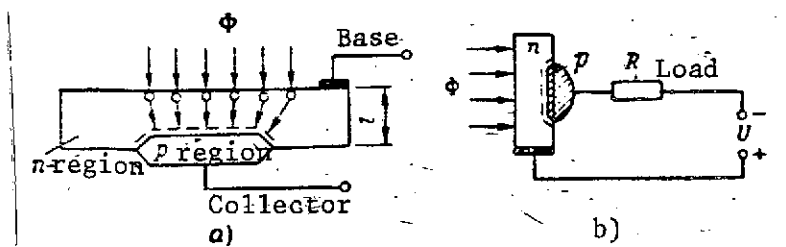


Fig. 4.16. Design and circuit of power supply of a photodiode: a. diagram of design; b. power-supply circuit.

being minority carriers in this region, are deeply diffused and, approaching the p-n junction, are carried away to the p region. The thickness of the n region must be less than the diffusion length and the holes must reach the p region before recombination. The increase in the current of the minority carriers

causes an additional voltage drop across the load resistor.

In operation in the valve and photodiode mode, the photodiodes are connected to the input of the amplifier in accordance with the circuits presented in Fig. 4.17. The expression for the current I in the circuit of the photodiode in the valve mode has the form [38]

/120

$$I = I_p - I_s (e^{U_R/U_T} - 1), \quad (4.95)$$

where U_R is the voltage drop across the load resistor from the current which flows in the internal circuit; $U_T = kT/e$ is the temperature potential; I_s is the saturation current which flows through the contact junction in the reverse direction; $I_p = SP$ is the photoelectric current caused by the radiation flux falling on the sensitive layer.

For the photodiode mode, the current in the outer circuit of the photodiode with its excitation by a radiation flux will be determined by the equation

$$I = I_p - I_s \left(e^{\frac{U_R - U}{U_T}} - 1 \right), \quad (4.96)$$

where U is the voltage of the external source.

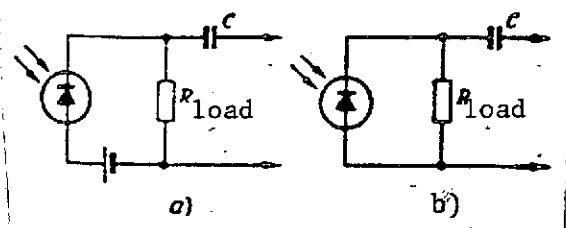


Fig. 4.17. Diagram of the connection of the photodiodes: a. in photodiode mode and b. in valve mode.

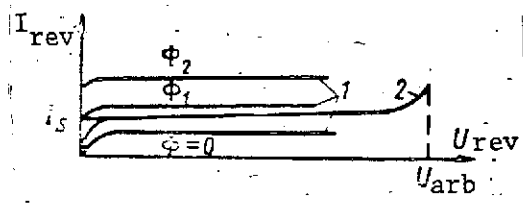


Fig. 4.18. Characteristics of a photodiode: 1. ideal; 2. actual characteristic of a dark current of a photodiode.

current has some slope. With some voltage U_{arb} , an irreversible thermal breakdown occurs in the p-n junction. Because of this, the photodiodes operate with voltages which are considerably less than the breakdown voltages.

The basic characteristics of the photodiodes are evaluated from the influence of the luminous flux or radiation flux, and the current of the photodiodes is taken as the response.

The threshold sensitivity of the photodiodes depends on the level of the fluctuation signal caused by the intrinsic noises, pertaining to which are shot, thermal, current and radiation noises.

The nature of shot noise was considered above. The expression which determines it has the form

The obtained equation provides the possibility of constructing the characteristic of the photodiode with different values of incident radiation Φ . If $\Phi = 0$, we obtain the current-voltage characteristic which is called dark (Fig. 4.18). However, under actual conditions the operation of the photodiode is influenced by the current of thermogeneration in the region of the junction which depends on the value of reverse voltage and is determined by the expression

$$I_p = k_p \sqrt{U}, \quad (4.97)$$

where k_p is the proportionality factor.

Therefore, the actual characteristic of a dark

$$\overline{I_s^2} = 2eI\Delta f,$$

where I is the current which flows through the photodiode.

The thermal noise of the photodiode is considered as applicable to the resistance of the basic semiconductor (base) R_b . The mean square value of the current of this noise will be

$$\overline{I_d^2} = 4kTR_b^{-1}\Delta f. \quad (4.98)$$

One of the basic components of the total noise current of the photodiode, especially with low frequencies of modulation of the radiation flux, is the current $1/f$ -noise.

It is believed that this type of noise is caused by fluctuations in the surface leakage of the current. The mean square value of this component is determined by the expression

$$\overline{I_i^2} = AVU \frac{\Delta f}{f}, \quad (4.99)$$

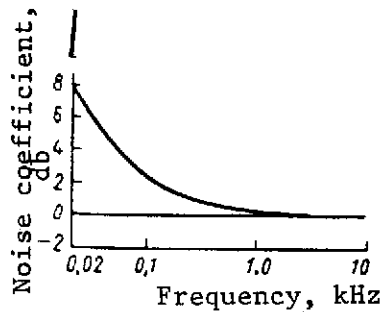
where U is the reverse voltage applied to the photodiode; A is the proportionality factor. /122

The radiation noise can be calculated from formula (4.48).

The mean square value of total noise current will be

$$\begin{aligned} \overline{I_n^2} = \overline{I_s^2} + \overline{I_d^2} + \overline{I_i^2} + \overline{I_r^2} = 2eI\Delta f + \\ + 4kTR_b^{-1}\Delta f + A \left\{ U \frac{\Delta f}{f} + 8kT\Phi S^2\Delta f \right\}. \end{aligned} \quad (4.100)$$

Let us note that the first three components are the basic ones, and in the region of low frequencies the main role is played by the noise current which, with an increase in frequency, is reduced to the level of white noise. In this case, the position of the boundary of predominance of noise current depends on the design and manufacturing technology of the photodiode. Thus, for example, the noise spectrum of a photodiode of indium antimonide (InSb) has a drop of excess noises to the level of white noise at a frequency on the order of 1 kHz (Fig. 4.19).



The threshold flux of photodiodes can be calculated from formula (4.68)

$$F_t = \frac{\sqrt{I_s^2}}{S^k}$$

Fig. 4.19. Noise spectrum of a photodiode of indium antimonide (InSb).

With the detection of small light signals modulated with a high frequency, the threshold sensitivity of the photodiode depends to a considerable degree on the value of the dark current which, in this case, causes the shot noise.

The dark current of a photodiode in the working range of voltages is considered constant. It is measured with small reverse voltages (usually with 1 V). The value of the dark current is sometimes characterized by the initial static resistance $R_{st} = 1/I_d$ (resistance to a direct current with $U = 1$ V). The value of the static resistance strongly depends on temperature ^{/123}

$$R_{st} = R_{st0} e^{(B/T - B/T_0)} \quad (4.101)$$

where R_{st0} is the initial static resistance with temperature T_0 ;

$B = \frac{T_1 T_2}{T_2 - T_1} \ln \frac{R_1}{R_2}$; and R_1 and R_2 are the resistance at temperatures T_1 and T_2 .

The dependence of the static resistance of a photodiode on temperature is presented in Fig. 4.20, and the nature of the change in dark current with increase in the temperature of the junction in Fig. 4.21.

The basic materials used to manufacture photodiodes are germanium and silicon. There are indications that gallium arsenide and germanium with gallium arsenide are also used for the creation of photodiodes [51].

The characteristic of the relative spectral sensitivity of photodiodes is shown in Fig. 4.22. All these photodiodes operate without cooling.

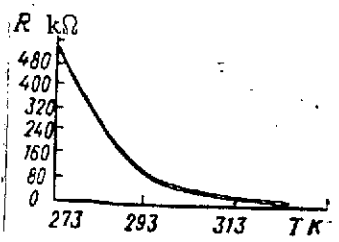


Fig. 4.20. Dependence of static resistance of a photodiode on temperature.

In addition, work [47] describes photodiodes on a base of such semiconductor materials as InSb, InAs, CsSe, and others. Rather deep cooling (to 77K) is required for their normal operation. The time constant τ of these photodiodes is extremely small and does not exceed 2 μ s. They possess high sensitivity in a broad band of the spectrum, which can be seen from the characteristics of relative spectral sensitivity presented in Fig. 4.23.

The direction of motion of the current carrier can be used for the creation of one more group of photoelectric receivers -- phototriodes. In these instruments, with their irradiation with a radiation flux the photocurrent not only is induced but is also amplified. Therefore, the integral sensitivity of the phototriodes reaches several amperes per lumen.

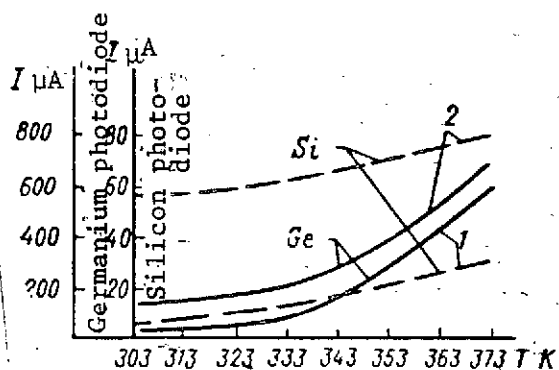


Fig. 4.21. Dependence of a dark current of germanium and silicon photodiodes on temperature: 1. with $F = 0.005$ lm; 2. with $F = 0$ lm.

The spectral characteristics of phototriodes are determined by the same factors as with photodiodes. Their threshold sensitivity depends on the level of the noises which have the same nature as those of photodiodes. The threshold flux of a phototriode is calculated from the formula

$$F_t^{(1)} = \frac{\sqrt{I^2}}{S_{pt} \sqrt{\Delta f}} \quad (4.102)$$

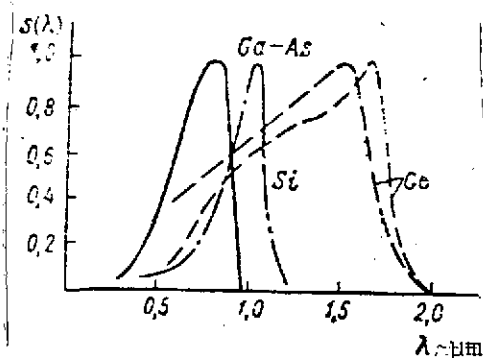


Fig. 4.22. Relative spectral sensitivity of photodiodes for the short-wave region of the spectrum.

Phototriodes can be connected in accordance with schemes with a free collector, free emitter, and with a free base. The first two schemes are similar to the connection of a phototriode in the diode mode. The connection of phototriodes in the triode mode differs in no way from the

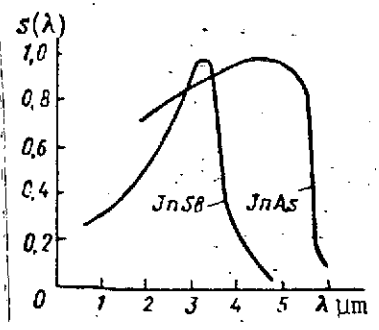


Fig. 4.23. Relative spectral sensitivity for the long-wave region of the spectrum.

connection of regular transistors. Most widespread is the scheme for connection with a common emitter.

Our industry is producing a germanium phototriode FT-1 (PT-1). Its characteristics are presented in the tables of work [20].

4.6. Photocells with a Longitudinal Photoelectric Effect (Inversion Photodiodes)

With the illumination of a semiconductor junction, a voltage arises between the two regions of the junction. With the nonuniform illumination of the sensitive layer, along with a transverse photo-emf, a photo-emf arises which is directed along the junction. This phenomenon received the name of longitudinal or lateral photoelectric effect.

Fig. 4.24a shows a diagram of an inversion photodiode on a germanium base of the n-type in which a region with p conductivity

/125

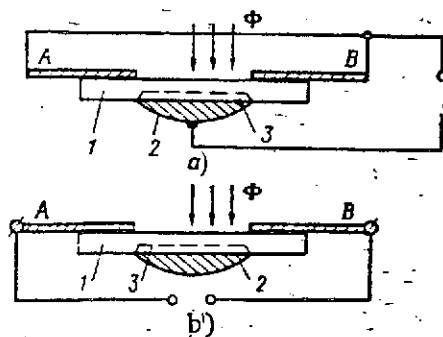


Fig. 4.24. Diagram of a photoelement with a longitudinal photoelectric effect: a. transverse photo-emf; b. longitudinal photo-emf; 1. n-layer of germanium; 2. indium; 3. layer of germanium.

has been created by the fusion of a drop of indium. With the illumination of the photocell on the germanium side, a transverse photo-emf arises between the electrode soldered to the indium and electrodes A and B. If the center of the light spot which falls on the photocell is shifted relative to the axis of symmetry, a longitudinal photo-emf appears between contacts A and B, whose sign changes with the passage of the light spot through the center (Fig. 4.24b). The value of this emf depends on the position of this spot with respect to the axis of symmetry (Fig. 4.25) and is determined by the expression

$$U_x = V_1 - V_2 = \frac{qI}{2\pi d} \ln \frac{d+x}{d-x}, \quad (4.103)$$

where V_1 and V_2 are the potentials of contacts 1 and 2 caused by the longitudinal photo-emf with the removal of the light spot to distance x from the center; $2d$ is the distance between the contacts; ρ is the resistivity of the n region; l is the thickness of the n region; and I is the total photocurrent.

The relation for the output voltage across the base electrodes as a function of the position of the light spot $U_x = f(x)$ has received the name of inversion characteristic. The appearance of this characteristic is shown in Fig. 4.26. With small shifts of the spot relative to the center, equation (4.103) is transformed to the form

$$U_x = \frac{qI}{2\pi l} \frac{x}{d} \quad (4.104)$$

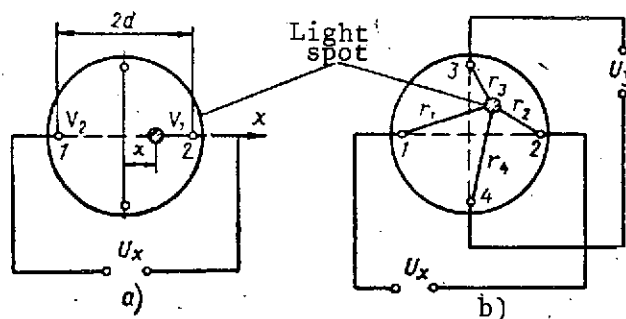


Fig. 4.25. Photo-emf which arises at the output of a photocell with longitudinal photoelectric effect: a. two-contact; b. four-contact; 1, 2, 3. contacts

coordinates of the light spot. The resulting voltages along the channels equal

$$U_x = \frac{qI}{2\pi l} \ln \frac{r_1}{r_2} \quad (4.105)$$

$$U_y = \frac{qI}{2\pi l} \ln \frac{r_3}{r_4} \quad (4.106)$$

Expressions (4.103), (4.104), or, in the general case, (4.105) and (4.106) are the equations of an inversion photodiode

Since in many cases photocells with a longitudinal photoelectric effect are used for the recording of small displacements of the light spot from center, this expression is extremely convenient for practical use.

If we arrange four contacts rather than two along the edges of the sensitive layer (two each on mutually perpendicular directions), as is shown in Fig. 4.25b, we obtain a two-dimensional photocell which permits determining the

/126

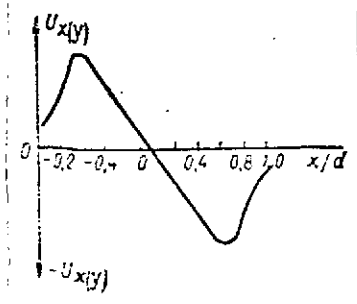


Fig. 4.26. Inversion characteristic of a photocell with longitudinal photoelectric effect.

from which we can obtain not only the values of output voltages U_x and U_y , but also data on the sensitivity, linearity, and slope of the inversion characteristic. From these equations, it follows that an increase in sensitivity can be obtained by increasing the resistivity of the n layer and reducing its thickness ℓ .

Since the photocurrent I depends on the value of the radiation flux which falls on the receiver, the value of the output signal will also depend not only on the position of the spot, but also on the radiation power in the spot. In this regard, this dependence remains linear with a change in the incident flux from the minimum (threshold) values by 3-4 orders of magnitude.

We transform these expressions in the following manner for convenience in using them. Let us present the photocurrent of the receiver in the form $I = i_{sp}\Phi$ (excluding the saturation section) and we introduce the designation

/127

$$\frac{e i_{\text{conv}}}{\pi \ell d} S_{\text{long}} \quad (4.107)$$

Then expressions (4.104), (4.105), and (4.106) take the corresponding form

$$U_x = S_{\text{long}} \Phi x; \quad (4.108)$$

$$U_x = S_{\text{long}} \Phi \frac{d}{2} \ln \frac{r_1}{r_2}; \quad (4.109)$$

$$U_y = S_{\text{long}} \Phi \frac{d}{2} \ln \frac{r_3}{r_4}, \quad (4.110)$$

where S_{long} is the sensitivity of a photocell with a longitudinal photoelectric effect measured in $\text{V} \cdot \text{W}^{-1} \text{mm}^{-1}$ or $\text{V} \cdot \text{lm}^{-1} \text{mm}^{-1}$. The sensitivity of some types of inversion photodiodes reaches several tens of $\text{V} \cdot \text{W}^{-1} \text{mm}^{-1}$ and the linear zone comprises approximately 20% of the distance between the contacts.

Relations (4.108), (4.109), and (4.110) show that the change in the strength of radiation in the spot has a substantial

influence on the value of the output signal which proves to be proportional to the incident radiation flux Φ . This effect leads to indeterminacy since the reason for the change in signal at the output remains unknown. Elimination of this indeterminacy is achieved in various ways. In a number of cases, when the photocell is used to determine direction to a powerful emitter, the effect of the saturation of the photocurrent is used. When operating in a saturation mode, the current of the photocell attains its maximum value and remains unchanged with insignificant fluctuations in the incident radiation flux. As a result, the signal at the output will depend only on the position of the spot on the sensitive layer. However, the applicability of the indicated method is extremely limited.

In practice, the task arises of determining the direction to low-power emitters or emitters sufficiently powerful but at great distances away and emitters the value of whose flux at the input is clearly insufficient for the operation of the photodiode in the saturation mode. This task arises in operation with radiation fluxes close to threshold fluxes. Here, the change in the dependence of the output signal on the value of the incident radiation flux is caused by fluctuations in the radiation flux and also by the change in the distance between the instrument and the emitter. In this case, the effect of inconstancy of the incident radiation flux can be excluded, using the signal from the output of the receiver which is caused by the transverse photoelectric effect.

For this, suppose that a radiation flux falls on the input /128 of a photocell which is focused by the optical system in the form of a spot whose center is removed some distance from the center of the photocell. Then the signals caused by the longitudinal photoelectric effect at the output of the receiver's channels will be determined by expressions (4.108) and (4.109).

At the same time, the signal which is read between electrodes 4(3) and 5 (Fig. 4.27) is caused by a regular transverse photoelectric effect and equals

$$U = S\Phi \quad (4.111)$$

where S is the integral sensitivity of the photocell for the transverse photoelectric effect.

Expressing Φ from (4.111) and substituting it in (4.109) and (4.110), we obtain

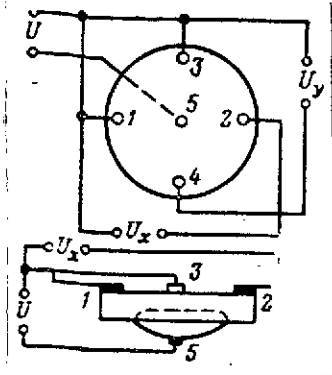


Fig. 4.27. Use of the transverse photoelectric effect to compensate for the change in value of the radiant flux which falls on the receiver: 1, 2, 3, 4, 5, - contacts.

$$\ln \frac{r_1}{r_2} = \frac{S}{S_{\text{long}}} \frac{2}{d} \frac{1}{U} U_x; \quad (4.112)$$

$$\ln \frac{r_3}{r_4} = \frac{S}{S_{\text{long}}} \frac{2}{d} \frac{1}{U} U_y. \quad (4.113)$$

Similarly, from (4.108) for the linear zone of the photocell, we will have

$$x = \frac{S}{S_{\text{long}}} \frac{1}{U} U_x. \quad (4.114)$$

Thus, if the signals over the channels caused by the longitudinal photoelectric effect are normalized by the signal of the transverse photoelectric effect and the obtained result is multiplied by a value constant for the given receiver, we obtain information which unambiguously determines the position of the radiation spot on the sensitive layer of the receiver.

What has been presented shows that, on the basis of inversion photodiodes, electro-optical instruments can be created which permit determining the angular coordinates of radiation objects relative to the zero axis. In this, the sign of the output signals will indicate the direction of misalignment. Feeding a constant voltage to the base contacts (1, 2, 3, 4), we can change the position of the zero point of the inversion characteristic which is necessary in a number of high-speed electro-optical instruments. Executing the electronic modulation of the output signal, in accordance with any given law, we can change the slope of the inversion characteristic and, consequently, the output signal, which permits using the photocells in circuits with alternating current amplifiers (without preliminary modulation of the radiation flux).

The threshold sensitivity of inversion photodiodes, just as ^{/129} with other photoelectric receivers, is determined by their noises. The basic components of the noises with this type of receiver are the same as with regular photodiodes. Furthermore, it is necessary to consider the zero drift which is characterized by the amount of displacement of the position of the point of zero potential under the influence of the change in the internal structure of the junction, temperature, and humidity with time.

A merit of the photocells with a longitudinal photoelectric effect, along with the possibility of determining the coordinates

of the radiating objects with simple instrumental realization, is the practical independence of the precision of measurement from the magnitude of the spot of scatter in whose form the radiation is focused on the sensitive layer.

At the present time, inversion photodiodes are made on the base of germanium, silicon, selenium, indium antimonide, and other materials. Their sensitivity sometimes reaches 40 V/(W·mm) with time constants of a few μ s. The threshold fluxes of germanium inversion photodiodes comprise approximately $\Phi_t \sim 2 \cdot 10^{-9}$ lm·mm for an emitter with $T_{col} = 2848$ K, and with silicon inversion photodiodes, $\Phi_t = (4-8) \cdot 10^{-10}$ W with the removal of the spot 9.5 mm from the center.

More detailed information on the design, operating principle, characteristics, and possible applications is presented in [47].

4.7. Thermal Radiation Receivers

The basic representatives of this group of radiation flux receivers which assure the conversion of the radiation falling on them to electrical signals are thermoelements and bolometers.

The specific thermo-emf which is characterized by the amount of emf which arises with a single temperature drop

$$U_{sp} = \frac{U_{th}}{\Delta T} \quad (4.115)$$

is usually small for metallic thermoelements and comprises several tens of microvolts per degree.

A thermo-emf also arises in the junctions of semiconductors. A higher specific thermo-emf is characteristic of them, which is explained by the dependence of the quantity and energy of current carriers on temperature. Moreover, in thermoelements of semiconductors, the addition of the emf of electronic and p-type semiconductors occurs.

The integral sensitivity of metallic thermoelements lies within limits of from 3 to 5 μ V/ μ W. With semiconductor thermoelements, it reaches several tens of μ V/ μ W. The values of the threshold fluxes of the photoelements lie within limits of from 10^{-8} to 10^{-9} W for any emitter, since the thermoelement is a non-selective receiver of radiation flux. -130

The time constants τ of different types of thermoelements fluctuate from fractions of a second to several milliseconds.

The shortcomings of the thermoelements are their low internal resistance, great time lag, and complexity of construction of sufficiently sensitive thermoelements. All this serves as a serious obstacle for their use in high-speed electro-optical equipment.

Such thermal receivers as bolometers are finding comparatively broad application in various types of electro-optical instruments, especially where long-wave infrared radiation is used.

The sensitive layer of a bolometer is a thin metallic or semiconductor film which is actually a thermistor. Usually, a bolometer consists of two heat-sensitive resistors. One of them is receiving and is subjected to the influence of a radiation flux, and the other (compensation) serves to compensate for the effect of temperature change of the external environment.

The change in resistance of the sensitive layer of the bolometer with its heating depends on the value of the temperature coefficient α which is determined by the expression

$$\alpha = \frac{1}{R} \cdot \frac{dR}{dT}, \quad (4.116)$$

where R is the resistance of the sensitive layer of the bolometer at temperature T .

For the majority of metals, the temperature coefficient of the resistor is expressed by the relation

$$\alpha = T^{-1}. \quad (4.117)$$

Therefore, for a temperature of $\sim 300\text{K}$, at which bolometers usually operate, the value of coefficient α with metallic sensitive layers is approximately 0.0033.

The resistance of the semiconductors in some limited temperature band follows the exponential law

$$R = R_0 e^{(B/T - B/T_0)}, \quad (4.118)$$

where $B = 3000K$ is a positive constant; R is the resistance of the semiconductor with temperature T_0 .

Differentiating (4.118) for variable T and substituting $1/R$ and dR/dT in (4.116), we obtain

$$\alpha = \frac{R_0 e^{(B/T - B/T_0)} (-B/T^2)}{R_0 e^{(B/T - B/T_0)}} = -\frac{B}{T^2},$$

whence, with consideration of the fact that $B = 3000K$, we have /131

$$\alpha = -\frac{3000}{T^2}. \quad (4.119)$$

Thus, with semiconductor materials, the coefficient of temperature resistance is negative and its absolute value is greater than with metals. Thus, with $T = 300K$; with semiconductors, $\alpha = 0.333$, i.e., an order of magnitude greater than with metals. Therefore, semiconductor bolometers possess greater sensitivity compared to metallic ones.

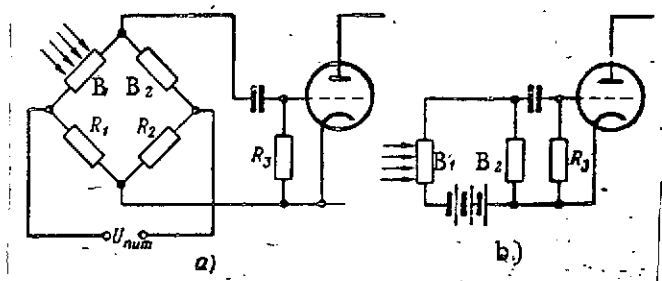


Fig. 4.28. Diagrams of the connection of bolometers to the input of and amplifier: a. bridge scheme; b. compensation bolometer accomplishes the work of a load resistor.

Signals read from the output of a bolometer, as a rule, are small and must first be amplified before their direct use in the circuit of the instrument. At the input of the amplifier, bolometers are connected either in accordance with a bridge scheme (Fig. 4.28a) or in accordance with a scheme in which the compensation elements plays the role of load resistor (Fig. 4.28b).

In the bridge connection scheme, with a pre-balanced bridge ($R_1 R_{B2} = R_2 R_{B1}$), the irradiation of the sensitive layer B_1 causes the unbalancing of the bridge and the appearance of a signal on the grid of the input tube of the amplifier. The simultaneous change of temperature of both sensitive layers (B_1 and B_2) under the influence of the external

environment does not cause the unbalancing of the bridge and, consequently, the appearance of a signal at the input of the amplifier.

The power supply of the bridge is accomplished either with a constant or with a variable voltage with a frequency of several hundreds or thousand Hz. So as not to use direct current amplifiers whose basic shortcoming is zero drift, the radiation flux is usually modulated. If the power supply of the bridge is accomplished with a constant voltage, the amplification of the signals from the output of the bolometer is accomplished on the modulation frequency. With the power supply with a variable voltage, the signal is amplified first on one frequency, for example, on the frequency of the power supply voltage, and then (after detection) on the modulation frequency. The connection of the bolometer to the input of the amplifier in accordance with the scheme presented in Fig. 4.28b causes a power supply with a constant voltage alone.

/132

The change in the resistance of bolometer B_1 by the value ΔR with irradiation causes the redistribution of the voltages between B_1 and B_2 and the signal appears at the input of the amplifier

$$U_{in} = LI\Delta R, \quad (4.120)$$

where I is the current which flows through bolometer B_1 ; L is the coefficient which depends on the connection scheme and the relationship of resistors R_{B1} , R_{B2} , and the load resistor.

With a bridge connection scheme and the equality $R_{B1} = R_{B2} = R_1 = R_2 = R$, and under the condition $R \gg R_3$, for the scheme (Fig. 4.28), $L = 1/2$. If the power supply voltage is U_B , then from (4.120) we find the value of the input signal

$$U_{in} = \frac{1}{2} I \Delta R = \frac{U_B}{4} \frac{\Delta R}{R}. \quad (4.121)$$

Inasmuch as the change in the resistance of the bolometer under the influence of an incident radiation flux is small, in changing in equation (4.116) to the final increases in resistance and temperature, we can write

$$\frac{\Delta R}{R} = \alpha \Delta T.$$

With consideration of this relation, from (4.121) we obtain the expression for the value of the signal from the bolometer at the input of the amplifier

$$U_{in} = \frac{1}{4} U_B \alpha \Delta T. \quad (4.122)$$

The basic characteristics in accordance with which a comparative evaluation of the bolometers is accomplished are the integral sensitivity, threshold flux, and time lag.

The integral sensitivity S of the bolometers is determined on the basis of (4.3).

Inasmuch as the bolometers in a broad spectral interval are nonselective receivers, the indication of the type of emitter according to which the measurements were conducted is not mandatory. The type of emitter and its characteristics must be indicated only in those cases where measurements of sensitivity are conducted with the presence of a selective filter in front of the sensitive layer of the bolometer.

Using (4.3) and the value U_{in} from (4.122), we have

$$S = U_B \frac{\alpha \Delta T}{4 \Phi}. \quad (4.123)$$

From the equation of the thermal state of the sensitive layer of the bolometer

$$c \frac{d(\Delta T)}{dt} + \beta \Delta T = \Phi, \quad (4.124)$$

where c is the heat capacity of the sensitive layer; β is the heat transfer coefficient.

123
/133

In the established mode $\left(\frac{d(\Delta T)}{dt} = 0 \right)$ we have

$$\Delta T = \Phi / \beta.$$

With consideration of the found relation on the basis of (4.123) we obtain

$$S = \frac{1}{4} U_B \frac{\alpha}{\beta} \quad (4.125)$$

The heat transfer coefficient β includes the component for temperature radiation of the sensitive layer and the component caused by the heat conductivity of the leads.

From expression (4.125), it can be seen that the integral sensitivity of the bolometer is proportional to the temperature coefficient of the resistance and the applied voltage and inversely proportional to the heat transfer coefficient β . To increase the integral sensitivity, it is necessary to reduce the heat transfer. This is attained by placing the sensitive layer of the bolometer in a vacuum, as a result of which losses in heating the ambient air are reduced, and also by the employment of thin connecting conductors with low heat conductivity.

The time lag of bolometers is determined by the final time of heating and cooling of the sensitive layer of the bolometers to modulated radiation. The expression for the integral sensitivity of bolometers with their irradiation with a variable radiation flux has the form

$$S_f = \frac{S_0}{\sqrt{1 + (2\pi f \tau)^2}} \quad (4.126)$$

where τ is the time constant equal to c/β ; S_0 is the integral sensitivity of the bolometer with frequency modulation close to $f = 0$.

From formula (4.126) it can be seen that with large time constants, sensitivity S_f is decreased significantly with an increase in frequency. In some cases, the sensitive layers of the bolometers are applied to highly conductive backings. This, naturally, leads to an increase in coefficient β and a reduction in the time constant τ . However, with a reduction in the time constant, the integral sensitivity S_0 is reduced just as many times. The increase in thermal scatter β permits increasing the power supply voltage of the bolometer which leads, as can be seen from formula (4.125), to an increase in integral sensitivity. As a result, despite some reduction in the value S_0 in a specific frequency band, a considerable gain in integral sensitivity is attained.

The threshold sensitivity of the bolometers is determined by the level of their intrinsic noises. The basic noises of bolometers are thermal, radiation, and current.

The thermal noises of bolometers are calculated from formula (4.52)

$$\overline{U_t^2} = 4kTR\Delta f,$$

where R is the resistance of the bolometer and T is its temperature.

The current noises of the bolometers depend on the characteristics of the material of the sensitive layer and are determined by the expression

$$\overline{U_i^2} = A_s R_B^2 I^2 \frac{\Delta f}{f}. \quad (4.127)$$

The spectral density of the current noise of a bolometer is described by the equation $G(f) = c/f$, and the necessary calculations of the magnitude of the current noises is performed from the formulas of Section 4.4.

Radiation noises are caused by fluctuations in the radiation flux which falls on the receiver and the radiation which arises during heat exchange of the sensitive layer of the bolometers with the environment.

The mean square value of the fluctuations in radiation flux from an object on the input of the bolometer is calculated from the formula

$$\sqrt{\Delta \Phi_{ob}^2} = \sqrt{16kT_{ob}\Phi_{ob}\Delta f}, \quad (4.128)$$

where Φ_{ob} is the radiation flux from the object which reaches the sensitive layer of the bolometer; T_{ob} is the temperature of the radiating surface of the object; k is Boltzmann's constant.

The second component, which is caused by the radiant heat exchange of the sensitive layer with area A which occurs with temperature T_1 and an environment having temperature T_2 , is

found in the following manner. In [37] it is shown that the fluctuations in radiation flux $\Delta\Phi_f^2$ caused by the absorbed radiation are determined by the expression

$$\overline{\Delta\Phi_f^2} = 8kT_2 A_{\Sigma} T_2^4 \Delta f = 8kT_2 \Phi_f \Delta f. \quad (4.129)$$

Fluctuations emitted by the body of radiation flux will be

$$\overline{\Delta\Phi_e^2} = 8kT_1 A_{\Sigma} T_1^4 \Delta f = 8kT_1 \Phi_e \Delta f. \quad (4.130)$$

Since expressions (4.129) and (4.130) are independent, they can be added, as a result of which we obtain the total value of the dispersion of the value of the fluctuations of the radiation flux due to heat exchange

$$\overline{\Delta\Phi_r^2} = \overline{\Delta\Phi_e^2} + \overline{\Delta\Phi_f^2} = 8kA_{\Sigma}(T_1^5 + T_2^5) \Delta f = 8k(T_1 \Phi_e + T_2 \Phi_f) \Delta f. \quad (4.131)$$

If the temperature of the sensitive layer and the environment equal each other, then /135

$$\overline{\Delta\Phi_r^2} = 16kT_1 \Phi_1 \Delta f. \quad (4.132)$$

On the basis of (4.128) and (4.132), we obtain the following expression for the dispersion of the total radiation noise

$$\overline{\Delta\Phi_r^2} = \overline{\Delta\Phi_{ob}^2} + \overline{\Delta\Phi_r^2} = 16k(T_{ob} \Phi_{ob} + T_B \Phi_B) \Delta f. \quad (4.133)$$

In working with a radiation flux close to the threshold values ($\Phi_{ob} \sim \Phi_f$), in uncooled bolometers the main role is played by fluctuations caused by the heat exchange (the second term in expression (4.133)).

The dispersion of the radiation noise, determined as $\overline{\Delta\Phi^2 S^2}$, will be

$$\overline{U_r^2} = \overline{\Delta\Phi_r^2 S^2} = 16k(T_{ob} \Phi_{ob} + T_B \Phi_B) \frac{S_0^2}{(\sqrt{1 + (2\pi f\tau)^2})^2} \Delta f. \quad (4.134)$$

Thus, the mean square value of the noise voltage of the bolometer through its basic components can be presented in the form

$$\sqrt{\overline{U_n^2} = \overline{U_T^2} + \overline{U_i^2} + \overline{U_r^2}} = (4kT_B R_B \Delta f + A_m R_B^{1/2} \Delta f / f + + 16k(T_{ob} \Phi_{ob} + T_B \Phi_B) \Delta f \frac{S_0^2}{(\sqrt{1 + (2\pi f \tau)^2})^2})^{1/2}. \quad (4.135)$$

In general form, the threshold flux of a bolometer in accordance with (4.19) will be

$$\Phi_{\bar{e}} = \frac{\sqrt{\overline{U_n^2}}}{S_f} = \frac{\sqrt{\left[\frac{4kT_B R_B + A_m R_B^{1/2} / f + 16k(T_{ob} \Phi_{ob} + T_B \Phi_B) \frac{S_0^2}{(\sqrt{1 + (2\pi f \tau)^2})^2}}{\Delta f} \right] \Delta f}}{S_0 \sqrt{1 + (2\pi f \tau)^2}} \quad (4.136)$$

or

$$\overline{\Phi_{\bar{e}}^2} = \frac{4kT_B R_B + A_m R_B^{1/2} / f}{S_0} \Delta f + 16k(T_{ob} \Phi_{ob} + T_B \Phi_B) \Delta f. \quad (4.136a)$$

We note that the basic types of noises with metallic bolometers are thermal, and with semiconductor bolometers, current.

Used as the materials for the manufacture of the sensitive layers in metallic bolometers are thin films of gold, nickel, bismuth, and several other metals. Used in semiconductor bolometers are oxides (oxides of manganese, nickel, cobalt), and also germanium, antimony, etc. The contact leads of the bolometers are usually made from silver or gold [20]. /136

Superconducting semiconductor bolometers are based on the use of the phenomenon of superconductivity. For pure metals, the transition to superconductivity occurs very rapidly, i.e., with an extremely small temperature drop. With some materials, the slope of this transition is less, which permits creating bolometers which are sensitive to a rather large temperature drop. The materials for the manufacture of sensitive layers of such bolometers are niobium and titanium nitride. Possessing a considerable threshold sensitivity (threshold flux on the order of $5 \cdot 10^{-10}$ W), these bolometers have a comparatively small time constant ($\tau \approx 0.5$ ms).

5.1. Purpose and Classification of Analyzers

With the use of analyzers, an analysis of the field of view is conducted, and signals are generated which correspond unambiguously to the angular coordinates of a radiating object relative to the axis of the instrument.

According to the method for discriminating error signals in electro-optical equipment the following types of analyzers are distinguished:

- Devices which react to a change in signal phase;
- Devices which react to the change in amplitude and polarity of the signal;
- Devices which use the change in signal frequency;
- Devices which react to a change in signal duration;
- Combined analyzers.

Usually, the composition of an analyzer includes a modulating device (radiation flux modulator), radiation receiver, and units of the electronic circuit which assure the shaping of error signals in the required coordinate system. The main element of an analyzer, which determines the method of shaping the error signals and the structure of the electronic circuit, is the radiation flux modulator. /137

Radiation flux modulation has a specific property in comparison with the modulation of electromagnetic radiation on radio frequencies since the radiation flux which falls on the radiation receiver changes slowly and does not contain high-frequency components.

The modulators are characterized by coefficients of modulation of the radiation flux from objects and backgrounds:

$$K_{m.o} = \frac{\Phi_{o \max} - \Phi_{o \min}}{\Phi_{o \text{ tot}}} \quad \text{or} \quad k_{m.b} = \frac{\Phi_{b \max} - \Phi_{b \min}}{\Phi_{b \text{ tot}}}, \quad (5.1)$$

where $K_{m.o}$ and $K_{m.b}$ are coefficients of the modulation of radiation fluxes from objects and backgrounds; $\Phi_{o \text{ tot}}$ and $\Phi_{b \text{ tot}}$ are the values of radiation fluxes from an object and background which fall on a modulator; $\Phi_{o \max}$ and $\Phi_{b \max}$ are the main values of radiation fluxes from an object and background which fall on a receiver during one modulation period; $\Phi_{o \min}$

and $\Phi_{b \min}$ are the minimum values of radiation fluxes from an object and background which fall on a radiation receiver during one modulation period. The condition $\Phi_{\max} = \Phi_{\text{tot}}$ is valid for many types of modulators.

Designs of modulators envision the possibility of different modulation of radiation fluxes from objects and backgrounds. The larger the modulation factor of flux from an object and the smaller the modulation factor of flux from the background, the more perfected is the design of the modulating device considered, since with a reduction in the value of $k_{m.b.}$ the level of radiation interference (external noise) is reduced on the input of the amplifier.

Two types of modulation of radiation flux find employment: sine-wave and square-wave (Fig. 5.1). With sine-wave modulation, the function of the change in radiation flux behind the modulator can be written in the following form:

$$\Phi(t) = \left(\frac{\Phi_{\max} + \Phi_{\min}}{2} + \frac{\Phi_{\max} - \Phi_{\min}}{2} \cos(\omega t - \theta) \right), \quad (5.2)$$

where ω is the modulation frequency and θ is the signal phase.

With square-wave modulation, the function of the change in radiation flux behind the modulator can be written in the form of an expansion in a Fourier series

$$\Phi(t) = \frac{\Phi_{\max} + \Phi_{\min}}{2} + \frac{\Phi_{\max} - \Phi_{\min}}{2} \sum_{k=1}^{\infty} (-1)^{k+1} \frac{\cos[(2k-1)\omega t - \theta_k]}{2k-1}, \quad (5.3)$$

where $k = 1, 2, 3 \dots$ is the natural series of numbers; θ_k is the phase of the k -th harmonic of the signal. /138

Rotating opaque disks with cuts of a specific shape, frequency rasters, cylinders, screens, fixed diaphragms with apertures, and others can be employed as modulators. With the use of fixed modulating diaphragms, modulation of the radiation flux is accomplished due to the displacement of the object's image over the surface of the diaphragm or the surface of the radiation receiver.

In some instruments, the radiation flux is not modulated. In this case, information on the coordinates of the radiating object is obtained thanks to the determination of the position

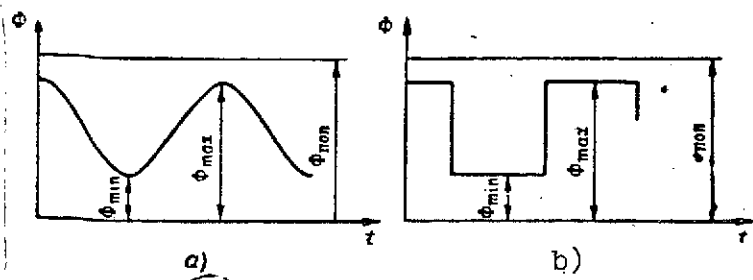


Fig. 5.1. Types of modulation of radiation flux: a. sine-wave; b. square wave.

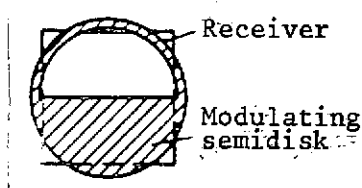


Fig. 5.2. Mutual position of a receiver and modulator made in the form of a rotating semidisk,

of the objects' image on the surface of the radiation receiver which is, for example, a mosaic or inversion photodiode.

5.2. Phase Analyzers

The shaping of error signals in analyzers of this type is based on the comparison of the phase of the operating signal with the phase of the reference signals. In the simplest type of phase analyzer, a rotating opaque semidisk (screen) is used as a modulator. The axis of rotation of the semidisk coincides with the optical axis of the lens and passes through the center of the sensitive layer of the receiver (Fig. 5.2). If the image of a point-radiating object is projected on the radiation receiver, then with the rotation of the semidisk, square-wave pulses, which are caused by the radiation of the object, go from the output of the receiver to the input of the amplifier.

The recurrence rate of these pulses is equal to the recurrence frequency of the semidisk, and the phase to the phasing angle of the object.

Various types of phase commutators which operate synchronously with the modulator are usually used as shaping and separating devices. Such commutators may be mechanical, electronic, or semiconductor devices.

/139

The simplest type is the collector-type mechanical phase commutator. It rotates synchronously with the modulating semidisk and operates in the mode of a full-wave rectifier. A schematic diagram of an analyzer is presented in Fig. 5.3. The load of the commutator, is connected between its brushes and the midpoints of the secondary windings of the output transformer of the amplifier. Schematically, this can be presented as shown in Fig. 5.4a. Thus, a voltage is fed to the commutator rings from the amplifier output with the use of brushes. Inasmuch as the first harmonic of the square pulses is used for the shaping of error signals, a narrow-band resonance amplifier of

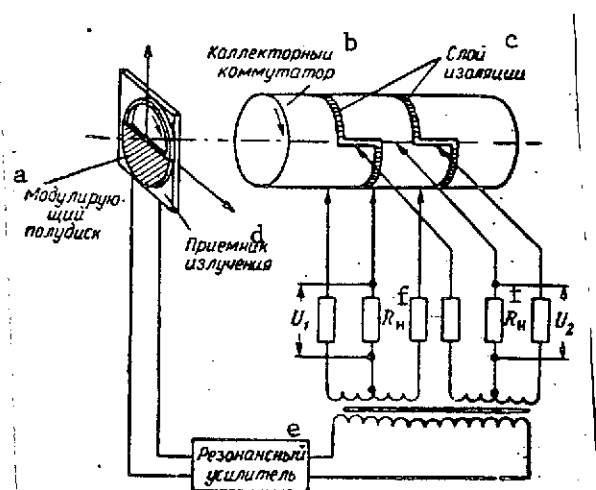


Fig. 5.3. Operating principle of a collector-type phase commutator: R_{load} - load resistor; U_1 - signal taken from load I of the channel; U_2 - signal taken from load II of the channel.

Key: a. Modulating semidisk; b. Collector commutator; c. Insulating layer; d. Radiation receiver; e. Resonance amplifier; f. R_{load}

throughout 2 and 3 of the fourth period through $R_{load 1}$ in the same direction as in the first period. A half-wave of voltage with a negative sign is created on the load resistor. With $\omega t = 3\pi/2$, the polarity on the ends of the transformer winding changes again, commutation occurs simultaneously with it, and a negative voltage again arises on the load resistor.

The current flows over the second channel in the first quarter of the period through the load resistor over circuit $R_{load 2}-R_2'$ in a positive direction. With $\omega t = \pi/2$, the polarity changes on the ends of the transformer winding, but commutation does not occur and, therefore, the current flows over the same circuit in the opposite direction, attaining its maximum value by the end of the half-period ($\omega t = \pi$). The negative quarter of the voltage wave $U_2(t)$ is created on load resistor $R_{load 2}$. When $\omega t = \pi$, commutation occurs and current flows over circuit $R_{load 2}-R_2$ through load resistor $R_{load 2}$ again in a positive direction. This will continue until the polarity changes on the transformer output, which will occur with $\omega t = 3\pi/2$. Finally,

photocurrents is used in the circuit. In this regard, the phase of the sine-wave voltage depends on the position of the object in the field of view and changes with a change in the sign of the error.

Let us examine the operation of a commutator with the presence of an error angle only for coordinate 1, when the phasing angle $\theta = \pi/2$ (Fig. 5.4b).

During the first quarter of the modulation period, the current flows through the load resistor $R_{load 1}$ from right to left (we take this direction of the current and the voltage U_1 corresponding to it as negative) /140 and a voltage drop with a negative sign is created on the load. With $\omega t = \pi/2$, the polarity of the signal on the ends of the transformer winding changes and occurring at the same time is commutation which leads to the case where the current over the circuit $R_1'-R_{load 1}$ flows

/141

in the last quarter of the modulation period, the current again flows through load resistor $R_{load,2}$ in a negative direction and so on.

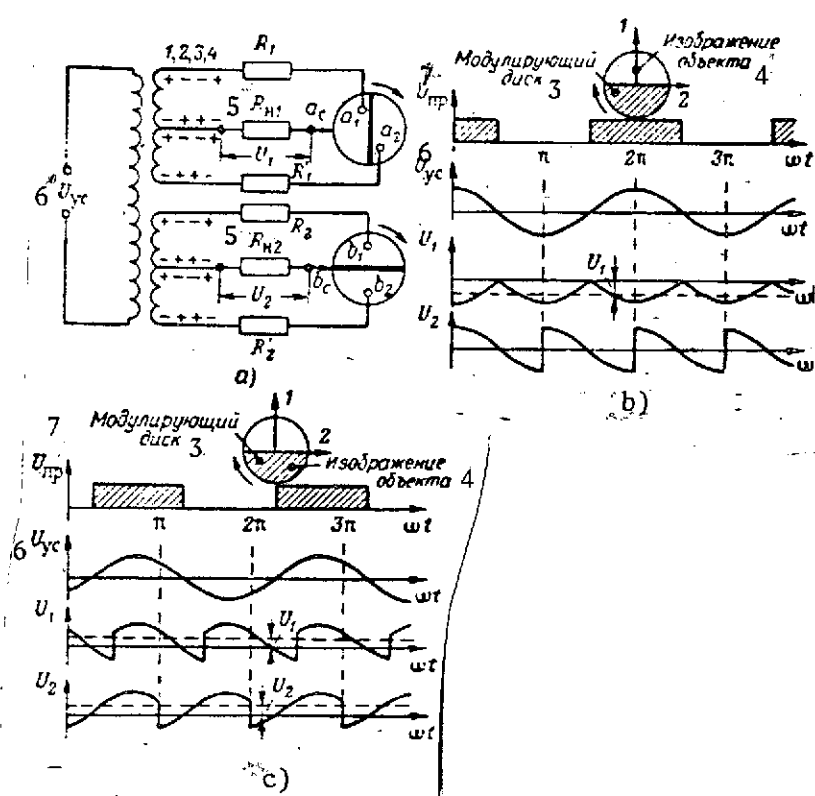


Fig. 5.4. Principle of discrimination of control signal in a phase analyzer: a. diagram of the connection of a load resistor; b. with an error in one coordinate; c. with an error in two coordinates; 1, 2. coordinates; 3. modulating disk; 4. image of object; 5. R_{load} ; 6. U_{ampl} ; 7. U_{rec}

On the basis of the procedure presented, curves of voltages over the channels have been constructed for the cases where $\theta = 0$ and $0 < \theta < \pi/2$. The corresponding graphs are presented in Fig. 5.4 a and b.

The constant components of voltages $U_1(t)$ and $U_2(t)$ for the channels will equal

$$U_m = \frac{1}{\pi} \int_0^\pi U_{max} \sin(\omega t - \theta) d(\omega t) = \frac{2U_{max}}{\pi} \cos \theta; \quad (5.4)$$

$$U_{02} = \frac{1}{\pi} \int_{-\pi/2}^{\pi/2} U_{\max} \sin(\omega t - \theta) d(\omega t) = \frac{2U_{\max}}{\pi} \sin \theta. \quad (5.5)$$

On the basis of the obtained formulas, we find that with $\theta = 0$, $U_1 = (2U_{\max})/\pi$ and $U_2 = 0$, and with $\theta = \pi/2$, $U_1 = 0$ and $U_2 = (2U_{\max})/\pi$, i.e., with the deviation of the object for one coordinate, the signal at the output of the analyzer appears only in one channel and turns out to be equal to zero in the second channel.

As can be seen from expressions (5.4) and (5.5), the constant components of error signals over the channels depend only on the phasing angle θ and do not depend on the size of the error angle, i.e., an instrument with the analyzer under consideration reacts only to the sign of the error angle. If the error angle equals zero (the image of the object is at the point of intersection of the optical axis with the center of the modulating disk), then with the rotation of the modulating disk, half the image will constantly fall on the sensitive layer of the receiver (no modulation of the radiation flux occurs) and there will be a constant signal on its output. In this case, the constant components over channels U_{01} and U_{02} will be equal to zero. The coefficient of modulation of the flux from the object depends on the shifting of the center of its image relative to the axis of rotation of the semidisk (Fig. 5.5).

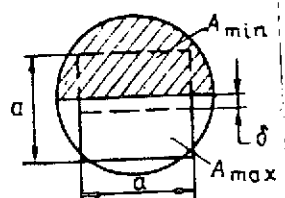


Fig. 5.5. For determination of the coefficient of modulation of the background.

If the radius of the circle of confusion r is small in comparison with the dimensions of the semidisk, the coefficient of modulation of the flux from the object $k_{m.o.} = 1$ over the entire area of the receiver except for its central portion.

The shortcomings of such a type of analyzer, caused by the design of the modulator, are unstable operation with small error angles and large dimensions of the object image and also modulation of the radiation flux from the background. /142

Let the deviation of the center of rotation of the semidisk from the center of the photoresistance by the amount of δ occur (see Fig. 5.5); then, even with a uniform background and receiver sensitivity identical over the entire area, we have

$$k_{mb} = \frac{A_{\max} - A_{\min}}{A_{\text{rec}}} = \frac{a \left(\frac{a}{2} + \delta \right) - a \left(\frac{a}{2} - \delta \right)}{a^2} = \frac{2\delta}{a}. \quad (5.6)$$

The flux from the background will be modulated due to the unequal sensitivity over the surface of the receiver and also as a consequence of the nonuniform background.

In some schemes, the shaping of the error signals is accomplished with the use of a full-wave demodulator, using electron tubes whose anode circuits are fed by square-wave voltage pulses. The diagram of such a demodulator is presented in Fig. 5.6.

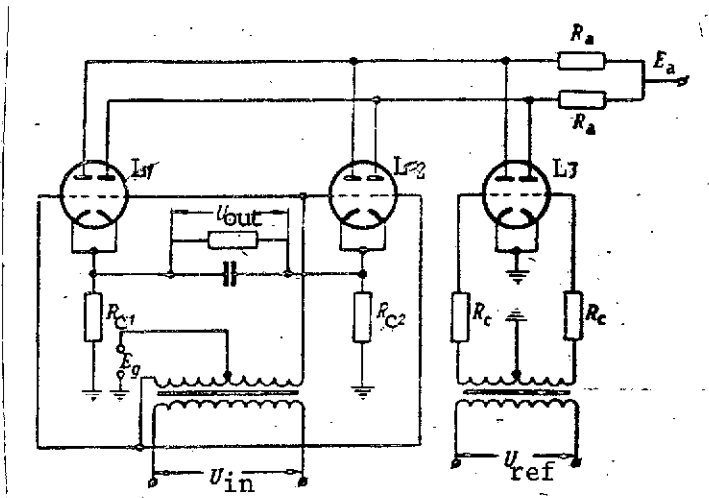


Fig. 5.6. Full-wave demodulator using electron tubes.

Square voltage pulses are shaped by a stage with a dual triode L3. The grid of this tube is under a zero initial bias. A reference voltage generated by a reference-voltage generator synchronously linked with the rotating modulator is fed to both grids of the dual triode L3 in antiphase. In this regard, the amplitude of the reference voltage is greater than the blocking voltage of the triodes. Therefore, during the negative half-periods of the reference voltage, the triodes are blocked and, during positive half-periods, open. When the triode is blocked, the

voltage on its anode equals E_a and during unblocking, it drops to E_0 . Since the voltage is fed to the grids of tube L3 in antiphase, the square pulses on the anode load will also be in antiphase.

The left and right anodes of the dual triodes L1 and L2 are connected respectively to the anodes of tube L3. Therefore, when the voltage on one of the anodes of tube L3 equals E_a , the halves of tubes L1 and L2 connected to it by the anodes are open, and the second halves of tubes L1 and L2 are blocked with respect to the anode voltage, since it equals E_0 .

If the voltage on the input of the demodulator equals zero ($U_{in} = 0$), equal currents flow through both tubes and, consequently, through the resistors which stand in the circuit of cathodes R_{C1} and R_{C2} . The voltage drops across resistors R_{C1} and R_{C2} are equal in value, the potential of points a and b are equal.

identical, and the output voltage equals zero (no current flows through the load resistor R_{load}).

Another types of phase analyzer is a device in which the modulation of the radiation flux is accomplished with the use of an inclined rotating flat modulating mirror and a fixed diaphragm with apertures (Fig. 5.7). The diaphragm has several apertures arranged along a circle and is installed in the focal plane of the lens. The dimensions of the apertures depend on the size of the circle of confusion of the system. With such a scheme, the instrument's field of view is determined by the radius of the diaphragm R and the focal length f of the lens /143

$$2W = 2\arctan \frac{R}{f} . \quad (5.7)$$

The angle of incline of the rotating flat mirror to the axis is such that if the object is located on the optical axis, its image in the focal plane with the rotation of the mirror will describe a circle which coincides with the external boundaries of the apertures of the diaphragm. The radiation flux is modulated with frequency

$$f_{car} = \frac{pn}{60} \quad (5.8)$$

where p is the number of apertures in the diaphragm; n is the number of revolutions of the mirror in one minute.

With the coincidence of the image of the object with the apertures in the diaphragm, half the value of the radiation flux which is focused by the optical system falls on the radiation receiver. With the displacement of the object from the axis, its image will describe a circle of the same radius, but the center of the circle will be displaced in a direction opposite to the displacement of the object. This leads to a change in the value of the flux which falls on the radiation receiver through the various apertures of the diaphragm. As a result, the carrier frequency f_{car} turns out to be additionally modulated for amplitude by the frequency of rotation of the mirror (Fig. 5.8). /144

$$f_{env} = \frac{n}{60} \quad (5.9)$$

Fig. 5.9 portrays the dependence of the coefficient of modulation of a radiation flux which arrives at the receiver on

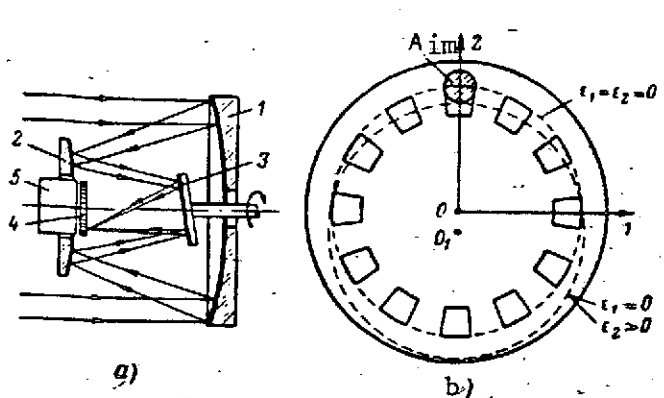


Fig. 5.7. Phase analyzer made on the basis of a fixed modulating diaphragm with apertures: a. diagram of the optical system; b. fixed modulating diaphragm; 1. main mirror of the objective; 2. secondary mirror; 3. inclined rotating mirror; 4. fixed modulating diaphragm; 5. receiver.

the amount of displacement x of the image of the object in the focal plane with the presence of an error angle. With $x = r$, where r is the radius of the circle of confusion, the modulation coefficient equals 1. If the error angle $\epsilon > r/f$, the overmodulation of the flux from the object is observed, in which regard the signal has the form of individual bunches of pulses of frequency f_{car} and the recurrence frequency of these bunches equals f_{env} .

The considered scheme of an analyzer permits accomplishing

the selection of objects from angular dimensions since the flux of radiation from the emitters having large dimensions is modulated only on the envelope frequency f_{env} .

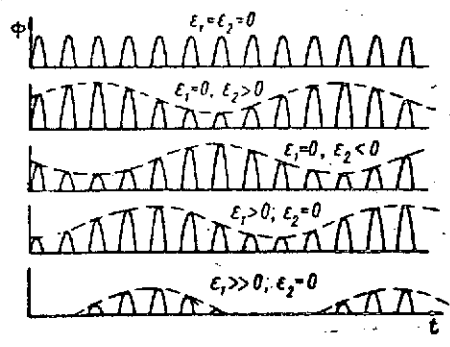


Fig. 5.8. Nature of the change in signals at the output of a receiver with different error angles.

The shaping of the control signal which characterizes the deviation of the object from the optical axis is accomplished with the aid of a system whose block diagram is presented in Fig. 5.10.

The signal modulated by frequencies f_{car} and f_{env} is amplified by a narrow-band resonance amplifier tuned on the f_{car} frequency. Such tuning can be accomplished, for example, by connecting a double T-shaped bridge with a resonant frequency equal to f_{car} in the feedback circuit of one of the amplifier stages. The typical appearance of the frequency response of such a bridge and the scheme for its connection are presented in Fig. 5.11.

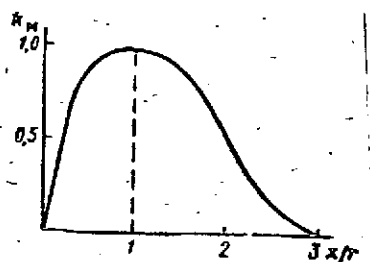


Fig. 5.9. Dependence of the modulation coefficient on the value of the error angle.

One more filter is connected in at the output of one of the amplifier stages which does not pass signals modulated only by frequency f_{env} . The role of this filter can be played by a double T-shaped bridge, but its resonant frequency equals f_{env} and it is not connected in the feedback circuit but directly between the amplifier stages.

The signal which has been filtered out goes from the amplifier output to the carrier-frequency detector, where the signal is discriminated from the object which is modulated by frequency f_{env} . This signal, which contains information about the position of the object after amplification, is fed to a separator which can be a collector-type mechanical commutator or a full-wave demodulator using electron tubes.

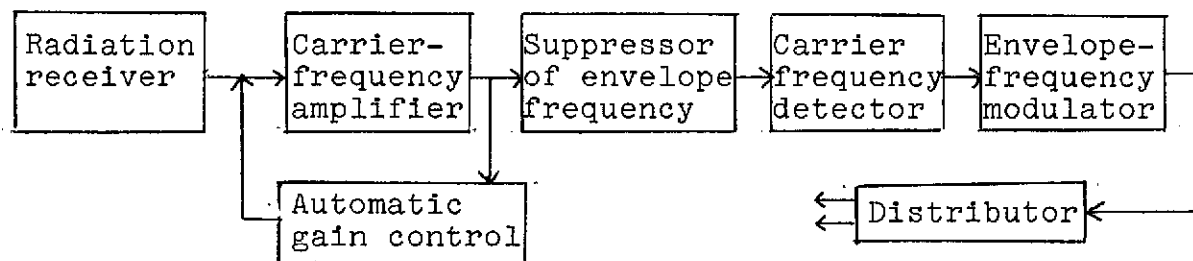


Fig. 5.10. Block diagram of the system for discriminating control signals.

In a number of cases, the shaping of signals which contain information about the magnitude and direction of the error is accomplished with the use of phase-sensitive detectors which use transistors (Fig. 5.12).

/146

In order to assure the operation of the scheme and the discrimination of the control signals which correspond to the direction of the error, a sine-wave reference voltage in the same polarity as shown in the diagram is fed to the collector-base intervals of each triode. Circles ring the signs which correspond to the second half-period, and those without circles are the polarity of the reference voltage during the first half-period for triodes T1, T2, T3, and T4.

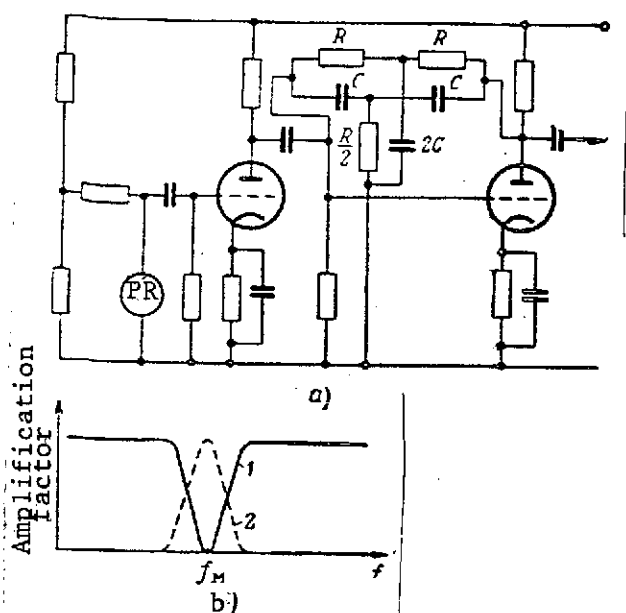


Fig. 5.11. Diagram of a resonance amplifier: a. connection of a dual T-shaped filter in the negative feedback circuit; b. typical appearance of the filter's frequency response.

Reference voltage U_{ref2} is shifted for phase by a quarter of a period in comparison with U_{ref1} . With regard to triodes T5-T8, these signs characterize the polarity of the reference voltages in the first and second quarters of the period.

The operating principle of the indicated phase-sensitive filter is based on the fact that with the potential of the base negative in comparison with the collector, the triode becomes conductive in the emitter-collector direction as well as in the opposite direction. Therefore, each pair of triodes (T1-T2 and so on) is conductive in those half-periods when the minus of the reference voltage is applied to the base. Each pair of triodes operates with its own half of the secondary winding of the transformer.

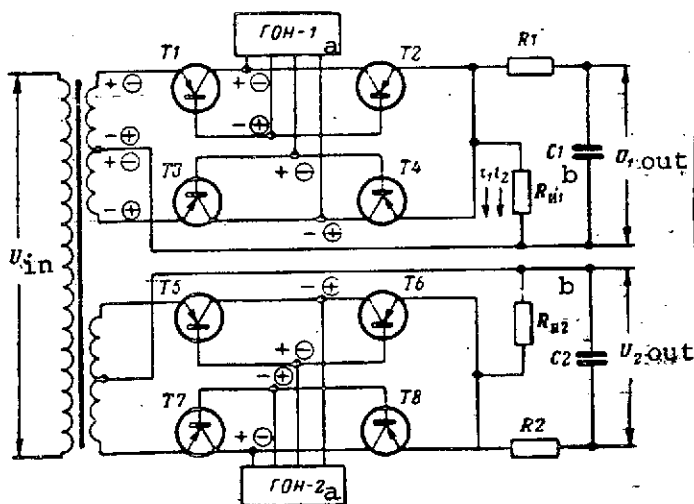


Fig. 5.12. Basic circuit of a phase-sensitive detector using transistors.

Key: a. Reference-voltage generator; b. R_{load} ...

When the input signal and reference voltage coincide for phase, and their polarity coincides with Fig. 5.12, then during the first half-period, triodes T1 and T2 are open and T3 and T4 are blocked. The signal from the output of the secondary transformer winding (its upper half) is discriminated on load resistor $R_{load\ 1}$ through which the current i_1 flows.

/147

In the second half-period, the polarity of the reference voltages and the input signal changes, triodes T3 and T4 are unblocked, and triodes T1 and T2 are blocked. The signal from the output of the lower half of the secondary winding (polarity shown by the signs in the circles) is discriminated through triodes T3 and T4 in the same polarity on resistor $R_{load 1}$ through which current i_2 will flow. In a similar manner, we can trace the character of change of the output signal over the second channel with a shift in phases between the input and reference voltages, equal to $\pi/2$, and also with the arbitrary phase of the input signal.

The operation of the given phase-sensitive detector is similar to the operation of a collector-type commutator and demodulator using electron tubes. Just as in the demodulators which have been considered, here the value of the constant component which is discriminated over each channel by circuit $R_1 C_1$ and $R_2 C_2$, respectively, depends only on the phase of the input signal which is determined by the direction of error.

5.3. Polar Analyzers

In analyzers of this type, at least four radiation receivers should be used with whose aid the two mutually perpendicular sides are fixed. The indicated fixation can be assured either by the direct placement of a four-area photoresistor in the focal plane of the lens (Fig. 5.13) or by the use of additional elements in the optical system which permit dividing the radiation flux and directing it in four directions. The elements of analyzers may be a tetrahedral mirror pyramid (Fig. 5.14a) or a bunched conductor of optical fibers (Fig. 5.14b), the input end of which is placed in the focal plane. The bunched conductor branches out in four component parts, the output ends of which are placed in front of the sensitive layers of the radiation receivers. Both these methods of dividing the radiation flux by direction and, in particular, the latter are extremely convenient when the radiation receivers are vacuum photocells, photomultipliers, and single-area photoresistors. /148

The radiation receivers of each line are connected in pairs to the input of two balance photocurrent amplifiers in accordance with the compensation scheme. Modulation of the radiation flux can be both external (with the use of a modulating device) and internal (electrical, due to the feeding of an alternating power-supply voltage of constant frequency and amplitude to the radiation receiver).

The operating principle of an analyzer consists of the following.

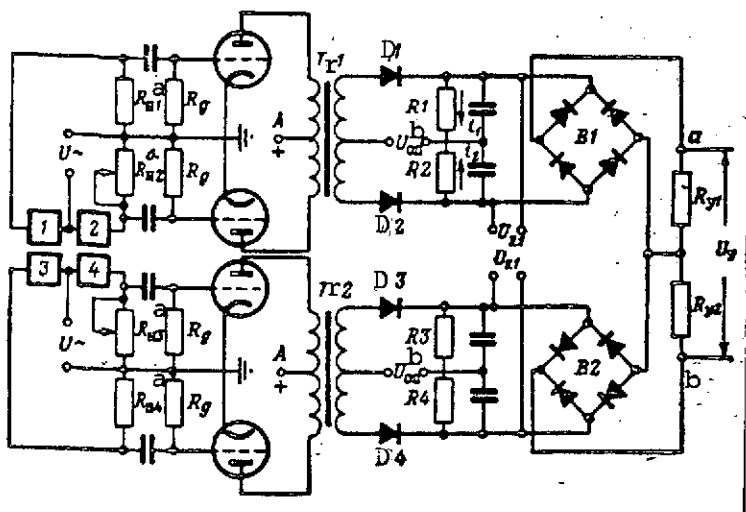


Fig. 5.13. Basic circuit of a polar analyzer: 1, 2, 3, and 4. areas of the photoresistor.

Key: a. $R_{load}...$; b. U_{ref}

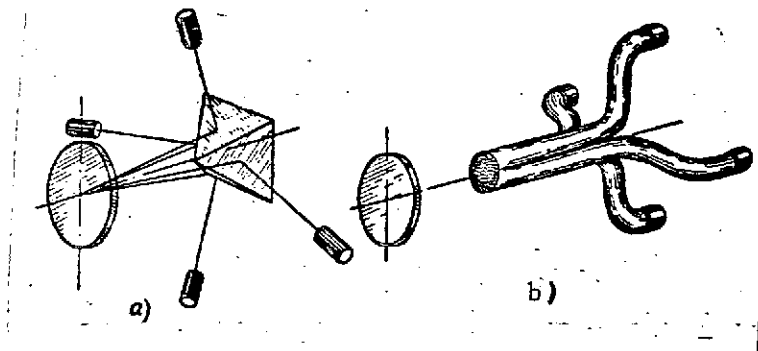


Fig. 5.14. Methods of dividing the radiation flux.

electrical modulation of the signals provide the possibility of taking the modulation factors of radiation flux from the object and background as equal to 1. The amplitude value of the voltage on the amplifier input, caused by the radiation of the background, will be

$$U_b = S_{b1}\phi_{b1} - S_{b2}\phi_{b2}, \quad (5.10)$$

If the object is located on the instrument axis, its image is projected to the gap which divides the sensitive areas of the receiver (zone of insensitivity) or, after the dividing elements, identical fractions of the radiation flux are directed to each of the four receivers. In this case, the signal on the output of the analyzer is not shaped. The shifting of the object from the optical axis causes the drift of the image from the zone of insensitivity. Let us examine the operation of the scheme under the condition that the radiation flux from an object falls on one of the receivers. As a result, a signal of specific polarity is shaped on the output. If the image is shifted to another receiver, then the polarity of the signal is changed to the opposite over one of the channels.

The compensation connection of the receivers and the

where S_{b1} and S_{b2} are the voltage sensitivities of the receivers with respect to the radiation of the background; Φ_{b1} and Φ_{b2} are the values of the radiation fluxes from the background which fall on the first and second receivers, respectively. Expression (5.10) can be written in the form

$$U_b = S_{b1}\Phi_{b1}k_d, \quad (5.11)$$

where $k_d = \frac{S_{b1}\Phi_{b1} - S_{b2}\Phi_{b2}}{S_{b1}\Phi_{b1}}$ is the coefficient of decompensation.

From (5.11), it follows that if the sensitivities of both receivers are identical ($S_{b1} = S_{b2}$) and the background is uniform, the radiation noises at the input of such a device equal zero.

The shaping of error signals over channels, for example, over a line, can be accomplished with the use of single-period demodulators using semiconductor diodes connected in the output of photocurrent amplifiers of each line. A reference voltage is fed to the midpoint of the secondary transformer winding, the frequency and phase of which coincides with the frequency and phase of the modulation voltage. /150

If the input signal U_s equals zero, the voltage between the cathodes and anodes of the diodes equals the reference voltage. During the positive half-periods of the voltage, currents of equal strength ($i_1 = i_2$) flow through the diodes and voltage drops across the resistors R will be identical in magnitude and opposite in sign; therefore, across the output of the demodulator, the voltage will be equal to zero. During the negative half-periods, both diodes are blocked and the output voltages are also equal to zero.

When the input signal does not equal zero and arrives in phase with the reference voltage, the voltage of the alternating current U_1 applied to diode D_1 exceeds voltage U_2 applied to diode D_2 . Therefore, $i_1 > i_2$. If the phases of the input signal and the reference voltage are opposite, the polarity of the output signal changes (Fig. 5.15). Since the input signal U_s and the reference voltage U_{ref} change in accordance with the law of sines

$$U_{ref} = U_{ref \max} \sin \omega t \quad (5.12)$$

$$U_s = U_{s \max} \sin (\omega t - \psi); \quad (5.13)$$

where

$$\psi = 0 \text{ rad}, 2\pi \text{ rad } (0^\circ, 180^\circ),$$

then adding them, we obtain

$$U_1 = (U_{\text{ref max}} \pm U_{\text{S max}}) \sin \omega t; \quad (5.14) \quad /151$$

$$U_2 = (U_{\text{ref max}} \pm U_{\text{S max}}) \sin \omega t. \quad (5.15)$$

The constant component of a rectified current with a capacitance connected in parallel with the resistor will be

$$i_0 = \frac{U_m}{\pi R_i} (\sin \varphi - \varphi \cos \varphi), \quad (5.16)$$

where R_i is the internal resistance of the diode; φ is the angle of cut-off which is determined by the relation

$$\varphi = \arccos \frac{i_0 R}{U_m} = \arccos \frac{U_0}{U_m}.$$

U_0 is the constant component of a rectified voltage.

From these relations, it follows that

$$\frac{U_0}{U_m} = f\left(\frac{R}{R_i}\right) = h$$

therefore,

$$U_{01} = k_u (U_{\text{ref max}} \pm U_{\text{S max}});$$

$$U_{02} = k_u (U_{\text{ref max}} \pm U_{\text{S max}}).$$

and the output voltage of the demodulator will be

$$U_{\text{out}} = \pm 2k_u U_{\text{S max}} \quad (5.17)$$

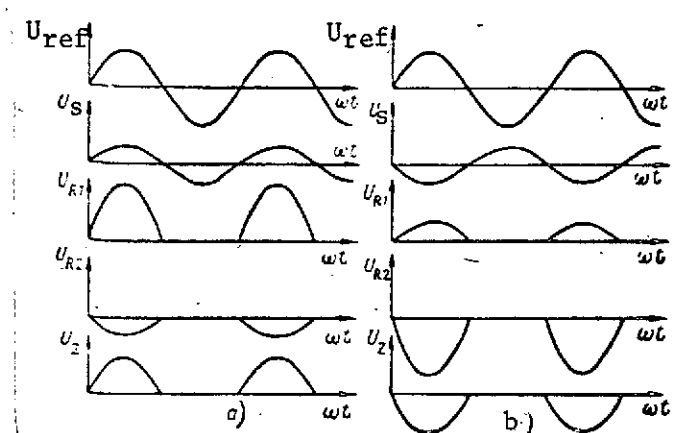


Fig. 5.15. Curves of voltages on various elements of a demodulator: a. phases of signal and reference voltage coincide; b. phases of signal and reference voltage are opposite to each other.

For the shaping of error signals over the second channel (in a mutually perpendicular plane) ring-type rectifiers using semiconductor diodes are connected at the output of line demodulators. The principle of discrimination of an error signal over this channel is the following.

When the image of an object is projected between lines, the output voltages of the demodulators equal zero, i.e., $U_{Z1} = U_{Z2} = 0$. If the image of the object is located on one of the

receivers (1 or 2) of the first line, then $U_{Z2} \neq 0$. As a result, behind the ring-type rectifier, the potential of point a will be higher than the potential of point b, regardless of on which receiver of the first line the image of the object is located. The passage of the image to either of the receivers (3 or 4) of the second line makes the potential of point b higher than the potential of point a and the polarity of the output signal U_y changes to the opposite.

The merit of the analyzer considered is a high degree of freedom from interference by a uniform radiating background. The shortcoming of the method is the independence of the error signals from the value of the error angle.

5.4. Scanning and Search Systems in Electro-optical Equipment

/152

Scanning and search systems find wide application in electro-optical equipment for various purposes. For the detection of radiating objects, the necessity often arises for their search in large zones of space. Attempts simultaneously to cover the entire scanning zone lead to a considerable increase in the quantity of false information, interference, and a reduction in the operating range due to the incidence of background radiation in the instrument and so forth. Therefore, to reduce the influence of the background and increase the range of operation of the system, attempts are made to see that at each moment in time the smallest possible region of space is projected on the radiation flux receiver.

Thus, it is necessary to scan a large zone of space but, from the point of view of the technological capabilities of the equipment, the dimensions of the zone being scanned at a given moment in time should be the smallest possible. This apparent contradiction is resolved by the employment of optical systems with small angles of instantaneous field of view successively directed to various sectors of space within the limits of the required region. Hence follows the designation of the scanning system which serves to assure the scanning of a given region of space by means of the successive displacement of the instantaneous field of view, in accordance with a specific law.

Scanning and search systems are classified by the scanning principle (by type), by type of trajectory of the instantaneous field of view, and by the scheme for accomplishing the scanning.

The following systems are distinguished by type of scanning:

- The simple scanning systems (with one fixed receiver);
- Raster systems in which the partitioning of the field of view is accomplished with the use of a raster (coding device) located in the plane of the image;
- Systems with mosaic radiation flux receivers.

In accordance with the law of displacement (nature of trajectory) of the instantaneous field of view in space, the following types of systems are distinguished:

- Line scanning;
- Line-frame scanning;
- Conical-rotational and conical-progressive scanning;
- Spiral scanning;
- With cycloidal and rosette trajectories of movement of the instantaneous field of view.

According to the scheme of accomplishment of the scanning, systems of scanning and search are divided into three basic groups: optomechanical, electro-optical, and electronic.

The displacement of the instantaneous field of view in space over one trajectory or another is accomplished by the displacement of the following elements and devices: /153

- By the displacement of the entire receiver;
- By the displacement of the entire optical system or objective;
- By the rotation (oscillatory motion) of one or several elements of the optical system;
- By the displacement of the radiation receiver and also by the commutation of the sensitive elements of mosaic receivers in a specific order.

Until recently, optomechanical scanning systems received the greatest popularity in electro-optical equipment. Electronic scanning systems are finding employment. The employment of electron-optical and piezoelectrical scanning systems is beginning.

The basic characteristics of a scanning and search system are:

- The angle of instantaneous field of view $2W_v$;
- The scanning angle or zone -- $2W_{sc}$ or $2W_{1sc}$ and W_{2sc} ;
- The trajectory and law of displacement of the instantaneous field of view in space;
- The scanning period T_s ;
- The overlap coefficient which characterizes the fraction of repeatedly scanned space;
- The efficiency of the cycle which determines that portion of the scanning cycle when useful information arrives in the instrument;
- The time constant of the scanning system (including the radiation receiver);
- The probability characteristics (probability of nontransmission of the target, instantaneous probability, search effort):

To assure the dependable operation of the instrument, the following requirements are made of the scanning system:

- Scanning the entire space in a given scanning zone without gaps;
- Minimum duration of scan of the required zone of space. Observance of this requirement is especially important in the detection of moving objects which can displace so much within the limits of the scanning zone during the time between two successive scans that they will not be detected by the instrument;
- The duration of the time interval when the object is within the limits of the instantaneous field of view should be sufficient to obtain the necessary quantity of information about it;
- The scanning system should assure high resolution for angular coordinates;
- The scanning system should be simple in design, dependable in operation, have small overall dimensions and mass, and be free of large dynamic overloads.

/154

Some of the simplest are systems with line scanning of space. In the line scanning method, sectors of space are successively scanned one after the other, the angular width of

which equals the angle of instantaneous field of view, and the length is determined by the size of the scanning angle. The passage from one line to another is accomplished by displacement of the instrument carrier.

Let us consider the diagrams presented in Fig. 5.16. The carrier (SC) moves at altitude H with velocity V relative to the earth. The direction with relation to which the scanning of the lines in space is accomplished comprises some angle α with the velocity vector of the carrier. The scanning of space is performed by the displacement of the instantaneous field of view of a system with size $2W_{V1} \cdot 2W_{V2}$ within the limits of the scanning angle $2W_{sc}$.

The linear dimensions of the instantaneous field of view on the earth's surface without consideration of its curvature can be found from expressions

$$a_0 = 2L_0 \tan W_{V2} \text{ and } b_0 = \frac{2L_0}{\sin \phi} \tan W_{V1}$$

where L_0 is the initial slant range.

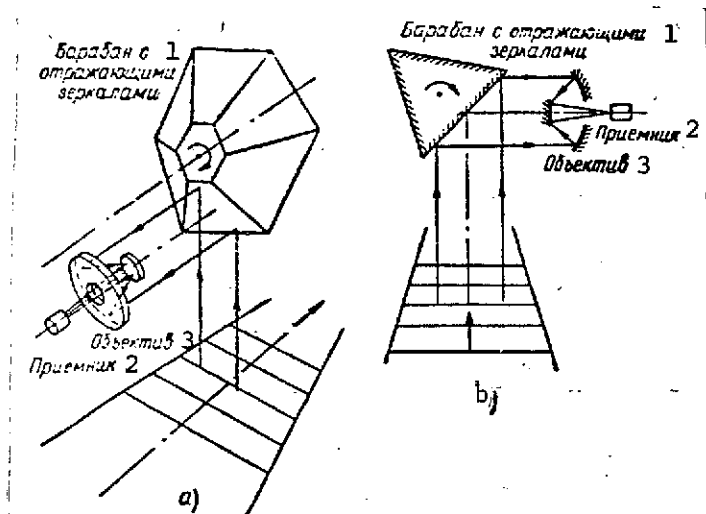


Fig. 5.16. Diagrams of scanning systems of electro-optical instruments: a. axis of rotation of the drum parallel to the optical axis; b. axis of rotation of the drum perpendicular to the optical axis.

Key: 1. Drum with reflecting mirrors; 2. Receiver; 3. Objective

With the use of a single-element radiation receiver in the instrument scheme, n lines will be scanned in space during each revolution of the drum. If a linear mosaic receiver consisting of m sensitive elements (a so-called "comb") is used in the instrument, then each surface of the drum simultaneously accomplishes the scanning of m adjacent lines, and the overall number of lines scanned during one revolution of the drum will be mn . Let us point out that with the simultaneous scanning of the lines, difficulties arise in the

recording and processing of the information; therefore, the equipment becomes considerably more complex.

In order to obtain information about each object located in the scanning zone at the output of the radiation receiver, the scanner should assure the finding of the object within the limits of the instantaneous field of view during a segment of time determined from the condition

$$\Delta t_{11} \geq k_{\tau} \tau \quad (5.18)$$

where Δt_{11} is the time of illumination of the receiver by the radiation flux from a given object, i.e., the time when this object is located in the field of view of the instrument; τ is the time constant of the receiver; k_{τ} is the positive coefficient which characterizes the exceeding of the duration of the illumination of the receiver by the radiation flux of the object in comparison with the time constant.

If the frequency of rotation of the scanning element is N/sec , the number of scanning elements of the dissociation scanned by the instrument in 1 sec is

$$Q = \frac{2\pi N}{2W_V}, \quad (5.19)$$

and the time of influence of the radiation flux from each point of space being scanned on the instrument will be

$$\Delta t_{11} = \frac{1}{Q} = \frac{W_V}{\pi N}. \quad (5.20)$$

With consideration of condition (5.18), we obtain the expression for the maximum permissible rotation frequency of the scanning element which is determined by the time constant of the receiver

$$N \leq \frac{W_V}{\pi k_{\tau} \tau}. \quad (5.21)$$

But the linear width of the terrain sector scanned by the instrument from flight altitude H during one revolution of the drum

comprises

$$l = 2W_v Hmn. \quad (5.22)$$

On the strength of the requirement for the contact of adjacent lines, it is necessary that the scanning rate, i.e., the width of the band scanned by the instrument in 1 sec, be no less than the speed of flight of the carrier /156

$$V \leq 2W_v HmnN.$$

From this relation, we obtain the expression which determines the minimum allowable frequency of rotation of the scanning element with which the scanning will be accomplished without gaps

$$N \geq \frac{V}{2W_v Hmn} \quad (5.23)$$

or, with consideration of the overlap of adjacent lines,

$$N \geq \frac{bV}{2W_v Hmn}, \quad (5.23a)$$

where b is the coefficient of overlap ($0 < b < 2$).

Formulas (5.21) and (5.23a) show that both the upper allowable limit of rotation frequency determined by the value of the time constant and the lower limit caused by the requirement for the contact of adjacent lines exist. Furthermore, the frequency of rotation of the scanning element is limited by mechanical possibilities. A frequency of rotation of 3000/sec is taken as such a limit for optomechanical systems with reflector size equal to 300 mm.

If we consider the extreme cases in formulas (5.21) and (5.23) then, equating their right sides to each other, we obtain

$$W_v = \sqrt{\frac{\pi k_r r V}{2mnH}}, \quad (5.24)$$

and, by the exclusion of W_V from (5.21) and (5.23a) and their joint solution, we find

$$N = \sqrt{\frac{V}{2\pi n m k_{\tau} H}} \quad (5.25)$$

As applicable to the scheme for the scanning system presented in Fig. 5.16b, the type of relations which connect the flight parameters with the characteristics of the instrument are maintained as approximately the same. The difference is caused by the change in the direction of displacement of the scanning element, as a result of which the sighting ray will displace at a rate twice as great in the latter scheme with the rotation of the drum. In this case, formulas (5.24) and (5.25) take the form

$$W_V = \sqrt{\frac{\pi k_{\tau} \tau}{H m n}} V; \quad (5.26)$$

$$N = \sqrt{\frac{V}{4H m n \pi k_{\tau} \tau}} \quad (5.27)$$

The latter relations permit calculating the basic parameters of the scanning system which satisfies the condition of contact of the adjacent lines.

/157

Of the values which determine the indicated parameters, some are given (V and H) and others, for example k_{τ} , cannot be taken as less than a specific value which will be equal to 2. The designer can only vary three parameters of the scanning instrument and, with their use, should assure the solution of the assigned problem.

The maximum allowable value of the angle of instantaneous field of view is determined by the required resolution of the system, and the minimum by the time constant of the receiver and the relationship of the altitude and speed of flight of the carrier.

To reduce the rate of rotation of the scanning element under the condition of assuring the scanning of space within given limits, we strive to increase the number of reflecting surfaces of the scanning element.

The maximum number of reflecting surfaces of the scanning element used in the scheme (see Fig. 16a) can be found from the formula

$$n_{\max} = \frac{360}{2W_{sc}} \quad \text{or} \quad n_{\max} = \frac{\pi}{W_{sc}}, \quad (5.28)$$

and as applicable to the scheme (see Fig. 5.16b), with consideration of the double velocity of the reflected beam, from the expression

$$n_{\max} = \frac{360}{W_{sc}} \quad \text{or} \quad n_{\max} = \frac{2\pi}{W_{sc}}. \quad (5.29)$$

To separate the lines and return the electronic circuit to the initial state prior to the start of the next line, it is necessary to provide for some reserve of time allotted to the scanning of each line. This is equivalent to the system accomplishing scanning within limits of the angle $W'_{sc} = W_{sc} + \Delta W_{sc}$.

With consideration of the reasons which have been presented, expressions (5.28) and (5.29) take the form

$$n_{\max} = \frac{180}{W_{sc} + \Delta W_{sc}} \quad \text{or} \quad n_{\max} = \frac{\pi}{W_{sc}} \quad (5.30)$$

$$n_{\max} = \frac{360}{W'_{sc}} \quad \text{or} \quad n_{\max} = \frac{2\pi}{W'_{sc}}. \quad (5.31)$$

The dependence of the maximum number of reflecting surfaces on the value of the scanning angle with various values of ΔW_{sc} , as applicable to the variations of scanning schemes being considered, is presented in Table 5.1.

With consideration of (5.30) and (5.31), formulas (5.24) and (5.26) take the form /158

$$W_{v1} = \sqrt{\frac{\tau \cdot k_t \cdot W'_{sc}}{H}} V; \quad (5.32)$$

$$W_{v2} = \sqrt{\frac{\tau \cdot k_t \cdot W'_{sc}}{2H}} V \quad (5.33)$$

and express the relation between all basic parameters of the scanning system and also the height and speed of flight of the carrier.

TABLE 5.1

Variations	ΔW_{sc}	Scanning angle $2W_{sc}$ rad							
		0,25	0,35	0,52	0,70	1,05	1,24	1,57	2,10
I see Fig. 5.16a	$\Delta W_{sc}=0$	0,418	0,313	0,208	0,156	0,105	0,087	0,070	0,052
	$\Delta W_{sc}=0,1W_{sc}$	0,400	0,295	0,208	0,140	0,087	0,070	0,052	0,052
	$\Delta W_{sc}=0,2W_{sc}$	0,382	0,295	0,192	0,140	0,087	0,070	0,052	0,035
	$\Delta W_{sc}=0,4W_{sc}$	0,350	0,210	0,175	0,122	0,087	0,052	0,052	0,035
II see Fig. 5.16b	$\Delta W_{sc}=0$	0,835	0,626	0,418	0,313	0,208	0,175	0,140	0,105
	$\Delta W_{sc}=0,1W_{sc}$	0,800	0,590	0,400	0,295	0,192	0,156	0,122	0,105
	$\Delta W_{sc}=0,2W_{sc}$	0,765	0,573	0,382	0,288	0,192	0,140	0,122	0,087
	$\Delta W_{sc}=0,4W_{sc}$	0,70	0,52	0,350	0,26	0,175	0,122	0,105	0,087

The basic merit of the line-scanning systems consists of the relative simplicity of the design execution of the scanner.

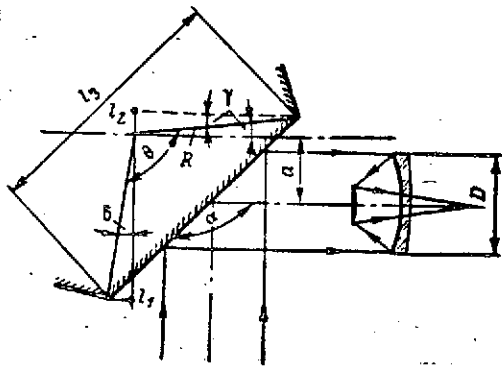
A shortcoming of the considered line-scanning systems is the necessity for the strict correspondence between the frequency of rotation of the scanning element and the speed of flight of the carrier with a given overlap of the lines.

Another substantial shortcoming is the presence of large-size rotating elements. We will show this by the example presented in Fig. 5.17.

The image of space being scanned will not be vignetted by the optical system in the case where the entrance pupil of the objective will be inscribed in the cross section of a pencil of rays reflected to the objective from a mirror with a change in the position of the scanning element within required limits. If the distance between the axis of rotation of the scanning element and the optical axis of the objective is designated by a , the indicated condition can be written in the form

/159

$$\left. \begin{array}{l} Ol_1 - a \geq D/2 \\ Ol_2 + a \geq D/2 \end{array} \right\} \text{ for the extreme position of the scanning element} \quad (5.34)$$



Having examined Fig. 5.17, we can write

$$Ol_1 = R \cos \delta \quad \text{and} \quad Ol_2 = R \sin \gamma$$

Adding term by term and subtracting the indicated inequalities, we find

Fig. 5.17. For the determination of the dimensions of the scanning element of the scanning system.

$$R(-\sin \gamma + \cos \delta) \geq D; \quad (5.35)$$

$$2a \leq R(\cos \delta - \sin \gamma), \quad (5.36)$$

where

$$\begin{aligned} \gamma &= \pi - \alpha - \frac{\pi - \theta}{2} = \pi/2 + \frac{\theta}{2} - \alpha; \\ \delta &= \theta - \pi/2 - \gamma = \frac{\theta}{2} + \alpha - \pi. \end{aligned}$$

Substituting the values γ and δ in expressions (5.35) and (5.36) and making certain transformations, we obtain

$$R \geq \frac{D}{2 \sin \frac{\theta}{2} \sin \alpha}, \quad (5.37)$$

$$2a \leq -R \cos \frac{\theta}{2} \cos \alpha \quad \text{and} \quad 2a \leq -\frac{D}{2} \cot \frac{\theta}{2} \cot \alpha. \quad (5.38) \quad (5.38)$$

In formula (5.37), the variable is the angle α , which characterizes the position of the plane of the mirror reflector relative to the optical axis of the objective. The maximum values of this angle can be given by the expression

/160

$$\alpha = \alpha_0 \pm \frac{\bar{W}_{sc}}{2},$$

where α_0 is the angle which determines the position of the mirror at which the middle of the scanning zone is projected on the radiation receiver.

Inasmuch as always $\alpha > \pi/2$, vignetting is most dangerous with the greatest angles α . Therefore, in order to exclude vignetting, it is necessary to accomplish calculations by formulas (5.37) and (5.38) for the case $\alpha = \alpha_{\max} = \alpha_0 + W_{sc}/2$, i.e.,

$$R \geq \frac{D}{2 \sin \theta/2 \sin (\alpha_0 + W_{sc}/2)}; \quad (5.39)$$

$$a \leq -\frac{D}{4} \cot \frac{\theta}{2} \cot \left(\alpha_0 + \frac{W_{sc}}{2} \right). \quad (5.40)$$

The minus sign in the inequality tells us that the optical axis of the objective passes below the axis of rotation of the scanning element.

Having examined Fig. 5.17, we can write

$$l_{\text{mir}} = 2R \sin \theta/2$$

whence, with consideration of (5.39), we find

$$l_{\text{mir}} = \frac{D}{\sin (\alpha_0 + W_{sc}/2)}$$

This relation shows that the length of the reflecting mirror depends both on the size of the scanning angle and on the angle which characterizes the initial position of the mirror surface of the scanning element. It is completely obvious that the width of this mirror should be at least the diameter of the objective. Also obvious is the necessity to satisfy the condition

$$\theta \geq W_{sc}$$

The parameters of the mirror drums calculated from formulas (5.39) and (5.40) (see Fig. 16a) with $2W_{sc} = 60 \cdot 1.74 \cdot 10^{-2}$ rad and $\alpha_0 = 135 \cdot 1.74 \cdot 10^{-2}$ rad are presented in Table 5.2.

From the table, it can be seen that even the diameter of a single mirror should be considerably larger than the diameter of the objective, not to mention the mirror drums.

TABLE 5.2

Number of reflecting surfaces and angle θ corresponding to this, rad	$2 (\theta=180 \times 1.74 \cdot 10^{-2})$	$3 (\theta=120 \times 1.74 \cdot 10^{-2})$	$4 (\theta=90 \times 1.74 \cdot 10^{-2})$	$6 (\theta=60 \times 1.74 \cdot 10^{-2})$
Diameter of mirror drum expressed in terms of the diameter of the objective	$2D_0$	$2.4D_0$	$2.86D_0$	$4D_0$
Distance α between axes expressed in terms of the diameter of the objective	0	$-0.5D$	$-0.866D$	$-1.5D$
Length of one mirror of the drum	$2D$			
Width of each mirror	D			

Another shortcoming of such scanning systems is the increase in the width of the band being scanned from the center from the edge of the scanning zone. If we disregard the earth's curvature, then with the deviation of the instantaneous field of view from the normal, the width of the band being scanned will change in accordance with the relation

/161

$$l_a = l_0 \frac{1}{\cos \alpha},$$

where l_0 is the width of the band being scanned during observation along the normal to the surface; α is the angle of deviation of the instantaneous field of view from the normal.

With consideration of the curvature of the earth's surface, the width of the band being scanned with the deviation of the instantaneous field of view changes according to the law

$$l_a = l_0 \frac{1}{\cos \alpha} + a \frac{2W_{VZ}}{\cos \alpha}, \quad (5.41)$$

where

$$a = R \cos^2 \alpha - H \sin^2 \alpha - \sqrt{(R \cos^2 \alpha - H \sin^2 \alpha)^2 - H^2 \sin^2 \alpha}$$

Let us point out that the second component with angles $\alpha \leq 45.1.74 \cdot 10^{-2}$ rad does not exceed 5-6 percent, and therefore need not be considered in a number of cases.

Along with the examined methods, line scanning of space can be accomplished with the use of multielement receivers or linear mosaics. A mosaic consisting of Q sensitive elements is placed in the focal plane of the objective in such a way that the required sector of space or terrain is projected on these elements.

The scanning of space by line is accomplished due to the commutation of the radiation receivers -- their sequential connection to the input of the amplifier. The passage from one line to another occurs with the displacement of the carrier (Fig. 1.18).

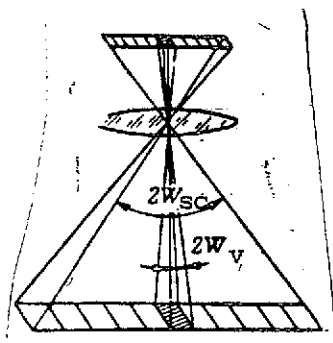


Fig. 5.18. Principle of scanning space in a system with a mosaic receiver.

Naturally, the instantaneous field of view of the instrument $2W_v$ in this case is limited by the dimensions of the sensitive layer of a separate receiver. If all elements are commutated N_k times per second, width ℓ of the band scanned during this time will be $\ell = \ell_{\text{line}} N$, where ℓ_{line} is the width of the band on the terrain scanned by the instrument at a given moment.

Considering that $\ell_{\text{line}} = 2W_v H$, we write the condition for the contact of adjacent lines in the form

$$V = N_k 2W_v H,$$

whence we obtain

$$N_k \geq \frac{V}{2W_v H}. \quad (5.42)$$

On the other hand, to satisfy the condition $t_{i1} > k\tau$, it is necessary that the following condition be satisfied

$$t_{i1} = \frac{1}{N_k Q} \geq k\tau,$$

whence it follows

$$N_k \leq \frac{1}{k\tau Q}.$$

$$(5.43)$$

Thus, the number of commutations of each element of a line is determined by the inequality

$$\frac{1}{k_{\tau} \tau Q} \geq N \geq \frac{V}{2W_{\nu} H}.$$

We note that the employment of such mosaics in comparison with the employment of single-element scanning instruments permits employing receivers with a large time constant along with the exclusion of large-size rotating parts.

A substantial shortcoming of the system being examined is the complication of the electronic system due to the presence of a commutator.

A common shortcoming of all scanning instruments with line scanning intended for the observation of ground objects is the fact that radiating objects are observed at various ranges which depend on the position of the object within the limits of the scanning angle. This circumstance leads to the difference of signals from identical objects arranged in different places of the scanning zone. Furthermore, with an increase in the angle of deviation of the instantaneous field of view from the normal, along with an increase in the distance to radiating objects, the thickness of the absorbing layer of the atmosphere in the path of propagation of the radiation flux increases. This furthers an even greater attenuation of the radiation flux from the object and a reduction in the signal at the output of the receiver.

Systems with a conical scanning of space (Fig. 5.19) can be considered devoid of this shortcoming. In these systems, the

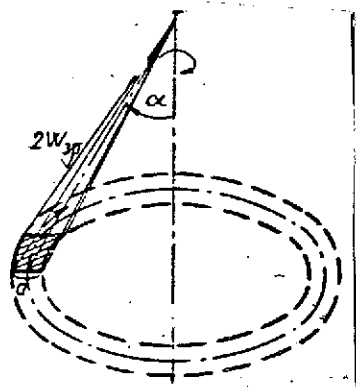


Fig. 5.19. Principle of scanning space in systems with conical scanning.

instantaneous field of view of the instrument rotates relative to a specific direction, called the scanning axis. In instruments intended for observations of the earth's surface, this axis is combined with the direction of the local vertical. In the general case, the instantaneous field of view is deflected from the axis of rotation by the angle α . Inasmuch as the angle α remains constant during rotation, the dimension of the area of the earth's surface projected on the receiver at each moment in time also remains unchanged (if the axis of rotation coincides with the normal to the earth's sphere). The basic relations between the flight

/163

parameters of the carrier and the characteristics of the scanning instrument can be obtained from the following considerations.

If the instantaneous field of view rotates with a rotation frequency of N/sec , the linear rate of its displacement over the earth's surface (without consideration of its curvature) is

$$V_v = 2\pi N H \tan \alpha \quad (5.44)$$

The angular velocity of the instantaneous field of view, determined by the expression

$$\omega_v = \frac{V_v}{L},$$

where $L = \frac{H}{\cos \alpha}$ is the distance from the instrument to the earth's surface with consideration of (5.44), turns out to be equal to

$$\omega_v = \frac{2\pi N H \tan \alpha}{L} = 2\pi N \sin \alpha. \quad (5.45)$$

Considering the size of the instantaneous field of view in the direction of rotation equal to $2W'_v$ and knowing the angular velocity ω_v , we find the time of illumination of the receiver by an emitter within its range from the formula

/164

$$\Delta t_{il} = \frac{2W'_v}{\omega_v} = \frac{W'_v}{\pi N \sin \alpha}.$$

Hence, on the basis of condition (5.18), we have

$$N \leq \frac{W'_v}{\pi k_r \tau \sin \alpha} \quad \text{or} \quad W'_v = N \pi k_r \tau \sin \alpha. \quad (5.46)$$

From the condition of the contact of adjacent lines, the rate of scan should be at least the speed of flight, i.e.

$$Nl \geq V, \quad (5.47)$$

where l is the width of the circular zone scanned by the instrument on the ground during one revolution of an instantaneous field of view. It is not difficult to show that

$$l = \frac{2HW_V'}{\cos^2 \alpha}, \quad (5.48)$$

where $2W_V'$ is the size of the instantaneous field of view in a radial direction. Considering the last expression, from (5.47) we have

$$N \geq \frac{V \cos^2 \alpha}{2HW_V'}. \quad (5.49)$$

Thus, the rate of rotation of an instantaneous field of view should satisfy the condition

$$\frac{W_V'}{\pi k_r \tau \sin \alpha} \geq N \geq \frac{V \cos^2 \alpha}{2HW_V'}. \quad (5.50)$$

With a square field of view ($W_V' = W_V''$), from (5.50) we obtain

$$W_V' = \sqrt{\frac{\pi k_r \tau V \sin \alpha \cos^2 \alpha}{2H}}, \quad (5.51)$$

$$N = \sqrt{\frac{V \cos^2 \alpha}{2H \pi k_r \tau \sin \alpha}}. \quad (5.52)$$

In a number of cases, when the satisfaction of the condition of contact of adjacent circular bands is not mandatory, for example, in plotting devices for the local vertical, relations (5.46) are used to establish the connection between various parameters of the instrument. However, here, in contrast to previously examined scanning systems, the value of coefficient k_r can sometimes be taken as not only less than 2, but also even 1. This is determined by the threshold sensitivity of the entire instrument, the amplification factor of the electronic circuit, and other factors. /165

Variations of the schematic solution of scanning systems with conical scanning are presented in Fig. 5.20.

5.5. Scanning and Search Systems Based on the Use of Fiber Optics

The use of fiber optics in scanning and search systems permits realizing various types of scanning comparatively simply. In this, the shortcomings inherent in the scanning systems which have been considered are either completely excluded or attenuated considerably. The use of fiber optics permits excluding from the instrument schemes large-size rotating parts and devices, and also increasing significantly the time efficiency of the scanning system.

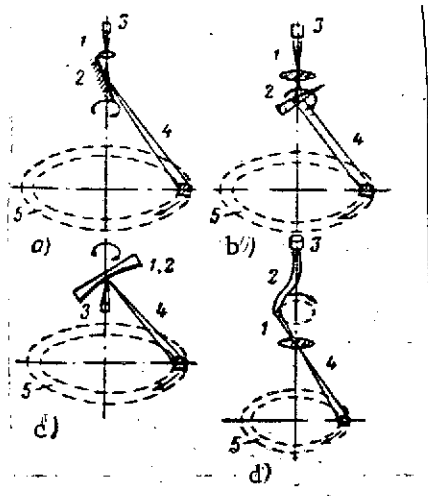


Fig. 5.20. Variation in the schematic solution of scanning systems with the conical scanning of space: a. with a flat mirror; b. with a rotating wedge; c. with a rotating off-axis parabolic mirror; d. with a rotating fiber bunched connector; 1. objective; 2. scanning element; 3. radiation receiver; 4. trajectory of the instantaneous field of view.

As an example, let us consider an electro-optical instrument with line scanning. A diagram of such a scanning device can be presented in the form shown on Fig. 5.21. Its composition includes an objective, fiber converter, optical commutator, and radiation receiver. The role of the scanner itself is played by a fiber image converter and optical commutator.

The fiber converter is a device which assures the change in the shape of the image from a line to a ring. For this, the

input ends of the fibers are collected in a bunched conductor having in its cross section the shape of a greatly elongated rectangle. Its small dimension is determined by the size of the angle of the instantaneous field of view, and its large dimension by the size of the scanning angle. The output ends of the fibers are assembled in a ring whose dimensions depend on the parameters of the optical system, scanning angle, and angle of instantaneous field of view of the instrument. With such a design of the converter, the image of the line is modified into a ring. If, with the use of the optical commutator, the radiation which emerges from the converter successively from each sector of the ring is directed at the radiation receiver, the

/166

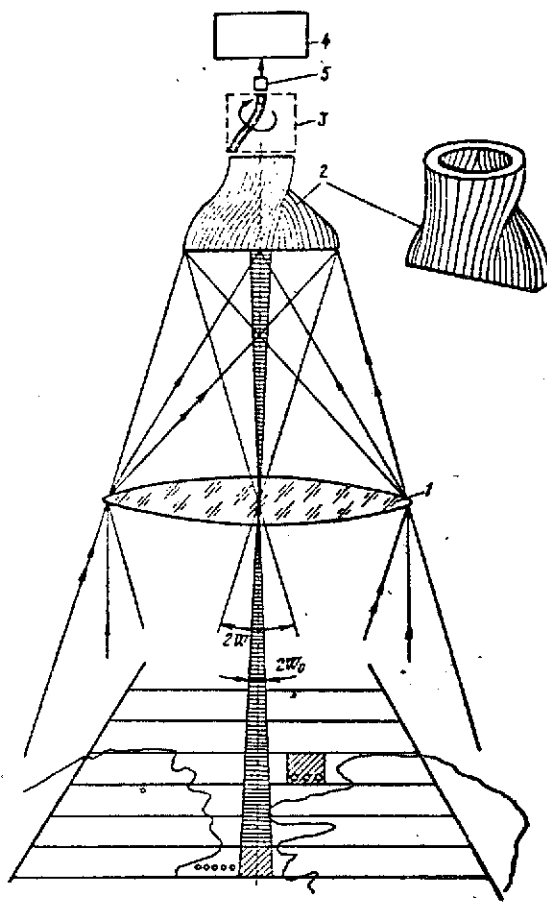


Fig. 5.21. Diagram of the scanning system with a fiber converter.

the entire line will be scanned during one revolution of the commutator. The role of the commutator can be accomplished either by a lens optical system with a diaphragm or by a bunched conductor which rotates relative to the optical axis of the objective.

In the focal plane of the objective, we can place not one, but several lines which will be collected into one ring successively one after the other at the output.

The width of the band /167 scanned by the instrument with the presence of m lines is determined by the expression

$$l = 2W_V m H,$$

and the width of the zone in angular measure

$$W = 2W_V m.$$

If we designate the frequency of rotation of the optical commutator by N , then on the strength of the condition for the contact of adjacent bands with a given speed of flight of the carrier V , we obtain the following relation

$$N \geq \frac{V}{2W_V H m} \quad \text{or} \quad N \geq \frac{u}{2W_V m}. \quad (5.53)$$

The number of scanning elements in the image in the given case is described by the equality.

$$Q = m \frac{W_{sc}}{W_v} \quad (5.54)$$

The number of scanning elements of which are scanned by the system in a second will be

$$Q_1 = NQ = Nm \frac{W_{sc}}{W_v},$$

whence the time of illumination of the receiver with one element turns out to be equal to

$$\Delta t_{ill} = \frac{1}{Q} = \frac{W_v}{NmW_{sc}} \quad (5.55)$$

From (5.55), with consideration of condition (5.18), we have

$$N \leq \frac{W_v}{k_r \tau m W_{sc}} \quad (5.56)$$

This relation determines the maximum allowable rate of rotation of the optical commutator on the strength of the time constant of the receiver. Equating the right sides of relations (5.53) and (5.56), we find

$$W_v = \sqrt{\frac{k_r \tau W_{sc} V}{2H}} \quad \text{or} \quad W_v = \sqrt{\frac{1}{2} k_r \tau \omega W_{sc}} \quad (5.57)$$

The expression obtained provides the opportunity to calculate the maximum allowable dimensions of the field of view of the scanning instrument with its given parameters and flight characteristics.

If we exclude W_v in formulas (5.53) and (5.56), then, solving them together, we obtain

$$N = \sqrt{\frac{V}{2Hm^2k_r\tau W_{sc}}} \quad \text{or} \quad N = \sqrt{\frac{\omega}{2m^2k_r\tau W_{sc}}} \quad (5.58)$$

Thus, in order to obtain information about all radiating objects located in a given scanning band with a specific receiver time constant, the rate of rotation of the optical commutator should satisfy condition (5.58).

Let us show that with the use of scanning systems based on the employment of fiber optics, the masses and dimensions of the rotating elements are considerably reduced. As an example, let us calculate the parameters of the converter and the commutator. If m lines of a fiber converter are placed in the focal plane of the objective, the overall number of scanning elements is determined by relation (5.54).

Considering that the area of one element of the dissociation is A_e , the overall surface of the receiving end of the fiber converter in the focal plane will be

$$A_{s.r.} = QA_e \quad (5.59)$$

$$A_e = a^2$$

where a is the size of one scanning in the focal plane.

Inasmuch as $a = 2f'W_v$, substituting the values of the quantities in (5.59), we find $m = 1$

$$A_{s.r.} = a^2 \frac{W_{sc}}{W_v} = \frac{(2f' \cdot W_v)^2}{W_v} \cdot W_{sc} = 4f'^2 W_v W_{sc} \quad (5.60)$$

Since the output end of the converter has the shape of a ring, its area can be found from the expression

$$A_{ring} = 2\pi\rho\delta, \quad (5.61)$$

where ρ is the mean radius of the ring; δ is the width of the ring in which the output ends of the converter fibers are collected.

In the employment of cylindrical fibers in the converter, the areas of the surface of its input and output ends are identical, i.e.,

$$A_{s.r.} = A_{ring}.$$

With consideration of (5.50) and (5.61), we obtain the relation for the determination of the value of the radius of the converter ring

$$\rho = \frac{2f'^2 W_v W_{sc}}{\pi \delta}. \quad (5.62)$$

If an objective with a focal length $f' = 500$ mm is employed in the instrument and the angle of the instantaneous field of view and scanning angle respectively equal $2W_v 2'$ and $2W_{sc} = 40.174 \cdot 10^{-2}$ rad, then with $\delta = 5$ mm, on the basis of (5.62), we obtain $\rho = 30$ mm.

Thus, the only rotating part in the instrument -- the optical commutator -- has a comparatively small diameter.

/169

The description of scanning systems with cycloid and spiral scans is presented in work [4].

CHAPTER 6. ELECTRO-OPTICAL INSTRUMENTS FOR THE ORIENTATION OF SPACECRAFT

6.1. The Purpose and Classification of Orientation Instruments

The orientation and stabilization of a spacecraft in space are necessary both for the solution of navigational problems and for assuring the normal functioning of equipment for specific purposes.

The orientation system, being a part of the system for the control of the SC, gives it a specific position in space and holds it in this position during the required time interval.

The orientation system permits:

- Accomplishing the stabilization of the SC in space;
- Reducing or completely excluding rotation relative to the center of mass;
- Orienting an orbital SC relative to the earth's surface in the accomplishment of observations and the conduct of meteorological reconnaissance;
- Orienting the SC in the accomplishment of astronomic observations;
- Orienting the SC before turning on mid-course propulsion systems during orbital and interplanetary flights;
- Accomplishing the constant orientation of the panels of the solar batteries in the direction of the sun;
- Assuring the orientation of the directional antennas toward the earth or other objects during communication;
- Accomplishing the orientation of unmanned interplanetary probes (UIP) during flights to other planets;
- Orienting the SC before turning on the retrofire rockets during landing;
- Assuring the orientation of the SC during the accomplishment of an approach in space and the mutual orientation of the SC in the execution of docking and so forth.

Both passive as well as active methods of orientation can be used for the accomplishment of orientation. Passive methods, based on the use of the gravitational field, light pressure, and so forth are characterized by small values of the orienting moments. A method based on the use of the gravitational field is beginning to find application. /170

Of the active methods, the basis of which is formed by the creation of orienting moments due to on-board sources of power (inertial, radiation, radar, and so forth), the greatest

propagation has been received by methods based on the employment of various electro-optical instruments.

Depending on the missions accomplished by the SC, its orientation may differ. The most widespread type of orientation of orbital SC is their orientation along the vertical and the course. In this case, the SC turns relative to the axis which is normal to the plane of orbit and remains stationary relative to the plane of orbit, i.e., it does not rotate around the local vertical.

A widespread type of orientation is single-axis orientation on a heavenly body when the SC has the possibility to rotate only around the axis directed at this body, remaining stabilized for the other two axes. We can point to orientation in the direction of the sun, moon, or a planet as examples of such orientation. Often such a type of orientation is used to assure the operation of solar batteries.

In general, the orientation system has three control channels in its composition, each of which includes measuring devices, amplifier-converters, and slave elements.

The operating principle of the orientation system consists of the fact that the measuring devices or data units generate error signals of the position of the axis being oriented relative to the given direction.

Next, the signals go to the amplifier-converters which directly control the operation of the slave elements. As a result of the action of the latter, the required orientation of the SC is attained relative to reference directions. Depending on specific conditions, the direction to the edge or to the center of a heavenly body or the direction to a star are selected as such reference directions.

In accordance with the initial astronomic reference point, electro-optical orientation instruments can be divided into the following groups:

- Instruments which use the earth as a reference point;
- Instruments which use some planet as the initial reference point;
- Instruments intended for determining the direction to the sun;
- Instruments which determine and fix the direction to individual stars or stellar fields.

In addition, there exists a division into groups according /171 to the band of the radiation spectrum used for work:

- Instruments which use the low-temperature radiation of planets and which operate in a broad band of the infrared region of the spectrum;
- Instruments which operate in the visible band of the spectrum and use the intrinsic radiation of the sun or the radiation of the sun reflected from the moon and planets;
- Instruments which operate from the visible radiation of the stars;
- Instruments intended for operation from radiation which lies in a narrow section of the spectrum (radiation of a laser, radiation of the carbon dioxide layer of the atmosphere).

In accordance with the type of SC, the following types of instruments are distinguished:

- Instruments for systems for the control and orientation of orbital SC both during flight in orbit as well as before descent to the earth. (Here, we refer to various types of resolvers of the vertical on board the SC, instruments for orientation of the longitudinal axis of the SC relative to the velocity vector, and instruments for the orientation of the SC from the sun and earth);
- Instruments of systems for the control and orientation of SC during interplanetary flights. (Here, we refer to systems for sun-star orientation, solar orientation, and instruments for orientation on the earth and planets);
- Instruments for orientation of the SC which are used for the execution of a controlled approach.

The last section of this chapter will consider the principles for the operation and design of electro-optical orientation instruments for various purposes as applicable to the latter classification.

6.2. Pulse Sensors of the Horizon

In a number of cases, stabilization of the SC in space is accomplished due to its rotation relative to one of its axes. A rotating SC stabilized in inertial space will continuously change its orientation relative to the earth. In order to determine the position of the axis of rotation of the SC relative to the local vertical, a pulsed electro-optical horizon sensor with a small field-of-vision angle is installed on board. The optical axis of the sensor comprises a right angle with the axis of rotation of the SC. As a result, with the rotation of the SC the field of view of the sensor will describe a complete circle, periodically intersecting the earth's surface. The sensor is an instrument

consisting of an objective in whose focal plane a radiation receiver is installed and an amplifying electronic circuit. With the intersection of the boundary between space and the surface of the earth by the instantaneous field of view, signals will arise on the output of the sensor. From these signals, the time intervals may be obtained during which the field of view is directed at the earth and into space. The angle between the axis of rotation of the SC and the local vertical is determined from the relationship of the time intervals, which provides the opportunity to determine the coordinates of the sectors of the earth's surface scanned by the satellite's apparatus from the known orbit parameters. /172

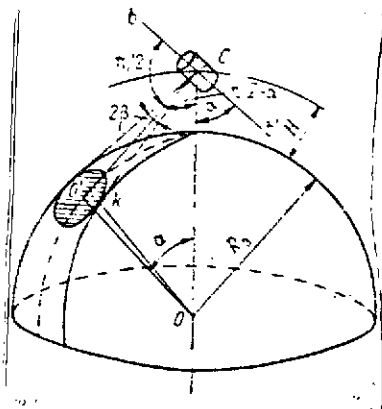


Fig. 6.1. Diagram of the determination of the position of the axis of rotation of a vehicle relative to the local vertical.

Fig. 6.1 shows the position of a spacecraft which is stabilized by rotation relative to axis bb' and which rotates through an orbit with altitude H . As a result of the rotation of the SC around axis bb' , the earth's surface will appear in the sensor's field of view at some moment of time t_1 and will remain there until moment t_2 , i.e., during interval

$$\Delta t_1 = t_2 - t_1.$$

After interval Δt_2 at moment t_3 , the sensor's field of view will again approach the horizon and will be directed at the earth and so on, in which regard

$$\Delta t_2 = t_3 - t_2.$$

The relationship between intervals Δt_1 and Δt_2 permits finding the size of the angle of rotation (2β) of the SC when the earth remains in the field of view of the horizon sensor. This relation has the form

$$\frac{\Delta t_1}{\Delta t_2} = \frac{\beta}{\pi - \beta}, \quad (6.1)$$

We find the value of angle α , which determines the position of the axis of rotation of the SC relative to the local vertical (using the geometric construction of Fig. 6.1), from the relation

$$\alpha = \arcsin \frac{\sqrt{2R_e H + H^2}}{(R_e + H) \cdot \cos \beta} \quad (6.2)$$

where R_e is the radius of the earth.

The described method for determining the axis of rotation of the SC relative to the local vertical found application in satellites of the "Tiros" types (US). Used as a horizon sensor on these SC is a compact (25 mm × 25 mm × 150 mm), light (230 g), narrow-band radiometer consisting of a germanium objective, immersion thermistor radiation receiver, and semiconductor amplifier. The field-of-vision angle of the sensor is 0.0225 rad [34]. Time intervals Δt_1 and Δt_2 are read from the distances between the positive and negative pulses which arise on the output of the amplifier with the intersection of the space-earth boundary. In this, a positive pulse arises with the crossing of the boundary in the space-earth direction, and a negative pulse in the earth-space direction. A typical appearance of the signals is presented in Fig. 6.2. Information obtained over the telemetry channel is transmitted to ground processing points where, on the basis of the indicated records, the orientation of the SC with respect to the earth is determined (the position of the axis of rotation of the SC relative to the local vertical is determined with an accuracy of ± 0.035 rad). The coordinates of the areas being observed are determined on the basis of these same records. /173

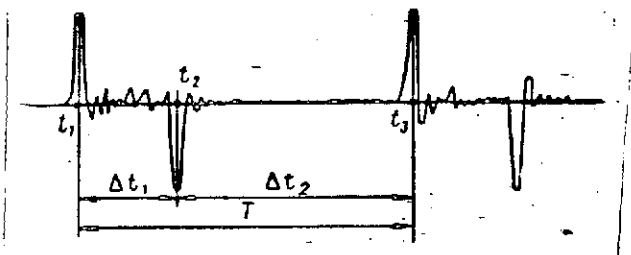


Fig. 6.2. Typical appearance of signals of a pulsed horizon sensor.

Signals from on board the SC are used to feed the corresponding commands to turn the measurement infrared and television equipment on and off. To obtain steady stabilization and satisfactory data in finding time intervals Δt_1 and Δt_2 , the frequency of rotation of the SC should be within the limits of 360-3600/sec.

From Fig. 6.1., it can be seen that with some invariable position of the axis of the SC in inertial space, on some sectors of the orbit the axis of the horizon sensor does not intercept the earth and the sensor does not issue any information. To exclude such a position on later orbits of the satellites, a block rather than one instrument is used consisting of two independent sensors whose optical axes are inclined at an angle of ± 0.38 rad from the normal to the axis of rotation.

Up to the present, instruments which permit immediately determining the position of the axis of yaw relative to the local vertical and generating the corresponding error signals have received wide application in space technology. These instruments have received the name of local-vertical resolvers. Several methods for constructing the local vertical are distinguished [32]. They include the following methods: the method of secants, following the horizon line with the use of scanning and nonscanning instruments and others.

6.3. Principles and Equipment for Determining the Local Vertical by the Method of Secants

The method of secants is also based on the use of the temperature contrast between the earth's surface and outer space and is used on SC which are stabilized with respect to the local vertical for the determination of the position of the axis being oriented (usually the axis of yaw) relative to the local vertical and the generation of the necessary error signals which control the operation of the stabilization system. In order to accomplish the stabilization of the SC relative to the local vertical, the error signals should be generated in two mutually perpendicular planes, i.e., along the roll and pitch channels.

For the realization of the method of secants, two electro-optical scanning instruments are installed aboard the SC. The sighting axes of these instruments intersect the earth's surface periodically in two mutually perpendicular planes during operation. Hence, it received its name of the method of secants. The scanning plane of one instrument is parallel to the plane in which the axes of yaw and roll lie, and the scanning plane of the second sensor is parallel to a plane which passes through the axis of yaw and pitch. The scanning instruments are installed on board in such a way that their axes, intersecting each other at a right angle, lie in one plane perpendicular to the yaw axis of the SC (Figs. 6.3, 6.4). The instantaneous field of view of each

of the instruments is deflected from the OO' axis by the angle α and rotates around it, describing a cone with the angle 2α at the apex. The value of angle α depends on a number of factors and may reach $\pi/2$.

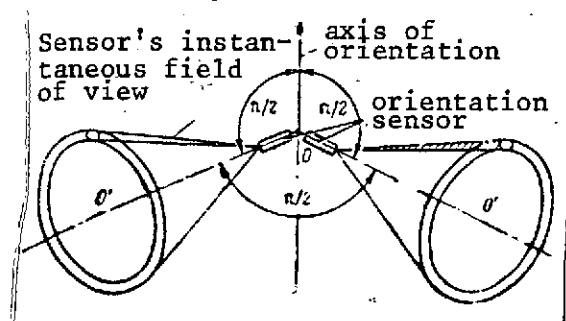


Fig. 6.3. Diagram of the arrangement of the sensors of an electro-optical resolver of the local vertical which operates with the intersections method.

During scanning, the instantaneous fields of view of the instruments are periodically directed

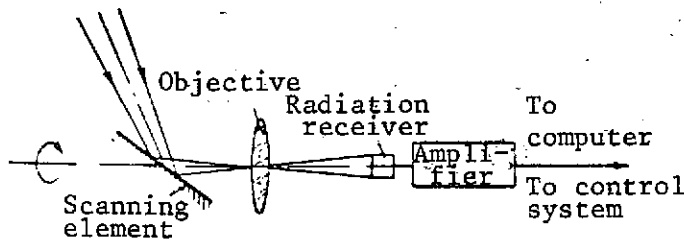


Fig. 6.4. Diagram of a sensor on board a space vehicle.

first at the earth's surface, then at space. During one scanning cycle, i.e., during a complete revolution of the scanning element, the instantaneous field of view crosses the horizon twice. When the earth's surface comes into the field of view, signals appear at the output of the instruments which are caused by the earth's thermal radiation. An idealized

shape of the signals at the output of the radiation receiver of one of the instruments is shown in Fig. 6.5. The duration of the pulses at the output of the receivers depends on the frequency of rotation of the instantaneous field of view and the angular dimensions of the earth's surface in the plane of its intersection by the sighting ray and the pulse repetition frequency is determined by the scanning frequency. The duration of pulse Δt from the output of the receiver, the value of angle 2β which corresponds to it (Fig. 6.6), and time segment $T - \Delta t$ are interconnected by the relation

$$\frac{\Delta t}{T - \Delta t} = \frac{\beta}{\pi - \beta}, \quad (6.3)$$

where T is the scanning period.

The value of angle 2β within whose limits the instrument's instantaneous field of view continues to remain directed toward the earth during scanning is a function of the altitude of flight of the SC and the angle of slope of the sighting axis to the axis of rotation of the instantaneous field of view. From the diagram presented in Fig. 6.6, we have

$$\beta = \arccos \frac{AK}{AE} = \arccos \frac{rH + h}{AE}, \quad (6.4)$$

where h is the rise of the earth segment measured from the plane in which the chord DE , which connects the points of intersection of the sensor's sighting axis with the earth's surface, lies; AE is the tangent to the earth's surface.

We find the quantities appearing in formula (6.4), using

Fig. 6.6

$$AE = L \cdot \sin \alpha \quad \text{and} \quad h = R_e (1 - \cos \gamma)$$

where

$$L = CE = \sqrt{2R_e H + H^2} \quad \text{and} \quad \cos \gamma = \frac{R_e}{R_e + H}$$

Substituting the found values in (6.4), we obtain

$$\beta = \arccos \frac{H + R_e \left(1 - \frac{R_e}{R_e + H}\right)}{\sin \alpha \sqrt{2R_e H + H^2}}, \quad (6.5)$$

whence, after simple conversions, we find

$$\beta = \arccos \frac{\sqrt{2R_e H + H^2}}{(R_e + H) \sin \alpha}. \quad (6.6)$$

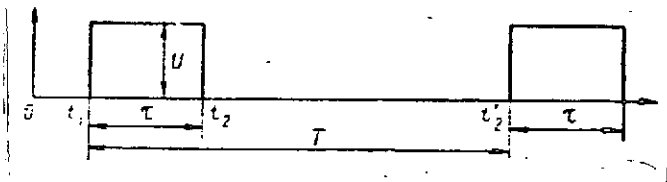


Fig. 6.5. Sequence of pulses read from the output of one of the radiation receivers of the vertical resolver.

With consideration of (6.6), ^{/177} from (6.3), we obtain

$$\frac{\Delta t}{T} = \frac{1}{\pi} \arccos \frac{\sqrt{2R_e H + H^2}}{(R_e + H) \sin \alpha}. \quad (6.7)$$

The dependence of the relative duration of the pulses from the output of the radiation receiver on

the size of the angle between the axis of rotation and the sighting angle of the sensor and also on the altitude of flight of the SC is shown in Fig. 6.7. From the graphs, it can be seen that with oscillations of the SC relative to the local vertical, the maximum values of the amplitudes of the oscillations with a given size of the angle depend on the altitude of flight and may achieve great values without causing a substantial change in the duration of the pulses.

The formation of the error signals of the axis of yaw of the SC with the local vertical in the method of secants can be accomplished in different ways. Applicable here are phase, time, and phase-time methods of forming the control signals.

$$f(t) = \frac{1}{2} \sum_{n=-\infty}^{\infty} \bar{A}_n e^{jn\omega_1 t}$$

where $\bar{A}_n = \frac{2}{T} \int_{t_1}^{t_2} f(t) e^{-jn\omega_1 t} dt$ is the complex amplitude of the n-th harmonic; $n = 1, 2, 3 \dots$ is the ordinal number of the harmonic; $\omega_1 = \frac{2\pi}{T} = 2\pi f$ is the frequency of the first harmonic; $T = t_2 - t_1$ is the pulse repetition period (scanning period).

From (6.7), it follows that with any altitude of flight of the SC, the duration of the pulses Δt will always be less than half the period T , and their sequence has the form shown in Fig. 6.5, where the moment of time relative to the start of the reading is designated by t_1 and the amplitude of the pulse by U . The corresponding time function of the given sequence is expressed in the following manner

$$f(t) = \begin{cases} U_m & \text{with } t_1 \leq t \leq t_2 = t_1 + \Delta t; \\ 0 & \text{with } t_2 < t < t_1 + T. \end{cases}$$

As applicable to the indicated sequence, the expression for \bar{A}_n takes the form

$$\bar{A}_n = \frac{2}{T} \int_{t_1}^{t_2} U_m e^{-jn\omega_1 t} dt = \frac{2U_m}{jnT\omega_1} (e^{-jn\omega_1 t_1} - e^{-jn\omega_1 t_2})$$

whence, considering that $t_2 = t_1 + \Delta t$, we have

$$\bar{A}_n = \frac{2U_m \Delta t}{T} \frac{\sin \frac{n\omega_1 \Delta t}{2}}{\frac{n\omega_1 \Delta t}{2}} e^{-jn\omega_1 (t_1 + \Delta t/2)} \quad (6.8)$$

Here, the constant component and parameters of the harmonics are determined by the relations

$$\text{- Constant component} \quad A = \frac{U_m \Delta t}{T}; \quad (6.9)$$

$$\text{- Amplitude of harmonics} \quad A_n = 2U_m \frac{\Delta t}{T} \left| \frac{\sin \frac{n\omega_1 \Delta t}{2}}{\frac{n\omega_1 \Delta t}{2}} \right|; \quad (6.10)$$

- Phase of harmonics $\theta_n = n\omega_1 \left(t_1 + \frac{\Delta t}{2} \right) + (n-1)\pi,$ (6.11)

where m is the ordinal number of the interval $\Delta\omega = \frac{2\pi}{\Delta t}.$

Since the reference signals in the phase method are a sine- /179 wave alternating voltage, only the first harmonic of the operating signal is usually used for the forming of the error signals. On the basis of (6.10) and (6.11), its parameters are characterized by the relations

$$U_1 = 2 \frac{U_m \Delta t}{T} \left| \frac{\sin \frac{\omega \Delta t}{2}}{\frac{\omega_1 \Delta t}{2}} \right|,$$

$$\theta_1 = \omega_1 (t_1 + \Delta t/2).$$

Whence, with consideration of (6.7), we obtain

$$U_1 = \frac{2U_m \Delta t}{T} \left| \frac{\sin \beta}{\beta} \right| = \frac{2U_m \Delta t}{T} \left| \frac{\sin \left(\arccos \frac{\sqrt{2R_e H + H^2}}{(R_e + H) \sin \alpha} \right)}{\arccos \frac{\sqrt{2R_e H + H^2}}{(R_e + H) \sin \alpha}} \right|, \quad (6.12)$$

$$\theta_1 = \omega_1 t_1 + \beta = \omega_1 t_1 + \arccos \frac{\sqrt{2R_e H + H^2}}{(R_e + H) \sin \alpha}. \quad (6.13)$$

Discrimination of the first harmonic is accomplished with the use of narrow-band resonance filters tuned to the required frequency which equals the scanning frequency. As a result, a sine-wave voltage is fed to the input of the device for the formation of the signal which is described by the relation

$$U = U_1 a \sin(\omega t + \theta_1),$$

where a is the amplification factor of the circuit.

If this voltage is fed to the input of a phase-sensitive detector which operates in the key mode and is controlled by signals of the reference voltage, the constant component of the

operating signal at its output proves to be proportional to the angle of phase shift θ_1 . Actually, by analogy with (5.4), we have

$$U_1 = \frac{U_1}{\pi} a \int_0^\pi \sin(\omega t + \theta_1) d(\omega t) = \frac{2U_1}{\pi} a \cos \theta_1. \quad (6.14)$$

Accordingly, for the second channel, we will have

$$U_{II} = \frac{2U_2}{\pi} a \cos \theta_2. \quad (6.15)$$

Designated in formulas (6.14) and (6.15) are: θ_1 and θ_2 are the components of the error angle of the SC with the local vertical for pitch and roll respectively; U_{1a} and U_{2a} are the amplitudes of the signals at the input of the phase-sensitive detectors in the pitch and roll channels. /180

An analysis of formulas (6.14) and (6.15) shows that the value of the output signal is linearly dependent on the error angle within limits of $\theta = \pm 0.6$ rad.

A functional diagram of the instrument which forms the error signals in accordance with the method considered is presented in Fig. 6.8. Instruments of the indicated type can give satisfactory results with the orientation of SC which rotate in orbits with altitudes of from 180-200 km up to several thousand km. The orbit may be circular as well as elliptical. The error in the determination of the position of the local vertical by instruments which realize the intersections method, with the phase method of forming control signals depending on the altitude of flight of the SC, lies within limits of from $\pm 1.72 \cdot 10^{-2}$ rad to $\pm 0.172 \cdot 10^{-2}$ rad [58, 59, 65].

Orientation instruments created in accordance with such a scheme were employed successfully to assure the orientation and stabilization of several elements in the experimental launchings of the Atlas, Thor, and Jupiter rockets, and also on the Mercury spacecraft. A layout diagram of one such instrument is presented in Fig. 6.9 [57, 63]. There is a window in the front wall of the instrument which is closed by a germanium filter. The scanning element in the instrument is an optical wedge of germanium with a taper angle of 0.26 rad. The radiation which has passed through the wedge is directed to the germanium layer of an immersion bolometer which simultaneously fulfills the role of instrument objective. All optical parts of germanium are coated for a wavelength of $\lambda = 12.5 \mu\text{m}$. Graphs of the change /181

in the coefficient of spectral transmission of one germanium part with two-sided transmission augmentation and of the entire optical system with transmission augmentation on a wavelength of $\lambda = 12.5 \mu\text{m}$ are presented in Fig. 6.10. With the use of the scanning element, the instantaneous field of view of the instrument which has dimensions of from 0.035 to 0.24 rad deviates from the normal by an angle of 0.96 rad. The scanning frequency in this instrument is 30 Hz. The power supply source and the electronic device in which the processing of the signals, which are read from the output of the radiation receiver, occurs comprise a compact unit assembled on printed circuits. The instrument is completely hermetically sealed and filled with dry nitrogen under a pressure of $1.29 \cdot 10^5$ – $1.35 \cdot 10^5$ Pa. To raise the dependability and effectiveness of operation of the instruments, ^{/182} blocking is provided for in their circuits in the event that the sun lands in the field of view.

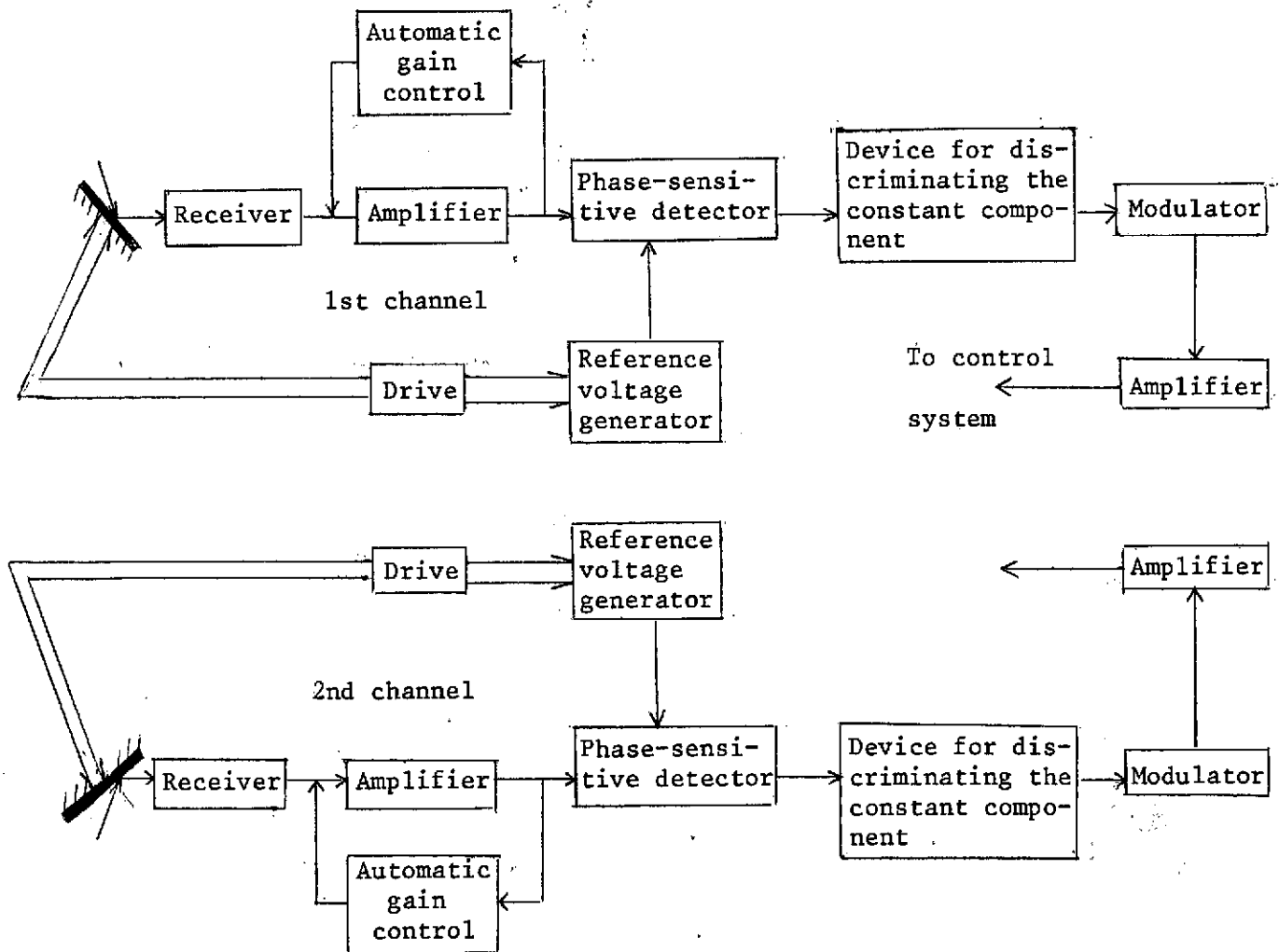


Fig. 6.8. Functional diagram of the resolver of the local vertical which operates with the method of secants.

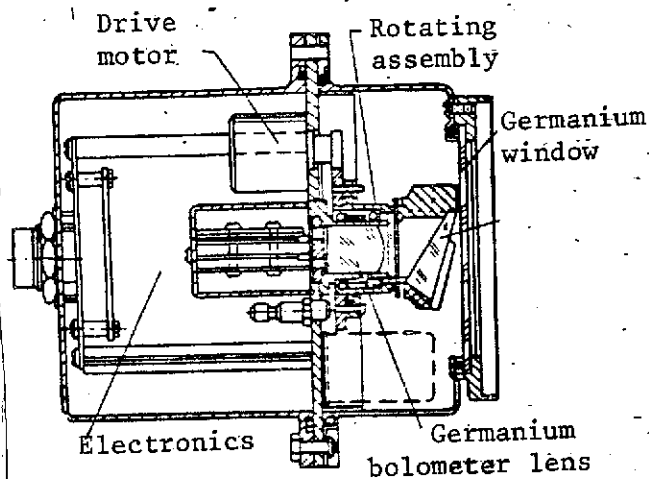


Fig. 6.9. Layout diagram of the scanning head of a local-vertical resolver which operates on the method of secants.

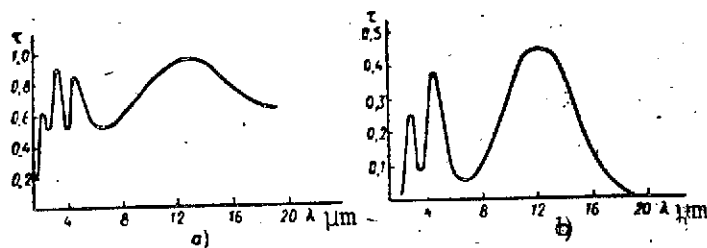


Fig. 6.10. Spectral transmission of germanium optical components exposed to a wavelength of $\lambda = 12.5 \mu\text{m}$: a. one component with exposure from both sides; b. complex optical system of four components.

On spacecraft which are rotating in circular orbits with a given altitude, error signals over the pitch and roll channels can be formed fundamentally with the use of only one instrument which operates according to the scheme presented in Fig. 6.11. In this case, the formation of the error signal over the roll channel is accomplished just as in the variation considered above, i.e., with the use of the phase method for discriminating the control signal. For forming the error signal over the pitch channel, use can be made of information on the duration of the pulses read from the output of the receiver. In order to obtain a control signal over this channel, pulses from the output of the receiver are also used here for triggering the generator of the reference signals which, together

with the amplified operating pulses, are fed to the coincidence circuit. The duration of the reference pulses should correspond exactly to the duration of the operating pulses from the output of the receiver with the correct orientation of the SC (i.e., with the matching of the axis of yaw with the direction of the local vertical), and for given parameters, the orbits are determined from the expression

$$\Delta t = \frac{T}{\pi} \arccos \frac{\sqrt{2R_e H + H^2}}{(R_e + H) \sin \alpha} \quad (6.16)$$

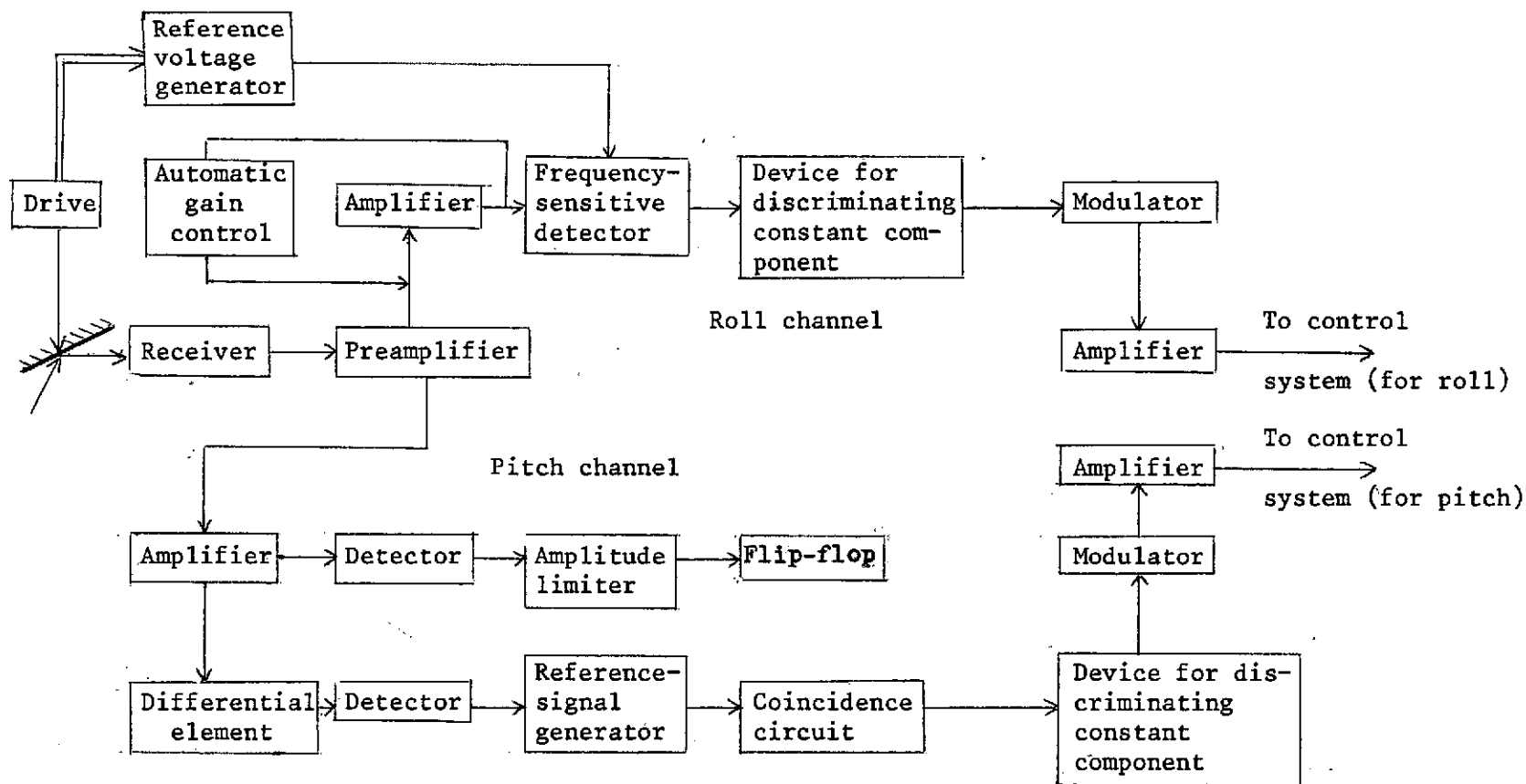


Fig. 6.11. Functional diagram of a system for forming control signals over two channels with the use of one scanning head.

The deviation of the axis of orientation of the SC from the local vertical for pitch causes an increase or decrease in the duration of the operating pulses from the output of the receiver. As a result of the comparison of the operating and reference signals, the constant component is discriminated whose value and sign determine the pitch error. A shortcoming of this method of forming error signals for pitch is the necessity to change the duration of the reference signals in accordance with the change in the altitude of the spacecraft above the surface of the earth (elliptical orbit).

The time method of forming error signals over the pitch and roll channels in the vertical resolvers which operate with the method of secants is based on the measurement of the time intervals between the reference (sighting) pulse and the pulse which arises on the output of the radiation receiver with the intersection of the earth's surface by the instrument's instantaneous field of view. We will explain the essence of the method with the aid of the diagram presented in Fig. 6.12a, which shows: lines tangent to the surface of the planet; the yaw axis of the SC which is oriented according to the local vertical; the reference sector.

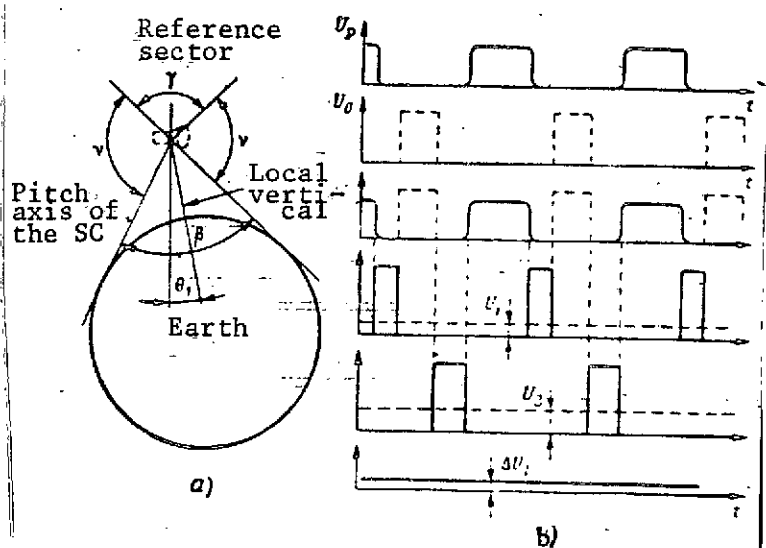


Fig. 6.12. Operating principle of the resolver of the local vertical which operates with the method of secants and is based on the use of the time method of forming control signals: a. essence of the method; b. nature of the output signals.

During scanning, the instantaneous field of view of the instrument periodically intersects the earth's surface, as a result of which pulses arise on the output of the radiation receiver whose duration is determined by expression (6.16). Furthermore, reference pulses are generated in the electronic circuit of the instrument. The position on the time axis and the duration of these pulses are determined by the position and angular

dimensions of the reference sector. Thus, in the electronic circuit of the resolver, with a given method of forming the error signals, series of periodically recurring electrical pulses are formed over each channel (Fig. 6.12b). The pulses shown by the dotted line pertain to the time intervals when the instantaneous field of view is located within the reference sector with angular dimension γ and apex at the point of intersection of the yaw axis with the local vertical. The pulses portrayed by the solid lines arise in those time intervals when the instantaneous field of view is directed at the earth's surface, i.e., when it passes through the sector between the two tangents to the surface of the planet. Let us point out that the radiation of the earth's surface is not perceived by the instrument with the location of the instantaneous field of view within the limits of the reference sector. The angle θ_1 between the yaw axis and the local vertical in the scanning plane being examined is the sought error angle and can be determined in the following manner.

If v_1 and v_2 designate the angles between the boundaries of the reference sector and the tangents to the surface of the planet, it is obvious that

$$\theta_1 = \frac{1}{2} (v_2 - v_1). \quad (6.17)$$

The pulses obtained from the output of the radiation receiver are used to form series of auxiliary pulses. The pulses in the auxiliary series have durations equal to the time intervals when the instantaneous field of view passes through sectors v_1 and v_2 , respectively. The auxiliary pulses which correspond to sector v_1 can be created, for example, by triggering a flip-flop at the moment which corresponds to the trailing edge of the reference pulse and by resetting the flip-flop by the leading edge of the pulse received from the planet. The pulses which correspond to sector v_2 are created by the trailing edge of the operating signal and the leading edge of the reference pulse. The reference pulse may be generated with the use of various sensors, for example, with the use of the magnetic sensor of the scanning mechanism. We also note that all auxiliary pulses have the same amplitude.

The mean value of the voltage of the sequence of pulses which correspond to sector v_1 is determined from the expression

$$U_1 = U \frac{v_1}{2\pi}, \quad (6.18)$$

where U is the amplitude of the auxiliary pulses; U_1 is the mean value of the voltage created by the sequence of pulses.

The sequence of pulses which correspond to sector v_2 causes /185 the mean voltage U_2 equal to

$$U_2 = U \frac{v_2}{2\pi} \quad (6.19)$$

Subtracting (6.18) from (6.19), we obtain

$$\Delta U_1 = U_2 - U_1 = \frac{U}{2\pi} (v_2 - v_1),$$

whence, with consideration of (6.17), we have

$$\Delta U_1 = \frac{U}{\pi} \theta_1 \quad (6.20)$$

This relation shows that the difference voltage ΔU is proportional to the error angle of the yaw axis of the SC with the local vertical in the scanning plane. In a similar manner, the error is determined in the other scanning plane where the second scanning instrument is used. Thus, voltages ΔU_I and ΔU_{II} completely describe the position of the yaw axis of the SC relative to the local vertical. These voltages are used for the forming of control signals in the system for stabilization over the pitch and roll channels.

6.4. Principles and Equipment for Determining the Local Vertical by the Method of Tracking the Horizon Line

The method is based on the use of the temperature contrast which exists between the earth's surface and outer space and can be realized with the use of three- or four-channel electro-optical resolvers of the local vertical. The simplest instrumental realization of the indicated method is the installation of a four-channel nonscanning instrument on board the SC whose fields of view of the channels are arranged in pairs in two mutually perpendicular planes. The optical axes of the channels deviate from the axis of the spacecraft being oriented (pitch axis) by the same angle. The size of the angle depends on the altitude of orbit and is so selected that with the correct

orientation of the spacecraft, the optical axes of the channels coincide with the tangents to the earth's surface. The angle of view of each sensor should be such that both the earth's surface with its surrounding atmosphere and outer space are projected to the radiation receiver simultaneously (Fig. 6.13). The second

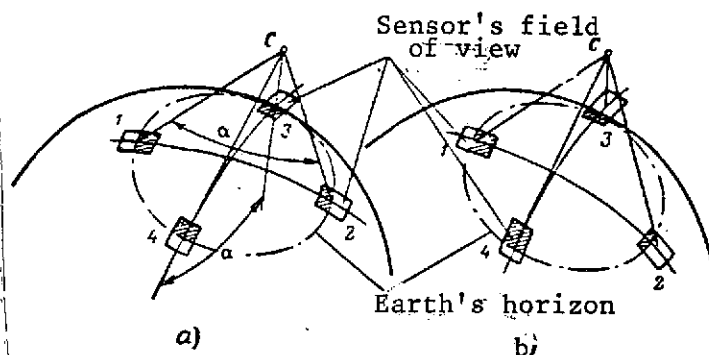


Fig. 6.13. Principle of construction of the local vertical with the use of a four-channel nonscanning instrument: a. precise orientation along the vertical of the SC; b. axis of the SC deflected from the vertical; 1, 2, 3, 4. fields of view.

condition on the strength of which the shape and dimensions of the field of view are selected is the condition of assuring the operation of the vertical resolver with a change in the altitude of orbit of the SC within certain given limits.

With the use of the four-channel instrument, on board the SC the position of the earth's horizon relative to the optical axes of the channels is constantly determined. The formation of error signals for pitch and roll can be accomplished with the use of the scheme

/186

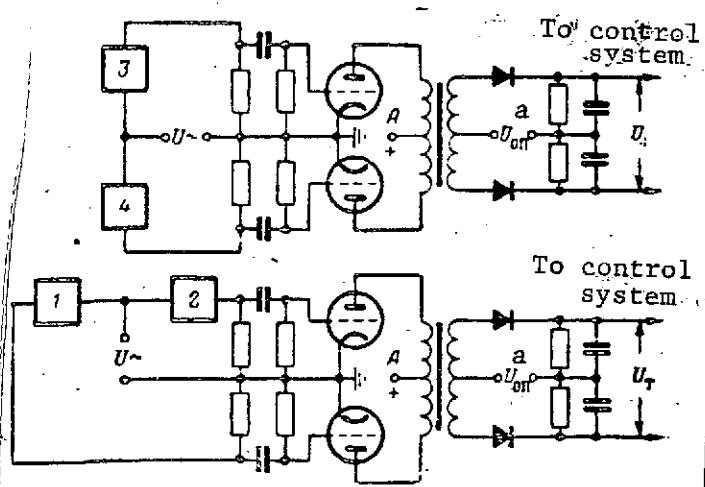


Fig. 6.14. Basic circuits of a system for the formation of control signals in a four-channel vertical resolver.

Key: a. U_{ref}

presented in Fig. 6.14. The radiation receivers of each pair of channels are connected at the input in opposition. One pair of receiver (channels 1 and 2) assures the formation of error signals for pitch, and the second (channels 3, 4) for roll.

With such a scheme, the output error signals prove to be proportional to the values of the angles of deviation of the yaw axis from the

direction of the local vertical for pitch and roll if the deviation does not exceed the dimensions of the field of view of one channel. When the value of the angle of deviation is larger between the axes of the channels, the output error signal is constant in value and equals its maximum value.

Actually, if the energy brightness B of the earth's surface within the limits of the fields of view of channels 1 and 2 are identical, the value of the signal from the output of each receiver will be proportional to the irradiated area of the sensitive layer which is determined by the size of the area of the earth's surface which is projected on the receiver. In turn, this area can be expressed in angular dimensions by the relation

$$A = W_0 W'_j c_1,$$

where W_0 and W'_j are the dimensions of the fields of view within whose limits the earth's surface is projected on the radiation receiver; c_1 is the proportionality factor.

The signals read from the outputs of the receivers of channels 1 and 2 can be presented in the form

/187

and

$$U_1 = S c_1 c_2 W_0 W'_1$$

$$U_2 = S c_1 c_2 W_0 W'_2$$

where S is the integral sensitivity of the radiation receivers (taken as the same for both receivers); c_2 is the proportionality factor which considers the parameters of the optical system.

Subtracting these equations, we get

$$\Delta U_1 = S c_1 c_2 W_0 (W'_1 - W'_2). \quad (6.21)$$

It is easy to see that the angle of deviation of the yaw axis from the local vertical θ is

$$\frac{w_1' - w_2'}{2} = \theta.$$

With consideration of the last relationship, from (6.21) we find

$$\Delta U_1 = 2Sc_1c_2W_0\theta. \quad (6.22)$$

One of the possible ways for creating such an instrument is the use of a wide-angle objective in whose focal plane four radiation receivers are placed by pairs in two mutually perpendicular directions. The distance between diametrically opposite receivers is determined by the parameters of the optical system and the angle which must be subtended by the earth's horizon α which depends on the altitude of orbit. As an example, Fig. 6.15 presents a scheme of a vertical resolver with a wide-angle objective [11, 35]. /188

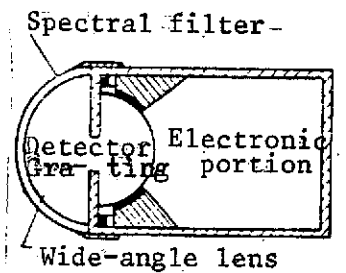


Fig. 6.15. Schematic diagram of a local vertical resolver with a wide-angle objective.

Bolometers connected by pairs in two bridge circuits are used as radiation receivers in the instrument. The deviation of the yaw axis of the SC from the direction of the local vertical causes the disruption of the balance of the bridge and the appearance of an error signal which is used to restore the correct orientation.

In order to exclude the influence of the sun on the operation of the instrument, in addition to the basic group of receivers, it contains one more group of four receivers turned by the angle $\pi/4$ with respect to the main group. When the sun's rays fall onto the field of view of one of the receivers of the first group, a signal is generated which puts the second group into operation. In this case, the error signals formed over the channels first go to the coordinate converter and only then to the servo elements.

The receiver of the vertical resolver itself as well as a special receiver can be used as a sensor which determines the presence of the incidence of solar rays in the field of view of the receivers of the first group. In the latter case, the fields of view of the channels of the device for protection from solar radiation should correspond to the fields of view of the individual receivers of the main group or exceed them somewhat.

The optical system of the instrument consists of a germanium lens objective and a germanium filter. The optical parts are coated for radiations with wavelengths of 14-15 μm . The instrument possesses minimum sensitivity to radiations with wavelengths of about 12 μm and a maximum in the region of 14-15 μm .

The instrument assures the determination of the vertical with a precision on the order of $3.1.74 \cdot 10^{-2}$ rad.

Another variation for the instrumental realization of the method for determining the position of the SC being oriented relative to the local vertical is possible. In this variation, use is made of an optical system which is common for all channels in whose focal plane the necessary number of radiation flux receivers is arranged. A diagram of the instrument's optical system is presented in Fig. 6.16.

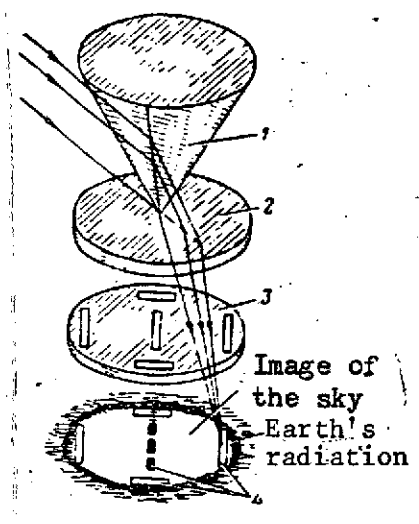


Fig. 6.16. Diagram of the construction of the local vertical with a cone-lens optical system: 1. optical cone with mirror coating; 2. lens objective and special filter; 3. germanium modulator; 4. receiver of earth's radiation.

The operating principle of such a vertical resolver consists of the fact that the radiation of the space located in front of the instrument is focused with the aid of the objective in the focal plane where the image of this space is also constructed. Thanks to the presence of a mirror cone, a sort of "reversing" of the image occurs. As a result, the image of the inner zone of space is constructed in the focal plane at some distance from the axis of the instrument. At the same time, the image of the outer zone of space is constructed close to the optical axis which either coincides with the axis of the SC being oriented or is parallel to it. /189

With the correct orientation of the SC, when the optical axis of the instrument coincides with the direction of the local vertical, the image of outer space will be constructed in the region of the focal plane near the axis and the image of the earth's surface not overlapped by the cone will be along the edges. Seven radiation receivers are placed in the focal plane. Four of them, which form the sides of a rectangle, are connected similar to the arms of a bridge. One

pair of diametrically arranged receivers is used for the orientation of the SC for pitch, and the other for roll.

The deviation of the axis of the SC being oriented from the direction of the local vertical causes a shift of the image in the focal plane and the appearance of signals on the outputs of the bolometers. These signals are initial for the forming of error signals and the subsequent control of the position of the SC.

The three remaining receivers are arranged on one line in the center of the focal plane. The central receiver perceives the radiation from space alone and the other two react to the earth's radiation which falls on them with a reduction in the altitude of flight when the dimensions of the image of outer space in the central zone of the focal plane are reduced.

With the presence of a wide-angle objective, the scheme of the instrument can be executed without a mirror cone. In the scheme of the given instrument, the cone is employed to reduce the dimensions of the image, and, consequently, to reduce the maximum value of the field of view of the objective with the maintenance of the required dimensions of the scanning zone. /190
At the same time, the optical system employed in the instrument is sufficiently wide-angle, which provides the possibility of using it on SC with low altitudes of flight. We note that the range of operating altitudes where the orientation of the SC can be accomplished with a given precision is determined by the size of the angle at the apex of the cone. An instrument with a lens optical system and mirror cone permits accomplishing the orientation of the SC relative to the local vertical at altitudes of orbit of from 80 to 1600 km, and in some variations (with a change in the angle of conicity) -- up to 160,000 km. An element sensitive to solar radiation is mounted on the outside on the base of the cone. With the incidence of solar radiation in the field of view, it generates a voltage which disconnects the germanium modulator.

Along with the interruption of the radiation flux which arrives at the instrument, the germanium modulator accomplishes one more function -- it eliminates the incidence of the intrinsic radiation of the elements of the instrument. The frequency of modulation of the radiation flux is 10 Hz.

The instrument possesses sensitivity to radiations in the spectrum band from $\lambda = 11$ to $\lambda = 20$ μm , where the intrinsic temperature radiation of the earth's surface lies. Therefore, the instrument is capable of operating on the day as well as on the night sides of the earth, assuring a precision of $0.1 \cdot 1.74 \cdot 10^{-2}$ rad. It can be presumed that the figure presented

characterizes the instrument error and not the precision of determining the position of the SC axis being oriented relative to the local vertical, which will be considerably greater.

The merits of the vertical resolvers considered are:

- Comparatively small masses and dimensions (mass ~ 3 kg; volume, 2 cubic decimeters);
- Small power consumption (does not exceed 6 W);
- Absence of rotating and moving parts, which extends the service life of the instrument;
- The possibility of using the instrument for checking position at the beginning and course correction at the end of the powered section of a rocket trajectory.

Among the shortcomings of the instrument, we should include its applicability only on spacecraft which are in circular orbits or orbits close to circular. Naturally, the deviation in height of orbit from the calculated one lowers the precision of orientation.

Attempts to eliminate these disadvantages or reduce their influence led to the creation of more complex instruments capable of forming error signals with high precision which determine the position of the yaw axis of the SC relative to the local vertical in a broad range of altitudes. An example of such a type of instrumental realization is the use of vertical resolvers consisting of three or four scanning tracking sensors. The diagram of the optical system of one such sensor is presented in Fig. 6.17 [62, 63]. /191

The instantaneous field of view of each sensor, with size $W_1 \times W_2$, which is limited by the dimensions of the sensitive layer of the receiver of radiation flux, fluctuates within radial directions with some amplitude W which characterizes the scanning zone of the sensor. Depending on the position of the earth's horizon within the limits of the zone scanned by each sensor, signals are generated in the system which are used for matching the middle of the zone being scanned with the horizon (earth-space boundary). The change of the signals from the output of the radiation flux receiver with time with a change in the position of the scanning zone relative to the horizon line is illustrated in Fig. 6.18.

The forming of error signals of the middle of the scanning zone with the horizon line can be accomplished, for example, with the comparison, for duration, of the operating signals read from the output of the receiver with the reference signals. In this case, the duration of the reference pulse should comprise half the scanning period, which corresponds to the matching of

the middle of the scanning zone with the horizon line. Feeding the operating signals together with the reference signals to the matching unit, pulses are obtained on its output whose duration characterizes the amount of deviation of the middle of the scanning zone from the horizon line, and the polarity determines the direction of the error. Thus, the constant component, being discriminated from the obtained series of pulses, describes both the value as well as the direction of the error.

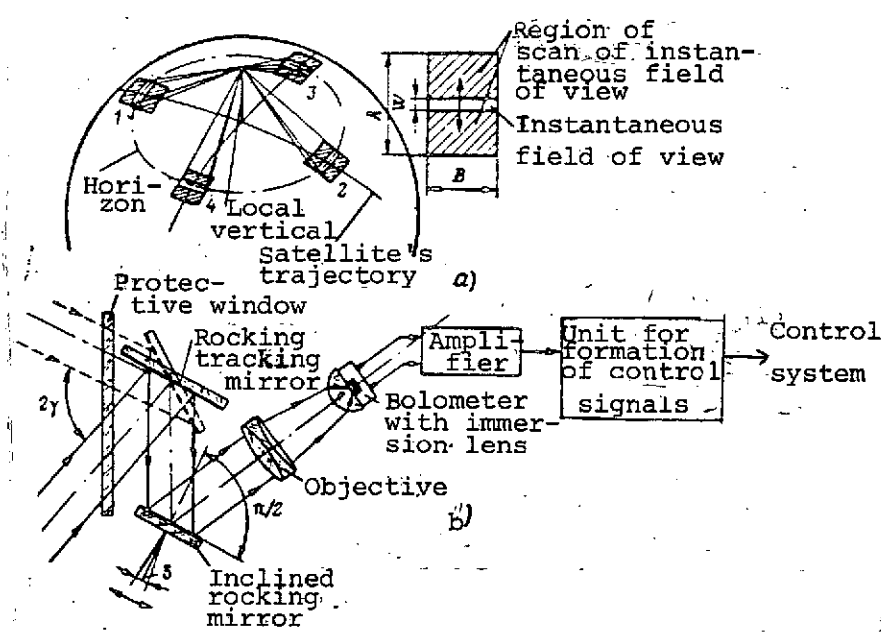


Fig. 6.17. Diagram of the construction of the local vertical with the use of four tracing horizon sensors: a. scheme; b. schematic diagram of the resolver.

The discriminated signal is fed to the reversible drive of a rocking tracking mirror, as a result of which the matching of the middle of the scanning zone with the horizon and its retention in such a position during the entire time of operation of the orientation system are assured.

The sizes of the angles α between the SC axis being oriented and the directions which pass through the middle of the scanning zones after their localization on the edges of the earth's disk characterize the position of this axis with respect to the local vertical. Since the yaw axis of the SC will coincide

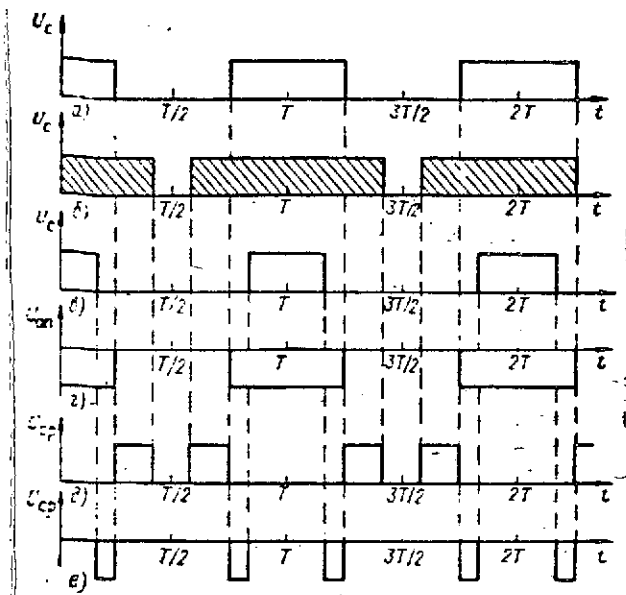


Fig. 6.18. Nature of the change of signals at the output of a radiation receiver with a change in the position of the scanning region relative to the horizon: a. mean position of the scanning region matched with the horizon; b. mean position of the scanning region shifted in the direction of the earth's surface; c. mean position of the scanning region shifted in the direction of space; d. pulses of reference signals; e. pulses on the output of the coincidence circuit which correspond to the position of the scanning region in case b; f. pulses on the output of the comparison circuit which correspond to the position of the scanning region in case c.

tages

with the direction of the local vertical only in the case of the equality of angles α_1 and α_2 , α_3 and α_4 , the signals which characterize the difference in these pairs will contain information about the magnitude and direction of the error. /193

The amount of deviation of the SC axis being oriented from the direction of the local vertical is described by a relation of the type

$$\theta_1 = \frac{\alpha_1 - \alpha_2}{2}, \quad (6.23)$$

where α_1 and α_2 are the angles between the SC axis being oriented and the directions to the horizon line; θ is the component of the angle of error of the axis being oriented with the direction of the local vertical in the plane of one pair of sensors.

If the rocking mirrors are connected to sensors whose output voltage is proportional to the angle of deviation of the mirror from the initial position,

$$\text{i.e., } U_1 = q \frac{\alpha_1}{2} \text{ and } U_2 = \frac{\alpha_2}{2},$$

the difference of these vol-

$$\Delta U_1 = U_1 - U_2 = q \left(\frac{\alpha_1 - \alpha_2}{2} \right) \quad (6.24)$$

characterizes the error of the SC axis being oriented with the local vertical in the plane of the given pair of sensors. From

(6.24), with consideration of (6.23), we obtain

$$\Delta U_1 = q \theta_1,$$

where q is the proportionality factor.

The described method of orientation can also be accomplished with the use of only three sensors whose axes are arranged at angles of $\pi/2$ rad to each other, and their projections on the plane normal to the axis being oriented comprise angles between each other equal to $2/3\pi$ rad. However, in this case the forming of the error signals over the channels becomes complicated.

The orientation equipment which realizes the second variety of the method being examined can assure the determination of the position of the SC axis being oriented with respect to the local vertical with flight altitudes from 120 to 36,000-40,000 km.

One of the instruments of this type [62, 63] can assure the matching of the middle of the scanning region with the horizon line with a precision of up to $1.74 \cdot 10^{-3}$ rad. The instantaneous field of view of each sensor with size of $8.7 \cdot 10^{-3} \times 5.2 \cdot 10^{-2}$ rad fluctuates in a radial direction within limits of the angle $7.85 \cdot 10^{-2}$ rad. A bolometer with a germanium immersion lens is used as a radiation receiver in the instrument.

The considered instrument, besides assuring the orientation of the SC with large flight altitudes which exceed considerably the maximum altitudes of the vertical resolvers which operate with the method of secants possesses one more substantial quality -- an increase in the period of service due to the absence of continuously rotating parts.

/194

Let us consider one more vertical resolver which accomplishes the tracking of the horizon line. Here, space is scanned with the rocking of small flat mirrors under the influence of an electromagnet. A diagram of such a sensor is shown in Fig. 6.19 [35]. Its composition includes a wide-angle lens objective, four flat rocking mirrors, and four radiation receivers. The mirrors and receivers operate in pairs, assuring the scanning of space in two mutually perpendicular planes.

The flat mirrors are fastened to symmetrically installed flat springs. One end of the spring is connected with the housing, and the other with a voice coil.

With the correct orientation of the SC, the objective 1 constructs an image of the earth. With the use of the rocking

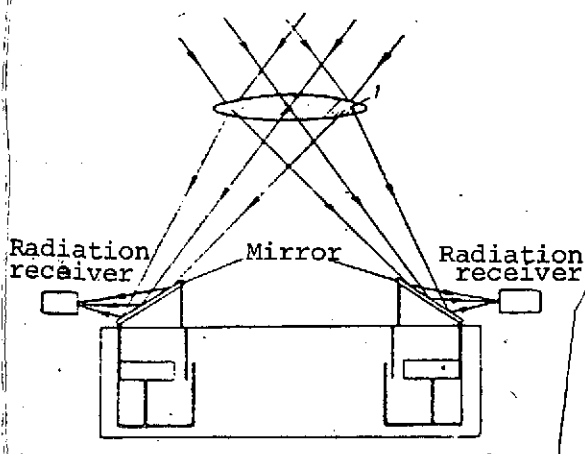


Fig. 6.19. Diagram of a resolver of the local vertical with flat rocking mirror:
1. objective.

mirrors, small sections of the image of the earth's edges land on the sensitive layers of the radiation receiver. Because of the synchronous rocking of the mirrors under the action of the oscillations of the voice coil, the scanning of diametrically opposite sections of the earth's horizon is assured. As a result of this, electrical pulses appear on the output of the receivers with recurrence rate equal to the scanning frequency. The duration of the pulses depends on the position of the SC axis being oriented relative to the direction of the local vertical. The durations of the pulses from the opposite radiation flux receivers

will equal each other only with the correct orientation of the SC. A functional diagram of the forming of control signals over one of the channels is presented in Fig. 6.20. Since the time method of forming error signals is employed here, the output signals should have identical amplitude, which is assured by the use of an amplitude limiter in the circuit. As a result, /195 neither the difference in the radiation fluxes perceived from the earth's surface nor the difference in amplification factors for the channels affects the operating precision of the instrument. The size of the error angle determines the difference in the durations of the pulses read from opposite receivers. The detection and subsequent discrimination of the constant component on RC filters gives a constant voltage proportional to the duration of the pulses read from the given receiver.

The constant voltage from the output of the filters is fed to the differential amplifier which generates an error signal. The amplitude and sign of the signal depend on the position of the instrument's optical axis (this axis is parallel to the SC axis being oriented). If the SC axis being oriented coincides with the direction of the local vertical, the signal on the output of the differential amplifier equals zero.

The rocking of the mirrors is accomplished on signals from a master oscillator whose role is fulfilled by the generator of sound vibrations. It generates a voltage of a specific frequency equal to the natural frequency of the resonance oscillations of the scanner, which reduces the power consumption.

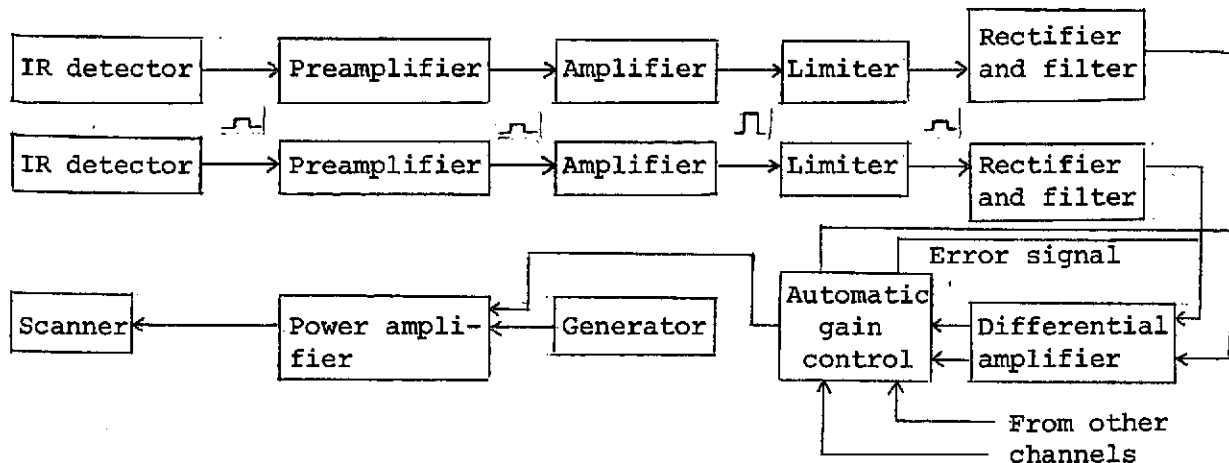


Fig. 6.20. Functional diagram of a system for forming control signals over one channel.

Envisioned in the scheme is the automatic regulation of amplification. Both the error signals and direct-current voltages from the output of all filters are fed to the AGC [automatic gain control] unit. On the basis of these data, the optimum amplitude of the oscillations of the mirrors is determined in a computer. With a considerable error over one or both channels, the mirrors oscillate with great amplitude. If error signals are absent and the constant components also equal zero, scanning is conducted with maximum amplitude. With small errors, the amplitude of the oscillations of the mirrors is reduced, as a result of which the precision of orientation is increased.

/196

6.5. Electro-Optical Instruments for Course Orientation of the SC

In connection with the expanded range of applied problems involving space vehicles, the on-board orientation systems should not only determine the position of the local vertical but also deviations for yaw, i.e., deviations of the roll axis from the orbital plane.

Existing methods for vehicle course orientation are based on the use of gyroscopic instruments which operate in combination with some resolver of the local vertical. However, these systems, not being distinguished by high precision and durability, require rather large expenditures of power.

Furthermore, various astronavigational methods based on tracking reference heavenly bodies and comparing measured angles

with programmed ones are employed. Along with the complexity of realization caused by the necessity to have an on-board computer and the relative difficulty in the assignment of programmed values of angles between the axes of the SC and the reference heavenly bodies, these methods possess a basic shortcoming and, namely, the selected reference heavenly bodies are not always directly visible from on board the SC.

A relatively simple method for orienting manned SC is the method based on the use of an optical attitude control, in whose focal plane a grid with parallel lines is installed. The instrument on board the SC is so installed that, with the correct orientation, the lines of the grid are parallel to the orbital plane and coincide with the direction of the relative velocity of the SC. The image of the earth's surface, constructed by the objective of the attitude control in the focal plane, continuously displaces during flight. The coincidence of the direction of displacement of the image with the longitudinal lines of the grid in the focal plane of the attitude control corresponds to precise orientation (to the coincidence of the axis of roll with the orbital plane).

Noncoincidence testifies to the disruption of course orientation which should be restored by turning the SC relative to the axis directed along the local vertical.

The indicated principle can be used for the course orientation of unmanned SC. Naturally, in this case the determination of the coincidence of the direction of displacement of the image with the reference direction should be accomplished automatically. The latter problem can be solved with the use of television-type electro-optical systems with line scan on board, the lines of which coincide for direction with the axis of roll. If the SC is oriented in flight so that its axis of roll lies in the orbital plane and the direction of the lines of scan coincide with the direction of relative velocity (Fig. 6.21), the video signals of lines in the same position on adjacent frames (with line scanning) or the two next lines (with line scanning) will be shifted by an amount proportional to the ratio of the velocity to the altitude of flight. Noncoincidence of the vector of relative velocity with the direction of the lines leads to a change in the video signals in a random manner in accordance with the random character of the earth's background which lands in the instrument's field of view. In this case, the comparison of the signals does not provide the opportunity to establish the constant value of the shift, which testifies to the disruption of orientation. Achieving the required coincidence of the video signals by turning the SC for course, its orientation can be restored.

/197

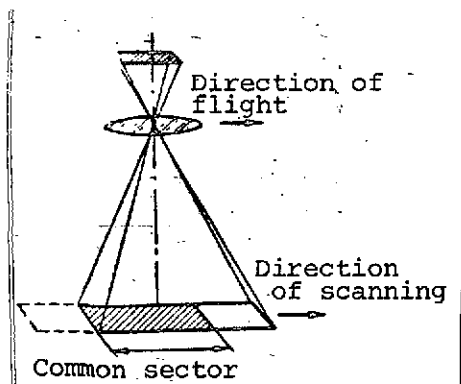


Fig. 6.21. Diagram for the principle of course orientation in accordance with the direction of run of the image.

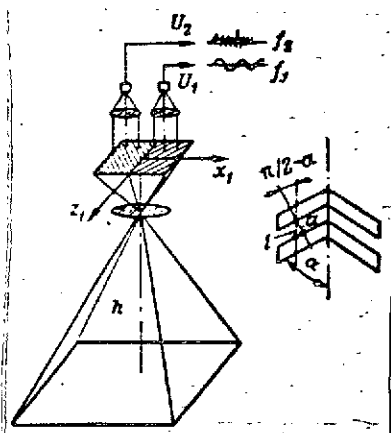


Fig. 6.22. Schematic diagram of an instrument for course orientation based on the use of frequency rasters.

A Method of Course Orientation Based on the Use of Frequency Rasters

This method of determining the direction of the vector of relative velocity is based on the use of modulation of a radiant flux which creates an image of the earth's surface.

The operating principle of the device which realizes the indicated method consists of the following. The composition of the instrument includes two electro-optical sensors. Installed in the focal plane of each of them is a frequency raster in the form of alternating transparent and opaque strips of the same width. The radiant flux goes from the output of the rasters to photoelectric receivers (Fig. 6.22).

The frequency of modulation of the radiation flux can be determined on the strength of the parameters of the raster. If the axis of symmetry of the frequency rasters coincides with the vector of relative velocity, the frequency of modulation of the radiation flux by both rasters is identical and equals

$$f_0 = \frac{1}{T}, \quad (6.26)$$

where T is the period of displacement of the image in the plane of the grid.

The period T is connected with the raster parameters and the velocity of the image by the relation

$$T = \frac{2l}{V_{im}}, \quad (6.27)$$

where L is the length of the path of the image within limits of one raster slit; V_{im} is the velocity of the image.

The velocity of the image in the focal plane can be determined from the expression

$$V_{im} = V_{SC} \frac{R_e}{H} \frac{f'_{ob}}{R_e + H}, \quad (6.28)$$

where V_{SC} is the relative velocity of the SC; $\frac{R_e}{R_e + H} V_{SC}$ is the rate of displacement of the sighting beam over the earth's surface; R_e is the radius of the earth; H is the altitude of flight of the SC above the earth's surface; f'_{ob} is the focal length of the instrument's objective.

If the angle of slope of the raster slits to the axis of symmetry is α , the length of the image path l will be

$$l = \frac{a}{\cos(\pi/2 - \alpha)} = \frac{a}{\sin \alpha}, \quad (6.29)$$

where a is the width of the slit.

With consideration of (6.27), (6.28), and (6.29), from (6.26) we obtain

$$f_0 = \frac{V_{SC} f'_{ob} R_e}{2aH(R_e + H)} \sin \alpha. \quad (6.30)$$

If the longitudinal axis of the SC deviates from the vector of relative velocity by the angle $\Delta\alpha$, then, due to the change in the length of the path l , the frequencies in the left and right channels will differ from f_0 and can be determined from the expressions

$$\begin{aligned} f_1 &= \frac{V_{SC} f'_{ob}}{2aH(R_e + H)} \sin(\alpha + \Delta\alpha) \text{ and} \\ f_2 &= \frac{V_{SC} f'_{ob}}{2aH(R_e + H)} \sin(\alpha - \Delta\alpha). \end{aligned} \quad (6.30a)$$

Then the difference frequency of the signals of the left and right channels is found from the expression /199

$$f_1 - f_2 = \frac{V_{sc} f'_{ob} R_e}{2aH(R_e + H)} 2 \cos \alpha \Delta \alpha. \quad (6.31)$$

Accepting that with small values of angles $\sin \Delta \alpha \approx \Delta \alpha$, after simple transformations from (6.31) we obtain

$$f_1 - f_2 = \frac{V_{sc} f'_{ob} R_e}{2aH(R_e + H)} 2 \cos \alpha \Delta \alpha. \quad [\text{sic}] \quad (6.32)$$

Expression (6.32) shows that the difference frequency of the signals over two channels is directly proportional to the angle of deviation of the axis of symmetry of the rasters from the vector of relative velocity. Naturally, to increase the precision of orientation, it is desirable that the difference in frequencies $f_1 - f_2$ be the greatest. From expression (6.32), it can be seen that this difference will be maximum with $\alpha = 0$. As follows from (6.30), frequencies f_0 , f_1 , and f_2 will be extremely close to zero.

On the strength of the condition for assuring simplicity in processing signals by means of the use of resonance amplifiers, it is necessary that the frequency of modulation of the signals over the channels be at least 12-15 Hz.

If we accept that the difference frequency should comprise at least 75-85% of the maximum value, the mean value of $\cos \alpha$ can be taken as equal to

$$\cos \alpha \approx 0.8.$$

In this case, $\sin \alpha = 0.6$ and, consequently, the radiation flux will be modulated with frequency $f_0 \approx 1.6 f_{\max}$. Taking $f_0 = 15$ Hz, we find that $f_{\max} = 25$ Hz.

We point out that the precision of determination of the angle of deviation of the SC axis from the orbital plane depends on the characteristics of the instrument. Thus, for example, if the focal length of the instrument's objective is $f'_{ob} = 250$ mm and the width of the slit $a = 0.25$ mm, then with $H = 300$ km and $V_{sc} = 8000$ m/sec:

$$\frac{V_{sc} R_e}{H(R_e + H)} = 25.5 \cdot 10^{-3} \text{ and } f_1 - f_2 = \frac{f'_{ob}}{a} 25.5 \cdot \cos \alpha \cdot \Delta \alpha.$$

Taking $\cos \alpha = 0.8$, we obtain

$$f_1 - f_2 = 25.5 \cdot 0.8 \cdot \Delta\alpha \approx 20 \Delta\alpha$$

If the system records a difference in frequencies of 1 Hz, in this case, under the given conditions,

$$\Delta\alpha = \frac{1}{20} = 0.05 \text{ or } \Delta\alpha \approx 0.052 \text{ rad}$$

A shortcoming of the method considered is the fact that the resonant frequencies are extremely small, and their difference with the disruption of course orientation also proves to be small, which hinders considerably the instrumental realization of electro-optical instruments for course orientation which possess high sensitivity. /200

A further development of the idea of using electro-optical instruments for course orientation of the SC is the use of correlation methods for forming the control signals.

Course Orientation of a Vehicle on the Basis of the Use of Correlation Methods for Forming Control Signals

Two identical optoelectronic instruments with sufficiently small field-of-vision angles are installed aboard a vehicle-oriented with respect to the local vertical and they are immobile with respect to the body. Each instrument consists of an objective and infrared radiation receiver.

The optical axes of both instruments are arranged in plane Ox_1y_1 of a system of coordinates connected with the SC and comprise some angle δ with the vertical (Fig. 6.23). The electrical voltage U on the output of each photoreceiver is proportional to the energy brightness of the section of the earth's surface which lands in the field of view. Therefore, with the movement of the SC above a heterogeneously radiating surface, the signals on the photoreceivers will be some random function of time $U_1(t)$ and $U_2(t)$. If the SC is oriented so that axis Ox_1 is directed along the vector of the relative velocity, the field of view of both instruments will pass sequentially over the very same terrain sectors and, in accordance with this, the same realization of a random function will be reproduced on the output of the receivers, but with a time shift equal to τ , which is determined by the mutual withdrawal of the fields of view and the

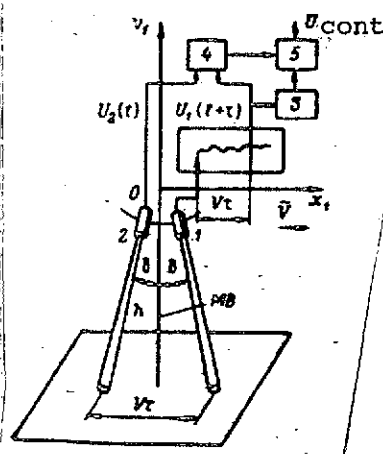


Fig. 6.23 Course orientation of a vehicle based on the use of the correlation of signals: 1, 2. Radiation receivers; 3, 4, 5. Signal processing unit.

speed of movement. If we assure the delay of signal $U_1(t)$ of the front instrument by the amount τ (for example, recording on a magnetic tape or magnetic drum), then comparing it with the current signal $U_2(t)$, generated by the second instrument, and establishing their identity, we can also fix the oriented position of the SC.

However, it should be kept in mind that even with the complete coincidence of the fields of view of the instruments within the limits of the same background band, we cannot achieve the exact coincidence of the signals $U_1(t + \tau)$ and $U_2(t)$, inasmuch as even if they are obtained from the same sections of the background, they are examined under different angles. Furthermore, a random change in individual emitters during time τ is possible. Therefore, it is more expedient to compare signals $U_1(t + \tau)$ and $U_2(t)$ not according to

algebraic difference, but with the use of the correlation coefficient $K_{U_1U_2}$, which statistically determines and compensates for possible cases of fluctuations of the background during some time segment T . To determine the sign of the angular deviation of axis Ox_1 from the velocity vector, one more channel is introduced into the scheme, arranging the field of view at the apexes of an isosceles triangle. Calculating the correlation coefficients $K_{U_1U_2}$ and $K_{U_2U_3}$ between signals $U_1(t + \tau)$, $U_2(t)$, and $U_1(t + \tau)$, $U_3(t)$, one can judge not only the value of the angular deviation, but also its sign. Actually, if $K_{U_1U_2} = K_{U_1U_3}$, this is evidence that the direction of the velocity vector coincides with the median of the triangle and corresponds to the oriented position of the SC. If $K_{U_1U_2} > K_{U_1U_3}$, this signifies that the SC is turned to the left with respect to the velocity vector, and if $K_{U_1U_2} < K_{U_1U_3}$, then the SC is turned to the right. /201

Among other methods for course orientation of a vehicle, we should include the use of various optical diaphragms which transform a luminous flux from the moving image of the surface in such a way that the position of the longitudinal axis of the SC relative to the direction of flight can be judged from the appearance and character of the random signal on the photoreceiver.

Simplest is the method based on the use of a slotted diaphragm. Its essence is the following. Located on board the

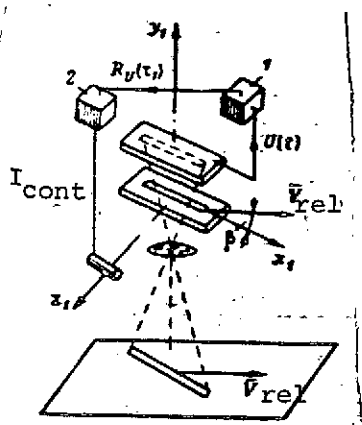


Fig. 6.24. Operating principle of a correlation course attitude control with a slotted diaphragm: 1. correlator; 2. processing unit.

moving SC which is oriented according to the local vertical is an electro-optical instrument whose optical axis coincides with the local vertical (Fig. 6.24). A slotted diaphragm, whose length is many times greater than its width is installed in the focal plane of the objective in front of the radiation receiver. In this case, the field of view of the system on the surface of the earth will be a greatly elongated rectangle whose length may comprise several kilometers or even tens of kilometers. The oriented position of the SC is considered to be the one in which the longitudinal axis of the slit, rigidly connected with the body of the SC, is directed along the vector of relative velocity. The property of the slotted diaphragm is the fact that with the oriented position of the SC a random signal on the output

of the photoreceiver is some smoothly changing curve in which the predominant value is had by low-frequency harmonics. With the transverse displacement of the slit, the components of harmonics of higher frequency become part of the random signal. Some intermediate values of the predominant frequencies will agree with the intermediate position of the slit relative to the velocity vector. The simplest physical explanation of this phenomenon is the following. Signal $U(t)$ obtained from the receiver of radiation energy is proportional to the total energy brightness of the elementary emitters which have landed within the limits of the field of view at a given moment. If this field of view is displaced along its longitudinal axis, each of the random emitters is located within its limits for a comparatively long time, creating some constant component. With the displacement of the slit-like field of view perpendicular to its longitudinal axis, the elementary random emitters are located within its limits only for a short time, which is determined by its small width. But, with intermediate position of the slit, the time of the emitters' location within the limits of the field of view will be determined by the angle of deviation from the velocity vector.

In the theory of random functions for a quantitative estimate of the nature of change by a random curve, it is customary to use its statistical characteristic -- the value of the autocorrelation function $R_U(\tau)$. If we record some time delay $\tau = \tau_1$, the value of function $R_U(\tau)$ for the smoothest curve will be the

greatest. With an increase in the frequency of the signal, which occurs with a deviation of the slit from the relative velocity vector, the value of the function $R_U(\tau_1)$ will be reduced. Thus, turning the SC for course until obtaining the maximum value of $R_U(\tau_1)$, we can determine the direction of the vector of relative velocity and orient the SC.

Along with the use of autocorrelation functions for determining the amount and direction of deviation of the longitudinal axis of the SC from the velocity vector, mutual correlation functions can also be used. In contrast to the preceding, in this case the instrument should have four fields of view, in which regard, within the limits of each field of view, the radiation lands on an individual receiver. The source of primary information is provided either by the random distribution of energy brightness of the underlying ground covers or by the random distribution of energy brightness of the firmament caused by the irregularity of arrangement of the stars in the firmament. The instrument's field of view is formed with the use of a diaphragm with slotted apertures installed in the focal plane of the objective. The slotted apertures in the diaphragm are arranged in two parallel pairs at some angle β , which lies within limits of up to 2π rad (Fig. 6.25).

/203

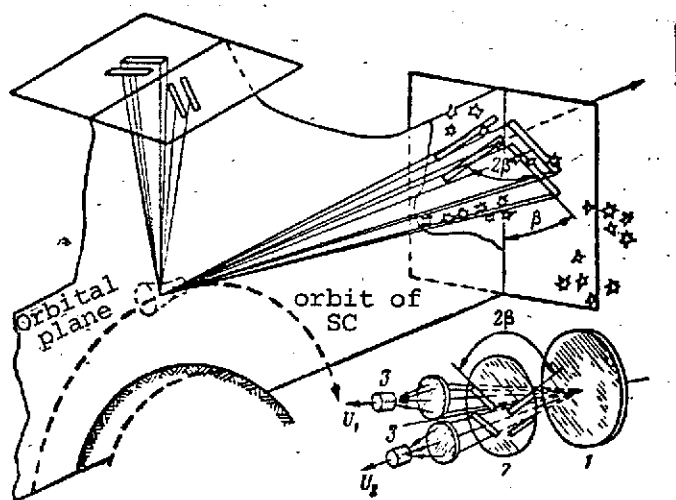


Fig. 6.25. Diagram of an electro-optical instrument for course orientation based on the use of the correlation between signals of slit-like fields of view: 1. objective; 2. diaphragm; 3. receivers.

The instrument is installed on board the SC so that the axis of the objective coincides with the direction of the SC axis which is oriented in accordance with the local vertical and the pairs of slits would be arranged symmetrically with respect to the axis of roll for angles $\pm\beta/2$.

If the starry sky is used as the source of primary information and the SC is oriented with regard to the local vertical, the instrument's field of view should be directed at the starry sky. The operating principle of the instrument consists of the following.

During the flight of a vehicle oriented relative to the local vertical, the image of the starry sky will displace in the focal plane of the instrument. The images of individual stars, passing through the slits of the diaphragm, will cause random signals on the output of the photoelectric receivers.

When the longitudinal axis of the SC (axis of roll) coincides with the orbital plane, the time intervals during which the images of the stars pass between the pairs of slits equal each other. With the deviation of the longitudinal axis of the SC from the orbital plane, the time intervals of the passage of the images of the stars between one pair of slits of the diaphragm is reduced and is increased between the slits of the other pair. These time intervals, which characterize the deviation of the longitudinal axis from the orbital plane, are determined on the basis of the measurement of the correlation between the random signals from the outputs of the receivers of radiation energy, using photoelectric multipliers. /204

The basic advantage of the described methods of course orientation of the SC are their complete autonomy and capability to operate on the illuminated as well as on the dark side of the earth. The heterogeneity of the radiating object is sufficient for the stable operation of such course sensors. Under actual flight conditions, it is always present.

6.6. Orientation Instruments Which Use the Sun as a Reference Point

Electro-optical instruments which use the sun as a reference point can be classified by purpose, precision in determining the direction to the sun, and scheme of construction.

Two groups are distinguished by purpose:

- Instruments which serve for the determination of the position of the SC in orbit or one of its structural axes in space;
- Instruments which assure the matching of one of the SC axes with the direction to the sun with a given precision.

All instruments are also divided into two groups according to the size of the zone of space instantaneously scanned:

- Instruments which instantaneously scan space within the limits of the entire sphere;
- Instruments whose instantaneous fields of view have different sizes and forms and do not span the entire sphere at once.

According to precision in determining the direction to the sun, instruments are divided into coarse, which determine direction with a precision up to several degrees; exact, with a precision up to several minutes; and precision, with a precision up to several fractions of a second.

Any of the enumerated groups of instruments can be constructed in accordance with one of the following schemes:

- Instruments of the diaphragm-receiver type;
- Instruments of the optics-receiver type;
- Instruments which measure the amount of radiation flux.

In the simplest case, a solar orientation instrument with circular scan can be realized with the use of several photosensitive elements which are arranged on the body of the SC in a specific manner. In this, in a number of cases, the high intensity of solar radiation permits getting by not only without /205 optical systems, but also without additional electronic amplifiers.

Thus, for example, if solar sensors are arranged on board an SC in pairs in each side and a shading diaphragm is placed in front of each pair as shown in Fig. 6.26, then in accordance with the logic of the formation of control signals, the orientation of one of the axes of the SC in the direction of the sun can be assured. Actually, with the identical sensitivity of opposing receivers, the signal at the output of the circuit changes in proportion to the difference of the irradiated areas of the radiation receivers

$$U = SE \left[\left(\frac{d}{2} + l\Delta\theta \right) - \left(\frac{d}{2} - l\Delta\theta \right) \right] \cos \alpha = 2ESl\Delta\theta \cos \alpha, \quad (6.33)$$

where S is the sensitivity of the radiation receivers; d is the size of the sensitive layer of the receiver; l is the distance from the shading diaphragm to the surface of the sensitive layer of the receiver; $\Delta\theta$ is the component of the error angle in the plane being examined; E is the irradiance created by the sun on the surface of the sensitive layers of the radiation receivers.

From this relation, it can be seen that the signal from the output of a pair of receivers is proportional to the error angle $\Delta\theta$.

If two pairs of receivers are placed relative to one of the axes with shading diaphragms in two mutually perpendicular directions, they will assure the formation of control signals in two mutually perpendicular planes, i.e., along two axes. /206

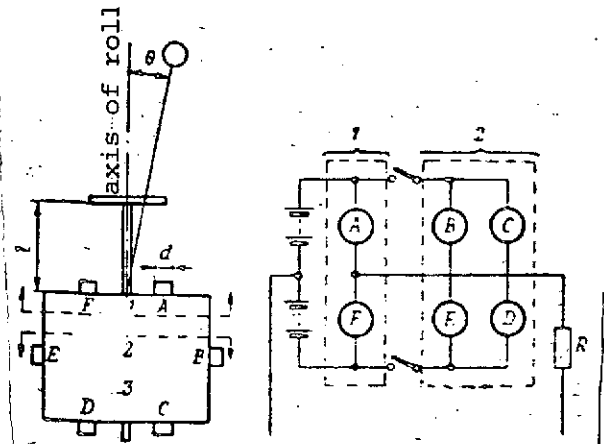


Fig. 6.26. Principle of construction of an instrument for orientation on the sun with the use of a shading diaphragm: 1, 2, 3. pairs of diaphragms.

This method of orienting on the sun was realized on the "Mariner-II" spacecraft. The roll axis was matched with the direction to the sun. This problem was solved with the use of two pairs of receivers (principal sensors) of which one provided a pitch signal and the other a yaw signal. The field of view of these two pairs was $\pi/4$ rad. The remaining part of the sphere was covered by similar pairs of receivers, the signals from which, going to the control system, caused the rotation of the SC in the direction

of matching the field of view of the central sensors with the direction to the sun. After the sun landed within the limits of this field, control of the angular position of the SC was accomplished on signals from the principal sensors right up to the matching of the roll axis with the direction to the sun.

The solar sensors employed on the "Mariner-II" spacecraft had the following characteristics:

Sensitivity (angular)	55 rad
Resistance of the sensitive field of the receiver	4.2-4.4 kΩ
Power consumption	0.058-0.061 W
Field of view	$\pi/4$ rad
Length of arms	28-41 cm
Length of sensitive layer of receiver	0.127 ± 0.005 cm
Mass	30 g

In flight, the system for controlling the orientation of the SC "locked on" the sun for 10 min, as a result of which the axis of roll proved to be directed at the sun.

The merits of the scheme for the attitude control which has been considered include simplicity of construction, low power consumption, and small mass. A shortcoming of the scheme is the necessity to have a large number of elementary sensors for the simultaneous scanning of space in a solid angle of 4π sr, which reduces the overall dependability of the system as a whole. Another shortcoming is also caused by the large number of sensors

in the system and consists of the fact that their arrangement on board imposes certain restrictions on the design of the SC.

Instruments of the diaphragm-receiver type for orientation on the sun are somewhat more complex. In these instruments, the shape and dimensions of the field of view of individual sensors are determined by the shape and dimensions of the diaphragms installed in front of the receivers (Fig. 6.27). The

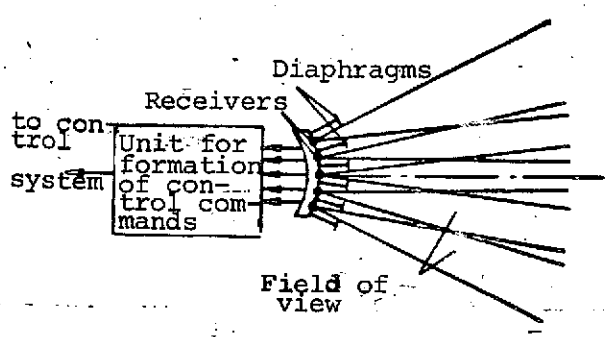


Fig. 6.27. Diagram of an instrument of the diaphragm-receiver type for orientation on the sun.

use of several radiation receivers with their own diaphragms provides the opportunity to divide the entire space into zones and obtain information on the position of the sun in a broad field of scan right up to a complete sphere.

To assure the least time in searching for the sun and reduce the number of sensors to the minimum, the field of view of each of them should be maximum. However, restrictions are imposed on the size of the field of view

which are connected with the interference immunity of the instrument. External interferences for solar instruments are the radiations of the planets and the moon. The solar radiation, reflected from these bodies is decisive (since their intrinsic radiation becomes perceptible for wavelengths of more than 3-5 μm , the use of cutoff filters or receivers which are insensitive in this region of the spectrum will obviate the influence of this factor on the operation of the instrument).

The maximum allowable dimensions of the field of view can be established on the strength of the following considerations. If we consider that the minimum signal from the sun on the output of the receiver should exceed the maximum value of the signal from the background by m times, we can write the initial condition in the form

$$m > \frac{\phi_{\text{eff min}}^s}{\phi_{\text{eff max}}^b} \quad (4.34)$$

where m is the signal/background relationship; $\phi_{\text{eff min}}^s$ is the minimum value of the effective amount of radiation flux from the

sun which falls on the radiation receiver; $\Phi_{\text{eff max}}^b$ is the maximum value of the effective amount of radiation flux caused by solar radiation reflected from the earth.

Since Φ_{eff}^s receives its minimum value when the sun is located at the edge of the field of view, the value $\Phi_{\text{eff min}}^s$ can be found from the expression

$$\Phi_{\text{eff min}}^s = E_s A_{\text{rec}} k_s \cos \frac{\alpha}{2} \cos \frac{\beta}{2} \quad (6.35)$$

where E is the irradiance created by the sun on a small area of the sensitive layer of the receiver with the normal incidence of the rays; A_{rec} is the area of the sensitive layer of the receiver; k_s is the utilization factor of the sun's radiation by the receiver; α and β are the angular dimensions of the field of view. /208

The signal from the background or, what is the same thing, the effective value of the radiation flux from the background on the radiation receiver will be maximum with the complete filling of the instrument's field of view with the radiating surface. In this case

$$\Phi_{\text{eff max}}^b = B_b A_{\text{rec}} \omega_v k_b. \quad (6.36)$$

If the background emitter is the earth's surface illuminated by the sun then, considering it as a diffuse reflector which follows Lambert's law and, on the strength of (1.16), we can write

$$B_b = \frac{E_s \rho_e}{\pi},$$

where ρ_e is the albedo of the earth's surface for visible solar radiation.

Also replacing ω_v by

$$\omega_v = \alpha \beta,$$

we write expression (6.36) in the form

$$\Phi_{\text{eff}}^b = \frac{E_s \rho_e}{\pi} A_{\text{rec}} \omega_v k_b = \frac{E_s \rho_e}{\pi} A_{\text{rec}} \alpha \beta k_b. \quad (6.37)$$

Substituting (6.35) and (6.37) in (6.34), we find

$$m \geq \frac{\Phi_{\text{eff min}}^c}{\Phi_{\text{eff max}}^b} = \frac{k_s \pi}{k_b \rho_e} \frac{\cos \alpha/2 \cos \beta/2}{\alpha \beta}, \quad (6.38)$$

$$m \geq \frac{k_s \pi}{k_b \rho_e} \frac{\cos \alpha/2 \cos \beta/2}{\omega_v}.$$

or

In a number of cases, for approximate estimates with some assumptions, it can be considered that $k_s = k_b$, then

$$m \geq \frac{\pi}{\rho_e} \frac{\cos \alpha/2 \cos \beta/2}{\alpha \beta} \quad \text{or} \quad m \geq \frac{\pi}{\rho_e} \frac{\cos \alpha/2 \cos \beta/2}{\omega_v}, \quad (6.39)$$

whence the allowable value of the instantaneous field of view will be

$$\omega_v \leq \frac{\pi}{m \rho_e} \cos \alpha/2 \cos \beta/2. \quad (6.40)$$

Formulas (6.39) and (6.40) permit determining the allowable dimensions of the instantaneous field of view with a given excess of the useful signal over the signal from the background. On the basis of relation (6.39), graphs have been constructed for various values of the angle β which characterize the change in the quantity $m \frac{\rho_e}{\pi}$ as a function of angle α (Fig. 6.28). Thus, if the albedo of the earth's surface is taken as equal to $\rho \sim 0.3$, the signal/background ratio, as can be seen from the graphs, can be assured as no less than 10 with $\beta = 15 \cdot 1.74 \cdot 10^{-2}$ rad, if $\alpha < 150 \cdot 1.74 \cdot 10^{-2}$ rad; with $\beta = 20 \cdot 1.74 \cdot 10^{-2}$ rad, if $\alpha < 140 \cdot 1.74 \cdot 10^{-2}$ rad; if $\beta = 30 \cdot 1.74 \cdot 10^{-2}$ rad, then $\alpha < 120 \cdot 1.74 \cdot 10^{-2}$ rad; and, finally, if $\beta = 40 \cdot 1.74 \cdot 10^{-2}$ rad, then $\alpha \leq 85 \cdot 1.74 \cdot 10^{-2}$ rad. /209

Depending on the shape and dimensions of the diaphragms and their mutual arrangement, various problems can be solved with the use of instruments of this type.

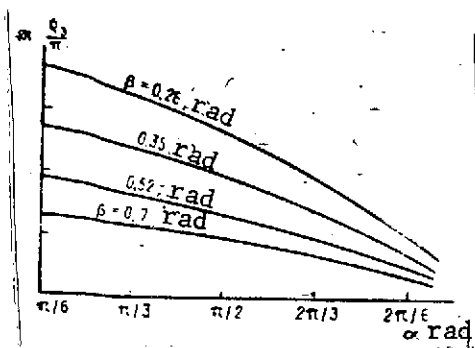


Fig. 6.28. Nature of change in allowable fields of view of solar instruments depending on m^0_e .

Thus, for example, if the diaphragms have the form of slits [61] and form fields of view in space as is shown in Fig. 6.29, then by imparting rotation to the SC relative to the y axis, we can discover the sun and match the x axis with the direction to it. In this, with the landing of the sun in the field of view of sensors I or II having scanning angles α_1 and α_2 , signals are formed in the control system which cause the turning of the SC toward the matching of the x axis with the direction to the sun. Naturally, the overall field of view in plane xOy should be at least π .

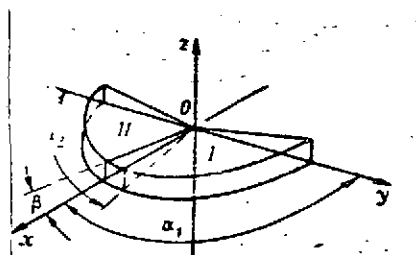


Fig. 6.29. Instrument for solar orientation with slit-like fields of view.

In order to determine the position of the sun relative to the SC, an instrument can be used whose simplified scheme is presented in Fig. 6.30. The sun's rays fall on a group of photodiodes through the luminous windows of a diaphragm. With the rotation of the SC, depending on the size of the angle between the axis of rotation and the direction to the sun, the sun's rays illuminate the various groups of photodiodes. Signals arise on the output of the illuminated photodiodes on the basis of whose processing the angle is determined between the axis of rotation and the direction to the sun. /210

In this indicator, the scanning angle within limits of from $+1.38$ to -1.38 rad is divided into individual sections of 0.047 rad each. To determine the direction to the sun, six coding slits are used with the use of which a three-element Gray code is formed. As a result, a binary signal is created which characterizes the position of the axis of rotation relative to the direction to the sun with a precision up to $\pm 1.74 \cdot 10^{-2}$ rad. When necessary, the precision of the reading can be increased to $\pm 0.2 \cdot 3.5 \cdot 10^{-3}$ rad through interpolation. A sun indicator of this type is used in a vehicle system described in [61].

To determine the direction to the sun relative to the axis of rotation of the SC, an instrument can be used which is constructed in accordance with a scheme with two intersecting fields of view which are formed by corresponding slotted

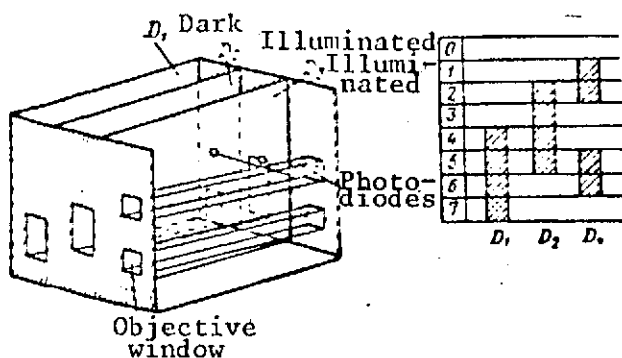


Fig. 6.30. Simplified diagram of an instrument for determining the position of the sun with the use of coding slits which form the Gray code.

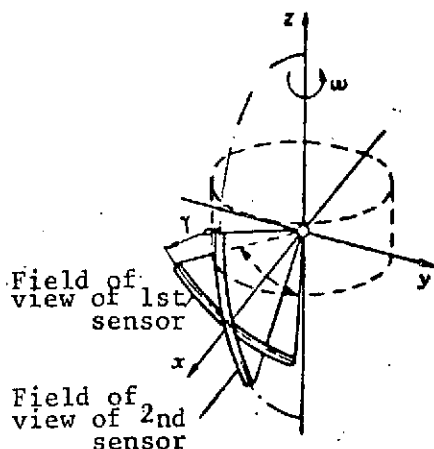


Fig. 6.31. Diagram of the arrangement of intersecting slit-like fields of view in an instrument which determines the position of the sun.

diaphragms. The dimensions of each field of view are $1.3 \cdot 0.0139$ rad. A diagram of the arrangement is presented in Fig. 6.31. In this, the field of view of one sensor lies in plane xOz and of the second is arranged at an angle γ to the first and with its axis is matched with the x axis. If the SC is given rotation relative to the axis, then from the difference in the moments of the landing of the sun in the fields of view and the appearance of the output signals of the

two receivers, we can determine the angle between the direction to the sun and the axis of rotation of the SC.

If we designate by ϕ the angle between the direction to the sun and the axis of rotation of the SC and by ψ_2 the angle of turn of the SC from the position in which the output signal of one sensor had maximum value to the position in which the output signal of the second sensor became maximum, then

$$\cot \phi = \sin \psi_2 \cot \gamma \quad (6.41)$$

The orientation of the SC is /211 determined and control commands are generated on the basis of this equation.

Such a principle for determining the position of the axis of rotation of a vehicle relative to the direction to the sun was used on the "Syncom" satellite. To increase reliability, two instruments are installed on the "Syncom" SC which determine the position of the sun relative to the x axis. Furthermore, three more such instruments displaced relative to each other by π rad [sic] are placed on board around the axis of rotation. These three

additional instruments in combination with the primary ones permit obtaining data on the position of the sun from all four quadrants.

In order to exclude rotation of the SC, to seek the sun, and determine its angular position, instruments can be used which permit scanning the entire sphere at once and issuing information on the position of the sun relative to the axis of the SC.

The system of solar orientation described in work [11] consists of two diametrically arranged instruments with scanning angles of $187 \pm 1.74 \cdot 10^{-2}$ rad, each scanning the entire sphere at once with an overlap of 0.245 rad. A typical scheme of one such instrument is presented in Fig. 6.32.

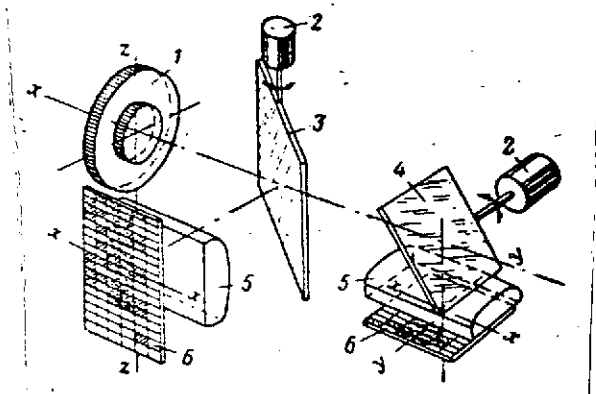


Fig 6.32. Typical diagram of a wide-field instrument for orientation on the sun: 1. wide-angle objective; 2. step-by-step motors(2); 3. semitransparent mirror; 4. mirror with hollow reflector; 5. anamorphic cylindrical lenses; 6. photovoltaic cells.

The optical axis of the instrument coincides with the direction of the x axis of the spacecraft. The axis of rotation of a semitransparent mirror coincides with the z axis, and of mirror 4 with the y axis of the SC.

Cylindrical lenses employed in the instrument convert the point image of the sun which is constructed by a wide-angle objective into a line which overlaps the entire width of the receiver's sensitive layer.

We note that such an instrument can be realized with the use of a wide-angle objective and one receiver with a longitudinal photoelectric effect, the signals from which provide information on the size and direction to

the sun with the instrument axis (Fig. 6.33). The nonlinear dependence of the value of the input signals on the error angles (amount of shift of the spot relative to the center of the layer) causes the need to introduce into the make-up of the orientation system computers with large storage which permit the unambiguous determination of the coordinates of the sun in the instrument's field of view from the magnitude and polarity of the signals from the output of the receiver.

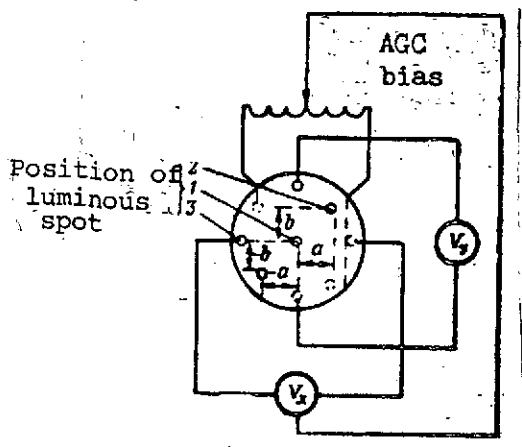


Fig. 6.33. Operating principle of an instrument for orientation on the sun with the use of a photocell with longitudinal photoelectric effect: a, b. coordinates of luminous spot.

The basic shortcomings of the /212 instrument which has been considered are the dependence of the parameters of the receiver on temperature and the dependence of the output signal not only on the angle of deviation but also on the power of the incident radiation. The latter dependence is excluded rather easily with the normalization of the output signal in accordance with the value of the voltage or current which is caused by the transverse (regular) photoelectric effect. Despite this, in a number of cases, such instruments may not satisfy the requirements made of instruments for solar orientation. Therefore, more complex instruments are used with a discrete output which is provided by binary photovoltaic cells.

Such instruments are free of the indicated shortcomings and assure the necessary precision.

These cells are made with the engraving of a special grid on the sensitive layer of the receiver. However, there may also be another variant.

A sensitive layer is applied to a single backing which is slit in several places for the entire depth to the backing so that a number of independent sensitive layers of equal width are obtained. Then, the entire receiver is covered from above by a diaphragm with openings which represent a code grid. The openings in it are arranged in strips above the corresponding sensitive layers of the receiver. A diagram of a binary photovoltaic cell is presented in Fig. 6.34.

If there are six sensitive layers and there are openings in each section which are separated by opaque strips (respectively, 32, 16, 8, 4, 2, and 1), this is equivalent to the presence of the corresponding number of pairs of strips sensitive and nonsensitive to radiation. Consequently, the resolution /213 of the sensor will equal

$$\frac{\pi}{2^N - 1} = \frac{\pi}{2^6 - 1} = \frac{\pi}{63} = 0.05 \text{ rad}$$

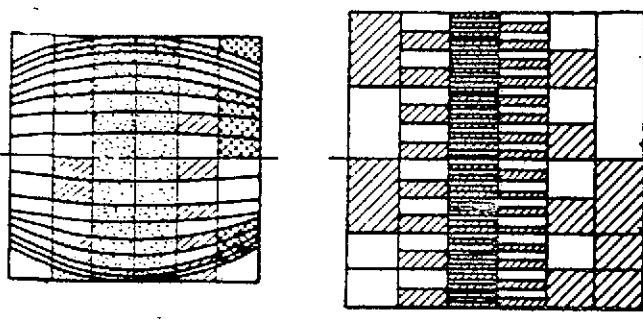


Fig. 6.34. Binary photovoltaic cell.

Since an optical system with cylindrical optical parts provides distortion of the image on the edges of the field of view, the shape of the openings in the diaphragm or the engraving of the receiver are made with consideration of this distortion.

following (see Fig. 6.32). When the sun is located at an arbitrary point of the field of view, its image is constructed with the use of an objective 1, mirrors 3 and 4, and cylindrical lenses 5 in the form of focal lines in the planes of disposition of the sensitive layers of the binary photovoltaic cells. Inasmuch as at the initial moment, mirrors 3 and 4 comprise an angle of $\pi/4$ rad with the optical axis, the position of the focal lines in the form of which the sun is depicted on the sensitive layer of the receiver will depend on the position of the sun in the field of view.

The operating principle of the instrument considered consists of the

If there is an error only for the z coordinate (sun in plane xOz), the focal line on the left cell 6 will coincide with its middle with axis zz and will prove to be shifted along this axis. In this regard, its removal from the center depends on the size of the error angle between the x axis and the direction to the sun. At the same time, the focal line on the right cell 6, coinciding with axis xx , proves to be shifted along it in such a way that the center of this line will not coincide with the axis yy which passes through the middle of the receiver. In this case, a signal is generated which is fed to the step-by-step motor of the mirror 4 and it will turn around until the middle of the focal line coincides with the axis yy .

After this, the output signal from the cell 6 permits determining the position of the sun relative to the optical axis unambiguously with a precision of up to $3.1.74 \cdot 10^{-2}$ rad.

If there is an error in the y coordinate alone (sun in plane xOy), the opposite picture is observed. The focal line is matched with axis xx of the left cell but its middle is displaced along this axis from some distance from the axis. The distance is determined by the error angle. The error signal is now fed to the step-by-step motor of mirror 3 which turns it

around until the coincidence of the middle of the line of the sun's image with axis zz . On the right cell 6, the focal line, being symmetrically arranged relative to axis yy , proves to be displaced along it from the center of the receiver for the distance which is determined by the size of the error angle. In this case, the signal from cell 6 determines the amount of error:

With the arbitrary position of the sun in the field of view, the signals for the turning of mirrors 3 and 4 until the symmetrical arrangement of the lines of the sun's image relative to axes zz and yy , respectively, are fed to both step-by-step motors and information about the angular coordinates of the sun relative to the x axis is obtained from the output of the cells.

When the sun is in a zone overlapped by both instruments, the selection of the necessary control signals is accomplished by shifting the signals.

The described instruments possess the following characteristics:

Focal length	6.5 mm
Field-of-vision angle	$187 \cdot 1.74 \cdot 10^{-2}$ rad
Size of image (along the diameter)	17.6 mm
Relative aperture	1:6.3 or less
Resolution	60-100 lines/mm
Overall dimensions	length - 49 mm and diameter - 73.5 mm

Mirrors 3 and 4 are placed between the objective and the cylindrical lenses and provide the possibility for displacing the image by 18.6 mm along axes xx and yy .

Inasmuch as orientation on the sun with a precision of $3 \cdot 1.74 \cdot 10^{-2}$ rad may prove insufficient for the solution of some problems, precise sensors of the sun's position are used in aggregate with the instrument examined. These sensors (the diagram of one of them is presented in Fig. 6.35) are based and operate on the same principle and with the use of the same binary photovoltaic cells as the coarse ones. The only difference is that to assure the required precision in determining the sun's position, the field of view of this sensor is $6 \cdot 1.74 \cdot 10^{-2}$ rad, the focal length of the objective equals 185 mm, and the semitransparent mirror is stationary. As a consequence of the small field of view, no substantial distortions of the image are observed. Therefore, cells with straight grids (diaphragms) may be used. /215

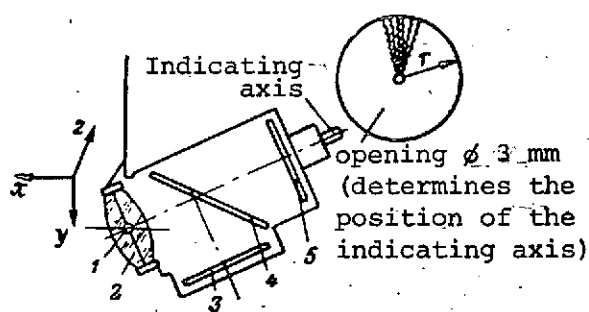


Fig. 6.35. Diagram of a precise position indicator: 1. point of suspension; 2. objective ($f = 18.5$ cm; $2W = 6.1 \cdot 1.74 \cdot 10^{-2}$ rad); 3. y sensor; 4. z sensor; 5. semi-transparent mirror.

Thus, the electro-optical sun seeker which is being examined includes coarse and precise sensors. The coarse sensor, catching the sun's radiation, puts out a signal from which the optical axis of the precise sensor of the discrete type coincides with the direction to the sun with a precision of $\pm 1.5 \cdot 1.74 \cdot 10^{-2}$ rad. The position of the precise sensor is fixed in this direction by the indicating axis which lands in one of the openings of

the recording collar. This collar is a hemisphere with an inner radius of 490 mm. Precise determination of the coordinates of the sun is accomplished with the use of two photovoltaic cells installed in two focal planes of the objective and arranged at an angle of $\pi/2$ rad to each other.

The block diagram of the instrument (precise or coarse channel) is presented in Fig. 6.36. The indicator system generates positive or negative signals relative to the average position in binary code. These signals go to the electronic circuit over 12 channels. The information which has arrived is processed in the logic unit, where control signals are formed which are fed both to the step-by-step motors (in the coarse instrument) and to control the orientation of the SC.

/216

The solar attitude control can also be used as a yaw sensor. However, in this case the velocities and angles of pitch and roll should be determined by other methods, for example, with the use of horizon-tracing instruments. In the determination of the angles of pitch and roll with a precision on the order of $5 \cdot 1.74 \cdot 10^{-2}$ rad, the error in measuring the angle of yaw should not exceed $4 \cdot 1.74 \cdot 10^{-2}$ rad. This error can be reduced by increasing the precision of measurement of the angles of pitch and roll.

In connection with the fact that two instruments are installed on board the SC which provide an overlap of $14 \cdot 1.74 \cdot 10^{-2}$ rad, in this zone, the sun is recorded at once by both sensors, which can be used for the approximate determination of the angular velocity of the SC during the measurement of the time

of a half turn of the SC, i.e., the time segment between the moments when the sun lands in the zone of overlap of the instruments.

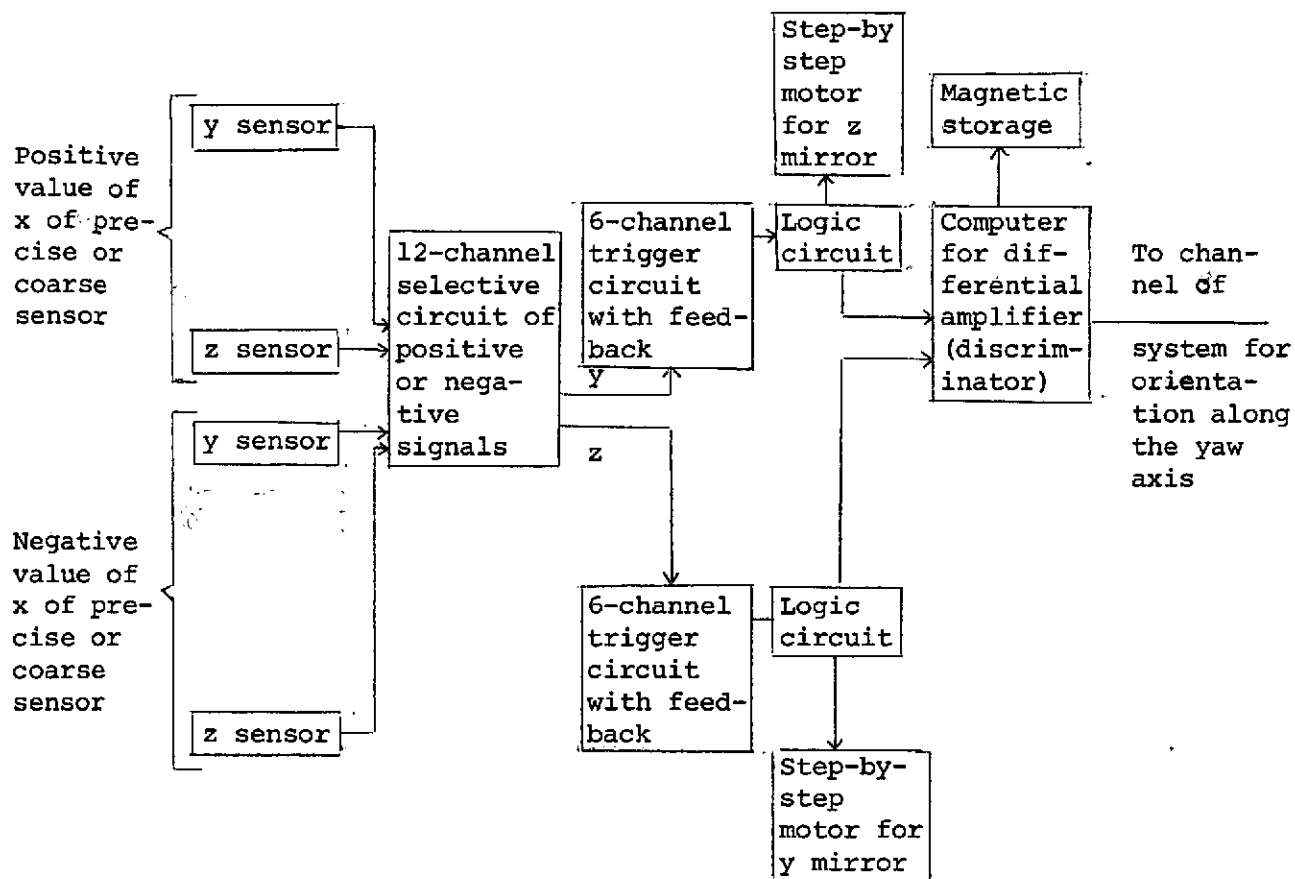


Fig. 6.36. Block diagram of an instrument to determine the sun's position.

As an example, let us consider a system for orientation on the sun which also consists of coarse and precise instruments (Fig. 6.37). The role of the coarse orientation sensors is accomplished by four photocells which assure the search of the sun and its landing in the field of view of the precise channel. The photocells are placed beneath a screen which covers them from the sun's rays in the case where the sun is in the field of view of the precise channel which equals $1.1.74 \cdot 10^{-2}$ rad. A two-mirror objective, photoelectric receivers, and an electronic unit are used in the precise channel.

/217

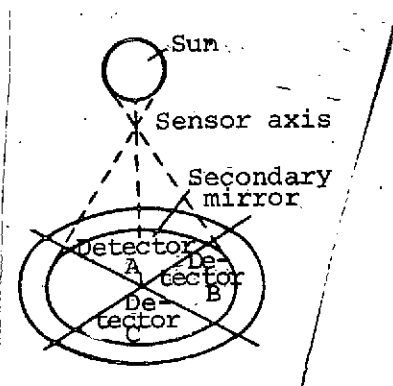


Fig. 6.37. Diagram of an instrument for solar orientation.

Used as radiation receivers are silicon photocells which are sensitive in the spectral band from 0.4 to 1.15 μm with maximum sensitivity on a wavelength of 0.85 μm .

Information about the angular coordinates of the sun relative to the axis of the sensor is generated on the signals of three sector photocells on which the sun's image is projected (Fig. 6.37). In this case, the error signal for the x coordinate is obtained with the comparison of the output signals of photo-

cells A and B, and for the y coordinate, of photocells B and C

Such a scheme for obtaining error signals causes a considerable influence of the difference in sensitivity of individual receivers on the precision of the instrument. To eliminate a possible change in sensitivity, a calibration system is used in

the instrument which permits compensating for the mutual change in the sensitivity of the receivers in the process of operation with the automatic adjustment of amplification of the signals. In this case, the signal of one of the photocells is taken as the reference signal. Calibration is accomplished with the use of a neon bulb which is fed by a pulsed voltage. The flashes of the bulb, which recur with a specific frequency, uniformly illuminate all receivers through the semitransparent mirror and cause the appearance of an alternating component in the signal on their outputs (in contrast to the constant component caused by the sun's radiation). The alternating signals go to a comparison device which provides the corresponding adjustment of amplification over the channels. The block diagram of the precise sensor of a solar orientation system is shown in

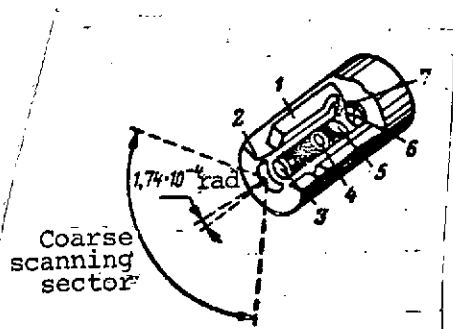


Fig. 6.38. Arrangement of receivers in the channel for precise solar orientation: 1. preamplifier unit; 2. photocells of the coarse system; 3. secondary mirror; 4. primary mirror; 5. semitransparent mirror; 6. photocells of the precise system; 7. calibration bulb.

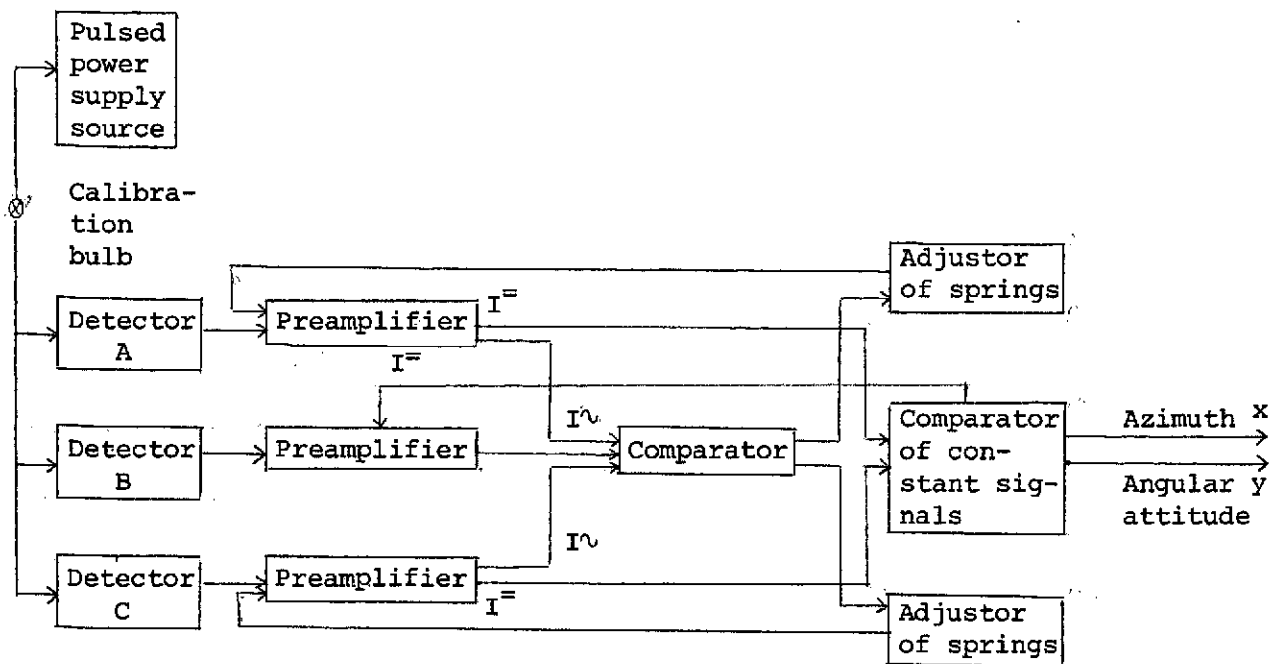


Fig. 6.39. Block diagram of a channel for precise solar orientation.

6.7. Electro-Optical Instruments for Orienting Spacecraft by the Stars

Electro-optical instruments for orienting a vehicle by the stars together with instruments for orientation by the sun are intended for the stabilization of the SC in space with a given position of its axes.

At each point of the flight trajectory of the SC which corresponds to a completely determined moment in time, the angle between the direction to the sun and a selected star will have a previously known value. If the optical axes of the solar and star instruments on board the SC are placed at an angle γ to each other which corresponds to the angle between the directions to the sun and the star at a given moment, then with the accomplishment of the orientation, the position of the SC in space will become known.

In order to accomplish the orientation of the SC in space with the use of the sun and a star as reference points, it is first necessary to orient the solar channel on the sun. Since the sun is the most powerful emitter within the limits of the solar system, its search and orientation on it cause no special

difficulties. On completion of orientation on the sun, to seek the star, rotation is imparted to the SC relative to the axis directed at the sun. In this, the field of view of the star channel of the sun-star orientation system will describe a conical surface in space which passes through the selected star. Thus, during a complete revolution, this star must fall within the limits of the field of view of the instrument.

Orientation of the SC on the sun and one of the stars provides the possibility of not only knowing the position of the SC in space, but also assigning it. To give the SC the required position in space, it is necessary to move the optical axes of the solar and star channels of the system which records the sun-SC-earth angle (SUE) on board simultaneously relative to the body of the SC (relative to all three axes) without changing the established value of the SUE angle. The movement of the fields of view of both channels relative to all three axes requires rather complex kinematics. /219

Another method is also possible to assure the given position of the SC in space in which the instruments of the system only record the SUE angle on board. Upon completion of orientation on the sun and star, the necessary turns of the SC relative to all three axes to the required position are accomplished on the commands of special sensors, for example, gyroscopic, with the introduction of the appropriate units. A shortcoming of this method is the impossibility of checking the position of the SC which it occupied in space after accomplishment of the turns.

However, regardless of the method of giving the SC the required position in space, the composition of the system should include an instrument which tracks the star along with the instrument for orientation on the sun.

Different circuit solutions of instruments for tracking a star are possible:

- Instruments based on the use of electronic scanning (with the use of dissectors and others);
- Instruments with mechanical modulating and scanning devices.

Let us consider a scheme for a star tracker intended for tracking a star and based on the use of an image dissector. The scheme for such an instrument should include: an objective, image dissector with a focusing-defocusing system, dissector power-supply unit, and an electronic circuit for discriminating control signals.

The basic element of the star tracker is the dissector which provides a field of view of the instrument of

$5.1.74 \cdot 10^{-2} \times 11.1.74 \cdot 10^{-2}$ rad. With this, thanks to electronic scanning, tracking is attained within the limits of a cone with an apex angle up to $28.1.74 \cdot 10^{-2}$ - $30.1.74 \cdot 10^{-2}$ rad in accordance with the change in the SUE angle.

In the operation of the instrument, its objective constructs the image of the sky in its focal plane where the end of a fiber-bunched conductor is located. The image constructed on the fibers is transmitted to the photocathode of the dissector and causes the emission of electrons. In this, the flux of electrons is proportional to the incident radiation flux. The constructed image is read by an electron beam.

If the star which has been selected as a reference point is not located on the axis of the instrument and its image is not constructed in the center of the photocathode, a sequence of pulses arises on the output of the photomultiplier. In this, an error signal is formed with the comparison of the phases of the operating and reference voltages. On the basis of these signals, control commands are generated which put the SC into a turn in the direction of reduction of the error. Most often, stars are selected as reference points which possess the greatest visible point brilliance (Sirius and Canopus). /220

The amplification stage is so constructed that, with the landing of the star in the field of view of the instrument, the rotation of the SC around the longitudinal axis stops and the lock-on on the star and its subsequent tracking are accomplished. This principle was realized in the star trackers of the "Mariner-IV" SC [60]. The search for the star began after localization of the axis of the solar channel in the direction of the sun with the forced rotation of the SC around this axis.

In electro-optical instruments for orientation on the stars with the use of modulating and scanning devices of the mechanical type, the search for a star is also accomplished by rotating the SC relative to the axis of roll oriented on the sun.

One of the variations of such instruments is intended for operation on point emitters, which stars are, and does not react to the radiation of extended sources (earth, moon) during flights in near-earth space. The instrument generates the necessary signals only in those cases where the irradiance created by a star which has fallen in its field of view lies within the limits of from 0.67 to 1.5 in comparison with the irradiance from the star Canopus.

With the landing of a star in the field of view of the instrument, it provides the following types of information:

- A signal about the presence of the star Canopus (or some other one) in the field of view;
- A signal which characterizes the angular position of the star in the plane of rotation and which is the input signal of the control system which assures the required orientation of the SC on the star;
- A signal proportional to the radiation flux of the section of the sky which has landed in the instrument's field of view.

A functional diagram of the instrument is presented in Fig. 6.40. The command for tracking a given star is given after a comparison of its radiation with the sun's radiation.

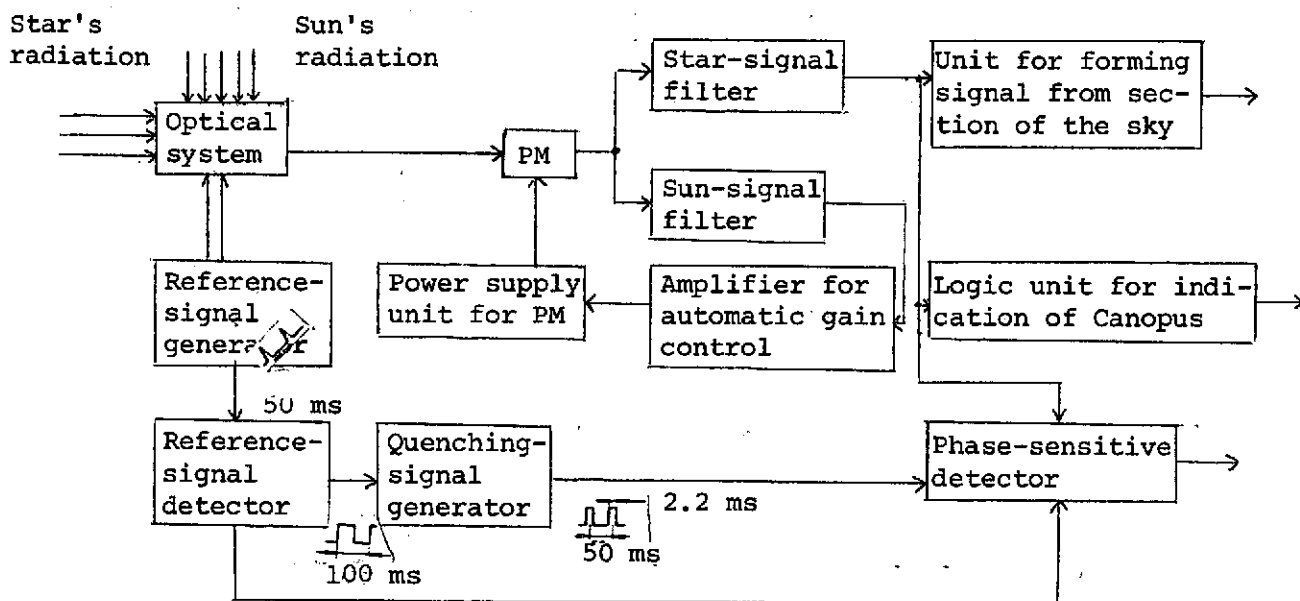


Fig. 6.40. Functional diagram of an instrument for orientation of an SC on a star.

The radiation of the star, passing through the protective glass after reflection from the rocking search mirror, is sent to the lens objective by the scanning mirror. A modulating disk is installed in the focal plane of the objective which assures modulation of the radiation flux from the star with a frequency of 3.9 kHz. The modulated radiation goes to the photocathode of the photomultiplier.

The solar radiation is also directed to the photocathode of the PM over its own channel with the aid of a miniature optical system through an attenuating filter and a system of optical parts. The possible effect of a change in the angle of incidence of the radiation is eliminated by the use of a diffuser of milky glass. A special corrective filter is used in the optical system, thanks to which the spectral composition of the solar radiation which has entered the instrument is modified and, at the output, becomes similar to the spectral composition of the radiation of the star Canopus. The solar radiation is modulated similar to the radiation of the star with the aid of a modulating disk. The radiation which is modulated with a frequency of 2.3 kHz is focused on the photocathode in the same place where the image of the star is constructed.

Thanks to the different modulation frequencies, the signals from the star and sun can be separated on the output of the PM by special electrical filters tuned to the corresponding modulation frequencies.

The signal from the output of the solar channel is used for the automatic adjustment of the amplification of the amplifier which controls the high-voltage power supply unit of the photomultiplier and, consequently, its amplification factor. This circuit maintains the signal in the solar channel at a fully determined level.

In this case, the output signal of the star channel is proportional to the irradiance ratio of the sun and the star.

For the formation of the three signals mentioned earlier, the voltage which corresponds to the star channel, modulated with a frequency of 3.9 kHz is fed from the output of the PM to three independent electronic circuits (see Fig. 6.40). Modulation of the radiation is accomplished by a scanning mirror which rocks with the aid of a cam of a specific shape which assures the linear law of scanning in a large part of the field of view. The scanning period equals 50 ms; in this, the duration of the return motion does not exceed 10% of it and comprises 4.4 ms. /222

When the amplitude of the signal in the star channel is within limits of the threshold values on the output of the presence unit, a signal appears which indicates the appearance of the star in the instrument's field of view.

Simultaneously with this, the signal from the output of the resonance filter is fed to a phase-sensitive detector to which the square pulses of the reference voltage also go. Thanks to the comparison of the operating and reference voltages, a

direct-current voltage is created on the output of the phase-sensitive detector which corresponds to the position of the star in the field of view. In proportion to the movement of the star from right to left, the output voltage changes from positive to negative and equals zero when the star is located in the center of the field of view.

Furthermore, as can be seen from the block diagram, the signal from the output of the filter is fed to the unit which forms a voltage proportional to the total radiation flux in the star channel. This voltage is transmitted over the telemetry channel to the earth and can be used to organize the search for the star on commands from earth. In this, the orientation of the longitudinal axis is accomplished in the direction to the sun and rotation around this axis is imparted to the SC with a velocity of $0.5 \cdot 1.74 \cdot 10^{-2}$ rad/sec. With the landing of some star in the field of view, information about it is transmitted to earth to verify whether it is the star Canopus.

Another method of checking consists of recording all stars which land in the field of view during the time of a complete revolution of the SC relative to the longitudinal axis. The chart which is thus obtained is compared with a control chart.

After the conduct of the correction for the check, the SC is again oriented on the sun and Canopus.

An instrument of this type was used on the "Surveyor" SC for orientation on the sun and a star in the execution of correction of the trajectory during the flight to the moon. It had a field of view of rectangular form with dimensions of $4 \cdot 1.74 \cdot 10^{-2}$ rad in the direction of rotation and $5 \cdot 1.74 \cdot 10^{-2}$ rad in the direction of search (parallel to the direction to the sun). The design of the instrument permits moving the field of view of the instrument within limits of $\pm 15 \cdot 1.74 \cdot 10^{-2}$ rad. This provides the opportunity to so tune the instrument that the lock-on on the star Canopus is assured with triggering during 48 days from the day of the adjustment of the instrument. The mass of the instrument is 2.0 kg.

The reliability of this instrument is 0.97 for a time interval equal to 66 h.

In flights in near-earth outer space, the use of the sun and star for orientation is not always convenient. Sometimes, orientation of the SC on stars alone is more rational. /223

For such orientation, a system may be used which consists of six tracking instruments capable of discovering stars and

tracking them. They are arranged in pairs relative to each axis and directed in the opposite directions.

Each direction finder is a two-stage tracking electro-optical instrument with a field of view of $1.1.74 \cdot 10^{-2}$ rad. The receiver of the instrument is fastened to a movable platform which can rock in two mutually perpendicular planes within limits of $\pm 43.1.74 \cdot 10^{-2}$ rad. The block diagram of one astrotracker is presented in Fig. 6.41 and a diagram of its optical system is shown in Fig. 6.42.

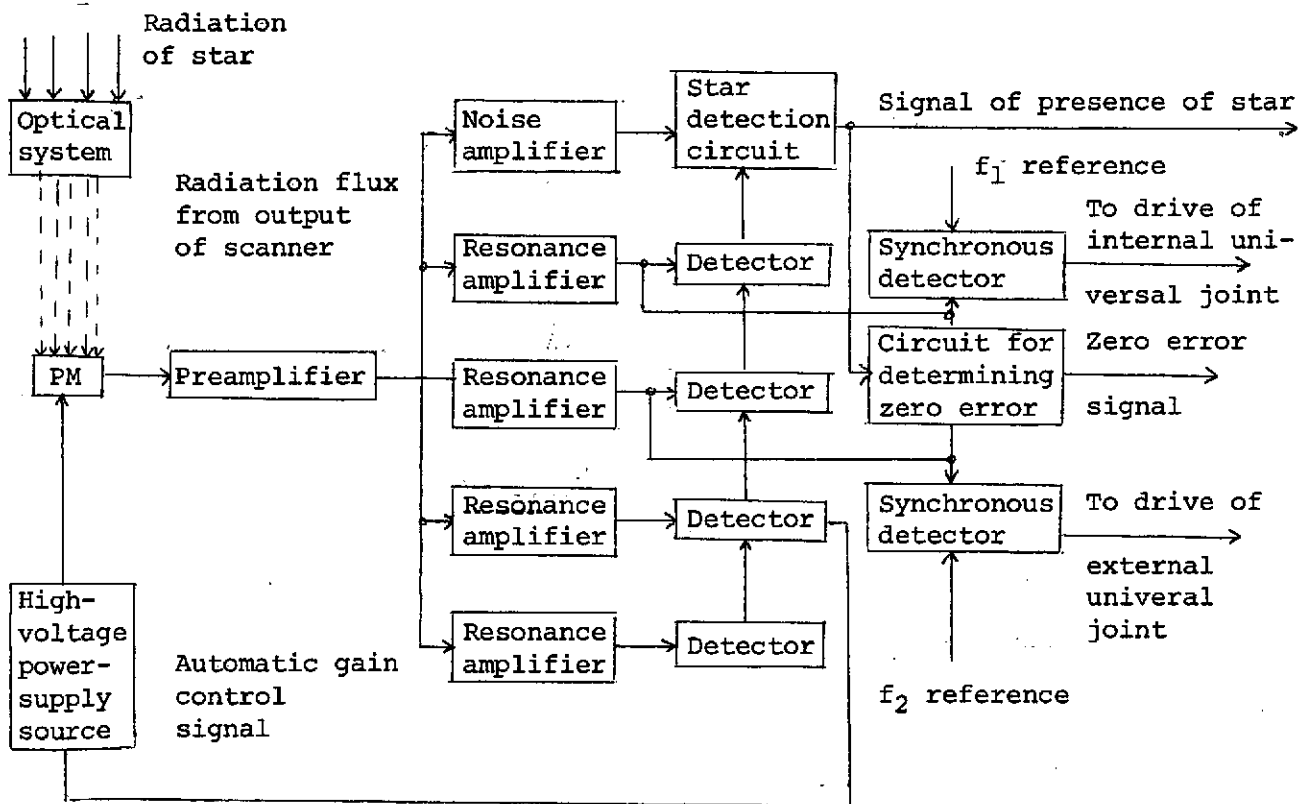


Fig. 6.41. Functional diagram of an astrotracker.

The primary mirror of parabolic form with a diameter of 87.5 mm with focal length $f' = 127$ mm directs the radiation of the star to a reflector of two mirrors which separate the radiation flux in two directions in mutually perpendicular planes. After reflection from the mirrors of the separating unit, the radiation flux in each channel is modulated with the aid of oscillating modulators arranged in the focal planes of the principal mirror.

In this, to exclude uncertainty, one of the modulators oscillates with frequency f_1 and the second with frequency $f_2 \neq f_1$. The modulated radiation is directed to the photocathode of the PM with the use of the optical system.

After preliminary amplification, the electrical signals which arise are fed to a resonance amplifier tuned to frequencies f_1 , $2f_1$, f_2 , $2f_2$ and also to the noise amplifier. The signal from the output of each amplifier is fed to the detector. The total signal from the output of all detectors is fed to the circuit for the formation of the "presence" signal. /224

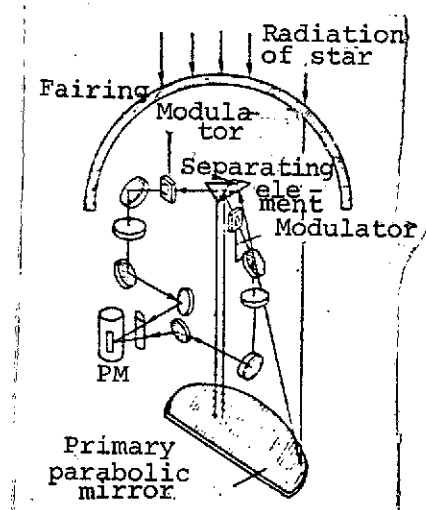


Fig. 6.42. Diagram of the optical system of an astrotracker.

In normal operating mode, when the image of the star is within the limits of the field being scanned, the level of the external noises is not great and the circuit for the formation of the "presence" signal puts out a signal for lock-on and search stops.

As soon as the image of the star occupies zero position with respect to the axis of the instrument, error signals no longer arise on frequencies f_1 and f_2 , as a result of which the signal of zero position of the star appears.

Identification signals on frequencies $2f_1$ and $2f_2$ are used for the automatic adjustment of the amplification factor of the automatic gain control during control of the power-supply unit of the PM. This is necessary to maintain steady tracking.

When radiation from the moon or from cloud cover on the earth falls into the field of view during search, the noise amplifier generates a signal which suppresses the presence circuit. As a result of the false signal, tracking does not arise and search can continue.

A synchronous detector is used in the circuit to increase reliability in discriminating operating signals. The reference voltage is fed to it over the synchronization circuit.

The astrotracker operates in two modes: search and tracking. In the search mode, when the axis of roll is oriented on the sun

and the axis of the astrotracker is given the required angle with respect to the axes of the SC, search and lock-on on the star are accomplished. When the astrotrackers simultaneously give out signals about locking on the star, rotation of the SC relative to the axis of roll stops and the system changes from the search mode to the tracking mode. With this, each astrotracker accomplished the tracking of its own star.

On obtaining signals from four astrotrackers, the control system automatically changes from solar orientation to orientation on stars. The astrotrackers assure the tracking of a star with a precision of $\pm 30.4.85 \cdot 10^{-6}$ rad. In this, normal functioning is maintained with angles between the directions to the star and sun of at least $30.1.74 \cdot 10^{-2}$ rad.

Orientation of the SC in space can also be accomplished with /225 the use of a star field rather than individual stars. In the realization of such a method, there is a chart of the corresponding section of the starry sky on board the SC. The search of the reference direction is accomplished by the system independently. In the search process, a comparison of the observable star field with the chart is performed. Matching of the visible star field with that prescribed is accomplished with the use of a comparatively simple electro-optical instrument, a disk (Fig. 6.43). The mutual arrangement of the openings corresponds exactly to the prescribed picture of the stars. The diameters of the individual holes in the standard chart are less than the width of the pencils which diverge from the image of each star at the places of their intersection with the plane of the chart. This provides the opportunity to obtain information about the slope of the sighting axis of the instrument relative to the star field.

With the correct orientation of the SC relative to the star field, the rays from each star pass through the corresponding openings in the standard chart and are collected by a condenser on the sensitive layer of the radiation receiver or in the correlation plane. A photomultiplier with an /226 antimony-cesium photocathode is used as a radiation receiver in the instrument. A modulating disk with a slotted raster applied to it is placed directly in front of the photocathode.

With correct orientation, all the beams land in a given zone of the photocathode and form one luminous spot on it. If a slope of the axis arises, caused by a change in the spatial orientation of the SC for roll or pitch, some decorrelation occurs: the spot is shifted in a direction opposite to the deflection of the star field from the axis being oriented and is slightly extended in the direction of the shift. This provides

an error signal which contains information both about the amount as well as the direction of slope of the SC relative to the reference direction.

The turning of the object relative to the reference direction (naturally, with this the standard chart also turns) causes an increase in the dimensions of the luminous spot in the plane of the photocathode of the PM which leads to a reduction of illumination in the spot. This is caused by the fact that it is not the central rays which pass through to the photocathode but the outer ones which go toward the optical axis at large angles. A reduction in the illumination and the imprecision of the spot lead to the appearance of an error signal which characterizes the value of the deflection angle.

In order to obtain information not only about the amount but also about the sign of the deflection angle, two identical groups of holes are made on the standard chart which correspond to the selected star field and are shifted relative to each other by some angle α (see Fig. 6.43b). This provides two separate correlation functions. The difference between the two outputs characterizes both the amount as well as the direction of turn of the object relative to the reference direction.

In the process of search, the disk with the standard chart is turned around the optical axis with the aid of a motor until the correct orientation relative to the star field is attained, which is determined from the position of the luminous spot on the photocathode and the illumination in the spot. For the operation of the instrument, the preliminary aiming of its sighting axis at the center of the selected star field with a precision of $10 \cdot 1.74 \cdot 10^{-2}$ rad is necessary. With flights within the limits of the solar system, this requirement is easily satisfied since in this case the SC will move in the plane of the ecliptic. A simple instrument for orientation on the sun can be used for the solution of this problem. With the aid of this instrument, the axis of suspension of the star instrument is directed at the sun and is kept in this position for some time. With completion of the orientation of the axis of suspension on the sun, the instrument for tracking the star field begins to rotate relative to the oriented axis, accomplishing the scanning of the circular zone of the sky where the selected star field is situated.

If the time of the start of the orientation is known, i.e., /227 if the orientation of the star field relative to the star point of space where the SC is located is known, the disk with the standard chart can be turned ahead of time relative to the optical axis by the required angle. As a result of this, after the accomplishment of one or two complete revolutions of the SC

around the axis oriented on the sun, the optical system for tracking the star field will prove to be approximately matched with the center of the star field. Subsequently, the SC is precisely oriented on the star field.

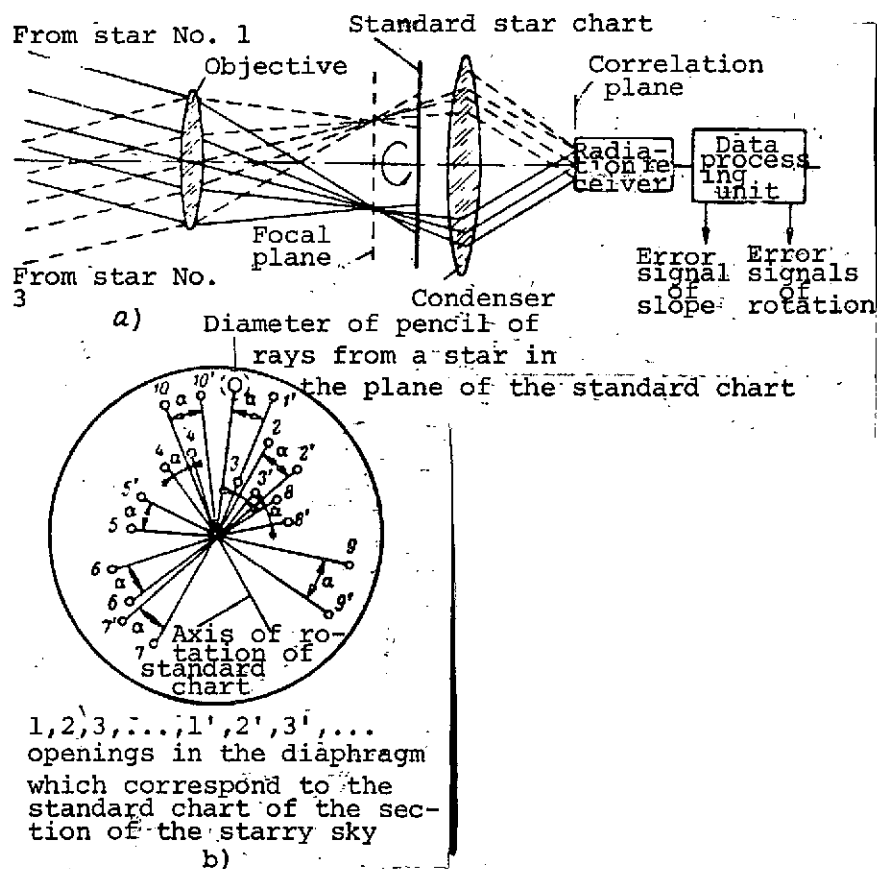


Fig. 6.43. Schematic diagram of an electro-optical instrument for orientation of a vehicle star field: a. diagram of the optical system; b. disk with two identical groups of openings which correspond to the chart of the starry sky; 1, 2, 3, ..., 1', 2', 2'... openings in the diaphragm which correspond to the standard chart of the section of the starry sky.

The correlation method for forming control signals used in the instrument considerably reduces the probability of interference on the part of the planets and other nonstellar sources

of light. Furthermore, this method assures increased sensitivity since the radiation of several stars is summed on the photocathode.

7.1. Types and Purpose of Special Electro-optical Instruments

Special electro-optical instruments are intended for the solution of problems which are connected with the basic functions of a given space ship. Depending on the purpose of the SC, this type of electro-optical equipment can be divided into several groups:

- Instruments for the detection and measurement of infrared, visible, or ultraviolet radiation of ground and space objects;
- Instruments for the meteorological investigation of the earth's surface and the atmosphere;
- Instruments for the determination of relative linear and angular coordinates of the SC.

The first group is made up of radiometric and photometric instruments which have different purposes and schemes in which regard, at the present time, radiometers have received greater propagation on unmanned SC. They are used to detect an object by the contrast of its intrinsic or reflected radiation with the background and they investigate and measure the characteristics of this radiation to obtain information about the object or solve other scientific and technical problems. Along with special radiometric equipment, the group of electro-optical instruments of weather AES [Automatic Earth Satellite] is made up of actinometers, reflexometers, photo-television instruments, and so forth. Assembled as a set on board the AES, these instruments assure the measurement of the radiation characteristics of the earth and the atmosphere, the investigation of the dynamics of change in the thermal balance of the earth, the movement and development of cloud cover, and so forth.

For a number of SC, one of the most difficult tasks is the accomplishment of rendezvous and docking. Along with radio-technical systems, these operations can be accomplished with the aid of special electro-optical equipment, for example, rangefinders and locators which assure control of the movement of the carrier until docking. A special group of instruments which accomplish the measurement of parameters relative to the movement of the SC is made up of various electro-optical instruments with lasers which will be examined below.

The variety and specific properties of the problems solved with the use of special electro-optical equipment of the SC does not permit examining in the space of one chapter, all possible variations of equipment of this type which is employed and projected. Therefore, in a number of cases the presentation of the material is limited to information on theory and the bases of

construction which permit the easy clarification of the operating principles of the instruments which are already known from other fields of application.

7.2. Principles of Construction of On-Board Radiometric Equipment

One of the types of electro-optical equipment which is employed on space carriers consists of instruments for the detection and recording of the thermal radiation of ground objects. They are used in meteorology to obtain thermal charts of the cloud cover and the earth's surface and to determine the thermal radiation and reflection coefficients of sections of the earth's surface. The high degree of resolution obtained with the use of such instruments permits obtaining images not only of sections of the landscape but also of individual heat-radiating objects.

Despite the variety of methods of construction and procedures for recording the signals which are received, the instruments of this type are based on the use of one common principle which consists of the fact that, because of the difference in the temperature and emissivity coefficient of two adjacent sections of the surface of the landscape (an object with a background), the radiation receiver installed in the instrument records the corresponding difference in radiation fluxes which are emitted by these surfaces (objects).

Several principles for the construction of the instrument's circuit for the detection and recording of the thermal radiation of objects are known, for example, the electron-optical converter, evaporograph, the IR radar, and others [16,18,25]. However, for use on a space vehicle with the automatic recording and processing of information which is obtained, various types of radiometric instruments are employed which are divided into several /229 groups depending on the method of recording the signal, principle for scanning space, and the circuitry of the basic units.

According to method of recording, instruments of this type can be divided into two groups: 1) thermographic in which the information which is received is recorded by a video tape recorder, oscillograph, or other recording device; 2) thermovisual instruments or televisions in which the construction of the image of the heat-radiating object is accomplished. In the latter, it is necessary to use a television channel for the transmission of information to earth or the delivery of photographs of the picture which has been obtained.

According to the principle for scanning space, radiometric instruments are divided into instruments with a constant angle of coverage (without scanning) and scanning radiometers. Multi-element (mosaic) radiation receivers are usually used in instruments of the first group to increase the angle of coverage. In

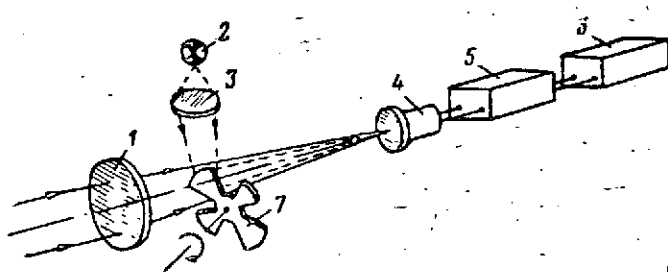


Fig. 7.1. Block diagram of a radiometer. 1. objective; 2. standard emitter; 3. condenser; 4. radiation receiver; 5. amplifier unit; 6. signal-recording units; 7. mirror modulator.

scanning radiometers, the scanning of space within limits of a given solid angle is accomplished with the use of a special scanning system. Depending on the design of the scanning system radiometric instruments can be divided into instruments with optical-mechanical, electronic, or luminous scanning.

Photo resistors which are sensitive to infrared rays, thermistors, bolometers, and also special semiconductor-type receivers or mosaic targets of electron tubes of vidi-

con, thermicon, and other systems are used as radiation receivers in radiometric systems. The characteristics of the receiver determine the spectral operating range of the instrument, its threshold sensitivity, and a number of other basic parameters.

Figure 7.1 presents the block diagram of a radiometer with a constant angle of coverage and one radiation receiver. The radiation flux from the object is collected by the objective 1 and is focused onto the sensitive surface of the receiver 4. A mirror modulator 7 is installed between the objective and the receiver and rotates around an axis which is placed at an angle of $\pi/4$ rad to the optical axis of the objective. With rotation, the blades of the modulator interrupt the radiation flux which is falling on the receiver and this permits using circuits on alternating current in the amplifier units 5 and recording units. For calibration of the instrument and to determine the absolute values of the signal being recorded, provision is made for a standard emitter 2 in the circuit of the radiometer, the radiation flux from which is sent to the receiver with the use of the modulator during those periods when the modulator interrupts the radiation flux from the objective. /230

Figure 7.2 presents the block diagram of a radiometric instrument of the second group - a thermovisual instrument with an optical-mechanical scanning system. The radiation flux from the object falls on a rotating prism 4 which is fastened in a universal joint 3. The flux which has been reflected from the faces of the prism is collected by the objective 7 and is focused on the radiation receiver 6. Scanning by frame is provided by the rocking of the prism 4 around the optical axis of the objective through the angle α_f with the use of the drive 1. Scanning by line is assured by the rotation of the prism from the drive 13. Pulses which characterize the processes of scanning by frame and line

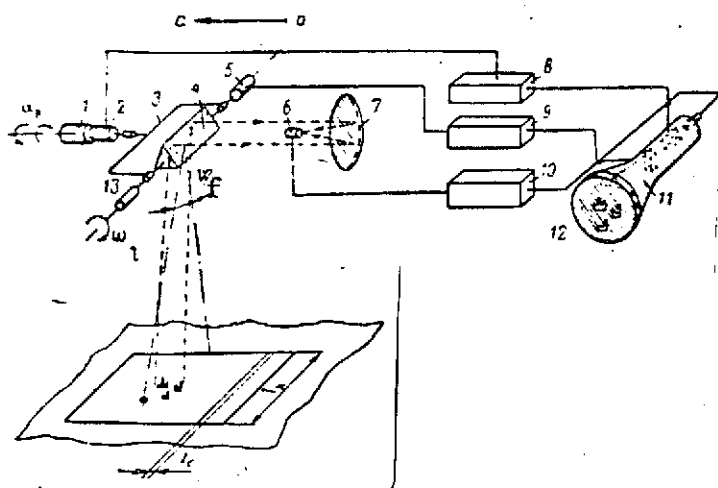


Fig. 7.2. Block diagram of a thermovisual instrument with an optical-mechanical scanning system: 1. scanning drive by frame; 2. pulse sensor by frame; 3. universal joints; 4. rotating mirror prism; 5. sensor of scanning pulses by line; 6. radiation receiver; 7. mirror objective; 8. unit for the control of frame scan; 9. unit for the control of line scan; 10. unit for amplification of signals from radiation receiver; 11. cathode-ray tube; 12. image of heat-radiating objects of the screen of the tube; 13. drive for scan by line; aa. direction of movement of the carrier.

are transmitted by pulsed sensors 2 and 5 to units 8 and 9 which control the scanning system of the cathode-ray tube 11 on whose screen the image (heat chart) of the object is created. The angle of coverage for frame W_f is determined by the turning limits of the prism 4 and the size of the line λ_1 - by the instantaneous field-of-vision angle of the instrument $W_1 = d_r$, where d_r is the diameter

f_i of the receiver and f' is the focal length of the objective. In some schemes, /231 a multi-element radiation receiver is used instead of a single element receiver and this permits simplifying the scanning mechanism. Thus, in the instrument of the "Eastman-Kodak" Company (USA) a "Ruler" of 50 receivers is used which assures the scanning by line. Scanning by frame is accomplished through a mechanical system in the form of a rod which oscillates at a frequency of 4-5 Hz. Each receiver has its own amplification channel with the output to the indicator [16,18].

An example of a television with an electronic scanning system is the instrument of the "Westinghouse" Company (USA) with a phothermionic tube [18] whose schematic is shown in Fig. 7.3. The radiation flux 1 from the object after the objective 3 is focused on the target 7 of the phothermionic electron tube 6 which is sensitive to the incident radiation. At the same time, the line-frame scanning with the luminous spot is created from the tube 14 which creates the luminous spot on its screen and which is controlled by the sweep generator 13 with the use of an optical system consisting of objective 16 and mirror 4. With this, the photoemission current from the target will be modulated by the thermal image created by the objective 2,3 on its surface. The output signal of the electron tube 6 controls the beam of the kinescope 11 on whose screen the visible image 12 of the heat-radiating object is also created.

be constructed with the use of a "thermicon" tube having a target of mosaic elements which are sensitive to infrared rays. Scanning and commutation are accomplished in the normal manner with the use of an electron beam which bypasses the target just as in transmitting television tubes of the vidicon type. Systems with electron scanning provide the opportunity to obtain high scanning rates and better resolution.

The construction of the image of a heat-radiating object can also be accomplished with the use of a luminous scanning system. In this case, an electron tube is placed after the objective with a semiconductor target and luminescent screen on which the luminous image is created. The scanning of the image is accomplished by the luminous scan which has first passed through an optical "shutter," the absorption or transmission of which is modulated by the infrared radiation from the object.

The threshold sensitivity and other parameters of the scheme of radiometric instru-

ments are calculated by methods which are common to electro-optical equipment (see below). For a simple radiometer, the monochromatic threshold irradiance which is equivalent to the noise equals [18, 25]:

$$E_{it} = \frac{\sqrt{W_{inst} f}}{D_o^2 q D_p^k} \quad (7.1)$$

The value of the signal/noise ratio for a point source is

$$m_{ps} = \frac{D_o^2 D_p J_s \tau_s k}{L^2 \sqrt{W_{inst}}} q \quad (7.2)$$

and for an extended source

$$m_{ps} = \frac{D_s D_p B_s \tau_a k \sqrt{W_{inst}}}{\sqrt{\Delta f} q} \quad (7.3)$$

where W_{inst} is the instantaneous field-of-vision angle;

- Δf - transmission banned, Hz;
- $D^* \lambda$ - detecting capabilities of the receiver;
- q - relative aperature;
- D_p - diameter of the entrance pupil;
- τ_a - transmission coefficient of the atmosphere along the route;
- I_2 and B_2 - luminous intensity and luminance respectively.

Coefficient $k = \frac{\pi \sigma_p}{4} k_1$, where the value k_1 considers the error in the dimension and form of the receiver and entrance pupil, use coefficient, noise characteristic of the receiver, and so forth. For a thermovisual system with electron scanning the threshold luminance of the object, equivalent to the noise, i. e., perceived at the limit of sensivity, is. /233

$$\Delta B_{\lambda} = \frac{m \sqrt{C}}{D_s D_p \tau_a k \sqrt{W_{inst}}} \quad (7.4)$$

where C is the capacity of the system's information channel.

For a system with mechanical scanning

$$\Delta B_{\lambda} = \frac{m \sqrt{W_{60v}}}{k D_s D_p \sqrt{nT}} q, \quad (7.5)$$

where T is the time for scanning a frame within limits of the angle of coverage; n - the number of elements in the receiver (channels of the system).

Knowing the value of the threshold luminance of the object, we can calculate the extreme minimum differences in the temperatures of the object and the background which are recorded by the instrument. Thus, for example, defining the inertia of the instrument by the condition for the buildup of the signal $[\beta = 1 - e^{-t/\tau}]$, where t is the duration of the pulse which depends on the dimensions of the object, field-of-vision angle, and scanning rate and τ - the time constant of the receiver amplifier system, we can determine the difference in the radiation densities which have been discovered.

$$\Delta R = 4m\Phi_t^e \sqrt{\Delta f_n} \frac{\beta}{D_p w_{inst}}, \quad (7.6)$$

where $\Delta R = \int_0^\infty \Delta r_\lambda s(\lambda) \tau_s(\lambda) \frac{d\lambda}{\lambda}$, i.e., expressed in effective quantities Φ_t^e - the radiation flux of the equivalent power of noise (for a receiver with an area of 1 cm² with a transmission band of 1 Hz).

From the theory of thermal radiation it is known that for gray emitters

$$\Delta R = \epsilon \xi 4\sigma T^2 \Delta T, \quad (7.7)$$

where ϵ is the coefficient of emissive power;

$$\epsilon = 5.67 \cdot 10^{-12} = \frac{W}{(\text{cm}^2 \cdot \text{K}^4)} \quad - \text{ Boltzmann's constant}$$

$$\xi = 0.82 \int_0^\infty \varphi_\lambda s(\lambda) \tau_s(\lambda) \tau_o(\lambda) \frac{d\lambda}{\lambda} \quad - \text{ the coefficient which considers the degree of use by a receiver of the different radiation of two emitters.}$$

The expressions which have been presented permit the determination of the relation for the extreme minimum difference in the temperatures of the object and the background (of two adjacent objects) detected by the thermovisual instrument /234

$$\Delta T_{min} = \frac{21.6 \cdot 10^{10} m \Phi_t^e \sqrt{\Delta f}}{T^3 D_p w_{inst} q \epsilon \beta} \quad (7.8)$$

The value $\frac{\xi \beta}{\Phi_t^e} = Q$ is the criterion of quality in the selection of a radiation receiver. For bolometers

$$Q \cong 8.1 \cdot 10^7 \text{ cm} \cdot \text{Hz}^{1/2} \cdot \text{W}^{-1/2}, \text{ and for photoresistor of the PbTe type}$$

$$Q = 2.7 \cdot 10^8 \text{ cm} \cdot \text{Hz}^{1/2} \cdot \text{W}^{-1/2}. \quad \text{The procedure for calculating the para-}$$

eters of thermovisual instruments is presented in greater detail in [25].

7.3. Instruments for the Measurement of Thermal Characteristics of the Earth's Surface and the Atmosphere

The launching of weather AES expands considerably the possibilities of the weather services in the preparation of short-range and long-range weather forecasts on a global scale.

Among the large quantity of information which is received from an AES and used for the preparation of forecasts, an important place is occupied by information about the thermal condition of the earth's surface and the atmosphere which is provided by on-board electro-optical equipment. For instance, on a number of weather satellites of the United States, an entire complex of electro-optical equipment has been used which includes a five-channel radiometer with a small field of view, a two-channel radiometer with a wide field of view, a set of television equipment, and an infrared horizon sensor [34].

The five-channel narrow-field radiometer is an electro-optical instrument consisting of five independent radiometers with optical modulation of the perceived signal and intended for the measurement of radiation of the earth and the upper layers of the atmosphere in five spectral bands. Each of the channels has two fields of view ($5.174 \cdot 10^{-2} \text{ rad}$ (5°)), in which regard in the oriented direction of the axes of the AES one of the fields of view of the instrument is directed toward the earth and the other, toward space. The radiation which arrives from the earth is continuously compared with the radiation from space which is equated to absolute zero. This permits measuring the absolute values of the amounts of the earth's radiation regardless of the temperature of the satellite. A diagram of one of the channels of a five-channel radiometer is presented in Fig. 7.4 [34]. The earth's radiation 2 arrives at the radiometer on one of the faces of the prism 1 while radiation from space 3 arrives on another face of this same prism. After reflection from the prism, the radiation from earth and space fall on a rotating modulating disk 4. The radiation which comes from the earth is reflected from the mirror half of the disk and falls on the upper half of the lens while the radiation which comes from outer space is reflected by the black half of the disk and falls on the lower half of the lens. Thus, when the disk rotates, reflected radiation from each direction arrives alternately at the receiver. The entire modulating disk, including its darkened portion, is always in the field of view of the receiver. Consequently, the intrinsic radiation of the disk is not modulated and therefore information about it does not pass through the alternating current amplifier. The modulated signal is proportional to the difference in the radiation fluxes which arrive from the earth and from outer space. The variable voltage which arises in a thermistor bolometer is proportional to the differences in the radiation

/235

fluxes which are absorbed by the small receiver area with two different positions of the disk modulator: the position depicted in Fig. 4.7 and diametrically opposite.

All five channels of the radiometer are almost identical. The only difference is that they operate in different spectral bands and each one provides strictly determined information. The discrimination of different spectral regions is attained by the combination of the transmission factors of the materials of the lenses and optical filters.

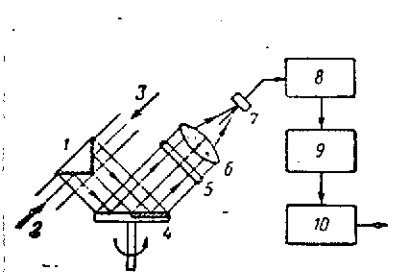


Fig. 7.4. Block diagram of one of the channels of a five-channel radiometer: 1. reflecting prism; 2. signal which arises from the earth; 3. signal which arises from space; 4. modulating disk; 5. optical filter; 6. objective; 7. radiation receiver; 8. preamplifier; 9. tape recorder; 10. transmitter.

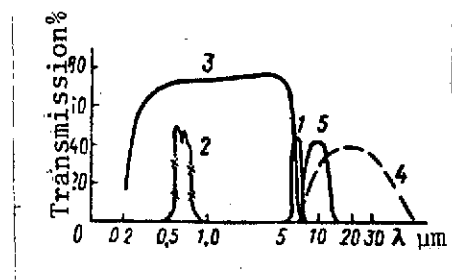


Fig. 7.5. Curves of the transparency of optical elements of the five channels of a radiometer.

Channel 1 is tuned [33] to a band of 5.7-6.9 μm (Fig. 7.5) and is intended for measuring the radiation in the band of absorption by water vapor. Channel 2 passes

the radiation in the "window of transparency" of the atmosphere (8-12 μm) and is intended for measurement of the radiation of the earth and the upper layer of the atmosphere, and channel 3 (0.2-5.0 μm) for the measurement of solar radiation reflected from the earth. Channels 4 ($\Delta\lambda = 0.6-0.8 \mu\text{m}$) - 5 ($\Delta\lambda = 7.5-30 \mu\text{m}$) measure respectively the solar radiation reflected from the earth and the total radiation of the earth and the atmosphere.

With the movement of the AES in its orbit, the optical systems of almost all channels of the radiometer scan the same region on the earth's surface with a size of about 50 x 50 km. /236

The two-channel radiometer is an instrument consisting of two radiometers and intended for determining the balance between the solar radiation reflected from the earth's surface and the earth's intrinsic radiation. Figure 7.6 presents a diagram of a radiometer and the spectral characteristics of the channels. The main parts of the instrument are two thermistor receivers

1 and 2, one painted black and the other white and situated in the apexes of two cones. The optical axes of the cones are directed toward the earth parallel to the satellite's axis of rotation. Serving as the optical condenser is an aluminized cone made from a plastic film with an aperture angle of $50 \cdot 1.74 \cdot 10^{-2}$ rad (50°) which also determines the field of view of the radiometer. The black and white coatings of the receivers perform the role of sensitive elements which overlap the spectral band of $0.2-50 \mu\text{m}$. One of them (with black coating) absorbs the shortwave solar radiation and the earth's intrinsic radiation but absorbs the earth's longwave radiation just as the first one. When the radiometers face the night side of the earth, their readings are identical since practically all the earth's intrinsic radiation lies in the long-wave region of the spectrum (more than $3 \mu\text{m}$). If the radiometers face the illuminated side of the earth, the white receiver, as formerly, absorbs only the earth's radiation while the black one still reacts to the reflected solar radiation. The earth's albedo and then the temperature of the underlying surface of the "earth-atmosphere" system are determined from the difference in the readings of the white and black receivers.

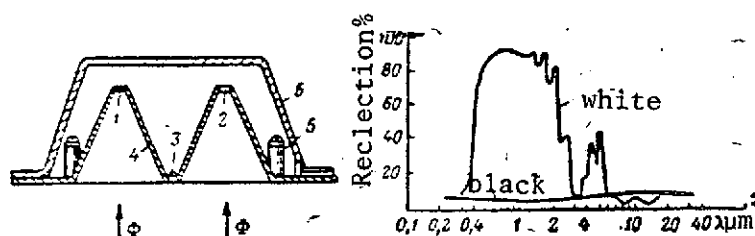


Fig. 7.6. Diagram of a two-channel wide-angle radiometer and its spectral characteristics: 1, 2. thermistor receivers with black and white coatings respectively; 3. point thermistor; 4. cone; 5. compensation for ohmic components; 6. housing.

The sensor of the earth's infrared horizon serves for the determination of the orientation of the satellite's axis of rotation relative to the local vertical. The operating principle and design of the sensor are examined in Chapter 6. Here, we will only note that inasmuch as the instrument scans the earth with a small field of view ($2.26 \cdot 10^{-2}$ rad) the information obtained is also used to determine the thermal condition of the sections being scanned.

It is known [34] that when the earth's infrared horizon enters the instrument's field of view, the horizon sensor forms a positive signal and, on leaving - a negative signal. These signals also serve for determining the orientation of the AES. The information read from the sensor between the indicated pulses, when the field of view of the instrument passes over the earth, is used to determine the thermal condition of the sections of the surface being scanned.

Similar electro-optical equipment is also used on Soviet weather AES of the "Meteor" system: actinometric, television, and others.

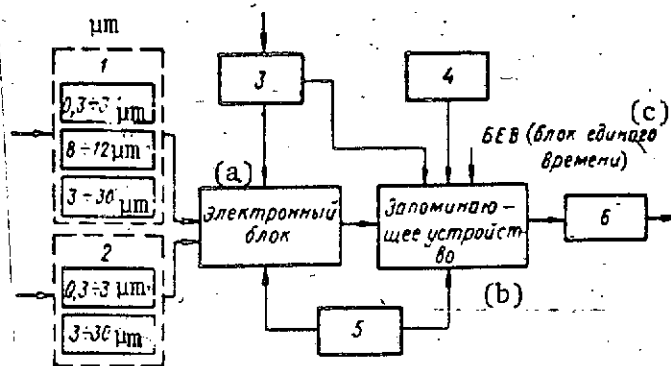


Fig. 7.7. Block diagram of actinometric equipment: 1. narrow-field scanning instrument; 2. wide-field instrument; 3. on-board programmer; 4. unit of temperature sensors; 5. power-supply unit; 6. transmitter.

Key: a. electronic unit;
b. storage;
c. BEV (common time unit).

equipment. Coverage of the earth's surface from on board the SC is accomplished with the use of a narrow-field scanning radiometer which operates in the spectral bands of 0.3-3 μm , and 3-30 μm , with the movement of the scanning element in a direction perpendicular to the movement of the SC.

With its fields of view, the wide-field instrument encompasses the entire earth and provides information about the radiation of the "earth-atmosphere" system in spectral bands of 0.3-2 μm and 3-30 μm .

All the information of the actinometric equipment is tied to on-board common time by feeding special signals to the storage (S) from the common time unit.

The electronic unit of the equipment is intended for the conversion and processing of information arriving at it and the output of formed signals to the storage which, during the period of the passage of the SC above the territory of the USSR, gives the information to the telemetry channel for transmission to earth.

The unit of temperature sensors is intended for the formation of electrical signals in the temperature mode of the narrow-field and wide-field instruments and their output to the S.

Actinometric equipment is a set of electro-optical instruments which absorb radiation with a body which is close in its properties to an ideal black body and which convert it to thermal energy. Actinometric equipment is intended for measuring the values of the intrinsic radiation of the earth's surface and the upper layer of the clouds in the spectral band of 8-12 μm and the intensity of the total radiation of the earth and the upper layers of the clouds in the band of 3-30 μm .

A typical block diagram of actinometric equipment is presented in Fig. 7.7. The equipment consists of a narrow-field scanning and wide-field radiometers, electronic unit, and auxiliary

Besides this equipment, on board the AES there is a set of electro-optical instruments intended for observation of the cloudiness on the shady side of the earth [33,34]. In its operating principle, this equipment differs in no way from the previously considered (see Fig. 7.2) infrared scanning equipment. However, the specific tasks which they accomplish on board the AES presume some differences in its design formulation and supplementary units. A typical block diagram of on-board infrared equipment for obtaining an infrared image of cloudiness on the shady side of the earth is presented in Fig. 7.8.

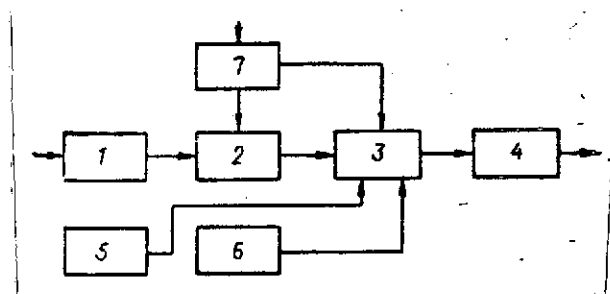


Fig. 7.8. Block diagram of infrared equipment: 1. electro-optical scanning equipment; 2. amplifier-converter unit; 3. storage; 4. transmitter; 5. unit of temperature sensors; 6. on-board common time unit; 7. on-board programmer.

is transmitted from the S to ground equipment where it is converted to a visible image.

The receiver of the equipment accomplishes scanning perpendicular to the direction of flight of the AES. With this, a scanning strip 1100 km wide is scanned.

The thermal radiation of the underlying surface of the "earth-atmosphere" system is converted to electrical signals by the receiver which are proportional to the value of the radiation flux. These signals are then processed in the amplifier-converter unit and fed to the S. At a specific moment in time, the collected information is transmitted from the S to ground equipment where it is converted to a visible image. /239

The photos of the cloud formations obtained with the use of infrared equipment are less detailed than television photos but are sufficiently detailed for the analysis of large atmospheric formations (cyclones, typhoons, and so forth).

7.4. Instruments for Controlling the Approach of Space Ships

Electro-optical systems for controlling the approach can be divided into two basic groups:

- Instruments for the control of the approach of cooperating space ships or instruments of the docking systems;
- Instruments for controlling the approach of noncooperating SC.

In order to execute the approach of SC, it is necessary to bring them out into a zone where the on-board means will prove to be capable of executing mutual search and detection with the subsequent formation of the necessary control commands.

For the solution of tasks for the approach, the instruments of the docking system should assure:

- The search and detection of the target SC;
- The guidance of the maneuvering SC to the target SC;
- The determination of the parameters of the relative movement of the approaching SC (range, angular coordinates, and their derivatives).

Depending on the methods for search and detection, the following electro-optical systems for controlling the approach of the SC are distinguished:

- Passive systems, where the target SC is detected from its intrinsic or reflected solar radiation;
- Active with a passive response when the complex of instruments on the maneuvering SC includes an active emitter whose radiation, after reflection from the target SC, again falls on the maneuvering SC and is used to generate the necessary information. With this, special corner reflectors may be installed on the target SC which increase the effective area of reflection and permit a considerable increase in the operating range of the system;
- Active with active response when on board the target SC, along with a system for tracking the maneuvering SC, an emitter is used which directs the radiation toward it.

In both types of active systems, both monochromatic emitters for example lasers, as well as sources which radiate in a broad band of the spectrum may be used. /240

In one of the variants of the system for controlling the approach of the SC during docking [66] it was assumed that the electro-optical locator of the "Martin" Corporation would be used (Fig. 7.9). This locator permits obtaining information about the range, relative velocity, angular coordinates, and rate of their change with distances between ships of from 50 km to 7 meters. Used as an emitter in the transmitter of the locator is a Xenon flash lamp installed in the focal plane of a parabolic mirror with a diameter of 18 cm which forms a directional radiation beam. In this case, a unit of corner reflectors is installed on board the target SC. The pulsed light signal of the transmitter which is reflected by this unit is received on the maneuvering SC by the mirror optical system of the receiver. The focused luminous flux is divided into three parts. Each part is directed to its own radiation receiver for which photomultipliers are used here.

If the components of the luminous flux which fall on the photocathodes of the PM are not equal, an error signal arises which is used to match the axes of the receiver and transmitter

of the locator with the direction to the unit of corner reflectors of the target SC. With the precise matching of the locator's line of sight with the direction to the target SC, no error signal arises.

A range of from 50 km to 30 meters is determined by this locator by a method on the basis of measurement of the time of propagation of the radiation to the target SC and return. A distance of less than 30 meters is determined from the amplitude of the reflected signal since it is difficult to accomplish the precise measurement of time segments of less than 0.2 μ s. The relative velocity is determined with the differentiation of data on range.

The locator is installed on rotatable supports which provide the opportunity to move the transmitter and receiver over two coordinates within limits of $\pm 15 \cdot 1.74 \cdot 10^{-2}$ rad ($\pm 15^\circ$), assuring the scanning of space in a zone of $\pm 15 \cdot 1.74 \cdot 10^{-2}$ rad ($\pm 15^\circ$) for elevation angle and azimuth. Scanning is accomplished by the line-frame scanning method. In this, the shifting of the instantaneous field of view through the angle of elevation to scan the next line is accomplished discretely, at the end of each scanning cycle for azimuth. The lock-on on the target occurs when it falls in the field of view of the receiver.

A shortcoming of this type of electro-optical locator is the comparatively short operating range due to the low density of the radiation flux in the beam of the transmitter and the influence of the background, the radiation flux from which may reach significant values and greatly reduce the correlation between the signal and the noise.

To a considerable degree, these shortcomings can be eliminated with the use of a laser as the emitter.

Electro-optical instruments for controlling the approach of noncoordinating SC are also constructed with the use of lasers. This group of optoelectronic instruments is considered below.

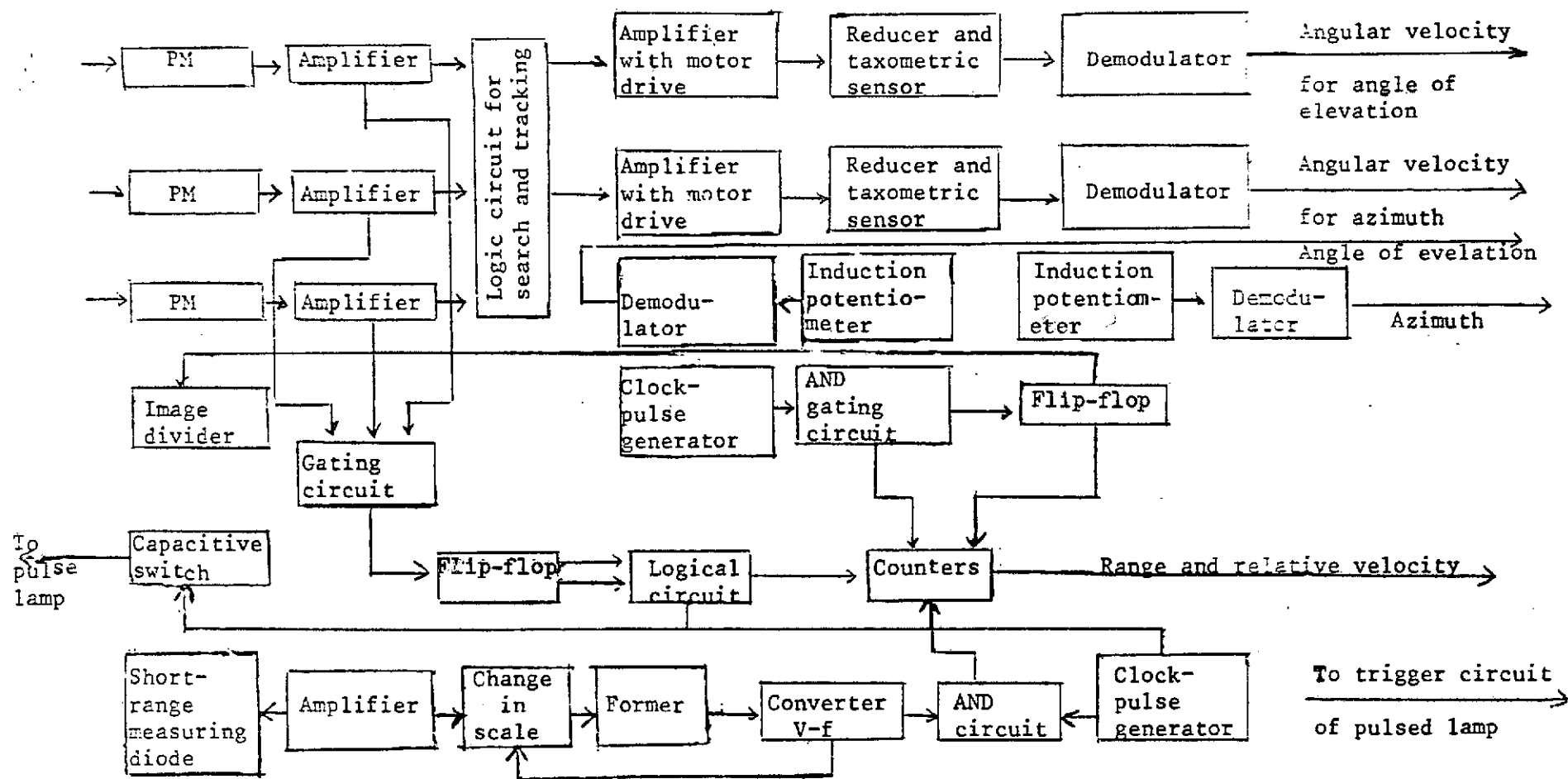


Fig. 7.9. Functional diagram of an electro-optical locator for docking a space vehicle.

8.1. Block Diagram of an Electro-Optical Locator with a Laser

The basis of optical location, just as the basis of radar, is formed by three principles. The first principle is the reflection of electromagnetic waves. The target and surrounding background reflect the electromagnetic waves which have fallen on them differently, as a result of which a contrast arises between them which permits discriminating the target signal. The smaller the wavelength, the greater the reflectivity; therefore, in desiring to obtain a large reflected signal, we should use short-wave generators. Since the optical band of waves is four orders of magnitude shorter than centimeter radio waves, there is the possibility of constructing locators with a greater operating range and better resolution.

Forming the basis of the principle of location is the use of the straight-line propagation of electromagnetic waves. If we direct a narrow beam of waves toward a target, the wave reflected by the target and received by the locator permits determining the direction to the target. The precision of determination of the direction to the target depends on the width of the beam. The narrower it is, the more precisely is the direction to the target determined. To narrow a beam in radar location, an antenna is used whose directivity factor is determined by the expression

$$G = \frac{4\pi A}{\lambda^2}, \quad (8.1)$$

where G is the front-to-rear ratio; A is the area of the antenna.

In order to increase the directivity of the antenna with a given wavelength λ , it is necessary to increase its diameter. Thus, for example, to obtain the angular opening of a beam on the order of one degree with the use of radio waves of the centimeter band, it is necessary to have an antenna diameter of about 10 m. On the strength of Eq. (8.1), we can increase the directivity of the radiation of the locator considerably, using shorter wavelengths. Calculations show that if the area of the antenna (input lens of the objective) $A = 10 \text{ cm}^2$, then using a generator with $\lambda = 1 \text{ }\mu\text{m}$, one can obtain the directivity of the locator 10^4 times higher than with the use of a generator with $\lambda = 1000 \text{ }\mu\text{m}$. Consequently, the use of waves of the optical band in location opens the possibility of constructing high-precision locators and, what is especially important for on-board equipment, with small overall dimensions of the transponders.

The basis of the third principle of location is formed by the use of the constancy of the rate of propagation of electromagnetic waves which permits constructing various range measurers. For example, if the radar operates on pulses, then to determine the range the following relationship is used

$$L = \frac{c\Delta t}{2}, \quad (8.2)$$

where c is the rate of propagation of electromagnetic waves; Δt is the time interval between the sending of the pulse and the reception of reflected signal.

From (8.2), it follows that for the construction of a locator with good range resolution, the pulses of the radiating waves should be as short as possible, since (with the necessary width of transmission band of the receiver) the precision in determining range depends on the duration of the pulse. It is known that with radiation in the optical band, the time for the passage of the excited particles from the upper to the lower energy level is about 10^{-9} sec; therefore, the use of a laser as a radiation source opens the potential opportunity to construct locators with high-range resolution /244

The following block diagram (Fig. 8.1) forms the basis of the electro-optical locator. The locator consists of transmitting, receiving, and display units and a power-supply unit. The transmitting unit is intended for the conversion of electrical energy to a monochromatic, narrow-band radiation flux and the accomplishment of the scanning of a given sector of space with this flux to irradiate targets. The transmitting unit consists of the laser, internal and external modulators, transmitting optical system, and scanner. The laser receives energy from the excitation source and generates electromagnetic oscillations of the optical band in a pulsed manner or continuously. The Q-modulator assures the generation of oscillations in such a way as to obtain a duration of pulse on the order of 10^{-9} sec in the case where the locator operates in the pulsed mode. The second modulator is intended for the amplitude modulation of the radiation on the output of the laser. The transmitting optical system forms the angular distribution of the radiation into the required distribution, assuring the necessary directional diagram.

The receiving unit is intended for the reception of the radiation reflected by the target and the background, the separation of the useful signal and noise, the conversion of the optical radiation to an electrical signal, and the discrimination,

from this signal of information on range, velocity, and angular coordinates of the target. This unit consists of an optical receiving system, optical interference filter, radiation receiver, and units for the measurement of range, velocity, and angular coordinates.

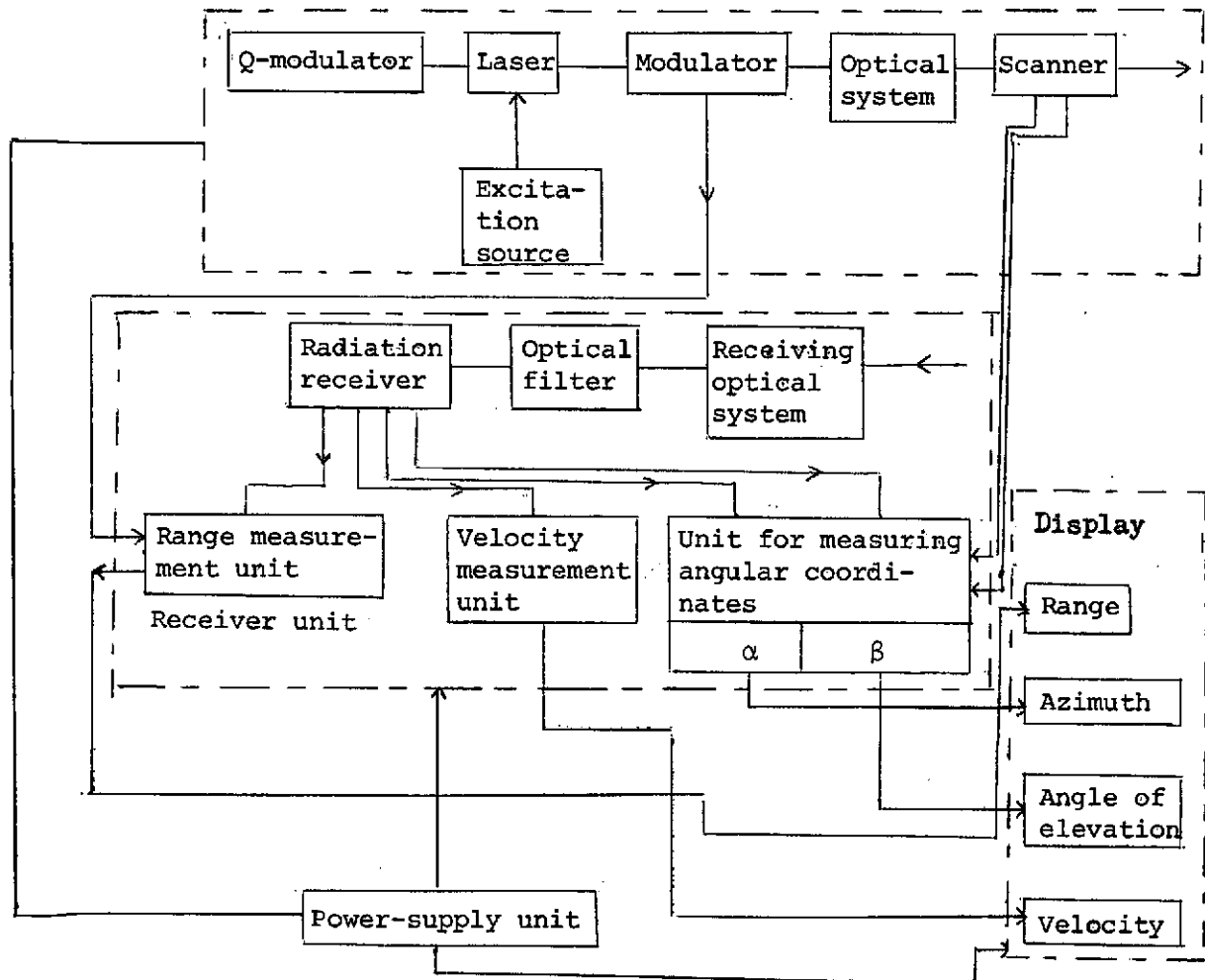


Fig. 8.1. Block diagram of an optoelectronic locator.

The display is intended for observing the results of the measurements if they are used by the operator to control the

SC or else this information goes to a computer and then to the control system.

The power-supply unit assures the conversion of direct current from the storage and solar batteries to direct and alternating current of the required voltage.

Depending on which parameters of the target are measured by the on-board locator, the following are distinguished: range-finders (which determine only the distance between the SC's), Doppler locators (which measure the relative velocity of the SC's), and the locators themselves (which measure the angular coordinates and the distance between the SC's). The basic characteristics of the optical locator are the zone of action, time of scan, precision in determining the coordinates, resolution, noise immunity, and dependability. By zone of action, we mean the region of space within whose limits the operation of the on-board locator is accomplished. Its limits are determined by the maximum and minimum ranges of operation of the locator and the limits of the scanning angle. The extension of the zone and its angular dimensions are determined by the purpose of the on-board locator. Thus, for example, a rangefinder which determines the distance between the SC and the moon should have a considerable operating range and angular coordinates of the zone of action which approach zero. At the same time, the on-board locator for vehicle docking in orbit should have an operating range on the order of hundreds of kilometers, but the angular dimensions of the zone of action should be such as to assure the discovery of the second SC. /245

The scanning time is considered to be the time during which the optical beam accomplishes a one-time scan of a given region of space.

The selection of the scanning time is determined by the mobility of the target. The higher the velocity and maneuverability of the target, the smaller should the assigned scanning time be. Frequently, the scanning time is determined by the probability characteristic of not missing the target.

The coordinates being determined depend on the requirements made of the on-board locator. If it is necessary to determine the distance to the moon, it is sufficient to know but one coordinate. For docking in orbit, the locator should assure the measurement of four coordinates: two angular, range, and velocity.

The precision of determining coordinates is characterized by the values of systematic and random errors which arise in measurement. Systematic errors can be determined by calculations or experimentally and, consequently, can be considered. Random

errors are caused by reasons which do not submit to calculations; therefore, each individual measurement has a random character. The average results of a large number of measurements remain practically constant and they can be estimated.

The required precision in the measurement of coordinates is caused by the purpose of the optical locator and should be especially high with on-board locators which assure the automatic docking of vehicles in orbit.

By resolution, we mean the possibility for the distinct determination of coordinates of closely situated targets. Corresponding to each coordinate is its own resolution. Range resolution is characterized numerically by the minimum distance between two targets arranged in a radial direction in which it is possible to determine the ranges to them distinctly. The resolution for angular coordinates is characterized by the minimum difference in the angles at which the distinct determination of the positions of these targets in space is possible. The resolution for velocity is characterized by the minimum difference of the radial velocities of two targets with the identical angular coordinates in which the distinct observation and position fixing of these targets is possible.

/246

It is customary to characterize the noise immunity of an on-board locator by the degree of its efficiency with the presence of natural (sun, moon, stars) and artificial noise. Solar illumination is most dangerous to the operation of optical locators; however, high monochromatic quality of the radiation sources of the laser permits, using interference filters, cutting off the wide-band solar radiation and increasing considerably the signal/noise ratio. The dependability of the on-board locator is its property of preserving its characteristics within established limits under conditions of operation in space.

The characteristics of an on-board locator are the wavelength of the emitted electromagnetic energy, the amount of energy, radiation power, scanning method, methods for determining coordinates, directivity of the locator, threshold and spectral sensitivity of the receiver, overall dimensions and mass of the locator, power consumption, and type of recorder. The parameters and values of these characteristics are so selected as to satisfy completely the general requirements made of an on-board optical locator. In the process of operation, an on-board locator accomplishes the search for the target in a given sector and, having detected it, it continuously tracks it, in the process of which the measurement of angular coordinates and the distance to the target is accomplished. The task of determining the distance between the locator and the target is reduced to

the measurement of the change in the corresponding parameter, for example, the time interval between the transmitted (sounding) and reflected pulses or the differences in the phases or frequencies of these signals.

In accordance with this, lasers are divided into three groups:

- With the pulsed method of measuring range;
- With the phase method of measuring range;
- With the use of the Doppler effect.

8.2. Electro-Optical Locators Which Measure Range by the Pulsed Method

The block diagram of the rangefinder part of an optical locator in which the pulsed method of measuring range is used is presented in Fig. 8.2. The radiation from the source of excitation which is arranged around the active material converts the material to an excited state. However, generation does not occur because the Q-modulator which is located between the active material and the reflecting prism is in a blocked state (its transparency equals zero). The Q of an open resonator¹ also equals zero and there are no conditions for the generation of stimulated radiation. Conditions are created for generation only at the moment that the Q-modulator is turned on, and this is done by a jump in a short time interval. All the energy accumulated in the active material is de-excited in a very short time interval, which comprises only 10^{-8} - 10^{-9} sec. The radiation of the generator is focused with the aid of the transmitting optical system and directed toward the target. A portion of the radiation is diverted to the PM intended for the formation of the

/247

¹ The Q of an open resonator, i.e., the degree of its tuning, which depends on the parallelism of the mirrors and the transparency of the medium between the mirrors is determined by the relationship

$$Q = \frac{2\pi n}{\lambda} \left(\frac{2dL}{\beta} \right)^{1/2},$$

where n is the index of refraction; d is the diameter of the mirrors; L is the distance between the mirrors; β is the angle of nonparallelism of the mirrors.

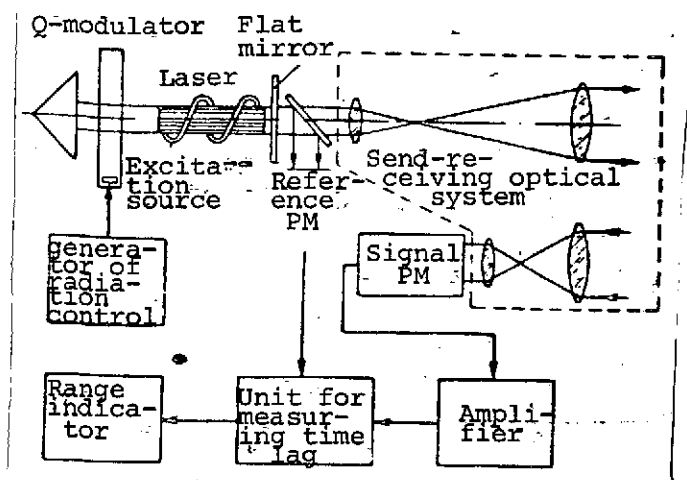


Fig. 8.2. Block diagram of the rangefinder portion of a locator with the use of the pulsed method of measuring range.

reference signal. The signal goes to the unit for measuring the time lag and puts the generator of pedestal pulses into operation. The radiation reflected by the target is perceived by the receiving optical system and directed to the signal PM, which converts the optical radiation to an electrical signal which passes through an amplifier to the unit for measurement of the time lag. This signal stops the operation of the pedestal pulse generator.

The measured time interval is compared with the number of reference oscillations of the generator of the main range-marker frequency. In this case, the range is determined as the time difference between the transmission and reception of signals, and its value can be digitally displayed on the range indicator. With the use of a cathode-ray tube as a recording device, a sawtooth voltage is fed to it which creates a linear or circular scan to determine the time interval between the reference signal and the signal reflected by the target. From relationship (8.2), it follows that an error in measuring distance will be determined by the equation

$$\Delta L = \frac{L}{c} \Delta c + \frac{c \Delta t}{2}. \quad (8.3)$$

An analysis of the last expression shows that an error in measuring distance depends on the error Δc in determining the rate of propagation of optical emissions in the environment in which the locator is operating and the instrumental error of the locator which depends on the stability of the frequency of the reference oscillations and the time resolution of the locator, i.e., the degree of its technical perfection is determined. If we assume that the instrumental error equals zero, then

$$\Delta L = \frac{L}{c} \Delta c, \quad \frac{\Delta L}{L} = \frac{\Delta c}{c}. \quad (8.4)$$

Numerous measurements of the rate of propagation provided the results which are presented in Table 8.1.

TABLE 8.1.

Author of measurements	Year	Velocity of light km/sec	Probable error km/sec
Rosa-Dorsey	1906	299710	10
Michelson	1926	299796	15
Anderson	1940	299776	6
Bergstrand	1949	299793	2
Kartashev	1952	299788	5
Velichko	1958	299792.7	0.3
Rank	1964	299792.8	0.4
Karolyus	1967	299792.5	0.15

At the present time, taken as the most probable value of the velocity of light in a vacuum is $c = 299792.5 \pm 0.4$ km/sec.

For precise operation of the rangefinder portion of the locator, it is necessary to synchronize the start of the operation of the sweep generator with the pedestal pulse. The precision of operation of the optical locator will depend on the precision of synchronization, the amount of delay of the signal in the rangefinder circuit, on the scale, and on the readout method. Rangefinder error due to imprecision of synchronization occurs in the case where ranges are judged from the distance between the signal of the pulse reflected by the target and the start of scanning. The amount of this error equals

$$\Delta L_c = \frac{c \Delta t_c}{2}, \quad (8.5)$$

where Δt_c is the synchronization error which equals the time interval between the start of the sounding pulse and the start of the scanning.

To exclude this error, the sweep generator is often started, not by a laser emission, but somewhat earlier. Then, two clear pulses may be obtained on the screen of the tube, one pedestal, caused by the start of generation of the laser, and the other by the signal reflected by the target. To start the sweep generator in this case, a pulse triggered by the laser is used. The rangefinder error caused by the delay in the rangefinder circuit equals /249

$$\Delta L_d = \frac{c \Delta t_d}{2}, \quad (8.6)$$

where Δt_d is the delay error of the signal in the rangefinder circuit.

To estimate the influence of this error, it is important to know not only its value, but also its constancy in the process of operation of the rangefinder. Rangefinder errors caused by scale imprecision can be found in the following manner. The distance by which the spot on the screen of the tube will be displaced is determined by two parameters: scale (M) and range to the target. The scanning scale, in turn, is determined by the relationship

$$M = \frac{2V_s}{e}, \quad (8.7)$$

where V_s is the scanning rate. But $e = MD$, where e is the segment on which the spot will be displaced on a screen with diameter D. Then

$$\Delta L_M = -L \frac{\Delta M}{M}, \quad (8.8)$$

where ΔM is the scale error.

The precision and constancy of the scanning rate are determined by the parameters of the sweep generator. In connection with the fact that it is rather difficult to assure the high stability of these parameters, it is necessary to have the possibility in the instrument to adjust the scale and accomplish its check with the aid of a special calibrator. Readout errors are determined by the method of reading the distance, scale value, and steepness of the leading edge of the sounding and reflected pulses. The steepness of the leading edge of the pulse reflected by the target is determined by the steepness of the sounding pulse and by the degree of the distortions which arise /250

in the reflection of the pulse from the target, with the passage of the radiation flux in the environment, and in the end-receiving optical system and amplifier channels. The distortions of the leading front of the sounding and reflected pulses in the medium are neglected as a result of their insignificance. Distortions introduced by the process of reflection of the flux from the target should be considered in the case where the linear dimensions of the object in the direction of irradiation are commensurate with the wavelength.

8.3. Electro-optical Locators Which Measure Range by the Phase Method

The operating principle of a phase optical rangefinder, whose simplified block diagram is presented in Fig. 8.3, is reduced to the following. The radiation of the laser is modulated by the generator of the range-marker frequency, in which regard the voltage on the modulator and, consequently, the output emission is modulated in accordance with the law

$$U_1 = U_m \sin(\omega_M t + \varphi_m), \quad (8.9)$$

where ω_M is the range-marker frequency; ϕ_{01} is the initial phase.

Reflected from the target, the radiation falls on the send-receiving device of the optical rangefinder which converts it to an electrical signal

$$U_2 = U_m \sin[\omega_M(t - t_L) + \varphi_m - \varphi_r - \varphi_{ref}] \quad (8.10)$$

where ϕ_{ref} is the angle of phase shift of the range-marker oscillation which arises with reflection from the object; ϕ_r is the phase delay of the range-marker oscillation in the circuits of the optical rangefinder.

Voltages U_1 and U_2 go to the input of the phasemeter which, /251
in accordance with the phase difference, puts out a signal which is proportional to the distance to the target

$$L = \frac{c}{2\omega_M} (\varphi_m - \varphi_r - \varphi_{ref}), \quad (8.11)$$

where

$$\varphi_d = \omega_M L + \varphi_r + \varphi_{ref}$$

The operating precision of the rangefinder is determined by

- 1) The precision of the range-marker frequency

$$\Delta L = - \frac{c}{2\omega_M^2} (\varphi_d - \varphi_r - \varphi_{ref}) \Delta\omega_M \quad (8.12)$$

where ω_M is the error in the range-marker frequency.

Then,

$$\frac{\Delta L}{L} = - \frac{\Delta\omega_M}{\omega_M} \quad (8.13)$$

i.e., the relative rangefinder error equals the relative range-marker frequency error;

- 2) The precision of measurement of the phase difference.
- We can write that

$$\Delta L = \frac{c}{2\omega_M} (\Delta\varphi_d - \Delta\varphi_r - \Delta\varphi_{ref}) \quad (8.14)$$

where $\Delta\varphi_d$ is the error in measuring the phase difference; $\Delta\varphi_r$ is the phase delay error in the rangefinder circuits; $\Delta\varphi_{ref}$ is the phase shift error in reflection.

The component $\Delta\varphi_d$ is determined by the technical parameters of the phasemeter. Component $\Delta\varphi_r$ depends on the stability of the phase characteristic of the rangefinder, and component $\Delta\varphi_{ref}$ on how precisely the reflecting properties of the target are considered. In the measurement of the distance to a moving target, one more error is introduced whose source is the Doppler frequency. Investigations show that the second and third components in the expression are values of the second order of smallness in comparison with the first; therefore, in preliminary calculations, they can be ignored. From the expression being analyzed, one more conclusion can be drawn to the effect that the rangefinder error is decreased with an increase in the range-marker frequency. It can be noted that the change to longer wavelengths provides a gain in raising the precision of

the measurements. But this also has its negative aspect. As a matter of fact, the unambiguity in the measurement of the phase difference is possible only within the limits of an angle of 2π rad; otherwise, an ambiguous range reading arises. In order to avoid an ambiguous reading, it is necessary to satisfy the condition

$$\left| \varphi_{p \max} - \varphi_{d \min} = \frac{2\omega_M}{c} (L_{\max} - L_{\min}) \leq 2\pi \right| \quad (8.15)$$

With $L_{\min} = 0$, this condition takes the form

$$\frac{2\omega_M}{c} L_{\max} \leq 2\pi \quad (8.16)$$

This expression provides the opportunity to determine the maximum value of the range-marker frequency.

$$\omega_M = \frac{c\pi}{L_{\max}} \quad (8.17)$$

Thus, to increase the precision of the measurements, it is necessary to increase the range-marker frequency, and to satisfy the condition of unambiguity of measurement, it must be reduced. The way out of this situation is usually as follows: two, and sometimes three, range-marker frequencies are used. The first serves for coarse determination of the range, the second for a more precise determination, and the third for an even more precise measurement of range. In order to assure unambiguity in the determination of range, the period of the following range-marker frequency should be deliberately larger than the possible errors which arise in the determination of the time lag from the coarse scale.

A diagram of a phase rangefinder is presented in Fig. 8.4.

The source of radiation is a semiconductor laser. Its radiation is modulated by a master oscillator. The radiation reflected from the target is received by the optical system and focused on a photomultiplier.

A feature of this device is the fact that the processes of phase detection and the heterodyning of the signals occur directly in the near-cathode space of the photomultiplier. A portion of the voltage from the master oscillator is fed to a

mixer. Fed to the mixer simultaneously is a voltage which is destabilized by a quartz-crystal oscillator. A voltage at an intermediate frequency of 100 kHz is formed at the output of the mixer which is fed through a phase shifter and phase commutator to special electrodes of the photomultiplier. A voltage from the heterodyne is fed to the other electrode. As a result, the photocurrent which is induced in the photomultiplier by the radiation received from the target modulated with the frequency of the master oscillator will again be modulated a second time by the high-frequency electrical field at the photocathode which is created by the heterodyne.

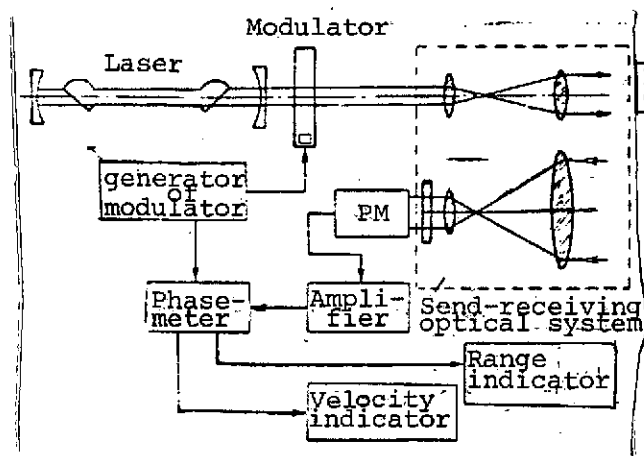


Fig. 8.3. Block diagram of an on-board locator for linkup.

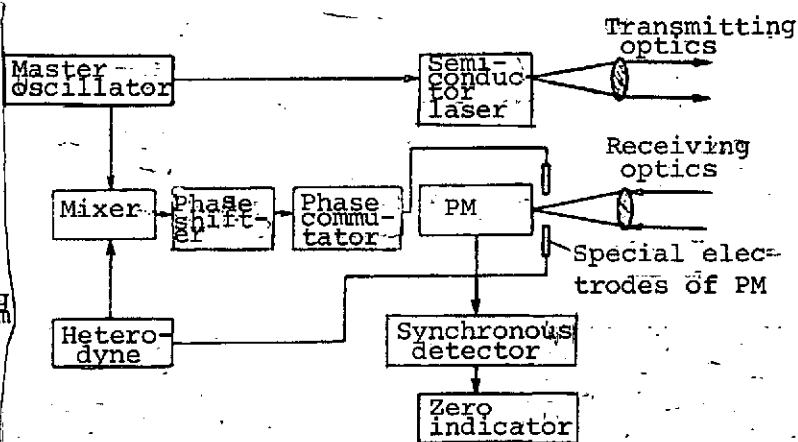


Fig. 8.4. Block diagram of the range-finder portion of a locator with the use of the phase method for measuring range.

An alternating component of the photocurrent appears with the difference frequency of the master oscillator and heterodyne, i.e., with a frequency of 100 kHz. The phase of this alternating component will depend on the distance being measured since heterodyning does not change the phase of the oscillations which participate in the bias. The alternating component of the photocurrent obtained in this way interacts with the electrical field which is created by the voltage fed to the corresponding electrode from the mixer through the phase shifter and phase commutator. /253

With this, phase detection occurs, i.e., the photocurrent will depend on the difference in phases between the reference and reflected signals. The phase shifter permits changing the

phase of the reference signal smoothly, which provides the possibility of measuring distance with high precision.

For a more precise determination of the mismatch of the phases, the phase of the reference signal is modulated by the phase modulator (phase commutator) which changes the phase of the reference voltage by 2π rad with a frequency of 1 kHz. With this, a component of the current appears in the photomultiplier with a frequency of 1 kHz with amplitude which depends on the difference in phases between the reference and reflected signals. Its value has sharply expressed maximums with a difference in the phases between the reference and reflected signals of π and 3π rad, which increases the precision of comparison of the phases. For a further increase in precision and greater noise immunity of the system, the signal from the load of the photomultiplier is fed to a synchronous detector and is then recorded by the null indicator. In this, three modulation frequencies of 30, 29.9, and 27 MHz are used for the solution of unambiguity. This permits obtaining a resolution of 1500, 50, and 5 m.

8.4. Electro-optical Locators with the Use of the Doppler Effect /254

Locators of this type are intended for the measurement of the relative velocity of SC's.

In accordance with the Doppler effect, if the target approaches the locator the frequency increases and vice versa.

The change in frequency is determined by the relationship

$$\Delta\nu = \frac{2V\nu}{c}, \quad (8.18)$$

where V is the relative tangential velocity of the target's movement; c is the velocity of light; ν is the frequency of electromagnetic oscillations.

This relation shows that a change in the frequency with the movement of the object is determined by the velocity of movement of the objects and is directly proportional to it. But this effect also depends on the frequency of the electromagnetic oscillations of the radiation used. The greater the frequency, the clearer the effect is manifested. Radio waves of the centimeter band have frequencies on the order of 10^{15} Hz. Therefore, with the use of optical Doppler locators, we can measure extremely low velocities of movement.

A diagram of a Doppler locator is presented in Fig. 8.5. The radiation of a gas laser is directed to a semitransparent

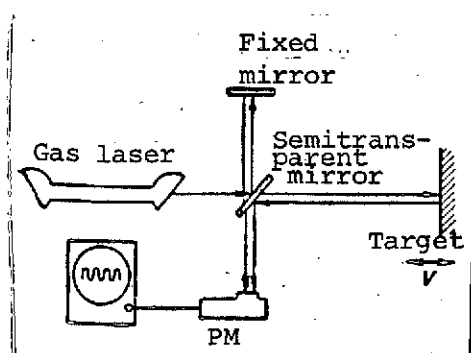


Fig. 8.5. Diagram of a Doppler rangefinder with semiconductor laser.

mirror which splits the beam in two. One is directed toward the target, and the second at a fixed mirror installed on the locator. Reflected from it, the beam falls on the radiation receiver -- the PM. This beam provides the pedestal frequency. With the movement of the target, a change occurs in the frequency of the first beam which, being reflected from the semitransparent mirror, also lands on the radiation receiver. Thus, two beams having different frequencies are combined on the receiver. This leads to the arising of two beat frequencies as a result of the addition. The frequency of the beats is proportional to the velocity of movement of the target.

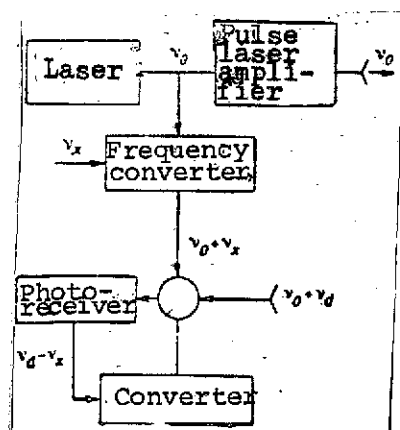


Fig. 8.6. Diagram of coherent locator.

Fig. 8.6. presents a block diagram [12] of a coherent locator. The laser, operating in continuous mode, generates a signal on the optical frequency v_0 which goes to the pulse laser amplifier and the latter, in turn, generates a pulsed optical signal on the carrier frequency v_0 . The frequencies of the oscillations which are reflected from the target are shifted relative to the frequency v_d being transmitted by the Doppler frequency. The carrier frequency of the reflected signal equals $v_0 + v_d$. Radiation from the laser is also fed to the frequency converter to which, in addition to this, a signal with frequency v_x (compensating) goes.

After frequency conversion, a signal with frequency $v_0 + v_x$ goes to the summing device. This signal is summed with the signal reflected from the target, and the resulting signal goes to a photoreceiver for which a photomultiplier is usually used. As a result of the difference in the two signals, the signal $v_d - v_x$ is read from the output of the PM which carried information about

the relative velocity of movement of the target. With the use of such a system, on the SC the maximum value of measured relative velocity can attain a value of 18 km/sec, which corresponds to the relative velocity for two low-altitude satellites which are moving in opposite directions.

The Doppler frequency shift on a wave of $0.69 \mu\text{m}$ attains $5 \cdot 10^{10}$ Hz in this case. With the closing of one of the satellites with the other, the relative velocities may be very insignificant, on the order of 0.1 m/sec. In this case, the Doppler frequencies attain values of $3 \cdot 10^5$ – $5 \cdot 10^{10}$ Hz. Even the most low-inertia PM cannot record the upper frequencies, since the maximum values of the frequencies which the PM's pass are $3 \cdot 10^8$ Hz.

8.5. Electro-Optical Equipment for Docking with a Laser

The use of a laser as an emitter in the on-board electro-optical equipment of an SC permitted the effective solution of a number of complex technical problems in controlling the closing of the spacecraft. One of the most promising trends in this field is the creation of electro-optical locators to assure the docking of the SC's. Let us examine the electro-optical equipment of a docking system of cooperating SC based on the employment of semiconductor lasers. Since the SC's are cooperating, the logic of the operation of the equipment envisages its emplacement on both ships. In this, it is envisioned that the electro-optical equipment will assure the mutual orientation of both ships which are docking, and the equipment of the maneuvering SC will put out information for controlling the closing.

/256

A block diagram of the equipment is presented in Fig. 8.7 [66]. Installed on board the maneuvering SC is a locator which assures tracking of the target SC, the measurement of the range to it, and the relative closing velocity. The width of beam of the locator's transmitter is $0.5 \cdot 1.7 \cdot 10^{-2}$ rad (0.5°).

Installed on board the target SC is a unit of corner reflectors and a system for angle tracking which assures tracking the maneuvering SC from the radiation of its transmitter. The unit of corner reflectors consists of seven prisms with hexagonal faces which reflect beams in the opposite direction. The distance between the parallel sides of the hexagon of the input face of one of the prisms equals 6 cm, and of the entire unit, 18 cm. The precision in manufacturing the prisms is such that the angle between the incident and reflected beams does not exceed $9.6 \cdot 10^{-6}$ rad. The angle of divergence of the beams reflected by the unit of corner reflectors is approximately $1.7 \cdot 10^{-5}$ rad.

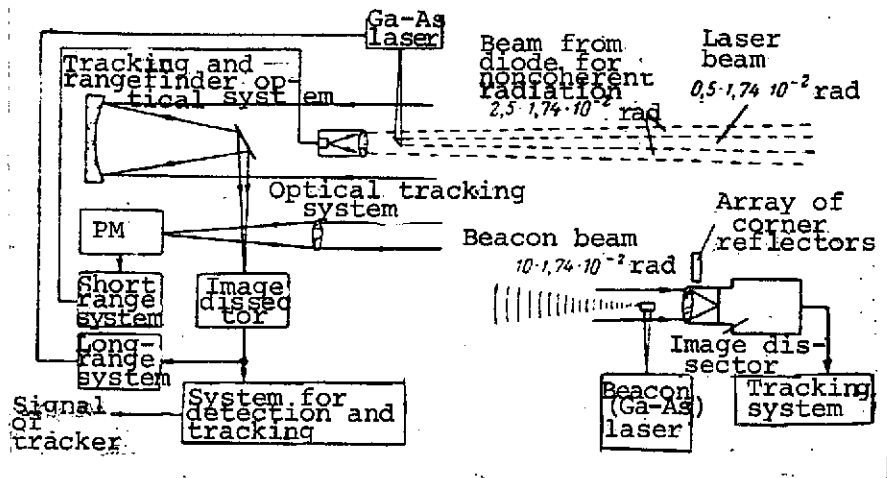


Fig. 8.7. Block diagram of electro-optical equipment for vehicle docking which uses semiconductor lasers.

For the most dependable and rapid orientation of the SC's relative to each other, additionally installed on board the target SC is a beacon which operates in the pulsed mode. The beacon's radiation is propagated within the limits of a cone with an apex angle of $10 \cdot 1.74 \cdot 10^{-2}$ rad (10°).

The beacon is a laser diode array with uncooled elements of gallium arsenide (Ga-As) which radiates on a wavelength of $\lambda = 0.9 \mu\text{m}$. The maximum value of the radiation flux released by the beacon is 1 kW. The width of the spectral band of radiation of the entire array is increased to approximately 20 Å. Since each diode emits in an angle of approximately $20 \cdot 1.74 \cdot 10^{-2}$ rad (20°), the corresponding objective is used to obtain the required angular dimension of the beam. Inasmuch as the field-of-vision angle of the angle tracking system of the maneuvering SC equals $10 \cdot 1.74 \cdot 10^{-2}$ rad (10°), prior to the start of docking the SC's should be oriented in a direction with each other with a precision of at least $\pm 10 \cdot 1.74 \cdot 10^{-2}$ rad.

/257

The principle of operation of this system consists of the following. If, at the initial moment, the radiation from the transmitter of the maneuvering SC which is propagated in an angle of $0.5 \cdot 1.74 \cdot 10^{-2}$ rad (0.5°) does not fall on the target SC, then to match the beam with the direction to the target SC, a beacon is used. It emits 1000 double pulses per second, each with a duration of 100 ns. The leading edges of the two pulses in a pair are divided by a time interval equal to 1 μs (Fig. 8.8).

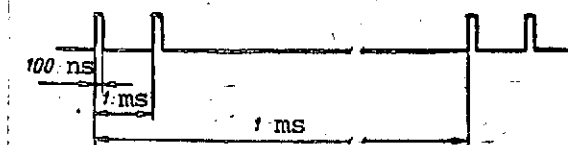


Fig. 8.8. View of double pulses of radiation of locator's transmitter.

The use of double radiation pulses of a synchronous detector permits improving considerably the discrimination of the useful signals. With such a frequency and duty factor, the radiation power (with a power in the pulse of 1 kW) is 200 MW and the power consumed by the array equals approximately 5 W.

The pulsed signals of the beacon which reach the receiver of the locator are used in the tracking system of the maneuvering SC for its turn along two axes until the matching of the narrow beam with the direction to the target SC.

As soon as the radiation of the transmitter of the maneuvering SC falls on the target, a part of it returns with the aid of the unit of corner reflectors and goes to the receiver of the maneuvering SC. The radiation from the locator's transmitter falls in the receiver of the angle tracking system of the target SC and is used to control the angular position so that the unit of corner reflectors is always directed toward the maneuvering SC.

With the installation of a sufficient number of corner reflectors on the target SC, the angle-tracking system need not be used. But at short distances which occur in the docking process, its employment is necessary to exclude possible errors /258

In essence, the angle-tracking system is an electro-optical tracking device with electronic scanning whose circuit is intended for operation from a pulsed source. The sensitive element in this system is served by a photomultiplier with a dissector with a silver-oxygen-caesium photocathode. A narrow-band interference filter is used to reduce the influence of background illuminations in the optical system. The field of view of the receiver of the angle tracking system, equal to $10 \cdot 1.74 \cdot 10^{-2}$ rad (10°), is formed with the use of an objective with a focal length of $f' = 90$ mm and relative aperture $q = 1:0.95$.

Included as part of the equipment installed on board the maneuvering SC is an angle tracking system and a system for measuring the parameters of relative motion.

The same diode array as on the beacon of the target SC is used as the emitter of the locator on the maneuvering SC. It operates in the same pulsed mode as the beacon, assuring radiation

with a power of 300 W in a pulse, with the propagation of the radiation flux in the pencil with a vertex angle of $0.5 \cdot 1.74 \cdot 10^{-2}$ rad (0.5°). Despite the lesser power, the radiation force in comparison with the beacon is greater by two orders of magnitude.

The angle tracking system is similar to the system of the target SC and serves for the initial detection of the beacon and for tracking it with the subsequent change to tracking the target SC from the radiation reflected by the unit of corner reflectors. In the receiver of the angle tracking system of the maneuvering SC, an optical system is used which assures a field of view of $10 \cdot 1.74 \cdot 10^{-2}$ rad (10°) in detection, and in tracking $0.75 \cdot 1.74 \cdot 10^{-2}$ rad (0.75°).

A block diagram of an angle tracking system during operation in detection and tracking modes is presented in Fig. 8.9 (a, b).

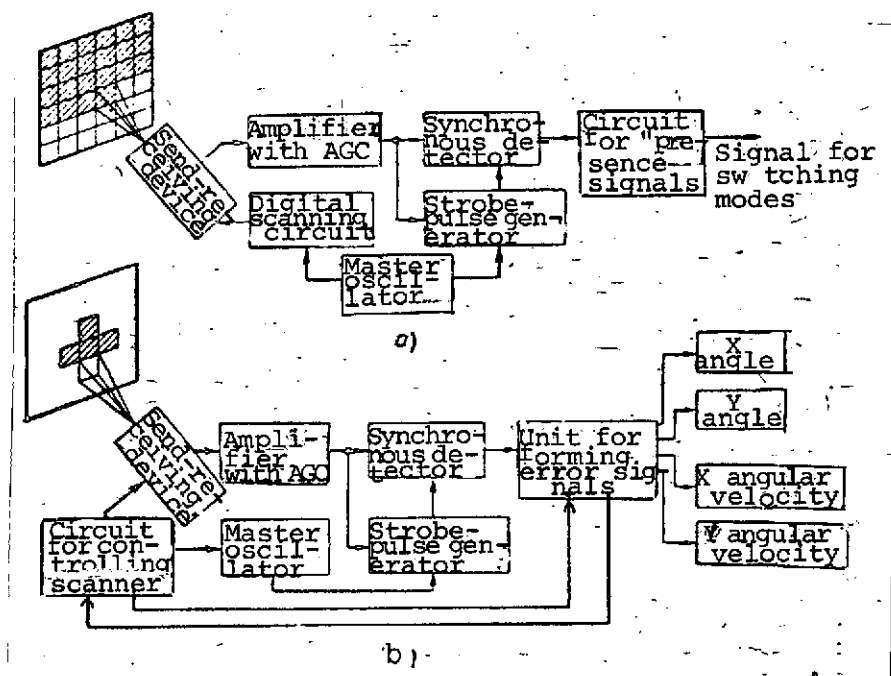


Fig. 8.9. Block diagram of a tracking system:
a. detection mode; b. tracking mode.

The optical system of the receiver consists of an objective with a focal length of 90 mm and a relative aperture of 1:0.95 and a projection system with a Cassegrain mirror objective having a focal length of 640 mm and a relative aperture of 1:3.6. Installed in the focal plane of this objective is a photomultiplier

with a dissector, type F-4004, the signals from whose output are used both in the angle tracking system and in the range measuring unit.

The size of the scanning diaphragm of the dissector is such that electrons from the section of the photocathode with an area less than 0.001 mm^2 fall in the multiplier at each moment in time. In this, the instantaneous field of view proves to be equal to several $\pi/64,800 \text{ rad}$ (seconds of arc). The use of a deflecting system in the dissector permits "looking through" various sections of the photocathode with the scanning diaphragm, /259 which is equivalent to scanning a given (10-degree) scanning zone with the instantaneous field of view. At the same time, the presence of a dissector along with the detection of the target SC provides the opportunity to determine error angles and accomplish tracking within the limits of the scanning zone.

The small value of the instantaneous field of view reduces considerably the influence of the background illuminations and furthers an increase in the precision of the angle tracking and the determination of the coordinates of the target SC.

The zone of coverage is scanned by the instantaneous field of view by the line-frame scanning method with the discrete change from one element of sweep to another (Fig. 8.9a). In order to exclude the possibility of an omission, the scanning of adjacent sections is accomplished with sufficient overlap. The stepped displacement of the instantaneous field of view is regulated by the feeding of pulses from the master oscillator and is selected so that at least one pair of pulses of radiation flux emitted by the locator's transmitter or the beacon manages to arrive at the receiver from one section of space. A video signal from the output of the dissector goes to the preamplifier and then is amplified by a three-stage amplifier with automatic adjust- /260 ment of amplification.

To increase the noise immunity of the system and for the more effective discrimination of the useful signals, a synchronous detector is included in the circuit which uses information about the width and synchronization of the arriving pulses. If a pair of pulses with amplitude no less than the given threshold value and with the same time interval between them as is given by the master oscillator arrives at the circuit which gives out the signal of the presence of the target, a "presence" signal appears at the output of the circuit. The appearance of the signal causes a change from the detection mode to angle tracking.

Transverse scanning is conducted in this mode within the limits of a small frame (see Fig. 8.9b) whose size comprises about 3% of the linear dimension of the entire scanning zone. In this

regard, the small frame may be in any section of the scanning zone depending on the location of the target at the moment of its detection. As the target displaces within the limits of the scanning zone, the frame will also displace in such a way that the target remains in the center all the time. In this mode, signals from the output of the synchronous detector, along with information from the control circuit, are fed to the unit for the formation of error signals. Then these signals, in the form of direct-current voltages proportional to the deviation of the target image from the center of the frame, are again fed to the circuit for the control of transverse scanning, assuring the matching of the center of the frame with the direction to the target.

Furthermore, signals are generated in the circuit in the form of direct-current voltages which characterize the angular position of the small frame within the limits of the scanning zone (X and Y angles) and the angular velocities of the displacement of the target in the scanning zone (X and Y velocities). These voltages, proportional to the measurable values, passing through a converter, go to the computer of the system for controlling the movement of the maneuvering SC in the form of output signals of the angle tracking system.

With the start of the angle tracking of the target SC by the locator, the long-range system is turned on, the block diagram of which is presented in Fig. 8.10. It assures the measurement of range with resolution on the order of 10 m and of the closing velocity with distances between the SC's of up to 120 km. The pulsed method of measuring range and closing velocity is realized in the circuit of this system.

From the output of the master oscillator, the signals go to a synchronous counter which performs the role of divider and to the strobe-pulse generator. The pulses of the synchronous counter are fed to the generator of double pulses. This generator generates pairs of pulses with a duration of 10 ns each and divided by 16 single pulses of the master oscillator, which corresponds to a time interval between the leading edge of approximately 1 μ s. The double pulses, recurring with a frequency of 1 kHz, are fed to two parallel laser excitation circuits with silicon-controlled rectifiers (SCR) which are triggered sequentially by the first and second pulses. /261

The current which flows through the diodes of the array depends on the amount of voltage on the discharge capacitors of the excitation circuit, which is regulated by the voltage of the AGC controlled from the locator's receiver. The radiation pulses reflected from the target SC are received on the maneuvering SC

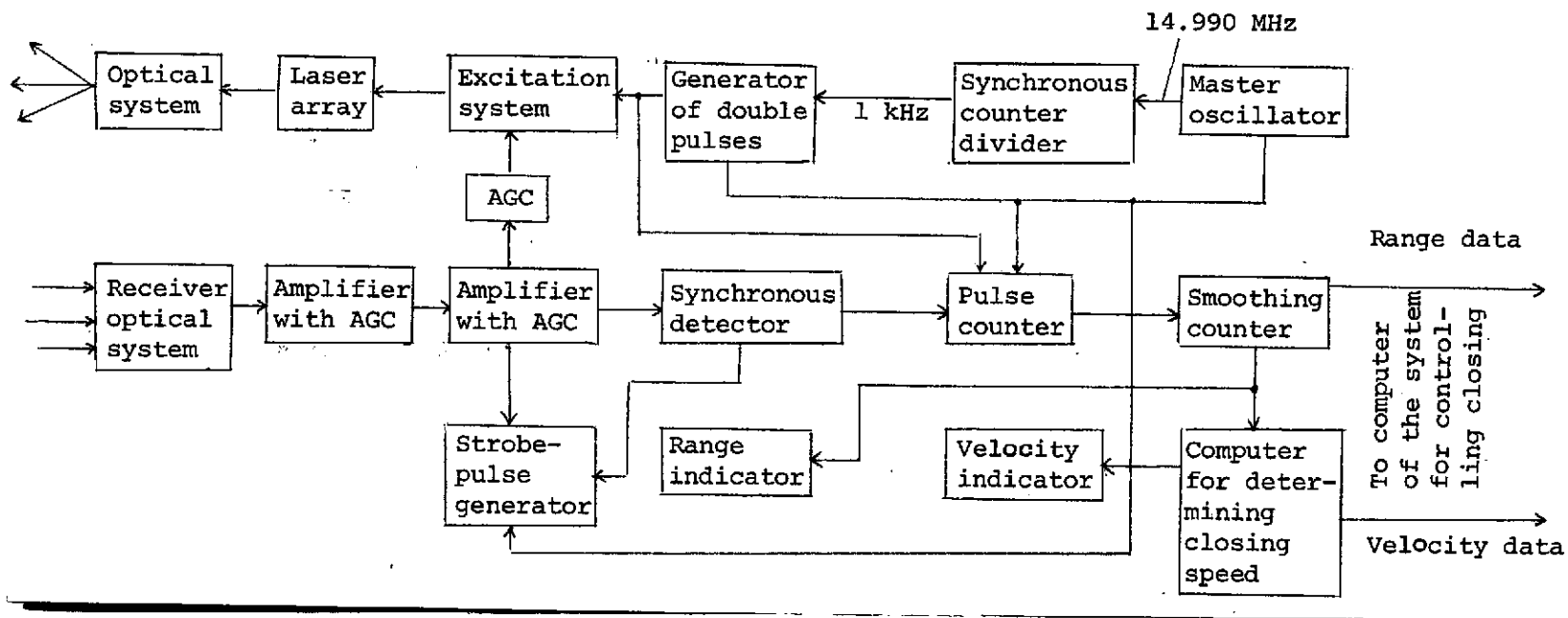


Fig. 8.10. Block diagram of a long-range system.

and go through an amplifier to the synchronous detector. The input signal of this detector is a pulse which characterizes the time of arrival of the leading edge of the first of the double pulses.

The time to the target SC is determined by the measured time interval between the emission and the received pulse with the use of a pulse counter. The counter is started by an emitted pulse and is stopped with the arrival of the reflected pulse. The interval is filled with pulses from the master oscillator which are also fed to the counter. Since the frequency of the master oscillator is 14.990 MHz, one period, with consideration of the double course of the beam, corresponds to 10 m. From the output of the pulse counter the information goes to a smoothing counter, where data on the range are averaged from the results of every 100 measurements.

Simultaneously with this, information about range is fed to a computer for determining the closing velocity which, on the basis of a comparison of the last and preceding readings, generates data about the amount and sign of the velocity.

As closing occurs, when the distance between the SC's is reduced to a value which assures dependable discrimination of the useful signals in the short-range unit, the long-range system is cut off. A block diagram of a short-range system is presented in Fig. 8.11. It assures the continuous measurement of range and closing velocity with distances between the SC from approximately 3 km to docking, with range resolution of 0.1 m and resolution for velocity of 0.01 m/sec.

A diode of incoherent radiation of gallium arsenide is used as the radiation source here. It emits within the limits of a cone with an apex angle of $2.5 \cdot 1.74 \cdot 10^{-2}$ rad (2.5°), which is coaxial with the beam of a pulsed laser. The power of emission of the diode equals ~ 40 MW with an excitation current of 2 A. The radiating junction of the diode is in optical contact with a hemispheric lens, which reduces losses to reflection. For forming the pencil, a fast objective is used with focal length $f' = 50$ mm and relative aperture $q = 1:1$. /262

After reflection from the target SC, the radiation of the diode is sent with the aid of a light-dividing device to a ten-stage photomultiplier with a silver-oxygen-caesium photocathode.

As a result of the heterodyning, a signal is obtained on the output of the main mixer with a frequency of 4.747 kHz and having the same phase characteristics as the signal received on a frequency of 3.747 MHz. Such a method of heterodyning permits

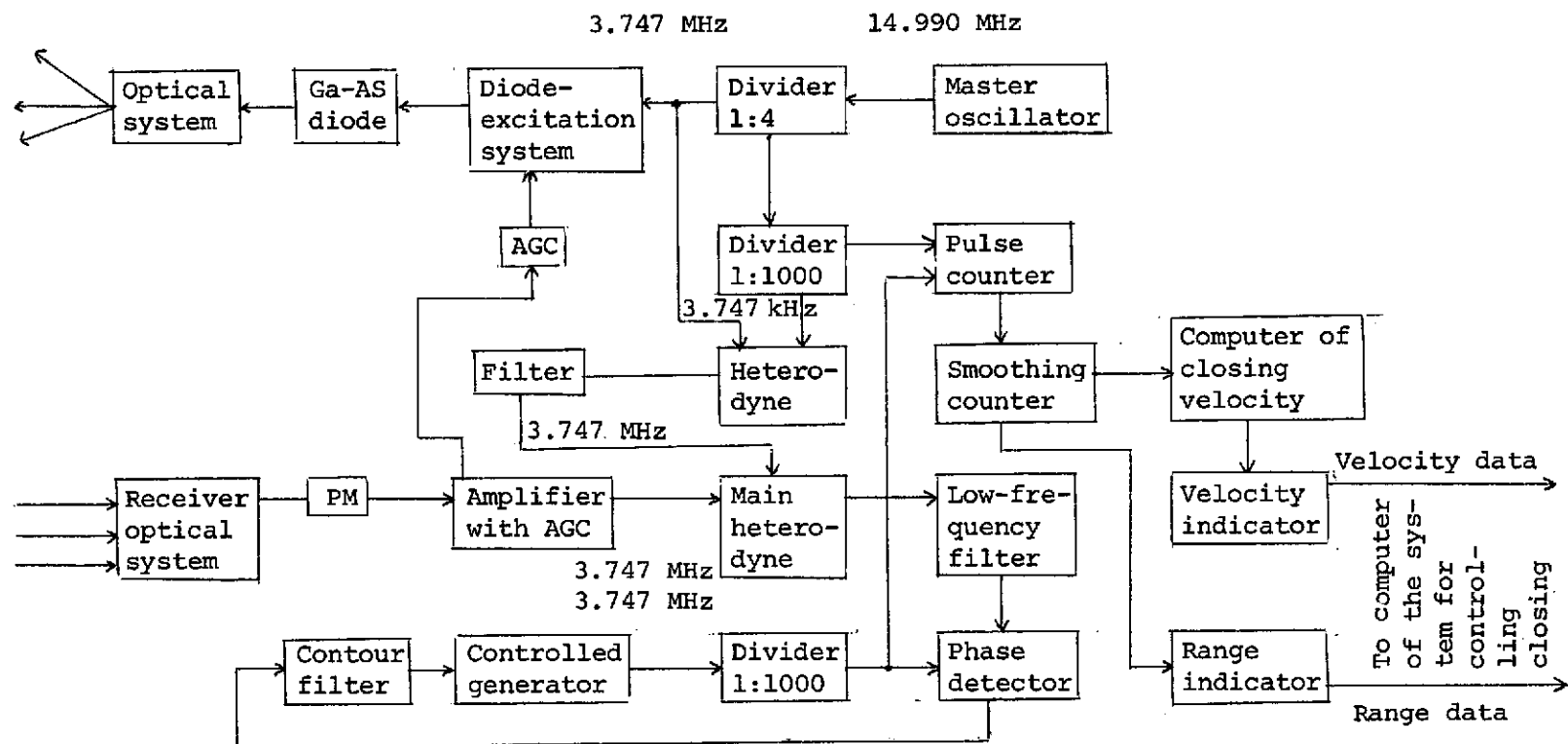


Fig. 8.11. Block diagram of a short-range system.

obtaining high-range resolution. The connections between the units and their interaction are shown in the block diagram. We will only point out that the contour filter is tuned to a frequency of 3.747 MHz and serves for the conversion of the sine form of the signal to a square shape.

The rate of closing is determined on the basis of a comparison of successive range readings. Information about the range and velocity is fed to a computer of the system for controlling closing for use on the final stage of rendezvous and docking

This electro-optical system has the following characteristics:

- Operating range 120 km;
- Range-measurement error 0.5% at distances from 120 to 3 km and 0.1 m from 3 km to docking;
- Error in determining angular docking coordinates $10 \cdot \frac{\pi}{648,000}$ (10").

rad (10").

CHAPTER 9. A METHOD FOR CALCULATING THE RADIATION CHARACTERISTICS

9.1. A Method for Calculating the Amount of Solar Radiation Perceived by the Instruments after Reflection from the Earth's Surface and Clouds

The power of the solar radiation reflected from some surface and perceived by an electro-optical instrument depends not only on the parameters of the instrument but also on the characteristics of the reflecting surface. Thus, for example, if the field of view of the instrument is directed toward the earth, then both the clouds and the surface of the earth with the atmosphere may fall within its limits.

If the field of view of the instrument is directed toward clouds illuminated by the sun, then we can approach the calculation of the radiation reflected from them in the following manner. Since the clouds are a diffuse reflector with a reflection coefficient ρ_0 , on the basis of (1.21) we find their luminance

$$B_0 = -\frac{E_S}{\pi} \rho_0, \quad (9.1)$$

where E_S is the irradiance created by the sun.

The irradiance created by the clouds in the plane of the entrance pupil of the instrument depends on the dimensions of the radiating surface. However, radiation from not all sections of this surface will fall on the receiver. The radiation flux will fall on it only from the sector which is limited by the instrument's instantaneous field of view. The irradiance created in the plane of the entrance pupil by the radiation which comes from this section of the surface will be called the active irradiance. The expression which determines the active irradiance E_a has the appearance

$$E_a = \frac{\Phi_a}{A_{ent0}} = \frac{E_S}{\pi} \rho_0 \omega_p, \quad (9.2)$$

where Φ_a is the radiation flux reflected from the clouds and falling in the instrument; A_{ent0} is the area of the entrance pupil of the instrument.

When a portion of the field of view is directed at the cloud cover and a portion at the cloudless section of the earth's surface, the active irradiance at the instrument entrance will be

$$E_a = \frac{\Phi_a}{\Delta \Omega} = \frac{E_s}{\pi} [q_0 n_e + q_0 (1 - n_e) \rho_e] \quad (9.3)$$

where n_e is the coefficient which characterizes the fraction of the field of view occupied by the cloud cover; ρ_e is the coefficient of reflection of solar radiation by the "earth's surface-atmosphere" system.

Naturally, if we consider the radiation reflected from the earth as interfering, the most difficult conditions for the operation of an electro-optical instrument will occur when the instantaneous field of view of the instrument is directed entirely at the clouds, i.e., $n_e = 1$ and

$$E_a = \frac{E_s}{\pi} q_0 \rho_e$$

The active irradiance will be maximum with the normal incidence of the sun's rays on the sections of the cloud cover which fall in the field of view. In this case $E_s = 0.135 \text{ W/cm}^2$ and the maximum possible value of the active irradiance at the entrance of the instrument will be

$$E_{a\max} = \frac{0.135}{\pi} q_0 \rho_e \cong 0.043 q_0 \rho_e \text{ W/cm}^2 \quad (9.4)$$

If we consider that the orbital plane of the SC is inclined toward the plane of the equator by the angles $i = 50.1.74 \cdot 10^{-2} \text{ rad} - 80.1.74 \cdot 10^{-2} \text{ rad}$ ($50^\circ - 80^\circ$), the probability of maximum illumination is very small. In the majority of cases, the angle between the direction being considered and the direction of incidence of the rays will be at least $20.1.74 \cdot 10^{-2} \text{ rad} - 30.1.74 \cdot 10^{-2} \text{ rad}$ ($20^\circ - 30^\circ$) and the coefficient of diffuse reflection $\rho_0 \leq 0.7$. The values of the effective irradiance which will occur under actual conditions are presented in Table 9.1.

If there is no cloud cover above the earth's surface, then the underlying surface and the atmosphere will fall in the instrument's field of view. In the first approximation, the

value of the active irradiance can be determined from formulas similar to (9.2) and (9.3):

$$E_a = \frac{E_s}{\pi} [q_e n + q_0 (n-1)] \omega_p \quad (9.5)$$

and

$$E_a = \frac{E_s}{\pi} \omega_p q_e \quad (9.6)$$

TABLE 9.1. DEPENDENCE OF EFFECTIVE IRRADIANCE AT THE ENTRANCE OF THE INSTRUMENT ON THE SIZE OF THE INSTANTANEOUS FIELD OF VIEW.

Field-of-vision angle, $2W$ rad	$3 \cdot 10^{-4}$	$7.5 \cdot 10^{-4}$	$1.5 \cdot 10^{-3}$	$3 \cdot 10^{-3}$	$9 \cdot 10^{-3}$
Active irradiance E_{a1} W/cm ²	$1.74 \cdot 10^{-9}$	$1.11 \cdot 10^{-8}$	$4.38 \cdot 10^{-8}$	$1.74 \cdot 10^{-7}$	$1.56 \cdot 10^{-6}$
Field-of-vision angle, rad	$1.74 \cdot 10^{-2}$	$3.5 \cdot 10^{-2}$	$8.9 \cdot 10^{-2}$	0.174	0.35
Active irradiance E_{a1} W/cm ²	$6.0 \cdot 10^{-6}$	$2.5 \cdot 10^{-5}$	$1.0 \cdot 10^{-4}$	$6.0 \cdot 10^{-4}$	$2.5 \cdot 10^{-3}$

Relation (9.5) permits finding the active irradiance when clouds also fall in the field of view along with the earth's surface.

Formulas (9.2), (9.3), (9.5), and (9.6) can be used only for approximate estimates in those cases where the reflection coefficients change weakly with a change in wavelength and if a nonselective radiation receiver is employed in the instrument.

For more rigorous estimates, we consider the change in the reflectivity of the ground cover in accordance with the spectrum. In addition, the radiation which falls on the earth is attenuated selectively by the atmosphere during passage to the earth's surface and return. This should also be considered in the calculations.

In those cases where a radiation receiver having selective sensitivity is used in the instrument, the use of integral reflection coefficients can lead to significant errors.

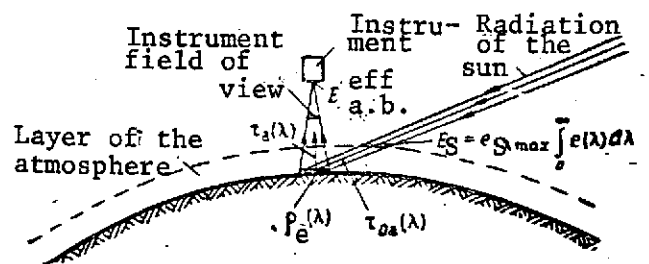


Fig. 9.1. For the determination of the effective value of active irradiance at the entrance of an instrument caused by reflected solar radiation.

Consideration of the spectral sensitivity of a radiation receiver leads to the necessity to change from regular irradiance at the entrance pupil of the instrument and radiation flux which falls on the receiver to effective values of irradiance and radiation flux.

In general the effective value of the active monochromatic irradiance at the entrance to the instruments (Fig. 9.1) will be /266

$$e_{\lambda a.b}^{\text{eff}} = e_{S_{\text{max}}} e_c(\lambda) \tau_a(\lambda) \rho_e(\lambda) \tau_{0a}(\lambda) \tau_0(\lambda) s(\lambda), \quad (9.7)$$

where $e_{\lambda a.b}^{\text{eff}}$ is the function of spectral density of the effective active monochromatic irradiance reduced to the entrance to the instrument; $e_{S_{\text{max}}}$ is the function of the spectral density of irradiance created by the sun on the boundary of the atmosphere on the wavelength of maximum radiation; $e_s(\lambda)$ is the function of spectral density of solar irradiance in relative units; $\tau_a(\lambda)$ is the spectral transparency of the atmosphere for the solar radiation which falls on the earth's surface; $\rho_e(\lambda)$ is the spectral reflection coefficient of the surface being examined; $\tau_{0a}(\lambda)$ is the spectral transparency of the atmosphere for the radiation which goes to the instrument; $\tau_0(\lambda)$ is the coefficient of the spectral transmission of the optical system of the instrument; $s(\lambda)$ is the relative spectral sensitivity of the radiation receiver.

The effective active irradiance can be determined by the integration of expression (9.7) for the variable

$$E_{a.b}^{\text{eff}} = \int_0^\infty e_{\lambda a.b}^{\text{eff}} d\lambda = \int_0^\infty e_{S_{\text{max}}} e_c(\lambda) \tau_a(\lambda) \rho_e(\lambda) \tau_{0a}(\lambda) \tau_0(\lambda) s(\lambda) d\lambda. \quad (9.8)$$

We multiply and divide the right side of equation (9.8) by the factor

$$\int_0^{\infty} e_{S_{\max}} e_S(\lambda) d\lambda \int_0^{\infty} e_{S_{\max}} e_S(\lambda) \tau_{0a}(\lambda) \varrho_e(\lambda) d\lambda$$

and, after certain transformations, we obtain

$$E_{a.b}^{\text{eff}} = \frac{e_{S_{\max}} \int_0^{\infty} e_C(\lambda) \tau_a(\lambda) \varrho_e(\lambda) \tau_{0a}(\lambda) \tau_0(\lambda) s(\lambda) d\lambda}{e_{S_{\max}} \int_0^{\infty} e_S(\lambda) \tau_{0a}(\lambda) \varrho_e(\lambda) d\lambda} \times$$

$$\times \frac{e_{S_{\max}} \int_0^{\infty} e_S(\lambda) \tau_{0a}(\lambda) \varrho_e(\lambda) d\lambda}{e_{S_{\max}} \int_0^{\infty} e_S(\lambda) d\lambda} e_{S_{\max}} \int_0^{\infty} e(\lambda) d\lambda,$$

/267

whence, after simplification, we have

$$E_{a.b}^{\text{eff}} = \frac{\int_0^{\infty} e_S(\lambda) \tau_a(\lambda) \varrho_e(\lambda) \tau_{0a}(\lambda) \tau_0(\lambda) s(\lambda) d\lambda}{\int_0^{\infty} e_S(\lambda) \tau_{0a}(\lambda) \varrho_e(\lambda) d\lambda} \times$$

$$\times \frac{\int_0^{\infty} e_S(\lambda) \tau_{0a}(\lambda) \varrho_e(\lambda) d\lambda}{\int_0^{\infty} e_S(\lambda) d\lambda} e_{S_{\max}} \int_0^{\infty} e(\lambda) d\lambda. \quad (9.9)$$

We note that $e_{S_{\max}} \int_0^{\infty} e(\lambda) d\lambda = E_S$ is the irradiance created by the sun beyond the limits of the earth's atmosphere and $e_{S_{\max}} \int_0^{\infty} e(\lambda) \tau_{0a}(\lambda) \varrho_e(\lambda) d\lambda = E_{a.\text{ref}}$ is the active irradiance reduced to the entrance of the instrument without consideration of attenuation by the atmosphere during propagation toward the instrument.

In (9.9) we call the integral ratio

$$\frac{\int_0^{\infty} e_S(\lambda) \tau_a(\lambda) \varrho_e(\lambda) \tau_{0a}(\lambda) \tau_0(\lambda) s(\lambda) d\lambda}{\int_0^{\infty} e_S(\lambda) \tau_{0a}(\lambda) \varrho_e(\lambda) d\lambda} = k(\varrho_e, i) \quad (9.10)$$

the coefficient of the receiver's utilization of the solar radiation reflected from the earth's surface.

The second cofactor in (9.9) is the integral coefficient of reflection of solar radiation by the earth's surface.

We designate it

$$Q_{in} = \frac{\int_0^{\infty} e(\lambda) \tau_{0a}(\lambda) \rho_e(\lambda) d\lambda}{\int_0^{\infty} e(\lambda) d\lambda} = \frac{e_{S\lambda_{max}} \int_0^{\infty} e(\lambda) \tau_{0a}(\lambda) \rho_e(\lambda) d\lambda}{e_{S\lambda_{max}} \int_0^{\infty} e(\lambda) d\lambda}. \quad (9.11)$$

Thus, from (9.9), with consideration of (9.10) and (9.11), we have

$$E_{a,b}^{eff} = ES k(\rho_e) Q_{in} \quad (9.12)$$

The obtained formula shows that the effective value of the active irradiance reduced to the entrance of the instrument equals the product of the irradiance created by the sun beyond the limits of the earth's atmosphere times the receiver's use coefficient of reflected radiation and times the integral reflection coefficient.

If the emitter is the moon rather than the sun, then all calculation formulas remain as written formerly, but in place of ES , $e_{S\lambda_{max}}$ and $e_S(\lambda)$, it is necessary to substitute E_λ , $e_{\lambda_{max}}$ and $e_\lambda(\lambda)$ in them, which correspond to the irradiance created by the moon.

9.2. Calculation of the Amount of Solar Radiation Reflected by Artificial Objects and Perceived by the Instrument

Let us consider a method for calculation using as an example in this case the reflection of solar radiation from objects with a cylindrical and spherical forms which possess diffuse reflection.

Assume that an emitter which has the form of a cylinder and the instrument are mutually arranged as shown in Fig. 9.2 where we assume the following designations: γ is the angle between object-sun direction and the object-instrument direction, i.e., the sun-object-instrument angle; Q is a plane perpendicular to

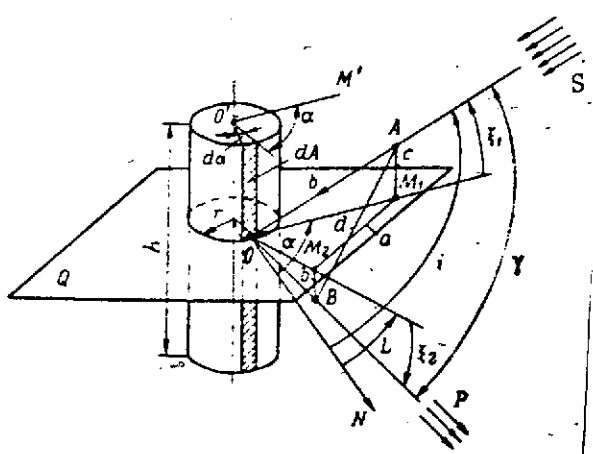


Fig. 9.2. Diagram of the reflection of solar radiation from a cylindrical object.

the axis of the cylinder; ξ_1 and ξ_2 are the angles between plane Q and the directions to the sun and instrument, respectively; i is the angle between normal N to the reflecting area element and the direction to the sun; ϕ is the angle between the normal N and the projection of the object-instrument direction to plane Q; δ is the angle in plane Q between the projections of the object-sun and object-instrument directions to it; α is the angle in plane Q between the normal N and the projection of the object-sun direction.

/269

Considering the cylinder as a secondary emitter, we can write that the force of emission dI from the area element dA will be

$$dI = B dA \cos i, \quad (9.13)$$

where

$$dA = H r_0 d\alpha;$$

H and r_0 are the height and radius of the cylinder

$$\cos i = \cos \alpha \cos \xi_1;$$

B is the energy brightness of the area.

If we accept that the object is a diffuse reflector, then with illumination by the sun, its energy brightness will be

$$B = \frac{E_S}{\pi} \cos \xi \cos \varphi.$$

Substituting in (9.13) the values which go into its quantities, we find

$$dI = \frac{ES}{\pi} q H r_0 \cos \xi_1 \cos \xi_2 \cos \varphi \cos \alpha d\alpha. \quad (9.14)$$

Considering that $\phi = \alpha - \delta$, we rewrite expression (9.14) in the form

$$dI = \frac{ES}{\pi} q H r_0 \cos \xi_1 \cos \xi_2 [\cos \delta \cos^2 \alpha + \sin \delta \cdot \sin \alpha \cos \alpha] d\alpha.$$

Integrating this expression, we find the total radiation intensity of the object in the direction of the instrument

$$I = \frac{ES}{\pi} q H r_0 \cos \xi_1 \cos \xi_2 \left[\cos \delta \int_{\alpha_1}^{\alpha_2} \cos^2 \alpha d\alpha + \sin \delta \int_{\alpha_1}^{\alpha_2} \sin \alpha \cos \alpha d\alpha \right]$$

or

$$I = \frac{ES}{\pi} q H r_0 \cos \xi_1 \cos \xi_2 \left[\left(\alpha + \frac{\sin^2 \alpha}{2} \right) \cos \delta + \frac{\sin^2 \alpha}{2} \sin \delta \right]_{\alpha_1}^{\alpha_2}. \quad (9.15)$$

The upper limit of integration of α_2 is established from the condition that with the angle $\alpha > \pi/2$, the surface of the object in the direction of the instrument will not emit anything; therefore, we take $\alpha_2 = \pi/2$. The lower limit is determined by the position of the sun with respect to the instrument. Since the maximum angle from direction OC, when the sun is still creating illumination on the side surface of the cylinder, should not exceed $\pi/2$, the lower limit, as follows from the drawing, will be

$$\alpha_1 = \delta - \frac{\pi}{2}.$$

With consideration of the established values of the limits, /270 from (9.15) we will have

$$I = \frac{ES}{\pi} q H r_0 \cos \xi_1 \cos \xi_2 \left[\left(\pi - \delta + \frac{\sin 2\delta}{2} \right) \cos \delta + \sin^3 \delta \right]. \quad (9.16)$$

With this the value of the angle δ is determined from the given values γ , ξ_1 and ξ_2 in the following manner.

On directions OC and OP, we lay off segments of identical length $OA = OB = b$. From points A and B, we drop perpendiculars to plane Q and designate them $AM_1 = c$, $BM_2 = d$, $M_1M_2 = a$. In order to establish the relation between angles γ , ξ_1 , ξ_2 and angle δ , we express segment AB by segments c, d, and a, and also from triangle AOB. From the drawing, it follows that

$$AB^2 = (c+d)^2 + a^2 \text{ и } AB^2 = 2b^2 - 2b^2 \cos \gamma.$$

Equating the right sides of these equations, we obtain

$$(c+d)^2 + a^2 = 2b^2(1 - \cos \gamma), \quad (9.17)$$

where

$$\begin{aligned} c &= b \sin \xi_1; & d &= b \sin \xi_2; \\ a^2 &= b^2 \cos^2 \xi_1 + b^2 \cos^2 \xi_2 - 2b \cos \xi_1 \cdot \cos \xi_2 \cos \delta. \end{aligned}$$

Substituting the values c, d, and a in (9.17) and removing parentheses, we find

$$\begin{aligned} b^2 \sin^2 \xi_1 + b^2 \sin^2 \xi_2 + 2b^2 \sin \xi_1 \cdot \sin \xi_2 + b^2 \cos^2 \xi_1 + \\ + b^2 \cos^2 \xi_2 - 2b^2 \cos \xi_1 \cos \xi_2 \cos \delta = 2b^2(1 - \cos \gamma). \end{aligned} \quad (9.18)$$

After making certain transformations, from (9.18) we obtain

$$\begin{aligned} \text{or} \quad & 1 + \sin \xi_1 \sin \xi_2 - \cos \xi_1 \cdot \cos \xi_2 \cdot \cos \delta = 1 - \cos \gamma \\ & \sin \xi_1 \cdot \sin \xi_2 - \cos \xi_1 \cos \xi_2 \cdot \cos \delta = -\cos \gamma, \end{aligned}$$

from which we have

$$\cos \delta = \frac{\cos \gamma + \sin \xi_1 \sin \xi_2}{\cos \xi_1 \cos \xi_2} = \frac{\cos \gamma}{\cos \xi_1 \cos \xi_2} + \operatorname{tg} \xi_1 \operatorname{tg} \xi_2. \quad (9.19)$$

Thus, relation (9.16) in aggregate with formula (9.19) provides the opportunity to find the intensity of the reflected radiation.

If the surface of the object reflects selectively with reflection coefficient $e(\lambda)$, formula (9.16) is written as applicable to monochromatic radiation

$$i_\lambda = \frac{e_S}{\pi} \varrho(\lambda) H r_0 \cos \xi_1 \cos \xi_2 \left[\left(\pi - \delta + \frac{\sin 2\delta}{2} \right) \cos \delta + \sin^3 \delta \right] \quad (9.20)$$

and then converted to the effective value of irradiance reduced to the entrance of the instrument which, by analogy with (9.19), can be presented in the form

/271

$$E_{S_j}^{\text{eff}} = \frac{e_{S_{\max}} \int_0^\infty e_S(\lambda) \varrho(\lambda) \tau_a(\lambda) \tau_0(\lambda) s(\lambda) d\lambda}{\pi L^2 e_{S_{\max}} \int_0^\infty e_C(\lambda) d\lambda} \int_0^\infty e_{S_{\max}} e_S(\lambda) d\lambda \times \quad (9.21)$$

$$\times H r_0 \cos \xi_1 \cos \xi_2 \left[\left(\pi - \delta + \frac{\sin 2\delta}{2} \right) \cos \delta + \sin^3 \delta \right]. \quad (9.21)$$

Designating $\left| \frac{\int_0^\infty e_C(\lambda) \varrho(\lambda) \tau_a(\lambda) \tau_0(\lambda) s(\lambda) d\lambda}{\int_0^\infty e(\lambda) d\lambda} = k \right|$ the coefficient of

utilization of the radiation reflected from the object by the receiver, from (9.21) we obtain

$$E_S^{\text{eff}} = \frac{E_S}{\pi L^2} H r_0 k \cos \xi_1 \cos \xi_2 \left[\left(\pi - \delta + \frac{\sin 2\delta}{2} \right) \cos \delta + \sin^3 \delta \right]. \quad (9.22)$$

9.3. A Method for Calculating the Amount of Radiation Intensity with Reflection from Objects of Spherical Form

The radiation flux which reaches the entrance of the instrument after reflection from objects of a spherical form will be the sum of two components depending on the state of their surface:

a flux caused by mirror reflection and a flux due to diffuse reflection.

Let us first consider the case of determining the amount of reflected flux from an object with mirror reflection when both the receiver and the emitter are on the same axis (Fig. 9.3).

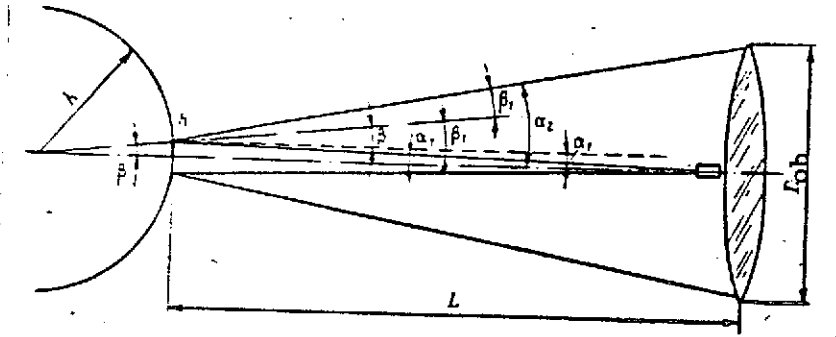


Fig. 9.3. Mirror reflection of radiation from objects of spherical form.

As follows from the sketch, only the radiation flux which is propagated within the limits of a solid angular aperture falls on the receiver after reflection from an object. This solid angle is characterized by the plane angle

$$\alpha_2 = \frac{D_{ob}}{2L}, \quad (9.23)$$

where L is the distance between the instrument and the object; D_{ob} is the diameter of the entrance pupil of the objective.

With a given radius of the sphere, the radius of the area h on the surface of the sphere from which the reflected radiation will be propagated at angles to the axis not exceeding α_2 depends on the diameter of the receiving objective of the receiver. Actually, radius h is determined by the angle α_2 , which equals $\alpha_2 = \beta + \beta_1$. /272

Since

$$\beta_1 = \beta + \alpha_1, \quad (9.24)$$

then

where

$$\alpha_1 = \frac{h}{L}$$

Substituting the values of α_2 from (9.23) and α_1 in (9.24), we find

$$\frac{D}{2L} = 2\beta + \frac{h}{L} \quad (9.25)$$

With small angles of β we can consider that $\beta = h/R$, then

$$\frac{D}{2L} = 2\frac{h}{R} + \frac{h}{L} \text{ or } \frac{D}{2L} = h \left(\frac{2}{R} + \frac{1}{L} \right)$$

Hence, we find the radius of the area on the surface of a sphere with reflection from which the radiation falls on the objective of the receiver

$$h = \frac{DR}{2(2L + R)}$$

Since $R \ll L$, then ignoring the value R in the denominator of the last formula, we obtain the expression for the calculation of h

$$h = \frac{RD}{4L} \quad (9.26)$$

This means that the ideal mirror sphere with radius R is equivalent in its reflectivity to a flat circular mirror with a diameter of $2h$. Table 9.2 presents comparative data on the dimensions of the sphere and reflecting area at various distances.

The size of the reflecting area of radius h is

/273

$$A_r = \pi h^2 = \pi \frac{R^2 D^2}{16L^2} \quad (9.27)$$

If the radiation intensity of the emitter I_{ob} is known, then the value of the radiation flux which reaches the receiver after reflection from the object (without consideration of attenuation in the medium) will be

$$\Phi_{\text{rec}} = I_{\text{ob}} \rho_m \omega_r \quad (9.28)$$

where ρ_m is the coefficient of mirror (directional) reflection of radiation flux by the objective; $\omega_r = \frac{A_r}{L^2}$ is the solid angle within whose limits the radiation flux which is propagated from the transmitter falls on the objective.

TABLE 9.2. VALUES OF DIAMETERS OF REFLECTING AREA IN mm DEPENDING ON THE DISTANCE TO THE OBJECT WITH VARIOUS DIMENSIONS OF SPHERICAL OBJECTS AND $D_{\text{ob}} = 0.5$ m

L km	0,2	0,3	0,4	0,5	1,0	2,0	5,0	10
$R = 1$ m	1,25	0,85	0,62	0,50	0,25	0,125	0,050	0,025
$R = 2,5$ m	3,12	2,12	1,56	1,25	0,62	0,312	0,125	0,062
$R = 5$ m	6,25	4,25	3,12	2,50	1,25	0,625	0,250	0,125

With consideration of attenuation of the radiation by the medium, expression (9.28) takes the form

$$\Phi_{\text{rec}} = I_{\text{ob}} \rho_m \tau_e^2 \quad (9.28a)$$

where τ_e is the coefficient of transmission of the radiation by the medium with propagation in one direction.

From (9.28) and (9.28a), with consideration of (9.27), we have

$$\Phi_{\text{rec}} = I_{\text{ob}} \pi \frac{R^2 D^2}{16 L^4} \rho_m \quad (9.29)$$

and

$$\Phi_{\text{rec}} = I_{\text{ob}} \pi \frac{R^2 D^2}{16 L^4} \rho_m \tau_e^2 \quad (9.29a)$$

With the use of a laser as an emitter, on the basis of (1.4), the radiation intensity of the transmitter will be

$$I_{ob} = \frac{\Phi_{laser}}{\omega} = \frac{\Phi_{laser}}{\pi \frac{\theta_p^2}{4}} = \frac{4\Phi_{laser}}{\pi \theta_p^2} \quad (9.30)$$

where ω_p and θ_p are respectively the solid and plane angles of divergence of the beam of the irradiator. /274

From (9.29) and (9.29a), considering (9.30), we find

$$\Phi_{rec} = \frac{\Phi_{laser} R^2 D_{ob}^2}{4L^2 \theta_p} q_m \quad (9.31)$$

and

$$\Phi_{rec} = \frac{\Phi_{laser} R^2 D_{ob}^2}{4L^2 \theta_p} q_m \tau_e^2 \quad (9.31a)$$

Sometimes, irradiators are used with mirror reflectors and a luminous element with luminance B . In these cases, the radiation intensity of the irradiator is found from the formula

$$I_{tr} = B_{tr} A_{pr} q_{pr} \quad (9.32)$$

where A_{pr} is the area of the exit opening of the projector; q_{pr} is the coefficient which considers the loss of radiation in the irradiator itself and on the reflector.

With the use of such an irradiator, from (9.29), (9.29a), and (9.32), we will have

$$\Phi_{rec} = \pi \frac{B_{pr} A_{pr} R^2 D_{ob}^2}{16L^4} q_m \quad (9.33)$$

and

$$\Phi_{rec} = \pi \frac{B_{pr} A_{pr} R^2 D_{ob}^2}{16L^4} q_m \tau_e^2 \quad (9.33a)$$

It can also be shown that, on the basis of (9.29) and (9.29a), the radiation intensity with mirror reflection from an object of

spherical shape will be

$$\left| L_{\text{ref.m}} = I_{\text{ob}} \frac{R^2 \rho_m}{4L^2} \right| \quad \text{and} \quad \left| I_{\text{ref.m}} = I_{\text{ob}} \frac{R^2 \tau_c}{4L^2} \rho_m \right| \quad (9.34)$$

Second, let us consider the case where an object reflects diffusely (Fig. 9.4).

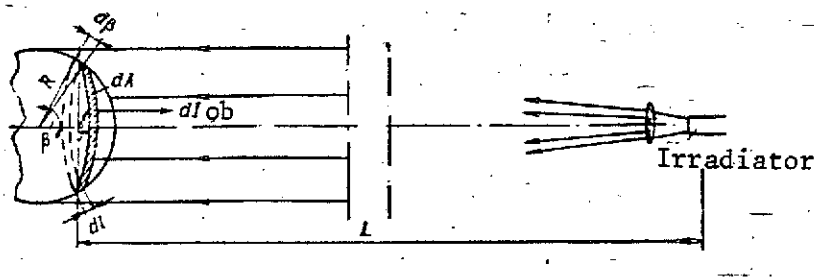


Fig. 9.4. Diffuse reflection of radiation from objects of spherical shape.

The irradiance created by the transmitter is determined in an arbitrary point of a spherical surface by the formula

1275

$$E = \frac{I_{\text{tr}}}{L^2} \cos \alpha, \quad (9.35)$$

where α is the angle between the normal to the surface and the direction of propagation of the beam.

Assuming that the coefficient of diffuse reflection of the surface is ρ_d , on the basis of (9.1) we write the expression for the luminance of this surface as a secondary emitter

$$B_{\text{ref}} = \frac{E}{\pi} \rho_d$$

whence, considering (9.35) we obtain

$$B_{\text{ref}} = \frac{I_{\text{tr}}}{\pi L^2} \tau_e \rho_d \cos \alpha_1. \quad (9.36)$$

Taking the elementary area dA (elementary circular zone with width $d\ell$) as an equally bright emitter, we find the intensity of the radiation reflected toward the instrument from the formula

$$dI_{\text{ref}} = B_{\text{ref}} dA \cos \alpha, \quad (9.37)$$

where $dA = 2\pi r d\ell$; $r = R \sin \alpha$ is the radius of the circular zone; $d\ell = R d\alpha$.

Expanding (9.37), we write

$$dI_{\text{ref}} = 2B\pi R^2 \sin \alpha \cos \alpha d\alpha. \quad (9.38)$$

Since the emitter and receiver are in the immediate proximity of each other, the limits of change of angles α and α_1 are practically identical during irradiation and reflection. Then the total intensity of reflected radiation is found by integrating expression (9.38)

$$I_{\text{ref}} = \int dI_{\text{ref}} = \int_0^{\pi/2} 2B\pi R^2 \sin \alpha \cos \alpha d\alpha,$$

whence, with consideration of (9.36), we will have

$$\begin{aligned} I_{\text{ref}} &= \int_0^{\pi/2} \frac{I_{\text{tr}} R^2 \tau_e \rho_d \sin \alpha \cos \alpha}{L^2} d\alpha = \\ &= \frac{I_{\text{tr}} R^2 \tau_e \rho_d}{L^2} \int_0^{\pi/2} \sin \alpha \cos \alpha d\alpha. \end{aligned}$$

Integration of this expression provides

/276

$$I_{\text{ref}} = \frac{2I_{\text{tr}}R^2}{3L^2} \tau_e \quad (9.39)$$

where I_{tr} is the radiation intensity which is calculated, depending on the type of emitter, from formulas (9.30) and (9.32).

The value of the radiation flux reflected diffusely from the object and reaching the receiver is calculated from the formula

$$\Phi_d = \frac{I_{\text{ref}} \tau_e}{L^2} A_{\text{en.ap}} = \frac{I_{\text{ref}} \pi D_{\text{ob}}^2}{4L^2}$$

whence, with consideration of (9.39), we obtain

$$\Phi_d = \frac{\pi I_{\text{tr}} R^2 D_{\text{ob}}^2}{6L^4} \tau_e \tau_e^2 \quad (9.40)$$

In practice, both mirror as well as diffusive reflection occurs simultaneously. Then the total intensity of reflected radiation will be

$$I_z = I_{\text{ref m}} + I_{\text{ref d}}$$

Substituting here the values for $I_{\text{ref m}}$ and $I_{\text{ref d}}$ from (9.34) and (9.39), we find

$$I_z = I_{\text{tr}} \frac{R^2 \tau_e}{4L^2} \tau_m + \frac{2}{3} I_{\text{tr}} \frac{R^2 \tau_e}{L^2} \tau_d = I_{\text{tr}} \frac{R^2 \tau_e}{2L^2} \left(\frac{\tau_m}{2} + \frac{4\tau_d}{3} \right) \quad (9.41)$$

The total value of radiation flux on the receiver entrance on the basis of (9.29) and (9.40) can be calculated using the relation

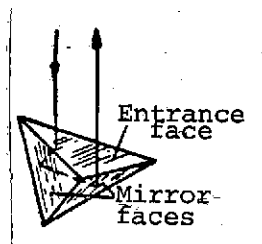
$$\Phi_z = \Phi_m + \Phi_d = I_{\text{tr}} \tau \frac{R^2 D_{\text{ob}}^2}{16L^4} \tau_m^2 \tau_e + I_{\text{tr}} \tau \frac{R^2 D_{\text{ob}}^2}{6L^4} \tau_e^2 \tau_d$$

whence

$$\Phi_r = I_{tr} \frac{\pi R^2 D^2 \tau_e^2}{2L^4} \left(\frac{Q_m}{8} + \frac{Q_d}{3} \right). \quad (9.42)$$

9.4. Calculation of Radiation Intensity with Reflection from Corner Reflectors

To increase the operating range of electro-optical instruments of the active type on objects which should be detected, in a number of cases special devices are installed in the form of corner reflectors or "tail light" reflectors. They are a set of four-sided glass prisms on all faces of which mirror-reflecting coatings have been applied except to the entrance face. All three mirror faces comprise right angles with each other (Fig. 9.5). The basic property of such prisms is that the pencil of rays which falls on the entrance face, after reflections from the mirror faces, leaves the prism in the opposite direction. /277



The divergence of the reflected pencil increases somewhat as a result of the diffraction effect and the imprecision in manufacturing the "tail light" reflectors and will comprise the value

$$\theta_{ref} = \theta_d + \theta_m, \quad (9.43)$$

Fig. 9.5. Corner reflector

where θ_d and θ_m are components of the angle of divergence of the reflected pencil caused by diffraction and imprecision in manufacture.

The first component can be calculated from the known formula

$$\theta_d = \frac{\lambda}{d \cos \beta},$$

where λ is the wavelength of the incident radiation; d is the linear dimension of the entrance face of one reflector; β is the angle between the beam and the normal to the reflector.

If λ is measured in μm and d in cm, then after the matching of the dimensions, we obtain

$$\theta_d = \frac{\lambda}{d \cos \beta} 10^{-4}. \quad (9.44)$$

The second component depends on the quality of manufacture of the reflector. Assuming that the divergence of the pencil due to imprecision of manufacture of the reflector is n seconds of arc, we have

$$\theta_{\text{ref}} = 10^{-4} \left(\frac{\lambda}{d \cos \beta} + 0.05n \right). \quad (9.45)$$

With the derivation of the relation for calculating the intensity of reflected radiation, in this case we will consider that the elementary reflectors on the object are assembled in a unit with the area of the reflecting surface equal to A_{ref} . On the basis of (1.4), we find that the irradiance created on the object by the transmitter of the instrument of the active type will be

$$E_{\text{ob}} = \frac{4\Phi}{\pi \theta_r^2 L^2} \tau_e, \quad (9.46)$$

where θ_r is the angle of divergence formed by the optical system of the transmitter and directed toward the object; θ_{tr} is the radiation flux emitted by the transmitter within the limits of angle θ_r .

It is not difficult to show that the main share of the radiation which is propagated in the direction of the instrument is reflected by a corner reflector. The value of the reflected flux is determined from the expression /278

$$\Phi_{\text{ref}} = E_{\text{ob}} A_{\text{ref}} \rho_{\text{ref}} = \frac{4\Phi_{\text{tr}} A_{\text{ref}} \tau_e \rho_{\text{ref}} \cos \beta}{\pi \theta_r^2 L^2}, \quad (9.47)$$

where ρ_{ref} is the coefficient of reflection of the radiation of the transmitter by the "tail light" reflector.

Considering that the reflected radiation is propagated in a pencil with angle of divergence θ_{ref} , we find the radiation intensity reflected by the object in the direction of the instrument

$$I_{\text{ref}} = \frac{4\Phi_{\text{ref}}}{\pi\theta_{\text{ref}}^2} \quad (9.48)$$

where $\frac{\pi}{4}\theta_{\text{ref}}^2 = \omega_{\text{ref}}$ is the solid angle within whose limits the laser radiation reflected by the object is propagated in the direction of the instrument.

Substituting in (9.48) the values of the quantities from (9.45) and (9.47), we have

$$I_{\text{ref}} = \frac{16\Phi_{\text{ref}} A_{\text{ref}}^2 \tau_a \tau_0 \tau_f \tau_r}{\pi^2 \theta_{\text{ref}}^2 \left(\frac{\lambda}{d \cos \beta} + 0.05n \right)^2 L^2} 10^8 \quad (9.49)$$

By analogy with (1.8), the value of the radiation reflected by the object which falls on the receiver will be

$$\Phi_{\text{rec}} = I_{\text{ref}} \frac{A_{\text{ant.ap}}}{L^2} \tau_a \tau_0 \tau_f \tau_r$$

whence, after substitution of I_{ref} from (9.49), we obtain

$$\Phi_{\text{rec}} = \frac{16\Phi_{\text{ref}} A_{\text{ref}}^2 A_{\text{en.ap}} \tau_a^2 \tau_0 \tau_f \tau_r}{\pi^2 \theta_{\text{ref}}^2 \left(\frac{\lambda}{d \cos \beta} + 0.05n \right)^2} 10^8 \cos \beta \quad (9.50)$$

At present, corner reflectors are made so precisely that the divergence of a beam after reflection is increased by only 2"-5" of arc, that is, $n = 2-5$ seconds of arc.

The reflecting faces of the "tail light" reflectors are coated with a mirror coating with reflection coefficient $\rho_{\text{ref}} = 0.9$.

With consideration of this, we obtain

$$I_{\text{ref}} = \frac{1.45\Phi_{\text{ref}} A_{\text{ref}}^2 \tau_a \tau_0 \tau_f \tau_r}{\theta_{\text{ref}}^2 \left(\frac{\lambda}{d \cos \beta} + 0.25 \right)^2 L^2} 10^8 \quad (9.51)$$

$$\Phi_{\text{rec}} = \frac{1.45\Phi_{\text{ref}} A_{\text{ref}}^2 A_{\text{en.ap}} \tau_a^2 \tau_0 \tau_f \tau_r}{L^4 \theta_{\text{ref}}^2 \left(\frac{\lambda}{d \cos \beta} + 0.25 \right)^2} 10^8 \cos \beta \quad (9.52) \quad /279$$

These permit calculating the intensity of reflection of the radiation by a corner reflector and the value of the radiation flux attained by the receiver after reflection from the object.

9.5. A Method for Calculating the Functions of the Spectral Density of Selective and Gray Emitters

Frequently, for some selective or gray emitter, one of its integral characteristics is known (emitted flux Φ , luminous intensity I , energy brightness B , energy luminosity R , or irradiance E) and its distribution over the spectrum is given in relative units, i.e., the function of relative spectral density is known and it is required to estimate the radiation of this source in a comparatively narrow angle and have data on its spectral characteristics expressed in absolute units.

With such a posing of the problem, the necessity arises, on the basis of the indicated initial data, to find the corresponding function of spectral density (in absolute units), which corresponds to finding the scale of the function of the relative spectral density. The function of spectral density permits estimating the characteristic of interest in the required band of the spectrum. Let us consider the method of determining the function of spectral density with the following example.

Assume that we know the luminous intensity of the source I and its relative spectral distribution given by the function of relative spectral density $i_{rel}(\lambda)$ (Fig. 9.6). It is required to find the function of spectral density of luminous intensity $i(\lambda)$ and its maximum value.

In accordance with (1.23), we have

$$I = \int_0^{\infty} i(\lambda) d\lambda \quad (9.53)$$

We transform this expression in the following manner. Referring the current value of the function of spectral density of luminous intensity $i(\lambda)$ to its maximum value $i_{max}(\lambda)$, we

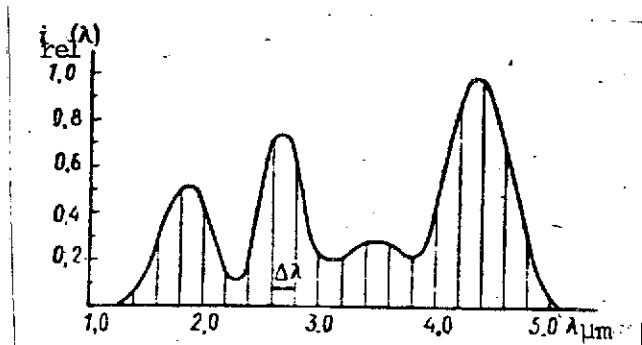


Fig. 9.6. Function of relative spectral density of luminous intensity.

obtain the function of relative spectral density of the luminous intensity $i_{\text{rel}}(\lambda)$:

$$i_{\text{rel}}(\lambda) = \frac{i(\lambda)}{i_{\text{max}}(\lambda)}, \quad (9.54)$$

whence we have

$$i(\lambda) = i_{\text{max}}(\lambda) i_{\text{rel}}(\lambda). \quad (9.55)$$

Substituting (9.55) in (9.53), we find

$$I = i_{\text{max}}(\lambda) \int_0^{\infty} i_{\text{rel}}(\lambda) d\lambda. \quad (9.56)$$

The solution of this equation relative to $i_{\text{max}}(\lambda)$ gives

$$i_{\text{max}}(\lambda) = \frac{I}{\int_0^{\infty} i_{\text{rel}}(\lambda) d\lambda}. \quad (9.57)$$

Inasmuch as in the majority of cases the function $i_{\text{rel}}(\lambda)$ and any other function of relative spectral density has no analytical expression, the integral of the denominator in formula (9.57) is usually calculated by graphical integration.

Setting ourselves the integration step $\Delta\lambda$, let us analyze the entire band of the spectrum where $i_{\text{rel}}(\lambda) \neq 0$ for intervals with width $\Delta\lambda_j$. Replacing the integral by the summation sign with the selected integration step, we can write

$$\int_0^{\infty} i_{\text{rel}}(\lambda) d\lambda \simeq \sum_{j=1}^n i_{\text{rel}}(\lambda_j) \Delta\lambda_j, \quad (9.58)$$

where $i_{\text{rel}}(\lambda_j)$ is the values of the ordinate of the function $i_{\text{rel}}(\lambda)$ read from the graph and corresponding to the middle of intervals $\Delta\lambda_j$.

With an integration step invariable for the spectrum ($\Delta\lambda_j = \Delta\lambda$) = const, carrying $\Delta\lambda$ beyond the summation sign, from (9.58) we have

$$\int_0^{\infty} i_{\text{rel}}(\lambda) d\lambda \simeq \Delta\lambda \sum_{j=1}^n i_{\text{rel}}(\lambda_j). \quad (9.59)$$

Thus, the integral of the denominator is the product of the width of the integration step times the sum of the ordinates of the function for all division intervals.

Substituting (9.59) in (9.57), we obtain

$$I_{\max}(\lambda) = \frac{I}{\Delta\lambda \sum_{i=1}^n i_{\text{rel}} \lambda_j} \quad (9.60)$$

We obtain the relation for finding the current values of the function of spectral density of radiation intensity $i(\lambda)$ from (9.55) with consideration of (9.60). It will have the form

$$i(\lambda) = i_{\text{rel}}(\lambda) \frac{I}{\Delta\lambda \sum_{i=1}^n i_{\text{rel}}(\lambda_j)} \quad (9.61)$$

By analogy with (9.60) and (9.61), formulas can be obtained for calculating the functions of spectral density of other radiation characteristics: radiation flux of energy brightness, energy luminosity, irradiance. For example, for radiation flux, the formulas will have the form

$$\phi_{\max}(\lambda) = \frac{\Phi}{\Delta\lambda \sum_{i=1}^n \phi_{\text{rel}}(\lambda_j)}; \quad (9.62)$$

$$\phi(\lambda) = \phi_{\text{rel}}(\lambda) \frac{\Phi}{\Delta\lambda \sum_{i=1}^n \phi_{\text{rel}}(\lambda_j)} \quad (9.63)$$

Example. It is required to determine the intensity of radiation of a selective source in the band of the spectrum from $\lambda_1 = 4.2 \mu\text{m}$ to $\lambda_2 = 4.5 \mu\text{m}$ if it is known that its luminous intensity in the band from 2 to 5.5 μm equals $I = 5 \cdot 10^5 \text{ W/sr}$ and its distribution over the spectrum is characterized by curve 1 in Fig. 9.7.

We will solve this problem in the following sequence:

1) If the scale of curve 1 is arbitrary, then taking its greatest value as unity, we construct the function of relative spectral density of luminous intensity $i_{\text{rel}}(\lambda)$ in a unit scale (curve 2);

2) Assigning integration step $\Delta\lambda = 0.1 \mu\text{m}$, we read from the graph the values of the function i_{rel} (ordinates of curve 2) which correspond to the middles of the intervals and tabulate them in Table 9.3:

TABLE 9.3.

λ_j	2.0	2.1	2.2	2.3	2.4	2.5	2.6	2.7	2.8	2.9	3.0	3.1	3.2	3.3	3.4	3.5	3.6
$i_{\text{rel}}(\lambda_j)$	0.33	0.22	0.21	0.22	0.28	0.35	0.35	0.38	0.36	0.31	0.22	0.18	0.17	0.20	0.21	0.22	0.21
λ_j	3.7	3.8	3.9	4.0	4.1	4.2	4.3	4.4	4.5	4.6	4.7	4.8	4.9	5.0	5.1	5.2	5.3
$i_{\text{rel}}(\lambda_j)$	0.21	0.20	0.18	0.22	0.35	0.79	1.00	0.84	0.43	0.22	0.12	0.05	0.03	0.02	0.01	0.00	0.00

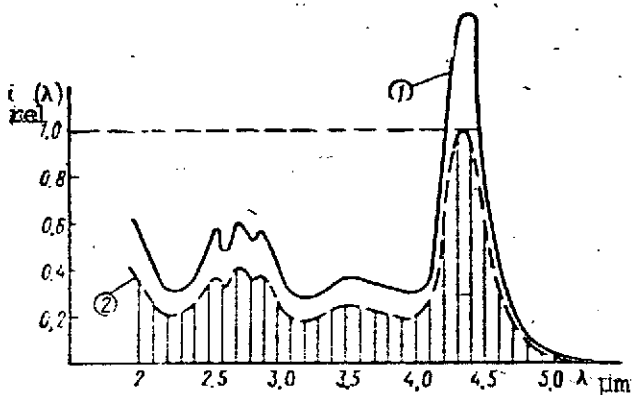


Fig. 9.7. Graphs of spectral distribution of luminous intensity: 1. spectral distribution of luminous intensity at an arbitrary scale; 2. function of relative spectral density of luminous intensity (on a unit scale).

3) Summing all values of $i_{\text{rel}}(\lambda)$, we find that

/282

$$\sum_{i=1}^n i_{\text{rel}}(\lambda_i) = 10$$

4) From formula (9.60), we determine the maximum value of the function of spectral density of luminous intensity

$$i_{\text{max}}(\lambda) = \frac{I}{\Delta\lambda \sum_{i=1}^n i_{\text{rel}}(\lambda_i)} = \frac{5 \cdot 10^5}{0.1 \cdot 10} = 5 \cdot 10^5 \text{ W/(sr} \cdot \mu\text{m)}$$

5) Using relation (9.55), we find the values of the function of spectral density of energetic luminous

intensity on arbitrary wavelengths

$$i(\lambda) = i_{\text{max}}(\lambda) i_{\text{rel}}(\lambda) = 5 \cdot 10^5 \cdot i_{\text{rel}}(\lambda) \text{ W/(sr} \cdot \mu\text{m)}$$

6) For calculating luminous intensity $I_{\Delta\lambda}$ in the band of the spectrum from $\lambda_1 = 4.2 \mu\text{m}$ to $\lambda_2 = 4.5 \mu\text{m}$, considering (9.60) we use the formula

$$I_{\Delta\lambda} = i_{\max}(\lambda) \Delta\lambda \sum_{j=1}^m i_{\text{rel}}(\lambda_j) = 5 \cdot 10^5;$$

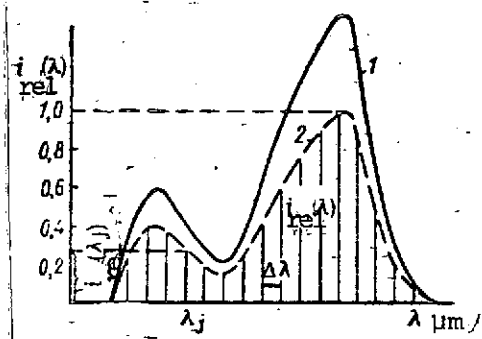
7) In the indicated band of the spectrum from $\lambda_1 = 4.2 \mu\text{m}$ to $\lambda_2 = 4.5 \mu\text{m}$, we determine the value of $\sum_{j=1}^m i_{\text{rel}}(\lambda_j) = 0.79 + 1.00 + 0.84 = 2.63$ (corresponding values from (λ_1) isolated in the table);

8) We find the required luminous intensity from the formula

$$I_{\Delta\lambda} = 5 \cdot 10^5 \cdot 0.1 \cdot \sum_{j=1}^m i_{\text{rel}}(\lambda_j) = 5 \cdot 10^5 \cdot 0.1 \cdot 2.63 \approx 131\,000 \text{ W/sr.}$$

9.6. Determination of the Characteristics of the Radiation of a Source from the Known Value of the Functions of Spectral Density /283

We will consider that one of the functions of relative spectral density, for example, the luminous intensity constructed in an arbitrary scale (curve 1, Fig. 9.8), and the value of monochromatic radiation intensity in the band of the spectrum $\Delta\lambda_j$ on wavelength λ_j are known, i.e., $i_{\text{rel}}(\lambda)$ and $I_{\Delta\lambda_j}$ are given. It is required to determine $i_{\max}(\lambda)$, $i(\lambda)$, and I .



From the known value of the intensity of monochromatic radiation $I_{\Delta\lambda_j}$ in the band $\Delta\lambda_j$ we find the value of the function of spectral density of the luminous intensity on the wavelength λ_j :

$$i(\lambda_j) = \frac{I_{\Delta\lambda_j}}{\Delta\lambda_j} \quad (9.64)$$

Fig. 9.8. Functions of relative spectral density of radiation: 1. in an arbitrary scale; 2. in a unit scale.

If a graph of relative spectral density of luminous intensity is presented in an arbitrary scale, then it is necessary, taking the greatest of its maximums as unity, to construct the function of relative spectral density in a unit scale (curve 2).

We determine the value of function $i_{rel}(\lambda)$ on wavelength λ , and, using relation (9.55), we find

$$i_{max}(\lambda) = \frac{i(\lambda_j)}{i_{rel}(\lambda_j)}. \quad (9.65)$$

From the value of $i_{max}(\lambda)$ now known, on the basis of (9.60) we determine the luminous intensity of the source

$$I = i_{max}(\lambda) \Delta\lambda \sum_{j=1}^m i_{rel}(\lambda_j), \quad (9.66)$$

and from formula (9.55), with consideration of (9.65), we obtain the expression for calculating the values of the function of spectral density of luminous intensity on any wavelength

$$i(\lambda) = \frac{i(\lambda_j)}{i_{rel}(\lambda_j)} i_{rel}(\lambda_j). \quad (9.67)$$

Similarly, we obtain the formula for the calculation of other characteristics of sources of radiation. For radiation flux, for example, these formulas can be written in the form

/284

$$\begin{aligned} \phi_{max}(\lambda) &= \frac{\phi(\lambda_j)}{\phi_{rel}(\lambda_j)}; \\ \Phi &= \phi_{max}(\lambda) \Delta\lambda \sum_{j=1}^n \phi_{rel}(\lambda_j) \end{aligned}$$

and

$$\phi(\lambda) = \frac{\phi(\lambda_j)}{\phi_{rel}(\lambda_j)} \phi_{rel}(\lambda_j).$$

(9.68)

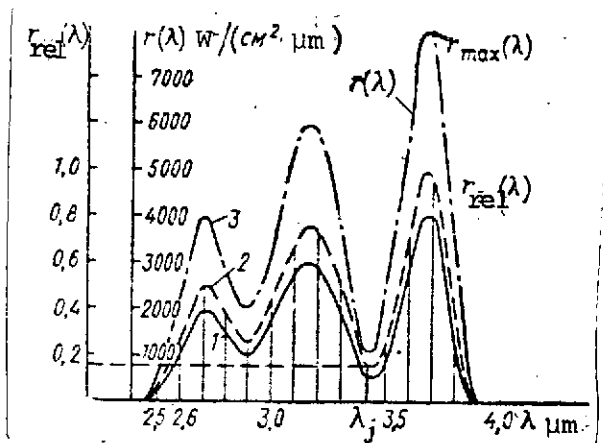


Fig. 9.9. Curves of the spectral density of the energy luminosity of a source (for the solution of the problem):

1. relative spectral energy luminosity in arbitrary scale;
2. function of relative spectral density of energy luminosity;
3. function of spectral density of energy luminosity.

Example. Assume that the relative spectral distribution of energetic radiosity $r_{rel}(\lambda)$ given by the graph (Fig. 9.9) is known. It is also known that on wavelength $\lambda_j = 3.4 \mu m$ the monochromatic energetic radiosity in the band of the spectrum $\Delta\lambda_j = 0.01 \mu m$ is $R_{\Delta\lambda_j} = 12.0 W/cm^2$.

It is required to determine R , $r_{max}(\lambda)$ and $r(\lambda)$:

1) We construct a graph of the function of relative spectral density of energy luminosity $r_{rel}(\lambda)$ (so that its maximum value equals 1.0);

2) We determine the value of the function $r_{rel}(\lambda_j)$ on wavelength $\lambda_j = 3.4 \mu m$. From the graph, we have $r_{rel}(\lambda_j) = 0.15$;

3) From the given $R_{\Delta\lambda_j}$ and $\Delta\lambda_j$, by analogy with (9.64) we find

$$r(\lambda_j) = \frac{R_{\Delta\lambda_j}}{\Delta\lambda_j} = \frac{12.0 W/cm^2}{0.01 \mu m} = 1200 W/(cm^2 \cdot \mu m);$$

4) Using an expression analogous to (9.65), from the known $r(\lambda_j) = 1200 W/cm^2 \cdot \mu m$ and from $r_{rel}(\lambda_j) = 0.15$, we find /285

$$r_{max}(\lambda) = \frac{r(\lambda_j)}{r_{rel}(\lambda_j)} = \frac{1200}{0.15} = 8000 W/(cm^2 \cdot \mu m);$$

5) We divide the entire band of the spectrum where $r_{rel}(\lambda) \neq 0$ into intervals with step $\Delta\lambda = 0.1 \mu m$ and we find the values of function $r_{rel}(\lambda_j)$ which correspond to the middles of the intervals (ordinates of the curve from the graph) and we tabulate them

λ_j	2.5	2.6	2.7	2.8	2.9	3.0	3.1	3.2	3.3	3.4	3.5	3.6	3.7	3.8	3.9	4.0
$r_{rel}(\lambda_j)$	0.12	0.40	0.48	0.32	0.32	0.53	0.75	0.63	0.30	0.15	0.45	0.96	0.70	0.05	0.00	0.00

6) Adding all values of $r_{rel}(\lambda_j)$, we find

$$\sum_{j=1}^n r_{rel}(\lambda_j) = 6.20;$$

7) Using the results of parts 4 and 6, we compute

$$R = r_{max}(\lambda) \Delta\lambda \sum_{j=1}^n r_{rel}(\lambda_j) = 8000 \text{ W}/(\text{cm}^2 \mu\text{m}) \cdot 0.1 \cdot 6.20 = 4960 \text{ W}/\text{cm}^2;$$

8) Using the relation

$$r(\lambda) = \frac{r(\lambda_j)}{r_{rel}(\lambda_j)} r_{rel}(\lambda) = 8000 \cdot r_{rel}(\lambda) \text{ W}/(\text{cm}^2 \mu\text{m}).$$

we find the values of the function of spectral density of energy luminosity.

9.7. A Method for Determining the Radiation Characteristics of Emitters Which Are Nonuniformly Heated

Let us examine the simplest case where the temperature of the radiating surface changes linearly with regard to one of the coordinates. As an example, let us take a flat rectangular radiating surface, whose temperature changes linearly along dimension H (Fig. 9.10) and let us determine the energy brightness for it.

On the radiating surface, we discriminate the area element dA and on the basis of (1.12) we write the expression for the determination of the luminous intensity of this area along the normal to the surface

$$dI = \frac{R(T)}{\pi} dA = \frac{\epsilon\sigma T^4}{\pi} dA, \quad (9.69)$$

where $dA = Hd\ell$ is the area of the radiating surface element; T is the temperature of the radiating surface element dA .

With a linear change in temperature along dimension H from T_1 to T_2 , the current temperature value at height h from the base will be /286

$$T = T_1 + ah, \quad (9.70)$$

Fig. 9.10. For the determination of the characteristics of radiation of nonuniformly heated flat emitters with a rectangular shape.

where

$$a = \frac{T_2 - T_1}{H} = \frac{\Delta T}{H}.$$

Substituting the values dA and T in (9.60), we obtain

$$dI = \frac{\epsilon \sigma l}{\pi} \left[T_1 + \frac{T_2 - T_1}{H} h \right]^4 dh. \quad (9.71)$$

The luminous intensity of the entire surface is found by integrating expression (9.71) for the variable h :

$$I = \int_h dI = \frac{\epsilon \sigma l}{\pi} \int_0^H \left(T_1 + \frac{\Delta T}{H} h \right)^4 dh. \quad (9.72)$$

Integration provides

$$I = \frac{\epsilon \sigma l H}{5\pi(T_2 - T_1)} \left(T_1 + \frac{T_2 - T_1}{H} h \right)^5 \Big|_0^H.$$

After substitution of the limits of integration we obtain

$$I = \frac{\epsilon \sigma l H}{5\pi} \frac{T_2^5 - T_1^5}{T_2 - T_1}. \quad (9.73)$$

or

$$I = \frac{\epsilon_0 l H}{5\pi} (T_2^4 - T_2^3 T_1 + T_2^2 T_1^2 + T_2 T_1^3 + T_1^4). \quad (9.74)$$

Introducing the designation $\Delta T = T_2 - T_1$, by means of simple conversions from (9.74) we will have

$$I = \frac{\epsilon_0 l H}{5\pi} T_1^4 \left[1 + \left(1 + \frac{\Delta T}{T_1} \right) + \left(1 + \frac{\Delta T}{T_1} \right)^2 + \left(1 + \frac{\Delta T}{T_1} \right)^3 \times \right. \quad (9.75)$$

$$\left. \times \left(1 + \frac{\Delta T}{T_1} \right)^4 \right]; \quad (9.76)$$

$$I = \frac{\epsilon_0 l H}{5\pi} T_1^4 (1 + p + p^2 + p^3 + p^4),$$

where $p = 1 + \frac{\Delta T}{T_1}.$

On the other hand, if the temperature is the same over the entire radiating surface, the luminous intensity is determined by the expression /287

$$I = \frac{\epsilon_0 l H}{\pi} T^4. \quad (9.77)$$

From a comparison of (9.76) and (9.77), it is obvious that for a nonuniform heated radiating surface we can select that value of equivalent temperature at which the luminous intensity of the surface proves to be identical to the luminous intensity of a surface with temperature nonuniform over the surface. Equating the right sides of equalities (9.76) and (9.77) we obtain

$$\frac{T_{\text{equiv}}^4}{5} = \frac{T_1^4}{5} (1 + p + p^2 + p^3 + p^4). \quad (9.78)$$

We note that even in the simplest case, when the temperature changes linearly along the radiating surface, the equivalent temperature differs from the mean temperature of the surface and, what is more, the luminous intensities differ. What has been said is graphically confirmed by the data in Fig. 9.11 where the character of change of the equivalent temperature of

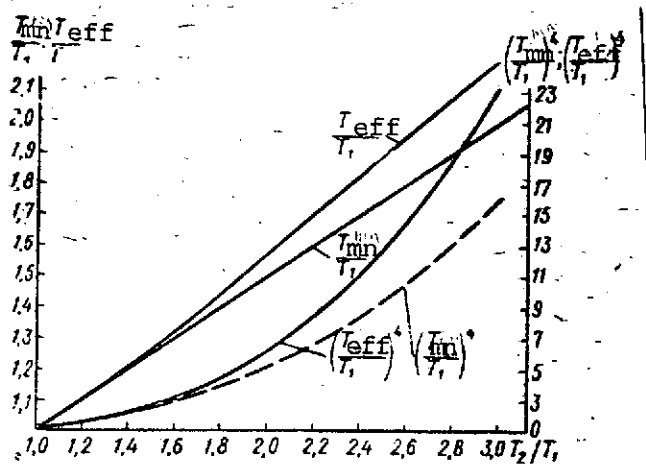


Fig. 9.11. Character of change of effective and mean temperatures and energy brightness which correspond to these temperatures.

the surface with an increase in the difference between the minimum and mean temperatures of the surface is shown. This same figure shows a graph of the relative change in luminous intensity with increase in ΔT for a surface with temperatures T_{equiv} and T_{mn} .

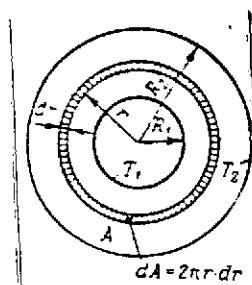
Calculations show that the difference between T_{equiv} and T_{mn} reaches 5% with $\Delta T = 2$ and with $\Delta T = 1.6$, does not exceed 2.5%. At the same time, the luminous intensity with

/288

the same values of ΔT differ already by 10 and 20%.

Hence, the conclusion can be drawn that with insignificant temperature differentials within the limits of the radiating surface being considered, the nonuniformity of heating can be considered by the introduction of mean temperature and with large differentials, it is expedient to use equivalent temperature.

Let us consider a circular idealized emitter whose temperature changes linearly along the radius.



In order to determine the luminous intensity of the entire area we first find the energy brightness of a circular zone element (Fig. 9.12) and we integrate it for the entire surface of the circle.

With a linear temperature change along the radius, its value within the limits of the circular zone element dA will be

Fig. 9.12. For a determination of the characteristics of radiation of a nonuniformly heated flat circular emitter.

$$T = T_1 + \frac{T_2 - T_1}{R_2 - R_1} (r - R_1), \quad (9.79)$$

where T_1 is the temperature of the radiating surface at distance R_1 from

the center; T_2 is the temperature at the edge of the radiating area at distance R_2 from the center; r is the radius of the circular zone element.

The luminous intensity of the circular zone element with temperature of the radiating surface T will be

$$dI = \frac{\epsilon \sigma T^4}{\pi} dA, \quad (9.80)$$

where $dA = 2\pi r dr$; dr is the width of the circular zone.

From (9.80), with consideration of (9.79), we have

$$dI = \frac{2\pi\epsilon\sigma}{\pi} \left[T_1 + \frac{T_2 - T_1}{R_2 - R_1} (r - R_1) \right]^4 r dr,$$

then the luminous intensity of the circle with linearly changing temperature will be

$$I = \int_A dI = 2\epsilon\sigma \int_{R_1}^{R_2} \left[T_1 + \frac{T_2 - T_1}{R_2 - R_1} (r - R_1) \right]^4 r dr. \quad (9.81)$$

The solution of equation (9.81) provides

/289

$$\begin{aligned} I = 2\epsilon\sigma \left\{ T_1^4 \frac{R_2^2 - R_1^2}{2} + 4T_1^3 \frac{T_2 - T_1}{R_2 - R_1} \left[\frac{R_2^3 - R_1^3}{3} - \frac{R_2^2 - R_1^2}{2} R_1 \right] + \right. \\ + 6T_1^2 \left(\frac{T_2 - T_1}{R_2 - R_1} \right)^2 \left[\frac{R_2^4 - R_1^4}{4} - \frac{2}{3} R_1 (R_2^3 - R_1^3) + \frac{1}{2} R_1^2 (R_2^2 - R_1^2) \right] + \\ + 4T_1 \left(\frac{T_2 - T_1}{R_2 - R_1} \right)^3 \left[\frac{R_2^5 - R_1^5}{5} - \frac{3}{4} R_1 (R_2^4 - R_1^4) + R_1^2 (R_2^3 - R_1^3) - \right. \\ \left. - \frac{1}{2} R_1^3 (R_2^2 - R_1^2) \right] + \left(\frac{T_2 - T_1}{R_2 - R_1} \right)^4 \left[\frac{R_2^6 - R_1^6}{6} - \frac{4}{5} R_1 (R_2^5 - R_1^5) + \right. \\ \left. + \frac{3}{2} R_1^2 (R_2^4 - R_1^4) - \frac{4}{3} R_1^3 (R_2^3 - R_1^3) + \frac{1}{2} R_1^4 (R_2^2 - R_1^2) \right] \left. \right\}. \end{aligned}$$

carrying T_1 outside the brackets and designating $T_2 - T_1 = \Delta T$, we obtain

$$I = \varepsilon \sigma T_1^4 \left\{ 1 + 8 \frac{\Delta T}{T_1} \frac{1}{R_2 - R_1} \left[\frac{R_2^3 - R_1^3}{3} - \frac{R_2^2 - R_1^2}{2} R_1 \right] + \right. \\ + 12 \left(\frac{\Delta T}{T_1} \right)^2 \frac{1}{(R_2 - R_1)^2} \left[\frac{R_2^4 - R_1^4}{4} - \frac{2}{3} R_1 (R_2^3 - R_1^3) + \right. \\ + \left. \frac{1}{2} R_1^2 (R_2^2 - R_1^2) \right] + 4 \left(\frac{\Delta T}{T_1} \right)^3 \frac{1}{(R_2 - R_1)^3} \left[\frac{R_2^5 - R_1^5}{5} - \right. \\ - \frac{3}{4} R_1 (R_2^4 - R_1^4) + R_1^2 (R_2^3 - R_1^3) - \left. \frac{1}{2} R_1^3 (R_2^2 - R_1^2) \right] + \\ + \left(\frac{\Delta T}{T_1} \right)^4 \frac{1}{(R_2 - R_1)^4} \left[\frac{R_2^6 - R_1^6}{6} - \frac{4}{5} R_1 (R_2^5 - R_1^5) + \right. \\ + \left. \frac{3}{2} R_1^2 (R_2^4 - R_1^4) - \frac{4}{3} R_1^3 (R_2^3 - R_1^3) + \frac{1}{2} R_1^4 (R_2^2 - R_1^2) \right] \left. \right\}. \quad (9.82)$$

simplifying the expression in the brackets, we will have

$$I = \varepsilon \sigma T_1^4 (R_2^2 - R_1^2) \left\{ 1 + \frac{4}{3} \frac{\Delta T}{T_1} \frac{2R_2^3 - 3R_2^2 R_1 + R_1^3}{(R_2^2 - R_1^2)(R_2 - R_1)} + \right. \\ + \left(\frac{\Delta T}{T_1} \right)^2 \frac{3R_2^4 - 8R_2^3 R_1 + 6R_2^2 R_1^2 - R_1^4}{(R_2^2 - R_1^2)(R_2 - R_1)^2} + \\ + \frac{1}{5} \left(\frac{\Delta T}{T_1} \right)^3 \frac{4R_2^5 - 15R_2^4 R_1 + 20R_2^3 R_1^2 - 10R_2^2 R_1^3 + R_1^5}{(R_2^2 - R_1^2)(R_2 - R_1)^3} + \\ + \left. \frac{1}{30} \left(\frac{\Delta T}{T_1} \right)^4 \frac{5R_2^6 + 24R_2^5 R_1 + 45R_2^4 R_1^2 - 40R_2^3 R_1^3 + 15R_2^2 R_1^4 - R_1^6}{(R_2^2 - R_1^2)(R_2 - R_1)^4} \right\}. \quad (9.83)$$

If the radiating disk is continuous, i.e., $R_1 = 0$, the expression (9.83) is simplified considerably and takes the form

$$I = \varepsilon \sigma T_1^4 R_2^2 \left[1 + \frac{8}{3} \left(\frac{\Delta T}{T_1} \right) + 3 \left(\frac{\Delta T}{T_1} \right)^2 + \frac{4}{5} \left(\frac{\Delta T}{T_1} \right)^3 + \frac{1}{6} \left(\frac{\Delta T}{T_1} \right)^4 \right]. \quad (9.84)$$

By analogy with the preceding, the equivalent temperature of a nonuniformly heated disk will be

$$T_{\text{equiv}} = T_1^4 \left[1 + \frac{8}{3} \frac{\Delta T}{T_1} + 3 \left(\frac{\Delta T}{T_1} \right)^2 + \frac{4}{5} \left(\frac{\Delta T}{T_1} \right)^3 + \frac{1}{6} \left(\frac{\Delta T}{T_1} \right)^4 \right]. \quad (9.85)$$

If the temperature differential from the center of the disk to the edges does not exceed 0.04 and it can be ignored, then

$$T_{\text{equiv}} = T_1^4 \left[1 + \frac{8}{3} \frac{\Delta T}{T_1} + 3 \left(\frac{\Delta T}{T_1} \right)^2 \right]. \quad (9.86)$$

With $0.5T_1 < T_2 - T_1 \leq T_1$, we can ignore the last term in the brackets, the relative value of which does not exceed 0.025.

Finally, with $T_2 - T_1 > T_1$, it is necessary to calculate the equivalent temperature with consideration of all components, i.e., from formula (9.85).

The luminous intensity of the disk with the temperature of the radiating surface which changes linearly from the center to the edges, expressed through the equivalent, will be

$$I = \epsilon \sigma R_2^2 T_{\text{equiv}}^4 \quad (9.87)$$

If the shape of the radiating surface differs from a rectangle or a circle and the law of temperature change is not linear, the approach to the solution of the problem remains as formerly. It is necessary to find the law of change of the dimensions of the radiating area element and the law of change of the surface temperature, place them in agreement with each other and, taking the integral from an expression of the type (9.59) in which dA and T will correspond to the situation being examined, to find the desired radiation characteristic.

CHAPTER 10. ENERGY CALCULATION FOR ELECTRO-OPTICAL INSTRUMENTS

10.1. The Problems of Energy Calculation

The problems of energy calculation of electro-optical equipment are the determination of the values of some parameters with which the required relationship between the useful signal and the signal caused by the internal (intrinsic noises of the receiver) and external (background radiation) interference is assured at the output of the radiation receiver. These problems are reduced to the calculation of either the threshold sensitivity and range of action of the instrument with given parameters or to finding the values of these parameters in accordance with given range of action or threshold sensitivity. /291

The range of action and threshold sensitivity of an electro-optical instrument are its most important characteristics. Both these concepts are practically identical, but one of them (range of action) is used in work on radiating objects at finite distances away, while the second is used most often as applicable to equipment intended for operation with infinitely distant emitters, for example, with the stars.

In the energy calculation of electro-optical instruments, the following cases may be encountered:

- The observed object is projected on a nonradiating background;
- The object is projected on a uniformly radiating background;
- The radiating background on which the object is projected is nonuniform.

In any of the indicated cases, the initial data for the power calculation of electro-optical equipment are data which characterize the radiation of the object, background, spectral transparency of the environment and elements of the optical system, and sensitivity of the receiver. Included in the data on radiation of the object are:

- The spectral composition of the radiation which is described by one of the functions of spectral density: radiation flux $\phi(\lambda)$, energetic luminous intensity $i(\lambda)$, energy brightness $b(\lambda)$, irradiance $r(\lambda)$;
- Area of the radiating surface A_r ;
- Emittance coefficient $\epsilon(\lambda)$;
- Contrast-frequency characteristic.

Let us note that the spectral composition of the radiation of ideal black and gray bodies can be determined if the temperature T of the radiating surface is known.

Therefore, for such emitters, the temperature of the radiating surface T is usually given instead of the functions $\phi(\lambda)$, $b(\lambda)$ and so forth.

10.2. Calculations of the Range of Action and Threshold Sensitivity of Instruments in the Absence of a Background

The first stage of the energy calculation is reduced to the determination of the amount of radiation flux from the object which falls on the radiation receiver.

Inasmuch as the spectral composition of the radiation flux of an object is generally described by an arbitrary function of spectral density and, in the path of propagation, undergoes selective attenuation in the medium and elements of the optical system, it is necessary to conduct all reasonings and derivations of relations as applicable to a monochromatic radiation flux with the subsequent change to integral radiation. /292

The monochromatic radiation flux from an object which falls on the instrument is determined as the function of spectral density of energy brightness $b(\lambda)$ and the dimensions of the radiating surface A_r , and also as the value of the solid angle ω within whose limits the flux which is propagated from an object falls on the electro-optical instrument (Fig. 10.1).

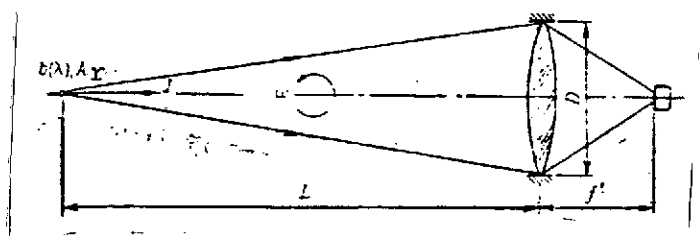


Fig. 10.1. For the derivation of the equation of the range of action of an electro-optical instrument.

For an IBB or gray body with a known temperature, function $b(\lambda)$ is described by the relation

$$b(\lambda) = \frac{r(\lambda, T)}{\pi}$$

monochromatic radiation flux which enters the instrument, without consideration of attenuation by the medium, will be

$$d\Phi_\lambda = i(\lambda) \omega d\lambda = A_r b(\lambda) \omega \cos \alpha d\lambda \quad (10.1)$$

Designating in the expression which has been obtained

$$A_{\text{r}} b(\lambda) \omega \cos(\alpha) = \phi(\lambda), \quad (10.2)$$

we have

$$d\Phi_{\lambda} = \phi(\lambda) d\lambda = A_{\text{r}} b(\lambda) \omega \cos \alpha d\lambda, \quad (10.3)$$

where $\omega = \frac{A_{\text{en.ap}}}{L^2}$; $A_{\text{en.ap}}$ is the area of the entrance pupil of the instrument on which the solid angle ω is based; L is the distance from the instrument to the radiating object.

With consideration of the attenuation of the flux in the medium and components of the optical system and keeping in mind the designations which have been introduced from (10.3), we obtain the relation which determines the amount of radiation flux which reaches the receiver: /293

$$d\Phi_{\lambda, \text{rec}} = \phi(\lambda) \tau_e(\lambda) \tau_0(\lambda) d\lambda = \frac{A_{\text{rad}} A_{\text{en.ap}}}{L^2} b(\lambda) \tau_e(\lambda) \tau_0(\lambda) \cos \alpha d\lambda, \quad (10.4)$$

where $\tau_0(\lambda)$ and $\tau_e(\lambda)$ are, respectively, the functions of spectral transmission of the radiation flux of the optical system and the medium.

This relation is often also used in the following form

$$\begin{aligned} d\Phi_{\lambda, \text{rec}} &= \phi(\lambda) \tau_e(\lambda) \tau_0(\lambda) d\lambda = \\ &= \frac{A_{\text{en.ap}}}{L^2} \phi(\lambda) \tau_e(\lambda) \tau_0(\lambda) d\lambda. \end{aligned} \quad (10.5)$$

The value of the monochromatic radiation flux effective for a given receiver will be

$$d\Phi_{\lambda, \text{eff}} = \phi(\lambda) \tau_e(\lambda) \tau_0(\lambda) s(\lambda) d\lambda. \quad (10.6)$$

Then, the effective value of the complex radiation flux which falls on the receiver can be calculated by integrating

expression (10.6) for all wavelengths, i.e.,

$$\Phi_{\text{eff}} = \int_0^{\infty} \phi(\lambda) \tau_e(\lambda) \tau_0(\lambda) s(\lambda) d\lambda. \quad (10.7)$$

Multiplying and dividing the right side of equality (10.7) by the same value $\int_0^{\infty} \phi(\lambda) d\lambda$, we obtain

$$\Phi_{\text{eff}} = \frac{\int_0^{\infty} \phi(\lambda) \tau_e(\lambda) \tau_0(\lambda) s(\lambda) d\lambda}{\int_0^{\infty} \phi(\lambda) d\lambda} \int_0^{\infty} \phi(\lambda) d\lambda. \quad (10.8)$$

The relation of the integrals in this expression is nothing but the utilization coefficient of the receiver for actual radiation with consideration of attenuation of the flux by the medium and components of the optical system

$$k_r = \frac{\int_0^{\infty} \phi(\lambda) \tau_e(\lambda) \tau_0(\lambda) s(\lambda) d\lambda}{\int_0^{\infty} \phi(\lambda) d\lambda}. \quad (10.9)$$

and the integral $\int_0^{\infty} \phi(\lambda) d\lambda$ is the total radiation flux of the object at the entrance of the instrument without consideration of its attenuation by the medium, i.e., /294

$$\int_0^{\infty} \phi(\lambda) d\lambda = \Phi_r$$

With consideration of the designations which have been introduced from (10.8), we have

$$\Phi_{\text{eff}} = \Phi_r k_r \quad (10.10)$$

where

$$\Phi_r = A_{\text{enap}} I_{\text{ob}} L^{-2}$$

We can come to a similar result in a different way. If we make the selective attenuation of the flux by the medium and the optical system similar to the attenuation of the flux by a filter which operates together with the radiation receiver, the relative spectral sensitivity of such a reduced receiver can be presented in the form

$$s'(\lambda) = s(\lambda) \tau_e(\lambda) \tau_o(\lambda). \quad (10.11)$$

Thus, considering at the entrance to the instrument the flux unattenuated by the atmosphere which is characterized by the function $\phi(\lambda)$ for the effective values of the monochromatic and complex radiation fluxes, we will have, respectively

$$\begin{aligned} d\Phi_{\text{eff}} &= \phi(\lambda) s'(\lambda) d\lambda, \\ \Phi_{\text{eff}} &= \int_0^\infty \phi(\lambda) s'(\lambda) d\lambda. \end{aligned}$$

Multiplying and dividing the right side of the last equality by the quantity $\int_0^\infty \phi(\lambda) d\lambda = \Phi_r$ we obtain

$$\Phi_{\text{eff}} = \Phi_r \frac{\int_0^\infty \phi(\lambda) s'(\lambda) d\lambda}{\int_0^\infty \phi(\lambda) d\lambda} = \Phi_r k_r, \quad (10.12)$$

where the expression for the coefficient of utilization of the receiver for an actual emitter is written in the usual form, but after the substitution of the value $s'(\lambda)$ it becomes identical with (10.9).

The second stage of the power calculation consists of the direct determination of the range of action.

In order to discriminate the signal from the objects against a background of noises at the output of the instrument, the effective value of the radiation flux from it should exceed the effective value of the threshold flux of the receiver by a given number of times m /295

or

$$\begin{aligned} \Phi_{\text{eff}} &\geq m \Phi_{\text{t. eff}} \\ \Phi_r k_r &\geq m \Phi_{s.t} k_s \end{aligned} \quad (10.13)$$

where m is the signal-noise relationship; $\Phi_{s.t}$ is the threshold flux of the receiver in accordance with the standard emitter; k_r and k_s are the utilization coefficients for the radiation of an actual and standard source.

The value of the coefficient m depends on the purpose of the instrument and the problems solved by it. In detection, for the dependable discrimination of the useful signal from the noises, $m = 5-10$ is taken; during measurements the coefficient m reaches 20-50 or more.

From (10.13), we obtain

$$\Phi_r = m \Phi_{s.t} \frac{k_s}{k_r} \quad (10.14)$$

Considering that $\Phi_r = I\omega$ and $\omega = A_{\text{en.ap}} L^{-2}$, we find

$$I \frac{A_{\text{en.ap}}}{L^2} m \Phi_{s.t} \frac{k_s}{k_r} \quad (10.15)$$

Here $\Phi_{s.t}$ is the threshold flux of the receiver for the radiation of a standard source when it is connected into the actual circuit of an electro-optical instrument. The value of $\Phi_{s.t}$ can be presented in the general form as

$$\Phi_{s.t} = \Phi_{s.t}^{(1)} k(\Delta f) \quad (10.16)$$

where $k(\Delta f)$ is a coefficient which considers the change in the modulation frequency and width of the transmission band of the amplifier in comparison with the standard measurement conditions. If the width of the frequency band of the amplifier is small in comparison with the modulation frequency, then $k(\Delta f) = \sqrt{\Delta f}$ is taken as this coefficient. In those cases where the modulation frequency f_M differs from the standard f_0 , the indicated coefficient is taken in the form

$$k(\Delta f) = \sqrt{\frac{f_0}{f_m} \Delta f}$$

Keeping (10.16) in mind, from (10.15) we obtain the relation

$$L = \sqrt{\frac{IA_{\text{en.ap}} k_r}{m\Phi_{\text{st}} k(\Delta f) k_r}} \quad (10.17)$$

which permits calculating the range of action of the instrument with given parameters of the emitter, medium, and receiver.

For the case where the emitter is a source at an infinite distance, for example, a star, the effective value of radiation flux is determined from the expression /296

$$\Phi_{\text{eff}} = EA_{\text{en.ap}} k_r \quad (10.18)$$

where $E = \frac{E^{\lambda}}{K_{\text{max}}(\lambda)\eta}$ is the irradiance created by the star at the entrance of the instrument; η is the eye's utilization coefficient of the radiation of a star having color temperature T ; E^{λ} is the illumination created by the star at the entrance of the instrument.

Since $E^{\lambda} = 10^{\frac{-13.75 + m_s}{2.5}}$ then

$$\Phi_{\text{eff}} = 10^{\frac{-13.75 + m_s}{2.5}} \frac{1}{K_{\text{max}}(\lambda)\eta} A_{\text{en.ap}} k_r \quad (10.19)$$

Equating the effective value of the flux from the emitter to the effective threshold flux, by analogy (10.14) we will have

$$A_{\text{en.ap}} = \frac{m\Phi_{\text{st}}^{(1)} k(\Delta f) k_r}{k_r 10^{\frac{-13.75 + m_s}{2.5}}} K_{\text{max}}(\lambda)\eta \quad (10.20)$$

The presented relation provides the opportunity to calculate the area of the instrument's entrance pupil with which the discrimination of the useful signal against a background of intrinsic noises of the radiation receiver and the electronic circuit is assured.

A similar formula can be obtained for the case where the object is projected on a nonradiating background if the required range of action of the instrument is given

$$A_{\text{en.ap}} = \frac{L^2 m \Phi_{s.t}^{(1)} k(\Delta f) k_s}{I k_r} \quad (10.21)$$

If the parameters of the instrument including the area of the entrance pupil are given, in this case we can calculate the threshold sensitivity of the instrument which is characterized by the required level of irradiance at the instrument entrance in accordance with the formula

$$E = \frac{m \Phi_{s.t}^{(1)} k(\Delta f) k_s}{A_{\text{en.ap}} k_r} \quad (10.22)$$

Relations (10.17), (10.20), (10.21), and (10.22) permit calculating the range of action, required area of the entrance pupil, and the threshold of irradiance under conditions where the background is absent or when its influence can be neglected.

10.3. Calculation of the Range of Action and Threshold Sensitivity with the Influence of a Uniform Background /297

With the influence of a uniform background, the relations which determine the range of action of the instrument with given parameters (area of the entrance aperture which assures the required range of action and threshold irradiance) remain basically similar to (10.17), (10.20), (10.21), and (10.22). However, several differences also appear in them which are caused by the constant illumination of the receiver as well as by the presence of some background level on which the emitting object should be detected.

The presence of constant illumination leads to a worsening of the threshold sensitivity of the receiver, i.e., to an increase in the threshold flux. With consideration of the influence of the background, the threshold flux of the receiver $\Phi_{s.t}^b$ will be

$$\Phi_{s.t}^b = \Phi_{s.t} k(\Phi_b) \quad (10.23)$$

where $k(\Phi_b)$ is the coefficient which characterizes the worsening of the threshold flux of the receiver due to constant background illumination.

The energy brightness of the space surrounding the object leads to a reduction in contrast as a result of a reduction in the differential of the energy brightness of the object in comparison with the surrounding space.

The amount of constant illumination caused by the flux from a radiating uniform background can be calculated in the following manner. If the background fills the entire field of view of the instrument (Fig. 10.2), the radiation flux from each area element of the background will be

$$d\Phi_b = dI_b \omega, \quad (10.24)$$

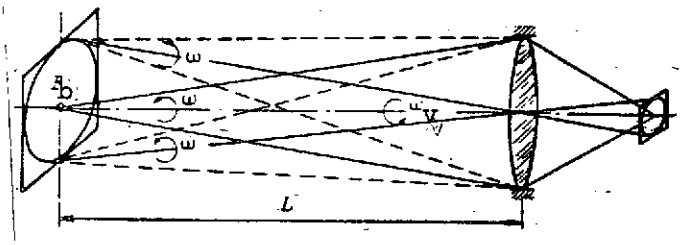


Fig. 10.2. Determination of the amount of radiation flux of a background which lands in the instrument.

ground flux which reaches the instrument is determined from the expression

$$\Phi_b = I_b \omega, \quad (10.25)$$

where $I_b = A_b B_b$ is the luminous intensity of the background in the direction of the instrument; B_b is the brightness of the background; A_b is the area of the radiating background which is limited by the instrument's field of view; ω is the solid angle within whose limits the radiation of the background lands in the instrument.

where dI_b is the luminous intensity of the background from the area element.

With small field-of-vision angles of the instrument, the solid angle ω which rests on the entrance pupil of the instrument will be approximately the same for all points of the radiating surface of the background. The back-

/298

Since $\omega = A_{\text{en.ap}} L^{-2}$, equality (10.25) can be rewritten in the form

$$\Phi_b = B_b A_b \frac{A_{\text{en.ap}}}{L^2} \quad (10.26)$$

Since $A_b/L^2 = \omega_v$, from (10.26) we have

$$\Phi_b = B_b A_{\text{en.ap}} \omega_v \quad (10.27)$$

Hence, by analogy with (10.12), we write the expression for the effective value of radiation flux of the background which acts on the radiation receiver

$$\Phi_{\text{eff}} = \Phi_b k_b = B_b A_{\text{en.ap}} \omega_v k_b \quad (10.28)$$

where k_b is the coefficient of utilization of the radiation flux of the background of the radiation receiver.

The background flux which is determined by expressions (10.27) and (10.28) not only influences the worsening of the threshold flux of the receiver, but it also leads to a change in the value of the useful signal.

With the presence of the object being detected (Fig. 10.3)

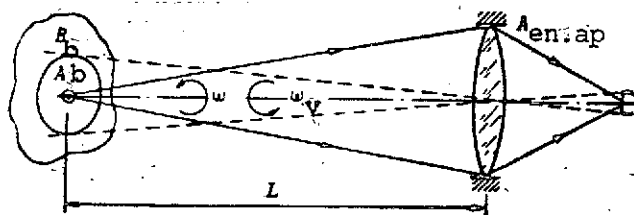


Fig. 10.3. For the derivation of the formula for the range of action with the presence of a radiating background.

in the field of view of the instrument, a radiation flux will arrive at the radiation receiver which is the sum of two components: the radiation flux from the object and the flux from that portion of the background which is not screened by the object. The effective value of the radiation flux of the object which arrives

at the radiation receiver and which is determined by relation (10.12) is written in the form

$$\Phi_{r,eff} = \Phi_r k_r$$

The effective value of the background flux, with consideration of screening by the object, will be

$$\Phi_{r,eff}^b = B_b A_{en.ap}^b k_b (\omega_v - \omega_{ob}) \quad (10.29)$$

where ω_{ob} is the solid angle subtended by the radiating surface of the object.

The total amount of the effective radiation flux with the presence of an object in an instrument's field of view will be /299

$$\Phi_{eff} = \Phi_{r,eff} + \Phi_{r,eff}^b = \Phi_r k_r + B_b A_{en.ap}^b \omega_v k_b - B_b A_{en.ap}^b \omega_{ob} k_b \quad (10.30)$$

The electro-optical instrument should now react not to the total radiation flux of the object, but to its increase over the level of the background flux, which is the difference

$$\Delta \Phi_{r,eff} = \Phi_{eff} - \Phi_{eff}^b$$

or, in accordance with (10.30) and (10.28),

$$\Delta \Phi_{r,eff} = \Phi_r k_r - B_b A_{en.ap}^b \omega_{ob} k_b \quad (10.31)$$

Substituting the values Φ_r and ω_{ob} in (10.31) from formulas

$$\Phi_r = \frac{B_b A_{ob}}{L^2} A_{en.ap} \quad \text{and} \quad \omega_{ob} = \frac{A_{ob}}{L^2}$$

we obtain

$$\Delta \Phi_{r,eff} = \frac{A_{ob} A_{en.ap} B_b k_r}{L^2} - B_b k_b \quad (10.32)$$

The last expression determines the effective amount of excess of radiation flux from the object above the level of flux of the background.

Formulas (10.17), (10.20), (10.21), and (10.22), from which the parameters of the electro-optical instrument should be calculated with the presence of a uniform radiating background in accordance with (10.23) and (10.32), take the form:

In the calculation of the range of action --

$$L = \sqrt{\frac{A_{\text{en.ap}} A_{\text{ob}} (B_{\text{ob}} k_r - B_{\text{b}} k_b)}{m \Phi_{\text{s.t}}^{(1)} k(\Delta f) k(\Phi_{\text{b}}) k_{\text{s}}}} \quad (10.33)$$

With the calculation of the area of the entrance pupil of the instrument which operates on an emitter at an infinite distance --

$$A_{\text{en.ap}} = \frac{m \Phi_{\text{s.t}}^{(1)} k(\Delta f) k(\Phi_{\text{b}}) k_{\text{s}}}{k_{\text{s}}} \quad (10.34)$$

In calculating the area of the entrance pupil of the instrument which operates on an emitter located at distance L -- /300

$$A_{\text{en.ap}} = \frac{L^2 m \Phi_{\text{s.t}}^{(1)} k(\Delta f) k(\Phi_{\text{b}}) k_{\text{s}}}{l_{\text{ob}} k_r} \quad (10.35)$$

For determining the threshold irradiance at the entrance to the instrument --

$$E_{\text{t}} = \frac{m \Phi_{\text{s.t}}^{(1)} k(\Delta f) k(\Phi_{\text{b}}) k_{\text{s}}}{A_{\text{en.ap}} k_r} \quad (10.36)$$

With vacuum photocells and photomultipliers, the constant illumination from the background has an effect on the value of the basic component of the noises -- the current of the shot effect. The increase of this component is caused by the increase in the total photocurrent. The background illumination also has an effect on the increase in radiation noise which, with high temperatures of the background emitters, becomes comparable with the shot noise. In this case, the value of the thermal noise in comparison with the shot and radiation noise can be disregarded.

Consideration of the influence of background illumination on the value of the threshold flux of a vacuum photocell or photomultiplier is accomplished by the calculation of a new value $\Phi_{s.t}^b$ with the presence of radiation of the background by the formula

$$\Phi_{s.t}^b = \sqrt{\frac{[2e(i_T + \Phi_b S_{PM}) + 8kT_b \Phi_b S] \Delta f}{S_{PM} S_{PC}}}, \quad (10.37)$$

where Φ_b is the radiation flux from the background which falls on the photocathode; T is the temperature of the background; k is Boltzmann's constant equal to $1.38 \cdot 10^{-23} \text{ J K}^{-1}$; S_{PM} is the integral sensitivity of the PM to the radiation of the background; S_{PC} is the integral sensitivity of the photocathode of the PM toward the radiation of the background.

The value of the threshold flux $\Phi_{s.t}^b$ calculated in this manner is substituted in formulas (10.33), (10.35), and (10.36) instead of the product $\Phi_{s.t} k(\Phi_b) k(\Delta f)$.

Consideration of the influence of background illumination on the photoresistor is extremely difficult and the analytical expressions which permit doing this can be obtained in convenient form only in some particular cases. Much more often, this influence is considered by using the experimentally obtained relations and graphs. Such graphs for some models of cooled and uncooled photoresistors are presented in Fig. 10.4.

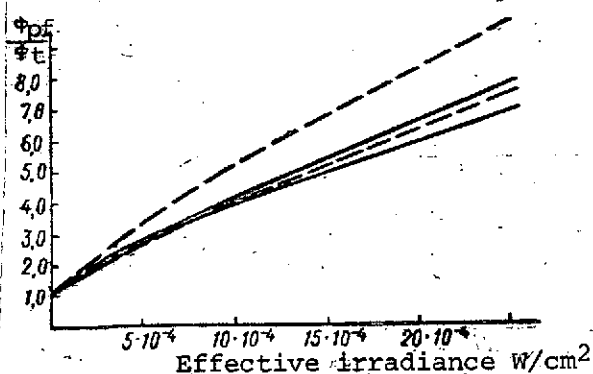


Fig. 10.4. Effect of constant illumination on the threshold sensitivity of photoresistors.

In those cases where the law of change of the resistance of a sensitive layer under the influence of an incident radiation flux is known, consideration of the influence of constant illumination can be accomplished from the change in integral sensitivity and the noises of the receiver.

/301

It is known that the sensitivity of the photoresistors is sometimes characterized by the relative change in their resistance under the influence of incident radiation flux and is determined as

$$S_R = \frac{\Delta R_b}{R_b \Delta \Phi}, \quad (10.38)$$

where S_R is the relative integral sensitivity; R_b is the resistance of the sensitive layer during its irradiation by flux Φ ; ΔR_b is the value of the change in resistance R_b of the sensitive layer under the influence of the increase $\Delta \Phi$ of the radiation flux.

The typical relation $R_b = f(\Phi)$ has the form presented in Fig. 10.5) [51]. Curve $R_b = f(\Phi)$ can be divided into three sections. On the first of them, which corresponds to small constant illuminations, function $R_b = f(\Phi)$ is linear and is described by the expression

$$R_b = R_r - k\Phi, \quad (10.39)$$

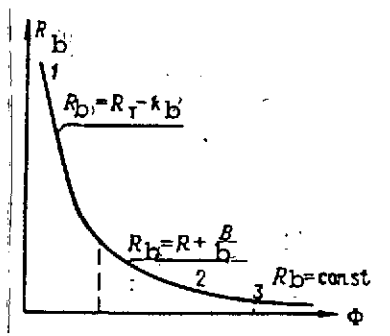


Fig. 10.5. Change in resistance of the sensitive layer of a photoresistor with a change in the value of incident radiation flux.

where R_r is the dark resistance of the sensitive layer; k is the constant coefficient (steepness of the characteristic).

With an increase in the value of constant illumination, function $R_b = f(\Phi)$ can be approximated by the relation

$$R_b = R_r + B\Phi^{-1}, \quad (10.40)$$

where B is the constant coefficient (for the given photoresistor).

Finally, on the third section R_b is approximately constant, since a further increase in the value of the incident flux does not lead to a noticeable change in the resistance of the sensitive layer. /302

Let us examine the method for considering the effect of constant illumination on the characteristics of a receiver as applicable to a section of linear change of resistance.

With the influence of radiation flux $\Delta \Phi$ on a receiver, the resistance of its sensitive layer on the basis of (10.39) will be

$$R_{\Delta\Phi} = R_r - k\Delta\Phi,$$

where $k\Delta\Phi = \Delta R_b$ is the change in the resistance of the receiver with incidence flux $\Delta\Phi$.

Substituting the value ΔR_b in (10.38), we obtain

$$S_R = \frac{k\Delta\Phi}{R_r\Delta\Phi} = \frac{k}{R_r}. \quad (10.41)$$

If a constant flux Φ_b falls on the sensitive layer from the background, its relative integral sensitivity can be expressed by the relation

$$S_{R_b} = \frac{\Delta R_b}{R_b\Delta\Phi}.$$

Substituting here the values of quantities R_b and ΔR_b , we find

$$S_{R_b} = \frac{a}{R_r} \frac{1}{1 - \frac{k}{R_r}\Phi_b}.$$

whence, with consideration of (10.41), we have

$$S_{R_b} = S_R \frac{1}{1 - S_R\Phi_b}. \quad (10.42)$$

In order to determine the voltage sensitivity of the receiver and its change under conditions of constant background illumination, it is necessary to proceed from a specific scheme for connecting the photoresistor. Usually, a load resistor is connected in series with the receiver from which the signal goes to the input of the amplifier (Fig. 10.6).

/303

The value of the signal at the input will be

$$u_s = u_r - u_b = \frac{u R_l k \Delta\Phi}{(R_r + R_l)(R_r - k\Delta\Phi + R_l)}.$$

Then the integral sensitivity of the photoresistor

$$S = \frac{u_S}{\Delta\Phi} = - \frac{uR_0k}{(R_T + R_0)(R_T + R_0 - k\Delta\Phi)} \quad (10.43)$$

With small fluxes $\alpha\Delta\Phi < R_T$, therefore

$$S = \frac{k}{R_T} \frac{uR_0R_T}{(R_T + R_0)^2} = S_R u \frac{R_0R_T}{(R_T + R_0)^2} \quad (10.44)$$

With considerable constant illuminations (at the end of the linear section) we have

$$\Delta u_S = \frac{uR_0k\Delta\Phi}{(R_0 + R_0)(R_0 + R_0 - k\Delta\Phi)}$$

Under these conditions, the integral sensitivity will be

$$S^b = \frac{\Delta u_S}{\Delta\Phi} = \frac{uR_0R_T}{(R_0 + R_0)(R_0 + R_0 - k\Delta\Phi)}$$

or

$$S^b = \frac{\Delta u_S}{\Delta\Phi} = S_R \frac{uR_0R_T}{(R_0 + R_0)(R_0 + R_0 - k\Delta\Phi)} \quad (10.45)$$

If $k\Delta\Phi < R_0$, then

$$S^b = S_R \frac{uR_0R_T}{(R_0 + R_0)^2} \quad (10.46)$$

We find the nature of change of the integral sensitivity by taking the relation of expressions (10.46) and (10.44)

$$\frac{S^b}{S} = \frac{(R_T + R_0 - k\Delta\Phi)^2}{(R_T + R_0)^2}$$

after a few simple transformations, we obtain

$$S^b = S \left(1 - \frac{k\Phi}{R_T + R_L} \right)^2 = S \left(1 - \Phi S_R \frac{R_T}{R_T + R_L} \right)^2. \quad (10.47)$$

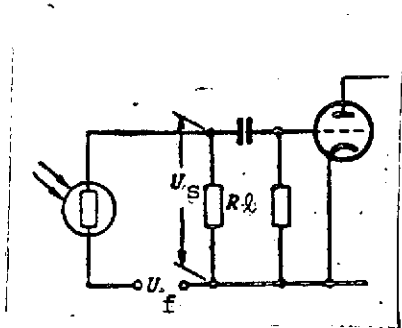


Fig. 10.6. Diagram of the connection of a photoresistor to the input of an amplifier.

This relation shows that with an increase in constant illumination, even on the section of linear change in the resistance, the integral sensitivity of the photoresistor drops.

Along with the change in integral sensitivity with illumination, the level of the intrinsic noises of the photoresistor also changes. In Section 4.4 it was shown that the current noise of the receiver is determined by the expression /304

$$\bar{i}_i^2 = A i^2 \frac{\Delta f}{f}.$$

The value of the current i which flows through an irradiated receiver (see 10.6) will be

$$i = \frac{u}{R_T + R_L},$$

and with the presence of illumination, the current will be altered by the relation

$$i_b = \frac{u}{R_T + R_L - k\Phi_{\text{eff}}^b}.$$

Then the relation of the mean squares of the current noise with the presence of background illumination and with its absence will be found as

$$\frac{\bar{i}_{ib}^2}{\bar{i}_i^2} = \frac{A k_b^2 \Delta f f}{A i^2 \Delta f f} = \frac{i_b^2}{i^2} = \frac{(R_T + R_L)^2}{(R_T + R_L - k\Phi_{\text{eff}}^b)^2},$$

whence, expanding the denominator, we have

$$\frac{\overline{i_b^2}}{\overline{i^2}} = \frac{1}{\left(1 - \frac{k\Phi}{R_T + R_L}\right)^2} \quad (10.48)$$

Considering (10.41), relation (10.48) can be rewritten in the form

$$\frac{\overline{i_b^2}}{\overline{i^2}} = \frac{1}{\left(1 - S_R \Phi \frac{R_T}{R_T + R_L}\right)^2} \quad (10.48a)$$

On the basis of (10.47), we obtain

$$\frac{\overline{i_b^2}}{\overline{i^2}} = \frac{S}{S^b} \text{ or } \overline{i_b^2} = \overline{i^2} \frac{S}{S^b} \quad (10.49)$$

Since, with an increase in background illumination, integral sensitivity S^b drops, consequently, the current noises will increase.

Proceeding analogously, we find the value of thermal noise with the presence of a constant background illumination. The dispersion of the current of thermal noise on the photoresistor is described by the relation (4.52)

$$\overline{i_T^2} = 4kTR^{-1}\Delta f.$$

Hence, it can be seen that with illumination the thermal noise changes as a result of the change in resistance of the sensitive layer which, in the absence of irradiation, equals R_R and, with the presence of a constant background illumination, $R_b = R_T - k\Phi$. Naturally, the relation of the dispersions of the current of thermal noise of a photoresistor not irradiated $\overline{i_T^2}$ and irradiated $\overline{i_{T,b}^2}$ will be determined by the relation of the corresponding resistors R_T and R_b , i.e.,

$$\frac{\overline{i_{T,b}^2}}{\overline{i_T^2}} = \frac{R_b^{-1}}{R_T^{-1}} = \frac{R_T}{R_T - k\Phi} \quad (10.50)$$

From (10.50) and (10.41), we have

$$\left| \frac{\overline{i_{r,b}^2}}{\overline{i_r^2}} = \frac{1}{1 - S_R \Phi} \right| \quad (10.51)$$

Whence, considering (10.42), we find

$$\left| \overline{i_{r,b}^2} = \overline{i_r^2} \frac{S_{R,b}}{S_R} \right| \quad (10.52)$$

In those cases where the values of the relative integral sensitivities are unknown, for the determination of $\overline{i_{r,b}^2}$ we can use the relation (10.51) in which S_R is expressed from (10.44), then

$$\left| \overline{i_{r,b}^2} = \overline{i_r^2} \frac{u R_r R_\ell}{u R_r R_\ell - S_b^2 (R_r + R_\ell)^2} \right| \quad (10.53)$$

With the presence of constant background illumination, considerable values can be attained by the radiation noises which are caused by the fluctuations in the flux from the background and are described by the relation

$$\Delta \Phi_b^2 = 16 k T \Phi_b \Delta f.$$

The change in the level of intrinsic noises of the receiver and its integral sensitivity under the action of background illumination leads to a change in the threshold flux. It is rather difficult to obtain a convenient expression for calculating coefficient $k(\Phi)$ in general form. It is simpler to calculate the value of the threshold flux of the receiver under new conditions from the formula

$$\left| \Phi_{s,\tau} = \Phi_{s,\tau}(\Phi) = \frac{\sqrt{\Sigma \overline{i_{r,b}^2}}}{S_b} R_\Phi \right| \quad (10.54)$$

in which it is necessary to place the following noises $\overline{i_{r,b}^2}$ and the integral sensitivity calculated for the conditions of constant background illumination.

If one of the types of noise is predominant, then under such conditions analytical relations may be obtained.

Thus, for example, if current noise is the main one, the relation which determines the threshold flux will be

$$\Phi_{s.t}^b = \frac{\sqrt{i_{ib}^2}}{S^b} R_{\ell} \quad (10.55)$$

Substituting here the value $\overline{i_{ib}^2}$ from (10.49) and multiplying and dividing the right side by the value S , we find

$$\Phi_{s.t}^b = \frac{\sqrt{i_{ib}^2} S}{S} R_{\ell} \frac{\sqrt{S/S^b}}{S^b}.$$

Whence, we obtain

$$\Phi_{s.t}^b = \Phi_{s.t} \left(\frac{S}{S^b} \right)^{3/2}. \quad (10.56)$$

Thus, if the current noise is the main one, the coefficient $k(\Phi_b)$, applicable to the scheme under consideration, equals

$$k(\Phi_b)_i = \left(\frac{S}{S^b} \right)^{3/2}. \quad (10.57)$$

From this expression, with consideration of (10.47) and (10.44), we can also obtain another entry $k(\Phi)_i$:

$$k(\Phi)_i = \frac{1}{\left(1 - \frac{\Phi S}{u} \frac{R_r + R_{\ell}}{R_{\ell}} \right)^3}. \quad (10.57a)$$

Similarly, for the case of the predominance of thermal noise, we obtain

$$k(\Phi)_i = \frac{S}{S^b} \sqrt{\frac{S_{R_b}}{S_R}}$$

or

$$k(\Phi)_r = \frac{S}{S^b} \sqrt{\frac{1}{1 - S_R^b}} \quad (10.58)$$

The last expression can be presented in the form of a dependence on the parameters of the connection scheme. For this, we find the ratio S/S^b from (10.47) and the value S_R from (10.44); then, after substituting them in (10.58), we obtain

$$k(\Phi)_r = \left[\left(1 - \frac{\Phi S R_r}{u R_\theta} \right)^2 \sqrt{1 - \frac{\Phi S (R_\theta + R_r)^2}{u R_\theta R_r}} \right]^{-1} \quad (10.58a)$$

Knowing the predominant type of noises in the case under consideration, we find the corresponding coefficient $k(\Phi)$ from formulas (10.57) and (10.57a) or (10.58) and (10.58a). We use the found values of $k(\Phi)$ in calculating one of the parameters of the instrument using relations (10.33), (10.34), (10.35), and (10.36). /307

If the current and thermal noises are comparable with each other, then having used relation (10.54), we can calculate a new value of the threshold flux of the receiver with background illumination, i.e., the product $\Phi_b^* = \Phi_t k(\Phi)$.

Naturally, the value of the background illumination should be calculated according to relation (10.27) and taken as S^b is the integral sensitivity of the receiver for the radiation of the background being considered.

The relations which have been presented are valid as applicable to the connection scheme presented in Fig. 10.6. With other schemes for connection, the method of approach to the determination of $k(\Phi)$ is retained, but the relations will be somewhat different.

The value of the coefficient $k(f)$ can be determined in the following manner. In general, we will assume that an instrument is being considered which assures the scanning of space within limits of the solid angle ω_{sc} by the instantaneous field of view ω_v during time T_k .

The overall number of elements in the scanning zone which are scanned by the instantaneous field of view will be

If the angles ω do not exceed 1 sr in value, then with sufficient precision, the transition from solid angles to plane angles with axisymmetrical fields may be accomplished in accordance with the relation

$$\omega = \frac{\pi}{4} (2W)^2,$$

where $2W$ is the plane angle at the apex of the solid angle in rad.

With uniform distribution of time T_k on the scanning of all elements of the sweep N_e , one element is scanned during time Δt_e , determined from the expression

$$\Delta t_e = \frac{T_k}{N_e},$$

whence, after the substitution of N_e

$$\Delta t_e = T_k \frac{(2W_v)^2}{(2W_{sc})^2} = T_k \frac{W_v^2}{W_{sc}^2}. \quad (10.59)$$

The lower limit of the transmission band $\Delta f - f_l$ of the amplifier should assure the passage of the first harmonic and is determined from the expression

$$f_l = \frac{1}{T_k}. \quad (10.60)$$

The upper limit of the transmission band f_u depends on the duration of the pulse received from an element of the sweep and the degree of conformance of the optical and electrical signals. The value f_u can be calculated using the relation /308

$$f_u = \frac{k_f}{\Delta t_e}, \quad (10.61)$$

where $k_f = 0.5-2$ is the coefficient which characterizes the agreement of the shape of the input and output signals of the electronic circuit. Substituting in the last expression the value Δt_e from (10.59), we obtain

$$f_u = \frac{k_f W_{sc}^2}{T_k W_v^2} \quad (10.62)$$

If the scanning of zone ω_{sc} is accomplished by the instantaneous field of view ω_v with some overlap m_0 , it is equivalent either to an increase in the scanning zone by this value or to a reduction in the instantaneous field of view which is caused by an increase in the sweep elements in the scanning zone to the value

$$N'_e = (1 + m_0) \frac{\omega_{sc}}{\omega_v} \quad (10.63)$$

then

$$\Delta t_e = T_k \frac{W_v^2}{(1 + m_0) W_{sc}^2} \quad (10.64)$$

$$f_u = \frac{k_f (1 + m_0) W_{sc}^2}{T_k W_v^2} \quad (10.65)$$

The width of the transmission band will be

$$\Delta f = f_u - f_l \quad \text{or} \quad \Delta f = \frac{1}{T_k} \left[\frac{k_f W_{sc}^2}{W_v^2} - 1 \right] \quad \text{and} \quad \Delta f' = \frac{1}{T_k} \left[\frac{k_f W_{sc}^2 (1 + m_0)}{W_v^2} - 1 \right] \quad (10.66)$$

In the majority of cases, the one can be disregarded and then

$$\Delta f = \frac{k_f W_{sc}^2}{T_k W_v^2} \quad \text{and} \quad \Delta f' = \frac{k_f (1 + m_0) W_{sc}^2}{T_k W_v^2} \quad (10.67)$$

In instruments with modulation of the radiation flux, the width of the transmission band is determined by the resonance characteristic of the filter tuned to the frequency of the first harmonic. The narrower the band Δf , the less the noise and the better the threshold sensitivity. /309

The coefficient $k(\Delta f)$ is determined from the known width of the transmission band Δf .

10.4. Calculation of the Range of Action and Threshold Sensitivity with the Observation of an Object on a Nonuniformly Radiating Background

When the background on which an observed object is projected is not uniform, this is equivalent to the influence of a fluctuating radiation flux of illumination on the receiver. This flux can be presented as the sum of two components: the constant Φ_0^b and the variable $\Delta\Phi^b$:

$$\Phi^b = \Phi_0^b + \Delta\Phi^b \quad (10.68)$$

The first component causes a worsening of sensitivity, and the second participates directly in the formation of the interference signal.

In this case, the meansquare value of the interference signal (noise signal) will be determined by the relation

$$\sqrt{\overline{I_{ns}^2}} = \sqrt{\sum \overline{I_{jb}^2} + \overline{\Delta\Phi_b^2} \left(S_s^b \frac{k_b}{k_s} \right)^2} \quad (10.69)$$

where $\sum \overline{I_{jb}^2}$ is the mean square of the internal noises of the receiver with consideration of the effect of constant illumination; $\overline{\Delta\Phi_b^2} \left(S_s^b \frac{k_b}{k_s} \right)^2$ is the mean square value of the external noise (interference signal caused by fluctuations of background illumination); S_s^b is the integral sensitivity of the receiver with respect to emission of a standard source with the presence of background illumination; k_s and k_b are the coefficients of utilization of the receiver with respect to emission of a standard source and background.

Then the threshold flux of the electro-optical instrument with consideration of (10.69) on the basis of (4.19) will be

$$\Phi_{s,t}^b = \frac{\sqrt{\sum \bar{i}_{jb}^2 + \Delta\Phi_b^2 \left(\frac{S_s^b k_b}{k_s} \right)^2}}{S_s^b} \quad (10.70)$$

If the components of the internal and external noises are comparable with each other, the threshold flux of the receiver is calculated from formula (10.72) and it is used in the determination of the range of action, threshold sensitivity, or other characteristics of the instrument.

Carrying the first component from under the radical, we obtain /310

$$\Phi_{s,t}^b = \frac{\sqrt{\bar{i}_{jb}^2}}{S_s^b} \sqrt{1 + \frac{\Delta\Phi_b^2 (S_s^b k_b)^2}{k_s^2 \sum \bar{i}_{jb}^2}} \quad (10.71)$$

whence, considering (10.55), we have

$$\Phi_{s,t}^b = \Phi_{s,t}^{b_0} \sqrt{1 + \frac{\Delta\Phi_b^2 (S_s^b k_b)^2}{k_s^2 \sum \bar{i}_{jb}^2}} \quad (10.72)$$

where $\Phi_{s,t}^{b_0}$ is the threshold flux of the instrument according to a standard emitter with the presence of constant background illumination.

In formula (10.72), the multiplier in the form of a radical considers the worsening of threshold sensitivity due to fluctuations in background radiation. In this, the value of $\Phi_{s,t}^{b_0}$ for photoemission devices is found from formula (4.75), for photomultipliers, from expressions (10.37), and finally, for photoresistors, from one of the relations (10.56) or (10.58).

If the components caused by the internal and external noises are comparable with each other, the threshold flux $\Phi_{s,t}^b$ is calculated from formulas (10.70) and (10.72).

In those cases where the component due to external noise (second term in radicands) is considerably less than the component caused by internal noises, the threshold flux is calculated by the method which considers only the effect of constant illumination (see Section 10.3).

If external noises prevail, i.e., the second term in the radicands of the relations (10.71) or (10.72) are considerably greater than unity, the value of fluctuations of flux from the background is taken as the threshold flux.

It is obvious that, in this case, for the dependable discrimination of the useful signal from the fluctuation interference of the background, it is necessary to attain an excess of the signal above the interference level such that

$$\Phi_{r,eff} = m \Delta \Phi_{eff}^b$$

Substituting here the values of $\Phi_{r,eff}$ from (10.10) and determining $\Delta \Phi_{eff}^b$, as

$$\Delta \Phi_{eff}^b = n \Phi_{eff}^b, \quad (10.73)$$

where n is the depth of modulation of the radiation flux from the background, with consideration of (10.28), we obtain

$$1 - \frac{A_{en.ap} k_r}{L^2} = m \Delta \Phi_{eff}^b = m B_f A_{en.ap} \omega_b^k n, \quad (10.74)$$

whence we find

/311

$$L_b = \sqrt{\frac{I k_r}{m B_b \omega_b^k n}}. \quad (10.75)$$

From this formula, it can be seen that the range of action of the instrument depends only on the relationship of the fluxes from the object and background and does not depend on the area of the instrument's entrance pupil. Therefore, by the value L_b here we should understand the greatest distance beginning from which the signal from the object becomes a given number of times greater than the signals caused by the nonuniformities of the energy brightness of the background.

The effective value of the flux from the background on the receiver by analogy with (10.28) is expressed by the relation

$$\Phi_{\text{eff}}^b = \Phi_{k_b}^b$$

where $k_b = \frac{\int_0^\infty \phi_b(\lambda) \tau_e(\lambda) \tau_0(\lambda) s(\lambda) d\lambda}{\int_0^\infty \phi_b(\lambda) d\lambda}$ is the coefficient of utilization of the receiver for radiation of the background.

The flux from the background, reduced for effectiveness of influence on the receiver to the radiation of a standard source, will be

$$\Phi_{\text{rec}}^b = \Phi_{k_s}^b \frac{k_b}{k_s}$$

or, with consideration of (10.27), we obtain

$$\Phi_{\text{rec}}^b = B_F A_{\text{enap}} \frac{\omega}{y} \frac{k_b}{k_s} \quad (10.76)$$

The value of Φ_{rec}^b calculated from this relationship is substituted in the formulas which consider the influence of constant illumination on the characteristics of the receiver.

If the observed object is projected on a nonuniformly radiating background, the threshold flux and sensitivity of the electro-optical instrument are calculated by formulas ((10.33) (10.34), (10.35), and (10.36), which consider the effect of constant illumination. In this, we first determine the value of the constant component of the flux from the background on the input of the radiation receiver Φ_{rec}^{b0} , from which the calculation of either the coefficient $k(\Phi)$ or new values of Φ_t and S are also conducted. If the fluctuations of flux from the background have a low-frequency character, consideration of the effect of background illumination on the parameters of the equipment is conducted according to the maximum value of the flux from the background which falls in the instrument.

With comparatively high-frequency fluctuations of the radiation flux caused by the nonuniformities of the background, besides the worsening of the sensitivity of the receiver, it is 312 still necessary to consider the interference signals caused by the heterogeneities of the background.

If the differentials of the radiation flux from the background cause signals on the output of the instrument which are comparable with the noise level, the calculation of the

threshold sensitivity of the instrument is conducted with consideration of this interference component.

Thus, in order to obtain an answer about the true range of action of the instrument which is operating under conditions of a nonuniform radiating background, it is necessary to find the relationship between the effective values of the actual threshold flux of the receiver and the increase in flux from the background, i.e., between $\Phi_{s,t}k(\Delta f)k(\Phi)k_s$ and $\Delta\Phi_b k_b$, or to calculate the range of action from formulas (10.33) and (10.75). In the first case, if

$$\Delta\Phi_b k_b > \Phi_{s,t}k(\Delta f)k(\Phi)k_s$$

then the true range is the range calculated from formula (10.75). In the calculation of range by expressions (10.33) and (10.75), the smallest of them is taken as the true range of action.

With the necessity to assure the maximum range of action limited only by the parameters of the radiation receiver, the attempt is made to reduce the value of the variable component of the radiation flux from the background to such a degree that it becomes less than the threshold flux of the instrument. As is clear from expression (10.75), this can be achieved only with a reduction in the dimensions of the instantaneous field of view of the instrument (if the background fills the entire field of view). The maximum allowable value of the instantaneous field of view is found with the joint solution of relations (10.33) and (10.75)

$$\left. \begin{aligned} L &= \sqrt{\frac{A_{ob}A_{enap}(B_{ob}k_r - B_b k_b)}{m \cdot \Phi_{s,t}^{(1)} k(\Delta f) k(\Phi) k_s}}; \\ L_b &= \sqrt{\frac{A_{ob}k_r B_{ob}}{m B_b \omega_v k_b}} \end{aligned} \right\}$$

the first of which determines the maximum range of action and the second, the minimum.

Squaring the right sides of the indicated relations and equating them to each other, we find the maximum allowable value of the instantaneous field of view, which will equal

$$\omega_v \leq \frac{\Phi_{s.t}^{(1)} k(\Delta f) k(\Phi_b) k_s}{A_{en.ap} B_b k_b n \left(1 - \frac{B_b k_b}{B_{ob} k_r}\right)} \quad (10.77)$$

In those cases where $B_b k_b < B_{ob} k_r$, expression (10.77) is simplified somewhat and takes the form

$$\omega_v \leq \frac{\Phi_{s.t}^{(1)} k(\Delta f) k(\Phi) k_s}{A_{en.ap} B_b k_b n} \quad (10.78)$$

Inasmuch as coefficient $k(\Phi)$ depends on the value of the radiation flux from the background which falls on the receiver, the calculations of the allowable solid angle of the field of view is conducted in two or three procedures. In the first procedure, the value of $k(\Phi)$ is taken as equal to 1 and the first approximation ω_1 is found. Then, with consideration of this value, we calculate the value of the radiation flux of constant illumination from which either the coefficient $k(\Phi)$ or a new value of the threshold flux of the receiver under conditions of illumination by a constant background, i.e., the product $\Phi_{s.t}^{(1)} k(\Phi)$ is determined. After this, we calculate the refined value of the maximum allowable solid angle of the field of view of the instrument (second approximation). This value is extremely close to the true value. /313

The greatest difficulty is caused by calculating the function $\Phi_{r.eff} = f(\Phi)$ or, what is the same thing, the functions $\Phi_{r.eff} = f(\omega)$ or $\Phi_{r.eff} = f(W)$. To construct this function, we calculate several values of $\Phi_{r.eff}$ from formula (10.54) or (10.37) which correspond to the minimum possible, maximum, and two intermediate values of ω from which the desired relation is also constructed.

The graphs of the functions constructed in Fig. 10.7 permit the extremely simple determination of the range of action of the instrument. Let us assume that the field-of-vision angle of the instrument is W_1 . For receiver 1, $\Phi_{r.eff} < \Delta \Phi_{eff}^b(\omega_1)$, and for receiver 2 $\Phi_{r.eff} > \Delta \Phi_{eff}^b(\omega_1)$. Therefore, the range of action of the instrument with the use of receiver 1 is limited by the radiation of the background, the effective value of the flux from which will be a given number of times less on the range L_1 from the object. The order in finding this range is shown on the graph by the dotted line with arrows. Inasmuch as with the second receiver $\Phi_{r.eff} > \Delta \Phi_{eff}^b(\omega_1)$, the range of action of the instrument is determined from the intersection of the graphs of the functions $\Phi_{eff} = f(L)$ and $\Phi_{r.eff} = f(\Phi)$ and equals L_1' . /314

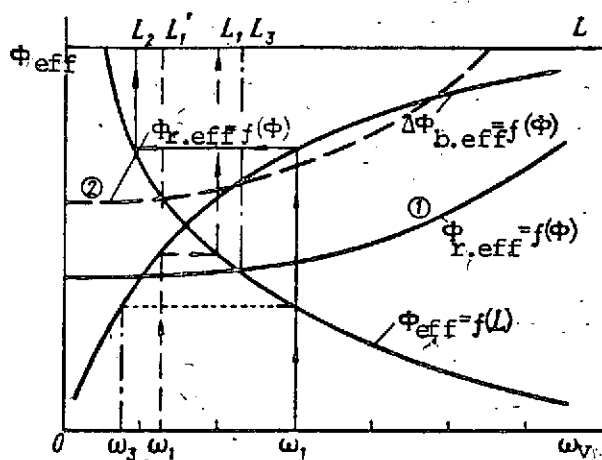


Fig. 10.7. Nomogram for determining the range of action and allowable size of the instantaneous field of view of the instrument.

If the instantaneous field of view of the instrument is W_2 and the value of the function $\Delta\Phi_{b,eff}^{b0}(W_2)$, which corresponds to it, exceeds the effective values of the threshold fluxes $\Phi_{r,eff}(W_2)$ of both receivers, the range of action of the instrument is determined by the flux from the background and equals L_2 . The order for finding it on the graph is shown by the solid line with the arrows.

Finally, with small fields of view, for example W_v , when $\Delta\Phi_{b,eff}^{b0}$ is less than the effective values of the threshold fluxes of both receivers, the range of action depends only on the characteristics of the receivers. The instrument's range of action with the employment of receivers 1 and 2 is found from the intersection of the function $\Phi_{eff} = f(L)$ with the function $\Phi_{r,eff} = f(\Phi)$ of both receivers. As applicable to the graph which has been presented, the indicated ranges prove to be equal to L_3 and L_1 , respectively.

As a result of the relative difficulty in calculating the range of action and the threshold sensitivity of electro-optical equipment with consideration of the effect of a constant background illumination and fluctuations of the background, it is more convenient sometimes to use the nomogram method for determining the required parameters of electro-optical equipment. The essence of this method consists of the following.

For the selected radiation receiver, we calculate the relations $\Phi_{eff} = f(L)$, $\Delta\Phi_{b,eff}^{b0} = f(\omega)$ and $\Phi_{r,eff} = f(\Phi) = f(\omega)$ from formulas (10.10), (10.74), and (10.54), respectively, and construct them on the graph (Fig. 10.7). The value of the solid angle of the field of view which determines the constant background illumination $\Phi_{b,eff}^{b0}$ and the variable component of the background illumination $\Delta\Phi_{b,eff}^{b0}$ are laid off on this graph along the abscissa. The values of the effective quantities of fluxes from the object, background, and threshold flux of the instrument are laid off along the ordinate. The distance to the radiation source is laid off along the second abscissa. Calculation of the functions $\Phi_{eff} = f(L)$ and $\Delta\Phi_{b,eff}^{b0} = f(\omega)$ causes no special

difficulties, since the first of them expresses the quadratic dependence on L . For its construction, it is sufficient to calculate one value of Φ_{eff} and, changing it proportionally to the square of the change of value (L/L_1) , construct the desired function $\Phi_{\text{eff}}(L) = \Phi_{\text{eff}}(L_1)(L/L_1)^2$.

Inasmuch as the second function $\Delta\Phi_{\text{eff}}^b \equiv \omega$, then calculating one value of $\Delta\Phi_{\text{eff}}^b$ which corresponds to the solid angle ω_1 , the current value of $\Delta\Phi_{\text{eff}}^b$ is calculated from the formula

$$\Delta\Phi_{\text{eff}}^b(\omega) = \Delta\Phi_{\text{eff}}^b(\omega_1) \frac{\omega}{\omega_1}. \quad (10.79)$$

If the field of view is given not by the solid angle ω but by a plane angle $2W$, then, with consideration of the connection between these angles with small values of the angles $\omega \approx W^2$, the current values of $\Delta\Phi_{\text{eff}}^b$ are determined from the expression

$$\Delta\Phi_{\text{eff}}^b(W) = \Delta\Phi_{\text{eff}}^b(W_1) \left(\frac{W}{W_1} \right)^2. \quad (10.80)$$

With the use of the nomogram which has been considered, we can also solve the inverse problem: to determine the maximum allowable value of the instantaneous field of view of the instrument with which the required range of action is assured or the range of action depends only on the parameters of the receiver.

10.5. Calculation of the Threshold Sensitivity of Instruments Which Operate with Areal Emitters

The problem of the calculation of threshold sensitivity arises in the calculation of instruments intended for the detection of ground objects from their infrared radiation, for making thermal charts of the terrain, and also in calculating electro-optical resolvers of the local vertical which operate from the intrinsic infrared radiation of the earth's surface and the atmosphere.

In this case, the value of the useful radiation flux on the input of the instrument without consideration of attenuation by the medium is calculated by formula (10.27) and for determination of the effective value of radiation flux on the radiation receiver, we use the expression

$$\Phi_{r,eff} = A_{enap} \omega_v \int_0^\infty b(\lambda) \tau_e(\lambda) \tau_0(\lambda) \tau_b(\lambda) s(\lambda) d\lambda = A_{enap} \omega_v B_r k_r \quad (10.81)$$

where $k_r = \frac{\int_0^\infty b(\lambda) \tau_e(\lambda) \tau_0(\lambda) \tau_b(\lambda) s(\lambda) d\lambda}{\int_0^\infty b(\lambda) d\lambda}$ is the utilization coefficient of radiation by the receiver.

To discriminate the operating signal, it is necessary to assure the excess of the effective value of operating flux over the effective threshold flux of the receiver by a given number of times on the strength of the allowable probability of a false alarm, i.e., it is necessary to satisfy condition (10.13) where /316

$$\Phi_{r,eff} = \Phi_{s,t}^{(1)} k(\Delta f) k_s$$

Solving equation (10.13) together with (10.27), we obtain the relation for the calculation of the minimum allowable area of the entrance pupil of the instrument

$$A_{enap} = \frac{m \Phi_{s,t}^{(1)} k(\Delta f) k_s}{\omega_v B_r k_r} \quad (10.82)$$

Sometimes, to increase the sensitivity of the instrument, the necessity arises to obtain operating signals with required amplitude not with complete but with the partial filling of the field of view of the instrument. If we designate the coefficient of filling by m_{fil} ($m_{fil} < 1$), the new value of the solid angle with which condition (10.13) should be satisfied will be

$$\omega'_v = \omega_v m_{fil}$$

and formula (10.82) for the calculation of the minimum allowable area of the entrance pupil will take the form

$$A_{enap} \geq \frac{m \Phi_{s,t}^{(1)} k(\Delta f) k_s}{m_{fil} \omega_v B_r k_r} \quad (10.83)$$

Relations (10.82) and (10.83) are applicable in determining the parameters of the instrument in the change from nonradiation to radiating underlying surfaces. Such cases occur, for example, in resolvers of the local vertical when the scanning instantaneous field of view of the instrument crosses the space-earth surface boundary.

If the problem arises of discriminating more heated sections of the surface against a background of less heated surfaces, i.e., with the presence of a constant component, then the calculation formulas, naturally, should be modified somewhat.

For simplicity of argument, we will assume that at one moment in time the entire field of view is directed at a less heated surface, and at another at the more heated surface. Then

$$\left. \begin{aligned} \Phi_{r.\text{eff}} &= A_{\text{enapv}} B_{r,k_{r2}} \\ \Phi_{r.\text{eff}} &= A_{\text{enapv}} B_{r,k_{r1}} \end{aligned} \right\} \quad (10.84)$$

The instrument should assure the generation of a signal which is caused by the increase in the effective value of the radiation flux with the transfer from one sector to another, i.e., it should discover the increase in radiation flux

$$\Delta \Phi_{r.\text{eff}} = \Phi_{r.\text{eff}2} - \Phi_{r.\text{eff}1} = A_{\text{enapv}} (B_{r,k_{r2}} - B_{r,k_{r1}}). \quad (10.85)$$

In this, the minimum of these fluxes, in this case $\Phi_{r.\text{eff}}$, ^{/317} plays the role of constant illumination whose influence is expressed in the worsening of the threshold flux of the receiver. With consideration of this worsening, the effective value of the threshold flux of the receiver should be taken by analogy with (10.23) as equal to

$$\Phi_{r.\text{eff}} = \Phi_{s.t} k(\Delta f) k_r k(\Phi_r). \quad (10.86)$$

Further, proceeding as in the preceding case, we achieve satisfaction of the condition

$$\Delta \Phi_{r.\text{eff}} \geq m \Phi_{r.\text{eff}}$$

Whence, with consideration of (10.85) and (10.86), we find

$$A_{\text{enap}} \geq \frac{m \Phi_{\text{S.C.}}^{(1)} k(\Delta f) k_{\text{S}} k(\Phi_{\text{R}})}{\omega_{\text{V}} (B_{\text{R}, k_{\text{R}_2}} - B_{\text{R}, k_{\text{R}_1}})} \quad (10.87)$$

We note that the most difficult conditions for the operation of equipment of this type are in the detection of small differentials of energy brightness with comparatively high brightness levels. As an example, let us consider the case where the underlying surface is a gray emitter, in which regard the coefficients of blackness of two adjacent sectors equal each other, i.e., $\epsilon_2 = \epsilon_1 = \epsilon$.

Then, using relation $B = \frac{\epsilon \sigma T^4}{\pi}$, the expression standing in the parentheses of the denominator of relation (10.87) is presented in the form

$$B_{\text{R}, k_{\text{R}_2}} - B_{\text{R}, k_{\text{R}_1}} = \frac{\epsilon \sigma}{\pi} (T_2^4 k_{\text{R}_2} - T_1^4 k_{\text{R}_1}).$$

Assuming that $T_2 = T_1 + \Delta T$, where $\Delta T \ll T_1$, we find

$$B_{\text{R}, k_{\text{R}_2}} - B_{\text{R}, k_{\text{R}_1}} = \frac{\epsilon \sigma}{\pi} [(T_1 + \Delta T)^4 k_{\text{R}_2} - T_1^4 k_{\text{R}_1}]. \quad (10.88)$$

For the assumption ($\Delta T \ll T_1$) accepted with sufficient precision, it can be considered that

$$k_{\text{R}_2} = k_{\text{R}_1} = k_{\text{R}}.$$

Then, carrying k_{R} out of the parentheses, after simple conversions, ignoring the last terms of the expansion, from (10.88), we obtain

$$B_{\text{R}, k_{\text{R}_2}} - B_{\text{R}, k_{\text{R}_1}} = \frac{\epsilon \sigma}{\pi} k_{\text{R}} (4T_1^3 \Delta T + 6T_1^2 \Delta T^2).$$

whence

$$B_{r_1} k_{r_1} - B_{r_2} k_{r_2} = \frac{4\epsilon\sigma}{\pi} k_{r_1} T_1^3 \Delta T \left(1 + \frac{3}{2} \frac{\Delta T}{T_1} \right). \quad (10.89)$$

If we consider that ΔT does not exceed $0.03T_1$, then ignoring /318 the second term, we have

$$B_{r_1} k_{r_1} - B_{r_2} k_{r_2} = \frac{4\epsilon\sigma}{\pi} T_1^3 \frac{\Delta T}{T} k_r = 4B_r k_r \frac{\Delta T}{T}. \quad (10.90)$$

Substituting the obtained value in (10.87), we find

$$A_{\text{enap}} \geq \frac{\frac{m\Phi_{s_1}^{(1)} k(\Delta f) k_s k(\Phi\Phi)}{\omega_{\text{v}} B_r k_r 4\Delta T}}{T}. \quad (10.91)$$

Formula (10.91) shows that the smaller the recorded temperature differential, the larger the minimum allowable area of the entrance aperture.

On the other hand, the higher the temperature of the radiating surface, the greater the value of constant illumination Φ_{r1} and the stronger the increase in the threshold flux of the receiver.

We note that the values of coefficients $k(\Delta f)$ and $k(\Phi_{r1})$ which consider the change in threshold sensitivity of the receiver which is operating in a specific scheme of connection and under specific conditions are calculated from the formulas of Section 10.3.

CHAPTER 11. CALCULATION OF THE CHARACTERISTICS OF TRANSPARENCY OF THE ATMOSPHERE

11.1. A Method for Determining the Coefficients of Transparency of the Atmosphere for Monochromatic and Complex Radiations

In Chapter 2 it was shown that with propagation in the atmosphere radiation flux is attenuated both due to scattering on molecules of gases and particles and due to absorption by various components of the atmosphere. Inasmuch as radiation flux is attenuated selectively, we will determine the transparency of the atmosphere for monochromatic radiation.

Since the basic components of the attenuation of radiation flux in the atmosphere are known (see Section 2.4) on the basis of (2.13), we can write the following formula for calculating spectral transparency of the atmosphere

$$\tau_a(\lambda) = \prod_{i=1}^n \tau_{sc i}(\lambda) \prod_{j=1}^k \tau_{tr j}(\lambda) = \tau_{sc 1}(\lambda) \tau_{sc 2}(\lambda) \tau_t(\lambda)_{H_2O} \tau_t(\lambda)_{CO_2} \cdot \tau_t(\lambda)_{O_3} \quad (11.1)$$

where $\tau_{sc 1}(\lambda)$ and $\tau_{sc 2}(\lambda)$ are the coefficients of transmission of a monochromatic radiation flux by the atmosphere with consideration of attenuation due to molecular $\tau_{sc 1}(\lambda)$ and aerosol $\tau_{sc 2}(\lambda)$ scatter; $\tau_t(\lambda)_{H_2O}$ is the coefficient of transmission of a monochromatic radiation flux by the atmosphere with consideration of attenuation due only to the absorption of radiation by water vapor; $\tau_t(\lambda)_{CO_2}$ and $\tau_t(\lambda)_{O_3}$ are the same coefficients but with consideration of attenuation due to absorption by carbon dioxide and ozone, respectively. /319

The value of coefficient $\tau_{sc 1}(\lambda)$ which determines the Rayleigh scatter on molecules of gases is calculated by the formula

$$\tau_{sc 1}(\lambda) = e^{-\tau_{sc 1}(\lambda)L}, \quad (11.2)$$

where

$$\tau_{sc 1}(\lambda) = \frac{32\pi^2(n^2-1)^2}{3N\lambda^4} \quad (11.3)$$

is the attenuation factor due to scatter; $N = 2.9 \cdot 10^{19} \text{ cm}^{-3}$ is the density of the air with normal pressure, expressed by the particles in one cm^3 ; $n = 1.0003$ is the refractive index of the air.

The values of the attenuation factor $d_{sc1}(\lambda)$ calculated from formulas (11.3) and (11.2) for various wavelengths and the coefficients of transmission of a monochromatic radiation flux by the atmosphere with different ranges which correspond to them are presented in Table 11.1.

TABLE 11.1. ATTENUATION FACTORS AND COEFFICIENTS OF TRANSMISSION OF MONOCHROMATIC RADIATION FLUX BY THE ATMOSPHERE WITH MOLECULAR SCATTER.

$\lambda, \mu\text{m}$	0.35	0.55	0.75	1.0	1.2	3.0	5.0
$\alpha_{sc1}(\lambda), \text{km}^{-1}$	$79.3 \cdot 10^{-3}$	$12.3 \cdot 10^{-3}$	$3.30 \cdot 10^{-3}$	$1.09 \cdot 10^{-3}$	$5.25 \cdot 10^{-4}$	$1.33 \cdot 10^{-5}$	$1.73 \cdot 10^{-6}$
$\tau_{sc1}(\lambda); L=10 \text{ km}$	0.45	0.89	0.97	0.99	1.0	1.0	1.0
$\tau_{sc1}(\lambda); L=40 \text{ km}$	0.04	0.4	0.855	0.95	0.99	1.0	1.0

From the table it can be seen that in the visible region of the spectrum molecular scattering is sufficiently great, reduces transparency substantially, and should be considered in calculations. At the same time, losses to molecular scatter in the infrared region of the spectrum can be ignored since they are small.

Transmission coefficient $\tau_{sc2}(\lambda)$, which considers losses to aerosol scatter alone, can be calculated from a formula similar to (11.2)

$$\tau_{sc2}(\lambda) = e^{-\alpha_{sc2}(\lambda)L} \quad (11.4)$$

However, in order to calculate the values of coefficient $\alpha_{sc2}(\lambda)$ necessary in this case, it is necessary to know the number, dimensions, and composition of the substance of the aerosol particle on which the scattering of the radiation occurs. Moreover, single relations for the calculation of values $\alpha_{sc2}(\lambda)$ applicable to various particles do not exist. All this causes great difficulties and practically excludes the analytical method of determining transmission coefficients $\tau_{sc2}(\lambda)$.

Most accessible is the method of determining the transmission factor $\tau_{sc}(\lambda) = \tau_{sc1}(\lambda)\tau_{sc2}(\lambda)$ (with consideration of total attenuation of radiation due to molecular and aerosol scatter) based on

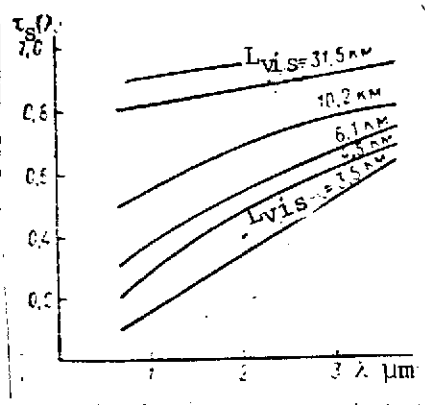


Fig. 11.1. Change in coefficient $\tau_{sc}(\lambda)$ depending on meteorological range of visibility.

the use of data on the meteorological range of visibility L_{vis} .¹

A certain connection exists between $\tau_{sc}(\lambda)$ and the meteorological range of visibility L_{vis} which is also extended to the infrared region of the spectrum. The values of coefficients $\tau_{sc}(\lambda)$

depending on L_{vis} are presented in Fig. 11.1. The indicated graphs were constructed for the case where the distance L_s between the object and the receiver is 1.85 km with a thickness of the layer of

precipitated water vapor $w = 17$ mm. If the real range L differs from $L_s = 1.85$ km, the value of the transmission coefficient is determined by recalculation using Bouguer's law

$$\begin{aligned} \tau_{sc}(\lambda) &= [\tau_{sc}^{(1)}(\lambda)]^L = [\tau_{sc}^s(\lambda)^{1/1.85}]^L = \\ &= [\tau_{sc}^s(\lambda)]^{\frac{L}{1.85}} \end{aligned} \quad (11.5)$$

where $\tau_{sc}(\lambda)$ is the coefficient of transmission of a monochromatic radiation flux by a layer of the atmosphere L km thick; $\tau_{sc}^{(1)}(\lambda)$ is the coefficient of transmission of a monochromatic flux by a layer of the atmosphere of unit thickness; $\tau_{sc}^s(\lambda)$ is the value of the transmission coefficient of a monochromatic radiation flux read from the graph.

We will show the use of formula (11.5) by an example. Assume it is required to determine the atmosphere's passage of a monochromatic flux with wavelength $\lambda = 1.25 \mu\text{m}$ with meteorological range of visibility $L_{vis} = 10.2$ km if the distance between the emitter and the receiver is $L = 5.5$ km.

¹By meteorological range of visibility L_{vis} , we mean the greatest range of visibility, during the day, of dark objects with angular dimensions exceeding $9 \cdot 10^{-3}$ rad. and projecting on the background of the sky at the horizon.

For radiation with wavelength $\lambda = 1.25 \mu\text{m}$ with $L_{\text{vis}} = 10.2 \text{ km}$, from the graph (see Fig. 11.1) we find $\tau_{\text{sc}}(\lambda) = 0.6$. Next, using Bouguer's law, we determine the transmission coefficient $\tau_{\text{sc}}^{(1)}(\lambda)$ with $L = 1 \text{ km}$:

$$\tau_{\text{sc}}^{(1)}(\lambda) = \tau_{\text{sc}}^s(\lambda = 1.25 \mu\text{m})^{1/1.85} = 0.6^{\frac{1}{1.85}}$$

Inasmuch as $\tau_{\text{sc}}(\lambda) = [\tau_{\text{sc}}^{(1)}(\lambda)]^L = [\tau_{\text{sc}}^s(\lambda)]^{\frac{L}{1.85}}$, with $L = 5.5 \text{ km}$, we have

$$\tau_{\text{sc}}(\lambda) = 0.6^{5.5/1.85} = 0.216$$

The value of the coefficient of transmission of radiation flux by the atmosphere is affected by the amount of water vapor in the path of propagation of the radiation. If under real conditions the thickness of the layer of precipitated water vapor w differs from $w_s = 17 \text{ mm}$, with which the graphs are constructed, this difference is considered with a special factor

$$\tau_{\text{sc H}_2\text{O}} = 0.998^{-(w_s - w)} = 0.998^{-(17 - w)}$$

Then the formula for the change from coefficient $\tau_{\text{sc}}^s(\lambda)$ found graphically (see Fig. 11.1) to the real coefficient $\tau_{\text{sc}}(\lambda)$ will have the appearance

$$\tau_{\text{sc}}(\lambda) = [\tau_{\text{sc}}^s(\lambda)]^{L/1.85} \cdot 0.998^{-(17 - w)} \quad (11.6)$$

The coefficients of transmission of a monochromatic radiation flux by the atmosphere with consideration of attenuation of the radiation due to absorption by water vapor $[\tau_{\text{ab}}(\lambda)_{\text{H}_2\text{O}}]$ and carbon

dioxide $[\tau_{\text{ab}}(\lambda)_{\text{CO}_2}]$ can be determined from Tables 6 and 7 of the

Appendix where the values of the indicated coefficients for various wavelengths are presented. However, for this in one case it is necessary to know the effective thickness of the layer of precipitated water vapor in the path of propagation of the radiation flux, and in the other -- the thickness of the layer of air reduced to the ground layer.

11.2. Calculation of the Quantity of Water Vapor on Horizontal, Sloping, and Vertical Paths

If the absolute humidity² m_0 at the earth's surface is known, the overall amount of water vapor in a column of atmosphere with thickness L and resting on area A can be determined from the formula

$$m = m_0 A$$

If all the water vapor located in the column is concentrated, /322 the volume it occupies will be

$$v = \frac{m_0 L A}{d},$$

where d is the specific density of the water.

Hence, the thickness of the layer of precipitated water

$$w = \frac{v}{A} = \frac{m_0}{d} L.$$

Since the values which go into the formula have different dimensionalities: m_0 (g/m^3), d (g/cm^3) and L (km), after their agreement, we obtain

$$w = w_0 L \quad (11.7)$$

Here w is the thickness of a layer of precipitated water vapor in mm in a layer of the atmosphere with thickness L ; w_0 is the specific thickness of a layer of precipitated water vapor in mm/km numerically equal to the value of absolute humidity m_0 .

In those cases where the absolute humidity is unknown, the amount of precipitated water can be calculated from the formula

²Absolute humidity m_0 is calculated from the formula $m_0 = m_{0\text{sat}} \frac{f\%}{100}$, g/m^3 where $m_{0\text{sat}}$ is the absolute humidity with air temperature K ; and f is the relative humidity.

$$w = m_N L \frac{288}{T}, \quad (11.8)$$

where m_N is the normal absolute humidity at the earth's surface; and T is the absolute air temperature.

Relations (11.7) and (11.8) are applicable for the calculation of the thickness of the layer of precipitated water vapor on horizontal paths near the ground.

With the necessity to determine the thickness of a layer of precipitated water vapor on horizontal paths at altitude H above the earth's surface, the distribution of humidity with altitude should be considered which, for a standard atmosphere, follows the law

$$m_H = m_0 e^{-\beta H}, \quad (11.9)$$

where m_N is the absolute humidity at altitude H ; $\beta = 0.45 \text{ km}^{-1}$ is a coefficient which characterizes the change in humidity with altitude.

Sometimes relation (11.9) is presented in the form

$$m_H = m_0 \cdot 10^{-H/5} \quad (11.9a)$$

Both these formulas are identical, and are easily converted one to the other, and can be used absolutely equally in calculations of absolute humidity aloft.

Considering (11.7), by analogy with (11.9), we write the expression for the thickness of a layer of saturated water vapor on a horizontal path at altitude H : /323

$$w_H = w_0 e^{-\beta H L} \quad (11.10)$$

Furthermore, we should also consider a reduction in the absorptivity of water vapor with altitude, which is described by relation (2.15). Substituting (11.10) in (2.15), we obtain the formula which determines the effective thickness of a layer of precipitated water vapor in the path of propagation of radiation flux on a horizontal path at altitude H above the earth's surface:

$$w_H^{\text{eff}} =$$

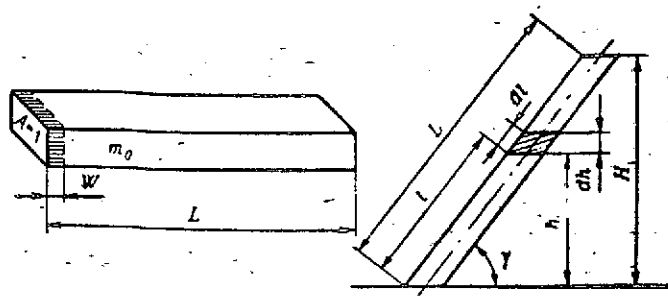


Fig. 11.2. For the determination of the effective thickness of a layer of absorbing substance in the path of propagation of radiation (sloping path).

or, substituting the value $\beta = 0.45$, we have

$$w_H^{\text{eff}} = w_0 e^{-0.5154 H_L} \quad (11.11)$$

The effective thickness of precipitated water vapor on sloping paths in the atmosphere can be calculated in the following manner.

On the basis of (11.11), the effective thickness of a layer of precipitated water vapor in an elemental layer of the atmosphere dl (Fig. 11.2) located at altitude H will be

$$dw_H^{\text{eff}} = w_0 e^{-0.5154 h} dl \quad (11.12)$$

where $h = l \cos \gamma$ is the current value of altitude; γ is the angle between the normal to the earth's surface and the direction of propagation of the radiation.

Then the general effective thickness of the layer of precipitated water vapor in the atmosphere on a sloping path without consideration of the curvature of the earth's surface is found by integrating expression (11.12)

$$w^{\text{eff}} = w_0 \int_0^L e^{-0.5154 l \cos \gamma} dl = w_0 \frac{e^{-0.5154 H_1} - e^{-0.5154 H_2}}{0.5154 \cos \gamma} \quad (11.13)$$

If $H_1 = 0$, then

$$w^{\text{eff}} = w_0 \frac{1 - e^{-0.5154 H}}{0.5154 \cos \gamma} \quad (11.14)$$

Cofactors $\frac{1 - e^{-0.5154 H}}{0.5154 \cos \gamma}$ and $\frac{e^{-0.5154 H_1} - e^{-0.5154 H_2}}{0.5154 \cos \gamma}$ are sometimes called

the range reduced to the surface layer for content of water vapor.

In work [10] it is shown that with consideration of the curvature of the earth with angles $\gamma \leq 1.4$ rad, the effective

thickness of a layer of precipitated water vapor can be calculated from the formula

$$w^{\text{eff}} = w_0 e^{-0.5154H} \cdot \frac{\left[1 - \frac{\xi_0}{\xi^*} e^{-(\xi^* - \xi_0)} \right]}{0.5154 \cos \gamma}, \quad (11.15)$$

where

$$\begin{aligned} \xi^* &= \xi + \xi_0; \quad \xi = L \left(\frac{0.5154}{2R_3} \right)^{1/2} \sin \gamma; \\ \xi_0 &= \left(\frac{0.5154R}{2} \right)^{1/2} \cot \gamma. \end{aligned}$$

The values of the effective thickness of the layer of precipitated water vapor calculated from formulas (11.13) or (11.15) are initial for determination of the transmission coefficient of the atmosphere $\tau_t(\lambda)H_2O$ from Table 6 of the Appendix and also for finding the coefficient $\tau_{sc}(\lambda)$.

11.3. A Method for Calculating the Mass of Air and Carbon Dioxide on Horizontal, Sloping, and Vertical Paths

It is known that air pressure changes exponentially with altitude with the index of the exponent $0.123H$, i.e.,

$$p_H = p_0 e^{-0.123H}. \quad (11.16)$$

The thickness of a layer of air on horizontal paths, located at altitude H above the earth's surface and reduced to the surface layer, with consideration of (11.16), can be calculated by the formula

$$L_{\text{red}} = L_H e^{-0.123H} \quad (11.17)$$

where L_H is the distance at which the propagation of the radiation flux is examined and L_{red} is the length of the near-ground horizontal path which, for a mass of air, is equivalent to the length of path L_H at altitude H .

With sloping paths, by analogy with (11.13) and (11.14), the following formulas can be obtained for the calculation of the length of the optical path of radiation reduced to the surface layer:

-- in altitude range from H_1 to H_2

/325

$$L_{\text{red}} = \frac{e^{-0.123H_1} - e^{-0.123H_2}}{0.123 \cos \gamma}, \quad (11.18)$$

-- in altitude range from 0 to H

$$L_{\text{red}} = \frac{1 - e^{-0.123H}}{0.123 \cos \gamma}. \quad (11.19)$$

Calculated from formulas (11.17), (11.18), and (11.19), the thickness of the layer of air in the path of propagation of radiation reduced to the surface layer can be used in the determination of the values of the transmission coefficient of the atmosphere with consideration of losses for scatter alone, i.e., of coefficient $\tau_{sc}(\lambda)$.

With some refinements, the indicated formulas are applicable for the calculation of transparency of the atmosphere in considering losses due to absorption by carbon dioxide, i.e. by coefficients $\tau_t(\lambda)\text{CO}_2$. The indicated refinement consists of consideration of the change in absorbing properties of the carbon dioxide with altitude which is described by the function

$$\frac{L_{\text{eff}}}{L_H} = e^{-0.19H}$$

With consideration of this relation, the effective length of the optical path reduced for absorptivity of carbon dioxide to the surface layer will be, on the basis of (11.7)

$$L_{\text{red.eff}} = L_H e^{-0.123H} e^{-0.19H} = L_H e^{-0.313H}. \quad (11.20)$$

Formula (11.20) is valid for horizontal paths located at altitude H above the earth's surface.

By analogy with (11.18) and (11.19), with sloping traces the expressions for the calculation of the effective length of the optical path, reduced for absorptivity of carbon dioxide to the surface layer of the atmosphere, will have the form

-- altitude range from H_1 to H_2

$$L_{\text{red.eff}} = \frac{e^{-0.313H_1} - e^{-0.313H_2}}{0.313 \cos \gamma} \quad (11.21)$$

-- altitude range from 0 to H

$$L_{\text{red.eff}} = \frac{1 - e^{-0.313H}}{0.313 \cos \gamma} \quad (11.22)$$

Relations (11.20), (11.21), and (11.22) permit calculating the effective length of the optical path of radiation in the atmosphere reduced for absorptivity of CO_2 to the surface layer. These values of $L_{\text{red.eff}}$ are initial for determining coefficients $\tau_t(\lambda)\text{CO}_2$ from Table 7 of the Appendix.

Thus, the relation obtained provides the opportunity, in the 326 first approximation, of calculating the transparency of the atmosphere for monochromatic radiation on horizontal as well as on sloping and vertical paths. Sometimes, the tables of spectral coefficients of the transparency of the atmosphere are compiled depending on the value of the absorbing mass expressed in atm-cm. The change from distances and thicknesses of attenuating layers to the absorbing mass is accomplished from formulas of the type

$$w' = f' L p_0 10^3 \quad (11.23)$$

where f' is the coefficient which characterizes the content of absorbing substance in the environment, expressed in percent; L is the effective length of the optical path in km, and p_0 is the pressure in atmospheres.

Data on the content of various components in the atmosphere are presented in Chapter 2.

CHAPTER 12. SELECTION OF RADIATION RECEIVERS AND CALCULATION OF THEIR CHARACTERISTICS

12.1. A Method for Calculating Spectral Sensitivity and Monochromatic Threshold Flux of Photocells and Photomultipliers

By analogy with (4.3), the integral sensitivity for the luminous flux F can be expressed by a relation

$$S^1 = \frac{U}{F} \quad (12.1)$$

In order to change the integral sensitivity which is estimated from the influence of the radiation flux of the same source, it is necessary to consider the connection between the luminous flux and the radiation flux which is established by the formula

$$F = \Phi K_{\max}(\lambda) \eta. \quad (12.2)$$

Substituting the value F in (12.1), we have

$$S^1 = \frac{U}{\Phi K_{\max}(\lambda) \eta}, \quad (12.3)$$

whence, with consideration of (4.3), we find

$$S^1 = \frac{S}{K_{\max}(\lambda) \eta} \quad \text{or} \quad S = S^1 K_{\max}(\lambda) \eta \quad (12.4)$$

In this expression, $K_{\max}(\lambda) = 683 \text{ lm/W}$ is the maximum sensitivity of the eye; η is the efficiency of the eye for a given emitter.

Formulas (12.4) establish the connection between the integral sensitivities of the receiver for luminous flux and radiation flux of the same emitter. /327

Since spectral sensitivity S_λ is expressed by the integral sensitivity in accordance with the equality

$$S_\lambda = \frac{S}{k} s(\lambda).$$

replacing the value S in it with its value from expression (12.4), we obtain

$$S_{\lambda} = S_1 \frac{K_{\max}(\lambda) \eta}{k} s(\lambda). \quad (12.5)$$

Here η_s is the efficiency of the eye for radiation from a standard source. This formula permits calculating the spectral sensitivity of photocells and photomultipliers using reference data. In this regard, as follows from the formula, it is sufficient to calculate one value of the function S_{λ} with $s(\lambda) = 1$, and to obtain the remainder by multiplication of the calculated maximum sensitivity times the value of the function $s(\lambda)$.

For example, for the photomultiplier FEU-25 (spectral characteristic of the photocathode S-6), the placement in formula (12.5) of the values: integral sensitivity of the photocathode $S_{pc}^1 = 3 \mu A/lm$; coefficient $\eta_s = 0.0243$ and $K_s = 0.0158$ provides

$$S_{\lambda} = 35 \cdot 10^{-6} \frac{683 \cdot 0.0243}{0.0158} s(\lambda) = 0.037 s(\lambda) \text{ A/W}$$

The threshold values of the monochromatic radiation flux can be calculated from expression (4.22)

$$\Phi_{\lambda t} = \Phi_t \frac{k}{s(\lambda)}$$

Since on the basis of (12.2) $F_t = \Phi_t K_{\max}(\lambda) \eta$,

$$\Phi_{\lambda t} = F_t \frac{k_s}{K_{\max}(\lambda) s(\lambda)} \quad (12.6)$$

where F_t , k_s is the threshold luminous flux and utilization coefficient of the receiver for a standard emitter.

Relation (12.6) provides the opportunity to determine the monochromatic threshold fluxes of the photocells and photomultipliers, and the variable value here is only the function $s(\lambda)$. Therefore, to obtain the spectral distribution of the threshold sensitivity, it is sufficient to calculate $\Phi_{\lambda t}$ with $s(\lambda) = 1$, i.e., the minimum monochromatic threshold flux. Then, calculating /328

the values $\frac{\Phi_{\lambda t \min}}{s(\lambda)}$, we find the desired distribution of threshold radiation flux for the spectrum.

12.2. Calculation of the Characteristics of Radiation Receivers

The values of integral sensitivity and threshold flux presented in certificates and reference books are measured from the effect of luminous flux or radiation flux of a standard radiation source.

Under real conditions, the functions of the spectral density of the radiation flux of emitters $\phi_r(\lambda)$ in accordance with which the instrument operates can be distinguished from the similar function $\phi_s(\lambda)$ of a standard source. In such cases, to evaluate the possibilities of employing a given receiver for operation with real emitters, the recalculation of its characteristics is performed.

In order to establish the connection between the characteristics and the receiver for real and standard emitters, let us use some of the relations from Section 4.2. On the basis of (4.7) and considering (4.9), we write the expressions which determine the integral sensitivities of the receiver for standard S_s and real S_r emitters:

$$S_s = S_{\lambda \max} \frac{\int_0^{\infty} \phi_s(\lambda) s(\lambda) d\lambda}{\int_0^{\infty} \phi_s(\lambda) d\lambda} = S_{\lambda \max} k_s; \quad (12.7)$$

$$S_r = S_{\lambda \max} \frac{\int_0^{\infty} \phi_r(\lambda) s(\lambda) d\lambda}{\int_0^{\infty} \phi_r(\lambda) d\lambda} = S_{\lambda \max} k_r, \quad (12.8)$$

where $S_{\lambda \max}$ is the maximum spectral sensitivity of the receiver; k_s and k_r are the utilization coefficients of the receiver for standard and real emitters, respectively.

Coefficients k_s and k_r in general are not equal to each other since they are calculated for emitters with different $\phi(\lambda)$. At the same time, $S_{\lambda \max}$, being a characteristic of the receiver itself, does not depend on the parameters of the emitter. Therefore, in (12.7) and (12.8), $S_{\lambda \max}$ is the same.

Expressing $S_{\lambda_{\max}}$ from (12.7) and placing its value in (12.8), we obtain

$$S_r = S_s \frac{k_r}{k_s} \quad (12.9)$$

If the integral sensitivity of the receiver for the standard /329 source was measured in accordance with the influence of the luminous flux, then keeping in mind (12.4) from (12.9) we will have

$$S_r = S_s^1 K_{\max}(\lambda) \eta_s \frac{k_r}{k_s} \quad (12.10)$$

where $K_{\max}(\lambda) = 683 \text{ lm/W}$; η_s is the efficiency of the eye utilization coefficient for a standard source.

If it is necessary to determine the integral sensitivity of a receiver to the luminous flux of a real emitter, we proceed in the following manner.

On the basis of formula (12.4), which connects the integral sensitivities S and S^1 of the receiver, it is necessary to write these expressions as applicable to a standard and real emitter:

$$S_s = S_s^1 K_{\max}(\lambda) \eta_s \quad (12.11)$$

$$S_r = S_r^1 K_{\max}(\lambda) \eta_r \quad (12.12)$$

Solving (12.11) relative to $K_{\max}(\lambda)$ and substituting the value obtained in (12.12), we find

$$S_r = \frac{S_r^1}{S_s^1} S_s \frac{\eta_r}{\eta_s} \quad \text{or} \quad S_r^1 = \frac{S_r}{S_s} S_s^1 \frac{\eta_s}{\eta_r} \quad (12.13)$$

Since, on the basis of (12.9) $S_r/S_s = k_r/k_s$, from (12.7) we finally obtain

$$S_r^1 = S_s^1 \frac{k_r \eta_s}{k_s \eta_r} \quad (12.14)$$

This formula permits calculating the integral sensitivity of the receiver for the luminous flux of an actual emitter if we know the value S_s^1 .

To establish the connection between threshold fluxes of the receiver for standard and real emitters, we use the relation (4.21) and, on its basis, we write the expression which determines $\Phi_{s.t.}$ and $\Phi_{r.t.}$.

$$\Phi_{s.t.} = \frac{\sqrt{U_m^2}}{S_s} \quad (12.15)$$

$$\Phi_{r.t.} = \frac{\sqrt{U_n^2}}{S_r} \quad (12.16)$$

Since $\sqrt{U_n^2}$ is the same in both formulas, the joint solution of equations (12.15) and (12.16) provides /330

$$\Phi_{r.t.} = \Phi_{s.t.} \frac{S_s}{S_r}$$

whence, with consideration of (12.9), we find

$$\Phi_{r.t.} = \Phi_{s.t.} \frac{k_s}{k_r} \quad (12.17)$$

If the threshold flux of the receiver is evaluated from the effect of luminous radiation of a standard source, then to obtain the desired relation it is sufficient to place in formula (12.17) instead of $\Phi_{s.t.}$ its value from (1.34), then

$$\Phi_{r.t.} = \frac{F_{s.t.}}{K_{\max}(\lambda)\eta_s} \frac{k_s}{k_r} \quad (12.18)$$

In calculating the threshold flux for luminous radiation of a real source we find the relation necessary in this case by placing in (12.17) the values of the threshold fluxes $\Phi_{r.t.}$ and $\Phi_{s.t.}$, expressed by the luminous threshold fluxes:

$$\Phi_{r.t.} = \frac{F_{r.t.}}{K_{\max}(\lambda)\eta_r} \quad \text{and} \quad \Phi_{s.t.} = \frac{F_{s.t.}}{K_{\max}(\lambda)\eta_s}$$

Whence we obtain

$$F_{r.t.} = F_{s.t.} \frac{k_s \eta_r}{k_r \eta_s} \quad (12.19)$$

Thus, the threshold flux of the receiver for a real emitter can be calculated on the basis of data on the threshold flux for a standard source by one of the formulas (12.17), (12.18), or (12.19).

The specific conditions for the use of a radiation receiver in an instrument for a specific purpose are made up of the additional restrictions which it is necessary to consider. Such restrictions include the type and frequency of modulation of the radiation flux, the width of the transmission band of the amplifier, and others. Their influence is felt especially on the characteristics of the photoresistors and bolometers. The modulation frequency affects the integral sensitivity of the photoresistor as a result of its rather significant inertia. This effect is manifested as a reduction in the integral sensitivity S_f with an increase in the frequency modulation of f and is described by the relations

-- with sinusoidal modulation

$$S_f = \frac{S_0}{\sqrt{1 + (2\pi f\tau)^2}} \quad (12.20)$$

-- with a square shape of pulses of radiation flux

$$S_f = S_0 \frac{1 - e^{-\frac{1}{2f\tau}}}{1 + e^{-\frac{1}{2f\tau}}} \quad (12.21)$$

where S_0 is the integral sensitivity of the receiver with modulation frequencies close to $f = 0$. τ is the time constant of the receiver. /331

Therefore, in designing an instrument, we strive to select the modulation frequencies so that they do not have a significant effect on the reduction of integral sensitivity. Such a condition is satisfied by the maximum permissible modulation frequencies determined as

$$f_m = \frac{1}{3\tau} + \frac{1}{2\tau} \quad (12.22)$$

However, in a number of cases, condition (12.16) cannot be satisfied and this leads not only to a reduction in the integral sensitivity but also to a worsening of the threshold flux of the receiver and the instrument as a whole.

In Section 4.4, it was shown that with low modulation frequencies, the effect of current noises is manifested especially strongly. In order to consider their effect with a change in

modulation frequency, we refine formula (4.93) with consideration of (4.88):

$$\bar{U}_n^2 = \bar{U}_i^2 \frac{f_0}{f_m} + \bar{U}_r^2 + \bar{U}_t^2 \quad (12.23)$$

We write the expression for threshold flux with frequency of sinusoidal modulation f_M :

$$\Phi_{tI} = \frac{\sqrt{\bar{U}_n^2(f_m)}}{S_f} = \frac{\sqrt{\bar{U}_i^2 \frac{f_0}{f_m} + \bar{U}_r^2 + \bar{U}_t^2}}{S_0} \sqrt{1 + (2\pi f \tau)^2}. \quad (12.24)$$

If the frequency of modulation of the radiation current is such that the current noise is predominant and the remaining components can be disregarded, relation (4.18) takes the form

Inasmuch as

$$\left. \begin{aligned} \Phi_{tI}^{(1)} &= \frac{\sqrt{\bar{U}_i^2}}{S_0} \sqrt{\frac{f_0}{f_m}} \sqrt{1 + (2\pi f \tau)^2} \\ \frac{\sqrt{\bar{U}_i^2}}{S_0} &= \Phi_{tI}^{(1)} \end{aligned} \right\} \quad (12.25)$$

then

$$\Phi_{tI}^{(1)} = \Phi_{tI}^{(1)} \sqrt{\frac{f_0}{f_m}} \sqrt{1 + (2\pi f_m \tau)^2}. \quad (12.26)$$

If the basic type of noise is thermal, then

$$\Phi_{tI} = \Phi_{tI}^{(1)} \sqrt{1 + (2\pi f_m \tau)^2}. \quad (12.27)$$

In order to determine the threshold flux of the receiver with connection to the input of an amplifier with band transmission $f_2 - f_1$, it is necessary to calculate coefficient $k(\Delta f)$ according /332 to the previously presented formulas and multiply the right sides of expressions (12.24), (12.26), and (12.27) by it.

12.3. Quantum Effectiveness and Quantum Threshold Sensitivity and a Method for Their Calculation

When the source of radiation is a monochromatic emitter, for example a laser, such characteristics as quantum effectiveness, quantum threshold sensitivity, and their distribution over the spectrum are usually used.

Quantum effectiveness q is calculated from the formula

$$q = \frac{N_{qu.pe}}{N_{qu}} \quad (12.28)$$

where $N_{qu.pe}$ is the number of quanta actively absorbed by the sensitive layer; N_{qu} is the overall number of quanta.

Inasmuch as one quantum of radiation can dislodge only one photoelectron, quantum effectiveness can be characterized as the relation of the number of dislodged primary photoelectrons N_{pe} to the overall number of quanta which have fallen on the sensitive layer

$$q = \frac{N_{pe}}{N_{qu}} \quad \text{or} \quad q = \frac{1}{L_{qu}}$$

where $L_{qu} = N_{qu}/N_{pe}$ is the number of quanta per photoelectron on the average.

A relation exists between the number of photoelectrons dislodged from the sensitive layer of the receiver in a unit of time and the arising photocurrent I

$$N_{pe} = \frac{I}{e} \quad (12.29)$$

Here $e = 1.6 \cdot 10^{-19}$ C is the electron charge.

On the other hand, the monochromatic radiation flux Φ_λ and the number of radiation quanta corresponding to it are connected to each other by the equality

$$N_{qu} = \frac{\Phi_\lambda}{h\nu} = \frac{\Phi_\lambda}{hc} \lambda \Delta t \quad (12.30)$$

where $h = 6.6252 \cdot 10^{-34}$ J·c is Planck's constant; ν is the frequency of electromagnetic oscillations of a given monochromatic radiation; $c \approx 3 \cdot 10^{10}$ cm·c⁻¹ is the rate of propagation of

electromagnetic oscillations in a vacuum; λ is the wavelength of monochromatic radiation in cm; Δt is the time interval during which the radiation flux acts. /333

On the basis of (12.28), with consideration of (12.29) and (12.30), the quantum effectiveness of a receiver for a monochromatic radiation flux will be

$$q_\lambda = \frac{I}{\Phi_\lambda} \cdot \frac{hc}{e\lambda}. \quad (12.31)$$

Since $\frac{I}{\Phi_\lambda} = S_\lambda$, $q_\lambda = S_\lambda \frac{hc}{e\lambda}$. (12.32)

Substituting the numerical values of constants h , c and e here, we obtain

$$q_\lambda = S_\lambda \frac{1.242}{\lambda} 10^{-4}, \quad (12.33)$$

where λ is measured in cm. If the wavelength is measured in μm , formula (12.33) takes the form

$$q_\lambda = S_\lambda \frac{1.242}{\lambda}. \quad (12.34)$$

Replacing S_λ in this expression by its value from (4.15) and (12.5), we find

$$q_\lambda = S \frac{s(\lambda)}{k} \frac{1.242}{\lambda} \quad (12.35)$$

$$q_\lambda = S^1 \frac{K_{\max}(\lambda) \eta}{k} s(\lambda) \frac{1.242}{\lambda}. \quad (12.36)$$

Formulas (12.35) and (12.36) provide the opportunity to calculate the monochromatic quantum effectiveness of the receiver from the known integral sensitivities S and S^1 measured from the influence of radiation flux and luminous flux, respectively. Coefficients k and η are calculated for the radiation of the same source.

The expressions which determine the monochromatic quantum effectiveness of the receiver on the wavelength of maximum sensitivity, i.e., with $s(\lambda) = 1$, can be presented in the form

$$q_{\lambda \max} = \frac{S}{k} \frac{1.242}{\lambda_{\max}} \quad (12.37)$$

and

$$q_{\lambda \max} = \frac{S^1}{k} K_{\max}(\lambda) \eta \frac{1.242}{\lambda_{\max}} \quad (12.38)$$

In order to find the distribution of the function q_{λ} through the spectrum through the value $q_{\lambda \max}$ we take their relation. Then, from (12.35) and (12.37) or (12.36) and (12.38), we obtain

$$q(\lambda) = \frac{q_{\lambda}}{q_{\lambda \max}} = \frac{\lambda_{\max}}{\lambda} s(\lambda),$$

whence

$$q_{\lambda} = q_{\lambda \max} \frac{\lambda_{\max}}{\lambda} s(\lambda). \quad /334 \quad (12.39)$$

This relation shows that the spectral distribution of the quantum effectiveness is determined not only by the function of relative spectral sensitivity but also by the position of the section of the spectrum being considered on the wave scale.

The quantum threshold sensitivity can be found from expression (12.30)

$$N_{\lambda t} = \frac{\Phi_{\lambda t}}{hc} \lambda \Delta t \quad (12.40)$$

Substituting the values of the constants h and c here, we obtain

$$N_{\lambda t} = 5.03 \cdot 10^{18} \Phi_{\lambda t} \lambda \Delta t \quad (12.41)$$

From this expression, with consideration of (4.22) and (12.6), we find the expression for the calculation of monochromatic quantum threshold sensitivity for the standard threshold radiation flux or luminous flux:

$$N_{\lambda t} = 5.03 \cdot 10^{18} \Phi_{s.t.} \frac{k_s}{s(\lambda)} \lambda \Delta t \quad (12.42)$$

$$N_{\lambda t} = 5.03 \cdot 10^{18} F_{s.t.} \frac{k_s}{K_{\max}(\lambda) \eta_s s(\lambda)} \lambda \Delta t \quad (12.43)$$

The quantum threshold sensitivity on the wavelength of maximum sensitivity, i.e., with $s(\lambda) = 1$, will be

$$N_{t\lambda_{\max}} = 5.03 \cdot 10^{18} \Phi_{s.t.} k_{\lambda_{\max}} \Delta t \quad (12.44)$$

or

$$N_{t\lambda_{\max}} = 5.03 \cdot 10^{18} F_{s.t.} \frac{k_s}{K_{\max}(\lambda) \eta_s} \lambda_{\max} \Delta t \quad (12.45)$$

If we take the ratio of relationships (12.42) and (12.44), then

$$N(\lambda) \frac{N_{t\lambda}}{N_{t\lambda_{\max}}} = \frac{\lambda}{\lambda_{\max} s(\lambda)} \quad \text{or} \quad N_{\lambda t} = N_{t\lambda_{\max}} N(\lambda) \frac{\lambda}{\lambda_{\max} s(\lambda)} \quad (12.46)$$

12.4. A Method for Calculating Quantum Effectiveness from the Integral Radiation of a Source

The quantum effectiveness of a receiver for complex radiation, similar to integral sensitivity, characterizes the total reaction of the receiver to radiations of all wavelengths expressed by the ratio of the number of photoelectrons which arise to the overall number of actuating quanta.

To obtain the desired ratio, we will proceed on the principle of superposition, i.e., determine the number of photoelectrons which arise on each wavelength, sum them, and refer them to the overall number of actuating radiation quanta. /335

The number of radiation quanta in a monochromatic radiation flux is determined by the expression

$$N_{\lambda} = \frac{\Phi_{\lambda}}{h\nu} = \frac{\phi(\lambda) \lambda d\lambda}{hc}, \quad (12.47)$$

since $\Phi_{\lambda} = \phi(\lambda) d\lambda$ and $\nu = c\lambda^{-1}$.

If the quantum effectiveness of the receiver is described by function q_{λ} , the number of photoelectrons which arise under the influence of quanta of complex radiation is found as the integral

$$N_{pe} = \int_0^{\infty} N_{\lambda} q_{\lambda} d\lambda. \quad (12.48)$$

The function q_{λ} can be presented in the form

$$q_{\lambda} = q_{\lambda \max} q(\lambda), \quad (12.49)$$

where $q(\lambda) = q_{\lambda}/q_{\lambda \max}$ is the quantum effectiveness on wavelength λ as compared to the maximum.

Since on the basis of (12.37)

$$q_{\lambda \max} = \frac{S}{k} \frac{1.242}{\lambda_{\max}}, \text{ and } q_{\lambda} = \frac{S}{k} \frac{1.242}{\lambda} s(\lambda), \quad (12.50)$$

$$\text{then } q(\lambda) = \frac{\lambda_{\max}}{\lambda} s(\lambda).$$

Placing the values for $q(\lambda)$ and N_{λ} in (12.48), from (12.47) we have

$$N_{pe} = \frac{1}{hc} q_{\lambda \max} \lambda_{\max} \int_0^{\infty} \phi(\lambda) s(\lambda) d\lambda \quad (12.51)$$

Considering that $\int_0^{\infty} \phi(\lambda) s(\lambda) d\lambda = \Phi K$, we obtain

$$N_{pe} = q_{\lambda \max} \frac{\Phi K}{hc} \lambda_{\max}. \quad (12.52)$$

The last expression provides the opportunity to calculate the number of photoelectrons which arise in a unit of time under the influence of a radiation flux from the known quantum effectiveness on the wavelength of maximum sensitivity.

Sometimes N and q are determined in a different way. The number of photoelectrons in a unit of time is calculated by formula (12.29) written in the form /336

$$N_{pe} = \frac{\Phi S}{e}$$

We also come to this expression in the case where we place in (12.52) $q\lambda_{\max}$ from (12.50) and the values h and c .

The overall number of quanta N in complex radiation will be

$$N = \int_0^{\infty} N_{\lambda} d\lambda = \int_0^{\infty} \frac{\phi(\lambda)}{hc} \lambda d\lambda. \quad (12.53)$$

If the emitter is an IBB, $\phi(\lambda) = r(\lambda)A$; $r(\lambda) = C_1 \lambda^{-5} (e^{\frac{C_2}{\lambda T}} - 1)^{-1}$, then

$$N = \frac{A}{hc} \int_0^{\infty} \frac{C_1}{\lambda^5} \frac{\lambda}{\left(e^{\frac{C_2}{\lambda T}} - 1\right)} d\lambda. \quad (12.54)$$

Taking the designations: $\frac{C_2}{\lambda T} = q$; $\lambda = \frac{C_2}{qT}$; $d\lambda = -\frac{C_2}{q^2 T} dq$, from (12.54) we obtain:

$$N = \frac{A}{hc} \frac{C_1}{C_2^3} T^3 \int_0^{\infty} \frac{q^2}{e^q - 1} dq. \quad (12.55)$$

Since an integral of the form

$$\int_0^{\infty} \frac{q^n}{e^q - 1} dq = \Gamma(n+1) \sum_{t=1}^{\infty} \frac{1}{t^{n+1}} = n! \sum_{t=1}^{\infty} \frac{1}{t^{n+1}},$$

where $t = 1, 2, 3, \dots$ is the natural series of numbers, then

$$\int_0^{\infty} \frac{q^2}{e^q - 1} dq = 2 \left(1 + \frac{1}{2^3} + \frac{1}{3^3} + \frac{1}{4^3} + \dots \right) = 2,4041.$$

Then

$$N = 2,4041 \frac{A}{hc} \frac{C_1}{C_2^3} T^3. \quad (12.56)$$

We rewrite (12.56) in a somewhat different form

$$\begin{aligned} N &= 2,4041 \frac{6.455}{6.455} A \frac{1}{hc} \frac{C_1 C_2}{C_2^3 C_2} \frac{T^3 T}{T} = \\ &= A \frac{C_1}{C_2^4} T^4 6.455 \frac{C_2}{T hc} \frac{2,4041}{6.455}. \end{aligned}$$

Whence, considering (1.21), (1.6) and (1.20)

/337

$$\begin{aligned} 6.455 \frac{C_1}{C_2^4} T^4 &= \Phi, \\ C_2 &= \frac{hc}{k}; \quad A T^4 = \Phi, \end{aligned}$$

we obtain

$$N = 0.3724 \frac{\Phi}{kT}, \quad (12.57)$$

where k is Boltzmann's constant; T , the temperature of the emitter.

Knowing N_{pe} and N , we find the integral quantum effectiveness of the receiver from the expression

$$q = \frac{N_{pe}}{N} = \frac{\Phi S}{e} : \frac{KT}{0.3724\Phi} = 2,32ST \cdot 10^{-4}. \quad (12.58)$$

If we express q by $q\lambda_{max}$, then substituting N_{pe} in (12.58) from (12.52), after conversions we obtain

$$q = 1.87 q_{\lambda_{max}} k T \lambda_{max}. \quad (12.59)$$

Relations (12.58) and (12.59) provide the opportunity to calculate the integral quantum effectiveness of the receiver for

complex radiation, the spectral distribution of which follows Planck's law. If the function of spectral density of radiation flux does not follow Planck's law, the integral quantum effectiveness should be calculated from the formulas

$$q = \frac{N_{pe}}{N} = \frac{q_{\lambda_{max}} \frac{\Phi k}{hc} \lambda_{max}}{\frac{1}{hc} \int_0^{\infty} \phi(\lambda) \lambda d\lambda} = \frac{q_{\lambda_{max}} \Phi k \lambda_{max}}{\int_0^{\infty} \phi(\lambda) \lambda d\lambda}, \quad (12.60)$$

$$q = \frac{N_{pe}}{N} = \frac{\Phi S hc}{e \int_0^{\infty} \phi(\lambda) \lambda d\lambda} = 1,242 \cdot 10^{-4} \frac{\Phi S}{\int_0^{\infty} \phi(\lambda) \lambda d\lambda} \quad (12.61)$$

The formulas derived provide the opportunity of changing from integral quantum effectiveness for one emitter to quantum effectiveness for another emitter. Using relation (12.59), we write the expression for q as applicable to a standard and real emitters

$$q_e = 1.87 q_{\lambda_{max}} k_s T_s \lambda_{max} \quad (12.62)$$

$$q_r = 1.87 q_{\lambda_{max}} k_r T_r \lambda_{max}$$

and, solving them jointly, we find

/338

$$q_r = q_s \frac{k_r}{k_s} \frac{T_r}{T_s} \quad (12.63)$$

If a real emitter is not gray, then using one of the formulas (12.61), we write the equations

$$\begin{aligned} q_s &= 1.242 \cdot 10^{-4} \frac{\phi_s k_s \lambda_{max}}{\int \phi_s(\lambda) \lambda d\lambda} q_{\lambda_{max}} \\ q_r &= 1.242 \cdot 10^{-4} \frac{\phi_r k_r \lambda_{max}}{\int \phi_r(\lambda) \lambda d\lambda} q_{\lambda_{max}} \end{aligned} \quad (12.64)$$

after the joint solution of which we obtain

$$q_r = q_s \frac{\phi_r k_r}{\phi_s k_s} \frac{\int_0^{\infty} \phi_s(\lambda) \lambda d\lambda}{\int_0^{\infty} \phi_r(\lambda) \lambda d\lambda} = q_s \frac{k_r}{k_s} T_s \left[\frac{\phi_r}{\int_0^{\infty} \phi_s(\lambda) \lambda d\lambda} \right] \quad (12.65)$$

Expressions (12.63) and (12.65) provide the opportunity to calculate the quantum effectiveness for a real emitter if the quantum effectiveness of the receiver for a standard emitter is known.

And finally, the equivalent threshold flux Φ_t of the receiver is the quantum integral threshold sensitivity for the radiation of an IBB N_t , the expression for which can be obtained from (12.57)

$$N_t = 0.3724 \frac{\Phi_t}{kT} \quad (12.66)$$

Writing it down as applicable to the radiation of standard and real emitters and solving these relations jointly, we find

$$N_{r.t.} = N_{s.t.} \frac{k_s T_s}{k_r T_r} \quad (12.67)$$

12.5. Selection of the Optimum Radiation Receiver

For the correct selection of a radiation receiver, it is necessary to know the purpose and operating principle of the equipment, where the receiver should be used, the conditions for the operation of the equipment, duration of operation, and also the radiation characteristics of the objects and the background.

It is known that higher sensitivity is possessed by cooled radiation receivers. Therefore, their use in equipment permits improving its tactical and technical characteristics considerably. 339 However, the employment of such receivers in actual models of electro-optical equipment is connected with great difficulties. This problem is solved most simply in those cases where the instrument is intended for operation during a short period of time from fractions of an hour to several hours and the moment of the start of operation is known ahead of time. Then receivers cooled with dry ice, liquid air, liquid nitrogen, and so forth can be used with success. In instruments and devices intended for prolonged continuous operation, the use of cooled receivers is possible only with the presence of cooling devices which assure prolonged operation.

Thus, a preliminary evaluation of the conditions and duration of operation of the instrument as well as of the characteristics of the cooling devices permits drawing a conclusion about the possibility or impossibility of using a cooled radiation receiver.

To substantiate the type and selection of a specific model of receiver, an analysis of their parameters is conducted on the

basis of the characteristics of radiation of the objects on which the equipment should operate and of the background. In this, an attempt is made to see that, along with assuring the required range of action, the correlation between the useful signals and the interference signal is the greatest.

Therefore, despite the fact that operating conditions may differ, i.e., an object is projected on a non-radiating background or an object is projected on a uniform radiating background, or an object is projected on a nonuniform radiating background, the approach to the substantiation of the receiver being employed remains constant in all cases. Its basis is formed by the comparison of the useful signal with the interference signal or values equivalent to them. It is convenient to use the values of effective radiant fluxes which cause the indicated signals as such values. The difference in the substantiation of the receivers being employed depending on the situation will be determined only by the nature of the interference.

In the simplest case, when background radiation is absent and the sensitivity of the instrument is limited only by internal noise, substantiation of the receiver being employed is conducted on the basis of a comparison of the effective values of the radiant flux from the object and the threshold of the receiver expressed by the relations

$$\begin{aligned}\Phi_{r.\text{eff}} &= \Phi_r k_r \\ \Phi_{t.\text{eff}} &= \Phi_{s.t.} k_s\end{aligned}$$

The evaluation of the receivers is conducted as applicable to some specific instrument in which the width of the transmission band is the same for all possible receivers. Therefore, the receiver which is characterized by the maximum value of the relation /340

$$B_j = \frac{\Phi_{r.\text{eff}}}{\Phi_{t.\text{eff}}} = \frac{\Phi_r k_{rj}}{\Phi_{s.t.j} k_{sj}} \quad (12.68)$$

should be considered best.

Inasmuch as the value Φ_r is the same for all receivers, normalizing the value B_j in accordance with it we obtain a rather simple and convenient evaluation criterion

$$b_j = \frac{B_j}{\Phi_r} = \frac{k_{rj}}{\Phi_{s.t.j} k_{sj}} \quad (12.69)$$

This criterion characterizes the sensitivity of the instrument. The greater its value, the better. Therefore, from a group of preliminary selected receivers, the best are considered to be the receivers which are characterized by the largest values of the criterion b_j . It is not difficult to show that criterion b is the detecting capability of the receiver for a real emitter. Actually, since

$$\Phi_{r.t.} = \Phi_{s.t.} \frac{k_s}{k_r}$$

from (12.69) we have

$$b = \frac{1}{\Phi_{r.t.}} = D_r^*$$

In expressions (12.68) and (12.69), we mean by k_{rj} the coefficient of utilization of the radiation flux by the instrument as a whole with consideration of the effect of the environment, i.e.,

$$k_{rj} = \frac{\int_0^\infty \phi(\lambda) s(\lambda) \tau_a(\lambda) \tau_0(\lambda) d\lambda}{\int_0^\infty \phi(\lambda) d\lambda}$$

With the presence of a uniform or nonuniform radiating background in the instrument field of view, it is necessary to evaluate the receivers for their sensitivity to the radiation of the background. It is completely obvious that from this point of view the best will be the receivers which are least susceptible to the background. To evaluate the sensitivity of the receivers being compared to background radiation, we use the values of effective flux from the background and the value of effective threshold flux:

$$\Phi_{b.\text{eff}} = \Phi_b k_b$$

$$\Phi_{t.\text{eff}} = \Phi_{e.t} k_s$$

Taking the ratio of the values of effective fluxes, we obtain /341

$$a'_j = \frac{\Phi_{b.\text{eff}}}{\Phi_{t.\text{eff}j}} = \frac{\Phi_b k_{bj}}{\Phi_{s.tj} k_{sj}} \quad (12.70)$$

Inasmuch as the radiation flux from the background Φ_b which is caught by the instrument is determined only by the parameters of

the instrument, does not depend on the instrument, and is the same for all receivers, normalizing coefficients a'_j for the value Φ_b we obtain

$$a_j = \frac{a'_j}{\Phi_b} \frac{k_{jb}}{\Phi_{s.t} k_{js}} \quad (12.71)$$

We call coefficient a the criterion of susceptibility of receivers to the background radiation. The best with regard to perception of background radiation will be that receiver whose value of criterion a is the smallest.

If the background is nonuniform and its fluctuations may cause signals on the output of the instrument which are similar to signals from the objective, in selecting the receiver we can use one more criterion obtained on the basis of the first two. From the considerations which have been presented, it follows that the best for employment in the instrument is that receiver which is characterized by the largest value of one criterion and the smallest of the other. If, in a group which has been taken ahead of time for evaluation, the receiver is found whose criterion b has the greatest value in comparison with the others, and criterion a has the least, preference should be given to this very receiver. However, such agreements are not often encountered. Therefore, we should consider as best the receiver which is characterized by the greatest value of the ratio of criteria b and a , i.e.,

$$c_j = \frac{b_j}{a_j} \quad (12.72)$$

Substituting the values b and a in this expression, from (12.69) and (12.71) we have

$$c_j = \frac{k_{rj} \Phi_{sj} k_{sj}}{\Phi_{sj} j_{sj} k_{bj}} = \frac{k_{rj}}{k_{bj}} \quad (12.73)$$

The expression found for criterion c shows that the best one is the receiver which provides the greatest difference in susceptibility of radiation fluxes from the object and the background. Sometimes, the selection of the receiver is accomplished from the greatest values of the criteria b and c simultaneously.

When the radiation background along with the creation of interference signals causes an increase in the intrinsic noises and a worsening of sensitivity in addition, the substantiation of the rational radiation receiver should be accomplished from the maximum signal-interference ratio.

With the presence of constant background illuminations, the /342 basic and practically only criterion for the selection of a receiver is the first of the criteria examined above. The only difference is that the effective value of the threshold flux should be determined from expression (10.70)

$$\Phi_{t.\text{eff}} = \Phi_{s.t}^{(1)} k_s k(\Phi)$$

With consideration of this, the expression for the desired criterion takes the form

$$B_j = \frac{\Phi_{r.\text{eff}}}{\Phi_{t.\text{eff}}^{(1)}} = \frac{\Phi_r k_r}{\Phi_{s.t}^{(1)} k_s k(\Phi)} \quad (12.74)$$

After normalization of criterion B_j for value Φ_r , we obtain

$$b_j = \frac{k_r}{\Phi_{s.t}^{(1)} k_s k(\Phi)} \quad (12.75)$$

Thus, with the influence of constant background illuminations, we should consider as best the receiver with the greatest values of criterion b_j with a fixed value of constant illumination.

Inasmuch as the value of coefficient $k(\Phi)$ depends on the area of the entrance pupil of the objective as well as on the size of the angle of the instantaneous field of view, the evaluation of receivers for criterion b_j is best conducted with the use of graphs which have been normalized for $A_{\text{en.ap}}$ but depend on ω_v .

Thus, for photoelectric radiation receivers with an photo-emission value $k(\Phi)$ can be presented in the following manner:

$$k(\Phi) = \sqrt{1 + \frac{\int_0^\infty \phi_b(\lambda) s(\lambda) \tau_b(\lambda) d\lambda}{I_r}} = \sqrt{1 + \frac{S_{\lambda \max} \Phi_b k_b}{I_r}}$$

where $\Phi_b = B_b A_{\text{en.ap}} \omega_v$,

then

$$k(\Phi) = \sqrt{1 + \frac{S_{\lambda \max} B_b A_{\text{en.ap}} \omega_v k_b}{I_r}} \quad (12.76)$$

With the influence of constant illumination as applicable to photomultipliers and photocells, the expressions for criterion b_j will be

$$b_j = \frac{k_r}{\Phi_{s.t}^{(1)} k_s \sqrt{1 + \frac{S_{\lambda_{\max}} B_b A_{en. ap} 0^{\omega_v} k_b}{I_r}}} \quad (12.77)$$

or

$$b_j = \frac{k_r}{\Phi_{\lambda_{\min}}^{(1)} \sqrt{1 + \frac{S_{\lambda_{\max}} B_b A_{en. ap} 0^{\omega_v} k_b}{I_r}}} \quad (12.77a) \quad /343$$

If the background signal is considerably greater than the dark current, i.e., the second term of the radicand is greater than unity,

$$b_j = \frac{k_r}{\Phi_{s.t}^{(1)} k_s \sqrt{\frac{S_{\lambda_{\max}} B_b A_{en. ap} 0^{\omega_v} k_b}{I_r}}} \quad (12.78)$$

or

$$b_j = \frac{k_r}{\Phi_{\lambda_{\min}} \sqrt{\frac{S_{\lambda_{\max}} B_b A_{en. ap} 0^{\omega_v} k_b}{I_r}}} \quad (12.78a)$$

If the background is nonuniform and the fluctuations of its radiation can cause false signals, then from the group of receivers which possess the greatest values of criterion b_j we select the receivers with the least susceptibility to background radiation.

As was indicated earlier, such receivers are receivers whose value of criterion $c_j = k_{rj}/k_{bj}$ will be the least.

As applicable to photoelectric receivers with an photo-conduction, the method of selecting the optimum receiver with different background situations remains the same for photocells and photomultipliers with the only difference that coefficients $k(\Phi)$ for them should be calculated from the formulas of Section 10.3.

The considerations presented are valid when the lag of the receivers has practically no influence on the amplitude of the signals. When the duration of the influence of a radiant flux from an object on a receiver is comparable with the time constant or becomes less than it, the criteria for the evaluation of receivers need refinement.

The effect of the time constant on the amplitude of a signal can be considered as the corresponding reduction in the value of radiant flux from an object to the radiation receiver. In this connection, this reduction is determined by the relationship of the time constant and time of influence of the radiant flux from the object to the receiver. When the radiation receiver is a sluggish element, which is valid in the majority of cases, the indicated reduction can be considered by introducing a factor which characterizes the change in the output signal depending on the duration of the pulse. Then

$$\Phi_r^t = \Phi_r(1 - e^{-t/\tau}) \quad (12.79)$$

where t is the duration of the radiation pulse which acts on the receiver; τ is the time constant of the receiver. /344

Consequently, with a given duration t of the radiation pulses, we need to take as the effective value of the radiation flux from the object

$$\Phi_{r.\text{eff}}^t = \Phi_{r.\text{eff}}(1 - e^{-\frac{t}{\tau}}) = \Phi_{rk}(1 - e^{-\frac{t}{\tau}}). \quad (12.80)$$

If the real flux from an object which falls on the receiver is considered constant, which actually occurs, the effect of the lag of the receiver is best considered through the worsening of threshold sensitivity, i.e., through an increase in the value of the threshold flux

$$\Phi'_{s.t} = \frac{\Phi_{s.t}}{1 - e^{-\frac{t}{\tau}}} \quad (12.81)$$

Any of these ways for considering the effect of lag leads to the same result and the criteria which have been considered take the form:

-- in the absence of background

$$b_j = \frac{k_{rj} \left(1 - e^{-\frac{t}{\tau}}\right)}{\Phi_{s, t} k_{s^j}}; \quad (12.82)$$

$$a_j = \frac{k_{bj} \left(1 - e^{-\frac{t}{\tau}}\right)}{\Phi_{s, t} k_{s^j}}; \quad (12.83)$$

$$c = \frac{k_{rj}}{k_{bj}};$$

-- with the presence of uniform background

$$b_j = \frac{k_{rj} \left(1 - e^{-\frac{t}{\tau}}\right)}{\Phi_{s, t}^{(1)} \cdot k_{s^j} \cdot k(\Phi)} \quad (12.84)$$

-- with a nonuniform background

$$b_j = \frac{k_{rj} \left(1 - e^{-\frac{t}{\tau}}\right)}{\Phi_{s, t}^{(1)} \cdot k_{s^j} \cdot k(\Phi)}; \quad (12.85)$$

$$c_j = \frac{k_{rj}}{k_{bj}}.$$

The method described is also applicable when special optical /345 filters are used in aggregate with the receiver to change the signal/background ratio. The only difference in this case consists of finding the utilization coefficients of the receivers for the radiation of real sources which should be calculated from the formula

$$k_{rj} = \frac{\int_0^\infty \phi_r(\lambda) s_j(\lambda) \tau_a(\lambda) \tau_0(\lambda) \tau_{b_i}(\lambda) d\lambda}{\int_0^\infty \phi_r(\lambda) d\lambda}, \quad (12.86)$$

where $\tau_p(\lambda)$ is the spectral transparency of the filter.

Thus, if the receivers and the characteristics of the spectral transmission of the optical filters are known, the optimum combination can be found which permits either assuring maximum range of action or the greatest sensitivity or the smallest dimensions of the entrance pupil.

CHAPTER 13. SPECIAL FEATURES OF CALCULATING ELECTRO-OPTICAL INSTRUMENTS WITH LASERS

13.1. Special Features in Calculating Operating Range in the Absence of Background Radiation

The range of action of an electro-optical instrument with a laser, for example, a locator, is one of its basic parameters. Naturally, it depends both on the characteristics of the receiver and transmitter and the condition of the medium between the object and the locator and on the characteristics of the object itself and the background on which it is projected. The use of a laser as an emitter in electro-optical locators expands their possibilities substantially and, at the same time, leads to the appearance of changes in the circuits of the instruments and causes a number of distinguishing features in the computation method. These features are determined primarily by the high directivity and monochromatic quality of the radiation of the laser. Let us examine their effect on the method of calculating the range of action of the instruments (Fig. 13.1).

If the laser of a transmitter emits flux Φ_{laser} which falls entirely in the transmitting optical system, the radiation intensity of the transmitter in space, in accordance with (9.30), will be

$$I_t = \frac{4\Phi_{\text{laser}}\tau_t}{\pi\theta_t^2} \quad (13.1)$$

where τ_t is the transmission coefficient of laser radiation by the transmitter's optical system; θ_t is the plane angle of the apex of the solid angle ω_t of divergence of the transmitter beam.

The irradiance created on the object can be determined from the formula

$$E_{\text{ob}} = \frac{I_t}{L^2} = \frac{\Phi_{\text{laser}}\tau_t}{\omega_t L^2} \tau_e \cos \beta \quad (13.2)$$

where τ_e is the coefficient of transmission of laser radiation for the medium; β is the angle between the direction of the beam and the normal to the irradiated surface.

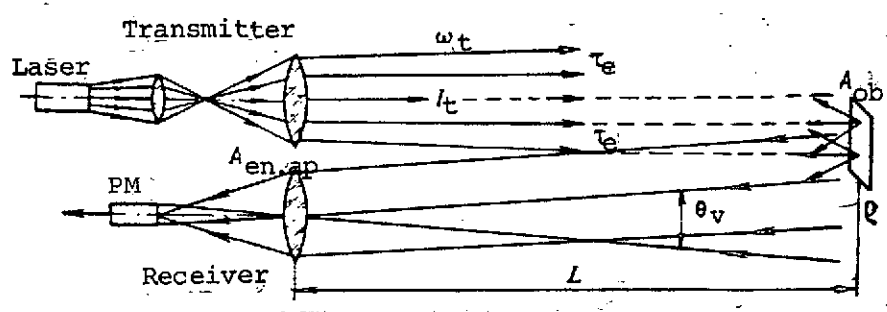


Fig. 13.1. For derivation of the equation of the range of action of an electro-optical locator.

After reflection from the object, some fraction of the laser radiation again returns to the locator. Only that portion of the reflected radiation falls on the locator's receiver which is propagated within the limits of the solid angle based on the entrance pupil.

The problem of determining the value of the reflected component at the entrance to the receiver is solved most simply in the case where the object is a plane surface.

If this surface reflects diffusely with coefficient ρ_d , the intensity of the reflected radiation in the direction to the locator will be

$$I_{ob} = \frac{E_{ob}}{\pi} A_{ob} \rho_d \cos \beta, \quad (13.3)$$

whence, with consideration of (13.2), we have

$$I_{ob} = \frac{\Phi_{laser} I_e}{\pi \omega_e L^2} A_{ob} \rho_d \cos^2 \beta. \quad (13.4)$$

The product

$$A_{ob} \rho_d \cos^2 \beta = A_{ob}^{eff} \quad (13.5)$$

is called the effective area of reflecting surface and we rewrite 1347 equation (13.4) in the form

$$I_{ob} = \frac{\Phi_{laser} A_{ob}^{eff}}{\pi \omega_t L^2} \tau_t \tau_e \quad (13.6)$$

Inasmuch as only that part of the reflected radiation falls on the receiver of the locator which is propagated within the limits of the solid angle based on an objective with area $A_{en.ap}$, the radiation flux of the transmitter on the entrance pupil of the receiver can be calculated by the formula

$$\Phi'_{rec} = \frac{I_{ob}}{L^2} A_{en.ap} \tau_e \quad (13.7)$$

where τ_e is the coefficient which considers attenuation of the radiation with reverse propagation.

Considering the attenuation of the laser radiation by the optical system and filter of the receiver with coefficients τ_0 and τ_f , we find the value of the flux which reached the receiver

$$\Phi_{rec} = \Phi'_{rec} \tau_0 \tau_f$$

whence, in accordance with equations (13.7) and (13.4), we have

$$\Phi_{rec} = \Phi_{laser} \frac{A_{ob}^{eff} A_{en.ap}}{\pi L^4 \omega_t} \tau_t^2 \tau_e \tau_0 \tau_f \quad (13.8)$$

Formula (13.8) shows that the laser radiation of the transmitter, reflected by the object and reaching the receiver, is attenuated in proportion to the fourth power of the distance between the object and the locator. The formula is valid in those cases where the angle of divergence of the locator beam exceeds the angular dimension of the object.

If the angle of divergence of the beam does not exceed the angular dimensions of the object, the reflected radiation will arrive at the receiver not from the entire surface of the object but only from its irradiated part, whose area is determined by the expression

$$A_{ob}^{ref} = \omega_t L^2 = \frac{\pi \theta^2 L^2}{4}$$

then

$$A_{ob}^{eff} = \omega_t L^2 \epsilon_d \cos^2 \beta = \frac{\pi \theta^2}{4} L^2 \epsilon_d \cos^2 \beta$$

Substituting the obtained value A_{ob}^{eff} in formula (13.8), we find

$$\Phi_{rec} = \Phi_{laser} \frac{A_{en.ap}}{\pi L^2} \tau_t \tau_e^2 \tau_0 \tau_f \rho_d \quad (13.9)$$

This expression is a particular case of a more general relation (13.8) which we will also use in the future. /348

For the dependable discrimination of the useful signal, it is necessary that the value Φ_{rec} exceed by m times the value of the threshold flux of the radiation receiver with a given width of transmission band of the electron channel

$$\Phi_{rec} \geq m \Phi_{\lambda t}^{(1)} k(\Delta f) \quad (13.10)$$

where m is the required signal/noise ratio; $\Phi_{\lambda t}^{(1)}$ is the monochromatic threshold flux of the receiver with transmission band $\Delta f = 1$; $k(\Delta f)$ is the coefficient which considers the worsening of the threshold flux with transmission band $\Delta f > 1$ Hz.

Solving equations (13.8) and (13.10) with respect to L , we obtain the formula for the calculation of the range of action of the locator

$$L = \sqrt{\frac{\Phi_{laser} \tau_t \tau_e^2 \tau_0 \tau_f}{m \Phi_{\lambda t}^{(1)} k(\Delta f) \pi \omega}} \quad (13.11)$$

If the reflecting surface of the object is not flat, formula (13.11), remaining just as written, in essence is transformed

somewhat due to the change in value A_{ob}^{eff} . We will show this using as an example an object having a spherical shape.

For it, the mirror and diffuse components of the intensity of reflected radiation are determined by relations (9.34) and (9.39), and the total radiation flux which falls in the instrument after reflection from the object by expression (9.42). Then, by analogy with (13.8), on the basis of (9.42) with consideration of (13.1), we write the formula for calculation of the amount of radiation flux which reached the radiation receiver after reflection from the object with a spherical form

$$\Phi_{rec} = \frac{\Phi_{laser} R^2 \tau_{fo} \tau_{en.ap}}{6^2 \pi L^4} \left(\frac{e_s}{4} + \frac{2}{3} e_d \right). \quad (13.12)$$

The joint solution of equations (13.10) and (13.12) leads to the formula for the range of action of an instrument which has the appearance

$$L = \sqrt[4]{\frac{16 \Phi_{laser} R^2 A_{en.ap} \tau_t \tau_e^2 \tau_o \tau_f}{m \pi^5 \Phi_{\lambda t}^{(1)} k(\Delta f)}}. \quad (13.13)$$

In this, $\Phi_{\lambda t}^{(1)}$ is calculated from the formulas presented in Chapter 12. In particular, for PM from formula (12.6) we obtain the relation

$$\Phi_{\lambda t}^{(1)} = F_{s.t} \frac{k_S}{K_{max}(\lambda) \tau_{S^s}(\lambda)} = \frac{k_S}{K_{max}(\lambda) \tau_{S^s}(\lambda)} \sqrt{\frac{5eI}{S_{PM}^s S_{pc}^s}}. \quad (13.14)$$

where I is the current strength.

The value of coefficient $k(\Delta f)$ as applicable to a PM is calculated from the formula $k(\Delta f) = \sqrt{\Delta f}$, where Δf is the required width of the transmission band, which can be determined from formula (10.69)

$$\Delta f = \frac{k_f (1 + m) \theta_{sc}^2}{T_k \theta_v^2}.$$

Placing it all in expression (13.13), we obtain the formula for calculating the range of action of a locator without consideration of background illumination

where T_k is the time for scanning a frame (pulse duration); $\Phi_{\lambda t}^{(1)}$ is the monochromatic threshold flux of a radiation receiver with a single amplifier transmission band; θ_t is the angle of divergence of the transmitter beam; θ_{sc} is the scanning angle; k_f is the coefficient which considers the shape of the pulse; m_0 is the coefficient of overlap of space in scanning.

Formula (13.15) permits calculating the range of action of a locator without consideration of the effect of illumination from the background. The coefficients k_s and n_s for various photocathodes of the PM which are necessary in this case are presented in Table 13.1.

TABLE 13.1

Emit- ter	η	Value of coefficient k for various spectral characteristics of photocathodes											
		C_1	C_2	C_3	C_4	C_5	C_6	C_7	C_8	C_9	C_{11}	C_{12}	C_{13}
Stand- ard "A"	0.0243	0.208	0.0176	0.0188	0.0416	0.0439	0.0158	0.0473	0.0176	0.0172	0.0418	0.0330	0.0114
Solar radia- tion	0.427	0.427	0.193	0.300	0.334	0.325	0.0240	0.380	0.241	0.274	0.325	0.335	0.240

Sometimes, to increase the range of action of instruments, special corner reflectors ("tail light" reflectors) are installed on the objects. With their use (see Chapter 9), the radiation flux on the input of the receiver can be found from formula (9.52).

$$\Phi_{\text{rec}} = \frac{16\Phi_{\text{laser}} A_{\text{refl}} A_{\text{en.ap}} \rho_{\text{refl}} \tau_0 \tau_f \tau_e^2 \tau_t}{L^4 \pi^2 \theta_t^2 \left(\frac{\lambda}{d \cos \beta} + 0.05n \right)^2} 10^8 \cos \beta$$

From this relation, considering (13.10) and substituting /350
instead of $k(\Delta f)$ its value from (10.67) $k(\Delta f) = \sqrt{\Delta f} = \frac{\theta_{sc}}{\theta_v} \sqrt{\frac{k_f(1+m_0)}{T_k}}$,
we find

$$L_{r,r} = \sqrt{\frac{16\Phi_{\text{laser}} A_{\text{refl}} A_{\text{en.ap}} \tau_t \tau_e^2 \tau_0 \tau_f \cos \beta \sqrt{T_k} \cdot 10^8}{m \Phi_{\lambda t}^{(1)} \pi^2 \theta_{sc} \left(\frac{\lambda}{d \cos \beta} + 0.05n \right)^2 k_f (1 + m_0)}} \quad (13.16)$$

The obtained formula permits calculating the range of action of an electro-optical locator against an object equipped with a unit of corner reflectors. The values which make up the formula are inserted in the following dimensions:

$$\begin{aligned} \Phi_{\text{laser}} &-- \text{W}; A_{\text{refl}} \text{ and } A_{\text{en.ap}} -- \text{m}^2; \Phi_{\lambda t}^{(1)} -- \text{W} \cdot \text{Hz}^{-1/2}; \\ k(\Delta f) = \sqrt{\Delta f} &-- \text{Hz}^{1/2}; \theta_t, \theta_{sc} -- \text{rad}; \lambda -- \mu\text{m}; d -- \text{cm}; \\ n &-- \text{seconds of arc}; k_t, m_0, m, \rho_{\text{refl}}, \tau_0, \tau_e, \tau_f, \\ &\tau_t -- \text{dimensionless}. \end{aligned}$$

Let us examine the employment of formula (13.16) using the following example. Assume that a gas laser (He-Ne) which operates in a continuous mode is used in a locator; the laser's $\Phi_{\text{laser}} = 20 \text{ mW}$ and $\theta_t = 3 \cdot 10^{-4} \text{ rad}$. The area of the entrance pupil of the objective of the locator's receiver is $A_{\text{en.ap}} = 100 \text{ cm}^2 = 0.01 \text{ m}^2$.

The FEU-46A is used as a radiation receiver ($\Phi_{\lambda t}^{(1)} = 1 \cdot 10^{-14} \text{ W/Hz}^{1/2}$). The optical system of the receiver and the filter is characterized by coefficients $\tau_0 = 0.8$; $\tau_f = 0.3$. On the object, a corner reflector is used on which $A_{\text{refl}} = 0.02 \text{ m}^2$, $\rho_{\text{refl}} = 0.9$, $d = 6 \text{ cm}$ and the manufacturing precision is characterized by the value $n = 2$. Setting $k_f = 1$, $m_0 = 0.5$, $\theta_{sc} = 0.078 \text{ rad}$ and the signal-noise ratio $m = 5$, $\tau_e = 1.0$, and $T_k = 0.1 \text{ sec}$, we have

$$L_{r,r} = \sqrt{\frac{16 \cdot 20 \cdot 10^{-3} \cdot 2 \cdot 10^{-2} \cdot 1 \cdot 10^{-14} \cdot 0.8 \cdot 1 \cdot 0.01 \cdot 0.8 \cdot 0.3 \cdot 10^8 \sqrt{0.1}}{5 \cdot 1 \cdot 10^{-14} \cdot 103 \cdot 3 \cdot 143 \cdot 9 \cdot 10^{-8} \cdot 270 \left(\frac{0.63}{6} + 2 \cdot 0.05 \right)^2 \sqrt{1 + 0.5}}} = 156 \text{ km.}$$

Thus, in the absence of interference, in this example, the locator provides a range of action $L_{r,r} = 156 \text{ km}$.

In order to evaluate the effectiveness of the use of corner reflectors, we use formulas (13.15) and (13.16).

Dividing the right and left parts term by term, we obtain

$$\frac{L_{r,r}}{L} = \sqrt{\frac{4A_{refl} \rho_{refl} 10^8 \cos \beta}{A_{ob} \rho_{refl} \cos^2 \beta \left(\frac{\lambda}{d \cos \beta} + 0.05n \right)}} \quad (13.17)$$

Considering $\beta = 0$, the areas of the reflecting surfaces equal to each other, i.e., $A_{refl} = A_{ob}$ and $\rho_{refl} = \rho_{refl}$ and assigning values n , λ , and d with which the expression in the parentheses will be no more than 1 (as a practical matter, it is 0.2-0.8), we find

/351

$$\frac{L_{r,r}}{L} = \sqrt{4 \cdot 10^8},$$

whence, $L_{r,r} = 1.4 \cdot 10^3 L$.

Thus, with the use of corner reflectors, the range of action increases considerably and, other conditions being equal, exceeds the range of action against an object without corner reflectors by more than two orders of magnitude.

13.2. Calculation of the Range of Action with the Presence of a Radiating Background

If the object against which a locator is operating is projected on a radiating background, along with the useful radiation background, radiation falls on the receiver which leads to an increase in noise and a worsening of the threshold sensitivity of the receiver. The appearance of background illumination causes the background component of the photocurrent and affects the value of the total current of the PM. For convenience in considering the effect of background illumination on the threshold flux, on the strength of certified characteristics and on the basis of expression (13.14), we write

$$F_{e.t.b}^{(1)} = \sqrt{\frac{5e(I_r + I_{bg})}{S_{PM} S_{pc}}}$$

whence we obtain

$$F_{e.t.b}^{(1)} = F_{s.t}^{(1)} \sqrt{1 + \frac{I_{fc}}{I_r}}, \quad (13.18)$$

where $F_{e.t.b}^{(1)}$ is the luminous threshold flux of the PM with the presence of background illumination and $\Delta f = 1$; $I_{fc} = S_b^l F_b = S_b \Phi_b$ is the photocurrent caused by the background illumination; S_b^l is the luminous integral sensitivity of the PM to background radiation, calculated from formula (12.14); F_b is the luminous flux from a background which falls on the photocathode of the PM; S_b is the integral sensitivity of the PM to radiation flux of the background determined by expression (12.10); Φ_b is the radiation flux from the background which falls on the photocathode.

It is known that with the complete filling of the field of view by the background, the value of the flux from it which falls on the receiver is determined by the relation /352

$$\Phi_b = B_b \omega_v A_{en.ap} \tau_0 \tau_f \text{ or } F_b = B_b \omega_v A_{en.ap} \tau_f \tau_0. \quad (13.19)$$

Thus, with the presence of background illuminations, the threshold sensitivity of the locator and, consequently, also its range of action depend not only on the characteristics of the background radiation, but also on the value of the angle of instantaneous field of view of the locator's receiver and the area of the entrance pupil of the objective.

We write (13.18), with consideration of formula (13.19), in the form

$$F_{e.t.b}^{(1)} = F_{s.t}^{(1)} \sqrt{1 + \frac{S_b^l k_s \tau_0 683 B_b \omega_v A_{en.ap} \tau_f \tau_0}{k_s I_r}} \quad (13.20)$$

or

$$F_{e.t.b}^{(1)} = F_{s.t}^{(1)} \sqrt{1 + \frac{S_b^l k_s \tau_0 683 B_b \omega_v A_{en.ap} \tau_0 \tau_f}{k_s B_b I_r}} \quad (13.20a)$$

Inasmuch as most often the background radiation is caused by scattered sunlight reflected from various objects, the

utilization coefficients necessary for this case can either be calculated by the method presented in Chapter 4 or taken from tables. For some standard photocathodes, the values of coefficients k_b and η_b for scattered solar radiation are given in Table 13.1 (bottom line).

In a number of cases, to reduce the effect of the background a narrow-band interference filter transparent for radiation with wavelength λ_{laser} with transmission band $\Delta\lambda_b$ from units of tens of Å is installed in the receiver in front of the radiation receiver. Then the value of constant background illumination in the spectral band $\Delta\lambda_b$ on wavelength λ_{laser} can be calculated in the following manner. For background illuminations whose function of spectral radiation density $r(\lambda)$ follows Planck's law, the share of radiation f_R taken over the spectral interval $\Delta\lambda_b$ can be calculated from the known formula (1.20).

The nature of change in the value of coefficients f_R , depending on the spectral composition of the radiations which is characterized by temperature T on various wavelengths λ with the width of the transmission filter $\Delta\lambda_b = 10$ Å is shown in Fig. 13.2¹. From the graphs, it can be seen that for scattered solar radiation whose spectral composition is characterized, for example, by temperature $T = 6000^\circ\text{K}$ on wavelengths of a gas laser (He-Ne), $\lambda_{\text{laser}} = 0.6328$ μm, and a ruby laser, $\lambda_{\text{laser}} = 0.6943$, coefficients $f_{R1} = 1.2 \cdot 10^{-3}$ ($\lambda = 0.6328$ μm) and $f_{R2} = 1.05 \cdot 10^{-3}$ ($\lambda = 0.6943$ μm).

Consequently, with the use of narrow-band filters it is necessary to consider their attenuation of the background, and then formulas (13.20) should take the form

/353

$$F_{e,t,b}^{(1)} = F_{s,t} \sqrt{1 + \frac{S_\lambda B_{\lambda,0} A}{h \nu_{\text{enap}} f_R(\lambda) \tau_0 \tau_f}}, \quad (13.21)$$

where $S_\lambda = S_s \frac{683 \eta_s}{k_s} s(\lambda)$ is the spectral sensitivity of the PM on the radiation wavelength of the laser; $s(\lambda)$ is the ordinate of the curve of relative spectral sensitivity of the PM on the radiation wavelength of the laser.

The needed values of S^λ for various PM can be read from the graphs presented in work [20].

¹ [Translator's note: Fig. 13.2 not presented in original text.]

Using relations (13.14) and (13.21), we obtain the final expression for calculating the value

$$\Phi_{t,b}^{(1)} = \frac{k_S}{s(\lambda) \eta_{S683}} \sqrt{\frac{5el_T}{S_{PM}^L S_{pc}^L}} \sqrt{1 + \frac{S_i B_i \omega A_{enap} f_R(\lambda) \tau_0 \tau_f}{I_T}} \quad (13.22)$$

or

$$\Phi_{t,b}^{(1)} = \Phi_{t,t}^{(1)} \sqrt{1 + \frac{S_i B_i \omega A_{enap} f_R(\lambda) \tau_0 \tau_f}{I_T}} \quad (13.22a)$$

The change in the value $\Phi_{t,t}^{(1)}$ depending on the wavelength for various PM calculated from the formula

$$\Phi_{t,t}^{(1)} = \frac{k_S}{s(\lambda) \eta_{S683}} \sqrt{\frac{5el_T}{S_{PM}^L S_{pc}^L}}$$

is shown in work [20].

A general formula for calculating the range of action of a locator with the presence of background is obtained from (13.15) with consideration of (13.22)

$$L = \sqrt[4]{\frac{4\Phi_{laser}^{eff} A_{ob}^{enap} \tau_e^2 \tau_0 \tau_f s(\lambda) \eta_{S683} \sqrt{T_K}}{m\pi^2 \theta_{sc} \sqrt{k_f(1+m_0)} k_s} \sqrt{\frac{5el_T}{S_{PM}^L S_{pc}^L}} \times \sqrt{1 + \frac{S_i B_i \omega A_{enap} f_R(\lambda) \tau_0 \tau_f}{I_T}}} \quad (13.23)$$

The range of action against objects with corner reflectors with consideration of equations (13.16) and (13.22a) can be determined from the formula

$$L = \sqrt[4]{\frac{16\Phi_{laser} A_{refl}^{enap} \tau_e^2 \tau_0 \tau_f \cos \beta \cdot 10^8 \sqrt{T_K} (\sqrt{k_f(1+m_0)})^{-1}}{m\Phi_{t,t}^{(1)} \sqrt{1 + \frac{S_i B_i \omega A_{enap} f_R(\lambda) \tau_0 \tau_f}{I_T}} \pi^2 \theta_{sc} \left(\frac{\lambda}{d \cos \beta} + 0.05n\right)^2}} \quad (13.24) \quad /354$$

These formulas show that the range of action of a locator increases not only with an increase in the power of the generator and area of the entrance pupil of the objective of the receiver, but also with a reduction in the angle of divergence, zone of scan, and reduction in the effect of the background through the use of narrower-band filters. They tie together the parameters of the locator, object, medium, and background situation and provide the opportunity to use the certified characteristics of the receivers in the calculations.

APPENDIX

TABLE 1. LUMINOUS EFFICIENCY AND EFFICIENCY OF THE EYE
FOR SOURCES WITH DIFFERENT TEMPERATURES

Tempera- ture of emitter, K	Efficien- cy of the eye	Luminous efficien- cy lm/W	Tempera- ture of emitter, K	Efficien- cy of the eye	Luminous efficien- cy, lm/W
1200	$6.10 \cdot 10^{-6}$	0.00417	5500	$1.30 \cdot 10^{-1}$	88.80
1300	$2.00 \cdot 10^{-5}$	0.01365	5750	$1.34 \cdot 10^{-1}$	91.50
1400	$5.50 \cdot 10^{-5}$	0.0383	6000	$1.36 \cdot 10^{-1}$	92.80
1500	$1.42 \cdot 10^{-4}$	0.0970	6500	$1.37 \cdot 10^{-1}$	93.60
1600	$2.82 \cdot 10^{-4}$	0.1923	7000	$1.35 \cdot 10^{-1}$	92.20
1700	$4.77 \cdot 10^{-4}$	0.3260	7500	$1.31 \cdot 10^{-1}$	89.50
1800	$6.00 \cdot 10^{-4}$	0.4105	8000	$1.26 \cdot 10^{-1}$	86.10
1900	$1.58 \cdot 10^{-3}$	1.050	8500	$1.21 \cdot 10^{-1}$	82.60
2000	$2.45 \cdot 10^{-3}$	1.675	9000	$1.14 \cdot 10^{-1}$	77.80
2100	$3.63 \cdot 10^{-3}$	2.480	9500	$1.07 \cdot 10^{-1}$	73.00
2200	$5.16 \cdot 10^{-3}$	3.620	10000	$9.88 \cdot 10^{-2}$	67.50
2300	$7.03 \cdot 10^{-3}$	4.800	11000	$9.48 \cdot 10^{-2}$	64.70
2360	$8.50 \cdot 10^{-3}$	5.810	12000	$8.90 \cdot 10^{-2}$	60.80
2400	$9.33 \cdot 10^{-3}$	6.370	13000	$7.60 \cdot 10^{-2}$	52.00
2500	$1.20 \cdot 10^{-2}$	8.20	14000	$6.74 \cdot 10^{-2}$	46.00
2600	$1.51 \cdot 10^{-2}$	10.30	15000	$5.83 \cdot 10^{-2}$	39.80
2700	$1.88 \cdot 10^{-2}$	12.80	16000	$5.11 \cdot 10^{-2}$	34.90
2850	$2.43 \cdot 10^{-2}$	17.00	17000	$4.45 \cdot 10^{-2}$	30.40
3000	$3.09 \cdot 10^{-2}$	21.10	18000	$3.85 \cdot 10^{-2}$	26.30
3100	$3.52 \cdot 10^{-2}$	24.10	19000	$3.33 \cdot 10^{-2}$	22.80
3200	$4.04 \cdot 10^{-2}$	27.60	20000	$3.06 \cdot 10^{-2}$	20.90
3300	$4.47 \cdot 10^{-2}$	30.50	25000	$1.73 \cdot 10^{-2}$	11.80
3400	$4.95 \cdot 10^{-2}$	33.80	30000	$1.18 \cdot 10^{-2}$	8.05
3500	$5.57 \cdot 10^{-2}$	38.00	35000	$8.61 \cdot 10^{-3}$	5.88
3750	$6.82 \cdot 10^{-2}$	46.70	40000	$5.37 \cdot 10^{-3}$	3.67
4000	$8.10 \cdot 10^{-2}$	55.30	45000	$3.84 \cdot 10^{-3}$	2.62
4250	$9.24 \cdot 10^{-2}$	63.20	50000	$3.58 \cdot 10^{-3}$	2.44
4500	$1.03 \cdot 10^{-1}$	70.50	55000	$3.18 \cdot 10^{-3}$	2.17
4750	$1.11 \cdot 10^{-1}$	75.80	60000	$2.64 \cdot 10^{-3}$	1.81
5000	$1.19 \cdot 10^{-1}$	81.30	65000	$2.11 \cdot 10^{-3}$	1.44
5250	$1.25 \cdot 10^{-1}$	85.40	70000	$1.33 \cdot 10^{-3}$	0.99

TABLE 2. CHARACTERISTICS OF SOME HEAVENLY BODIES POSSESSING
THE GREATEST BRILLIANCE

/355

Ordinal number	Stars and heavenly bodies	Hemis- phere	π_{vis}	v	Spectral class	Tempera- ture in K	Bolomet- ric cor- rection Δm	Illumi- nance lx	Irrad- iance W/cm ²	Color index		Color index c
										B-V	U-B	
1	Sirius (α Ma Canus Major)	S	-1.6	-1.43	A1	10300	-0.64	$1.15 \cdot 10^{-5}$	$1.73 \cdot 10^{-11}$	0.05	0.05	-0.12
2	Canopus (α Car - Carina)	S	-0.9	-0.73	0	7600	-0.09	$5.60 \cdot 10^{-6}$	$6.30 \cdot 10^{-12}$	0.30	0.02	0.12
3	Alpha Centauri (α Cen)	S	-0.3	-0.27	0	6000	-0.06	$4.00 \cdot 10^{-6}$	$4.30 \cdot 10^{-12}$	0.60	0.06	0.40
4	Vega (α Lyr - Lyra)	N	-0.14	0.04	A0	11000	-0.72	$3.00 \cdot 10^{-6}$	$4.64 \cdot 10^{-12}$	0.00	0.00	-0.15
5	Capella (α Aur - Auriga)	N	0.21	0.09	0	6000	-0.06	$2.90 \cdot 10^{-6}$	$3.12 \cdot 10^{-12}$	0.60	0.06	0.40
6	Arcturus (α Boo - Bootes)	N	0.24	-0.06	K2	3810	-0.72	$3.30 \cdot 10^{-6}$	$6.80 \cdot 10^{-12}$	1.16	1.20	1.15
7	Rigel (β Ori - Orion)	S	0.34	0.15	V3	12800	-1.16	$2.70 \cdot 10^{-6}$	$5.04 \cdot 10^{-12}$	-0.09	-0.29	-0.20
8	Procyon (α CMi - Canus Minor)	N	0.48	0.37	5	6540	-0.04	$2.25 \cdot 10^{-6}$	$2.40 \cdot 10^{-12}$	0.44	0.00	0.25
9	Achernar (α Eri - Eridanus)	S	0.60	0.53	V5	15600	-1.58	$1.95 \cdot 10^{-6}$	$5.30 \cdot 10^{-12}$	-0.16	-0.56	-0.35
10	Beta Centauri - β Cen	S	0.86	0.66	V1	22500	-2.48	$1.75 \cdot 10^{-6}$	$1.07 \cdot 10^{-11}$	-0.28	-1.00	-0.48
11	Altair (α Eri - Eridanus)	N	0.89	0.80	A7	8100	-0.22	$1.50 \cdot 10^{-6}$	$1.76 \cdot 10^{-12}$	0.19	0.08	-0.07
12	Betelgeuse (α Ori - Orion)	N	0.90	0.73	M2	3050	-3.00	$1.60 \cdot 10^{-6}$	$7.10 \cdot 10^{-12}$	1.57	1.86	1.7
13	Alpha Crux (α Cru)	S	1.40	0.87	V1	22500	-2.48	$1.40 \cdot 10^{-6}$	$8.54 \cdot 10^{-12}$	-0.28	-1.00	-0.48
14	Aldebaran (α Tau - Taurus)	N	1.06	0.85	K5	3550	-1.35	$1.40 \cdot 10^{-6}$	$3.52 \cdot 10^{-12}$	1.52	1.84	1.35
15	Pollux (α Gem - Gemini)	N	1.16	1.16	K0	4200	-0.54	$1.10 \cdot 10^{-6}$	$1.79 \cdot 10^{-12}$	1.01	0.86	1.05
16	Spica (α Vir - Virgo)	S	1.21	1.00	V1	22500	-2.48	$1.26 \cdot 10^{-6}$	$7.70 \cdot 10^{-12}$	-0.28	-1.00	-0.48
17	Antares (α Sco - Scorpius)	S	1.20	0.98	M1	3400	-1.70	$1.25 \cdot 10^{-6}$	$3.70 \cdot 10^{-12}$	1.48	1.21	1.40
18	Fomalhaut (α PSA - Piscis Austrinus)	S	1.29	0.87	A3	9100	-0.47	$1.40 \cdot 10^{-6}$	$1.82 \cdot 10^{-12}$	0.09	0.07	-0.05
19	Deneb (α Cyg - Cygnus)	N	1.33	1.26	A2	9700	-0.56	$1.00 \cdot 10^{-6}$	$1.41 \cdot 10^{-12}$	0.07	0.06	-0.10
20	Regulus (α Leo - Leo)	N	1.34	1.36	V7	13600	-1.24	$8.90 \cdot 10^{-7}$	$1.84 \cdot 10^{-12}$	-0.13	-0.47	-0.22

TABLE 3. CHARACTERISTICS OF A SOLID-STATE LASER

/356

		Basic characteristics									
Brand laser	Active substance	Radiation wavelength, λ , μm	Radiation energy, J	Pulse duration, sec	Radiation power in pulse, W	Beam divergence, rad	Frequency of pulses, Hz	Excitation energy, J	Power consumption, W	Overall dimensions, mm	Mass, kg
OGM-20	Ruby	0.6943	0.4	$20 \cdot 10^{-9}$	$2 \cdot 10^8$	$6 \cdot 10^{-4}$	1	800	1500	$523 \times 915 \times 1390$	110
GSI-1	Glass with admixture of neodymium	1.0600	75	$7 \cdot 10^{-4}$	10^6	$2,25 \cdot 10^{-2}$	0.1	1200	—	—	200
GOS-100.M	Glass with admixture of neodymium	1.0600	250	$1.5 \cdot 10^{-3}$	$1,7 \cdot 10^5$	—	0.01	30000	3000	—	—
GOR-300	Ruby	0.6943	300	—	—	$1.8 \cdot 10^{-2}$	0.003	—	700	$160 \times 610 \times 250$	38
IT-118	Calcium tungstate	1.0600	—	—	0.1 Continuous mode	—	—	—	—	—	10

* Radiation on wavelength $\lambda = 0.5300 \mu\text{m}$ obtained due to conversion of radiation of the master oscillator $s = 1.0600 \mu\text{m}$ with KDR crystals.

TABLE 4. BASIC CHARACTERISTICS OF GAS LASERS

/357

Brand laser	Basic characteristics							Power-supply source				Mass, kg
	Active substance	Radiation wavelength μm	Radiation power, W	Operating mode	Beam divergence, rad	Dimensions of radiating head	Mass of radiating head, kg	Type	Output power, W	Power consumption, W	Overall dimensions, mm	
OKG-11	He-Ne	0.6328	$2 \cdot 10^{-3}$	Continuous	$(1.5-3) \times 10^{-3}$	—	—	—	—	—	—	—
LG-35	He-Ne	0.6328 1.15	$(6-10) \times 10^{-3}$	Continuous	$(3-9) \times 10^{-4}$	$1530 \times 240 \times 308$	45	The same	—	530	$450 \times 370 \times 230$	20
LG-55	He-Ne	0.6328	$(1-2) \times 10^{-3}$	Continuous	$(1.5-3) \times 10^{-3}$	$363 \times 72 \times 58$	1.5	Direct current	—	66 BA	$297 \times 166 \times 150$	5
"Malakhit"	Ar	0.4545 + 0.5145	0.2—0.5	Continuous	—	$870 \times 412 \times 245$	40	—	—	—	—	—
"Prometei"-50	$\text{CO}_2 + \text{N}_2 + \text{He}$	10.6	50	Continuous	—	$1800 \times 150 \times 150$	—	Direct current	—	2000	$1100 \times 650 \times 850$	—

TABLE 5. CHARACTERISTICS OF SEMICONDUCTOR LASERS

/358

Brand laser	Working substance	Radiation wavelength, μm	Spectrum width, \AA	Operating mode	Frequency of pulses, kHz	Pulse duration, ns	Radiation power in pulse	Modulation frequency in continuous mode	Width of beam, rad	Cooling temperature, K	Efficiency	Overall dimensions, mm
S-51	Ga-As	0.90	—	Pulsed	2	100	200	2.0	$0.58 \times 2.9 \cdot 10^{-4}$	to 330		
		0.85	—	.	—	30	60	—	—	to 77	0.4	
		0.85	—	.	—	1000	20	—	—	to 77	0.4	
			—	.	0.01--0.1	50	4	—	$0.35 \times 0.35 \times 2.9 \cdot 10^{-4}$	300	0.002	
RCA	.	9.155	50	.	50	90	12	—	$0.35 \times 0.35 \times 2.9 \cdot 10^{-4}$	300	0.06	12×6×2.5
MVZ	.	0.65--0.85	8	.	—	50000	0.5	—	$0.35 \times 0.35 \times 2.9 \cdot 10^{-4}$	77	0.15	
PKG	.	0.85	5	.	10	100	10--12	—	—	300	0.15	170×110×200
"Kometa-1"	.	0.84--0.86	20	.	0.04--1.0	200	3	—	—		0.15	170×110×200

TABLE 6. COEFFICIENTS OF SPECTRAL TRANSMISSION OF THE ATMOSPHERE
DEPENDING ON THICKNESS OF LAYER OF PRECIPITATED WATER
VAPOR (AT SEA LEVEL)

/359

Wavelength λ	Thickness of layer of precipitated water vapor, W, mm.										
	0.1	0.5	1	5	10	20	50	100	200	500	1000
0.3	0.980	0.955	0.937	0.860	0.802	0.723	0.574	0.428	0.263	0.076	0.012
0.4	0.980	0.955	0.937	0.860	0.802	0.723	0.574	0.428	0.263	0.076	0.012
0.5	0.986	0.968	0.956	0.901	0.861	0.804	0.695	0.579	0.433	0.215	0.079
0.6	0.990	0.977	0.968	0.929	0.900	0.860	0.779	0.692	0.575	0.375	0.210
0.7	0.991	0.980	0.972	0.937	0.910	0.873	0.800	0.722	0.615	0.425	0.260
0.8	0.989	0.975	0.965	0.922	0.891	0.845	0.758	0.663	0.539	0.330	0.168
0.9	0.965	0.922	0.800	0.757	0.661	0.535	0.326	0.165	0.050	0.002	0
1.0	0.990	0.977	0.968	0.929	0.900	0.860	0.779	0.692	0.575	0.375	0.210
1.1	0.970	0.932	0.905	0.790	0.707	0.595	0.406	0.235	0.093	0.008	0
1.2	0.980	0.955	0.937	0.860	0.802	0.723	0.574	0.428	0.263	0.076	0.012
1.3	0.720	0.432	0.268	0.013	0	0	0	0	0	0	0
1.4	0.930	0.844	0.782	0.536	0.381	0.216	0.064	0.005	0	0	0
1.5	0.997	0.991	0.988	0.972	0.960	0.944	0.911	0.874	0.823	0.724	0.616
1.6	0.998	0.996	0.994	0.986	0.980	0.972	0.956	0.937	0.911	0.860	0.802
1.7	0.998	0.996	0.994	0.986	0.980	0.972	0.956	0.937	0.911	0.860	0.802
1.8	0.792	0.555	0.406	0.062	0.008	0	0	0	0	0	0
1.9	0.960	0.911	0.874	0.723	0.617	0.479	0.262	0.113	0.024	0	0
2.0	0.935	0.966	0.953	0.894	0.851	0.790	0.674	0.552	0.401	0.184	0.006
2.1	0.997	0.991	0.988	0.972	0.960	0.944	0.911	0.874	0.823	0.724	0.616
2.2	0.998	0.996	0.994	0.986	0.980	0.972	0.956	0.937	0.911	0.860	0.802
2.3	0.997	0.991	0.988	0.972	0.960	0.944	0.911	0.874	0.823	0.724	0.616
2.4	0.980	0.955	0.937	0.860	0.802	0.723	0.574	0.428	0.263	0.076	0.012
2.5	0.930	0.844	0.782	0.536	0.381	0.216	0.064	0.005	0	0	0
2.6	0.617	0.261	0.110	0	0	0	0	0	0	0	0
2.7	0.351	0.040	0.004	0	0	0	0	0	0	0	0
2.8	0.453	0.092	0.017	0	0	0	0	0	0	0	0
2.9	0.689	0.369	0.205	0.005	0	0	0	0	0	0	0
3.0	0.851	0.673	0.552	0.184	0.060	0.008	0	0	0	0	0
3.1	0.900	0.779	0.692	0.375	0.210	0.076	0.005	0	0	0	0
3.2	0.525	0.833	0.766	0.506	0.347	0.184	0.035	0.003	0	0	0
3.3	0.950	0.888	0.843	0.658	0.531	0.377	0.161	0.048	0.005	0	0
3.4	0.973	0.939	0.914	0.811	0.735	0.633	0.448	0.285	0.130	0.017	0.001
3.5	0.988	0.973	0.962	0.915	0.881	0.832	0.736	0.635	0.502	0.287	0.133

TABLE 6 [continued]

/360

Wavelength λ	Thickness of layer of precipitated water vapor, W, mm										
	0.1	0.5	1	5	10	20	50	100	200	500	1000
3.6	0.994	0.987	0.982	0.958	0.947	0.916	0.866	0.812	0.738	0.596	0.452
3.7	0.997	0.991	0.988	0.972	0.960	0.944	0.911	0.874	0.823	0.724	0.616
3.8	0.998	0.995	0.994	0.986	0.980	0.972	0.956	0.937	0.911	0.860	0.802
3.9	0.998	0.995	0.994	0.986	0.980	0.972	0.956	0.937	0.911	0.860	0.802
4.0	0.997	0.993	0.990	0.977	0.970	0.960	0.930	0.900	0.870	0.790	0.700
4.1	0.997	0.991	0.988	0.972	0.960	0.944	0.911	0.874	0.823	0.724	0.616
4.2	0.994	0.987	0.982	0.958	0.947	0.916	0.866	0.812	0.738	0.596	0.452
4.3	0.991	0.975	0.972	0.937	0.910	0.873	0.800	0.722	0.615	0.425	0.260
4.4	0.980	0.955	0.937	0.860	0.802	0.723	0.574	0.428	0.263	0.076	0.012
4.5	0.970	0.932	0.905	0.790	0.707	0.595	0.400	0.235	0.093	0.008	0
4.6	0.966	0.911	0.874	0.723	0.617	0.478	0.262	0.113	0.024	0	0
4.7	0.950	0.888	0.743	0.658	0.531	0.377	0.161	0.048	0.005	0	0
4.8	0.940	0.866	0.812	0.595	0.452	0.289	0.117	0.018	0.001	0	0
4.9	0.930	0.844	0.782	0.536	0.381	0.216	0.064	0.005	0	0	0
5.0	0.915	0.811	0.736	0.451	0.286	0.132	0.017	0	0	0	0
5.1	0.885	0.747	0.649	0.308	0.149	0.041	0.001	0	0	0	0
5.2	0.846	0.664	0.539	0.168	0.052	0.006	0	0	0	0	0
5.3	0.792	0.555	0.406	0.062	0.008	0	0	0	0	0	0
5.4	0.726	0.432	0.208	0.013	0	0	0	0	0	0	0
5.5	0.617	0.261	0.110	0	0	0	0	0	0	0	0
5.6	0.491	0.121	0.029	0	0	0	0	0	0	0	0
5.7	0.361	0.040	0.004	0	0	0	0	0	0	0	0
5.8	0.141	0.001	0	0	0	0	0	0	0	0	0
5.9	0.141	0.001	0	0	0	0	0	0	0	0	0
6.0	0.180	0.003	0	0	0	0	0	0	0	0	0
6.1	0.260	0.012	0	0	0	0	0	0	0	0	0
6.2	0.552	0.313	0.153	0.001	0	0	0	0	0	0	0
6.3	0.552	0.182	0.060	0	0	0	0	0	0	0	0
6.4	0.317	0.025	0.002	0	0	0	0	0	0	0	0
6.5	0.164	0.002	0	0	0	0	0	0	0	0	0
6.6	0.138	0.001	0	0	0	0	0	0	0	0	0
6.7	0.322	0.037	0.002	0	0	0	0	0	0	0	0
6.8	0.361	0.040	0.004	0	0	0	0	0	0	0	0
6.9	0.416	0.068	0.010	0	0	0	0	0	0	0	0
7.0	0.532	0.161	0.048	0	0	0	0	0	0	0	0

TABLE 7. COEFFICIENTS OF SPECTRAL TRANSMISSION OF THE ATMOSPHERE /361
WITH ATTENUATION OF RADIATION BY CARBON DIOXIDE DEPENDING ON
LENGTH OF PATH (AT SEA LEVEL)

Wave- length λ	Length of path, L, km											
	0.1	0.5	1	2	5	10	20	50	100	200	500	1000
0.3-1.2	1.000	1.000	1.000	1.000	1.000	1.000	1.000	1.000	1.000	1.000	1.000	1.000
1.3	1.000	1.000	0.999	0.999	0.999	0.998	0.997	0.996	0.994	0.992	0.987	0.982
1.4	0.996	0.992	0.988	0.984	0.975	0.964	0.949	0.919	0.885	0.838	0.747	0.649
1.5	0.999	0.998	0.998	0.997	0.995	0.993	0.990	0.984	0.976	0.967	0.949	0.927
1.6	0.996	0.992	0.988	0.984	0.975	0.964	0.949	0.919	0.885	0.838	0.747	0.649
1.7	1.000	1.000	0.999	0.999	0.999	0.998	0.997	0.996	0.994	0.992	0.987	0.982
1.8	1.000	1.000	1.000	1.000	1.000	1.000	1.000	1.000	1.000	1.000	1.000	1.000
1.9	1.000	1.000	0.999	0.999	0.999	0.998	0.997	0.996	0.994	0.992	0.987	0.982
2.0	0.978	0.951	0.931	0.903	0.847	0.785	0.699	0.541	0.387	0.221	0.053	0.006
2.1	0.998	0.996	0.994	0.992	0.987	0.982	0.974	0.959	0.942	0.919	0.872	0.820
2.2-2.6	1.000	1.000	1.000	1.000	1.000	1.000	1.000	1.000	1.000	1.000	1.000	1.000
2.7	0.799	0.569	0.419	0.253	0.071	0.011	0	0	0	0	0	0
2.8	0.871	0.695	0.578	0.432	0.215	0.079	0.013	0	0	0	0	0
2.9	0.997	0.993	0.990	0.985	0.977	0.968	0.954	0.927	0.898	0.855	0.772	0.688
3.0-3.9	1.000	1.000	1.000	1.000	1.000	1.000	1.000	1.000	1.000	1.000	1.000	1.000
4.0	0.998	0.996	0.994	0.991	0.986	0.980	0.971	0.955	0.937	0.911	0.852	0.802
4.1	0.983	0.961	0.944	0.921	0.876	0.825	0.755	0.622	0.485	0.322	0.118	0.027
4.2	0.673	0.445	0.182	0.059	0.003	0	0	0	0	0	0	0
4.3	0.098	0	0	0	0	0	0	0	0	0	0	0
4.4	0.481	0.115	0.026	0.002	0	0	0	0	0	0	0	0
4.5	0.957	0.903	0.863	0.807	0.699	0.585	0.439	0.222	0.084	0.014	0	0
4.6	0.935	0.989	0.985	0.978	0.966	0.951	0.931	0.891	0.815	0.783	0.663	0.539
4.7	0.935	0.989	0.985	0.978	0.966	0.951	0.931	0.891	0.815	0.783	0.663	0.539
4.8	0.976	0.945	0.922	0.891	0.828	0.759	0.664	0.492	0.331	0.169	0.030	0.002
4.9	0.975	0.913	0.920	0.886	0.822	0.750	0.652	0.468	0.313	0.153	0.024	0.001
5.0	0.999	0.997	0.995	0.994	0.990	0.986	0.979	0.968	0.954	0.935	0.897	0.855
5.1	1.000	0.999	0.998	0.998	0.996	0.994	0.992	0.988	0.984	0.976	0.961	0.946
5.2	0.986	0.968	0.955	0.936	0.899	0.857	0.799	0.687	0.560	0.420	0.203	0.072
5.3	0.937	0.993	0.989	0.984	0.976	0.966	0.951	0.923	0.891	0.846	0.760	0.666
5.4-7.0	1.000	1.000	1.000	1.000	1.000	1.000	1.000	1.000	1.000	1.000	1.000	1.000

TABLE 8. BASIC CHARACTERISTICS OF PHOTOMULTIPLIERS

/362

PM	Spectral character- istic	Size of photocath- ode	Utilization coefficient	$U_{\text{pow. sup.}}$, V	I_{ph} , A	S_{pc} , $\mu\text{A/lm}$	S_{PM} , $\mu\text{A/lm}$	$F_{\text{s.t}}$, $\text{lm/Hz}^{\frac{1}{2}}$	S_{pc} , $\mu\text{A/W}$	S_{PM} , A/W	$\phi_{\text{s.t}}$, $\text{W/Hz}^{\frac{1}{2}}$	S_{pc} , $\mu\text{A/W}$	S_{PM} , A/W	$\phi_{\text{s.t}}$, $\text{W/Hz}^{\frac{1}{2}}$
PM-15A	S 5	20	0.0402	1700	$1 \cdot 10^{-7}$	40	30	$8.20 \cdot 10^{-12}$	664	500	$4.95 \cdot 10^{-13}$	$1.73 \cdot 10^4$	$1.24 \cdot 10^4$	$1.98 \cdot 10^{-14}$
PM-17A	S 6	16×5	0.0158	1400	$3 \cdot 10^{-7}$	20	1000		332	$1.66 \cdot 10^4$	$2.08 \cdot 10^{-13}$	$2.1 \cdot 10^4$	$1.05 \cdot 10^6$	$3.30 \cdot 10^{-15}$
PM-25	S 6		0.0158	1700	$6 \cdot 10^{-9}$	35	4	$5.85 \cdot 10^{-12}$	580	66.4	$3.53 \cdot 10^{-13}$	$3.68 \cdot 10^4$	$4.70 \cdot 10^3$	$5.55 \cdot 10^{-15}$
PM-27	S 7	25	0.0473	1100	$5 \cdot 10^{-9}$	30	1	$1.15 \cdot 10^{-11}$	500	16.6	$6.95 \cdot 10^{-13}$	$1.06 \cdot 10^4$	$3.51 \cdot 10^2$	$3.34 \cdot 10^{-14}$
PM-31	S 6	25 cm^2	0.0158	1400	$5 \cdot 10^{-7}$	20	10	$4.47 \cdot 10^{-11}$	332	166	$2.70 \cdot 10^{-12}$	$2.1 \cdot 10^4$	$1.18 \cdot 10^4$	$4.25 \cdot 10^{-14}$
PM-46	S 6		0.0158		$1 \cdot 10^{-10}$	30	10	$5.16 \cdot 10^{-13}$	500	166	$3.12 \cdot 10^{-14}$	$3.16 \cdot 10^4$	$1.18 \cdot 10^4$	$4.90 \cdot 10^{-16}$
PM-46A	S 9		0.0172		$1 \cdot 10^{-10}$	30	10	$5.16 \cdot 10^{-13}$	500	166	$3.12 \cdot 10^{-14}$	$2.9 \cdot 10^4$	$9.65 \cdot 10^3$	$5.34 \cdot 10^{-16}$
PM-52	S 8	70	0.0176	1800	$6 \cdot 10^{-8}$	45	10	$1.03 \cdot 10^{-11}$	750	166	$6.20 \cdot 10^{-13}$	$4.25 \cdot 10^4$	$9.43 \cdot 10^3$	$1.09 \cdot 10^{-14}$
PM-62	S 1	10	0.208	1300	$6 \cdot 10^{-8}$	15	1	$5.65 \cdot 10^{-11}$	250	16.6	$3.42 \cdot 10^{-12}$	$1.2 \cdot 10^3$	80	$6.80 \cdot 10^{-13}$
PM-64	S 6	5	0.0158	1500	$5 \cdot 10^{-8}$	25	1000	$1.26 \cdot 10^{-12}$	415	$1.66 \cdot 10^4$	$7.60 \cdot 10^{-14}$	$2.6 \cdot 10^4$	$1.18 \cdot 10^6$	$1.20 \cdot 10^{-15}$
PM-67	S 6	10	0.0158	1250	$5 \cdot 10^{-9}$	20	3	$8.16 \cdot 10^{-12}$	332	50	$4.93 \cdot 10^{-13}$	$2.1 \cdot 10^4$	$3.50 \cdot 10^3$	$7.77 \cdot 10^{-15}$
PM-68	S 11	10	0.0418	1400	$1 \cdot 10^{-8}$	60	1	$1.15 \cdot 10^{-11}$	1000	16.6	$6.95 \cdot 10^{-13}$	$2.39 \cdot 10^4$	$4.00 \cdot 10^2$	$2.90 \cdot 10^{-14}$
PM-71	S 15	16	0.0156	1000	$1 \cdot 10^{-8}$	30	100	$1.63 \cdot 10^{-12}$		$1.66 \cdot 10^3$	$9.82 \cdot 10^{-14}$	$3.2 \cdot 10^4$	$1.06 \cdot 10^5$	$1.53 \cdot 10^{-15}$
				1300	$5 \cdot 10^{-7}$		1000	$3.65 \cdot 10^{-12}$	500	$1.66 \cdot 10^4$	$2.20 \cdot 10^{-13}$		$1.06 \cdot 10^6$	$3.42 \cdot 10^{-15}$

1. Alekseyev, K.B. and G.G. Bebenin, Upravleniye kosmicheskimi letatel'nyimi apparatami [Control of Spacecraft], Mashinostroyeniye, Moscow, 1964.
2. Beletskiy, V.V., Dvizheniye iskusstvennogo sputnika otnositel'no tsentra mass [Movement of an Artificial Satellite Relative to the Center of Mass], Nauka, Moscow, 1965.
3. Bramson, M.A., Infrakrasnoye izlucheniye nagretykh tel [Infrared Radiation of Heated Bodies], Nauka, Moscow, 1965.
4. Bramson, M.A., Spravochnyye tablitsy po infrakrasnomu izlucheniyu nagretykh tel [Reference Tables on Infrared Radiation of Heated Bodies], Nauka, Moscow, 1964.
5. Watanabe, K., "Processes of Absorption of Ultraviolet Radiation in the Upper Atmosphere," in the book Issledovaniye verkhney atmosfery s pomoshch'yu raket i sputnikov [Investigation of the Upper Atmosphere with the Aid of Rockets and Satellites], Foreign Literature Publishing House, Moscow, 1961.
6. Volosov, D.S. and M.V. Tsyvkin, Teoriya i raschet svetoopticheskikh sistem [Theory and Design of Light-Optics Systems] Iskusstvo, Moscow, 1960.
7. Voronkova, Ye.M. et al., Opticheskiye materialy dlya infrakrasnoy tekhniki [Optical Materials for Infrared Equipment], Nauka, Moscow, 1965.
8. Jamisson, J.E. et al., Fizika i tekhnika infrakrasnogo izlucheniya [Physics and Equipment of Infrared Radiation], Sovetskoye radio, Moscow, 1965.
9. Yefimov, M.V., Avtomaticheskiye sistemy s opticheskimi obratnymi svyazyami [Automatic Systems with Optical Feedbacks], Energiya, Moscow, 1969.
10. Zuyev, V.Ye., Prozrachnost' atmosfery dlya vidimyykh i infrakrasnykh luchey [Transparency of the Atmosphere for Visible and Infrared Rays], Sovetskoye radio, Moscow, 1966.
11. Ivandikov, Ya.M., Optiko-elektronnyye pribory dlya oriyentatsii i navigatsii kosmicheskikh apparatov [Electro-optical Instruments for Orientation and Navigation of Spacecraft], Mashinostroyeniye, Moscow, 1971.

12. Lashin, A.N. and B.F. Fedorov, Opticheskiye kvantovyye generatory v voyennom dele [Lasers in Military Affairs], Sovetskoye radio, Moscow, 1966.
13. Isayev, S.I. and N.V. Pushkov, Polyarnyye siyaniya [Polar Auroras], Izd-vo AN SSSR, Moscow, 1958.
14. Katys, P.G., Informatsionnyye skaniruyushchiye sistemy [Information Scanning Systems], Nauka, Moscow, 1965.
15. Karachentsev, I.D., "The Influence of Micrometeorites on Optical Surfaces," in the book Iskusstvennyye sputniki Zemli [Artificial Earth Satellites], Izd-vo AN SSSR, Issue 15, Moscow, 1963.
16. Kozelkin, V.V. and I.F. Usol'tsev, Osnovy infrakrasnoy tekhniki [Principles of Infrared Equipment], Mashinostroyeniye, Moscow, 1967.
17. Kondrat'yev, K.Ya. and K.Ye. Yanushevskaya, "Angular Distribution of Departing Thermal Radiation in Various Regions of the Spectrum," in the book Iskusstvennyye sputniki Zemli [Artificial Earth Satellites], Izd-vo AN SSSR, Issue 14, Moscow, 1962.
18. Kriksunov, L.Z. and I.F. Usol'tsev, Infrakrasnyye sistemy obnaruzheniya pelengatsii i avtomaticheskogo soprovozhdeniya dvizhushchikhsya ob'yektov [Infrared Systems for the Detection, Direction Finding, and Automatic Tracking of Moving Objects], Sovetskoye radio, Moscow, 1968.
19. Kulikovskiy, P.G., Spravochnik lyubitelya astronomii [Reference Book for the Amateur Astronomer], Fizmatgiz, Moscow, 1964.
20. Lazarev, L.P., Infrakrasnyye i svetovyye pribory samonavedeniya i navedeniya letatel'nykh apparatov [Infrared and Luminous Instruments for Homing and Guidance of Aircraft], Mashinostroyeniye, Moscow, 1966.
21. Luk'yanov, S.Yu., Fotoelementy [Photocells], Izd-vo AN SSSR, Moscow, 1948.
22. Makutov, D.D., Astronomicheskaya optika [Astronomic Optics], Z364 GTTI, 1959.
23. Markov, M.N., Priyemniki infrakrasnogo izlucheniya [Infrared Radiation Receivers], Nauka, Moscow, 1968.
24. Meshkov, V.V., Osnovy svetotekhniki, [Principles of Illumination Engineering], Part 1, Gosenergoizdat, Moscow, 1957.

25. Miroshnikov, M.M., "A New Trend in Infrared Equipment -- Television," Trudy Gosudarstvennogo Opticheskogo instituta im. S.I. Vavilova XXIX, Issue 158 (1965).
26. Mirtov, B.A., "Meteoric Matter and Problems of Geophysics of the Upper Layers of the Atmosphere," in the book Iskusstvennyye sputniki Zemli [Artificial Earth Satellites], Izd-vo AN SSSR, Issue 4, Moscow, 1960.
27. Mikhnevich, V.V. et al., "Some Results in Determining Parameters of the Atmosphere," in the book Iskusstvennyye sputniki Zemli [Artificial Earth Satellites], Izd-vo AN SSSR, Issue 3, Moscow, 1959.
28. Moroz, V.I., "About the Earth's Dust Shell," in the book Iskusstvennyye sputniki Zemli [Artificial Earth Satellites], Izd-vo AN SSSR, Issue 12, Moscow, 1962.
29. Nazarova, T.N., "Investigation of Meteoric Dust on Rockets and Artificial Earth Satellites," in the book Iskusstvennyye sputniki Zemli [Artificial Earth Satellites], Izd-vo AN SSSR, Issue 12, Moscow, 1962.
30. Frishman, N.G., "Distribution of Energy in Spectra of Polar Auroras in the Region of 3900-8707 A," Optika i spektroskopiya 6 (1959).
31. Olesk, A.O., Fotorezistory [Photoresistors], Energiya, Moscow, 1967.
32. Pavlov, A.V. and D.P. Shelkovnikov, "How to Calculate Integral Sensitivity," Tekhnika i vooruzheniye (3) (1961).
33. Petrov, V.P., Kosmicheskiye stantsii pogody [Weather Satellites], Izd-vo AN SSSR, Moscow, 1966.
34. Malkevich, M.C., ed., Rakety i iskusstvennyye sputniki v meteorologii [Rockets and Artificial Satellites in Meteorology], Foreign Literature Publishing House, Moscow, 1963.
35. Safronov, Yu.P., Yu.G. Andrianov, and D.S. Iyevlev, Infra-krasnaya tekhnika v kosmose [Infrared Equipment in Space], Voenizdat, Moscow, 1963.
36. Seleznev, V.P. and M.L. Kirst, Sistemy navigatsii kosmicheskikh letatel'nykh apparatov [Systems for the Navigation of Spacecraft], Voenizdat, Moscow, 1965.
37. Smith, R., F. Jones and R. Chesmer, Obnaruzheniye i izmereniye infrakrasnogo izlucheniya [Detection and Measurement of Infrared Radiation], Foreign Literature Publishing House, Moscow, 1959.

38. Soboleva, N.A., A.G. Berkovskiy, N.O. Chechik, et al., Fotoelektronnyye pribory [Photoelectronic Instruments], Nauka, Moscow, 1965.
39. Spravochnaya kniga po svetotekhnike [Reference Book on Illumination Engineering], Izd-vo AN SSSR, Moscow, 1956.
40. Elektrovakuumnyye pribory, spravochnik [Vacuum Tube Devices, Reference Book], Vol. III, Ministry of the Electronics Industry, 2nd edition, 1967.
41. Sputniki svyazi [Communication Satellites], Voenizdat, Moscow, 1966.
42. Tverskoy, P.N., ed., Meteorologiya [Meteorology], Gidrometeoizdat, Moscow, 1951.
43. Tikhodeyev, P.M., Svetovyye izmereniya v svetotekhnike [Light Measurements in Illumination Engineering], Gosenergoizdat, Moscow, 1962.
44. Tudorovskiy, A.I., Teoriya opticheskikh priborov [Theory of Optical Instruments], Izd-vo AN SSSR, Moscow, 1970.
45. Turygin, I.A., Prikladnaya optika [Applied Optics], Mashinostroyeniye, Moscow, 1965.
46. Fabri, Vvedeniye v fotometriyu [Introduction to Photometry], ONTI, 1934.
47. Frimmer, A.I. and I.I. Taubkin, ed., Poluprovodnikovyye foto-priyemniki i preobrazovateli izlucheniya (Sbornik statey) [Semiconductor Photoreceivers and Radiation Converters (Collection of Articles)], Mir, Moscow, 1965.
48. Khrigian, A.Kh., Fizika atmosfery [Physics of the Atmosphere], Gostekhizdat, Moscow, 1953.
49. Chechik, N.O., S.M. Faynshteyn, and T.N. Lifshits, Fotoelektronnyye umnozhiteli [Photomultipliers], Gostekhizdat, Moscow, 1957.
50. Churillovskiy, V.N., Teoriya opticheskikh priborov [Theory of Optical Instruments], Mashinostroyeniye, Moscow, 1966.
51. Yakushenkov, Yu.G., Fizicheskiye osnovy optiko-elektronnykh priborov [Physical Properties of Electro-Optical Instruments], Sovetskoye radio, Moscow, 1965.
52. Aviatsiya i kosmonavtika (10) (1965); (2) (1963).

53. Voprosy raketnoy tekhniki (6) (1963); (10) (1969).
54. Pol', A.I., "Results of Visual and Photometric Observation of Polar Auroras," Geomagnetizm i aeronomiya 1 (1961).
55. Raketnaya i kosmicheskaya tekhnika [Missile and Space Techno- /365
logy] 1964-1965.
56. Issledovaniye kosmicheskogo prostranstva [Investigation of
Outer Space], Journal of Abstracts (4, 7, 9) (1966).
57. Arck, M., "Simulator Proves Operation of Horizon Sensors,"
Automatic Control 15(3), 21-26 (1961).
58. Astheimer, R.W., "Infrared Horizon Sensors for Attitude
Determination," Peaceful Uses of Automatics in Outer Space,
Plenum Press, New York, 1966.
59. Astheimer, R.W., Infrared Horizon Sensor Techniques for Lunar
and Planetary Approaches [sic].
60. Beller, W. and R. Van Osten, "Mariner Carrier Planet Fly-by
Hopes," Missiles and Rockets 8(1,2) (1961).
61. Bishop, D.R., "Horizon Seeker Errors Arising Out of the
Statistical Properties of the Horizon," Amer. Astronaut. Soc.
[sic] 96 (1961).
62. Kendall, P.E. and R.E. Stalcup, "Attitude Reference Device for
Space Vehicles," Proc. IRE 48(4) (1960).
63. Kovit, B., "Infrared Horizon Sensor Guides Planetary Orbiting,"
Space Aeronautics 35(2), 131-133 (1961).
64. Newcomb, A.L. et al., "A Novel Moon and Planet-Seeking Attitude
Sensor for Use in Spacecraft Orientation and Control, IEEE
International Convention Records (4), 48-53 (1965).
65. Hanel, R.A., W.K. Bandech, and R.T. Conrath, "The Infrared
Horizon of the Planet Earth," NASA Preprint, Goddard Space
Flight Center, Greenbelt, Md., August 1962, pp. 1-20.
66. Navigation 3(3) (1966).
67. Wermser, E.M., "Infrared Instrumentation: A Sure Bet for
Spacecraft," Space Aeronautics 36(2), 127-142 (1961).
68. Peaceful Uses of Automatics in Outer Space, Plenum Press,
New York, 1966, p. 119.

69. Miller, B., "New IR Space Sensors Add to Reliability," Aviation Week, 68-71 (1964).
70. Schwarz, F. and T. Falk, "High Accuracy, High Reliability Infrared Horizon Sensors for Earth, Lunar and Planetary Use," Navigation 13(3), 246-259 (1966).